STUDIES TOWARD THE SYNTHESES OF ANTIARRHYTHMIC, ANTI-VIRULENCE, AND ANTICANCER SMALL MOLECULES

APPROVED BY SUPERVISORY COMMITTEE:

Laszlo, Kürti, Ph.D, Chair

Chuo, Chen, Ph.D

David, R. Corey, Ph.D

John, R. Falck, Ph.D, DIC

Dedicated to my family, friends, and loved ones.

STUDIES TOWARD THE SYNTHESES OF ANTIARRHYTHMIC, ANTI-VIRULENCE, AND ANTICANCER SMALL MOLECULES

by

ADENIYI MICHAEL ADEBESIN

DISSERTATION

Presented to the Faculty of the Graduate School of Biomedical Sciences

The University of Texas Southwestern Medical Center at Dallas

In Partial Fulfillment of the Requirements

For the Degree of

DOCTOR OF PHILOSOPHY IN

BIOLOGICAL CHEMISTRY

The University of Texas Southwestern Medical Center

Dallas, Texas

December, 2015

Copyright

ADENIYI MICHAEL ADEBESIN, 2015

All Rights Reserved

ACKNOWLEDGMENTS

I would like to express my warmest gratitude to Prof. J.R. Falck for his mentorship and patience with me during my work on the projects recorded in this dissertation. His emphasis on hard work, open-mindedness, creativity, and a hopeful attitude has helped me become a wiser and more independent scientist. Also, thanks to Prof. Laszlo Kürti for his many encouragements, support and invaluable ideas during and outside committee meetings. The gentleness and mental acuity of Prof. David Corey and Prof. Chuo Chen made committee meetings a fruitful and safe environment, and for this I thank you. I will also like to thank the members of my dissertation committee for always being very flexible with scheduling committee meetings and for taking the time to mentor me. You guys are the best.

I am thankful to Prof. W-H. Schunck and his coworkers for their promptness in the evaluation of the pharmacological properties of the 17,18-EEQ analogs. Their contributions were critical for the success of the project.

Many thanks to Prof. Sperandio, Regan Russell, Prof. Noelle Williams, Dr. Changguang Wang, and the other collaborators who contributed toward the biological studies of the inhibitors of QseC mediated virulence gene expression.

I am grateful to Dr. Ganesh Kumar, Dr. Jawahar L. Jat, Dr. Shyam Gandham, and Dr. Rami Neelapu for their preliminary work on approaches to the nigricanosides. Thanks also to Dr. Rambabu Dakarapu and Dr. Mahesh Paudyal for being the best collegues ever. You guys have made working in the Falck laboratory an exciting experience.

I will also like to thank Prof. Joseph Ready, Dr. Nancy Street, Carla Childers, and the Biochemistry Department at UTSW for giving me the opportunity to obtain an education at such a prestigious institution. Special thanks to Prof. Kathlynn C. Brown, Dr. Bethany Powell Gray, and Prof. Autumn Sutherlin for helping me lay a strong foundation in scientific research. Importantly, I thank Dr. Quyen Do, Drs. Cynthia and Gregory Powell, Sandy King, Prof. Eric Hardegree, Prof. Kim Pamplin, Prof. Perry Reeves, the Biology and Biochemistry Department at Abilene Christian University, Tracy Perry, Dr. Ronnie Brown, Aaron Falck, Dr. Kathleen Spivey Lee, and the Preston road Church of Christ for being a nurturing family to me in every possible way. Their support and good tidings are a dependable cornerstone.

December, 2015

STUDIES TOWARD THE SYNTHESES OF ANTIARRHYTHMIC, ANTIVIRULENCE, AND ANTICANCER SMALL MOLECULES

ADENIYI MICHAEL ADEBESIN, Ph.D
The University of Texas Southwestern Medical Center at Dallas, 2015

MENTOR: JOHN R. FALCK, Ph.D, DIC

This work is comprised of three projects: a) the development of antiarrhythmic analogs of 17(*R*),18(*S*)-epoxyeicosatetraenoic acid for the treatment of atrial fibrillation, b) the development of potent inhibitors of QseC mediated virulence gene expression, and c) studies toward a biomimetic total synthesis of nigricanoside A.

Antiarrhythmic analogs of 17(*R*),18(*S*)-epoxyeicosatetraenoic acid (17(*R*),18(*S*)-EEQ): Arrhythmias such as atrial and ventricular fibrillation are a leading cause of death in the United States of America. However, the available drugs for the treatment of these deadly conditions can paradoxically induce proarrhythmic effects, amongst other side effects, and are individually insufficient for treatment. Through a neonatal rat cardiomyocyte assay, 17(*R*),18(*S*)-EEQ was found to possess negative chronotropic effects, a characteristic of antiarrhythmic activity. My work on this project led to the development of potent and metabolically robust analogs of

17(*R*),18(*S*)-EEQ, which are currently being developed by OMEICOS Therapeutics GmbH, an early stage drug development company, for the treatment of atrial fibrillation.

Inhibitors of QseC mediated virulence gene expression:

Quorum sensing *E. coli* regulator C (QseC), a membrane-bound histidine sensor kinase, mediates the expression of various virulence genes in Gram-negative bacteria such as *Escherichia coli* (EHEC), *Salmonella typhimurium*, and *Francisella tularensis* which are pathogenic to humans. Therefore, QseC is a potential target of anti-virulence antibacterial strategies. In collaboration with the Sperandio laboratory, my work on this project led to the development of novel inhibitors of QseC mediated virulence gene expression. Some of the analogs synthesized in this project are currently being investigated by GlaxoSmithKline as anti-virulence agents.

Studies toward a biomimetic total synthesis of nigricanoside A:

Nigricanoside A, a novel ether-linked glycoglycerolipid with 7 unassigned stereocenters, was reported to possess potent ($IC_{50} \approx 3$ nM) antimitotic activity against MCF-7 and HCT-116 cancer cell lines. However, the rarity of the natural product precluded further structural and biological studies. With the aid of biomimetic hypotheses and literature precedents, the Falck laboratory reduced the stereochemical uncertainty associated with the structure elucidation of the nigricanosides. Furthermore, one of the biomimetic hypotheses inspired the development of a novel stereocontrolled distal epoxidation of conjugated dienols. Armed with this methodology, my work on this project led to the syntheses of the three major fragments of a nigricanoside.

TABLE OF CONTENTS

Acknowledgments........v

Abstract........vii

List of Figures........xii

List of Tables........xiv

List of Schemes........xv

CHAPTER 1 ANALOGS OF 17(*R*),18(*S*)-EPOXYEICOSATETRAENOIC ACID (EEQ) AS ANTIARRHYTHMIC AGENTS: CONJUGATES AND CARBOXYLIC ACID BIOISOSTERES........1

- 1.1 Abstract........1
- 1.2 Introduction........2
- 1.3 Literature Review........3
  - 1.3.1 The Human Heart........5
  - 1.3.2 Antiarrhythmic Drugs........8
  - 1.3.3 Antiarrhythmic Effects of PUFAs........11
- 1.4 Results and Discussion........14
  - 1.4.1 Chemistry........19
- 1.5 Conclusion........23
- 1.6 Experimental........23
- 1.7 References........49
- 1.8 Spectra........54

CHAPTER 2 INHIBITORS OF QSEC AS NOVEL ANTI-VIRULENCE AGENTS........81

- 2.1 Abstract........81
- 2.2 Introduction........82
  - 2.2.1 Anti-virulence Approaches........83

2.2.2 Inhibition of Virulence Gene Expression 84
2.2.3 Inhibition of Virulence Effectors 85
2.2.4 Anti-virulence and Bacterial Resistance 85
2.2.5 Targeting QseC as an Anti-virulence Approach 86
2.3 Literature Review 87
2.3.1 The Histidine Sensor Kinase QseCB 88
2.4 Results and Discussion 91
2.4.1 Structure-Activity Relationship Studies of LED209: Polarity Focused SAR91
2.4.2 Synthesis of Tritium Labeled LED209 for Drug-Receptor Studies 96
2.5 Conclusion 108
2.6 Experimental 110
2.7 References 131
2.8 Spectra 135
CHAPTER 3 STUDIES TOWARD A BIOMIMETIC TOTAL SYNTHESIS OF NIGRICANOSIDE A 169
3.1 Abstract 169
3.2 Introduction 170
3.2.1 Antimitotic Agents as Cancer Chemotherapeutics 170
3.3 Literature Review 173
3.3.1 Biomimetic Hypotheses 173
3.3.2 Other Synthetic Approaches to the Nigricanosides 179
3.3.3 Methods 182
3.4 Results and Discussion 186
3.4.1 Synthesis of the Glyceryl Galactoside Fragment (C) 187
3.4.2 Synthesis of C16 Fatty Acid Fragment 188
3.4.3 Synthesis of the C20 Fatty Acid Fragment 190
3.4.4 Regio- and Stereoselective Epoxidation of 11 and 27 192
3.4.5 Allylic Epoxide Opening 192
3.5 Conclusion 195
3.6 Experimental 196
3.7 References 217

3.8 Spectra..221

LIST OF FIGURES

Figure 1.1 17(*R*),18(*S*)-EEQ and analogs 2

Figure 1.2 The two classes of essential PUFAs. 4

Figure 1.3 Glycerolipids and sites of phospholipase activity 5

Figure 1.4 Non-pacemaker cardiac action potential 7

Figure 1.5 Class I antiarrhythmic drugs....8

Figure 1.6 Class II antiarrhythmic drugs 9

Figure 1.7 Class III antiarrhythmic drugs....10

Figure 1.8 Class IV antiarrhythmic drugs....10

Figure 1.9 Class V antiarrhythmic drugs 11

Figure 1.10 Functional regions of **1.01**. 14

Figure 2.1 Structures of LED209 and CF308 82

Figure 2.2 Targets of anti-virulence approaches....83

Figure 2.3 Synthetic inhibitors of some QS signals....84

Figure 2.4 QseC responds to AI-3 and the host stress hormones 87

Figure 2.5 QS signaling cascade in E. coli 89

Figure 2.6 Biosynthesis of AI-2. 90

Figure 2.7 Four segments of LED209....92

Figure 2.8 Structure and composition of CF308....100

Figure 2.9 Structures of adamantane containing antivirals....102

Figure 2.10 Real time qPCR and macrophage survival data for **2.54** and **2.38**..........................107

Figure 2.11 Structures of most potent EHEC drugs in this study..108

Figure 2.12 Inhibitors of AI-2 activation of LuxPQ...109

Figure 3.1 Proposed retrobiosynthesis of nigricanoside A..169

Figure 3.2 Some clinically relevant antimitotic agents..171

Figure 3.3 ELISA of cellular mitotic arrest 172

Figure 3.4 Proposed structure of the nigricanosides..172

Figure 3.5 Structural composition of the nigricanosides 174

Figure 3.6 Proposed biosynthesis of ω-4 C16 tri-oxygenated fatty acid of nigricanoside A 175

Figure 3.7 Structures of known trioxygenated C18 fatty acid metabolites.................................175

Figure 3.8 Potential precursors of the C20 fragment of the nigricanosides................................176

Figure 3.9 Apoptosis-inducing galactolipid from a cultured marine diatom..............................176

Figure 3.10 Proposed mechanism of formation of fatty acid ether bond....................................177

Figure 3.11 Brønsted acid catalyzed transformation of topsentolide A_2 to topsentolide C_2 178

Figure 3.12 Proposed mechanisms for formation of C8’-O-C6’’ etherbond..............................179

Figure 3.13 MacMillan and Ready synthesis of nigricanoside A..180

Figure 3.14 Kurashina et al synthesis of protected C16 fragment..181

Figure 3.15 Fujiwara and coworkers synthetic approach to the nigricanosides 181

Figure 3.16 Hepoxilin and trioxilin motifs in select bioactive natural products 182

Figure 3.17 Palladium catalyzed etherification of unsaturated α,β-unsaturated γ,δ-epoxy esters184

Figure 3.18 Interconversions between allylic epoxides and diols 185

LIST OF TABLES

Table 1.1 Chronotropic effects of 17,18-EEQ analogs on NRCMs and inhibition of soluble epoxide hydrolase (sEH)........16

Table 2.1. Modifications to thiourea moiety B........93

Table 2.2. Modifications to phenyl rings A and D........94

Table 2.3. Attachment of polar groups to rings A and D........95

Table 2.4. Conversion of sulfimidazolide **2.34** to LED 209........99

Table 2.5. Biological and metabolic studies of new scaffolds........101

Table 2.6. qPCR and survival data for adamantyl scaffolds........103

Table 2.7. Stability and biological activity of adamantyl scaffolds........105

Table 3.1 Allylic epoxide opening with carboxylic/carboxylate nucleophiles........193

LIST OF SCHEMES

Scheme 1.1 Linear/divergent synthesis of analogs. 21

Scheme 1.2 Convergent synthesis of analogs. 22

Scheme 2.1 Alkylation of lysine residues by LED209/OM188. 97

Scheme 2.2 Tritium labeled LED209* 97

Scheme 2.3 Failed attempts at the synthesis of **2.25**..98

Scheme 2.4 Synthesis of sulfimidazolide **2.34** as a surrogate for **2.25**...98

Scheme 3.1 Retrosynthetic analysis of nigricanoside A. 187

Scheme 3.2 Synthesis of glyceryl galactoside fragment..188

Scheme 3.3 Asymmetric synthesis of C16 fatty acid fragment. 189

Scheme 3.4 Synthesis of C16 fatty acid fragment contd. 190

Scheme 3.5 Synthesis of C20 fatty acid fragment. 191

Scheme 3.6 Synthesis of C20 fatty acid fragment contd. 192

Scheme 3.7 Formation of **28** and **29**. 192

Scheme 3.8 Allylic epoxide opening with alcohols...194

Scheme 3.9 Preliminary results on the formation of the *bis*-fatty acid ether of a nigricanoside .195

CHAPTER 1

ANALOGS OF 17(*R*),18(*S*)-EPOXYEICOSATETRAENOIC ACID (EEQ) AS ANTIARRHYTHMIC AGENTS: CONJUGATES AND CARBOXYLIC ACID BIOISOSTERES

1.1 Abstract

The cytochrome P450 metabolite of eicosapentaenoic acid (EPA), 17(*R*),18(*S*)-epoxyeicosatetraenoic acid (EEQ), is a potent arterial vasodilator and a potential antiarrhythmic agent. Previous structure-activity relationship (SAR) studies established that a *cis*-$\Delta^{11,12}$ -olefin and a 17(*R*),18(*S*)-epoxide were required for the maximum antiarrhythmic effect of 17,18-EEQ. Subsequent progress towards a structurally simpler analog of 17,18-EEQ identified oxamide **1.01** as a potent, non-chiral, and more robust analog of 17,18-EEQ. In this chapter, a series of conjugates and carboxylic acid bioisosteres of **1.01** was synthesized and evaluated as negative chronotropes in an *in vitro* arrhythmia model and for soluble epoxide hydrolase (sEH) inhibition. Compounds **1.11** and **1.12** possessed potent negative chronotropic effects at 30 nM with little inhibition of sEH at 1μM. The robustness and potency of these analogs should enable future *in vivo* and mechanism of action studies.

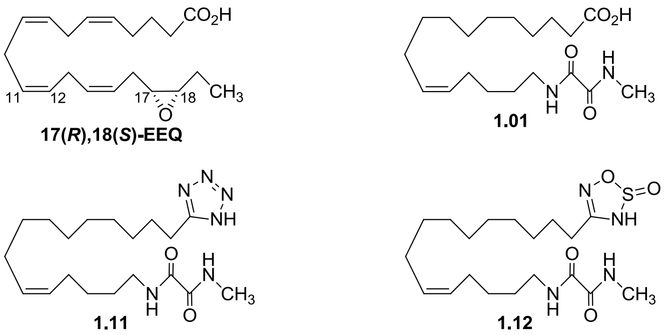

Figure 1.1
17(*R*),18(*S*)-EEQ and analogs.

1.2 Introduction

Heart disease is the major global cause of death with about 17.3 million deaths each year.[1] In the United States of America, sudden cardiac death (SCD) is a leading cause of death with a survival rate of 10% and sustained ventricular fibrillation (VF), a type of tachyarrhythmia, is the most common cause of SCD.[2] Ventricular fibrillation occurs when abnormal electrical impulses in the lower chambers of the heart prevent proper contraction and blood flow out of the heart. This often leads to organ damage and eventual fatality. On a molecular basis, dysfunctional ion channels and pumps are implicated in VF. The current treatments for VF and other kinds of arrhythmias are antiarrhythmic drugs and defibrillators (external and implantable) individually or in combination. However, the side effects and the propensity of the current antiarrhythmic drugs (pages 8-11) to cause future arrhythmias suggest the need for more effective treatments.[3] Omega-3- polyunsaturated fatty acid (ω-3-PUFA) therapy[4] has previously been suggested as a simpler and less invasive supplement to current treatments for VF. The ingestion of ω-3-PUFAs is associated with a plethora of cardiovascular benefits, *inter alia*, anti-inflammatory, antithrombotic, vasodilatory,[5] and lipid homeostatic[6] effects. Although the active principle (or principles) responsible for the cardio-protective effects of ω-3-fatty acids remains elusive, a large body of data suggests that enzymatic metabolites of PUFAs are involved.[7] Most biologically active metabolites of PUFAs are transient and highly labile autacoids, which complicates *in vitro* and *in vivo* biological studies. Thus progress in this area of eicosanoid research is dependent on the development of stable analogs with similar or more potent biological activities with respect to the endogenous metabolites, as well as validated biological assays and relevant animal models of diseases. Therefore, the Falck group and collaborators have established a medicinal chemistry program focused on the design and synthesis of chemically and metabolically robust pharmacological tools and novel drug candidates based upon PUFA metabolites. We previously showed that the cytochrome P450 metabolite of EPA, 17(*R*),18(*S*)-EEQ, is 1000-fold more potent as a negative chronotrope than the parent EPA.[7] Furthermore, preliminary SAR studies identified analog **1.01** as a potent, non-chiral negative chronotrope in *in vitro* assays. With **1.01** as a lead compound, modifications to the carboxylic terminal were examined to: 1) increase hydrophilicity, 2) obviate β-oxidation, 3) avoid esterification, and 4) provide mechanistic information on the possible mode of action of the analogs. Reported in this section is the development of second generation analogs of **1.01** and their evaluation in a neonatal rat cardiomyocyte arrhythmia assay, as well as a sEH inhibition assay.

1.3 Literature Review

Polyunsaturated fatty acids (PUFAs) are important small molecules that constitute the cellular lipid membranes present in all organisms. The two main classes of PUFA namely, the n-6 (ω-6) and the n-3 (ω-3), are derived biosynthetically from linoleic acid (LA, 18:2n-6) and α-linolenic acid (ALA, 18:3n-3) respectively. Elongation and desaturation of LA by elongase and desaturase enzymes forms arachidonic acid (AA, 20:4n-6) and docosapentaenoic acid (DPA, 22:5n-6), while similar enzymatic action on ALA forms eicosapentaenoic acid (EPA, 20:5n-3) and docosahexanoic acid (DHA, 22:6n-3) (Figure 1.1). Furthermore, in the leaves of certain plants, algae, and phytoplankton, LA can be converted to ALA.[4] The major dietary sources of n-6 PUFAs are vegetable and seed oils such as primrose oil, canola oil, and sunflower seed oil, while n-3 PUFAs are mostly obtained from fish oil and flax seed oil.

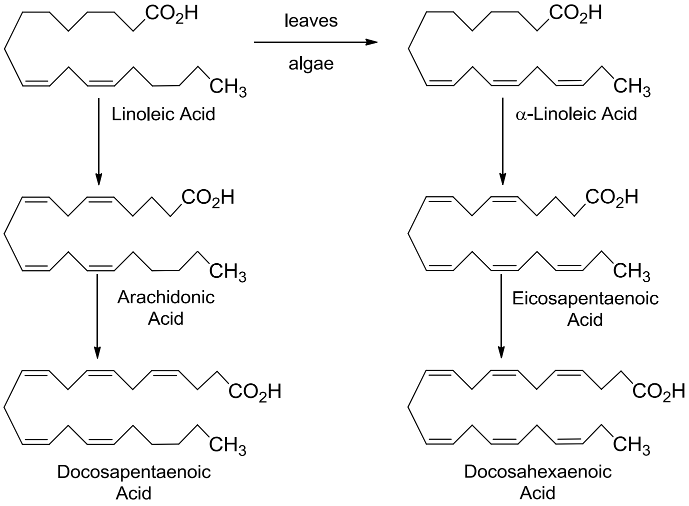
CO2H
leaves
algae
CH3
Linoleic Acid
α-Linoleic Acid
Arachidonic Acid
Eicosapentaenoic Acid
Docosapentaenoic Acid
Docosahexaenoic Acid

Figure 1.2
The two classes of essential PUFAs.

Apart from their role as structural components, energy stores, and protective media against electrical and chemical signals, PUFAs are important second messengers. PUFAs, like their saturated (SFA) and monounsaturated (MFA) relatives, are esterified to glycerol-phosphates and thus make up the glycerophospholipids (Figure 1.2) of cellular membranes. Upon signal stimulation (by hormones, growth factors, transcriptional factors, etc.) of a receptor (e.g., a G-protein coupled receptor, GPCR), a series of signal cascading events lead to activation of phospholipases (PLA1 or PLA2) that excise the acyl ester bonds of phospholipids releasing the esterified fatty acids. In the case of PUFAs, subsequent enzymatic conversions by cyclooxygenases (COX-1, COX-2), lipoxygenases, and cytochrome P450s (epoxygenases and hydroxylases) form biologically active autacoids that mediate myriad biological processes. In some cells, the PUFAs can be metabolized in their esterified state, or re-esterified after subsequent enzymatic metabolism.[8] Rapid inactivation of the PUFA metabolites by enzymes such as soluble epoxide hydrolases (sEH) and peroxisomal enzymes prevents persistence of these highly active metabolites. Thus, the biological activities of PUFAs in various cells/tissues/organs are highly dependent on the signals, the PUFA membrane-composition, and the presence of releasing/attaching and metabolic enzymes.

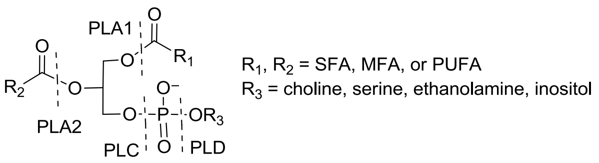
PLA1
PLA2
PLC
PLD
O
O
O
O⁻
O
R1
R2
OR3
P
R_1, R_2 = SFA, MFA, or PUFA
R_3 = choline, serine, ethanolamine, inositol

Figure 1.3
Glycerolipids and sites of phospholipase activity.

1.3.1 The Human Heart

The human cardiovascular system is composed of the heart, blood, and the blood vessels that transport blood around the body. The human heart is composed of two upper chambers (right and left atria) and two lower chambers (right and left ventricles). The right atrium receives deoxygenated blood from the superior and inferior vena cava and passes it through the right atrioventricular valve into the right ventricle. The blood then passes through the pulmonary semilunar valve and the pulmonary artery to the lungs. Upon reoxygenation of the blood by the lungs, the blood passes through the pulmonary vein to the left atrium, and moves through the mitral valve to the left ventricle where it is pumped to the rest of the body via the aorta.[9] A normal heart rate is between 60-90 beats/min, and a rate faster than 100 beats/min is considered tachycardia.[10] Efficient pumping of blood through the body is highly dependent on a rhythmic relaxation and contraction of the heart chambers. This rhythmic process is maintained by a unidirectional action potential. In the heart, action potentials originate from the sinoatrial node (SAN) in the right atrium and travel through the His-Purkinje network to the atrioventricular node (AV node). Conduction from the AV node to the ventricles causes ventricular contraction and blood flow. There are five major phases[11] of a cardiac action potential (Figure 1.4).

In phase 4, the resting membrane potential, most contractile cells (non-pacemaker cells) maintain a membrane potential of about -85 to -95 mV. This potential is maintained through active transport by ion exchange pumps such as the Na^+-K^+ (sodium-potassium) ion exchange pump, the Na^+-Ca^{2+} (sodium-calcium) exchanger current, and the I_{k1} inwardly rectifying K^+ current. Furthermore, the cells are said to be polarized with a high extracellular concentration of Na^+ ions and a high intracellular concentration of K^+ ions. Pacemaker cells on the other hand, spontaneously depolarize slowly due to increased inward Na^+ and Ca^{2+} currents and a slowly decreasing K^+ outward current until a threshold potential (around -40 mV) is reached and an action potential is initiated. [12]

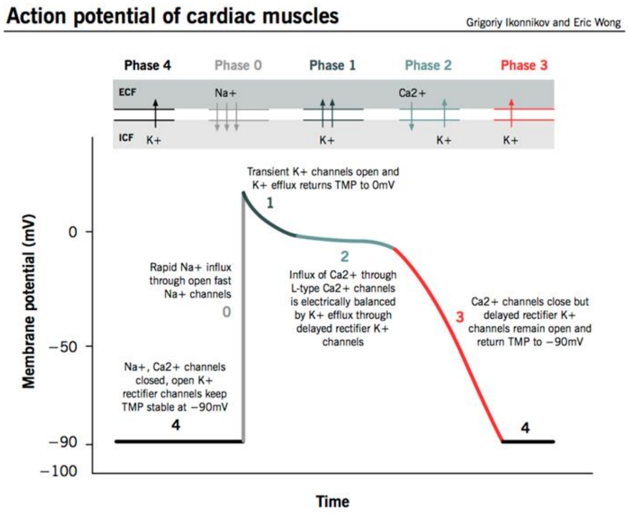

Figure 1.4
Non-pacemaker cardiac action potential (taken from Grigoriy Ikonnikov and Eric Wong, 2013).[13]

The stimulus for this gradual rise in potential often comes from the parasympathetic and sympathetic branches of the autonomous nervous system. In phase 0, rapid membrane potential depolarization occurs due to Na^+ influx via fast Na^+ channels resulting in a positive membrane potential. In pacemaker cells, however, influx of Ca^{2+} ions through the L-type calcium channels rather than Na^+ ions is responsible for phase 0.[11] Phase 1 of the action potential is characterized by initial repolarization due to an inactivation of the fast Na^+ channels (L-type Ca^{2+} channels in the case of pacemaker cells) and an outward flow of K^+ and Cl^- ions. Phase 2 is characterized by equilibrium between the inward movement of Ca^{2+} through L-type calcium channels, and the outward movement of K^+ through the slow delayed rectifier K^+ channel. The resulting large concentrations of intracellular calcium lead to the contraction of contractile cells. Note that this phase is absent in pacemaker cells. Phase 3 of the action potential, the rapid repolarization phase, is characterized by a closure of the L-type Ca^{2+} channels, and the opening of K^+ channels. Once the membrane potential is restored, the K^+ channels close, and the sodium-calcium exchanger and sodium-potassium pumps restore ion concentrations to the previous polarized state, which leads to a relaxation of contractile cells. Cardiovascular disease often develops from interruptions of blood flow to the heart by atherosclerotic plaques.[10] Prolonged ischemia of the heart results in cell death, and an interruption of the rhythmic process of the heart. Omega-3 PUFAs are believed to prevent and help treat cardiovascular disease through their actions on the heart cells, blood vessels, blood cells, and inflammation.[5]

1.3.2 Antiarrhythmic Drugs

There are five major classes of antiarrhythmic drugs according to the Vaughan Williams classification:[14]

Class I agents (Figure 1.5) interfere with ion transport through the Na^+ channel, which can result in a lengthening of the action potential (Class Ia agents), a shortening of the action potential (class Ib drugs), or a decrease in the rate of depolarization without an overall change in the length of the action potential (class Ic drugs).[15] Class I agents are used to treat ventricular arrhythmias, prevent paroxysmal recurrent fibrillation, and treat Wolff-Parkinson-White syndrome. Examples of class I agents include procainamide (class Ia), disopyramide (class Ia), lidocaine (class Ib), and flecainide (class Ic).

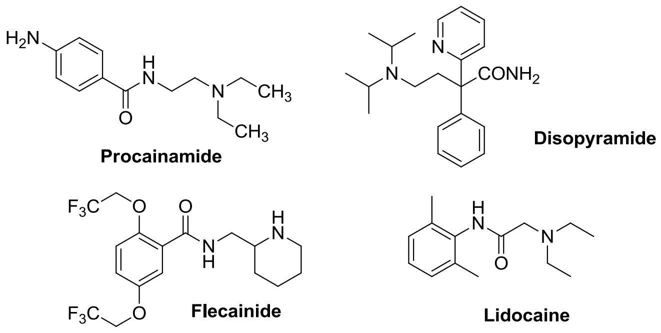

Figure 1.5
Class I antiarrhythmic drugs.

Class II agents (Figure 1.6) are inhibitors of catecholamine mediated actions at β_1-adrenergic receptors. Also, they decrease the slope of the pacemaker potential (phase 4) of the cardiac action potential. Of note is a recent report on the importance of class II agents for the suppression of the pro-arrhythmic effects of class 1 and 3 agents.[16] Class II agents are used to treat myocardial infarction and tachyarrhythmias. Examples of class II agents include atenolol, propranolol and metoprolol.

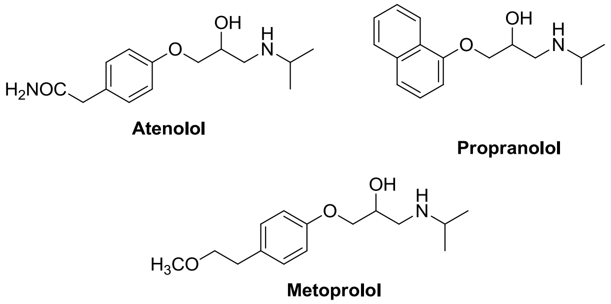

Figure 1.6
Class II antiarrhythmic drugs.

Class III agents (Figure 1.7) prolong the repolarization phase (phase 3) of the action potential by interfering with ion transport through the K^+ channel. This prevents re-entrant (looping signal) arrhythmias since a re-entrant rhythm is less likely to depolarize refractory cells. Class III agents are used to treat ventricular tachycardias, atrial fibrillation, and Wolff-Parkinson-White syndrome. Examples include amiodarone, sotalol, and dofetilide.[17]

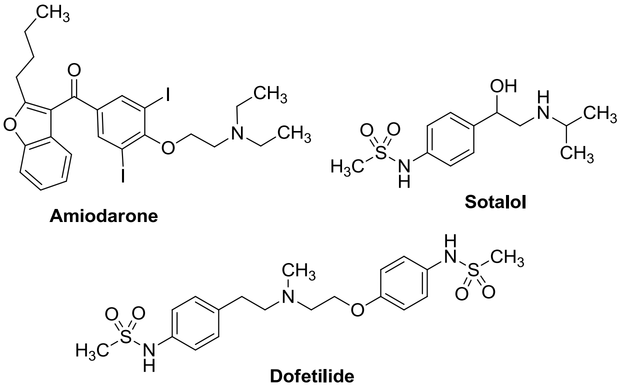

Figure 1.7
Class III antiarrhythmic drugs.

Class IV agents (Figure 1.8) are calcium channel antagonists, which decrease conduction through the AV node[18] and influence phase 2 of the cardiac action potential. These agents are inappropriate for conditions such as heart failure, since they decrease the contractility of the heart. Class IV agents are used to prevent recurrence of paroxysmal supraventricular tachycardia, and to reduce ventricular rate in patients with atrial fibrillation. Examples of class IV agents are verapamil and diltiazem.

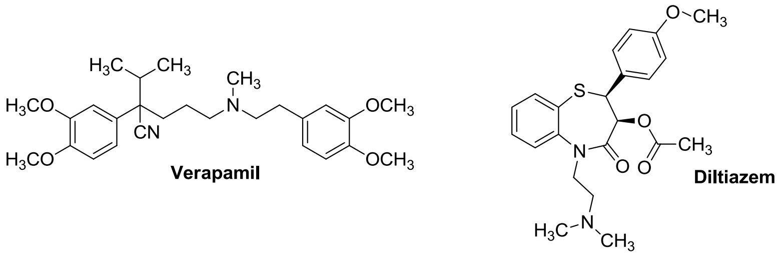

Figure 1.8
Class IV antiarrhythmic drugs.

Class V agents (Figure 1.9) consist of drugs with mechanisms of action that do not fit any of the classes discussed above. Examples include digoxin (reduces conduction through AV node), adenosine (treatment of supraventricular tachycardias)[19] and magnesium sulfate (prevents atrial fibrillation and supraventricular arrhythmias).[20]

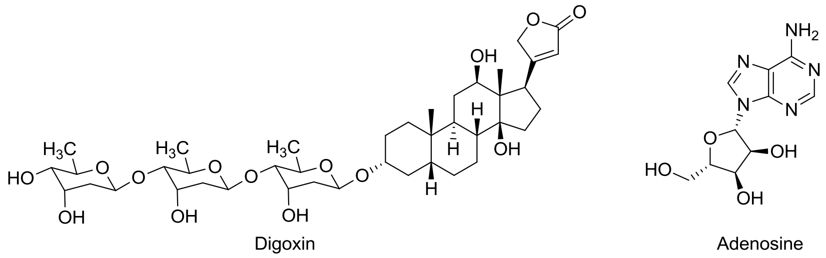

Digoxin

Adenosine

Figure 1.9
Class V antiarrhythmic drugs

1.3.3 Antiarrhythmic Effects of PUFAs

Reports about the lower incidence of cardiac mortality of Greenland Eskimos despite the high fat contents of their diets pioneered interests in the potential benefits of n-3 PUFAs on cardiac health.[21] In 1989, Burr and co-workers reported the first clinical cardiovascular trial to determine the effects of dietary fat, fish, or fiber on the prevention of myocardial infarction (MI).[22] At the end of the trial, there was a 29% reduction in mortality in men on the fish diet as compared to those on the other diets, although more non-fatal arrhythmias occurred in this group. This beneficial effect was attributed to a reduction in arrhythmic deaths.[4] Other clinical trials such as the GISSI-Prevenzione trial[23] and a review of the Physicians' Health Study[24] have reported reductions in cardiac deaths of 45% and 52%, respectively, due to n-3 PUFA consumption. Together these reports suggest a beneficial effect of n-3 PUFA consumption on the prevention of sudden cardiac death and overall cardiac mortality.

In 1994, Leaf and Kang published a neonatal rat cardiomyocyte (NRCM) assay developed to study the biochemical and physiological antiarrhythmic actions of n-3 PUFA. In this assay, individual cardiac myocytes from rats are cultured on a microscope coverslip for 48 h, after which the cells are adherent in spontaneously beating monolayer clumps. An inverted microscope is then used to monitor the amplitude and rate of contraction of individual myocytes in several clumps during perfusion with various media.[25] EPA and DHA (2-10 μM) containing media significantly reduced the contraction rate of the cells within 3 min of perfusion without major changes in the amplitude of contractions. Importantly, this negative chronotropic effect could be reversed by perfusing the cells with delipidated bovine serum albumin (BSA) within 2 min, which suggests a non-covalent mode of action of these PUFAs. Furthermore, EPA and DHA were able to "prevent and terminate tachyarrhythmias induced by high extracellular calcium concentrations or ouabin," in a similar fashion as the antiarrhythmic drug lidocaine.[25] Additional studies[26-28] in a dog animal model of sudden cardiac death further confirmed these preventive and therapeutic effects of EPA and DHA. Through a series of experiments,[29-32] Leaf and coworkers proposed that the n-3 PUFAs prevent fatal arrhythmias by inhibiting the fast, voltage-dependent sodium current and the L-type calcium currents. This inhibition prevents further transduction of an arrhythmic signal by a shift of the steady state inactivation curve to more hyperpolarized potentials.[4]

While there is obviously a significant effect of n-3 PUFA on Na^+ and Ca^{2+} channels of heart cells, the molecular mediators of this effect are currently unknown. A leading hypothesis suggests the involvement of n-3 PUFA metabolizing enzymes and distinct receptors for the metabolites.[33,34] In support of this hypothesis, recent studies have shown that 1) a switch in the lipid composition from n-6 PUFAs to n-3 PUFAs could occur in certain organs and tissues such as the kidney, lung, liver, and left ventricle with a n-3 PUFA rich diet, 2) n-3 PUFAs compete favorably for metabolism by n-6 PUFA metabolizing enzymes,[7] 3) 8,9-epoxyeicosatrienoic acid (8,9-EET, a cytochrome P450 metabolite of arachidonic acid) modulates Na^+ channel activity of rat cardiomyocytes *in vitro,*[35] and 4) the omega-3 PUFA metabolite binding sites and biological activities are different than those of the n-6 PUFAs.[36] Furthermore, the long-term beneficial effects of n-3 PUFAs could be a cumulative effect from other components of the cardiovascular system (i.e. blood vessels and blood components). EETs have been shown to modulate vascular tone and homeostasis.[37,38] It would be interesting to compare the effects of n-3 and n-6 PUFA metabolites in various cardiac diseased states involving these components.

Recent studies by the Schunck group[7] showed that various isoforms of cytochrome P450 metabolized EPA predominantly into 17,18-epoxyeicosatetraenoic acid (17,18-EEQ) in various organs. 17,18-EEQ was found to possess antiarrhythmic properties at low nanomolar concentrations in the NRCM assay. 17(*R*),18(*S*)-EEQ was identified as the negative chronotrope, while its enantiomer was mostly inactive. Furthermore, preliminary SAR studies in collaboration with the Falck laboratory using 17(*R*),18(*S*)-EEQ as a lead identified analog **1.01** as a non-chiral, yet potent negative chronotrope in *in vitro* assays. Analog **1.01** does not inhibit sEH at 5 μM, which eliminates a mechanism of action involving any direct effect on sEH metabolism of endogenous 17,18-EEQ. With **1.01** as a lead compound, modifications to the carboxylic terminal were examined to, 1) increase the hydrophilicity, 2) obviate β-oxidation, 3) avoid esterification, and 4) provide mechanistic information on the possible mode of action of the analogs.

1.4 Results and Discussion

The structure of **1.01** can be divided into 4 functional regions namely: 1) a carboxylic terminus, 2) a lipophilic region, 3) a cis-$\Delta^{11,12}$–olefin, and 4) an oxamide epoxide bioisostere near the terminus (Figure 1.10). The Falck group had previously established the importance of the carboxylic acid, the cis-$\Delta^{11,12}$ –olefin, and the oxamide (or other epoxide bioisostere) for antiarrhythmic activity.[7] In subsequent studies, I focused my attention on the carboxylic functional group. Conjugation of various polar moieties was examined with the aim of increasing the hydrophilicity of this class of analogs.

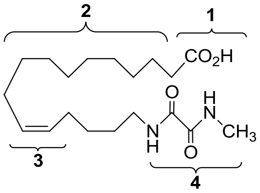

1.01

Figure 1.10
Functional regions of **1.01**.

As shown in Table 1.1, the more robust analogs oxamide **1.01**, the related urea **1.02**, and the 3-oxa analog **1.03** showed higher potency than the labile natural ligand 17(*R*),18(*S*)-EEQ. On the other hand, the more hydrophilic triethyleneglycol esters (**1.04-1.06**) and glycine conjugate (**1.07**) displayed similar activities as 17(*R*),18(*S*)-EEQ, although **1.04** showed a slight increase in sEH inhibition. LC–MS analysis of the **1.06**/assay prep incubate showed the presence of the hydrolyzed carboxylic acid **1.03**, which suggests that **1.04-1.06** are hydrophilic prodrugs that are converted to the active carboxylic acid in situ. A likely role for enzymatic conversion is further suggested by the moderate activity of tertiary amide **1.08** and the weakly active alanine conjugate **1.09**. An increase in steric congestion which curtails amidase hydrolysis could prevent efficient conversion to the parent acids, hence the decreased activity. Alternatively, a weak binding of the intact analogs to the appropriate receptor due to sterics could explain the result. However, the high potency of **1.10** suggests that increased acidity at the carboxylate terminus could override steric effects, which is consistent with previous observation[39] on the favorable influence of increased acidity at the carboxylate terminus on the biological activity of this class of analogs. Importantly, analogs **1.01-1.10** showed minor effects on sEH inhibition at the concentration (30 nM) used for the NRCM assay. Comparison of the bioactivity and sEH inhibition of the pair **1.01/1.02** and **1.04/1.05** suggested that oxamides might be better epoxide bioisosteres than ureas and have less untoward effect on sEH, thus, subsequent studies focused on oxamide analogs.

Next, the effect of replacing the carboxylic terminus with established bioisosteric groups was evaluated. Delightfully, heterocyclic isosteric analogs such as tetrazole **1.11** (-30.9±5.5 bpm) and oxathiadiazole **1.12** (-24.3±1.3 bpm) displayed strong potency and were more active than 17(*R*),18(*S*)-EEQ (-21.3±0.9 bpm). The biological activity decreased by more than 50% with oxadiazole **1.13** (-11.0±1.2 bpm), which might be partially due to its reduced acidity vs. **1.12**, and rebounded with benzothiazole **1.14** (-21.1±1.1 bpm). On the other hand, phenolic thio-ether **1.15** (-7.5±4.5 bpm) was the least active carboxylic isostere examined in this series. We speculate that the decreased activity of **1.15** could be the result of rapid metabolism of the 2-hydroxythiophenol ether moiety, and/or the lower acidity[39] of the phenol. Sodium sulfonate (**1.16**) and phosphonate (**1.17**) were as active as 17(*R*),18(*S*)-EEQ and, thus, allows one to discount esterification or incorporation into phospholipids as a necessary step for suppression of the beating rate. Inclusion of the $\Delta^{11,12}$–olefin into an ortho-substituted phenyl as demonstrated in **1.18** and **1.19** retained a significant part of the biological activity. These results re-enforce the presumed hairpin binding motif[36] of these analogs at the binding site, and suggests the presence of sufficient room in the lipophilic pocket for substitution at the *cis*-olefin. Unlike in the carboxylic series, conjugation (esterification) of the phosphonate (**1.20-1.22**) gave a more modest reduction in potency. Possibly, enzymatic and/or non-enzymatic hydrolysis of the phosphonate esters could be faster than that of the carboxylic conjugates resulting in a rapid conversion of **1.20-1.22** to the parent **1.17** (or mono ester); hence, a minor decrease in activity when compared with the carboxylic conjugates **1.04**, **1.05**, **1.07**, **1.08**, and **1.09** relative to **1.01** and **1.02**.

Table 1.1 Chronotropic effects of 17,18-EEQ analogs on NRCMs and inhibition of soluble epoxide hydrolase (sEH)

Compound	Structure	Change (beats/min)[a]	sEH inhibition (%)[b] at	
			1 µM	10 µM
17(*R*),18(*S*)-EEQ	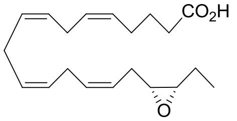	-21.3±0.9	NA	NA
1.01	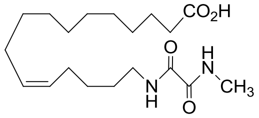	-33.7±1.3	-4.1±2.9	-8.3±6.3
1.02*	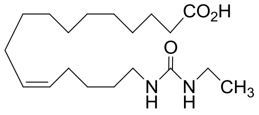	-27.0±1.2	4.7±1.7	23.4±2.9
1.03	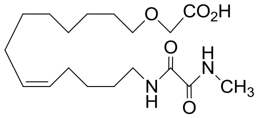	-31.2±3.0	NA	NA
1.04*	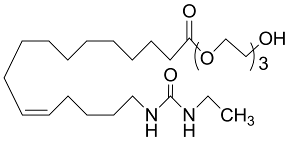	-19.8±1.0	26.5±2.5	76.6±3.0
1.05	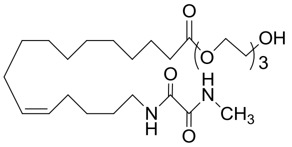	-19.3±1.4	NA	NA

1.06	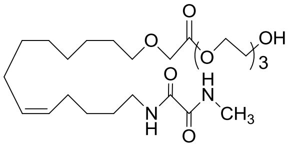	-24.7±0.9	NA	NA
1.07*	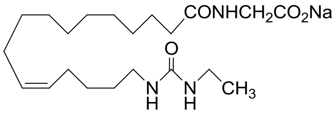	-21.1±1.4	0.9±6.0	19.2±5.0
1.08*	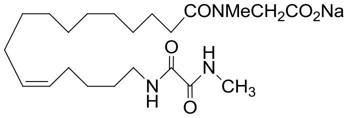	-15.6±4.3	-0.6±3.8	17.8±4.0
1.09*	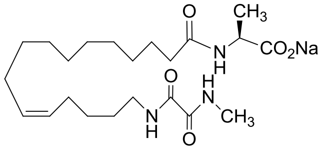	-1.1±1.5	1.9±5.7	18.7±3.4
1.10*	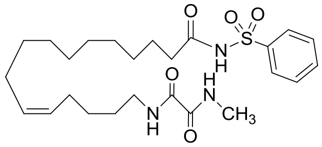	-23.1±1.2	-3.2±5.0	1.1.0±2.7
1.11	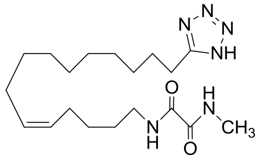	-30.9±5.5	-1.3±4.6	1.9±4.6
1.12	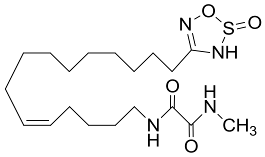	-24.3±1.3	-0.2±4.0	10.0±3.1
1.13	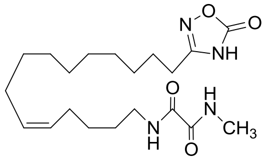	-11.0±1.2	-5.0±3.5	-9.2±4.1
1.14	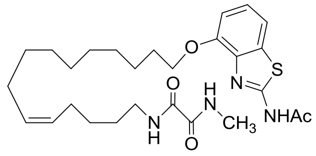	-21.1±1.1	17.0±3.1	61.8±2.8
1.15	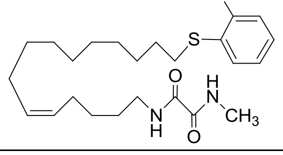	-7.5±4.5	0.4±4.1	1.5±3.8

1.16	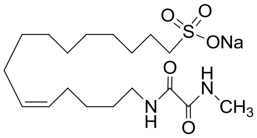	-20.7±0.9	5.2±1.8	0.0±3.8
1.17	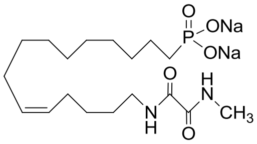	-21.3±1.0	6.8±3.2	37.7±2.9
1.18*	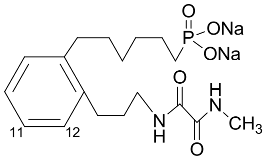	-24.5±0.8	-1.0±5.5	-2.2±2.2
1.19*	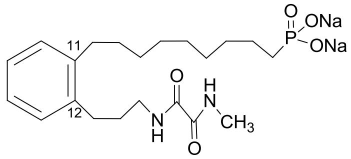	-21.8±1.0	1.3±5.8	1.8±2.6
1.20*	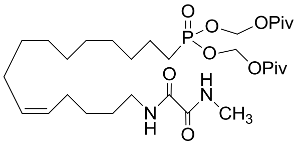	-23.5±1.0	5.1±2.1	38.4±6.7
1.21*	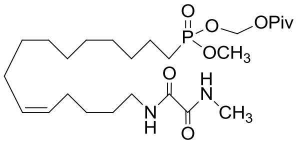	-16.2±0.9	5.4±2.8	18.6±3.6
1.22	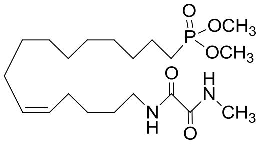	-18.0±0.9	5.0±1.7	6.4±2.7
1.23 (AUDA)	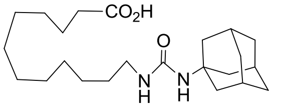	n.d.	98.4±0.1	n.d.

[a]Negative chronotropic effect of 17,18-EEQ analogs. n = 18-24 cardiomyocyte clusters originating from at least three independent NRCM preparations. Compounds were tested at a final concentration of 30 nM. Data presented as mean ± SD. [b]Inhibition tested with 14,15-EET as substrates for recombinant human sEH. Data represent mean ± SD; n = 4. AUDA, a highly potent sEH inhibitor is shown for comparison. Under the assay conditions, AUDA produced 84.6 ± 1.0% inhibition at 100 nM. NA = not available. [*]denotes analogs prepared by postdoctoral students.

With respect to the mechanism of action, it is noteworthy that esterification of the analogs, e.g., into cellular phospholipids as has been suggested might not be required for NC activity, since non-carboxylate analogs were sufficiently active. Furthermore, the rapid onset of activity supports a non-conjugative mechanism. Although a different mechanism of action could exist for carboxylate and non-carboxylate analogs, the similarity in the electrocardiograms for these two classes of compounds suggests a similar mechanism of action. Competition/antagonism experiments should be performed to further confirm this hypothesis. Importantly, it can be inferred from our data that sEH inhibition had negligible influence on the antiarrhythmic action of all the analogs. Our current proposal for the mechanism of action for this class of antiarrhythmic compounds is that they bind to a receptor that modulates the activities of ion channels or pumps. Alternatively, direct interaction with ion channels or pumps could be responsible for the observed biological activity. 17(*R*),18(*S*)-EEQ is known to dilate rat cerebral arteries and stimulate large-conductance K^+ (BK) channels.[40] Perhaps the antiarrhythmic action of the 17(*R*),18(*S*)-EEQ analogs could result from an overall modulation of K^+ channels like other class III antiarrhythmic agents. Future work will focus on exploring this mechanistic possibility. In light of the fatal proarrhythmic side effects of some of the currently available antiarrhythmic drugs, a major question which remains to be engaged is the arrhythmic induction potential of the 17(*R*),18(*S*)-EEQ analogs. In the absence of comprehensive *in vivo* data, the fact that treatment of arrhythmic cells with 17(*R*),18(*S*)-EEQ or the analogs restored the beating rate to basal levels and not below, at the concentrations tested *in vitro* is promising. Hopefully, further studies would shed some light on the mechanism behind this effect.

1.4.1 Chemistry

A general synthetic scheme for the compounds tested in this study is shown in scheme 1.1.

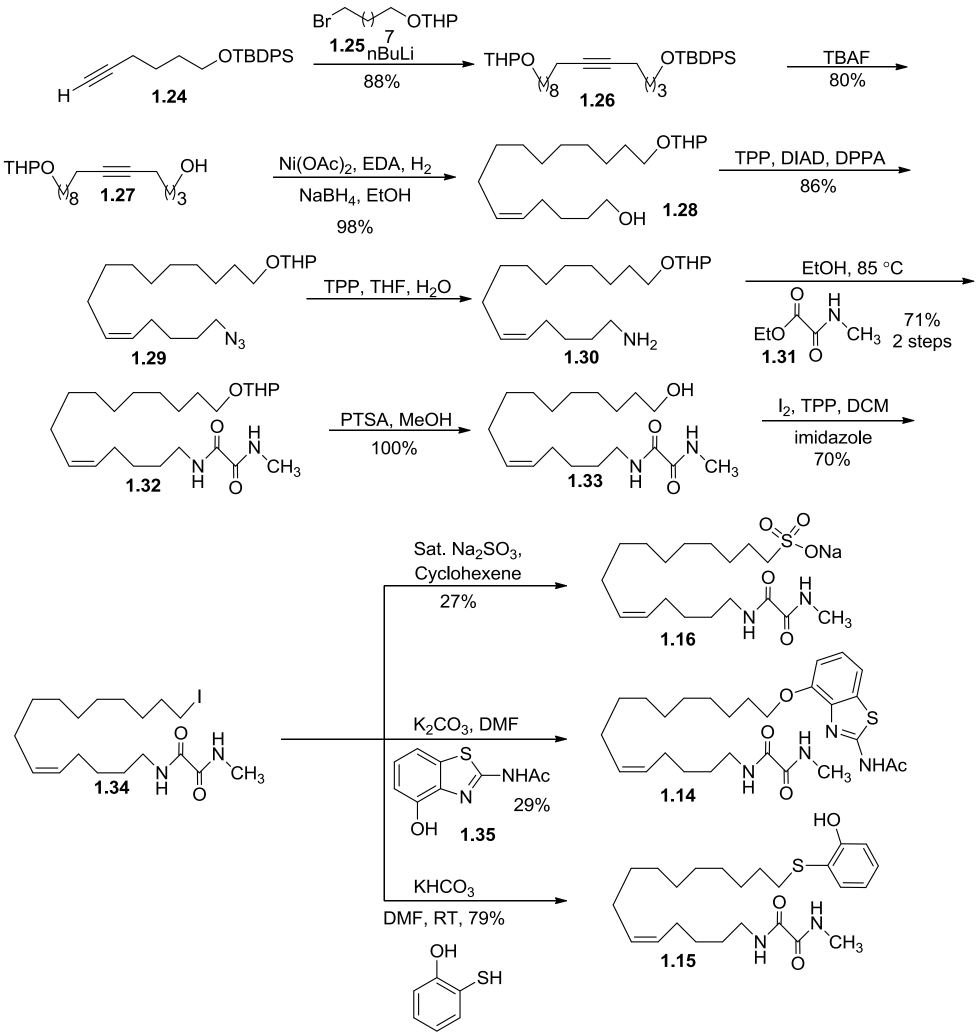
OTBDPS
H
1.24
Br
7
OTHP
1.25
nBuLi
88%
THPO
8
1.26
3
OTBDPS
TBAF
80%
THPO
8
1.27
3
OH
Ni(OAc)$_2$, EDA, H$_2$
NaBH$_4$, EtOH
98%
OTHP
OH
1.28
TPP, DIAD, DPPA
86%
OTHP
N$_3$
1.29
TPP, THF, H$_2$O
OTHP
NH$_2$
1.30
EtOH, 85 °C
EtO
O
H
N
CH$_3$
O
1.31
71%
2 steps
OTHP
N
H
O
O
H
N
CH$_3$
1.32
PTSA, MeOH
100%
OH
1.33
I$_2$, TPP, DCM
imidazole
70%
I
1.34
Sat. Na$_2$SO$_3$,
Cyclohexene
27%
O
O
S
ONa
1.16
K$_2$CO$_3$, DMF
S
N
NHAc
OH
1.35
29%
O
S
N
NHAc
1.14
KHCO$_3$
DMF, RT, 79%
OH
SH
HO
S
1.15

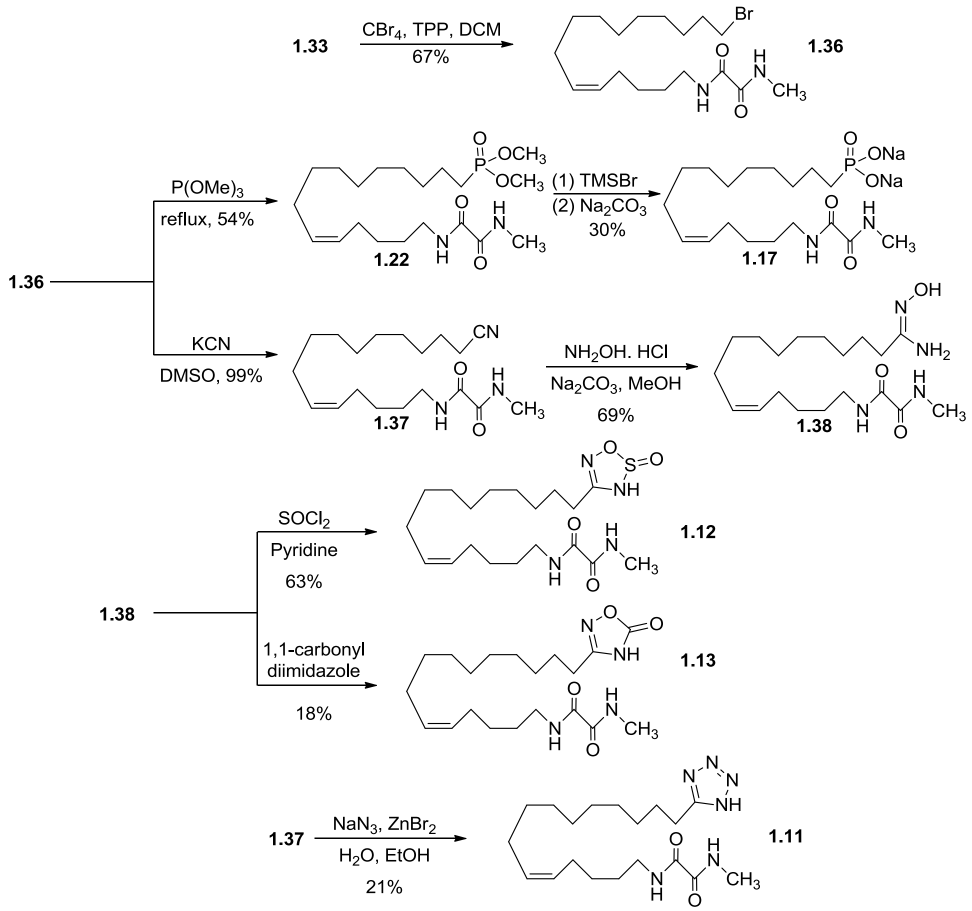
1.33
CBr$_4$, TPP, DCM
67%
1.36
Br
1.36
P(OMe)$_3$
reflux, 54%
1.22
(1) TMSBr
(2) Na$_2$CO$_3$
30%
1.17
KCN
DMSO, 99%
1.37
NH$_2$OH. HCl
Na$_2$CO$_3$, MeOH
69%
1.38
1.38
SOCl$_2$
Pyridine
63%
1.12
1,1-carbonyl diimidazole
18%
1.13
1.37
NaN$_3$, ZnBr$_2$
H$_2$O, EtOH
21%
1.11

Scheme 1.1
Linear/divergent synthesis of analogs.

Access to sufficient quantities of the analogs for animal studies was hindered by the linear nature of the synthetic route in Scheme 1.1. Therefore, a more convergent synthetic route was developed. The synthesis of **1.11** is representative of the new synthetic route (un-optimized) (Scheme 1.2).

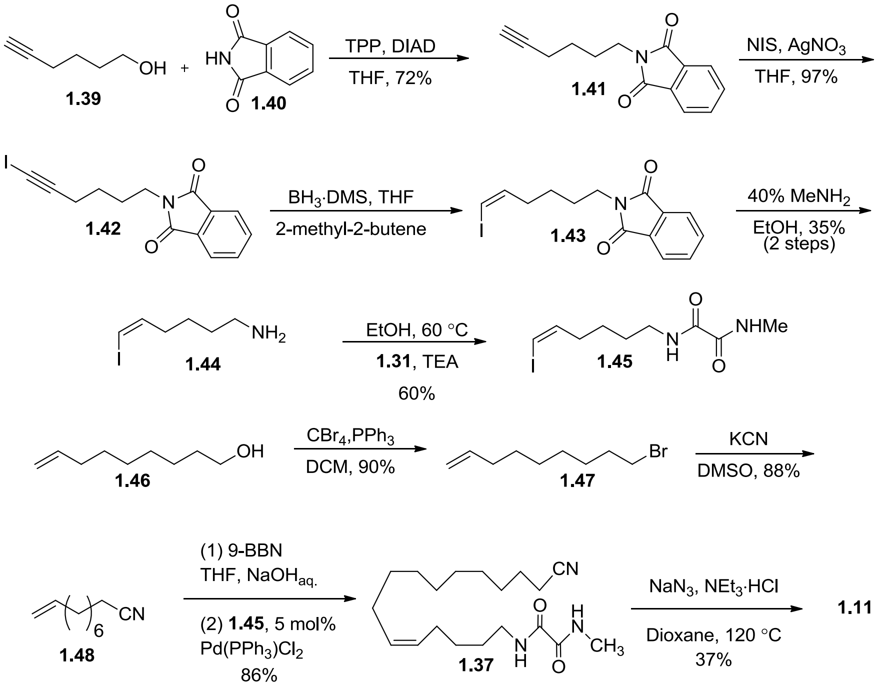
OH
1.39
+
HN
O
O
1.40
TPP, DIAD
THF, 72%
N
O
O
1.41
NIS, AgNO3
THF, 97%
I
1.42
BH3·DMS, THF
2-methyl-2-butene
1.43
40% MeNH2
EtOH, 35%
(2 steps)
NH2
1.44
EtOH, 60 °C
1.31, TEA
60%
NHMe
N
H
1.45
OH
1.46
CBr4,PPh3
DCM, 90%
Br
1.47
KCN
DMSO, 88%
6
CN
1.48
(1) 9-BBN
THF, NaOHaq.
(2) 1.45, 5 mol%
Pd(PPh3)Cl2
86%
CN
CH3
1.37
NaN3, NEt3·HCl
Dioxane, 120 °C
37%
1.11

Scheme 1.2
Convergent synthesis of analogs.

As shown in Scheme 1.2, **1.11** can be obtained from **1.37** through a tandem addition, cyclization process with NaN_3. Retrosynthetic disconnection at the olefin of **1.37** gives vinyl iodide **1.45** and the hydroboration product of **1.48**. In the synthetic direction, a Suzuki-Miyaura couplinig of both fragments furnished **1.37**. Cyanide **1.48** was synthesized in two steps from commercial 8-nonen-1-ol (**1.46**) through bromide **1.47**, while Vinyl iodide **1.45** was prepared in five steps commencing with phthalimide Mitsunobu substitution of commercial 5-hexyn-1-ol to give **1.41** from which iodo-alkyne **1.42** was obtained via treatment with *N*-iodosuccinimide with silver nitrate catalysis. Sequenctial stereospecific reduction of **1.42**, deprotection of the phthalimide group in the resultant *cis*-vinyl iodide **1.43**, and amidation with oxamide **1.31** resulted in **1.45**. With the above synthetic route, hundreds of milligrams of **1.11** were synthesized in approximately half the time compared with the linear synthetic scheme. Further pre-clinical *in vitro* and *in vivo* studies with **1.11** are currently ongoing.

1.5 Conclusion

Various conjugates and carboxylic acid bioisosteres of 17,18-EEQ were synthesized and evaluated as negative chronotropes in an *in vitro* arrhythmia model, and for soluble epoxide hydrolase (sEH) inhibition. Heterocyclic bioisosteres **1.11** and **1.12** showed potent negative chronotropic effects at 30 nM with little inhibition of sEH at 1μM, and are instructive on the potential mechanism of action of these analogs. Phosphonate analogs and conjugates were also potent negative chronotropes and will be further evaluated as “backup” scaffolds. Finally, a robust and convergent synthetic route to the analogs was developed, which should enable future *in vivo* and mechanism of action studies.

1.6 Experimental

General Methods and Materials. Proton and carbon nuclear magnetic resonance spectra (^{1}H and ^{13}C NMR) were recorded at 500 MHz and 126 MHz, respectively, or at 400 MHz and 101 MHz, respectively, in $CDCl_3$ with TMS as internal standard, unless otherwise stated. ^{1}H NMR data are reported as follows: chemical shift (ppm), multiplicity (s = singlet, br s = broad singlet, d = doublet, t = triplet, q = quartet, app q = apparent quartet, qn = quintet, app qn = apparent quintet, m = multiplet), and coupling constant (Hz). Melting points were measured using an automated melting point apparatus and are uncorrected. Analytical thin layer chromatography (TLC) used EMD Chemicals TLC silica gel 60 F_{254} plates (0.040-0.063 mm) with visualization by UV light and/or phosphomolybdic acid (PMA) solution followed by heating.

Chromatographic purifications utilized preparative TLC or flash chromatography using pre-packed SiO_2 columns on an automated medium pressure chromatograph. Unless otherwise noted, yields refer to isolated, purified material with spectral data consistent with assigned structures or, if known, were in agreement with published data. All reactions were conducted under an argon atmosphere in oven-dried glassware with magnetic stirring. Reagents were purchased at the highest commercial quality and used without further purification. Reaction solvents were dried by passage through a column of activated, neutral alumina under argon and stored under argon until use.

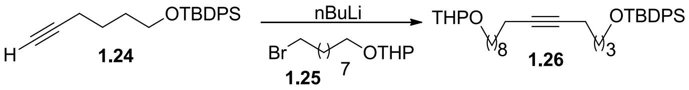

Synthesis of *tert*-butyldiphenyl[15-(tetrahydro-2*H*-pyran-2-yloxy)pentadec-5-yn-1-yloxy]silane (1.26)

n-Butyllithium (2.5M in hexanes, 3.89 mL, 9.72 mmol, 1.2 equiv) was added dropwise to a -78 °C solution of *tert*-butyl(hex-5-yn-1-yloxy)diphenylsilane[41] (2.70 g, 8.10 mmol) in THF (20 mL) and anhydrous hexamethylphosphoramide (HMPA, 10 mL). The reaction (blood red) was stirred at -78 °C for 30 min and at 0 °C for 2 h. The reaction was cooled to -78 °C and 2-(9-bromononyloxy)tetrahydro-2*H*-pyran[42] (2.50 g, 8.10 mmol) in THF (16.2 mL) was added slowly to the reaction via cannula. The reaction was stirred at -78 °C for 40 min and then allowed to gradually warm to rt overnight (18 h). The reaction was quenched with sat. NH_4Cl solution, diluted with water and extracted with EtOAc (3 × 20 mL). The combined organic extracts were dried over Na_2SO_4, filtered through a fritted funnel, and concentrated in vacuo. The crude product was purified via SiO_2 column chromatography with 2% EtOAc/hexanes to give the title compound (4.04 g, 88% yield) as a colorless oil.

^{1}H NMR (500 MHz, $CDCl_3$) δ 7.67 (dt, *J* = 7.9, 1.7 Hz, 2H), 7.39 (ddd, *J* = 14.1, 7.6, 6.0 Hz, 3H), 4.57 (dt, *J* = 4.7, 2.4 Hz, 1H), 3.87 (ddd, *J* = 10.8, 7.6, 2.7 Hz, 1H), 3.78 – 3.64 (m, 2H), 3.56 – 3.45 (m, 1H), 3.38 (dq, *J* = 9.3, 6.6 Hz, 1H), 2.22 – 2.07 (m, 2H), 1.90 – 1.39 (m, 8H), 1.39 – 1.23 (m, 9H), 1.04 (s, 5H), 0.92 – 0.81 (m, 2H); ^{13}C NMR (126 MHz, $CDCl_3$) δ 135.8 (2), 134.3, 129.8, 127.8 (2), 99.1, 99.06, 80.7, 80.2, 77.6, 77.3, 67.9, 67.89, 63.7, 62.6, 62.56, 45.4, 32.9, 32.0, 31.1, 30.02, 30.0, 29.75, 29.73, 29.66, 29.63, 29.41, 29.39, 29.1, 29.09, 27.1, 26.5, 26.47, 25.8, 25.77, 20.0, 19.5, 19.0, 18.8.

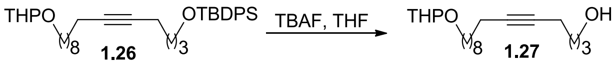

Synthesis of 15-(tetrahydro-2*H*-pyran-2-yloxy)pentadec-5-yn-1-ol (1.27)

A solution of *tert*-butyldiphenyl[15-(tetrahydro-2*H*-pyran-2-yloxy)pentadec-5-yn-1-yloxy]silane (6 g, 10.42 mmol) and tetra-*n*-butylammonium fluoride (3.14 g, 12.5 mL of a 1 M solution in THF, 12.5 mmol) in THF (150 mL) was stirred at rt under an argon atmosphere. After 5 h, the reaction mixture was quenched with saturated aqueous NH_4Cl (5 mL), washed with water (100 mL) and brine (75 mL). The aqueous layer was back-extracted with ether (2 × 75 mL). The combined organic extracts were dried over Na_2SO_4, concentrated under reduced pressure, and the residue was purified by SiO_2 column chromatography, using 5-10% EtOAc/hexanes as eluent to give the title compound (3.17 g, 80%) as a colorless oil. TLC: 40% EtOAc/hexanes, R_f ~ 0.4.

^{1}H NMR (500 MHz, $CDCl_3$) δ 4.57 (dd, *J* = 4.5, 2.8 Hz, 1H), 3.87 (ddd, *J* = 11.0, 7.5, 3.2 Hz, 1H), 3.72 (dt, *J* = 9.5, 6.9 Hz, 1H), 3.67 (t, *J* = 6.4 Hz, 2H), 3.53 – 3.46 (m, 1H), 3.37 (dt, *J* = 9.5, 6.7 Hz, 1H), 2.19 (tt, *J* = 6.9, 2.4 Hz, 2H), 2.13 (tt, *J* = 7.1, 2.4 Hz, 2H), 1.83 (qd, *J* = 7.9, 3.6 Hz, 1H), 1.75 – 1.63 (m, 3H), 1.62 – 1.48 (m, 6H), 1.48 – 1.40 (m, 2H), 1.39 – 1.22 (m, 7H); ^{13}C NMR (126 MHz, $CDCl_3$) δ 99.0, 80.7, 80.0, 67.9, 62.5, 62.4, 32.0, 30.9, 29.9, 29.6, 29.3 (2), 29.0, 26.4, 25.7, 25.6 (2), 19.8, 18.9, 18.7.

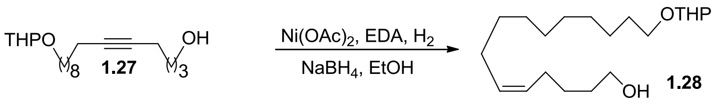

Synthesis of (*Z*)-15-(tetrahydro-2*H*-pyran-2-yloxy)pentadec-5-en-1-ol (1.28)

$NaBH_4$ (141 mg, 3.70 mmol, 0.8 equiv) was added to a solution of $Ni(OAc)_2$ (690 mg, 2.77 mmol, 0.6 equiv) in anhydrous EtOH (10 mL) in a two-necked flask under a H_2 atmosphere (1 atm). After 25 minutes, ethylenediamine (EDA, 0.93 mL, 13.9 mmol, 3 equiv) was added to the flask, followed by 15-(tetrahydro-2*H*-pyran-2-yloxy)pentadec-5-yn-1-ol (1.5 g, 4.62 mmol) in anhydrous EtOH (10 mL). After completion as judged by TLC analysis (2 h), the reaction was filtered through a column of silica gel and eluted with ethyl acetate. The filtrate was concentrated in vacuo to give the crude product (1.48 g, 98%) as a colorless oil. TLC: 20 % EtOAc/hexanes, R_f ~ 0.35.

^{1}H NMR (500 MHz, $CDCl_3$) δ 5.43 – 5.28 (m, 2H), 4.61 – 4.53 (m, 1H), 3.87 (ddd, *J* = 11.0, 7.6, 3.2 Hz, 1H), 3.73 (dt, *J* = 9.6, 7.0 Hz, 1H), 3.65 (t, *J* = 6.6 Hz, 2H), 3.55 – 3.45 (m, 1H), 3.38 (dt, *J* = 9.6, 6.7 Hz, 1H), 2.06 (app q, *J* = 7.0 Hz, 2H), 2.01 (app q, *J* = 6.7 Hz, 2H), 1.83 (tdd, *J* = 11.9, 7.1, 3.6 Hz, 1H), 1.71 (ddt, *J* = 12.0, 8.5, 3.1 Hz,1H), 1.63 – 1.48 (m, 8H), 1.46 – 1.38 (m, 2H), 1.38 – 1.24 (m, 12H); ^{13}C NMR (126 MHz, $CDCl_3$) δ 130.5, 129.6, 99.0, 67.9, 62.8 (2), 62.5, 32.6, 30.9, 29.9, 29.8 (2), 29.7, 29.5, 27.4, 27.2, 26.4, 26.1, 25.6, 19.8.

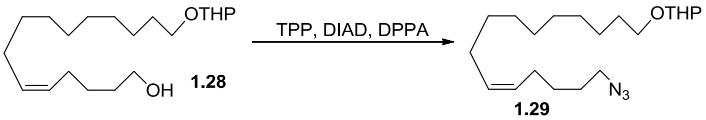

Synthesis of (*Z*)-2-(15-azidopentadec-10-enyloxy)tetrahydro-2*H*-pyran (1.29)

Diisopropyl azodicarboxylate (DIAD, 1.04 g, 5.15 mmol, 1.2 equiv) was added dropwise to a solution of triphenylphosphine (TPP, 1.35 g, 5.15 mmol, 1.2 equiv) in anhydrous THF (20 mL) at -20 °C. After 10 min, (*Z*)-15-(tetrahydro-2*H*-pyran-2-yloxy)pentadec-5-en-1-ol dissolved in THF (2.8 mL) was added dropwise to the reaction, and the resultant yellow suspension was stirred for 30 min at -20 °C. The reaction was warmed to 0 °C and diphenylphosphoryl azide (1.15 mL, 1.2 equiv) was added dropwise. The reaction was allowed to warm to rt overnight (16 h) and quenched with H_2O (11 mL). The organic layer was separated and the aqueous phase was extracted with Et_2O (4 × 20 mL). The combined organic fractions were dried over Na_2SO_4, filtered through a fritted funnel, and concentrated in vacuo. The crude product was purified via SiO_2 column chromatography using 2% EtOAc/hexanes to give a yellow oil (1.3 g, 86%). An analytical sample was purified by TLC to give the title compound as a colorless oil. TLC: 10% EtOAc/hexanes, R_f ~ 0.4.

^{1}H NMR (400 MHz, $CDCl_3$) δ 5.43 – 5.28 (m, 2H), 4.59 – 4.56 (m, 1H), 3.91 – 3.84 (m, 1H), 3.77 – 3.69 (m, 1H), 3.54 – 3.46 (m, 1H), 3.41 – 3.35 (m, 1H), 3.27 (t, *J* = 6.8 Hz, 2H), 2.10 – 1.95 (m, 4H), 1.88 – 1.78 (m, 1H), 1.76 – 1.68 (m, 1H), 1.65 – 1.48 (m, 8H), 1.46 – 1.38 (m, 2H), 1.38 – 1.24 (m, 12H); ^{13}C NMR (101 MHz, $CDCl_3$) δ 130.9, 129.0, 99.0, 67.8, 62.4, 51.5, 31.0, 29.9, 29.8, 29.7, 29.6 (2), 29.5, 28.6, 27.4, 26.9, 26.8, 26.4, 25.7, 19.9.

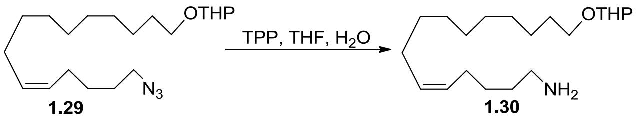

Synthesis of (*Z*)-15-(tetrahydro-2*H*-pyran-2-yloxy)pentadec-5-en-1-amine (1.30)

A mixture of the above azide (1.1 g, 3.13 mmol) and TPP (1.07 g, 4.07 mmol, 1.3 equiv) in THF (23 mL) was stirred at rt. After 2 h, H_2O (0.2 mL) was added and the reaction was continued overnight (20 h). The reaction was diluted with EtOAc, poured into brine (10 mL) and extracted with EtOAc (4 × 15 mL). The combined organic extracts were dried over Na_2SO_4, filtered through a fritted funnel, and concentrated in vacuo. The crude product was carried on to the next reaction without further purification. TLC: 5% MeOH/DCM, R_f ~ 0.1.

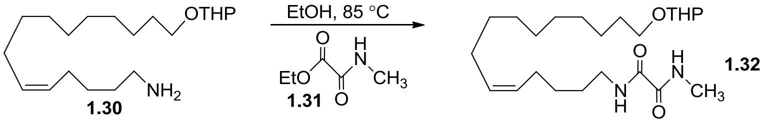

Synthesis of (*Z*)-*N*^{1}-methyl-*N*^{2}-(15-(tetrahydro-2*H*-pyran-2-yloxy)pentadec-5-enyl)oxalamide (1.32)

A mixture of the above crude **(*Z*)-**15-(tetrahydro-2*H*-pyran-2-yloxy)pentadec-5-en-1-amine (3.25 g, 10.0 mmol) and ethyl 2-(methylamino)-2-oxoacetate[43] (**1.31**, 1.57 g, 12.0 mmol) in anhydrous EtOH (50 mL) was refluxed for 8 h. The reaction was cooled to rt and concentrated in vacuo. The crude product was purified via SiO_2 column chromatography with 20-30% EtOAc/hexanes to give the title compound as a white solid (2.92 g, 71%; mp, 69.9-70.2 °C). TLC: 50% EtOAc/hexanes, R_f ~ 0.65.

^{1}H NMR (500 MHz, $CDCl_3$) δ 7.50 (br s, 2H), 5.42 – 5.28 (m, 2H), 4.59 – 4.56 (m, 1H), 3.91 – 3.84 (m, 1H), 3.77 – 3.69 (m, 1H), 3.54 – 3.46 (m, 1H), 3.41 – 3.35 (m, 1H), 3.32 (q, *J* = 7.0 Hz, 2H), 2.91 (d, *J* = 5.5 Hz, 3H), 2.05 (app q, *J* = 7.0 Hz, 2H), 2.00 (app q, *J* = 7.0 Hz, 2H), 1.88 –

1.78 (m, 1H), 1.76 – 1.68 (m, 1H), 1.64 – 1.47 (m, 8H), 1.44 – 1.22 (m, 14H); ^{13}C NMR (126 MHz, $CDCl_3$) δ 160.8, 159.9, 130.9, 129.1, 99.1, 67.9, 62.6, 39.8, 31.0, 29.9(2), 29.8, 29.7(2), 29.5, 29.0, 27.5, 27.1, 26.9, 26.5, 26.4, 25.7, 19.9.

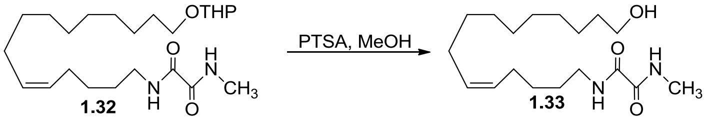

Synthesis of (*Z*)-*N*^{1}-(15-hydroxypentadec-5-enyl)-*N*^{2}-methyloxalamide (1.33)

p-Toluenesulfonic acid monohydrate (PTSA, 71.4 mg, 0.375 mmol) was added to a solution of the above THP-ether (1.0 g, 2.43 mmol) in anhydrous methanol (71.4 mL). The reaction was monitored by TLC every hour and was concentrated under vacuum after 2 h. The concentrate (white solid) was re-dissolved in EtOAc and passed through a pad of SiO_2 to give the title compound as a white solid (0.721 g, quantitative yield; mp, 115.9-116.0 °C). TLC: 50% EtOAc/hexanes, R_f ~ 0.25.

^{1}H NMR (500 MHz, $CDCl_3$) δ 7.45 (br s, 2H), 5.42 – 5.28 (m, 2H), 3.64 (q, *J* = 6.5 Hz, 2H), 3.32 (q, *J* = 6.5 Hz, 2H), 2.91 (d, *J* = 5.0 Hz, 3H), 2.06 (app q, *J* = 7.0 Hz, 2H), 2.00 (app q, *J* = 7.0 Hz, 2H), 1.61 – 1.52 (m, 6H), 1.44 – 1.23 (m, 12H); ^{13}C NMR (126 MHz, $CDCl_3$) δ 160.8, 159.9, 130.9, 129.1, 63.3, 39.8, 33.0, 29.8, 29.7, 29.6(2), 29.4, 29.0, 27.4, 27.1, 26.9, 26.4, 25.9.

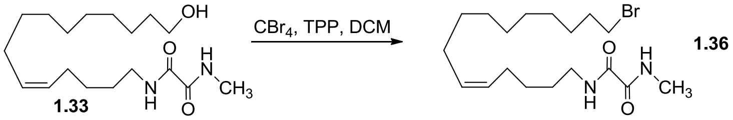

Synthesis of (*Z*)-*N*^{1}-(15-bromopentadec-5-enyl)-*N*^{2}-methyloxalamide (1.36)

Carbon tetrabromide (CBr_4, 0.942 g, 1.2 equiv) was added to a solution of TPP (0.745 g, 1.2 equiv) and (*Z*)-*N*^{1}-(15-hydroxypentadec-5-enyl)-*N*^{2}-methyloxalamide (0.740 g, 2.37 mmol) in anhydrous DCM (120 mL) and the mixture was stirred at rt for 24 h. The reaction was concentrated in vacuo and the crude product was purified via SiO_2 column chromatography with 20-25% EtOAc/hexanes to give the title compound as a white solid (0.596 g, 67% yield; mp, 77.5-77.6 °C). TLC: 50% EtOAc/hexanes, R_f ~ 0.7.

^{1}H NMR (400 MHz, $CDCl_3$) δ 7.45 (br s, 2H), 5.42 – 5.27 (m, 2H), 3.40 (t, *J* = 6.8 Hz, 2H), 3.31 (q, *J* = 6.8 Hz, 2H), 2.91 (d, *J* = 5.6 Hz, 3H), 2.09 – 1.96 (m, 4H), 1.85 (qn, *J* = 7.2 Hz, 2H), 1.62 – 1.52 (m, 2H), 1.47 – 1.37 (m, 4H), 1.37 – 1.23 (m, 10H); ^{13}C NMR (101 MHz, $CDCl_3$) δ 160.8, 159.9, 130.9, 129.1, 39.8, 34.3, 33.0, 29.9, 29.6(2), 29.5, 29.0, 28.9, 28.4, 27.4, 27.1, 26.9, 26.4.

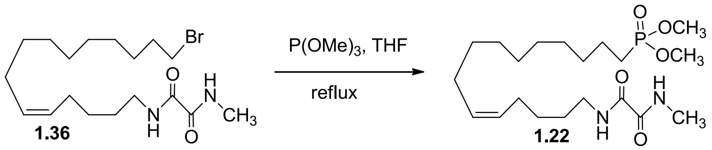

Synthesis of (*Z*)-dimethyl 15-(2-(methylamino)-2-oxoacetamido)pentadec-10-enylphosphonate (1.22)

Trimethyl phosphite [$P(OMe)_3$, 16 mL] was added to a solution of (*Z*)-*N*^{1}-(15-bromopentadec-5-enyl)-*N*^{2}-methyloxalamide (0.375 g, 1.1 mmol) in THF (16 mL). The reaction was refluxed (120 °C) in a sealed tube and monitored by TLC everyday over 3 days. After reaction completion as judged by TLC analysis, excess $P(OMe)_3$ was distilled off and the crude material (white paste) was subjected to the next reaction without further purification (0.250 g, crude yield ~ 54%.). An analytical sample was purified by TLC to give **1.22** as a low melting solid. TLC: 50% EtOAc/hexanes, R_f ~ 0.2.

^{1}H NMR (500 MHz, $CDCl_3$) δ 7.48 (br s, 2H), 5.39 – 5.26 (m, 2H), 3.72 (d, $J_{H\text{-}P}$ = 10.7 Hz, 6H), 3.30 (app q, *J* = 7.0 Hz, 2H), 2.90 (d, *J* = 5.0 Hz, 3H), 2.04 (app q, *J* = 7.5 Hz, 2H), 1.98 (app q, *J* = 7.5 Hz, 2H), 1.81 – 1.67 (m, 2H), 1.63 – 1.51(m, 4H), 1.43 – 1.21 (m, 14H); ^{31}P NMR (202 MHz, methanol-d_4, H_3PO_4 external standard) δ 36.48 (s); ^{13}C NMR (126 MHz, $CDCl_3$) δ 160.7, 159.9, 130.6, 129.0, 52.3 (d, ${}^{2}J_{C\text{-}O\text{-}P}$= 6.5 Hz), 39.6, 30.7 (d, ${}^{2}J_{C\text{-}C\text{-}P}$= 16.8 Hz), 29.8, 29.5, 29.4, 29.3, 29.1, 28.9, 27.3, 27.0, 26.8, 26.3, 24.7 (d, ${}^{1}J_{C\text{-}P}$= 140.2 Hz), 22.4 (d, ${}^{3}J_{C\text{-}P}$= 5.3 Hz).

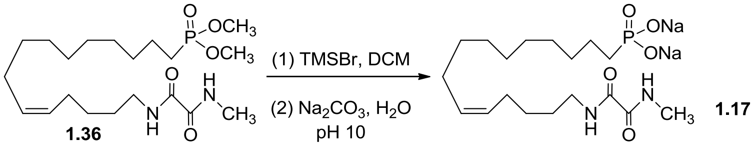

Synthesis of disodium (*Z*)-15-(2-(methylamino)-2-oxoacetamido)pentadec-10-enylphosphonate (1.17)

TMSBr (10 equiv, 0.5 mL) was added dropwise to a solution of (*Z*)-dimethyl 15-(2-(methylamino)-2-oxoacetamido)pentadec-10-enylphosphonate (0.250 g, 0.371 mmol) in DCM at 0 °C. After 75 min, the reaction was quenched with methanol and concentrated in vacuo. The crude product was triturated with DCM and decanted. The residue (mp, 130.6-130.7 °C) was dissolved in 1M aq. Na_2CO_3 (20 mL). Bio-Beads™ SM-2 absorbent (Bio-Rad, 20-50 mesh) was added to the solution and gently stirred for 30 min. The Bio-Beads™/compound mixture was collected on a Buchner fritted glass funnel and washed with water (3 × 20 mL). The product was eluted from the beads with methanol, and the eluent was concentrated to give **1.17** as a white solid (48.4 mg, 30%; mp, 240 °C [dec]).

Sodium salt:^{1}H NMR (500 MHz, methanol-d_4) δ 5.42 – 5.29 (m, 2H), 3.26 (t, *J* = 7.0 Hz, 2H), 2.82 (s, 3H), 2.13 – 1.97 (m, 4H), 1.87 – 1.75 (m, 2H), 1.69-1.43 (m, 4H), 1.42-1.23 (m, 14H); ^{13}C NMR (101 MHz, DMSO-d_6) δ 161.02, 160.15, 129.92, 128.81, 38.97, 31.86 (d, ${}^{2}J_{C\text{-}P}$ = 18.0 Hz), 30.95, 29.65, 29.45, 29.41, 29.33, 29.30, 29.0, 27.6 (d, $J_{C\text{-}P}$ = 169.0 Hz), 26.6, 26.4, 24.9, 24.6 (d, ${}^{3}J_{C\text{-}P}$ = 3.9 Hz).

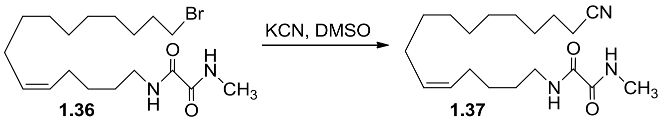

Synthesis of (*Z*)-*N*^{1}-(15-cyanopentadec-5-enyl)-*N*^{2}-methyloxalamide (1.37)

Potassium cyanide (KCN, 0.480 g, 7.35 mmol, 5 equiv) was added to a solution of (*Z*)-*N*^{1}-(15-bromopentadec-5-enyl)-*N*^{2}-methyloxalamide (0.550 g, 1.47 mmol) in anhydrous DMSO (30 mL) and the mixture was stirred overnight at rt. After completion as judged by TLC analysis, the reaction was diluted with H_2O (50 mL) and extracted with Et_2O (3 × 25 mL). The combined organic extracts were washed with H_2O (2 × 10 mL) and brine (15 mL). The organic phase was dried over anhydrous Na_2SO_4, filtered through a fritted funnel, and concentrated in vacuo. The crude product was purified via SiO_2 column chromatography with 20-25% EtOAc/hexanes to give the title compound as a white solid (0.467 g, 99%; mp, 88.8-88.9 °C). TLC: 50% EtOAc/hexanes, R_f ~ 0.55.

^{1}H NMR (400 MHz, $CDCl_3$) δ 7.43 (br s, 2H), 5.44 – 5.23 (m, 2H), 3.31 (q, *J* = 6.8 Hz, 2H), 2.91 (d, *J* = 5.2 Hz, 3H), 2.34 (t, *J* = 7.2 Hz, 2H), 2.09 – 1.96 (m, 4H), 1.71 – 1.60 (m, 2H), 1.61 – 1.49 (m, 5H), 1.49 – 1.36 (m, 3H), 1.36 – 1.22 (m, 8H); ^{13}C NMR (101 MHz, $CDCl_3$) δ 160.8, 159.9, 130.8, 129.1, 120.1, 39.8, 29.8, 29.6, 29.5, 29.4, 29.0, 28.9, 28.8, 27.4, 27.1, 26.9, 26.4, 25.6, 17.3.

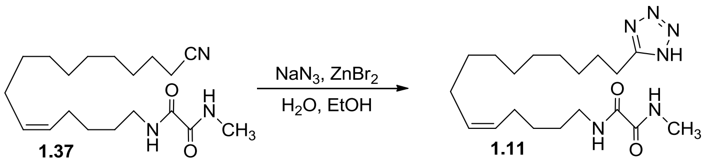

Synthesis of (*Z*)-*N*^{1}-(15-(1*H*-tetrazol-5-yl)pentadec-5-enyl)-*N*^{2}-methyloxalamide (1.11)

NaN_3 (30.3 mg, 0.466 mmol, 1.5 equiv) and a solution of $ZnBr_2$ (105 mg, 1.5 equiv) in H_2O (2.8 mL) were added to a solution of (*Z*)-*N*^{1}-(15-cyanopentadec-5-enyl)-*N*^{2}-methyloxalamide (100 mg, 0.311 mmol) in EtOH (1.7 mL). The reaction was refluxed in a sealed tube for 3 days. The reaction was cooled to rt and acidified with 10% HCl to bring the pH to 1. The reaction was diluted with H_2O (10 mL) and extracted with EtOAc (4 × 10 mL). The organic extracts were dried over Na_2SO_4, decanted, and concentrated in vacuo. The crude product was purified by TLC (eluent: 10% MeOH/DCM) to give **1.11** as a white solid (24.7 mg, 21%; mp, 127.3 °C).

^{1}H NMR (400 MHz, methanol-d$_4$) δ 5.42 – 5.25 (m, 2H), 3.23 (t, *J* = 7.2 Hz, 2H), 2.90 (t, *J* = 7.6 Hz, 2H), 2.80 (s, 3H), 2.09 – 1.95 (m, 4H), 1.81 – 1.69 (m, 2H), 1.60 – 1.47 (m, 2H), 1.41 – 1.22 (m, 12H); ^{13}C NMR (101 MHz, methanol-d$_4$) δ 162.1, 161.3, 160.4, 130.2, 129.1, 39.18, 29.7, 29.5, 29.4, 29.3, 29.2, 29.16, 29.0, 28.7, 27.0, 26.9, 26.6, 25.1, 24.8, 22.8.

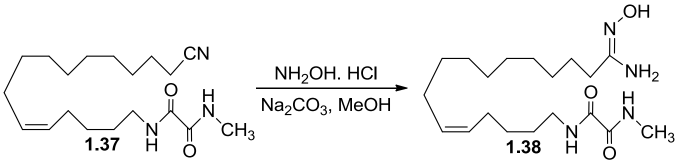

Synthesis of (*Z*)-*N*^{1}-((5*Z*,16*Z*)-16-amino-16-(hydroxyimino)hexadec-5-enyl)-*N*^{2}-methyloxalamide (1.38)

A mixture of (*Z*)-*N*^{1}-(15-cyanopentadec-5-enyl)-*N*^{2}-methyloxalamide (100 mg, 0.311mmol), $NH_2OH{\cdot}HCl$ (108 mg, 1.56 mmol, 5 equiv), and Na_2CO_3 (181 mg, 1.71 mmol, 5.5 equiv) in anhydrous methanol (2 mL) was refluxed in a sealed tube for 2 days. The reaction was filtered and the residue was washed with MeOH. Concentration of the filtrate gave a solid that was sequentially washed with water (10 mL) and DCM (3 × 10 mL). The solid (white) residue (76.0 mg, 69%; mp, 118.1-118.5 °C) was used in the next reaction without further purification. An analytical sample was purified by TLC (5% MeOH/DCM, R_f ~ 0.35).

^{1}H NMR (400 MHz, methanol-d_4) δ 5.42 – 5.29 (m, 2H), 3.25 (t, *J* = 7.1 Hz, 2H), 2.82 (s, 3H), 2.12 – 1.98 (m, 4H), 1.90 (s, 1H), 1.56 (p, *J* = 7.3 Hz, 6H), 1.44 – 1.26 (m, 16H); ^{13}C NMR (101 MHz, methanol-d_4) δ 161.2, 160.4, 156.5, 130.1, 129.1, 39.2, 30.6, 29.6, 29.4, 29.4, 29.3, 29.1, 29.0, 28.7, 27.1, 26.9, 26.85, 26.6, 25.1.

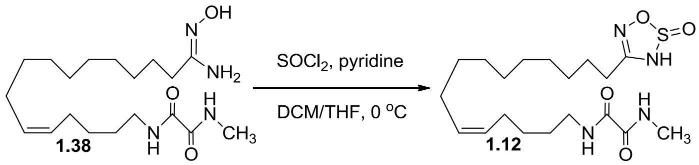

Synthesis of (*Z*)-*N*^{1}-methyl-*N*^{2}-(15-(2-oxido-3*H*-1,2,3,5-oxathiadiazol-4-yl)pentadec-5-en-1-yl)oxalamide (1.12)

Thionyl chloride ($SOCl_2$, 20 µL, 0.273 mmol, 1.3 equiv) dissolved in DCM (1 mL) was added slowly to a solution of crude *N*^{1}-((5*Z*,16*Z*)-16-amino-16-(hydroxyimino)hexadec-5-enyl)-*N*^{2}-methyloxalamide (74 mg, 0.210 mmol) and pyridine (43.6 µL, 0.546 mmol, 2.6 equiv) in THF (4 mL) at 0 °C. The reaction was continued at 0 °C for 1h 40 min and then concentrated in vacuo. The concentrate was diluted with water (5 mL) and extracted with EtOAc (5 × 5 mL). The combined organic extracts were dried over Na_2SO_4, decanted, and concentrated in vacuo. The crude product was purified by TLC to give **1.12** as a white solid (54.8 mg, 63%; mp, 92.7-92.9 °C). TLC: 5% MeOH in DCM, R_f ~ 0.6.

^{1}H NMR (500 MHz, CDCl$_3$) δ 8.38 (s, 1H), 7.50 (s, 2H), 5.41 – 5.28 (m, 2H), 3.41 – 3.21 (m, 2H), 2.91 (d, *J* = 5.2 Hz, 3H), 2.62 (t, *J* = 7.7 Hz, 2H), 2.06 (app q, *J* = 7.0 Hz, 2H), 2.01 (app q, *J* = 6.8 Hz, 2H), 1.69 (p, *J* = 7.7 Hz, 2H), 1.63 – 1.55 (m, 4H), 1.46 – 1.24 (m, 12H); ^{13}C NMR (101 MHz, CDCl$_3$) δ 160.7, 159.9, 152.9, 130.9, 129.2, 40.0, 29.4, 29.3, 29.2, 29.1, 29.0, 28.97, 28.9, 27.1 (2), 26.9, 26.6, 26.5, 24.0.

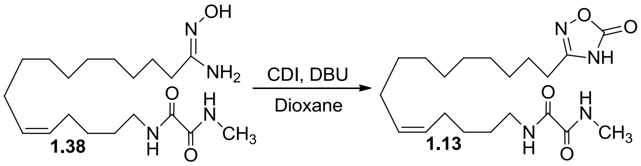

Synthesis of (*Z*)-*N*^{1}-methyl-*N*^{2}-(15-(5-oxo-4,5-dihydro-1,2,4-oxadiazol-3-yl)pentadec-5-en-1-yl)oxalamide (1.13)

1,8-Diazabicyclo[5.4.0]undec-7-ene (DBU, 51 μL, 0.340 mmol, 1.2 equiv) was added via syringe to a mixture of crude *N*^{1}-[(5*Z*,16*Z*)-16-amino-16-(hydroxyimino)hexadec-5-enyl]-*N*^{2}-methyloxalamide (100 mg, 0.280 mmol) and 1,1′-carbonyldiimidazole (55 mg, 0.340 mmol, 1.2 equiv) in anhydrous dioxane (1 mL). The reaction was stirred at rt for 30 min and at 100 °C for 10 min. The reaction was cooled to rt and concentrated in vacuo. The concentrate was directly purified by TLC to give **1.13** as a white solid (19.8 mg, 18%; mp, 125.6 °C). TLC: 5% MeOH/DCM, R$_f$ ~ 0.65.

^{1}H NMR (400 MHz, CDCl$_3$) δ 8.10 (s, 1H), 7.68 (s, 1H), 5.47 – 5.26 (m, 2H), 3.33 (q, *J* = 7.0 Hz, 2H), 2.93 (d, *J* = 5.1 Hz, 3H), 2.57 (app t, *J* = 7.6 Hz, 2H), 2.05 (dt, *J* = 12.9, 6.7 Hz, 4H), 1.69 (p, *J* = 7.7 Hz, 2H), 1.64 – 1.51 (m, 2H), 1.46 – 1.16 (m, 14H); ^{13}C NMR (101 MHz, CDCl$_3$) δ 1.63.4, 161.4, 160.0, 159.4, 130.8, 129.2, 39.9, 39.8, 29.8, 29.2, 29.15, 29.1, 29.03, 29.0, 28.94, 28.92, 28.5, 27.1, 26.88, 26.85, 26.0, 25.3.

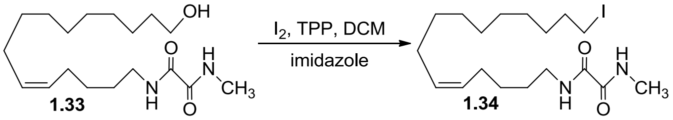

Synthesis of (*Z*)-*N*^{1}-(15-iodopentadec-5-en-1-yl)-*N*^{2}-methyloxalamide (1.34)

Iodine crystals (I_2, 1.75 g, 6.91 mmol,1.20 equiv) were added to a solution of (*Z*)-*N*^{1}-(15-hydroxypentadec-5-enyl)-*N*^{2}-methyloxalamide (1.80 g, 5.76 mmol), TPP (1.81 g, 1.2 equiv) and imidazole (0.784 g, 11.5 mmol, 2 equiv) in THF (180 mL) at 0 °C. The reaction was allowed to slowly warm to rt overnight. After the reaction was completed as judged by TLC analysis, the reaction was quenched with sat. aq. $NaHSO_3$ (10 mL) and concentrated in vacuo. The residue was diluted with water (70 mL), and extracted with EtOAc (3 × 20 mL). The combined organic extracts were dried over Na_2SO_4, filtered through a funnel, and concentrated in vacuo. The crude product was purified via SiO_2 column chromatography with 20-25% EtOAc/hexanes to give the title product (1.76 g, 70%; mp, 81.7 °C). TLC: 50 % EtOAc/hexanes, R_f ~ 0.65.

^{1}H NMR (500 MHz, $CDCl_3$) δ 7.43 (br s, 2H), 5.42 – 5.27 (m, 2H), 3.31 (q, *J* = 6.9 Hz, 2H), 3.19 (t, *J* = 7.0 Hz, 2H), 2.91 (d, *J* = 5.2 Hz, 3H), 2.05 (app q, *J* = 7.2 Hz, 2H), 2.00 (app q, *J* = 7.0 Hz, 2H), 1.82 (p, *J* = 7.2 Hz, 2H), 1.61 – 1.52 (m, 2H) 1.44 – 1.33 (m, 4H), 1.28 (d, *J* = 4.8 Hz, 10H); ^{13}C NMR (126 MHz, $CDCl_3$) δ 160.8, 160.0, 130.9, 129.1, 39.8, 33.8, 30.8, 29.9, 29.7, 29.6, 29.5, 29.1, 28.8, 27.5, 27.3, 27.1, 26.9, 26.4, 7.7.

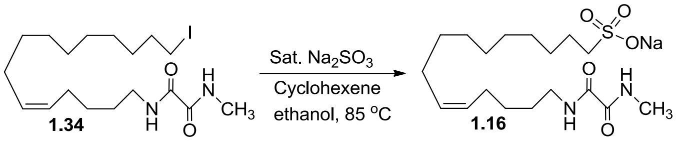

Synthesis of sodium (*Z*)-15-(2-(methylamino)-2-oxoacetamido)pentadec-10-ene-1-sulfonate (1.16)

A mixture of (*Z*)-*N*^{1}-(15-iodopentadec-5-en-1-yl)-*N*^{2}-methyloxalamide (0.2 g, 0.460 mmol), Na_2SO_3 (0.231 g, 1.83 mmol, 4 equiv), ethanol (3 mL), cyclohexene (0.932 mL, 9.20 mmol, 20 equiv) and water (1.5 mL) was heated at 85 °C in a sealed tube for 4 days. The reaction was cooled to rt and concentrated in vacuo. The titled product (51.0 mg, 27%, mp: 202-210 °C [dec]) was isolated via Bio-Beads™ SM-2 absorbent (Bio-Rad, 20-50 mesh) extraction.

^{1}H NMR (500 MHz, DMSO-d_6) δ 8.87 – 8.56 (m, 2H), 5.44 – 5.18 (m, 2H), 3.16 – 3.01 (m, 2H), 2.65 (d, *J* = 5.2 Hz, 3H), 2.39 – 2.28 (m, 2H), 2.03 – 1.88 (m, 4H), 1.59 – 1.36 (m, 4H), 1.35 – 1.13 (m, 14H); ^{13}C NMR (101 MHz, DMSO-d_6) δ 161.3 , 160.5, 130.3, 129.9, 52.2, 39.2, 29.8, 29.6, 29.3, 29.1, 29.0, 27.3, 27.1, 26.9, 25.8.

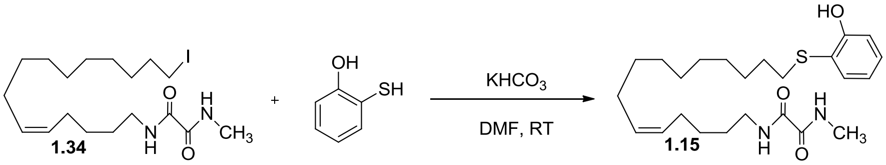

Synthesis of (*Z*)-*N*^{1}-(15-((2-hydroxyphenyl)thio)pentadec-5-en-1-yl)-*N*^{2}-methyloxalamide (1.15)

To a suspension of (*Z*)-*N*^{1}-(15-iodopentadec-5-en-1-yl)-*N*^{2}-methyloxalamide (400 mg, 0.920 mmol) and $KHCO_3$ (111 mg, 1.10 mmol, 1.2 equiv) in anhydrous DMF (3.50 mL) was added commercial 2-mercaptophenol (116 mg, 1 equiv) dropwise. The reaction was stirred overnight at rt. **Note:** The reaction went from a white suspension to a clear solution by the next day. After completion by TLC, the reaction was quenched with water, extracted with EtOAc (3 × 30 mL), dried over anhydrous Na_2SO_4, filtered through a Buchner fritted funnel, and concentrated under vacuum. The crude product was purified using a Teledyne Isco Combiflash® R_f chromatographic system (12 g SiO_2 column eluted with 15-20% EtOAc/hexane) to give **1.15** as a yellow solid (317 mg, 79%; mp, 62.4-62.7 °C). TLC: 50% EtOAc/hexanes, $R_f \sim 0.65$.

^{1}H NMR (500 MHz, $CDCl_3$) δ 7.46 (dd, J = 7.5, 1.5 Hz, 2H), 7.43 (br s, 1H), 7.29 – 7.22 (m, 1H), 6.98 (dd, J = 8.3, 1.3 Hz, 1H), 6.87 (td, J = 7.5, 1.3 Hz, 1H), 6.78 (s, 1H), 5.42 – 5.26 (m, 2H), 3.31 (q, J = 6.9 Hz, 2H), 2.91 (d, J = 5.2 Hz, 3H), 2.68 (app t, J = 7.5 Hz, 2H), 2.05 (app q, J = 7.2 Hz, 2H), 1.99 (app q, J = 6.8 Hz, 2H), 1.62 – 1.49 (m, 4H), 1.44 – 1.23 (m, 14H); ^{13}C NMR ($CDCl_3$, 126 MHz) δ 160.7, 159.8, 157.0, 135.9, 130.9, 130.7, 129.0, 120.7, 119.4, 114.8, 39.7, 36.8, 29.8, 29.7, 29.52, 29.51, 29.3, 29.2, 28.9, 28.7, 27.3, 27.0, 26.8, 26.3.

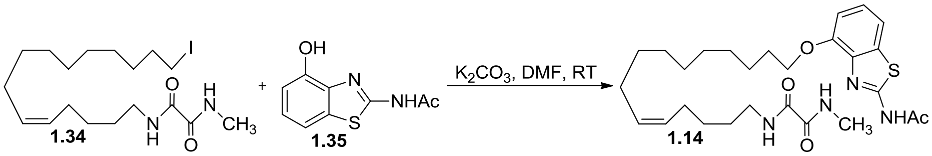

Synthesis of (*Z*)-*N*^{1}-(15-(2-acetamidobenzo[*d*]thiazol-7-yloxy)pentadec-5-en-1-yl)-*N*^{2}-methyloxalamide (1.14)

A mixture of (*Z*)-*N*^{1}-(15-iodopentadec-5-en-1-yl)-*N*^{2}-methyloxalamide (0.200 g, 0.458 mmol), *N*-(4-hydroxybenzo[*d*]thiazol-2-yl)acetamide[44] (0.122 g, 0.458 mmol), and K_2CO_3 (0.095 g, 0.687 mmol, 1.5 equiv) in DMF (3 mL) was heated in a sealed tube at 85 °C for 6 h. The reaction was cooled to rt, diluted with H_2O (20 mL), and extracted with EtOAc (3 × 20 mL). The combined organic extracts were dried over Na_2SO_4, decanted, and concentrated in vacuo. The crude product was purified via SiO_2 column chromatography with 50-60% EtOAc/hexanes to give **1.14** (68.6 mg, 29%). TLC: 50% EtOAc/hexanes, $R_f \sim 0.2$.

^{1}H NMR (500 MHz, CDCl$_3$) δ 11.34 (br s, 1H), 7.85 (br s, 1H), 7.59 (br s, 1H), 7.40 (d, *J* = 8.0 Hz, 1H), 7.24 (t, *J* = 8.0 Hz, 1H), 6.90 (d, *J* = 8.0 Hz, 1H), 5.40 – 5.26 (m, 2H), 4.13 (t, *J* = 6.5 Hz, 2H), 3.32 (q, *J* = 7.0 Hz, 2H), 2.89 (d, *J* = 5.0 Hz, 3H), 2.24 (s, 3H), 2.05 (app q, *J* = 7.2 Hz, 2H), 1.96 (app q, *J* = 7.0 Hz, 2H), 1.84 (p, *J* = 6.9 Hz, 2H), 1.56 (p, *J* = 7.3 Hz, 2H), 1.50 – 1.35 (m, 4H), 1.34 – 1.17 (m, 10H); ^{13}C NMR (126 MHz, CDCl$_3$) δ 169.2, 160.9, 160.1, 158.2, 151.6, 138.3, 133.7, 131.0, 129.1, 125.5, 125.0, 124.3, 113.6, 113.3, 108.2, 105.0, 69.0, 39.9, 29.8 (2), 29.7 (2), 29.5 (2), 29.0, 27.4, 27.1, 26.9, 26.5, 26.3, 23.6.

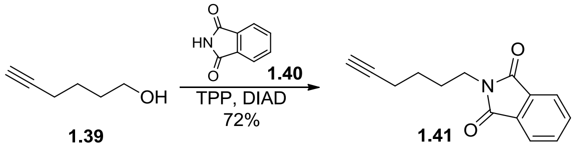

Synthesis of 2-(hex-5-yn-1-yl)isoindoline-1,3-dione (1.41)

Following literature precedent,[45] a solution of 5-hexyn-1-ol (**1.39**) (5.00 g, 50.9 mmol, 1 equiv) and diisopropyl azodicarboxylate (DIAD, 10.5 g, 52.0 mmol, 1.02 equiv) in anhydrous THF (30 mL) was slowly added via cannula to a 0 °C solution of phthalimide (**1.40**, 7.50 g, 51.0 mmol) and triphenylphosphine (TPP, 13.4 g, 1 equiv) in anhydrous THF (50 mL). The flask and cannula were washed with an additional portion of dry THF (20 mL) to ensure complete addition. The reaction was allowed to gradually warm to room temperature overnight. After a total of 18 h, all volatiles were evaporated and the residue was purified using a Teledyne Isco Combiflash® *R*f chromatographic system (80 g SiO$_2$ column eluted with hexanes, 2 min; 0-20% EtOAc/hexanes, 12 min; 20% EtOAc/hexanes, 6 min) to give **1.41** (8.30 g, 72%) as a white solid whose spectral values were identical to those reported.[46]

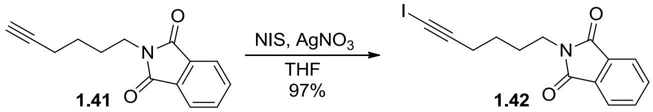

Synthesis of 2-(6-iodohex-5-yn-1-yl)isoindoline-1,3-dione (1.42)

Following literature precedent,[47] *N*-iodosuccinimide (NIS, 7.4 g, 1.5 equiv) was added in one portion to a rt solution of 2-(hex-5-yn-1-yl)isoindoline-1,3-dione (5.00 g, 22.0 mmol) and $AgNO_3$ (0.93 mg, 0.25 equiv) in anhydrous THF (120 mL). The reaction head space was flushed with argon and the reaction mixture was protected from light with an aluminum foil wrap. After 4 h, the reaction mixture was poured into H_2O (200 mL) and extracted with Et_2O (2 × 50 mL). The ethereal extracts were washed with brine (3 × 60 mL) (note: biphasic mixture turned brown). The combined aqueous phases were re-extracted with Et_2O (2 × 50 mL). The combined ethereal extracts were dried over Na_2SO_4, filtered, and concentrated on a rotary evaporator. The residue was purified using a Teledyne Isco Combiflash® R_f chromatographic system (80 g SiO_2 column eluted with hexanes, 2 min; 0-40% EtOAc/hexanes, 8 min; 40% EtOAc/hexanes, 10 min; 40-100% EtOAc/hexanes, 5 min; 100%, EtOAc, 3 min) to give the title compound (7.79 g, 97%; mp, 132.5-132.7 ºC) as a white solid.

^{1}H NMR (500 MHz, $CDCl_3$) δ 7.85 (ddd, *J* = 5.4, 3.0, 1.0 Hz, 2H), 7.72 (ddd, *J* = 5.5, 3.0, 1.0 Hz, 2H), 3.71 (t, *J* = 7.1 Hz, 2H), 2.42 (t, *J* = 7.0 Hz, 2H), 1.83 – 1.73 (m, 2H), 1.61 – 1.51 (m, 2H); ^{13}C NMR (100 MHz, $CDCl_3$) δ 168.6, 134.1, 132.3, 123.4, 94.0, 37.6, 27.9, 25.9, 20.6, -6.3.

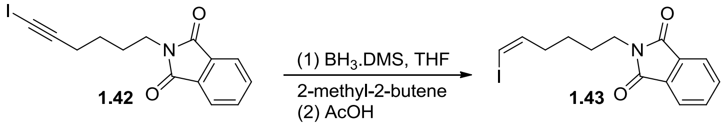

Synthesis of 2-(6-iodohex-5(*Z*)-en-1-yl)isoindoline-1,3-dione (1.43)

Following literature precedent,[48] neat 2-methyl-2-butene (4.20 mL, 2.80 equiv) was added over 5 min to a 0 °C solution of $BH_3 \cdot Me_2S$ (2.0 M in THF, 9.20 mL, 1.3 equiv) in THF (3 mL). After 1 h, the reaction mixture was warmed to room temperature and stirred for 90 min. After re-cooling to 0 °C, a solution of 2-(6-iodohex-5-yn-1-yl)isoindoline-1,3-dione (5.00 g, 1 equiv) in THF (30 mL) was added slowly over 5 min. Upon complete addition, the cold bath was removed and the reaction mixture was stirred at rt. After 2 h, the reaction was cooled again to 0 °C whereupon glacial AcOH (8.50 mL) was added slowly over 5 min (caution: gas evolution). After stirring overnight (14 h), the reaction mixture was diluted with H_2O (20 mL), then carefully poured into a stirring, saturated sodium bicarbonate solution (40 mL). The biphasic mixture was extracted with ether (2 × 40 mL) and the combined ethereal extracts were washed with water, brine, dried over anhydrous $MgSO_4$, filtered, and concentrated in vacuo. The residue was purified using a Teledyne Isco Combiflash® R_f chromatographic system (40 g SiO_2 column eluted with 0-20% EtOAc/hexanes, 8 min; 20% EtOAc/hexanes, 6 min) to give a mixture (4.52 g) of **1.43** and borane side-product. Further purification was postponed until the next step.

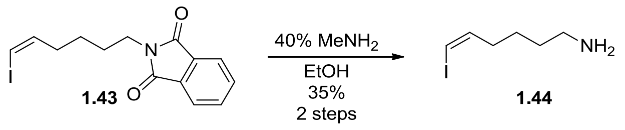

Synthesis of 6-iodohex-5(*Z*)-en-1-amine (1.44)

Following literature precedent,[49] 40% wt $MeNH_2$ in H_2O (15 mL) was added to a rt solution of crude 2-(6-iodohex-5(*Z*)-en-1-yl)isoindoline-1,3-dione (4.52 g) in EtOH (20 mL). After stirring overnight (18 h), the reaction mixture was poured into ice water (100 mL) and extracted with Et_2O (30 mL × 2). The combined ethereal extracts were washed with cold 1N HCl solution (20 mL × 2). The combined aqueous washes were adjusted to pH 8 with dilute, aq. NaOH. The solution was extracted with Et_2O (30 mL × 2), dried over anhydrous Na_2SO_4, filtered, and concentrated *in vacuo* to give the crude title product (1.12 g) as a brown oil that was used in the next step without further purification.

^{1}H NMR (500 MHz, $CDCl_3$) δ 6.29 – 6.08 (m, 2H), 2.71 (tt, *J* = 7.0, 1.8 Hz, 2H), 2.16 (app q, *J* = 6.5 Hz, 2H), 1.78 – 1.52 (m, 2H).

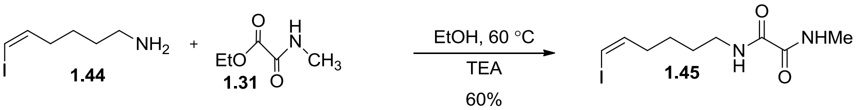

Synthesis of *N*^{1}-(6-iodohex-5(*Z*)-en-1-yl)-*N*^{2}-methyloxalamide (1.45)

Following literature precedent,[50] a solution of 6-iodohex-5(*Z*)-en-1-amine (1.12 g, 4.98 mmol), ethyl 2-(methylamino)-2-oxoacetate (**1.31**)[42] (0.620 g, 1.2 equiv), and triethylamine (0.83 mL, 1.2 equiv) in anhydrous ethanol (10 mL) was heated at 60 °C. After 20 h, the brown solution was cooled to rt and concentrated *in vacuo*. Purification of the residue using a Teledyne Isco Combiflash® R_f chromatographic system (25 g SiO_2 column eluted with 0-50% EtOAc/hexanes, 10 min; 50% EtOAc/hexanes, 10 min) gave **1.45** (0.930 g, 60%, mp: 99.7-99.8 °C) as a white solid.

^{1}H NMR (500 MHz, $CDCl_3$) δ 7.46 (br s, 2H), 6.32 – 6.02 (m, 2H), 3.34 (app q, *J* = 6.9 Hz, 2H), 2.91 (d, *J* = 5.3 Hz, 3H), 2.18 (dt, *J* = 7.5, 7.0 Hz, 2H), 1.68 – 1.59 (m, 2H), 1.54 – 1.42 (m, 2H); ^{13}C NMR (100 MHz, $CDCl_3$) δ 160.5, 159.7, 140.4, 83.1, 39.4, 34.1, 28.6, 26.2, 25.1.

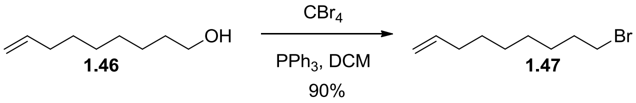

Synthesis of 9-bromonon-1-ene (1.47)

Carbon tetrabromide (CBr_4, 3.03 g, 9.14 mmol, 1.3 equiv) was added to a solution of TPP (2.40 g, 1.3 equiv) and commercial non-8-en-1-ol (**1.46**, 1.00 g, 7.03 mmol) in anhydrous DCM (90 mL). The mixture was stirred at rt for 24 h and then concentrated in vacuo. The crude product was re-dissolved in hexanes (30 mL), cooled to 0 °C and filtered through a Buchner fritted funnel. The residue was washed with cold hexanes (2 × 20 mL) and the combined filtrate was concentrated in vacuo to give the title product (1.3 g, 90%) as a colorless oil whose ^1H NMR data were consistent with those reported.[51]

^1H NMR (500 MHz, $CDCl_3$) δ 5.81 (ddt, J = 16.9, 10.2, 6.7 Hz, 1H), 5.06 – 4.89 (m, 2H), 3.41 (t, J = 6.9 Hz, 2H), 2.10 – 2.00 (m, 2H), 1.93 – 1.80 (m, 2H), 1.47 – 1.21 (m, 10H).

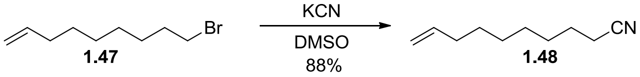

Synthesis of dec-9-enenitrile (1.48)

Potassium cyanide (KCN, 1.65 g, 25.3 mmol, 4 equiv) was added to a solution of 9-bromonon-1-ene (**1.47**, 1.30 g, 6.34 mmol) in anhydrous DMSO (90 mL) and the mixture was stirred overnight at rt. After completion as judged by TLC analysis, the reaction was diluted with H_2O (180 mL) and extracted with Et_2O (2 × 120 mL). The combined organic extracts were washed with brine (2 × 100 mL). The organic phase was dried over anhydrous Na_2SO_4, filtered through a Buchner fritted funnel, and concentrated in vacuo. The crude product was purified via SiO_2 column chromatography with 0-20% EtOAc/hexanes to give the title product[52] as a colorless oil (0.845 g, 88%). TLC: 20% EtOAc/hexanes, R_f ~ 0.55.

^{1}H NMR (500 MHz, $CDCl_3$) δ 5.80 (ddt, *J* = 16.9, 10.1, 6.7 Hz, 1H), 5.05 – 4.89 (m, 2H), 2.33 (t, *J* = 7.1 Hz, 2H), 2.12 – 1.98 (m, 2H), 1.72 – 1.60 (m, 2H), 1.50 – 1.26 (m, 8H).

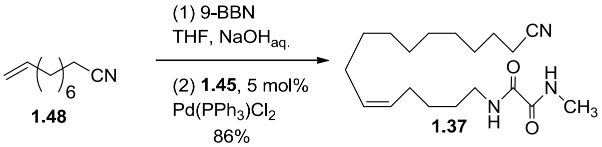

Synthesis of (*Z*)-*N*^{1}-(15-cyanopentadec-5-enyl)-*N*^{2}-methyloxalamide (1.37)

To an oven-dried flask containing dec-9-enenitrile (J) (358 mg, 2.37 mmol, 1.5 equiv) was added a solution of 9-BBN (0.5 M in THF, 3.00 equiv, 9.50 mL). After stirring at rt for 3 h, an aqueous solution of Na_2CO_3 (2.0 mL of 2 M soln prepared from argon sparged H_2O) was added. After 5 min, $Pd(PPh_3)_2Cl_2$ (55.5 mg, 5 mol%) was added followed by **1.45** (490 mg, 1.58 mmol). The resulting red solution was protected from light and the reaction was continued overnight (14 h) at rt, then at 50 °C for 1 h. After cooling to rt, the reaction mixture was concentrated *in vacuo* and the residue was purified using a Teledyne Isco Combiflash® *R*$_f$ chromatographic system (24 g SiO_2 column eluted with 0-20% EtOAc/hexanes, 5 min; 20% EtOAc/hexanes, 6 min; 20-50% EtOAc/hexanes, 5min; 50% EtOAc/hexanes, 8 min) to give ether **1.37** as an off-white solid. Re-purification on a 12 g column and eluting with 0-20% EtOAc/hexanes, 8 min; 20% EtOAc/hexanes, 4 min; 20-50%, 8 min gave the pure title product as a white solid (440 mg, 86%; mp, 88.8-88.9 °C). TLC: 50% EtOAc/hexanes, R_f ~ 0.55.

^{1}H NMR (400 MHz, $CDCl_3$) δ 7.43 (br s, 2H), 5.44 – 5.23 (m, 2H), 3.31 (q, *J* = 6.8 Hz, 2H), 2.91 (d, *J* = 5.2 Hz, 3H), 2.34 (t, *J* = 7.2 Hz, 2H), 2.09 – 1.96 (m, 4H), 1.71 – 1.60 (m, 2H), 1.61 – 1.49 (m, 5H), 1.49 – 1.36 (m, 3H), 1.36 – 1.22 (m, 8H); ^{13}C NMR (101 MHz, $CDCl_3$) δ 160.8, 159.9, 130.8, 129.1, 120.1, 39.8, 29.8, 29.6, 29.5, 29.4, 29.0, 28.9, 28.8, 27.4, 27.1, 26.9, 26.4, 25.6, 17.3.

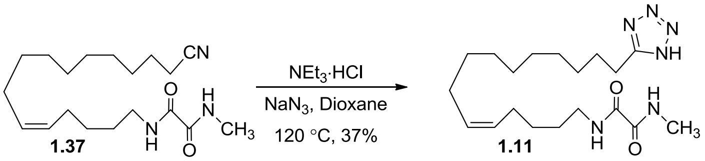

Synthesis of (*Z*)-*N*^{1}-(15-(1*H*-tetrazol-5-yl)pentadec-5-enyl)-*N*^{2}-methyloxalamide (1.11)

A mixture of NaN_3 (350 mg, 5.40 mmol, 3.9 equiv), $NEt_3\cdot HCl$ (860 mg, 4.6 equiv) and dioxane (8 mL) was heated at 120 °C in a sealed tube for 4 days. The reaction was cooled to rt and acidified with 10% HCl to bring the pH to 1. The reaction was diluted with H_2O (10 mL) and extracted with EtOAc (4 × 10 mL). The combined organic extracts were dried over Na_2SO_4, decanted, and concentrated in vacuo. The crude product was purified using a Teledyne Isco Combiflash® R_f chromatographic system (12 g SiO_2 column eluted with 0-100% EtOAc/hexanes, 10 min; DCM, 2 min; 0-10% MeOH/DCM, 10 min; 10%, 8 min) to give **1.11** as a white solid (195 mg, 37%; mp, 127.3 °C).

^{1}H NMR (400 MHz, methanol-d$_4$) δ 5.42 – 5.25 (m, 2H), 3.23 (t, *J* = 7.2 Hz, 2H), 2.90 (t, *J* = 7.6 Hz, 2H), 2.80 (s, 3H), 2.09 – 1.95 (m, 4H), 1.81 – 1.69 (m, 2H), 1.60 – 1.47 (m, 2H), 1.41 – 1.22 (m, 12H); ^{13}C NMR (101 MHz, methanol-d$_4$) δ 162.1, 161.3, 160.4, 130.2, 129.1, 39.18, 29.7, 29.5, 29.4, 29.3, 29.2, 29.16, 29.0, 28.7, 27.0, 26.9, 26.6, 25.1, 24.8, 22.8.

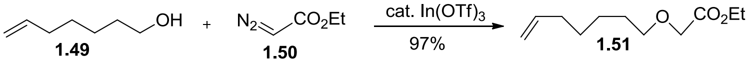

Synthesis of ethyl 2-(oct-7-en-1-yloxy)acetate (1.51)

Following literature precedent,[53] commercial 6-hepten-1-ol (1.92 g, 1.2 equiv) was added neat to a rt suspension of $In(OTf)_3$ (1.57 g, 20 mol%) in anhydrous toluene (20 mL). Ethyl diazoacetate (1.60 g, 14 mmol) was added slowly under an argon atmosphere over 5 min (caution: exothermic) to give a yellow solution. After 2 days, the reaction mixture was concentrated *in* *vacuo* and the residue was purified using a Teledyne Isco Combiflash® R_f chromatographic system (25 g SiO_2 column eluted with 0-10% EtOAc/hexanes, 5 min; 10% EtOAc/hexanes, 8 min) to give **1.51** (2.72 g, 97%) as a colorless oil.

^{1}H NMR (500 MHz, $CDCl_3$) δ 5.80 (ddt, J = 16.9, 10.2, 6.6 Hz, 1H), 5.08 – 4.84 (m, 2H), 4.22 (q, J = 7.1 Hz, 2H), 4.06 (s, 2H), 3.52 (t, J = 6.7 Hz, 2H), 2.13 – 1.96 (m, 2H), 1.72 – 1.52 (m, 2H), 1.48 – 1.33 (m, 4H), 1.28 (t, J = 7.1 Hz, 3H); ^{13}C NMR (100 MHz, $CDCl_3$) δ 170.7, 139.0, 114.5, 72.0, 68.5, 60.9, 33.8, 29.5, 28.8, 25.6, 14.3.

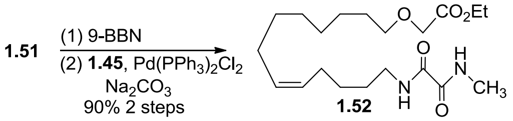

Synthesis of ethyl 2-((13-(2-(methylamino)-2-oxoacetamido)tridec-8(*Z*)-en-1-yl)oxy)acetate (1.52)

To an oven-dried flask containing ethyl 2-(oct-7-en-1-yloxy)acetate (**1.51**) (220 mg, 1.2 equiv) was added a solution of 9-BBN (0.5 M in THF, 2.4 equiv, 4.40 mL). After stirring at rt for 3 h, an aqueous solution of Na_2CO_3 (1.5 mL of 2 M soln prepared from argon sparged H_2O) was added. After 5 min, $Pd(PPh_3)_2Cl_2$ (33 mg, 5 mol%) was added followed by **G** (284 mg, 0.92 mmol). The resulting red solution was protected from light while another portion of aq. Na_2CO_3 (0.5 mL of 2 M soln) was added. The reaction was continued overnight (14 h) at rt, then at 50 °C for 4 h. After cooling to rt, the reaction mixture was concentrated *in vacuo* and the residue was purified using a Teledyne Isco Combiflash® R_f chromatographic system (24 g SiO_2 column eluted with 0-40% EtOAc/hexanes, 6 min; 40% EtOAc/hexanes, 8 min; 40-100% EtOAc/hexanes, 4 min) to give ether **1.52** (330 mg, 90%) as an off-white solid. An analytical sample was purified by preparative TLC to give **1.52** as a white, low melting solid (paste).

TLC: 50% EtOAc/hexanes, R_f ~ 0.49. ^{1}H NMR (500 MHz, $CDCl_3$) δ 7.45 (br s, 2H), 5.42 – 5.26 (m, 2H), 4.22 (q, *J* = 7.2 Hz, 2H), 4.06 (s, 2H), 3.52 (t, *J* = 6.7 Hz, 2H), 3.31 (dt, *J* = 7.0, 6.5 Hz, 2H), 2.91 (d, *J* = 5.1 Hz, 3H), 2.15 – 1.91 (m, 4H), 1.70 – 1.50 (m, 2H), 1.44 – 1.31 (m, 12H), 1.29 (t, *J* = 7.1 Hz, 3H); ^{13}C NMR (100 MHz, $CDCl_3$) δ 170.6, 160.5, 159.7, 130.6, 128.9, 72.0, 68.6, 39.5, 29.6, 29.5, 29.3, 29.2, 27.2, 26.8, 26.7, 26.1, 25.9, 14.2.

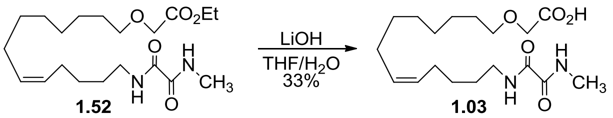

Synthesis of 2-[(13-(2-(methylamino)-2-oxoacetamido)tridec-8(*Z*)-en-1-yl)oxy]acetic acid (1.03)

To a rt solution of **1.52** (1.08 g, 2.80 mmol) in THF (60 mL) was added LiOH (90 mg, 3.76 mmol, 1.3 equiv) in H_2O (20 mL). After 48 h, the reaction was cooled to 4 °C and acidified to pH 4 using aq. 2 N HCl. The mixture was diluted with H_2O (10 mL) and extracted with EtOAc (20 mL × 3). The combined organic extracts were dried over Na_2SO_4, filtered through a fritted funnel, and concentrated *in vacuo*. The crude material was purified using a Teledyne Isco Combiflash® *R*f chromatographic system (24 g SiO_2 column eluted with 0-30% EtOAc/hexanes, 5 min; 30%, 5 min; DCM, 3 min; 0-10% MeOH/DCM, 10 min; 10%, 10 min; 10-20%, 5 min; 20%, 5 min) to give **1.03** (676 mg, 67%; mp, 94.6-94.7 °C) as a white solid.

^{1}H NMR (500 MHz, $CDCl_3$) δ 7.90 (s, 1H), 7.66 (s, 1H), 5.48 – 5.22 (m, 2H), 4.10 (s, 2H), 3.58 (t, *J* = 6.5 Hz, 2H), 3.32 (dt, *J* = 7.0, 6.5 Hz, 2H), 2.91 (d, *J* = 5.2 Hz, 3H), 2.16 – 1.90 (m, 4H), 1.71– 1.48 (m, 4H), 1.45 – 1.18 (m, 10H); ^{13}C NMR (75 MHz, methanol-d_4) δ 177.0, 160.3, 160.1, 130.6, 130.0, 72.5, 69.8, 39.5, 29.8, 29.6, 29.1, 27.7, 27.4, 27.2, 27.1, 26.8, 25.8, 25.0.

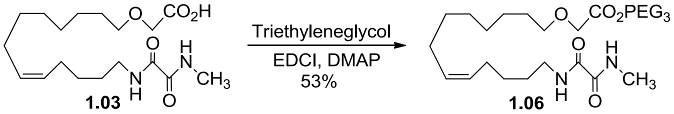

Synthesis of analog 1.06

A mixture of EDCI (275 mg, 1.3 equiv) and triethyleneglycol (1.5 mL, 10 equiv) was dried under high vacuum for 90 min. The reaction flask was flushed with argon and DMAP (175 mg, 1.3 equiv), acid **1.03** (395 mg, 1.1 mmol), and anhydrous CH_2Cl_2 (55 mL) were added. After 2 days, the reaction mixture was diluted with brine (20 mL) and 1N HCl (10 mL). The organic phase was separated and the aqueous phase was re-extracted with CH_2Cl_2 (20 mL × 2). The combined organic extracts were dried over Na_2SO_4, filtered, and concentrated *in* vacuo. The residue was purified using a Teledyne Isco Combiflash® R_f chromatographic system (12 g SiO_2 column eluted with 0-100% EtOAc/hexanes, 15 min; EtOAc, 15 min; 5% MeOH/DCM, 5 min) to give analog **1.06** (286 mg, 53%; mp, 65.3-65.8 °C) as a white solid, and a 70:30 mixture of product and starting material (107 mg).

^{1}H NMR (500 MHz, $CDCl_3$) δ 7.46 (s, 2H), 5.41 – 5.27 (m, 2H), 4.33 (t, *J* = 4.7 Hz, 2H), 4.11 (s, 2H), 3.77 – 3.70 (m, 4H), 3.70 – 3.64 (m, 4H), 3.61 (app t, *J* = 4.5 Hz, 2H), 3.52 (t, *J* = 6.7 Hz, 2H), 3.42 (t, *J* = 6.1 Hz, OH), 3.31 (dt, *J* = 7.0, 6.5 Hz, 2H), 2.91 (d, *J* = 5.2 Hz, 3H), 2.44 (s, 1H), 2.05 (dt, *J* = 7.5, 7.0 Hz, 2H), 2.00 (dt, *J* = 7.0, 6.5 Hz, 2H), 1.62 – 1.50 (m, 4H), 1.45 – 1.21 (m, 10H); ^{13}C NMR (125 MHz, $CDCl_3$) δ 170.9, 160.8, 159.9, 130.8, 129.1, 72.8, 72.2, 70.8, 70.5, 69.2, 68.3, 63.8, 61.9, 39.8, 29.8, 29.7, 29.5, 29.4, 29.0, 27.4, 27.1, 26.9, 26.4, 26.1.

1.7 References

1. Mozaffarian, D.; Benjamin, E. J.; Go, A. S.; Arnett, D. K.; Blaha, M. J.; Cushman, M.; de Ferranti, S.; Despres, J. P.; Fullerton, H. J.; Howard, V. J.; Huffman, M. D.; Judd, S. E.; Kissela, B. M.; Lackland, D. T.; Lichtman, J. H.; Lisabeth, L. D.; Liu, S.; Mackey, R. H.; Matchar, D. B.; McGuire, D. K.; Mohler, E. R III.; Moy, C. S.; Muntner, P.; Mussolino, M. E.; Nasir, K.; Neumar, R. W.; Nichol, G.; Palaniappan, L.; Pandey, D. K.; Reeves, M. J.; Rodriguez, C. J.; Sorlie, P. D.; Stein, J.; Towfighi, A.; Turan, T. N.; Virani, S. S.; Willey, J. Z.; Woo, D.; Yeh, R. W.; Turner, M. B. "Heart disease and stroke statistics — 2015 Update: a report from the American Heart Association." *Circulation* **2015**, *131*, e29-e322.

2. Newman, M. M. About SCA "Sudden cardiac arrest: A healthcare crisis." Sudden Cardiac Arrest Foundation. **2015**, accessed 19 June 2015,

   http://www.sca-aware.org/about-sca.

3. Fischer, T. H.; Neef, S.; Maier, L. S. "The Ca-calmodulin dependent kinase II: A promising target for future antiarrhythmic therapies." *J. Mol. Cell. Cardiol.* **2013**, *58*, 182-187.

4. Leaf, A.; Kang, J. X.; Xiao, Y.; Billman, G. E. "Clinical Prevention of Sudden Cardiac Death by n-3 Polyunsaturated Fatty Acids and Mechanism of Prevention of Arrhythmias by n-3 Fish oils." *Circulation* **2003**, *107*, 2646-2652.

5. Kris-Etherton, P. M.; Harris, W. S.; Appel, L. J. "Fish consumption, fish oil, omega-3 fatty acids, and cardiovascular disease." *Circulation* **2002**, *106*, 2747-2757.

6. Sampath, H.; Ntambi, J. M. "Polyunsaturated fatty acid regulation of genes of lipid metabolism." *Annu. Rev. Nutr.* **2005**, *25*, 317-340.

7. Arnold, C.; Markovic, M.; Blossey, K.; Wallukat, G.; Fischer, R.; Dechend, R.; Konkel, A.; Von Schacky, C.; Luft, F. C.; Muller, D. N.; Rothe, M.; Schunck, W. "Arachidonic Acid-metabolizing Cytochrome P450 Enzymes Are Targets of ω-3 Fatty Acids." *J. Biol. Chem.* **2010**, *285*, 32720-32733.

8. Karara, A.; Dishman, E.; Falck, J. R.; Capdevila. J. H. "Endogenous epoxyeicosatrienoyl-phospholipids: A novel class of cellular glycerolipids containing epoxidized arachidonate moieties." *J. Biol. Chem.* **1991**, *266*, 7561-7569.

9. Hall, J. E.; Guyton, A. C. (2011). *Guyton and Hall textbook of medical physiology* (12th edition). Philadelphia, PA: Saunders/Elsevier, 157. Print.

10. American Heart Association **2015**, *What is cardiovascular disease?*, accessed 19 June 2015,

http://www.heart.org/HEARTORG/Caregiver/Resources/WhatisCardiovascularDisease/What-is-Cardiovascular-Disease_UCM_301852_Article.jsp#.

11. Grant, A. O. “Basic Science for the Clinical Electrophysiologyist: Cardiac ion channels.” *Circ Arrhythmia Electrophysiol*. **2009**, *2*, 185-194.

12. Sherwood, L. (2012). Human Physiology, From Cells to Systems (8th [revised] edition). Belmont, CA: Brooks/Cole, Cengage Learning, 310-311. Print.

13. Ikonnikov, G.; Wong, E. “Physiology of cardiac conduction and contractility—Action potential of cardiac muscles.” McMaster Pathophysiology Review. **2013**, accessed 19 June 2015, http://www.pathophys.org/physiology-of-cardiac-conduction-and-contractility/actionpotential/.

14. Vaughan Williams, E. M. “The experimental basis for the choice of an anti-arrhythmic drug.” *Adv Cardiol*. **1970**, *4*, 275-289.

15. Milne, J. R.; Hellestrand, K. J.; Bexton, R. S.; Burnett, P. J.; Debbas, N. M. G.; Camm, A. J. “Class 1 antiarrhythmic drugs—characteristic electrocardiographic differences when assessed by atrial and ventricular pacing.” *Eur. Heart J.* **1984**, *5*, 99-107

16. Vrana, M.; Pikorny, J.; Marcian, P.; Fejfar, Z. “Class I and III antiarrhythmic drugs for prevention of sudden cardiac death and management of postmyocardial infarction arrhythmias. A review.” *Biomed Pap Med Fac Univ Palacky Olmouc Czech Repub* **2013** *157*, 114-124.

17. Lenz, T. L.; Hilleman, D. E. “Reviews of therapeutics. Dofetilide, a new class III antiarrhythmic agent.” *Pharmacotherapy* **2000**, *20*, 776-786.

18. Rowland, E. “Antiarrhythmic drugs-Class IV.” *Eur. Heart J.* **1987**, *8* (Supplement A), 61-63.

19. Conti, J. B.; Belardinelli, L.; Utterback, D. B.; Curtis, A. B. “Endogenous adenosine is an antiarrhythmic agent.” *Circulation* **1995**, *91*, 1761-1767.

20. Frick, M.; Darpo, B.; Ostergren, J.; Rosenqvist, M. “The effect of oral magnesium, alone or as an adjuvant to sotalol, after cardioversion in patients with persistent atrial fibrillation.” *Eur. Heart J.* **2000**, *21*, 1177-1185.

21. Bang, H. O.; Dyerberg, J.; Horne, N. “The composition of food consumed by Greenland Eskimos.” *Acta Med Scand* **1976**, *200*, 69-73.

22. Burr, M.; Fehily, A. M.; Gilbert, J. F., Roger, S.; Holliday, R. M.; Sweetnam, P. M.; Elwood, P. C.; Deadman, N. M. “Effects of changes in fat, fish, and fibre intakes on

death and myocardial reinfarction: Diet and Reinfarction Trial (DART)." *Lancet* **1989**, *334*, 757-761.

23. GISSI-Prevenzione Investigators. "Dietary supplementation with n-3 polyunsaturated fatty acids and vitamin E after myocardial infarction: results of the GISSI-Prevenzione trial." *Lancet* **1999**, *354*, 447-455.

24. Albert, C. M.; Hennekens, C. H.; O'Donnell, C. J.; Ajani, U. A.; Carey, V. J.; Willett, W. C.; Ruskin, J. N.; Manson, J. E. "Fish consumption and risk of sudden cardiac death." *JAMA* **1998**, *279*, 23-28.

25. Kang, J. X.; Leaf, A. "Effects of long-chain polyunsaturated fatty acids on the contraction of neonatal rat cardiomyocytes." *Proc Natl Acad Sci USA* **1994**, *91*, 9886-9890.

26. Billman, G. E.; Hallaq, H.; Leaf, A. "Prevention of ischemia-induced arrhythmias by n-3 fatty acids." *Proc Natl Acad Sci USA* **1994**, *91*, 4427-4430.

27. Billman, G. E.; Kang, J. X.; Leaf, A. "Prevention of ischemia-induced cardiac sudden death by n-3 polyunsaturated fatty acids." *Lipids* **1997**, *32*, 1161-1168.

28. Billman, G. E.; Kang, J. X.: Leaf, A. "Prevention of ischemia-induced cardiac sudden death by pure n-3 polyunsaturated fatty acids." *Circulation* **1999**, *99*, 2452-2457.

29. Xiao, Y-F; Kang, J. X.; Morgan, J. P.; Leaf, A. "Blocking effects of polyunsaturated fatty acids on Na^+ channels of neonatal rat ventricular myocytes." *Proc Natl Acad Sci USA* **1995**, *92*, 11000-11004.

30. Xiao, Y-F.; Wright, S. N.; Wang, G. K.; Morgan, J. P.; Leaf, A. "N-3 fatty acids suppress voltage-gated Na^+ currents in HEK293t cells transfected with the α–subunit of the human cardiac Na^+ channel." *Proc Natl Acad Sci USA* **1998**, *95*, 2680-2685.

31. Xiao, Y-F.; Wright, S. N.; Wang, G. K.; Morgan, J. P.; Leaf, A. "Co-expression with the β1 –subunit modifies the kinetics and fatty acid block of $hH1\alpha Na^+$ channels." *Am J Physiol Heart Circ Physiol.* **2000**, *279*, H35-H46.

32. Xiao, Y-F.; Gomez, A. M.; Morgan, J. P.; Lederer, W. J.; Leaf, A. "Suppression of voltage-gated L-type Ca^{2+} currents by polyunsaturated fatty acids in adult and neonatal rat cardiac myocytes." *Proc Natl Acad Sci USA* **1997**, *94*, 4182-4187.

33. Smith, W.L. "Cyclooxygenases, peroxide tone and the allure of fish oil." *Curr. Opin. Cell Biol.* **2005**, *17*, 174-182.

34. Li, Y.; Kang, J. X.; Leaf, A. "Differential effects of various eicosanoids on the production or prevention of arrhythmias in cultured neonatal rat cardiac myocytes." *Prostaglandins* **1997**, *54*, 511-530.

35. Lee, H-C.; Lu, T.; Weintraub, N. L.; VanRollins, M.; Spector, A. A; Shibata, E. F. "Effects of epoxyeicosatrienoic acids on the cardiac sodium channels in isolated rat ventricular myocytes." *J Physiol* **1999**, *519.1,* 153-168.

36. Falck, J. R.; Wallukat, G.; Puli, N.; Goli, M.; Arnold, C.; Konkel, A.; Rothe, M.; Fischer, R.; Muller, D. N.; Schunck, W-H. "17(R), 18(S)-Epoxyeicosatetraenoic acid, a potent eicosapentaenoic acid (EPA) derived regulator of cardiomyocyte contraction: Structure-Activity Relationships and Stable Analogues." *J. Med. Chem.* **2011**, *54*, 4109-4118.

37. Campbell, W. B; Gebremehdin, D.; Pratt, F.P.; Harder, D. R. "Identification of epoxyeicosatrienoic acids as endothelium-derived relaxing factors." *Circ Res.* **1996**, *78*, 415-423.

38. Scarborough, P. E.; Ma, J.; Qu, W.; Zeldin, D.C. "P450 subfamily CYP2J and their role in the bioactivation of arachidonic acid in extrahepatic tissues." *Drug Metab Rev.* **1999**, *31*, 205-234.

39. Falck, J. R.; Koduru, S. R.; Mohapatra, S.; Manne, R.; Atcha, R.; Manthati, V. L.; Capdevila, J. H.; Christian, S.; Imig, J. D.; Campbell, W. B. 14,15-Epoxyeicosa-5,8,11-trienoic acid (14,15-EET) surrogates: carboxylate modifications. *J. Med. Chem.* **2014**, *57*, 6965-6972.

40. (a) Lauterbach, B.; Barbosa-Sicard, E.; Wang, M. N.; Honeck, H.; Kärgel, E.; Theuer, J.; Schwartzman, M. L.; Haller, H.; Luft, F. C.; Gollasch, M.; Schunk, W.-H. Cytochrome P450-dependent eicosapentaenoic acid metabolites are novel BK channel activators. *Hypertension* **2002**, *39*, 609-613. (b) Hercule, H. C.; Salanova, B.; Essin, K.; Honeck, H.; Falck, J. R.; Sausbier, M.; Ruth, P.; Schunk, W.-H.; Luft, F. C.; Gollasch, M. The vasodilator 17,18-epoxyeicosatetraenoic acid targets the pore-forming BK alpha channel subunit in rodents. *Exp. Physiol.* **2007**, *92*, 1067-1076.

41. Nikas, S. P.; D'Souza, M.; Makriyannis, A. Enantioselective synthesis of (10*S*)- and (10*R*)-methyl-anandamides. *Tetrahedron* **2012**, *68*, 6329-6337.

42. Grube, A.; Timm, C.; Kock, M. Synthesis and Mass Spectrometric Analysis of Cyclostellettamines H, I, K and L. *Eur. J. Org. Chem.* **2006**, 1285-1295.

43. Yavari, I.; Bayat, M. New synthesis of highly functionalized 3-pyrrolin-2-ones. *Synthetic Communications* **2002**, *32*, 2527-2534.

44. Wang, H-L.; Katon, J.; Balan, C.; Bannon, A. W.; Bernard, C.; Doherty, E. M.; Dominguez, C.; Gavva, N. R.; Gore, V.; Ma, V.; Nishimura, N.; Surapaneni, S.; Tang, P.; Tamir, R.; Thiel, O.; Treanor, J. J. S.; Norman, M. H. Novel vanilloid receptor-1 antagonists: 3. The identification of a second-generation clinical candidate with improved physicochemical and pharmacokinetic properties. *J. Med. Chem.* **2007**, *50*, 3528-3539.

45. Altman, A. R.; Nilsson, L. B.; Overman, E. L.; Read de Alaniz, J.; Rohde, M. J.; Taupin, V. Total synthesis of (+)-Nankakurines A and B and (±)-5-*epi*-Nankakurine. *J. Org. Chem.* **2010**, *75*, 7519–7534.

46. Rozkiewicz, I. D.; Janczewski, D.; Verboom, W.; Ravoo, J. B; Reinhoudt, N. D. “Click” Chemistry by microcontact printing. *Angew. Chem. Intd. Ed.* **2006**, *45*, 5292–5296.

47. Webb, A. J.; Klijn, E. J.; Hill, A. P.; Bennett, L. J.; Goroff, S. N. Experimental studies of the ^{13}C NMR of iodoalkynes in Lewis-basic solvents. *J. Org. Chem.* **2004**, *69*, 660–664.

48. Devin, K. J. S.; Van Vranken, L. D. Palladium-catalyzed carbene insertion and trapping with carbon nucleophiles. *Org. Lett.* **2008**, *10*, 1909–1911.

49. Trybulski, J. E.; Reeder, E.; Blount, F. J.; Walser, A.; Fryer, R. I. 2-Benzazepines.1. Synthesis of 2-benzazepin-4-ones and 5-ones via 2-acetylenic benzophenones. *J. Org. Chem.* **1982**, *47*, 2441–2447.

50. Meddad-Belhabich, N.; Aoun, D.; Djimdé, A.; Redeuilh, C.; Dive, G.; Massicot, F.; Chau, F.; Heymans, F.; Lamouri, A. Design of new potent and selective secretory phospholipase A_2 inhibitors. 6-Synthesis, structure–activity relationships and molecular modeling of 1-substituted-4-[4,5-dihydro-1,2,4-(4*H*)-oxadiazol-5-one-3-yl(methyl)]-functionalized aryl piperazin/one/dione derivatives. *Bioorg. Med. Chem.* **2010**, *18*, 3588–3600.

51. Simon, K. A.; Burton, E. A.; Cheng, F.; Varghese, N.; Falcone, E. R.; Wu, L.; Luk, Y-Y. Controlling thread assemblies of pharmaceutical compounds in liquid crystal phase by using functionalized nanotopography. *Chem. Mater.* **2010**, *22*, 2434-2441.

52. Shimojo, H.; Moriyama, K.; Togo, H. Simple one-pot conversion of alcohols into nitriles. *Synthesis* **2013**, *45*, 2155-2164.

53. Muthusamy, S.; Arulananda Babu, S.; Gunanathan, C. Indium triflate: a mild and efficient Lewis acid catalyst for O-H insertion reactions of α-diazo ketones. *Tetrahedron Letters* **2002**, *43*, 3133–3136.

1.8 Spectra

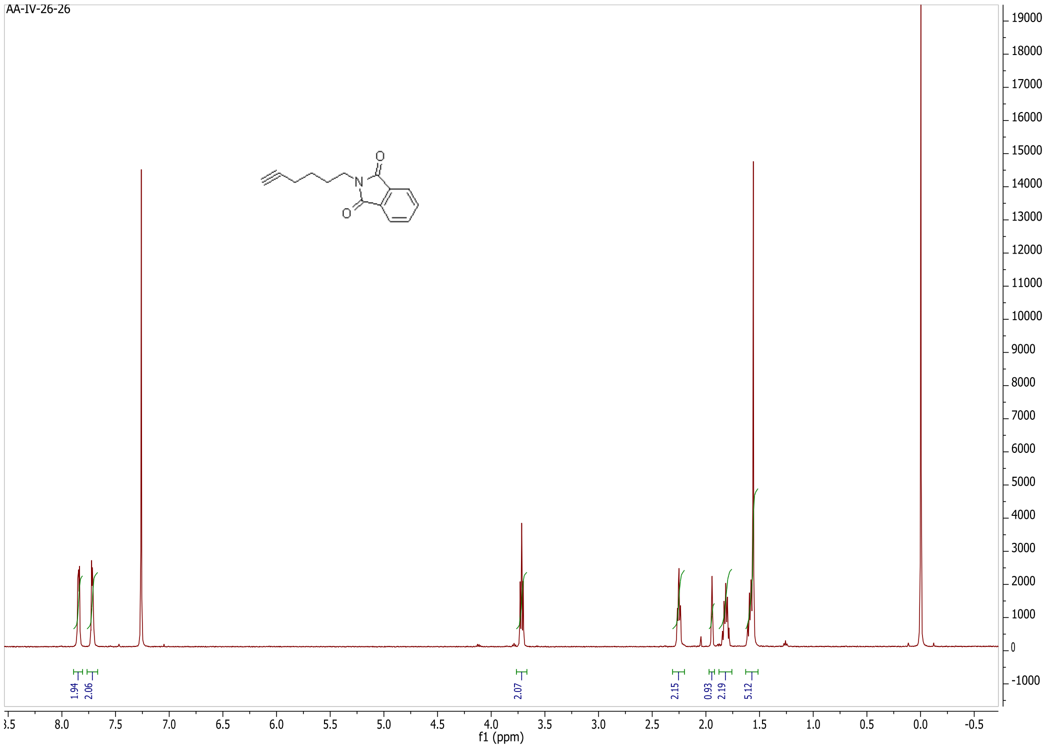
AA-IV-26-26
O
N
O
1.94
2.06
2.07
2.15
0.93
2.19
5.12
19000
18000
17000
16000
15000
14000
13000
12000
11000
10000
9000
8000
7000
6000
5000
4000
3000
2000
1000
0
-1000
8.5
8.0
7.5
7.0
6.5
6.0
5.5
5.0
4.5
4.0
3.5
3.0
2.5
2.0
1.5
1.0
0.5
0.0
-0.5
f1 (ppm)

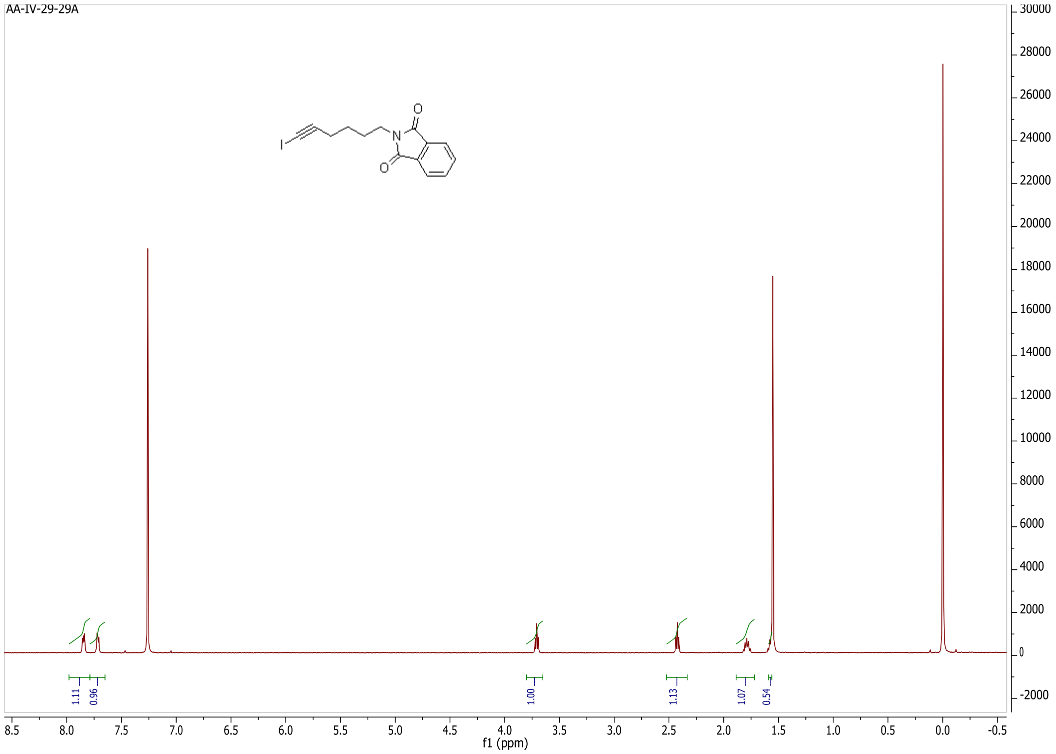
AA-IV-29-29A
I
O
N
O
1.11
0.96
1.00
1.13
1.07
0.54
30000
28000
26000
24000
22000
20000
18000
16000
14000
12000
10000
8000
6000
4000
2000
0
-2000
8.5
8.0
7.5
7.0
6.5
6.0
5.5
5.0
4.5
4.0
3.5
3.0
2.5
2.0
1.5
1.0
0.5
0.0
-0.5
f1 (ppm)

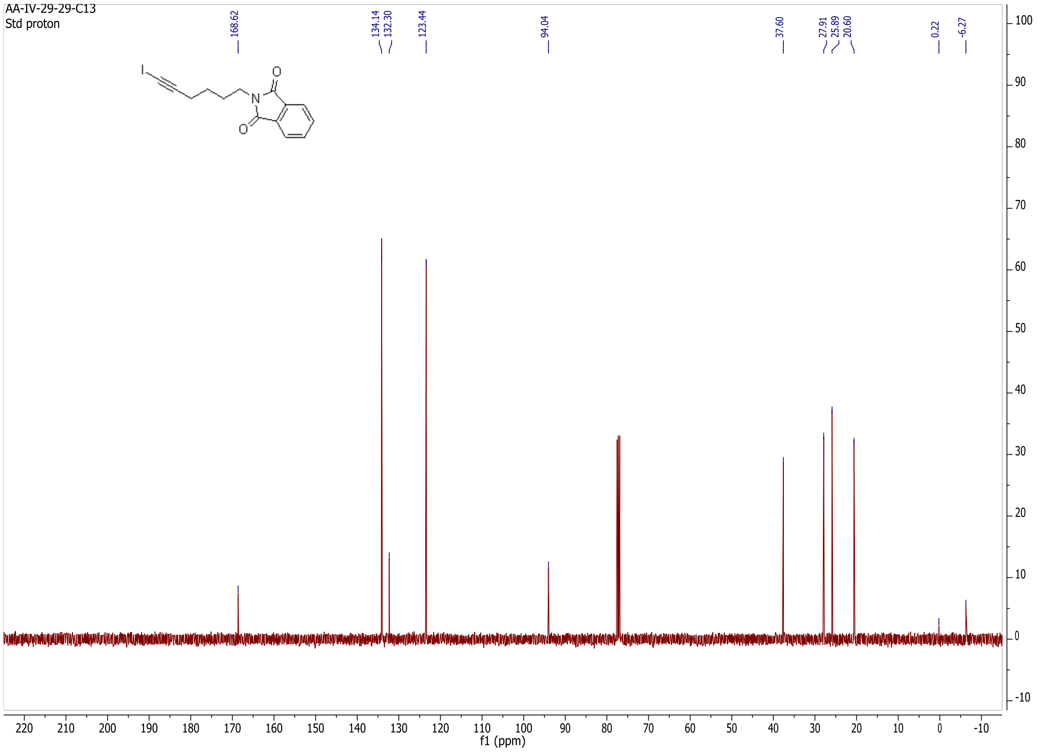
AA-IV-29-29-C13
Std proton
168.62
134.14
132.30
123.44
94.04
37.60
27.91
25.89
20.60
0.22
-6.27
I
N
O
O
f1 (ppm)

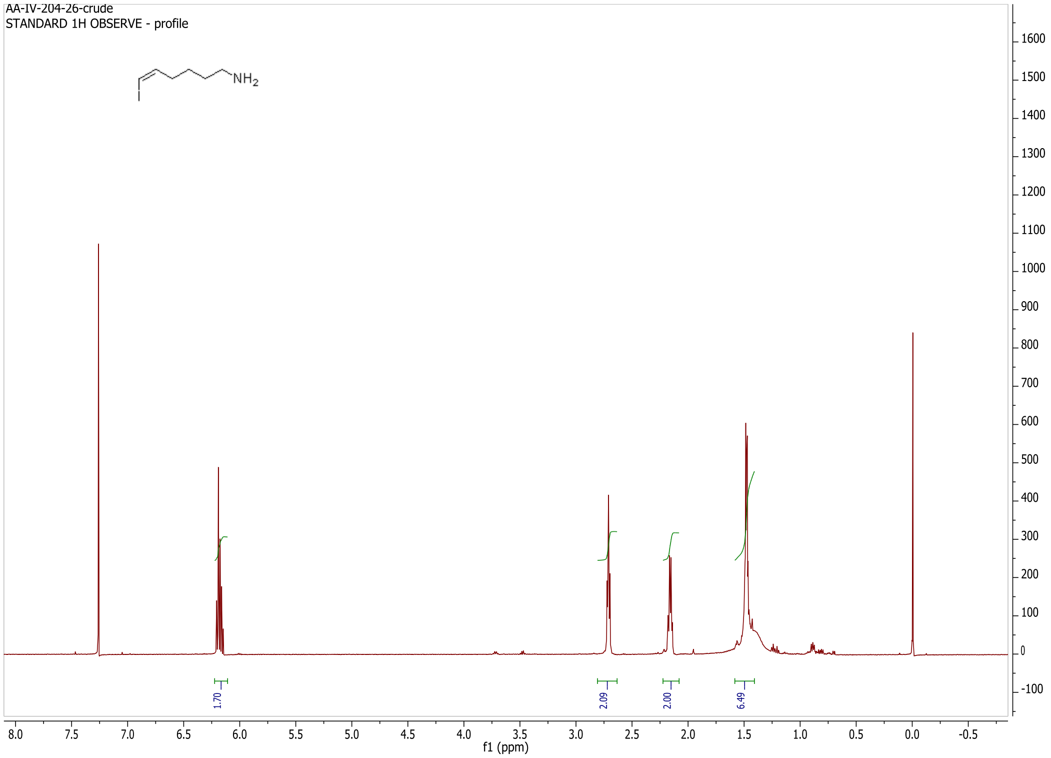
AA-IV-204-26-crude
STANDARD 1H OBSERVE - profile
NH2
I
1.70
2.09
2.00
6.49
f1 (ppm)

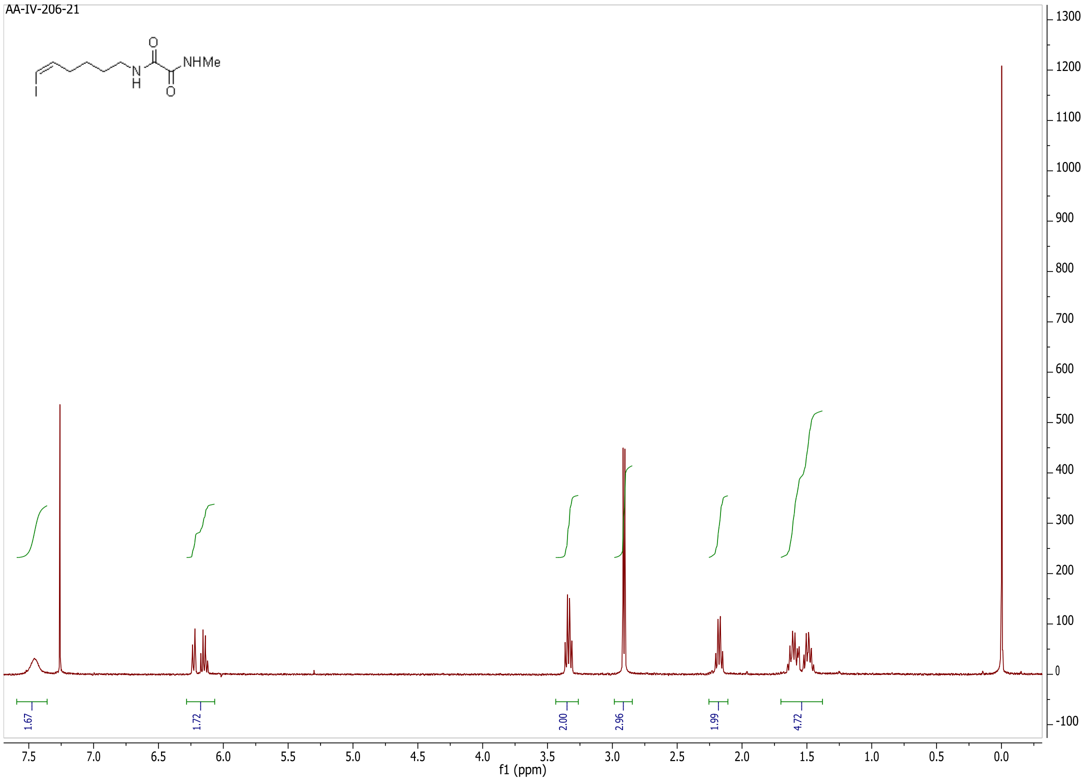
AA-IV-206-21
O
NHMe
N
H
O
I
1.67
1.72
2.00
2.96
1.99
4.72
7.5
7.0
6.5
6.0
5.5
5.0
4.5
4.0
3.5
3.0
2.5
2.0
1.5
1.0
0.5
0.0
f1 (ppm)
1300
1200
1100
1000
900
800
700
600
500
400
300
200
100
0
-100

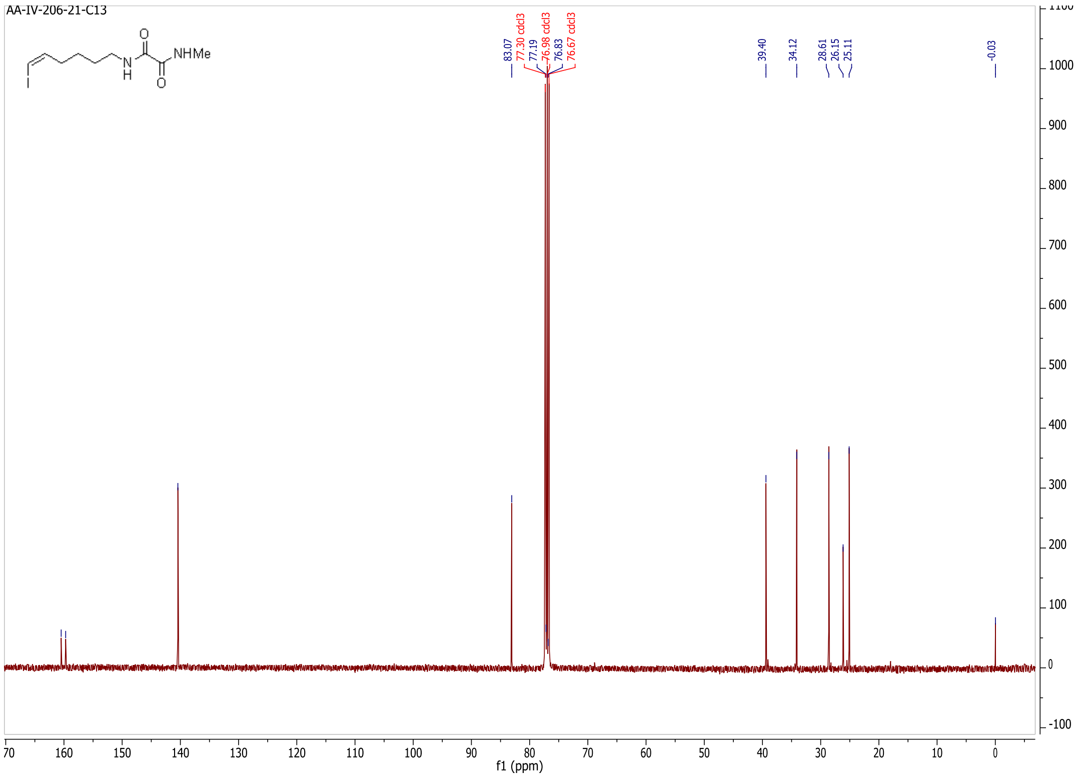
AA-IV-206-21-C13
O
NHMe
N
H
O
I
83.07
77.30 cdcl3
77.19
76.98 cdcl3
76.83
76.67 cdcl3
39.40
34.12
28.61
26.15
25.11
-0.03
70
160
150
140
130
120
110
100
90
80
70
60
50
40
30
20
10
0
f1 (ppm)
1100
1000
900
800
700
600
500
400
300
200
100
0
-100

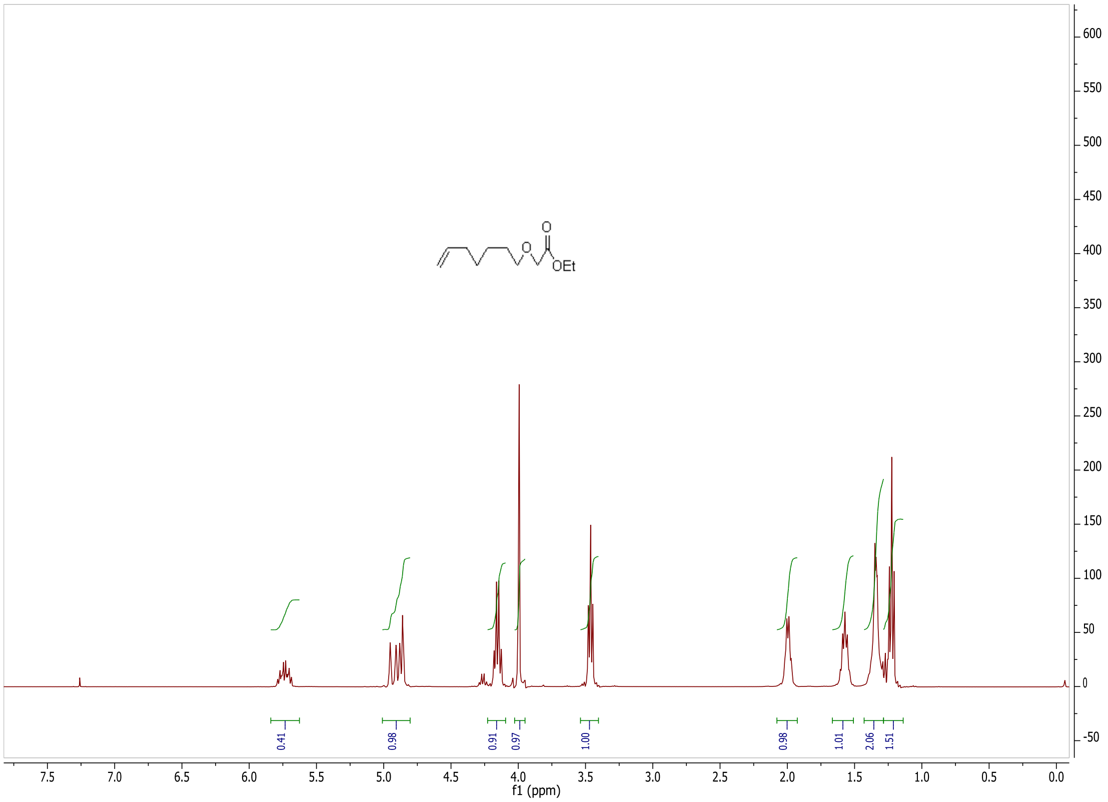
O
O
OEt
0.41
0.98
0.91
0.97
1.00
0.98
1.01
2.06
1.51
7.5 7.0 6.5 6.0 5.5 5.0 4.5 4.0 3.5 3.0 2.5 2.0 1.5 1.0 0.5 0.0
f1 (ppm)
600 550 500 450 400 350 300 250 200 150 100 50 0 -50

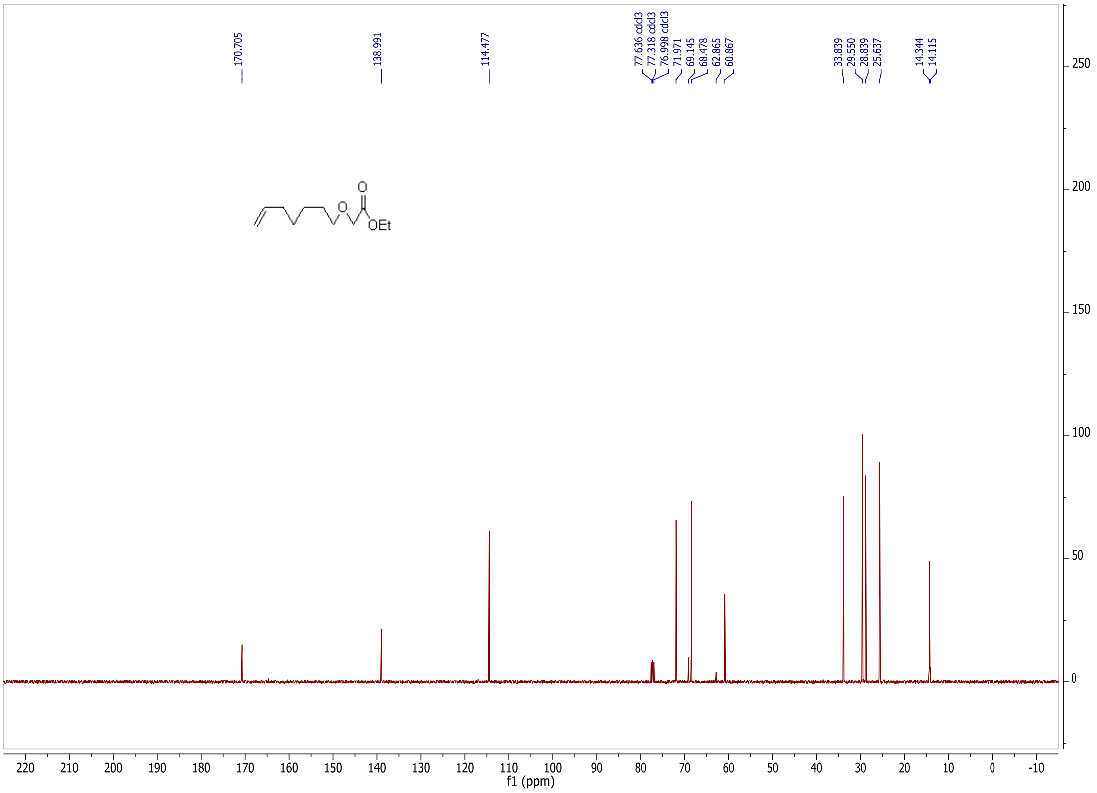
170.705
138.991
114.477
77.636 cdcl3
77.318 cdcl3
76.998 cdcl3
71.971
69.145
68.478
62.865
60.867
33.839
29.550
28.839
25.637
14.344
14.115
O
O
OEt
220 210 200 190 180 170 160 150 140 130 120 110 100 90 80 70 60 50 40 30 20 10 0 -10
f1 (ppm)
250 200 150 100 50 0

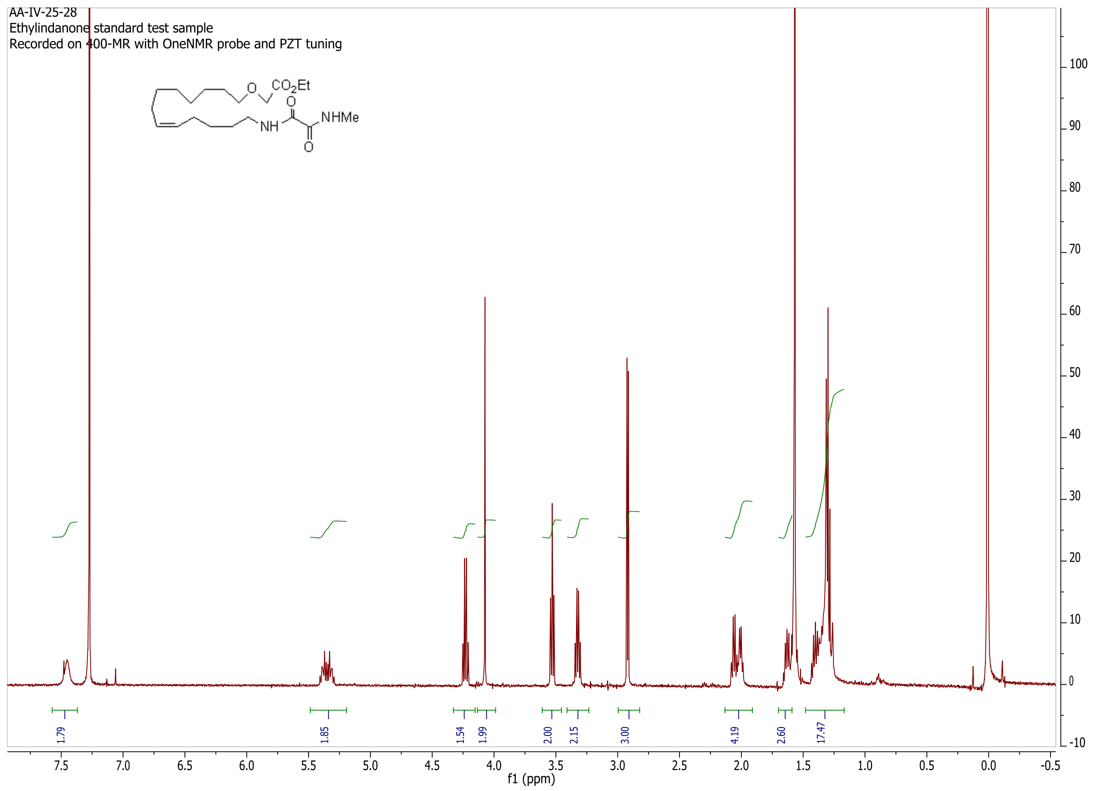
AA-IV-25-28
Ethylindanone standard test sample
Recorded on 400-MR with OneNMR probe and PZT tuning
O
CO2Et
O
NH
NHMe
O
1.79
1.85
1.54
1.99
2.00
2.15
3.00
4.19
2.60
17.47
7.5
7.0
6.5
6.0
5.5
5.0
4.5
4.0
3.5
3.0
2.5
2.0
1.5
1.0
0.5
0.0
-0.5
f1 (ppm)
100
90
80
70
60
50
40
30
20
10
0
-10

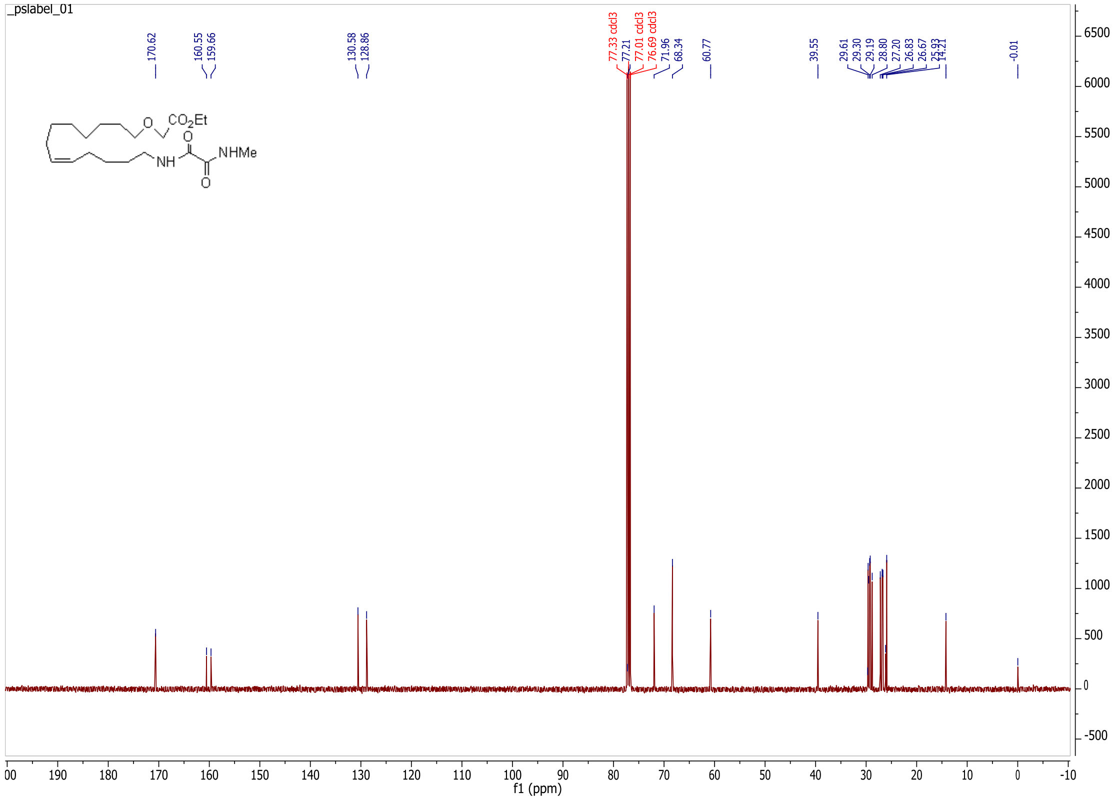
_pslabel_01
170.62
160.55
159.66
130.58
128.86
77.33 cdcl3
77.21
77.01 cdcl3
76.69 cdcl3
71.96
68.34
60.77
39.55
29.61
29.30
29.19
28.80
27.20
26.83
26.67
25.93
14.21
-0.01
O
CO2Et
O
NH
NHMe
O
00
190
180
170
160
150
140
130
120
110
100
90
80
70
60
50
40
30
20
10
0
-10
f1 (ppm)
6500
6000
5500
5000
4500
4000
3500
3000
2500
2000
1500
1000
500
0
-500

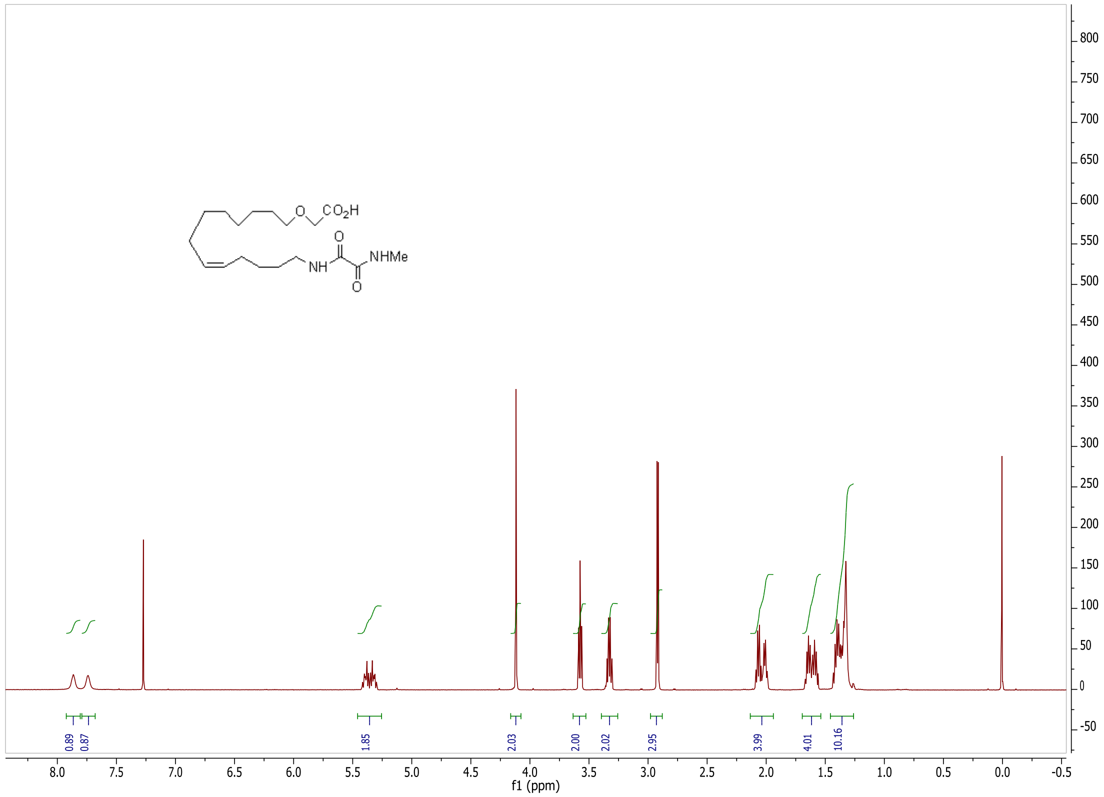
CO2H
O
NH
O
NHMe
O
0.89
0.87
1.85
2.03
2.00
2.02
2.95
3.99
4.01
10.16
8.0
7.5
7.0
6.5
6.0
5.5
5.0
4.5
4.0
3.5
3.0
2.5
2.0
1.5
1.0
0.5
0.0
-0.5
f1 (ppm)
800
750
700
650
600
550
500
450
400
350
300
250
200
150
100
50
0
-50

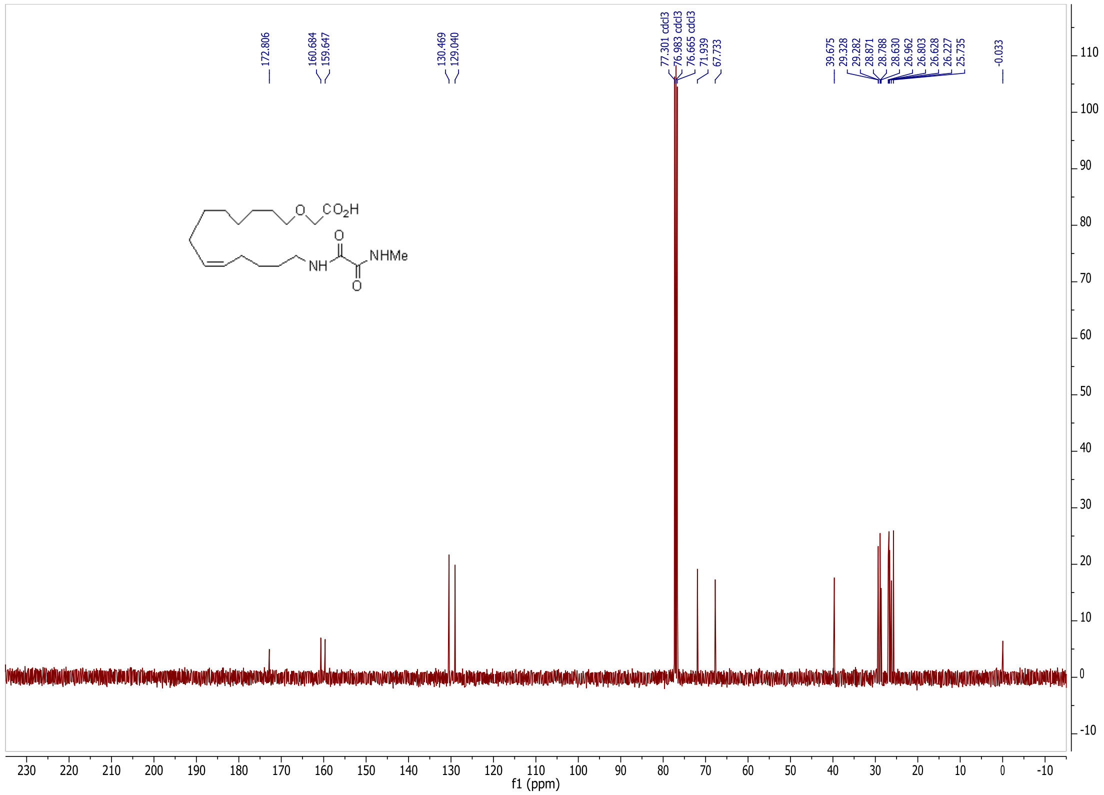
172.806
160.684
159.647
130.469
129.040
77.301 cdcl3
76.983 cdcl3
76.665 cdcl3
71.939
67.733
39.675
29.328
29.282
28.871
28.788
28.630
26.962
26.803
26.628
26.227
25.735
-0.033
CO2H
O
NH
O
NHMe
O
230
220
210
200
190
180
170
160
150
140
130
120
110
100
90
80
70
60
50
40
30
20
10
0
-10
f1 (ppm)
110
100
90
80
70
60
50
40
30
20
10
0
-10

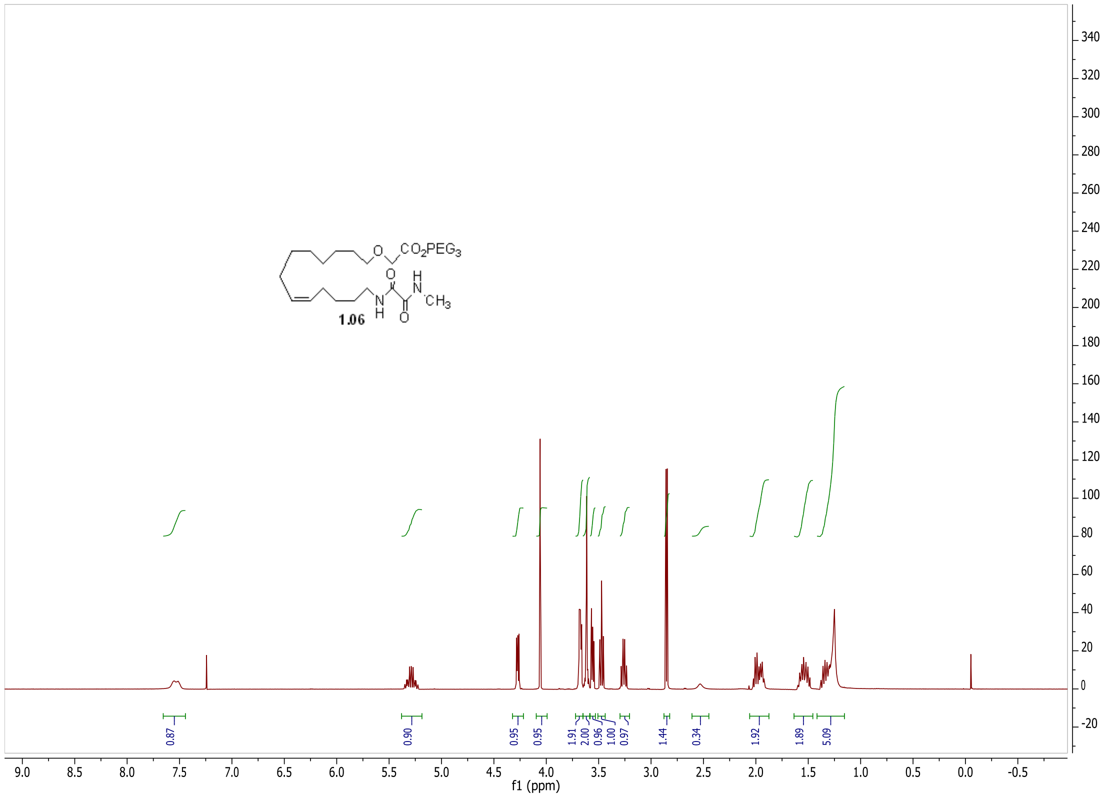
CO2PEG3
O
O
H
N
CH3
N
H
O
1.06
0.87
0.90
0.95
0.95
1.91
2.00
0.96
1.00
0.97
1.44
0.34
1.92
1.89
5.09
9.0
8.5
8.0
7.5
7.0
6.5
6.0
5.5
5.0
4.5
4.0
3.5
3.0
2.5
2.0
1.5
1.0
0.5
0.0
-0.5
f1 (ppm)
340
320
300
280
260
240
220
200
180
160
140
120
100
80
60
40
20
0
-20

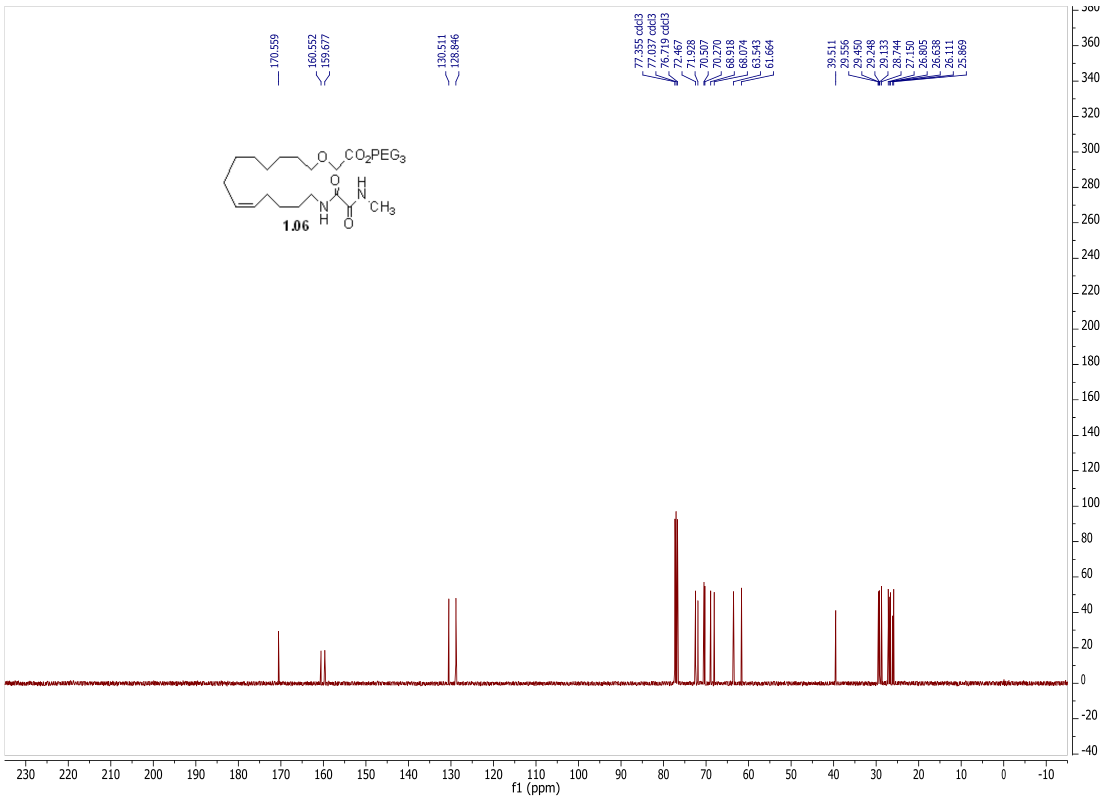
170.559
160.552
159.677
130.511
128.846
77.355 cdcl3
77.037 cdcl3
76.719 cdcl3
72.467
71.928
70.507
70.270
68.918
68.074
63.543
61.664
39.511
29.556
29.450
29.248
29.133
28.744
27.150
26.805
26.638
26.111
25.869
CO2PEG3
O
O
H
N
CH3
N
H
O
1.06
230
220
210
200
190
180
170
160
150
140
130
120
110
100
90
80
70
60
50
40
30
20
10
0
-10
f1 (ppm)
380
360
340
320
300
280
260
240
220
200
180
160
140
120
100
80
60
40
20
0
-20
-40

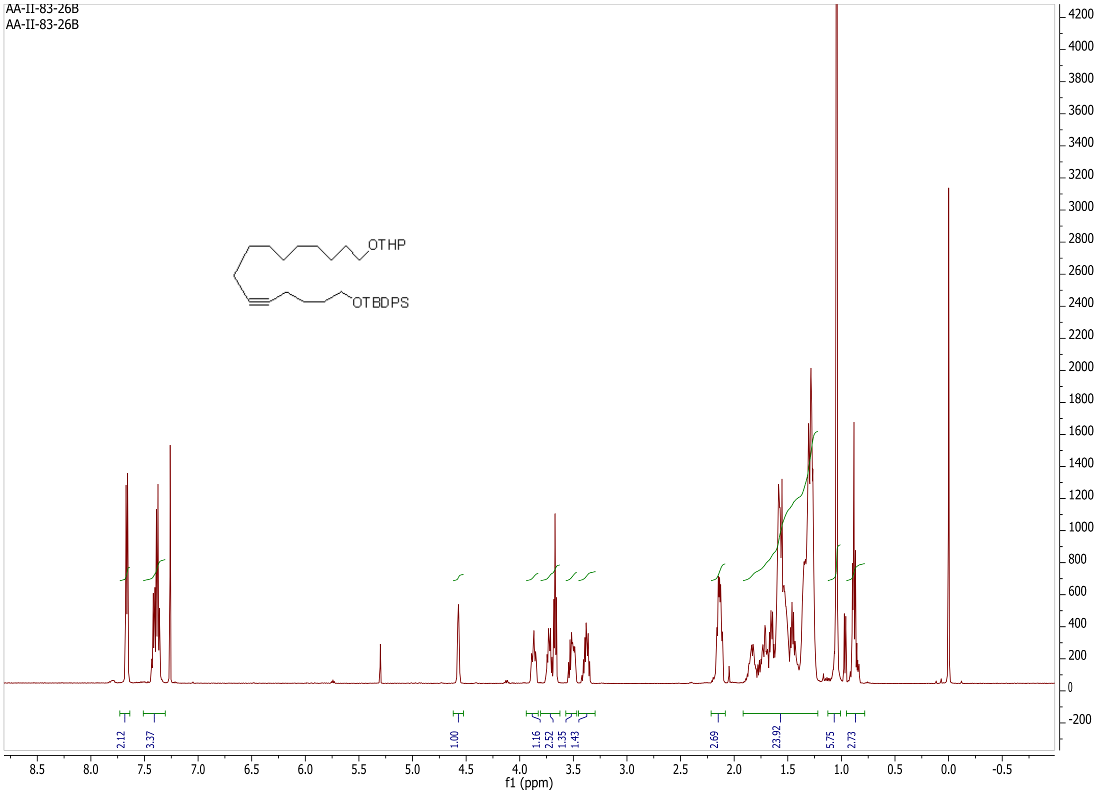
AA-II-83-26B
AA-II-83-26B
OTHP
OTBDPS
2.12
3.37
1.00
1.16
2.52
1.35
1.43
2.69
23.92
5.75
2.73
8.5 8.0 7.5 7.0 6.5 6.0 5.5 5.0 4.5 4.0 3.5 3.0 2.5 2.0 1.5 1.0 0.5 0.0 -0.5
f1 (ppm)
4200 4000 3800 3600 3400 3200 3000 2800 2600 2400 2200 2000 1800 1600 1400 1200 1000 800 600 400 200 0 -200

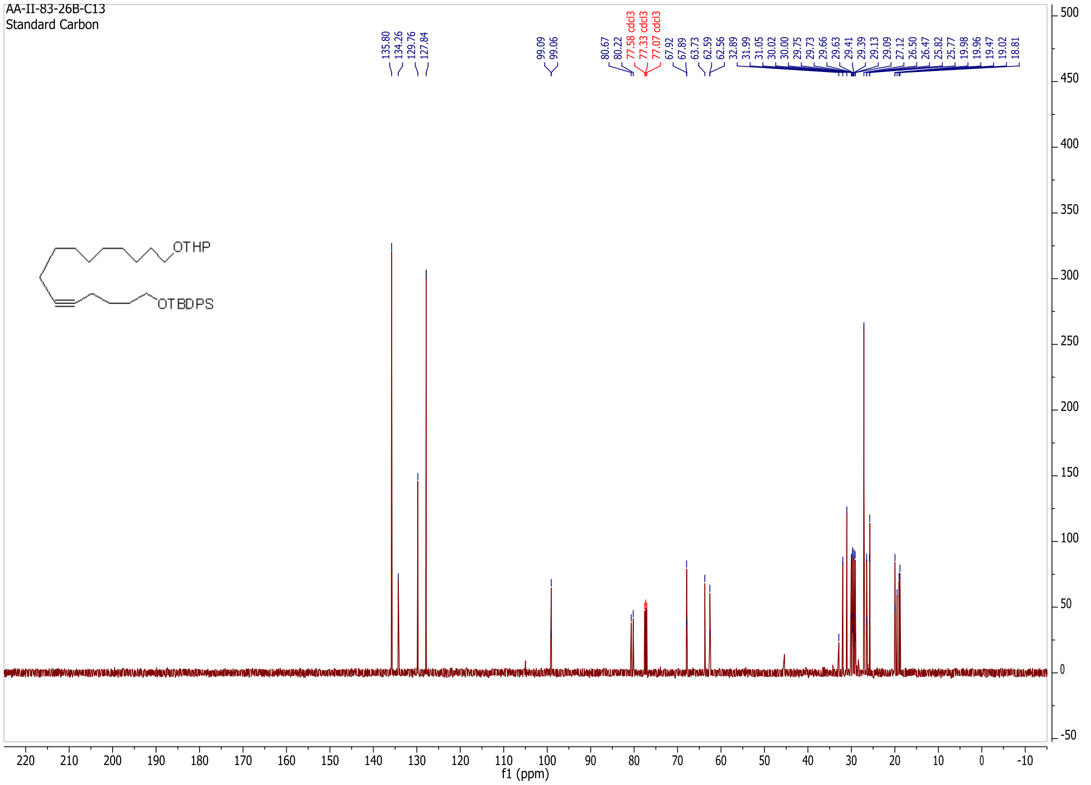
AA-II-83-26B-C13
Standard Carbon
135.80
134.26
129.76
127.84
99.09
99.06
80.67
80.22
77.58 cdcl3
77.33 cdcl3
77.07 cdcl3
67.92
67.89
63.73
62.59
62.56
32.89
31.99
31.05
30.02
30.00
29.75
29.73
29.66
29.63
29.41
29.39
29.13
29.09
27.12
26.50
26.47
25.82
25.77
19.98
19.96
19.47
19.02
18.81
OTHP
OTBDPS
220 210 200 190 180 170 160 150 140 130 120 110 100 90 80 70 60 50 40 30 20 10 0 -10
f1 (ppm)
500 450 400 350 300 250 200 150 100 50 0 -50

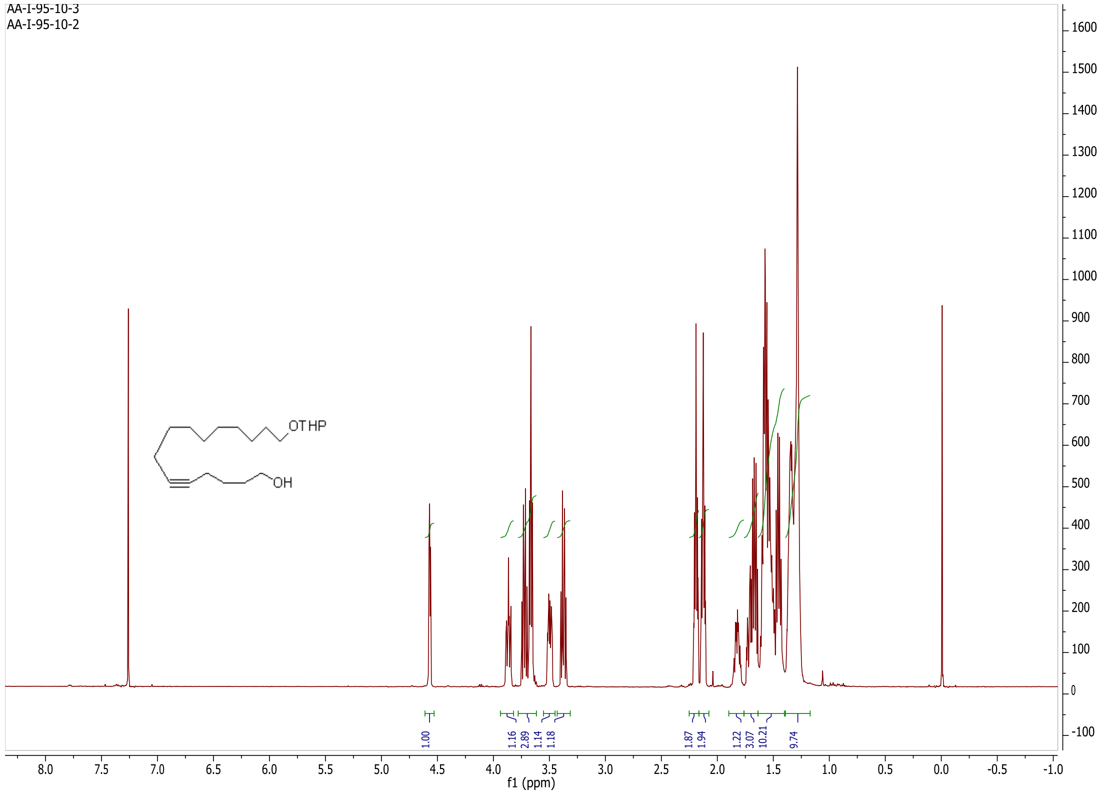
AA-I-95-10-3
AA-I-95-10-2
OTHP
OH
1.00
1.16
2.89
1.14
1.18
1.87
1.94
1.22
3.07
10.21
9.74
f1 (ppm)

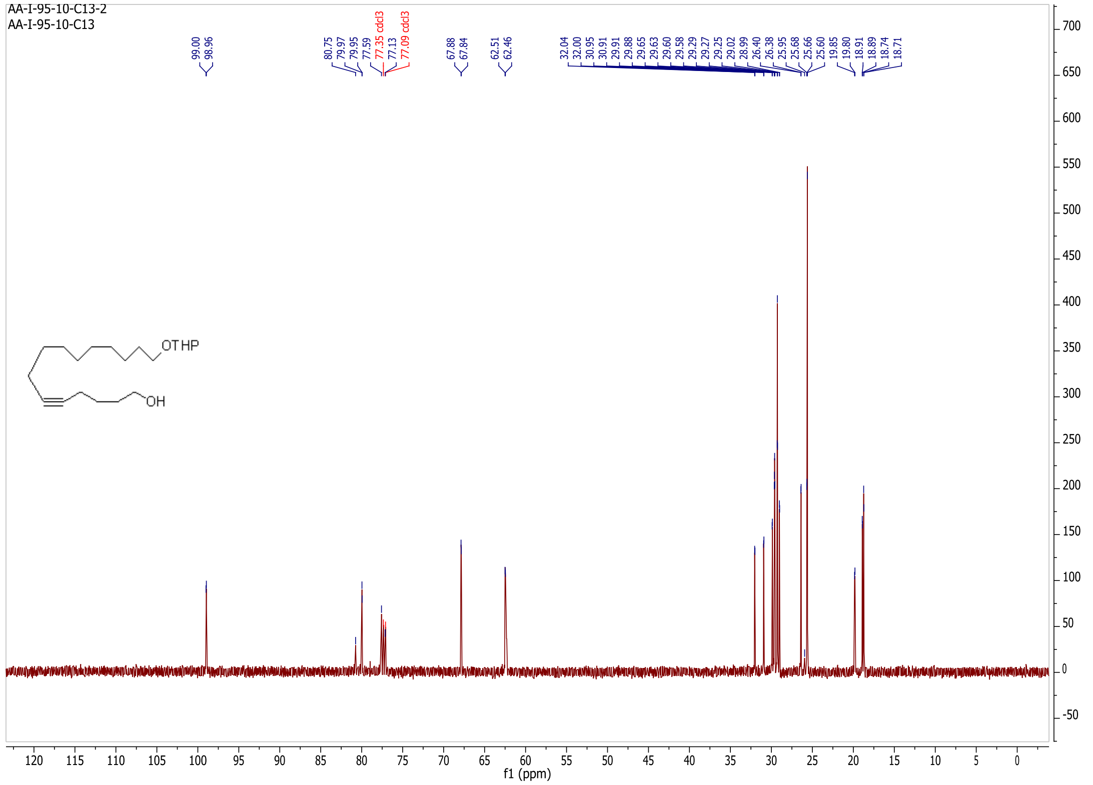
AA-I-95-10-C13-2
AA-I-95-10-C13
99.00
98.96
80.75
79.97
79.95
77.59
77.35 cdcl3
77.13
77.09 cdcl3
67.88
67.84
62.51
62.46
32.04
32.00
30.95
30.91
29.91
29.88
29.65
29.63
29.60
29.58
29.29
29.27
29.25
29.02
28.99
26.40
26.38
25.95
25.68
25.66
25.60
19.85
19.80
18.91
18.89
18.74
18.71
OTHP
OH
f1 (ppm)

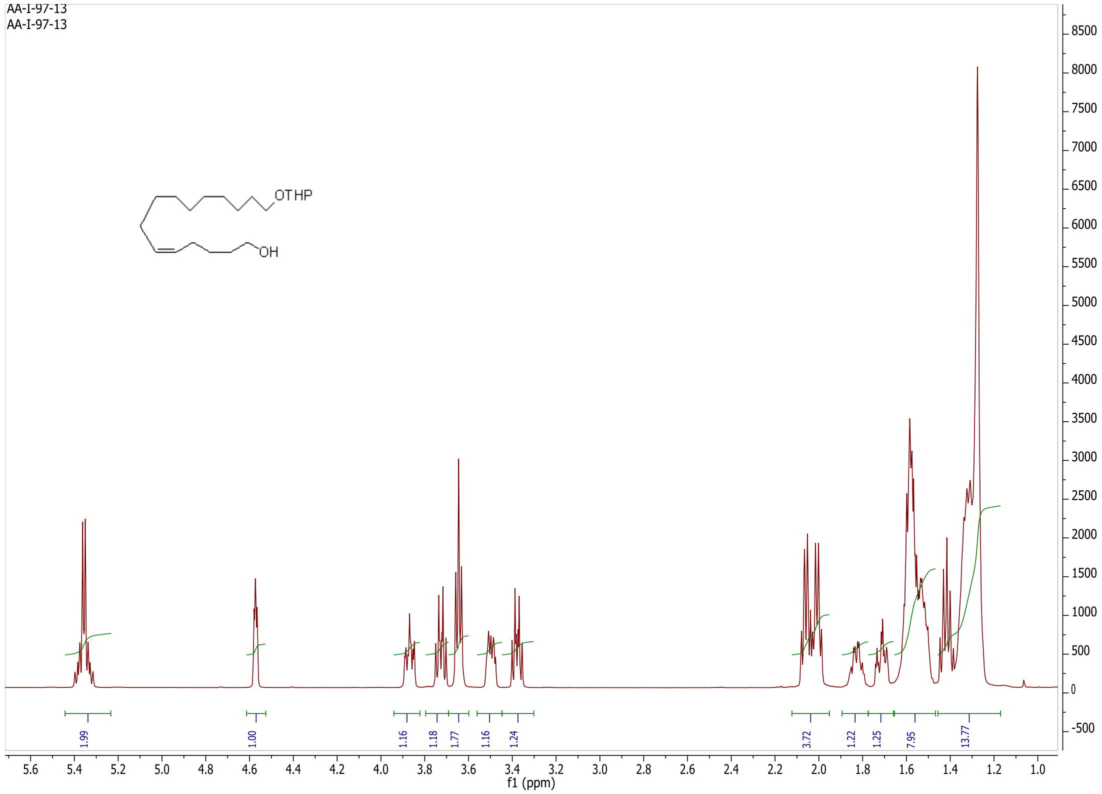
AA-I-97-13
AA-I-97-13
OTHP
OH
1.99
1.00
1.16
1.18
1.77
1.16
1.24
3.72
1.22
1.25
7.95
13.77
5.6 5.4 5.2 5.0 4.8 4.6 4.4 4.2 4.0 3.8 3.6 3.4 3.2 3.0 2.8 2.6 2.4 2.2 2.0 1.8 1.6 1.4 1.2 1.0
f1 (ppm)
8500 8000 7500 7000 6500 6000 5500 5000 4500 4000 3500 3000 2500 2000 1500 1000 500 0 -500

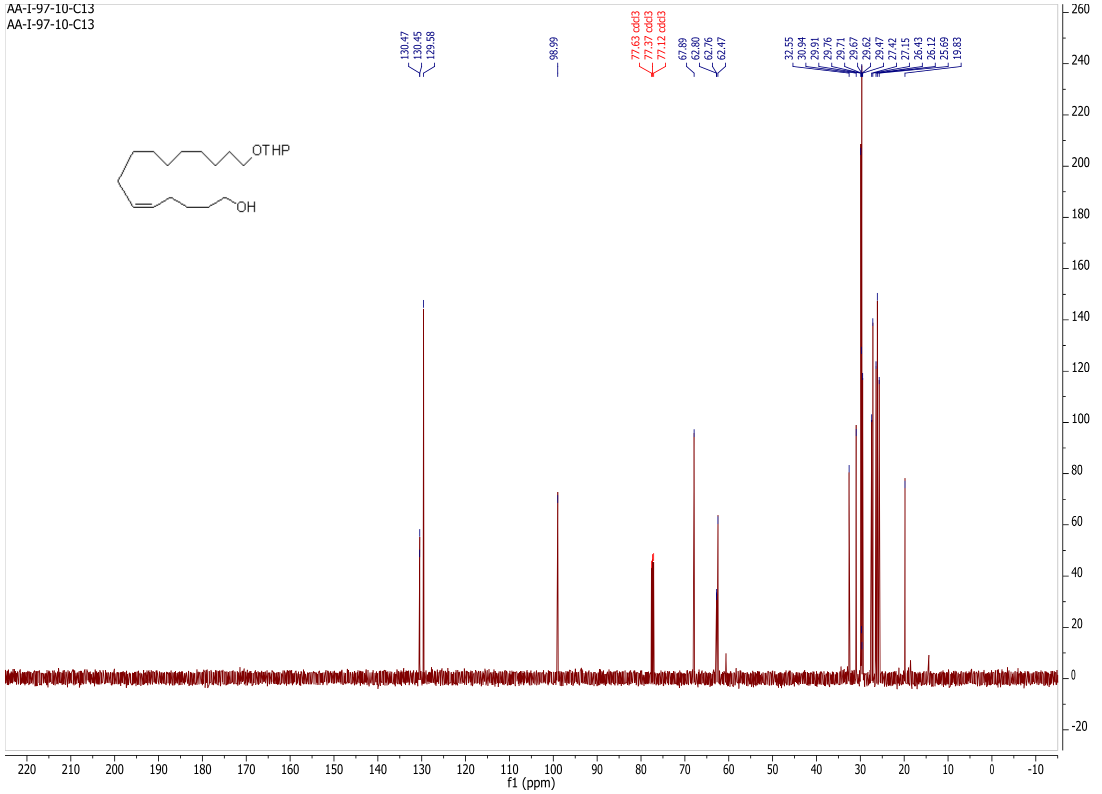
AA-I-97-10-C13
AA-I-97-10-C13
130.47
130.45
129.58
98.99
77.63 cdcl3
77.37 cdcl3
77.12 cdcl3
67.89
62.80
62.76
62.47
32.55
30.94
29.91
29.76
29.71
29.67
29.62
29.47
27.42
27.15
26.43
26.12
25.69
19.83
OTHP
OH
220 210 200 190 180 170 160 150 140 130 120 110 100 90 80 70 60 50 40 30 20 10 0 -10
f1 (ppm)
260 240 220 200 180 160 140 120 100 80 60 40 20 0 -20

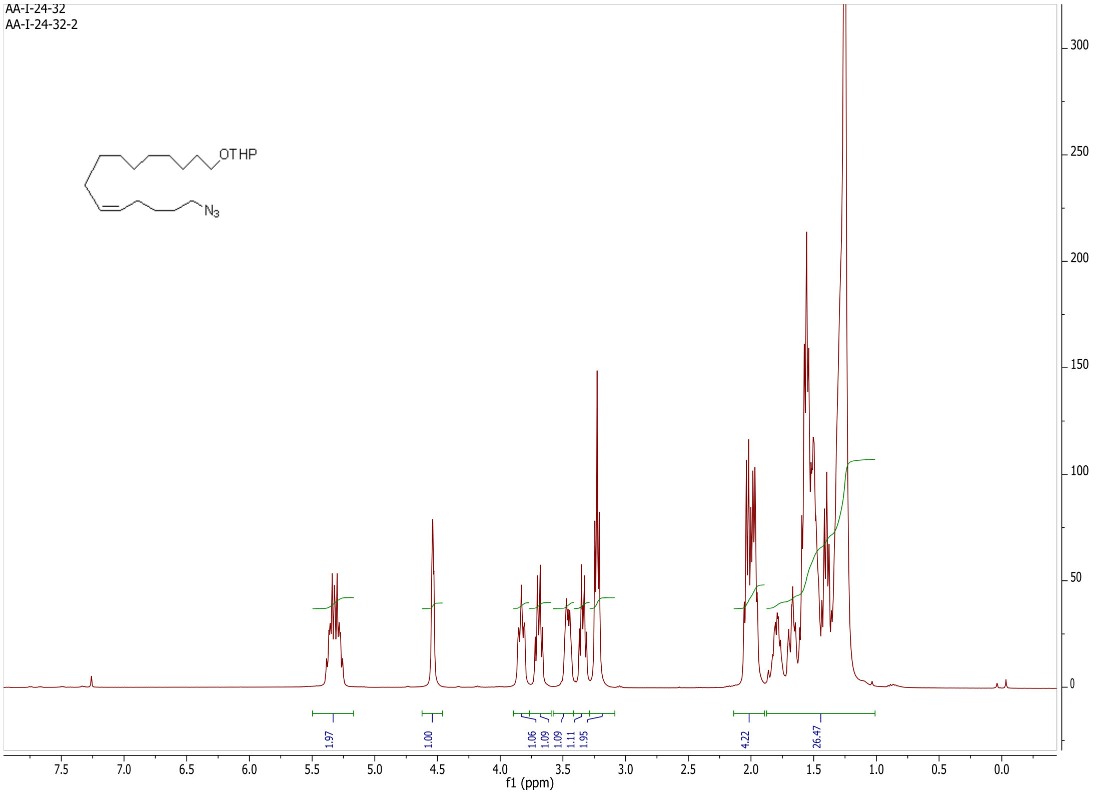
AA-I-24-32
AA-I-24-32-2
OTHP
N3
1.97
1.00
1.06
1.09
1.09
1.11
1.95
4.22
26.47
7.5
7.0
6.5
6.0
5.5
5.0
4.5
4.0
3.5
3.0
2.5
2.0
1.5
1.0
0.5
0.0
f1 (ppm)
300
250
200
150
100
50
0

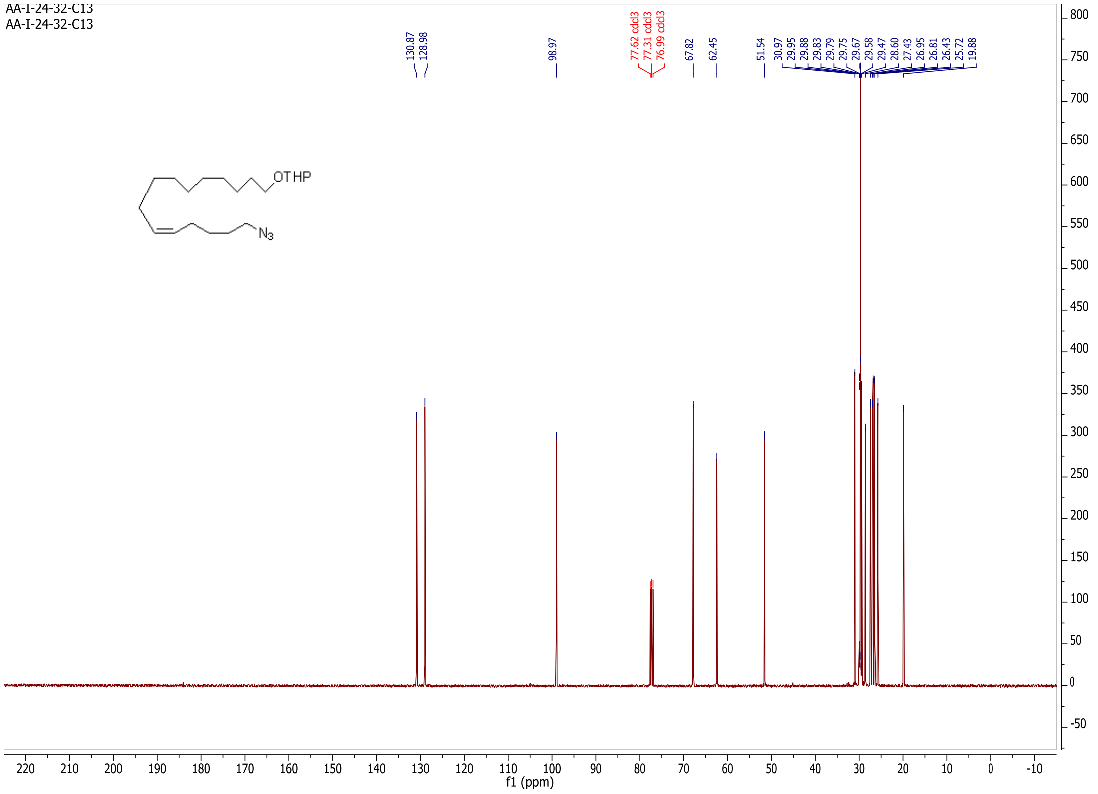
AA-I-24-32-C13
AA-I-24-32-C13
130.87
128.98
98.97
77.62 cdcl3
77.31 cdcl3
76.99 cdcl3
67.82
62.45
51.54
30.97
29.95
29.88
29.83
29.79
29.75
29.67
29.58
29.47
28.60
27.43
26.95
26.81
26.43
25.72
19.88
OTHP
N3
220
210
200
190
180
170
160
150
140
130
120
110
100
90
80
70
60
50
40
30
20
10
0
-10
f1 (ppm)
800
750
700
650
600
550
500
450
400
350
300
250
200
150
100
50
0
-50

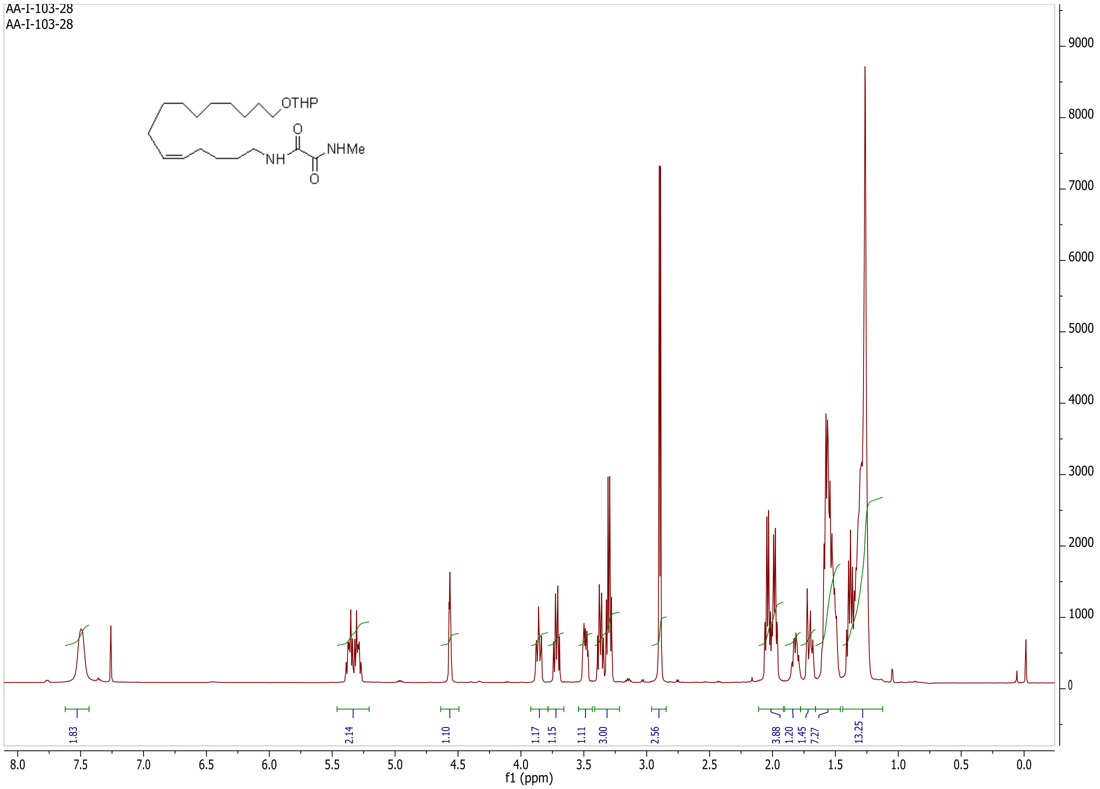
AA-I-103-28
AA-I-103-28
OTHP
O
NHMe
NH
O
1.83
2.14
1.10
1.17
1.15
1.11
3.00
2.56
3.88
1.20
1.45
7.27
13.25
9000
8000
7000
6000
5000
4000
3000
2000
1000
0
8.0
7.5
7.0
6.5
6.0
5.5
5.0
4.5
4.0
3.5
3.0
2.5
2.0
1.5
1.0
0.5
0.0
f1 (ppm)

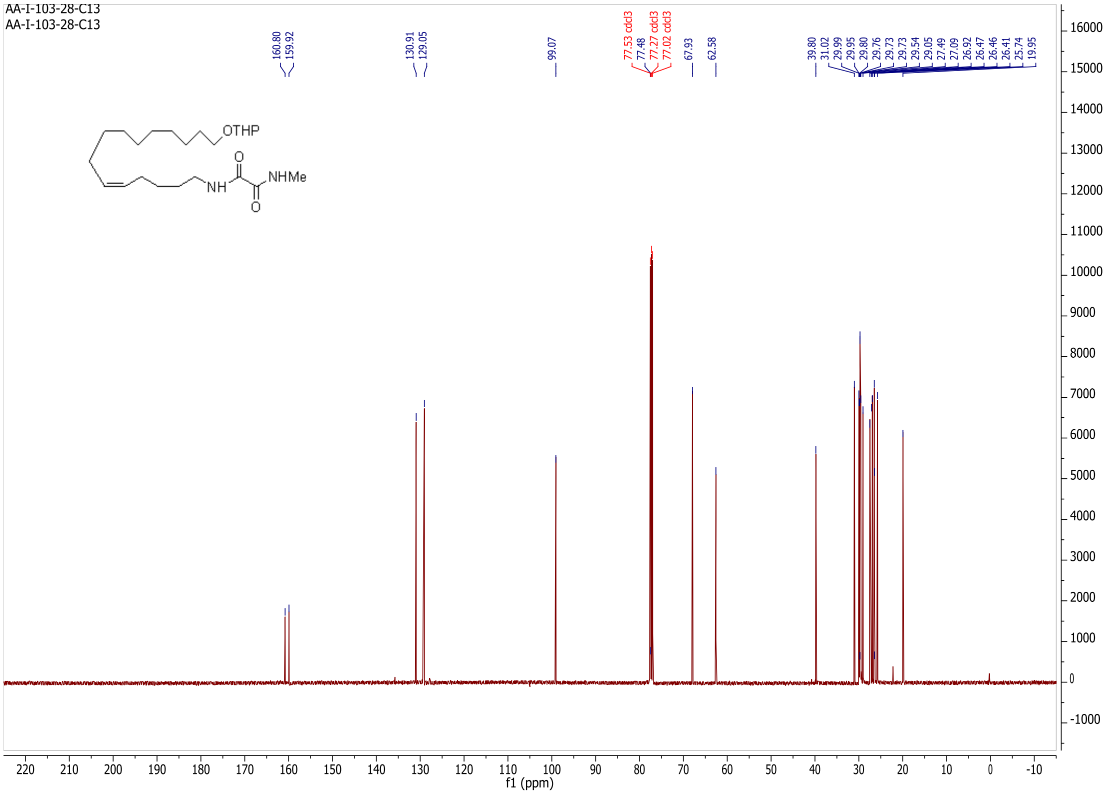
AA-I-103-28-C13
AA-I-103-28-C13
160.80
159.92
130.91
129.05
99.07
77.53 cdcl3
77.48
77.27 cdcl3
77.02 cdcl3
67.93
62.58
39.80
31.02
29.99
29.95
29.80
29.76
29.73
29.54
29.05
27.49
27.09
26.92
26.47
26.46
26.41
25.74
19.95
OTHP
O
NHMe
NH
O
16000
15000
14000
13000
12000
11000
10000
9000
8000
7000
6000
5000
4000
3000
2000
1000
0
-1000
220
210
200
190
180
170
160
150
140
130
120
110
100
90
80
70
60
50
40
30
20
10
0
-10
f1 (ppm)

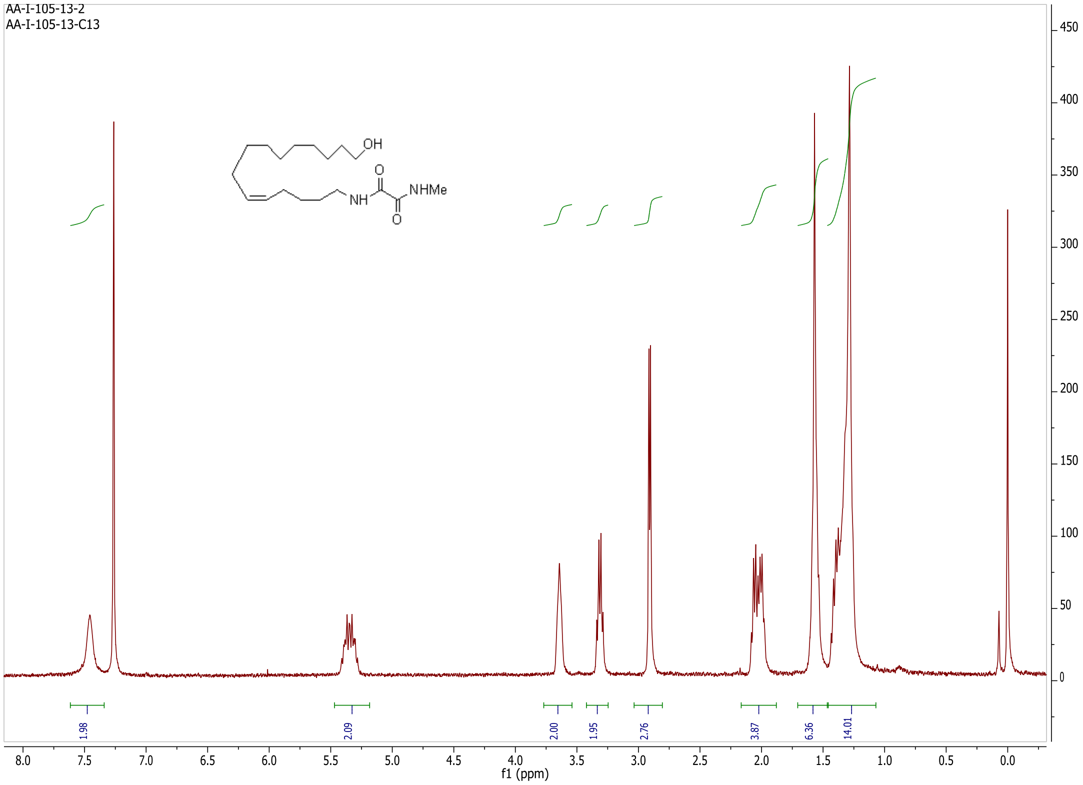
AA-I-105-13-2
AA-I-105-13-C13
OH
O
NH
NHMe
O
1.98
2.09
2.00
1.95
2.76
3.87
6.36
14.01
8.0
7.5
7.0
6.5
6.0
5.5
5.0
4.5
4.0
3.5
3.0
2.5
2.0
1.5
1.0
0.5
0.0
f1 (ppm)
450
400
350
300
250
200
150
100
50
0

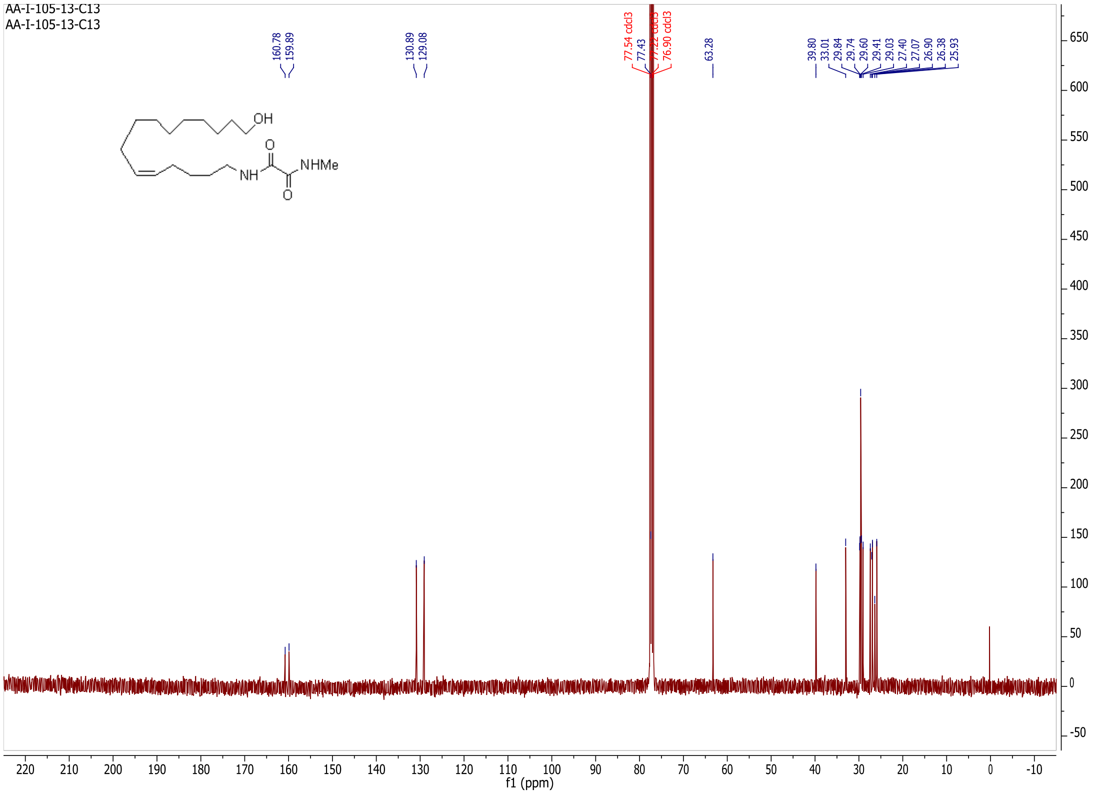
AA-I-105-13-C13
AA-I-105-13-C13
160.78
159.89
130.89
129.08
77.54 cdcl3
77.43
77.22 cdcl3
76.90 cdcl3
63.28
39.80
33.01
29.84
29.74
29.60
29.41
29.03
27.40
27.07
26.90
26.38
25.93
OH
O
NH
NHMe
O
220
210
200
190
180
170
160
150
140
130
120
110
100
90
80
70
60
50
40
30
20
10
0
-10
f1 (ppm)
650
600
550
500
450
400
350
300
250
200
150
100
50
0
-50

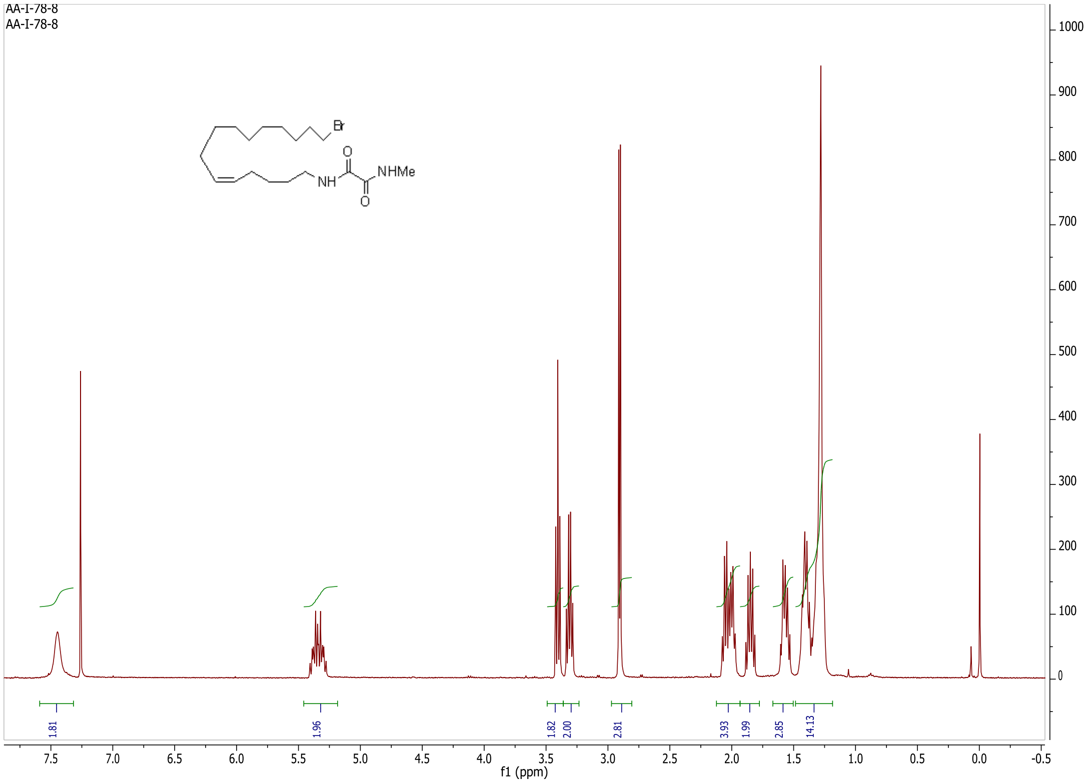
AA-I-78-8
AA-I-78-8
Br
O
NH
NHMe
O
1.81
1.96
1.82
2.00
2.81
3.93
1.99
2.85
14.13
7.5
7.0
6.5
6.0
5.5
5.0
4.5
4.0
3.5
3.0
2.5
2.0
1.5
1.0
0.5
0.0
-0.5
f1 (ppm)
1000
900
800
700
600
500
400
300
200
100
0

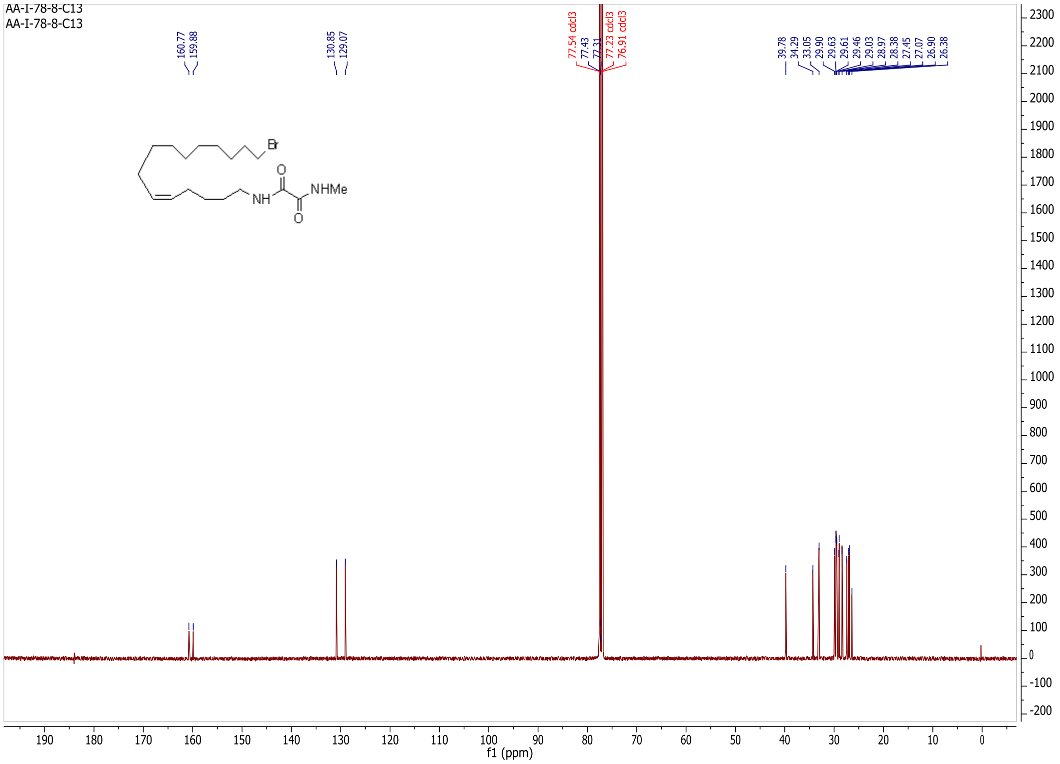
AA-I-78-8-C13
AA-I-78-8-C13
160.77
159.88
130.85
129.07
77.54 cdcl3
77.43
77.31
77.23 cdcl3
76.91 cdcl3
39.78
34.29
33.05
29.90
29.63
29.61
29.46
29.03
28.97
28.38
27.45
27.07
26.90
26.38
Br
O
NH
NHMe
O
190
180
170
160
150
140
130
120
110
100
90
80
70
60
50
40
30
20
10
0
f1 (ppm)
2300
2200
2100
2000
1900
1800
1700
1600
1500
1400
1300
1200
1100
1000
900
800
700
600
500
400
300
200
100
0
-100
-200

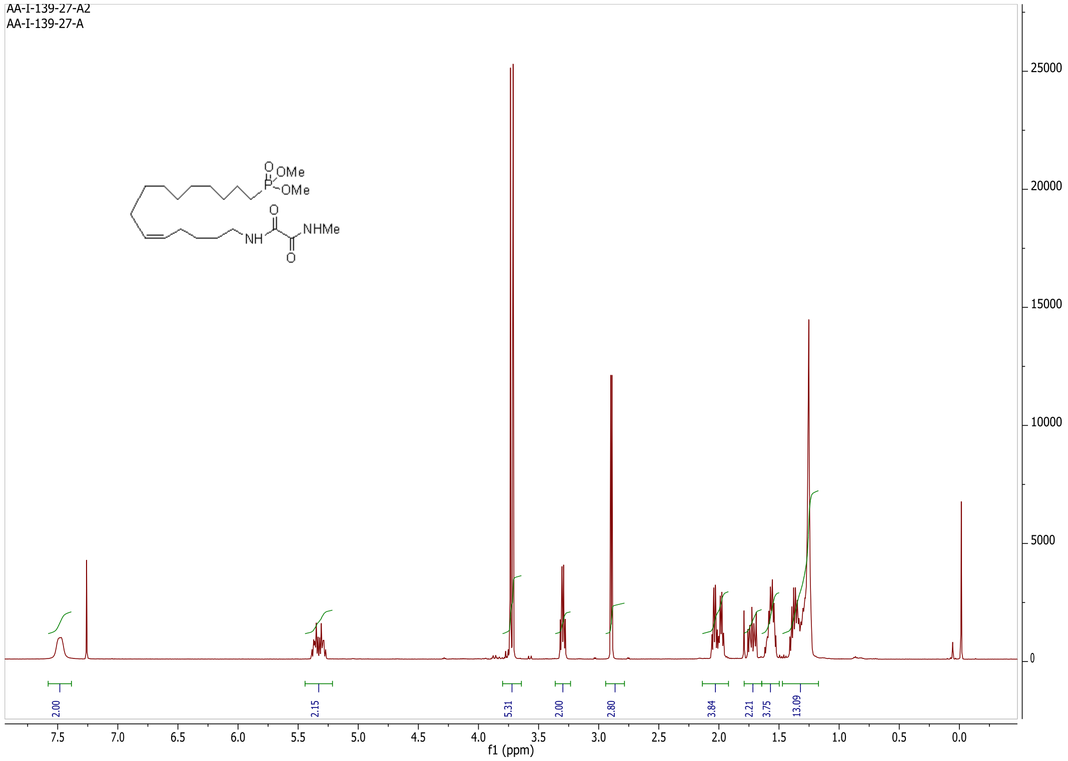
AA-I-139-27-A2
AA-I-139-27-A
OMe
OMe
P
O
NH
NHMe
O
O
25000
20000
15000
10000
5000
0
2.00
2.15
5.31
2.00
2.80
3.84
2.21
3.75
13.09
7.5
7.0
6.5
6.0
5.5
5.0
4.5
4.0
3.5
3.0
2.5
2.0
1.5
1.0
0.5
0.0
f1 (ppm)

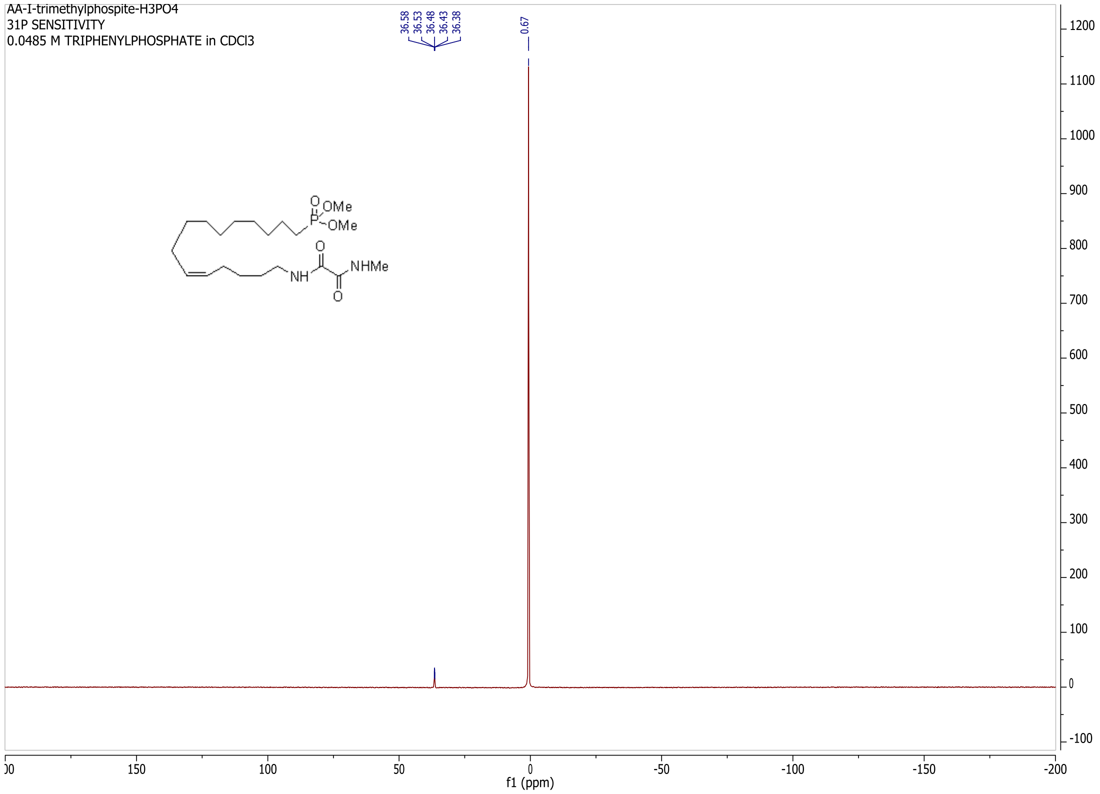
AA-I-trimethylphospite-H3PO4
31P SENSITIVITY
0.0485 M TRIPHENYLPHOSPHATE in CDCl3
36.58
36.53
36.48
36.43
36.38
0.67
OMe
OMe
P
O
NH
NHMe
O
O
1200
1100
1000
900
800
700
600
500
400
300
200
100
0
-100
00
150
100
50
0
-50
-100
-150
-200
f1 (ppm)

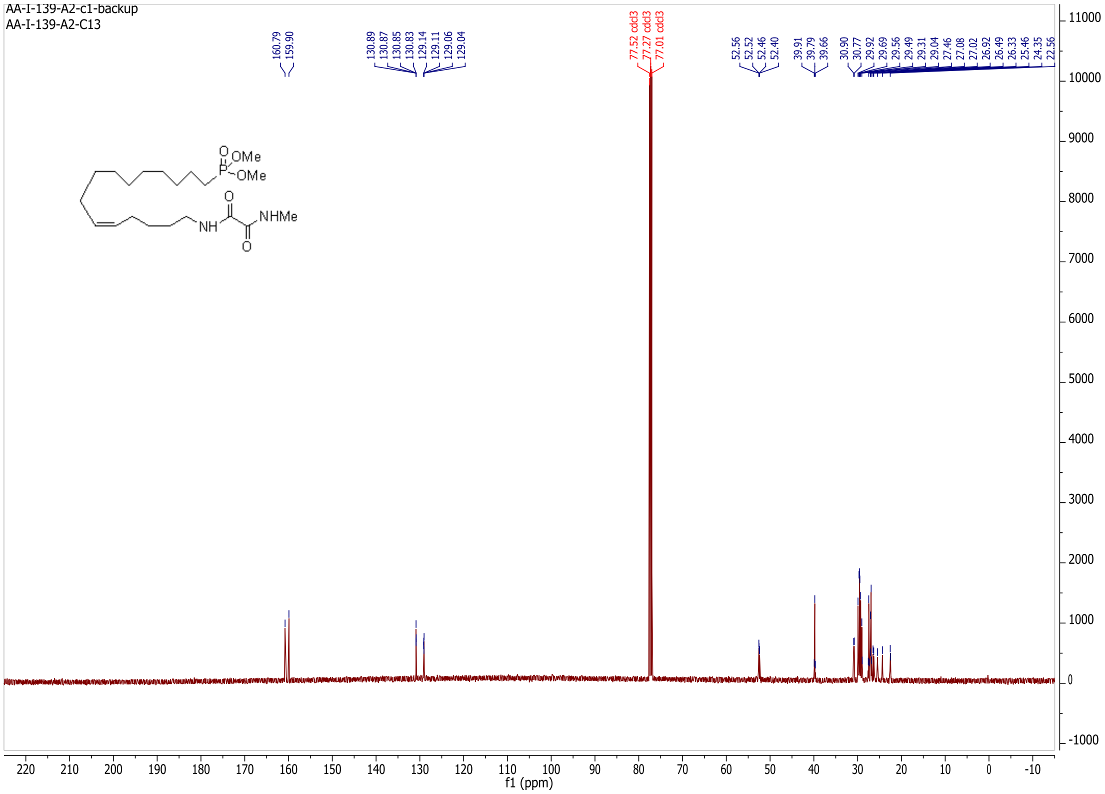
AA-I-139-A2-c1-backup
AA-I-139-A2-C13
160.79
159.90
130.89
130.87
130.85
130.83
129.14
129.11
129.06
129.04
77.52 cdcl3
77.27 cdcl3
77.01 cdcl3
52.56
52.52
52.46
52.40
39.91
39.79
39.66
30.90
30.77
29.92
29.69
29.56
29.49
29.31
29.04
27.46
27.08
27.02
26.92
26.49
26.33
25.46
24.35
22.56
O
OMe
P
OMe
O
NHMe
NH
O
f1 (ppm)

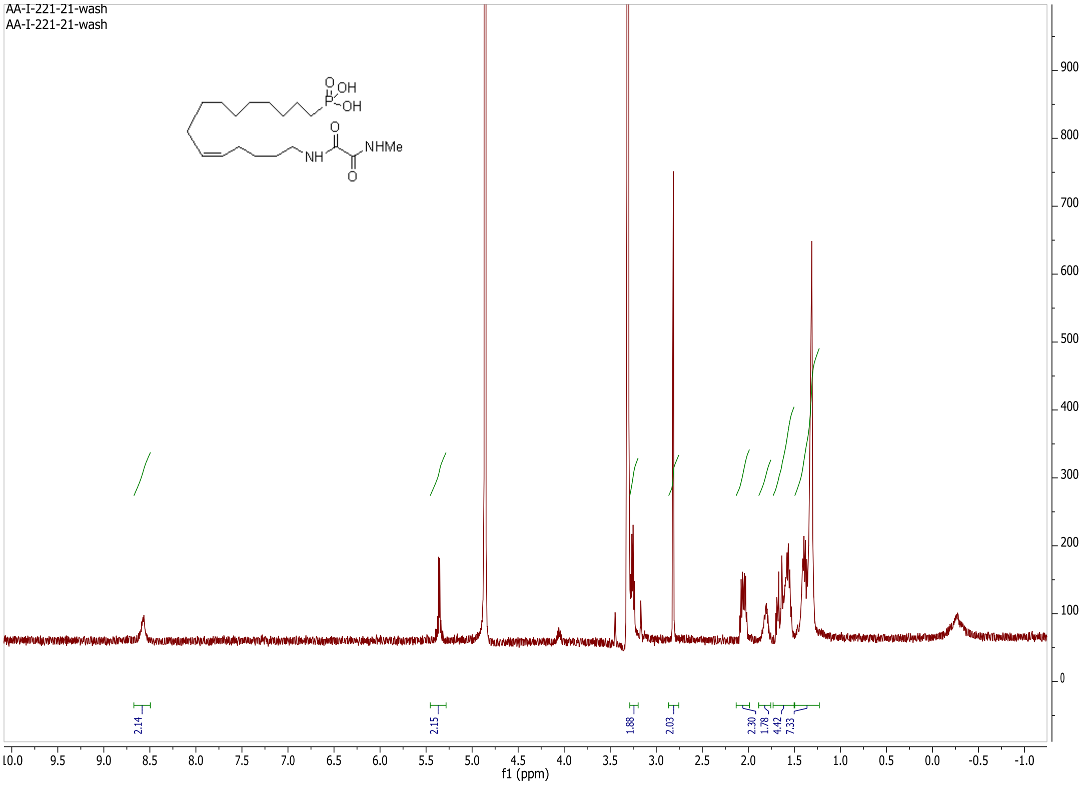
AA-I-221-21-wash
AA-I-221-21-wash
O
OH
P
OH
O
NHMe
NH
O
2.14
2.15
1.88
2.03
2.30
1.78
4.42
7.33
f1 (ppm)

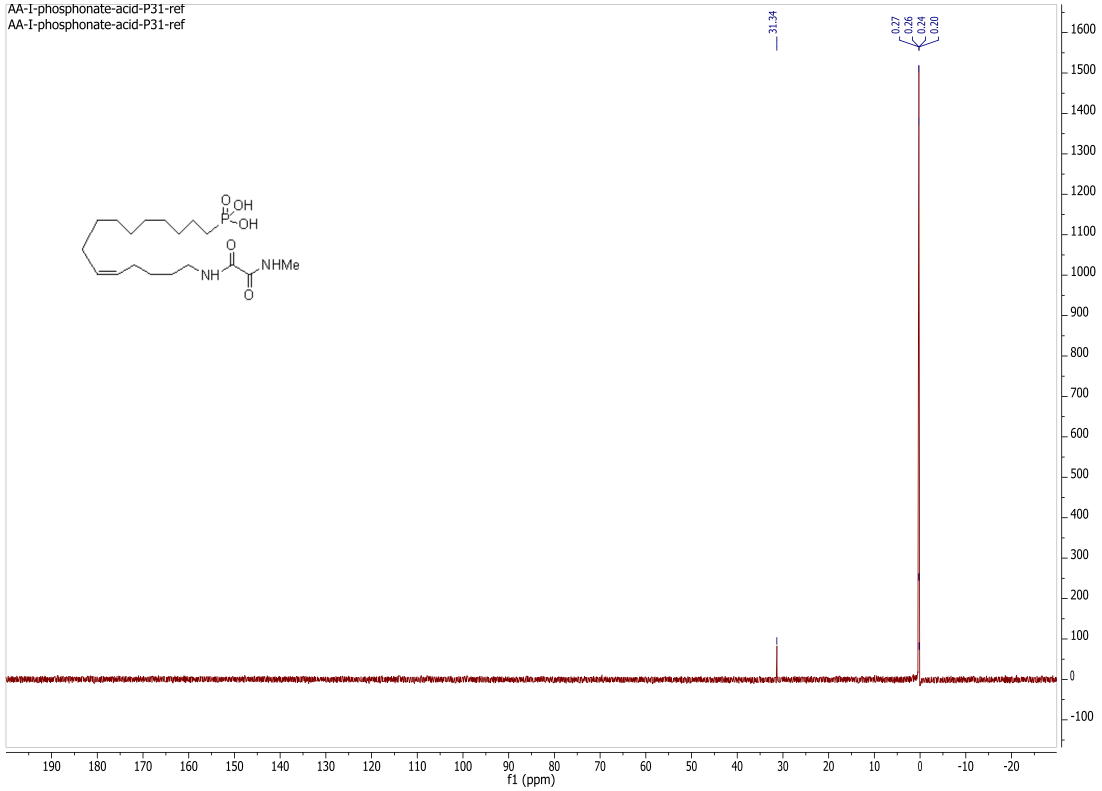
AA-I-phosphonate-acid-P31-ref
AA-I-phosphonate-acid-P31-ref
31.34
0.27
0.26
0.24
0.20
OH
OH
P
O
O
NH
NHMe
O
1600
1500
1400
1300
1200
1100
1000
900
800
700
600
500
400
300
200
100
0
-100
190 180 170 160 150 140 130 120 110 100 90 80 70 60 50 40 30 20 10 0 -10 -20
f1 (ppm)

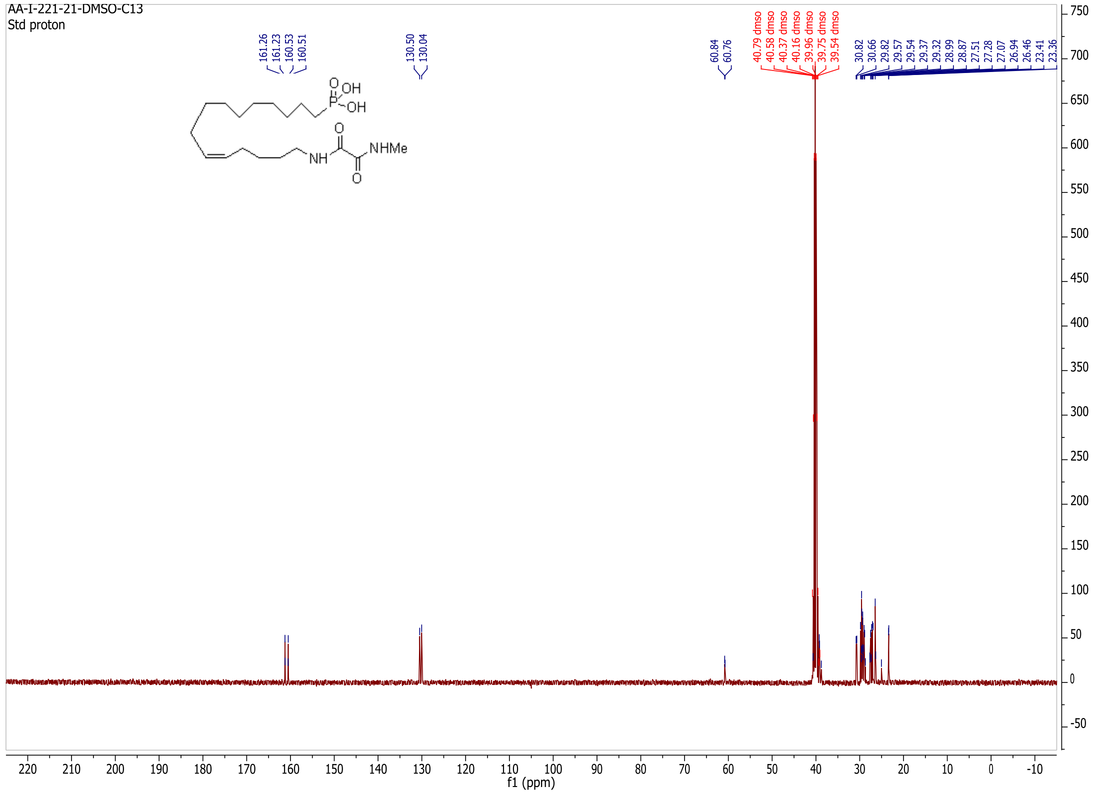
AA-I-221-21-DMSO-C13
Std proton
161.26
161.23
160.53
160.51
130.50
130.04
60.84
60.76
40.79 dmso
40.58 dmso
40.37 dmso
40.16 dmso
39.96 dmso
39.75 dmso
39.54 dmso
30.82
30.66
29.82
29.57
29.54
29.37
29.32
28.99
28.87
27.51
27.28
27.07
26.94
26.46
23.41
23.36
OH
OH
P
O
O
NH
NHMe
O
750
700
650
600
550
500
450
400
350
300
250
200
150
100
50
0
-50
220 210 200 190 180 170 160 150 140 130 120 110 100 90 80 70 60 50 40 30 20 10 0 -10
f1 (ppm)

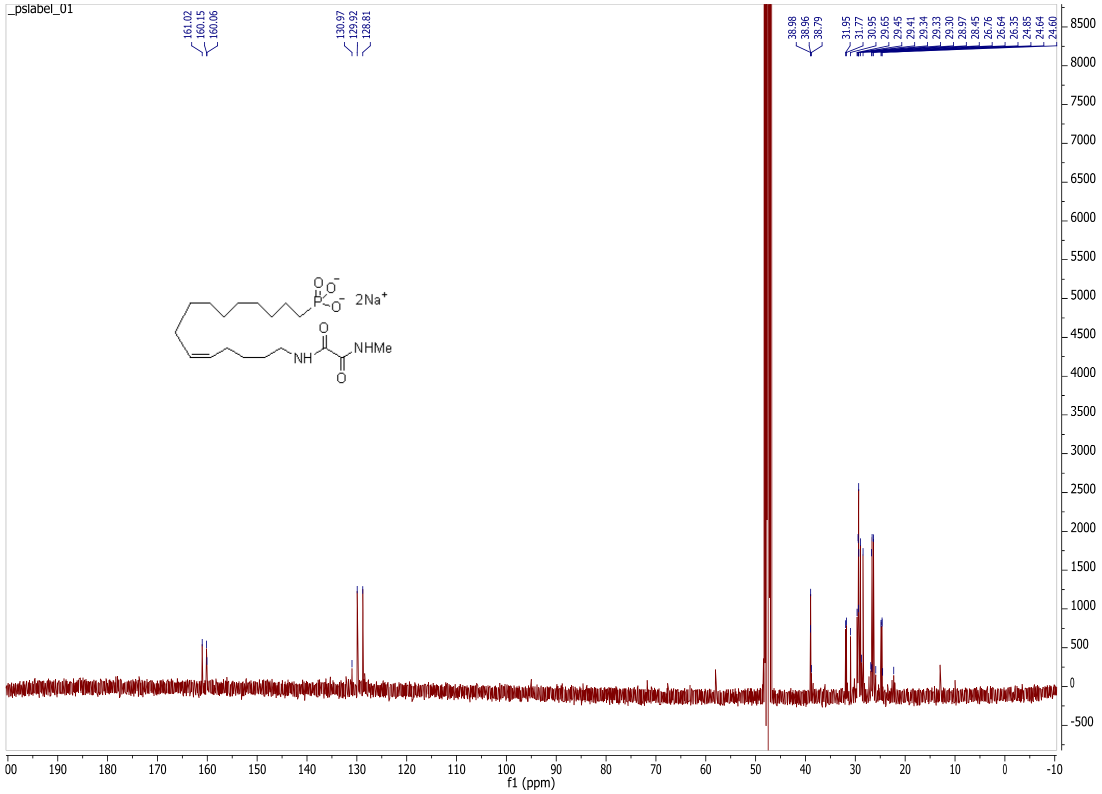
_pslabel_01
161.02
160.15
160.06
130.97
129.92
128.81
38.98
38.96
38.79
31.95
31.77
30.95
29.65
29.45
29.41
29.34
29.33
29.30
28.97
28.45
26.76
26.64
26.35
24.85
24.64
24.60
O
O⁻
O⁻
P
2Na⁺
O
NH
NHMe
O
200
190
180
170
160
150
140
130
120
110
100
90
80
70
60
50
40
30
20
10
0
-10
f1 (ppm)
8500
8000
7500
7000
6500
6000
5500
5000
4500
4000
3500
3000
2500
2000
1500
1000
500
0
-500

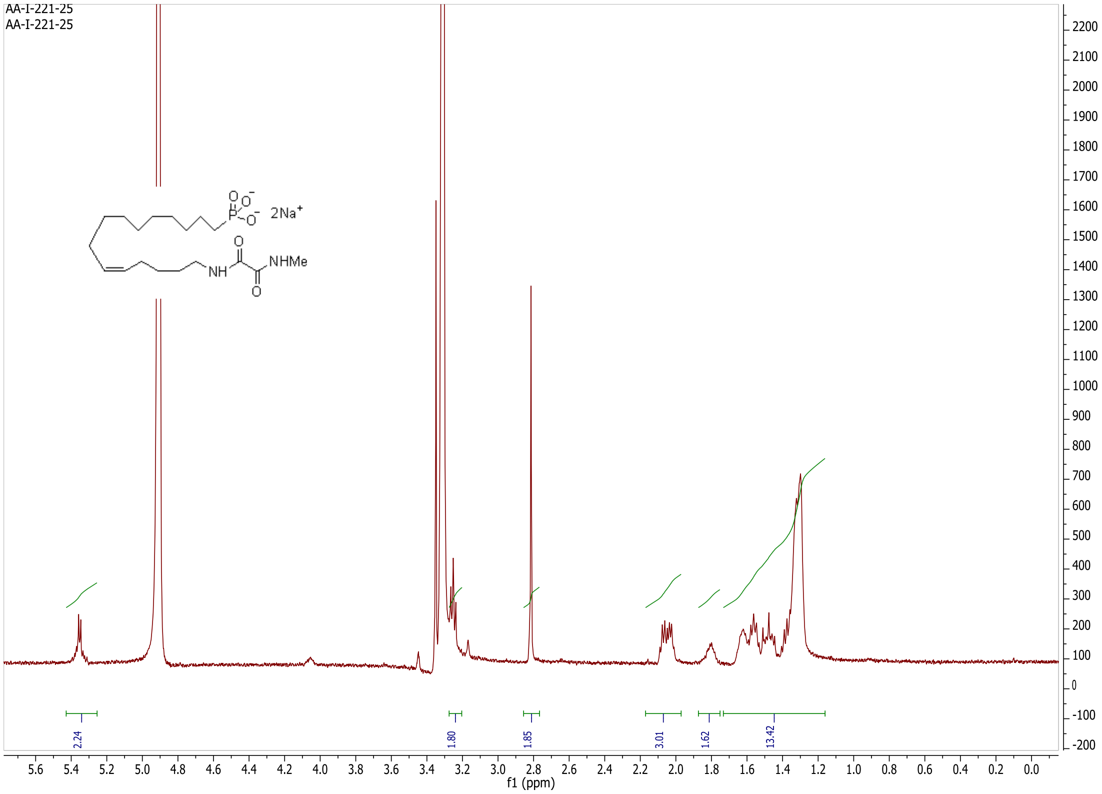
AA-I-221-25
AA-I-221-25
O
O⁻
O⁻
P
2Na⁺
O
NH
NHMe
O
2.24
1.80
1.85
3.01
1.62
13.42
5.6
5.4
5.2
5.0
4.8
4.6
4.4
4.2
4.0
3.8
3.6
3.4
3.2
3.0
2.8
2.6
2.4
2.2
2.0
1.8
1.6
1.4
1.2
1.0
0.8
0.6
0.4
0.2
0.0
f1 (ppm)
2200
2100
2000
1900
1800
1700
1600
1500
1400
1300
1200
1100
1000
900
800
700
600
500
400
300
200
100
0
-100
-200

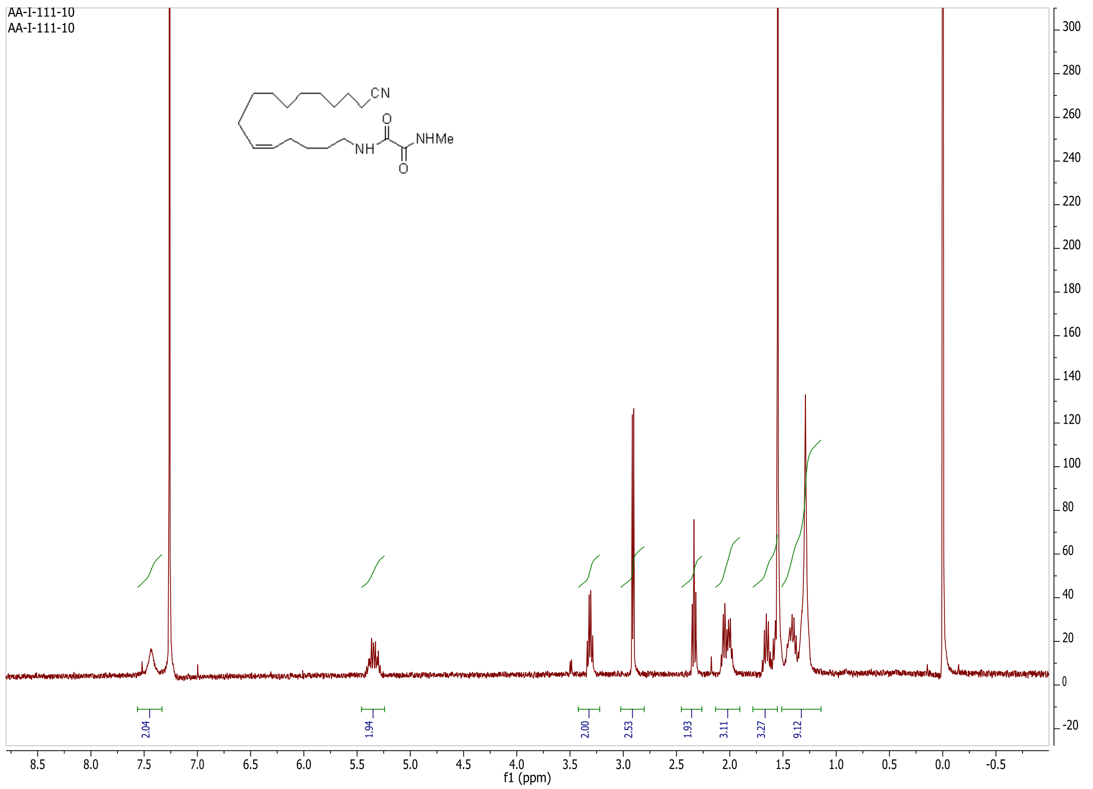
AA-I-111-10
AA-I-111-10
CN
O
NHMe
NH
O
2.04
1.94
2.00
2.53
1.93
3.11
3.27
9.12
8.5
8.0
7.5
7.0
6.5
6.0
5.5
5.0
4.5
4.0
3.5
3.0
2.5
2.0
1.5
1.0
0.5
0.0
-0.5
f1 (ppm)
300
280
260
240
220
200
180
160
140
120
100
80
60
40
20
0
-20

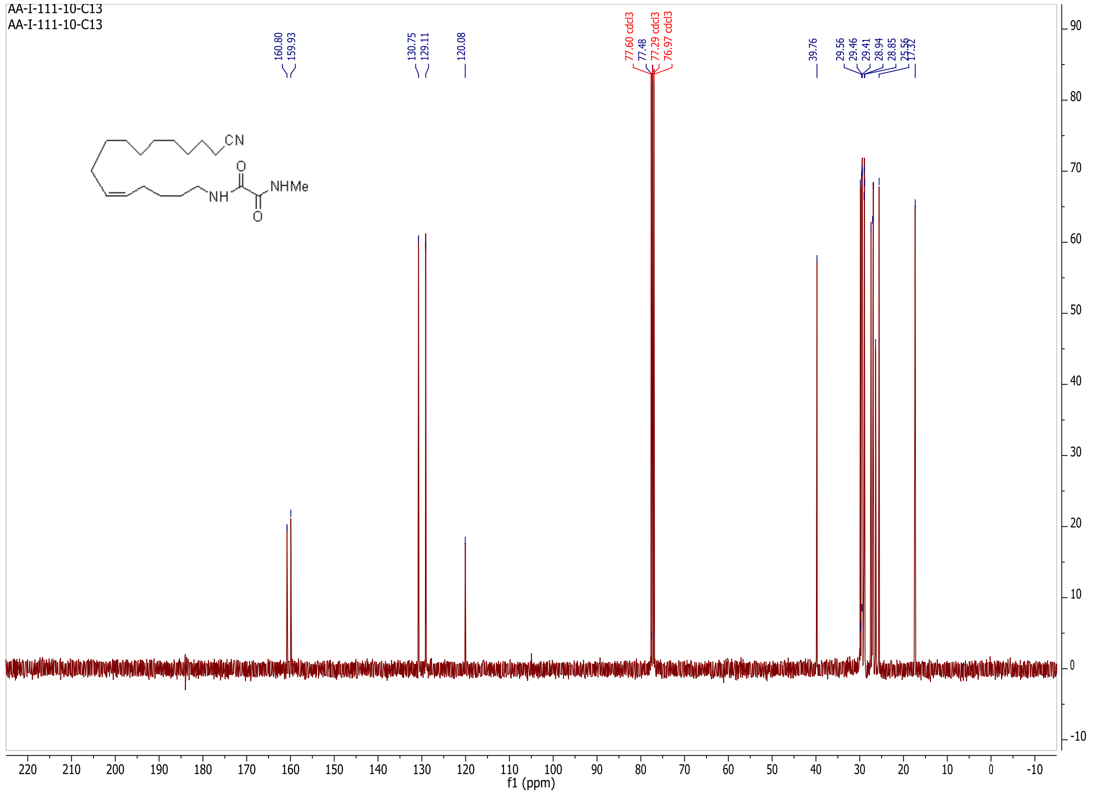
AA-I-111-10-C13
AA-I-111-10-C13
160.80
159.93
130.75
129.11
120.08
77.60 cdcl3
77.48
77.29 cdcl3
76.97 cdcl3
39.76
29.56
29.46
29.41
28.94
28.85
25.56
17.32
CN
O
NHMe
NH
O
220
210
200
190
180
170
160
150
140
130
120
110
100
90
80
70
60
50
40
30
20
10
0
-10
f1 (ppm)
90
80
70
60
50
40
30
20
10
0
-10

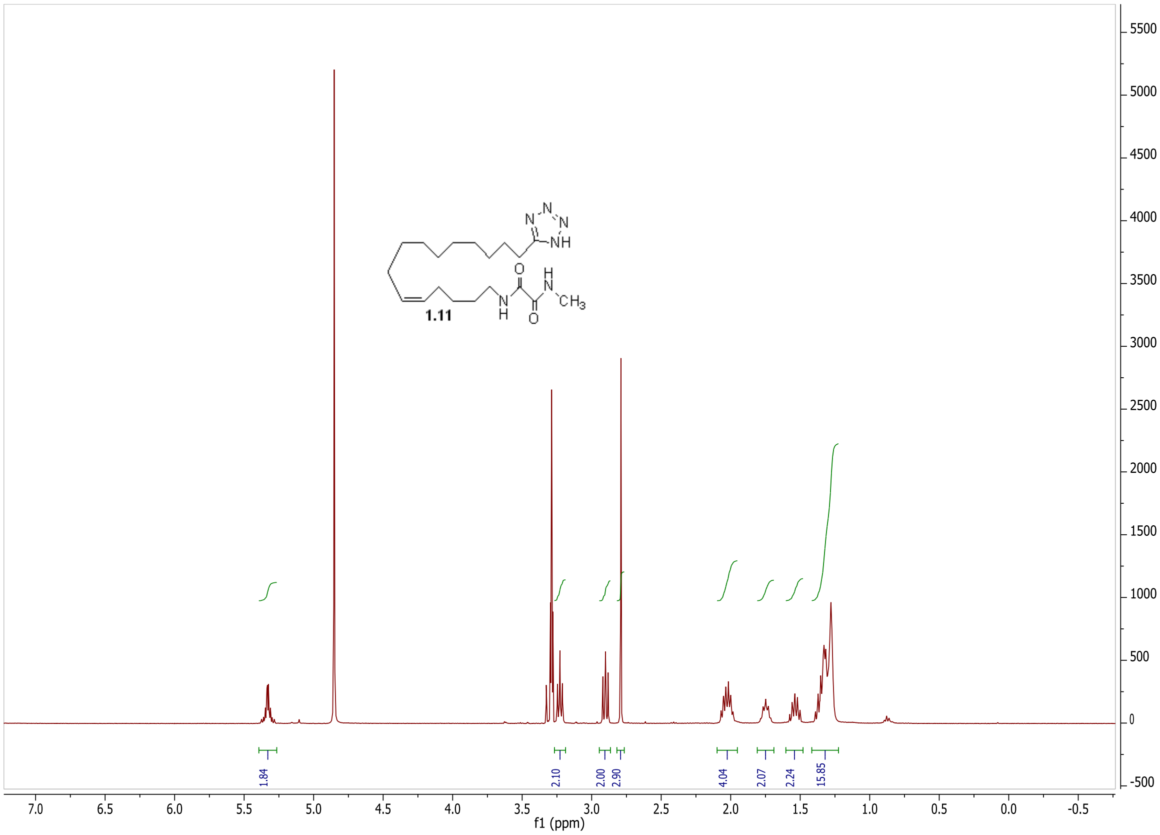
1.11
N
N
N
NH
O
H
N
CH3
N
H
O
1.84
2.10
2.00
2.90
4.04
2.07
2.24
15.85
7.0
6.5
6.0
5.5
5.0
4.5
4.0
3.5
3.0
2.5
2.0
1.5
1.0
0.5
0.0
-0.5
f1 (ppm)
5500
5000
4500
4000
3500
3000
2500
2000
1500
1000
500
0
-500

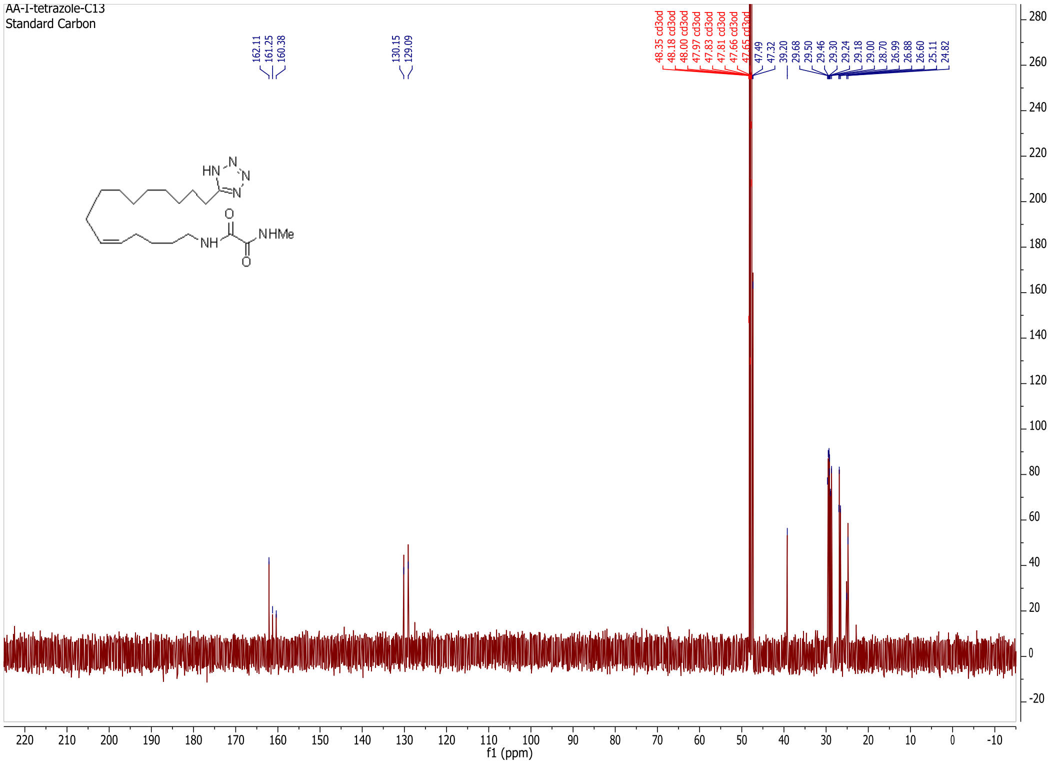
AA-I-tetrazole-C13
Standard Carbon
162.11
161.25
160.38
130.15
129.09
48.35 cd3od
48.18 cd3od
48.00 cd3od
47.97 cd3od
47.83 cd3od
47.81 cd3od
47.66 cd3od
47.65 cd3od
47.49
47.32
39.20
29.68
29.50
29.46
29.30
29.24
29.18
29.00
28.70
26.99
26.88
26.60
25.11
24.82
HN
N
N
N
O
NH
NHMe
O
220
210
200
190
180
170
160
150
140
130
120
110
100
90
80
70
60
50
40
30
20
10
0
-10
f1 (ppm)
280
260
240
220
200
180
160
140
120
100
80
60
40
20
0
-20

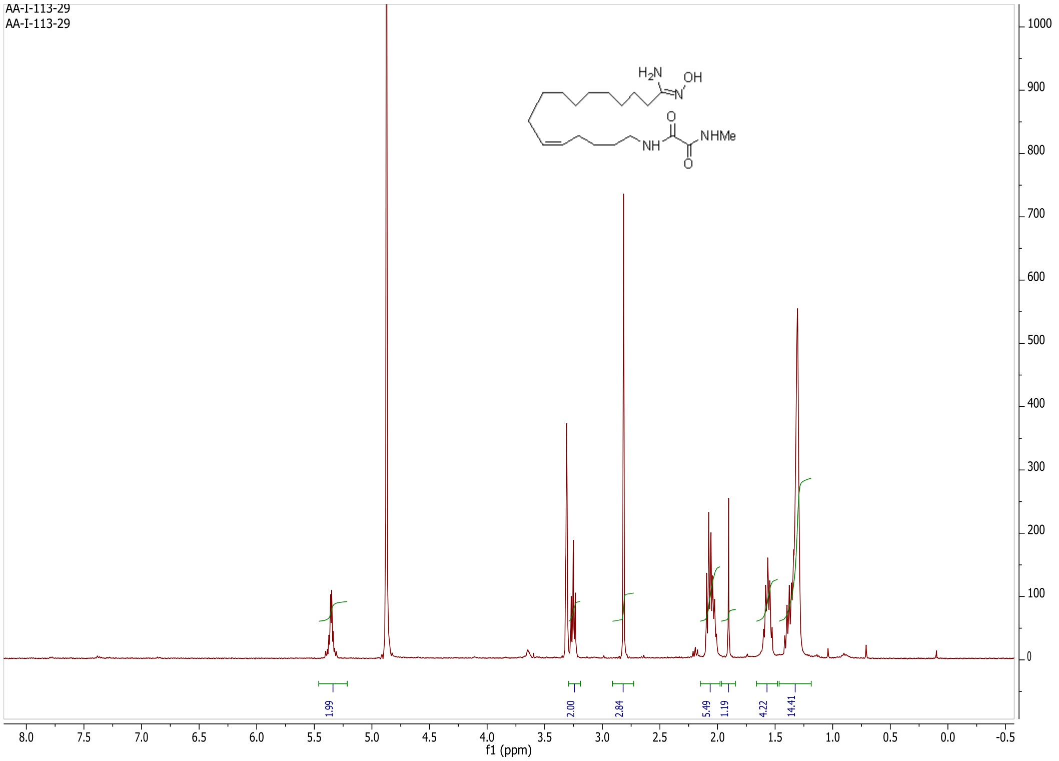

AA-I-113-29
AA-I-113-29
H2N
OH
N
O
NHMe
NH
O
1.99
2.00
2.84
5.49
1.19
4.22
14.41
8.0
7.5
7.0
6.5
6.0
5.5
5.0
4.5
4.0
3.5
3.0
2.5
2.0
1.5
1.0
0.5
0.0
-0.5
f1 (ppm)
1000
900
800
700
600
500
400
300
200
100
0

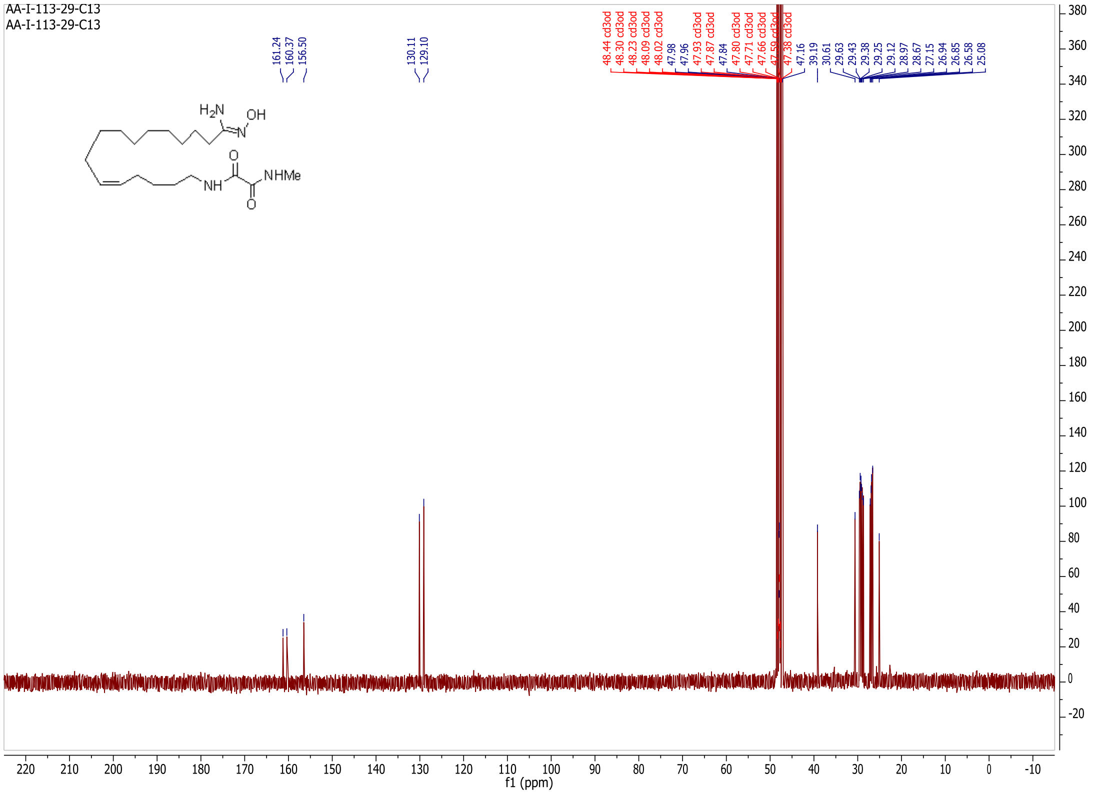

AA-I-113-29-C13
AA-I-113-29-C13
161.24
160.37
156.50
130.11
129.10
48.44 cd3od
48.30 cd3od
48.23 cd3od
48.09 cd3od
48.02 cd3od
47.98
47.96
47.93 cd3od
47.87 cd3od
47.84
47.80 cd3od
47.71 cd3od
47.66 cd3od
47.59 cd3od
47.38 cd3od
47.16
39.19
30.61
29.63
29.43
29.38
29.25
29.12
28.97
28.67
27.15
26.94
26.85
26.58
25.08
H2N
OH
N
O
NHMe
NH
O
220
210
200
190
180
170
160
150
140
130
120
110
100
90
80
70
60
50
40
30
20
10
0
-10
f1 (ppm)
380
360
340
320
300
280
260
240
220
200
180
160
140
120
100
80
60
40
20
0
-20

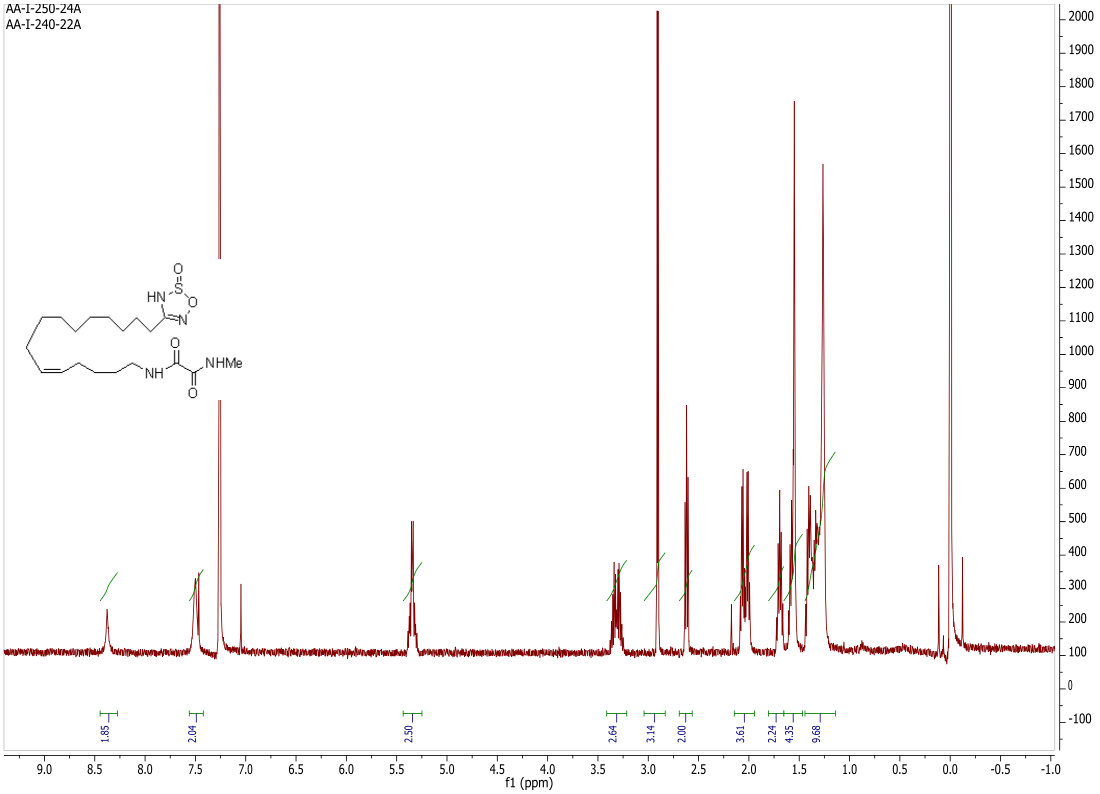
AA-I-250-24A
AA-I-240-22A
HN
S
O
O
N
NH
O
NHMe
O
1.85
2.04
2.50
2.64
3.14
2.00
3.61
2.24
4.35
9.68
9.0
8.5
8.0
7.5
7.0
6.5
6.0
5.5
5.0
4.5
4.0
3.5
3.0
2.5
2.0
1.5
1.0
0.5
0.0
-0.5
-1.0
f1 (ppm)
2000
1900
1800
1700
1600
1500
1400
1300
1200
1100
1000
900
800
700
600
500
400
300
200
100
0
-100

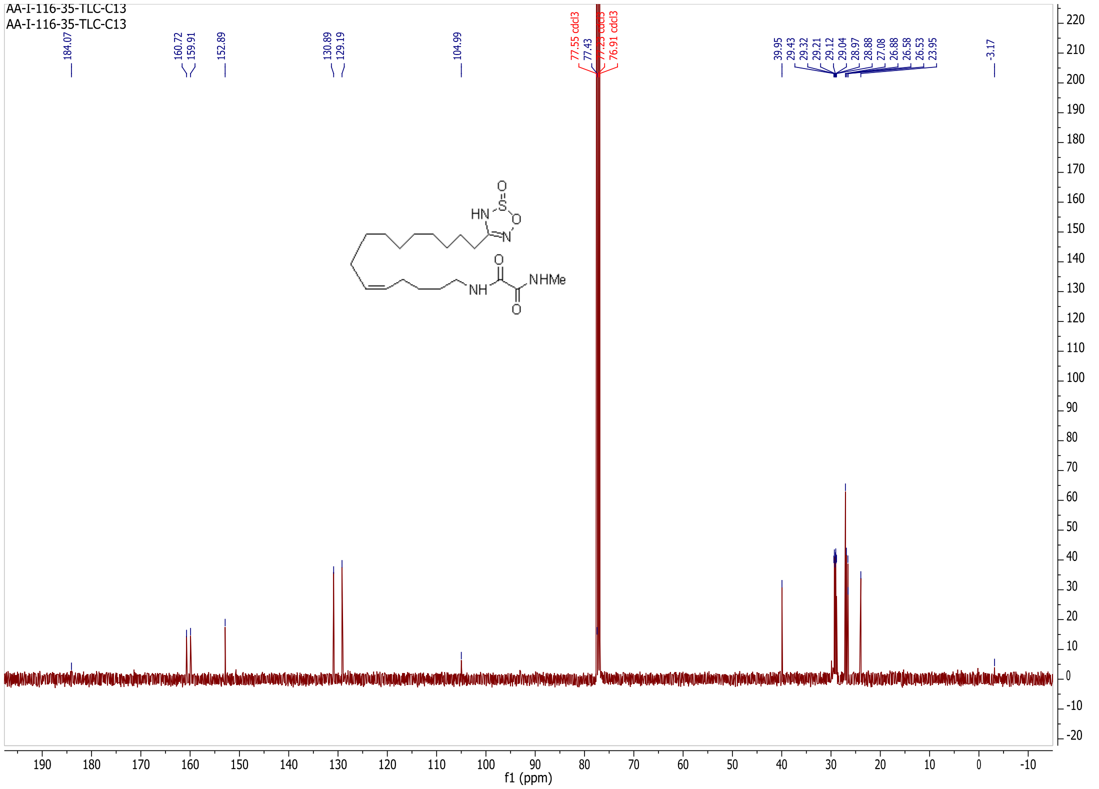
AA-I-116-35-TLC-C13
AA-I-116-35-TLC-C13
184.07
160.72
159.91
152.89
130.89
129.19
104.99
77.55 cdcl3
77.43
77.23 cdcl3
76.91 cdcl3
39.95
29.43
29.32
29.21
29.12
29.04
28.97
28.88
27.08
26.88
26.58
26.53
23.95
-3.17
HN
S
O
O
N
NH
O
NHMe
O
190
180
170
160
150
140
130
120
110
100
90
80
70
60
50
40
30
20
10
0
-10
f1 (ppm)
220
210
200
190
180
170
160
150
140
130
120
110
100
90
80
70
60
50
40
30
20
10
0
-10
-20

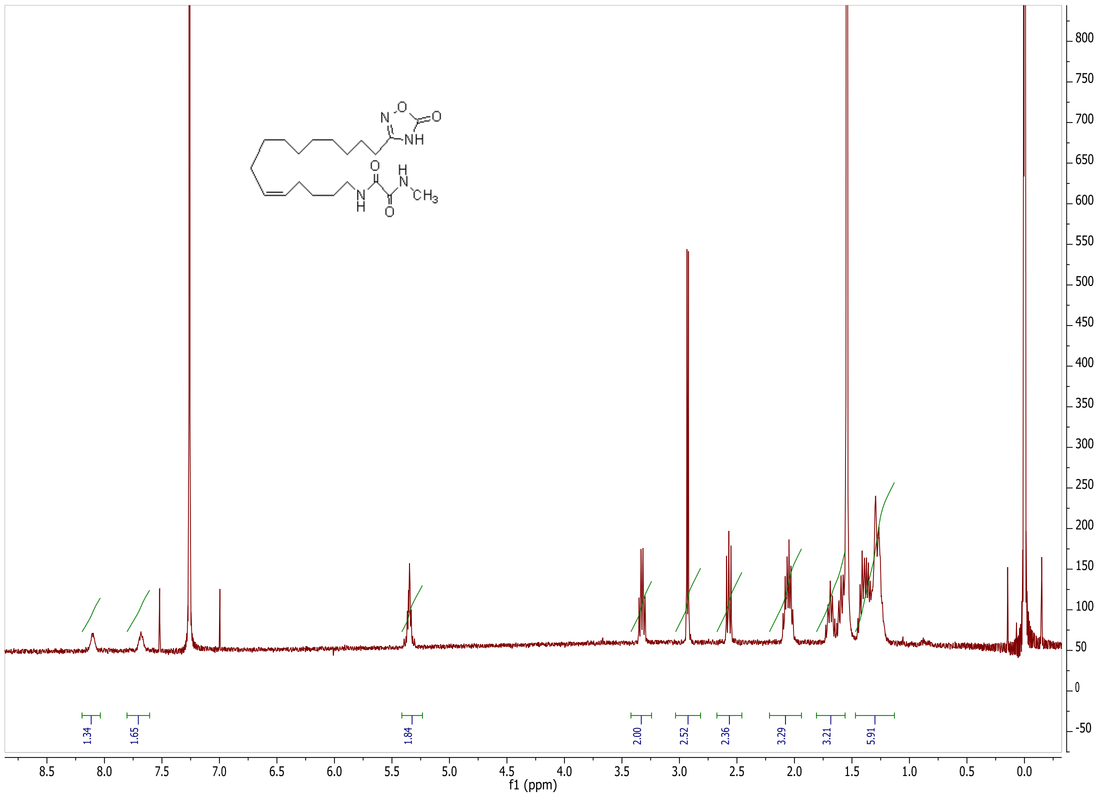

N
O
O
NH
O
H
N
CH3
N
H
O
1.34
1.65
1.84
2.00
2.52
2.36
3.29
3.21
5.91
8.5
8.0
7.5
7.0
6.5
6.0
5.5
5.0
4.5
4.0
3.5
3.0
2.5
2.0
1.5
1.0
0.5
0.0
f1 (ppm)
800
750
700
650
600
550
500
450
400
350
300
250
200
150
100
50
0
-50

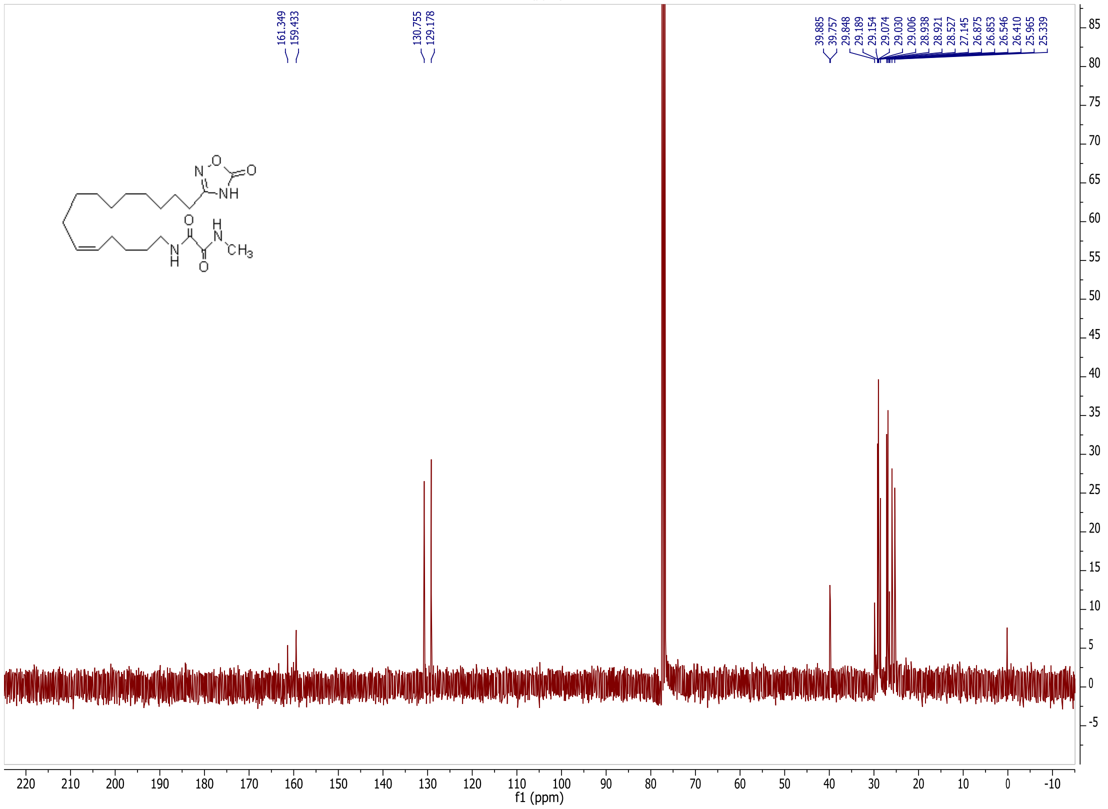

161.349
159.433
130.755
129.178
39.885
39.757
29.848
29.189
29.154
29.074
29.030
29.006
28.938
28.921
28.527
27.145
26.875
26.853
26.546
26.410
25.965
25.339
N
O
O
NH
O
H
N
CH3
N
H
O
220
210
200
190
180
170
160
150
140
130
120
110
100
90
80
70
60
50
40
30
20
10
0
-10
f1 (ppm)
85
80
75
70
65
60
55
50
45
40
35
30
25
20
15
10
5
0
-5

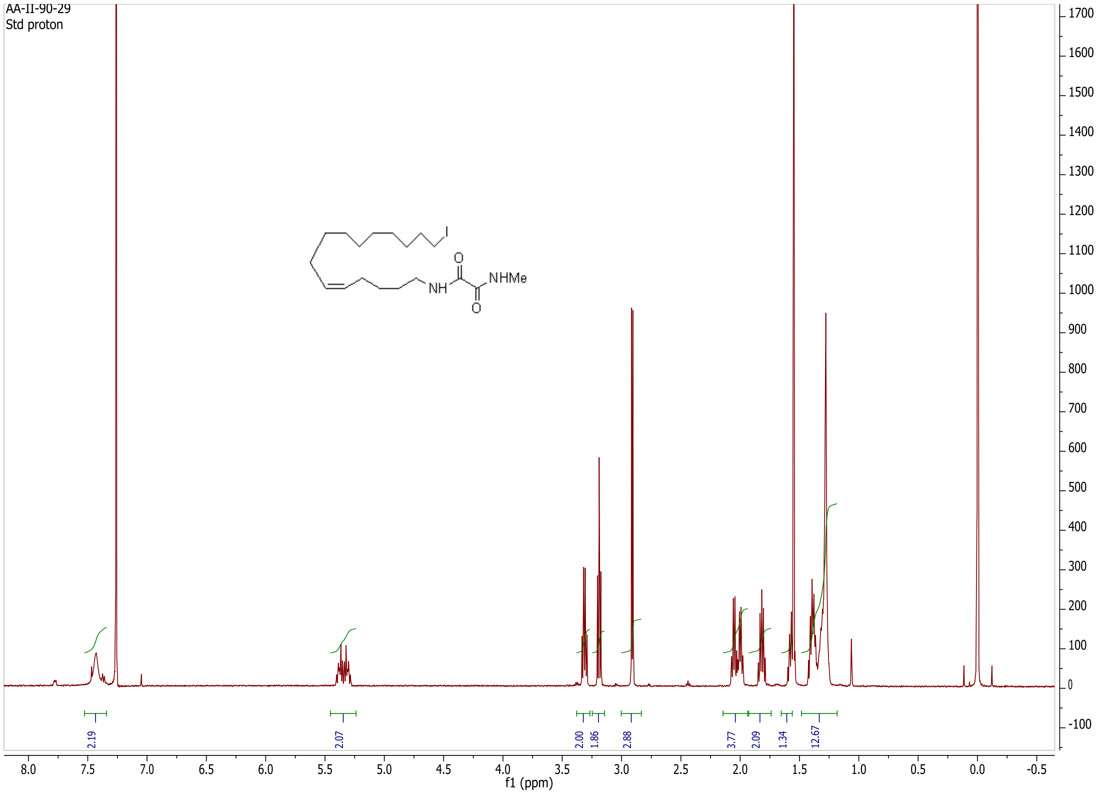
AA-II-90-29
Std proton
I
O
NH
NHMe
O
2.19
2.07
2.00
1.86
2.88
3.77
2.09
1.34
12.67
8.0
7.5
7.0
6.5
6.0
5.5
5.0
4.5
4.0
3.5
3.0
2.5
2.0
1.5
1.0
0.5
0.0
-0.5
f1 (ppm)
1700
1600
1500
1400
1300
1200
1100
1000
900
800
700
600
500
400
300
200
100
0
-100

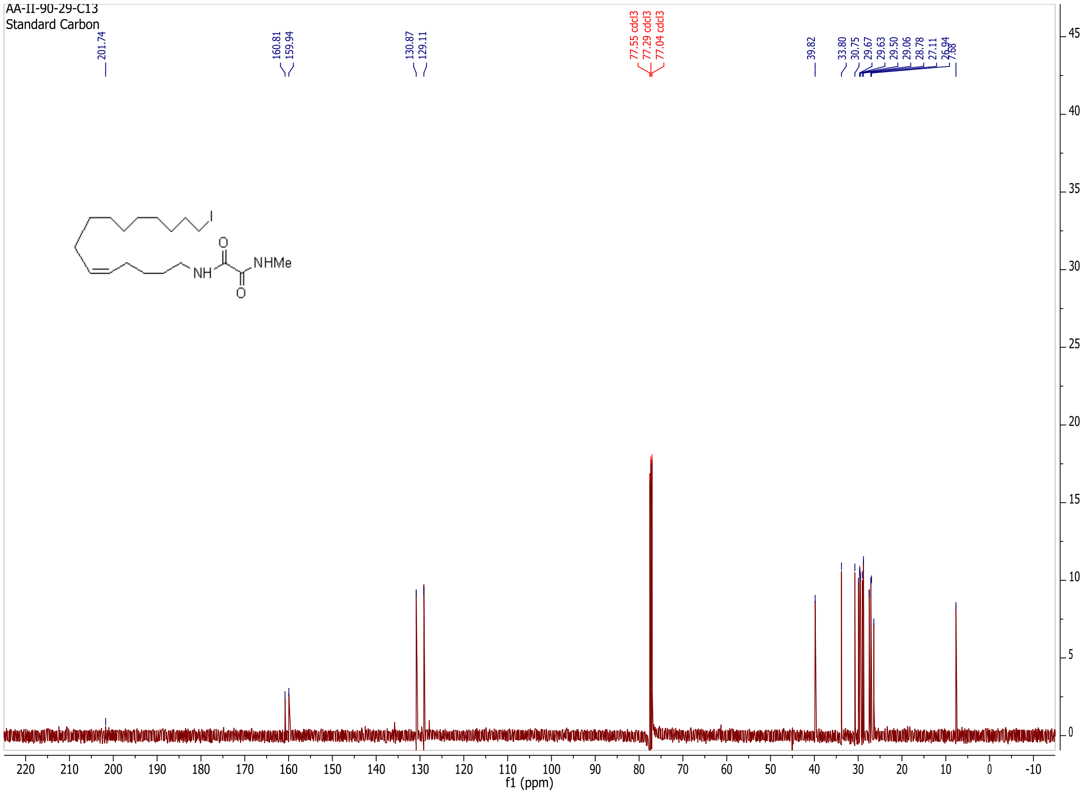
AA-II-90-29-C13
Standard Carbon
201.74
160.81
159.94
130.87
129.11
77.55 cdcl3
77.29 cdcl3
77.04 cdcl3
39.82
33.80
30.75
29.67
29.63
29.50
29.06
28.78
27.11
26.94
7.68
I
O
NH
NHMe
O
220
210
200
190
180
170
160
150
140
130
120
110
100
90
80
70
60
50
40
30
20
10
0
-10
f1 (ppm)
45
40
35
30
25
20
15
10
5
0

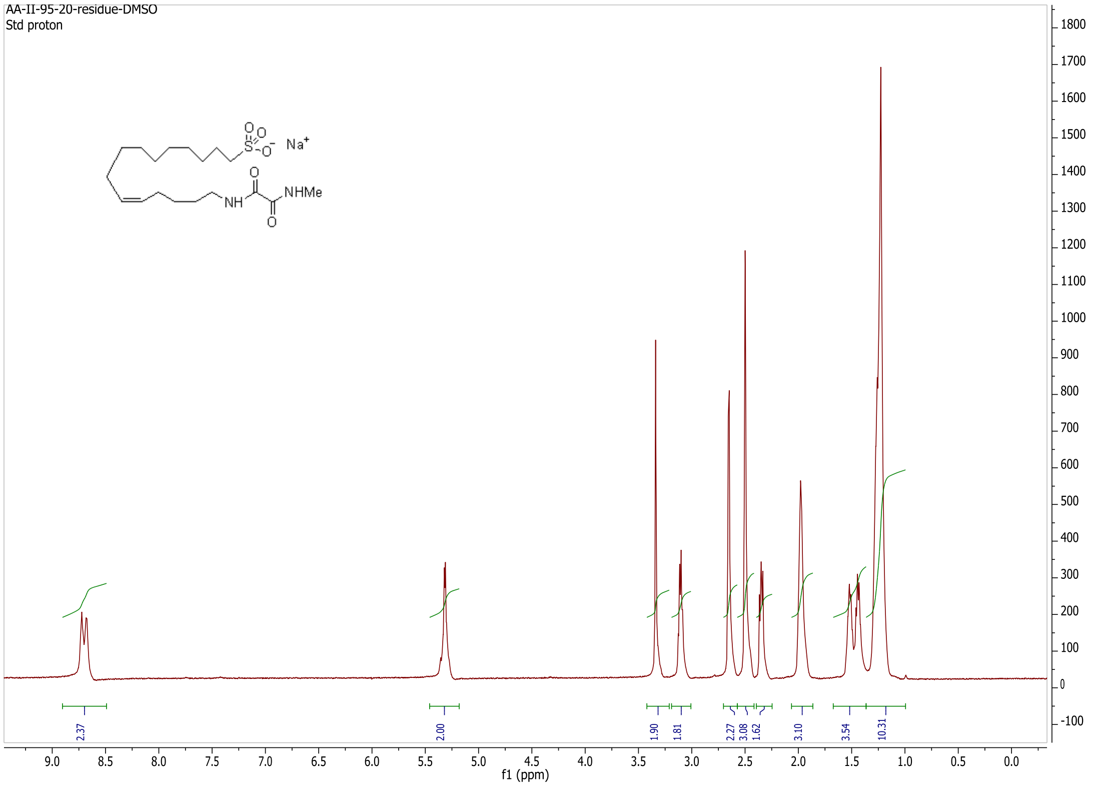
AA-II-95-20-residue-DMSO
Std proton
O O
S
O⁻
Na⁺
O
NH
NHMe
O
2.37
2.00
1.90
1.81
2.27
3.08
1.62
3.10
3.54
10.31
9.0 8.5 8.0 7.5 7.0 6.5 6.0 5.5 5.0 4.5 4.0 3.5 3.0 2.5 2.0 1.5 1.0 0.5 0.0
f1 (ppm)
1800 1700 1600 1500 1400 1300 1200 1100 1000 900 800 700 600 500 400 300 200 100 0 -100

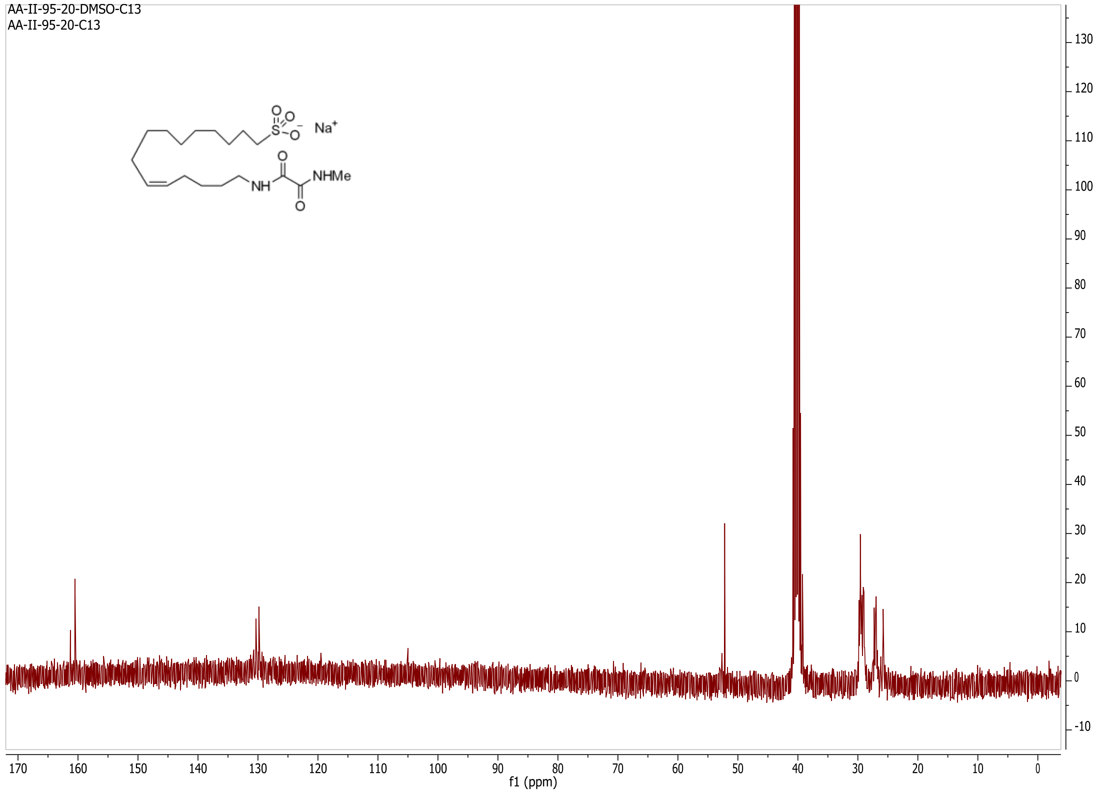
AA-II-95-20-DMSO-C13
AA-II-95-20-C13
O O
S
O⁻
Na⁺
O
NH
NHMe
O
170 160 150 140 130 120 110 100 90 80 70 60 50 40 30 20 10 0
f1 (ppm)
130 120 110 100 90 80 70 60 50 40 30 20 10 0 -10

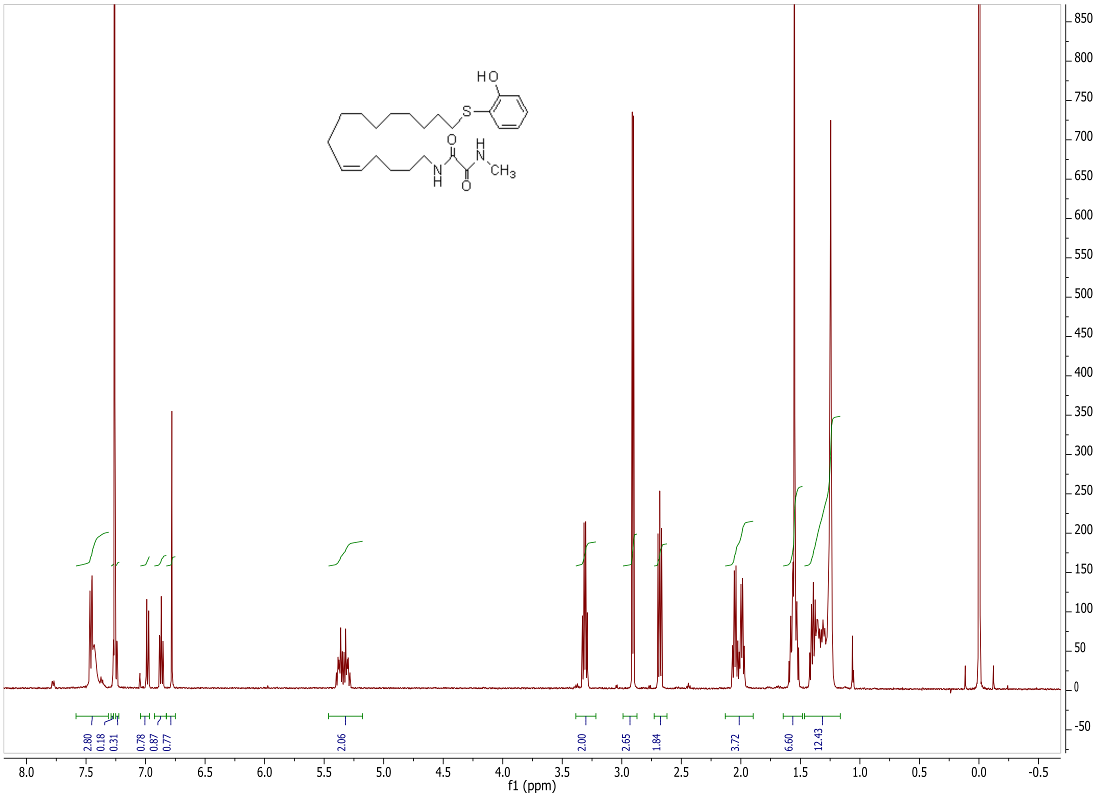
HO
S
O
N
H
H
N
CH3
O
2.80
0.18
0.31
0.78
0.87
0.77
2.06
2.00
2.65
1.84
3.72
6.60
12.43
8.0
7.5
7.0
6.5
6.0
5.5
5.0
4.5
4.0
3.5
3.0
2.5
2.0
1.5
1.0
0.5
0.0
-0.5
f1 (ppm)
850
800
750
700
650
600
550
500
450
400
350
300
250
200
150
100
50
0
-50

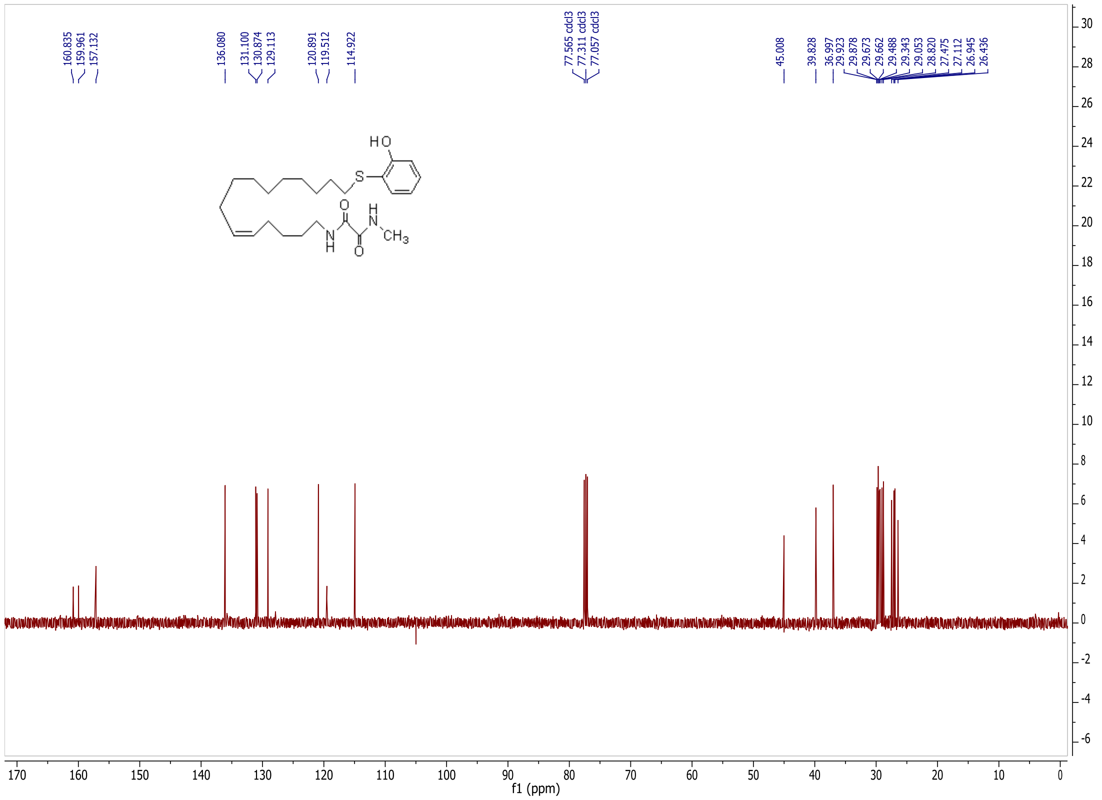
160.835
159.961
157.132
136.080
131.100
130.874
129.113
120.891
119.512
114.922
77.565 cdcl3
77.311 cdcl3
77.057 cdcl3
45.008
39.828
36.997
29.923
29.878
29.673
29.662
29.488
29.343
29.053
28.820
27.475
27.112
26.945
26.436
HO
S
O
N
H
H
N
CH3
O
170
160
150
140
130
120
110
100
90
80
70
60
50
40
30
20
10
0
f1 (ppm)
30
28
26
24
22
20
18
16
14
12
10
8
6
4
2
0
-2
-4
-6

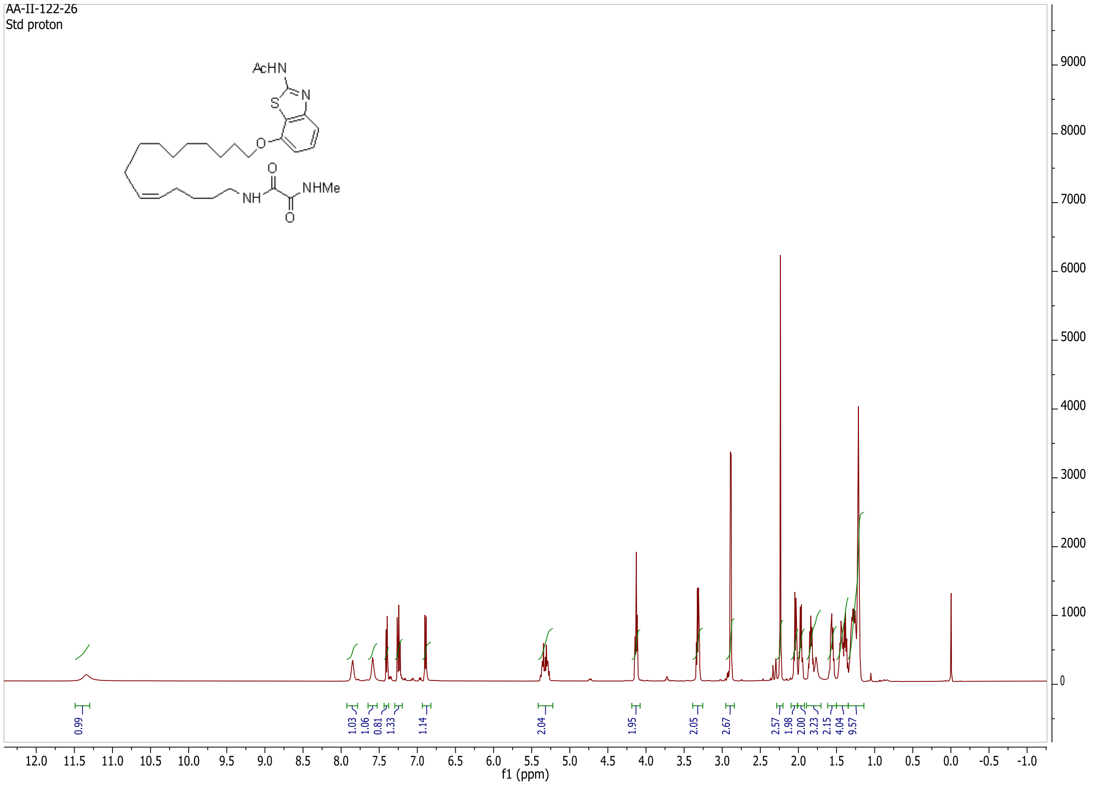
AA-II-122-26
Std proton
AcHN
S
N
O
NH
O
O
NHMe
0.99
1.03
1.06
0.81
1.33
1.14
2.04
1.95
2.05
2.67
2.57
1.98
2.00
3.23
2.15
4.04
9.57
f1 (ppm)

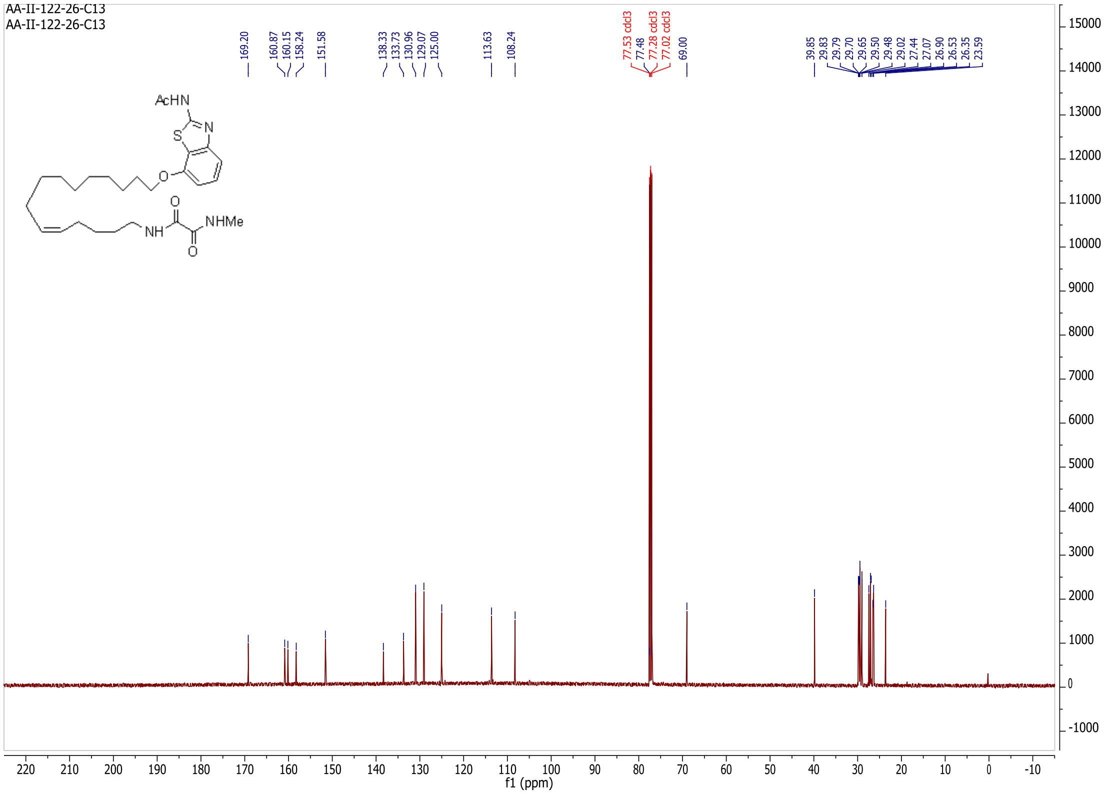
AA-II-122-26-C13
AA-II-122-26-C13
169.20
160.87
160.15
158.24
151.58
138.33
133.73
130.96
129.07
125.00
113.63
108.24
77.53 cdcl3
77.48
77.28 cdcl3
77.02 cdcl3
69.00
39.85
29.83
29.79
29.70
29.65
29.50
29.48
29.02
27.44
27.07
26.90
26.53
26.35
23.59
AcHN
S
N
O
NH
O
O
NHMe
f1 (ppm)

CHAPTER 2

INHIBITORS OF QSEC AS NOVEL ANTI-VIRULENCE AGENTS

2.1 Abstract

The bacterial quorum sensing receptor, *E. coli* regulator C (QseC), is a membrane-bound histidine sensor kinase that is conserved in at least 25 important human and plant pathogens. The activation of QseC by host adrenergic signaling molecules (epinephrine and norepinephrine) and the bacterial signaling molecule, auto-inducer 3 (AI-3), results in a virulent phenotype. It was previously shown that the inhibition of QseC mediated signaling by 5 pM of LED209, *N*-phenyl-4-{[(phenylamino)thioxomethyl]amino}-benzenesulfonamide, represses *in vitro* the expression of various virulence genes implicated in the pathogenesis of Gram-negative bacteria *Escherichia coli* (EHEC), *Salmonella typhimurium* and *Francisella tularensis*. In this work, structure-activity relationship (SAR) studies on LED209 and CF308 led to the discovery of two distinct classes of inhibitors and activators of QseC mediated virulence gene expression in *Salmonella* and EHEC. The *in vitro* activities of these analogs ranged from low picomolar to high nanomolar (5 pM to 500 nM). The analogs were synthesized via conventional amidation and urea formation methodologies, while quantitative polymerase chain reaction (qPCR) was used to assess the expression of various virulence genes. Structural studies showed that both classes were relatively intolerant of steric congestion but amenable to changes in electron density and polarity. With this information, a synthetic route to radiolabeled LED209 for further mechanistic studies was

developed. These findings will be germane for the development of clinically useful bacterial anti-virulence agents.

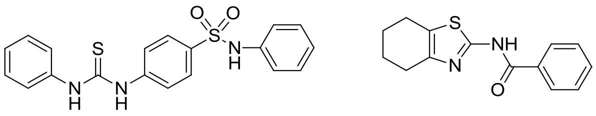
2.01 LED209 2.02 CF308

Figure 2.1
Structures of LED209 and CF308

2.2 Introduction

The constant development of structurally and mechanistically novel and effective anti-microbial agents is a task of vital interest to our modern, internationally-connected global society. Bacteria resistance to conventional antibiotics is a major problem that limits the effective treatment of bacterial infections in plants and animals including humans, and also leads to major economic losses. Since the discovery of penicillin by Alexander Fleming in 1928, the superfluous use of antibiotics[1] has stimulated rapid evolutionary changes in various bacteria species and resulted in the development of resistance at an alarming pace. Meanwhile, the available antibacterial tool box to efficiently compete with bacteria resistance has depreciated. As evident from the past century, the development of antibiotics using conventional bactericidal strategies is not sufficient to keep up with resistance; thus, new antibacterial tactics are needed.[2] Ideally, an effective tactic should be 1) effective against pathogenic bacteria, 2) selective against pathogenic bacteria while leaving symbionts and the host unharmed, 3) flexible and compatible with other therapies, and 4) exert less evolutionary pressure on bacteria, thereby curtailing the emergence of resistance. One such promising approach involves the inhibition of virulence gene expression.[3]

Recently, anti-virulence has emerged as a promising approach for combating bacterial infection and resistance. This method involves the inhibition/degradation of genes, proteins, and small molecules that promote the expression of bacteria virulent phenotype. Quorum sensing is generally involved in this process. As the population density of bacteria increases, small molecule mediated communication between the bacteria and the environment can lead to a switch from planktonic behavior to multicellular behavior.[4] Virulence gene expression and biofilm formation are often the results of this behavioral change and are critical for successful pathogenesis. Over the years, several laboratories have shown that the interruption of the quorum sensing pathway can impede successful pathogenesis of bacteria, both *in vitro* and *in vivo*.[5-11] Current work is focused on translating this basic science observation to the development of novel clinical anti-virulence agents for the control/prevention of bacterial infections.

2.2.1 Anti-virulence Approaches

The two major ways for inhibiting bacteria virulence are: 1) inhibition of virulence gene expression, and 2) inhibition of virulence protein effectors (Figure 2.2).

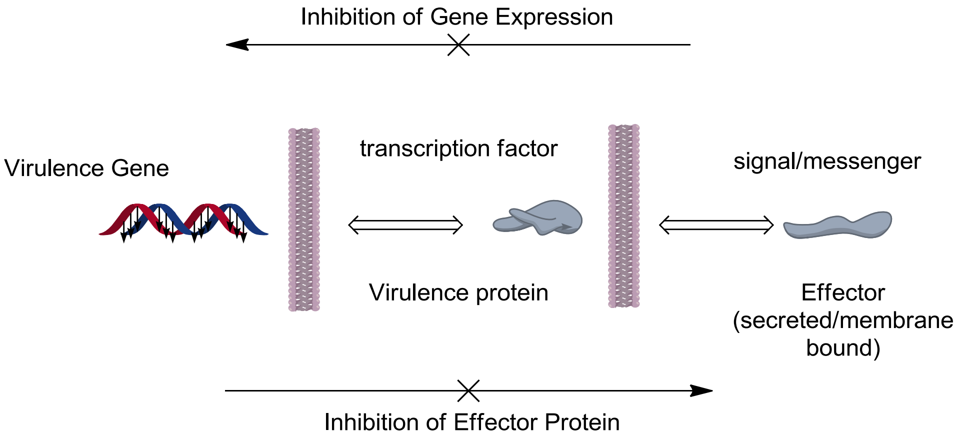
Inhibition of Gene Expression
Virulence Gene
transcription factor
signal/messenger
Virulence protein
Effector (secreted/membrane bound)
Inhibition of Effector Protein

Figure 2.2
Targets of anti-virulence approaches.

2.2.2 Inhibition of Virulence Gene Expression

The development of strategies to inhibit virulence gene expression is an active area of research. Most approaches involve disrupting the QS pathway by employing natural/bio-engineered QS systems and synthetic inhibitors. Examples of anti-virulence through natural/bio-engineered QS systems include the use of AHL (*N*-acylhomoserine lactone)-lactonase of Bacillus sp. strain 240B1 to degrade the AHL quorum signal,[6] the use of Bacillus sp. as probiotic in aquaculture,[7] and the use of Siomycin I produced by *Streptomyces* sp. strain Y33-1 to inhibit gelatinase of *Enterococcus faecalis*.[8] Examples of synthetic inhibitors include analogs of anthranilate required for the biosynthesis of the *Pseudomonas* quinolone signal (PQS),[9] noncompetitive inhibitors of the autoinducing peptide (AIP) activated AgrC receptor,[10] and *meta*-bromo-thiolactone inhibitors (a mimetic of 3OC12-HSL) of pyocyanin and biofilm formation in *Pseudomonas aeruginosa*[11] (Figure 2.3).

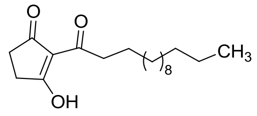

3-Acyltetronic Acid:
Inhibitor of AIP

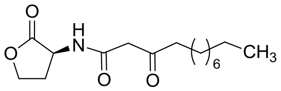

3OC12-HSL

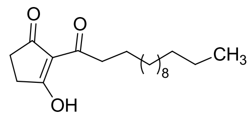

3-Acyltetronic Acid:
Inhibitor of AIP

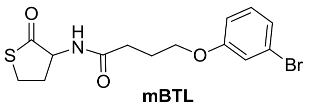

mBTL

Figure 2.3
Synthetic inhibitors of some QS signals.

2.2.3 Inhibition of Virulence Effectors

Virulence effectors are secretory or membrane-bound proteins and macromolecules that enhance or promote successful invasion and colonization by lytic bacteria. Most virulence effectors are toxins such as the Shiga toxin secreted by EHEC, anthrax toxin secreted by *Bacillus anthracis*, cholera toxin secreted by *Vibrio cholera*, and are the cause of the life-threatening conditions associated with infections by the foregoing bacteria. Other effectors such as VopC[12] and VopS[13] of *Vibrio parahaemolyticus* promote cell invasion and cell rounding. Due to the large molecular weights of virulence effectors, vaccination and antibody therapies are often employed as anti-virulence strategies. Also, the use of non-absorbable polymers that bind and sequester bacteria toxins is promising.[14] Such polymers prevent the cellular internalization of bacteria toxins and are excreted in the feces. An example is a polyacrylamide binder designed by Watanabe et al. to sequester both Stx1 and Stx2 in mice challenged with a lethal dose of EHEC.[15]

2.2.4 Anti-virulence and Bacterial Resistance

There are four major antimicrobial resistance strategies namely: 1) Inhibition of antimicrobial agent entry into cells, 2) ejection of antimicrobial agents via efflux pumps, 3) inactivation of antimicrobial agents, and 4) modification of antimicrobial targets. These strategies are often utilized singly or in combination by bacteria and other microbes to limit the effectiveness of antimicrobial agents. A major question generally posed by critics of anti-virulence as an antimicrobial strategy is whether anti-virulence would have any effect on bacterial resistance. Although there is not sufficient data on the effects of anti-virulence strategies on bacterial resistance processes, it is believed that the non-toxic nature of anti-virulence strategies would pose little evolutionary pressure on bacteria, and facilitate the survival of the more populous non-resistant bacteria at the expense of the less populous resistant bacteria. However, a report by Maeda et al.,[16] on the resistance of *P.aeruginosa* possessing mutant virulence genes *mexR* and *nalC* to a quorum sensing inhibitor (brominated furanone C-30) suggests the possibility of resistance to anti-virulence therapy. Furthermore, it should be noted that the success of anti-virulence approaches rely on other factors such as the ability of the host's immune system to eradicate the pathogenic bacteria, and competition between pathogenic and normal flora for nutrients. Since some fundamental life processes of bacteria are detrimental to animal and plant hosts, uncontrolled bacteria population growth is undesired. Thus, anti-virulence strategies might only be successful if they are used in combination with the current bactericidal strategies. Until the commercialization and exploration of the frequent use of anti-virulence therapy, the superiority of anti-virulence strategies over current anti-bacterial strategies cannot be confirmed. However, the potential advantages and current successes of anti-virulence therapy present a hopeful perspective in the fight against bacterial resistance, as well as a unique mechanistic approach to drug discovery.

2.2.5 Targeting QseC as an Anti-virulence Approach

The membrane-bound histidine sensor kinase, QseC, is part of a two component system that mediates quorum sensing and virulence gene expression in several Gram-negative bacteria. Upon activation by host stress hormones or AI-3 (Figure 2.4), QseC autophosphorylates and activates transcriptional regulators QseB, QseF, and KdpE via phosphorylation in EHEC.[17] This leads to the expression of genes required for motility, attachment and effacement, and secretion of Shiga toxin.

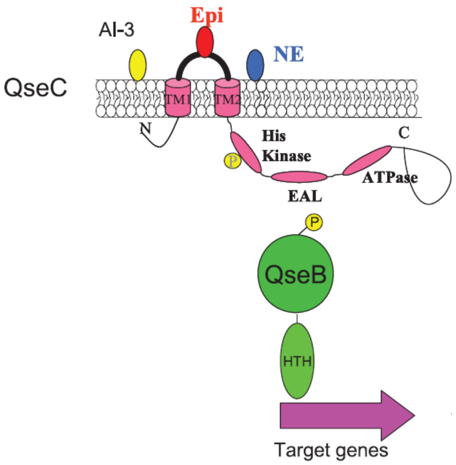

Figure 2.4
QseC responds to AI-3 and the host stress hormones: "From [*Science* **2008**, *321*, 1078-1080]. Reprinted with permission from AAAS."[5]

In previous studies by Sperandio et al.,[5] it was shown that the small molecule LED209 decreased the expression of these virulence genes at picomolar concentration, did not inhibit the growth of EHEC *in vitro*, and was relatively non-toxic to mice at micro-molar concentrations. However, LED209 slowly decomposes in solution (dimethyl sulfoxide), is poorly soluble, is a potential alkylating agent, and is rapidly absorbed from the GI tract of mice. My contributions to this research include 1) SAR studies of LED209 to improve stability and water solubility, 2) the synthesis of a molecular probe to aver our current understanding of the mechanism behind the exquisite potency of LED209, and 3) the discovery of a new class of inhibitors of QseC mediated virulence gene expression.

2.3 Literature Review

The detection and transduction of signals are phenomena common to every organism. Most signal transduction pathways consist of 1) a primary signal, 2) a primary signal receptor, 3) transducer(s), and 4) a genetic target. Prolonged interruption at any of these stages impairs proper signal transduction and might have severe consequences for the survival of an organism. In bacteria such as Enterohemorrhagic *Escherichia coli* (EHEC) O157:H7, signal transduction pathways are intimately involved in pathogenesis.[4] Therefore, the inhibition of the pertinent signal transduction pathway can help control bacteria pathogenesis. EHEC is responsible for the major symptoms of hemorrhagic colitis and hemolytic uraemic syndrome.[18] Virulence gene expression in EHEC leads to the formation of attaching and effacing (AE) lesions and the secretion of Shiga toxin (Stx) in the large intestine of animals. The genes that are responsible for the formation of AE lesions are encoded in a pathogenicity island called the locus of enterocyte effacement (LEE).[19] The genes responsible for the secretion of Stx are located within the late genes of a λ bacteriophage.[20] The LEE genes are regulated by the LEE-encoded regulator (Ler). The LEE region consists of five major operons: *LEE1* (*ler*), *LEE2*, *LEE3*, *LEE4*, and *tir* (*LEE5*). The quorum sensing signal AI-3 transcriptionally activates *ler* and *stx* through the two-component system QseCB.

2.3.1 The Histidine Sensor Kinase QseCB

Histidine sensor kinases (HK) are multifunctional receptors widely used by bacteria to detect and transduce signals. The histidine kinase QseC is part of a two-component quorum sensing system with QseB, and it is homologous with the PmrAB two-component system of *Salmonella typhimurium*.[21] QseC is the sensor kinase while QseB is the response regulator/transducer. QseC has a predicted molecular weight of 50 kDa and is composed of two transmembrane domains, a sensing periplasmic N-terminal, and a cytoplasmic/catalytic C-terminal. QseB is a cytoplasmic protein with an estimated molecular weight of 24 kDa.[21]

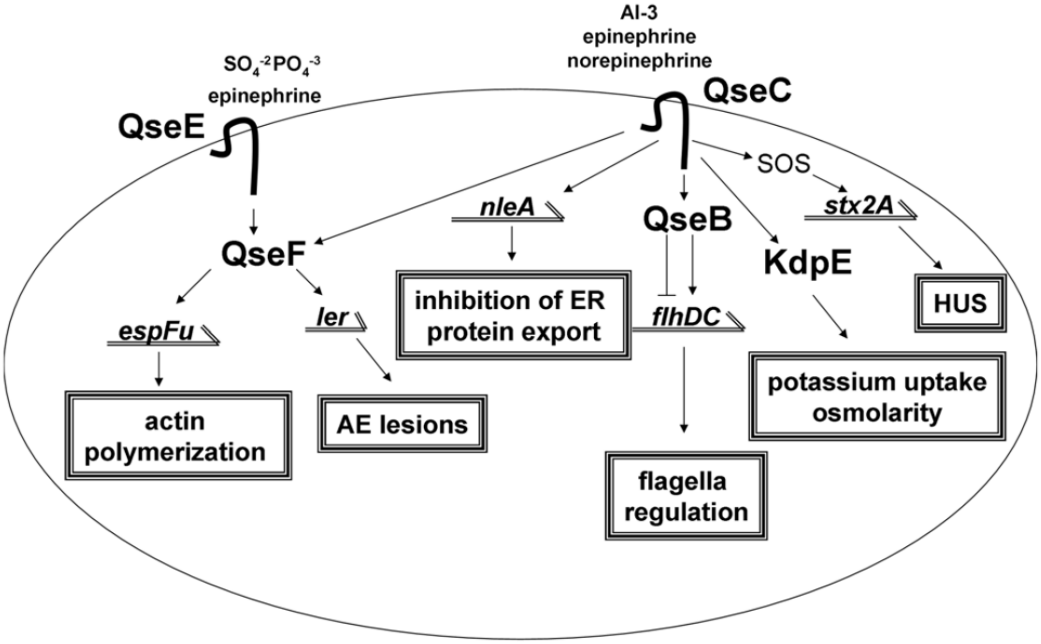
AI-3
epinephrine
norepinephrine
SO4-2PO4-3
epinephrine
QseE
QseC
SOS
nleA
QseB
stx2A
QseF
KdpE
HUS
inhibition of ER protein export
espFu
ler
flhDC
potassium uptake osmolarity
actin polymerization
AE lesions
flagella regulation

Figure 2.5
QS signaling cascade in E. coli.[22]

Recently, another HK two-component system consisting of QseE and QseF[23] was identified in E. coli which suggests the presence of a multi-faceted signaling system in E. coli (Figure 2.5).[22] QseCB is conserved in at least 25 important human and plant pathogens, while QseEF homologues are found in enterics. QseC senses the hormones norepinephrine and epinephrine, and the bacterial signal AI-3. AI-3, whose chemical structure is currently unknown, is believed to be a small molecule secreted by certain bacteria strains.[24] AI-3 can be obtained from the spent supernatant of AI-3 producing bacteria. The LuxS enzyme which is involved in the catabolism of S-adenosylmethionine (SAM) is involved in the syntheses of AI-3 and the furanosyl borate diester autoinducer-2 (AI-2, Figure 2.6).[25] LuxS is an iron-dependent metalloenzyme which belongs to the family of lyases.[26]

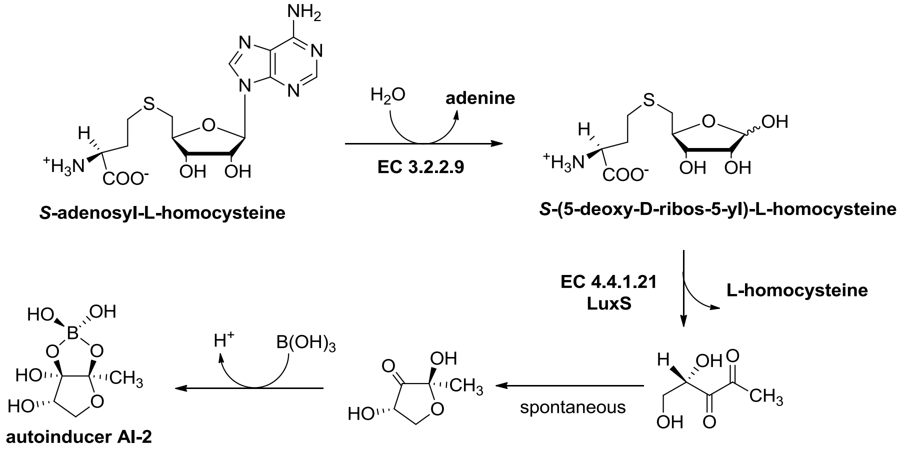

S-adenosyl-L-homocysteine
H2O
adenine
EC 3.2.2.9
S-(5-deoxy-D-ribos-5-yl)-L-homocysteine
EC 4.4.1.21
LuxS
L-homocysteine
spontaneous
H+
B(OH)3
autoinducer AI-2

Figure 2.6
Biosynthesis of AI-2.

It is unknown if QseCB responds to other classes of bacteria QS signals such as AHLs and oligopeptides, however, current data suggest that AI-3 is the main bacterial signal involved in QseC mediated virulence gene expression.[27] A better understanding of the signaling network of QseC would further validate QseC as a critical anti-virulence target. This is currently being pursued by Sperandio and coworkers.

A collective body of work has established the relationship between QseC (and its homologs) mediated signal transduction and virulence in certain bacteria strains.[3,5,17-18,21,24] Also, preliminary animal studies showed the involvement of QseC in bacteria pathogenesis,[3] and the upregulation of *qseC* expression in infected mice.[5] In concert with current work by various groups on the development of quorum sensing inhibitors as anti-infective agents, the Falck group in collaboration with the Sperandio group initiated a medicinal chemistry program to develop potent inhibitors of QseC signaling. In addition to the reasons discussed above, QseC was chosen as a target because: 1) there is no identified human homolog, 2) it is easily accessible to inhibitors due to its location on the cell membrane, and 3) it has a central role in virulence gene expression in organisms such as EHEC.

By means of a high-throughput screen of 150,000 small organic molecules at the University of Texas (UT) Southwestern, LED209 was identified as a relatively non-toxic, picomolar inhibitor of AI-3 mediated virulence gene expression. For further animal studies, a more soluble and drug-like version of LED209 was needed. Discussed in the next section are attempts to meet this need.

2.4 Results and Discussion

2.4.1 Structure-Activity Relationship Studies of LED209: Polarity Focused SAR

The structure of LED209 can be divided into four segments namely: A) a left phenyl substituent, B) a thiourea functional group, C) a para substituted sulfanilide middle segment, and D) a right phenyl group. The relative insolubility of LED209 can be attributed to the presence of planar, hydrophobic phenyl groups that can π-stack, and the tendency of the thiourea group to form possible polymeric species via intermolecular hydrogen-bonding. Similar hydrogen-bonding is typically exploited in organocatalysis with electron-deficient phenyl substituted thioureas.[28] Therefore, our approach towards developing a more soluble form of LED209 involved three main modifications: 1) replacement of the thiourea with a urea or thiazole ring system, 2) replacement of the left and right phenyl groups with a non-aromatic cyclohexyl, and 3) the addition of polar solubilizing groups. Bioactivity was determined through quantitative polymerase chain reaction (qPCR) comparison of virulence gene expression in non-treated and compound treated EHEC.[5]

LED209

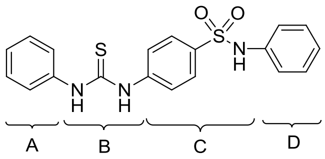

Figure 2.7
Four segments of LED209.

2.4.1.2. Bioisosteres of Thiourea Group

Due to the solubility and potential toxicity of thioureas, we began our SAR studies by replacing the thiourea with other bioisosteres. My goal was to develop a non-toxic, bioactive and more hydrophilic analog of LED209. As shown below (Table 2.1), constricting the thiourea segment into a ring as in **2.03-2.06** produced non-active, toxic compounds, which suggests the importance of some flexibility or reactivity at the thiourea for selectivity. Also, guanidine containing analogs **2.07** and **2.08,** as well as oxamide **2.12** were non-active. Fortunately, the urea bioisostere **2.09** was active, albeit with lower potency. We believe that urea **2.09** should be more hydrophilic than the thiourea **2.01** due to the higher electronegativity of the oxygen in the urea that facilitates better interactions with water molecules. The higher aqueous solubility of urea as compared to thiourea also supports this hypothesis. On the other hand, mono *N*-methylated urea **2.10** was an agonist of *ler* expression. Amide **2.11** was found to be toxic and was not further tested for activity. Thus, future SAR studies utilized **2.01** (LED209) and **2.09** as lead compounds.

Table 2.1. Modifications to thiourea moiety B.

ID	Structure	ler (qPCR)	Pedestal (qPCR)	Toxicity
2.01	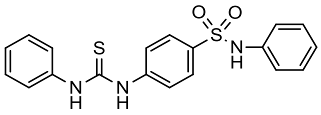	Inhibitor**	Inhibitor**	Non-Toxic
2.03#	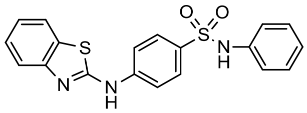	No change	ND	Toxic
2.04	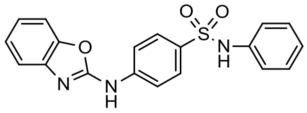	No change	ND	Toxic
2.05	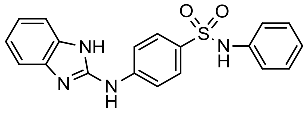	No change	ND	ND
2.06	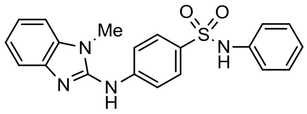	No change	ND	Toxic
2.07#	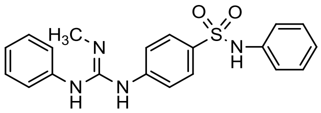	No change	ND	ND
2.08#	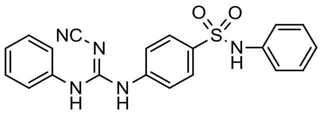	No change	ND	ND
2.09	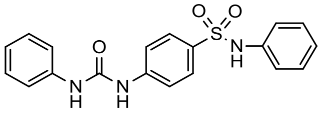	Inhibitor*	Inhibitor	ND
2.10#	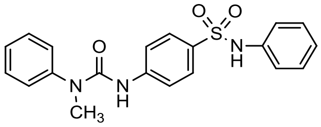	Activator+	ND	ND

2.11#	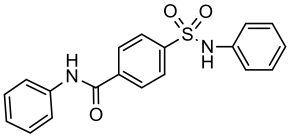	ND	ND	Toxic
2.12#	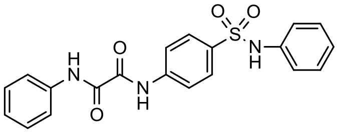	No change	ND	ND

* > 2-fold decrease, ** > 10-fold decrease. + > 2-fold increase. ND = not determined. Compounds were tested at 500 nM. # Synthesized by other group members.

2.4.1.3. Replacement of the Phenyl Groups with Polar Flexible Moieties

Next, replacement of the phenyl groups with more flexible, polar groups was examined (Table 2.2). Replacement of the D ring of **2.09** (**2.14**, **2.17**) produced active inhibitors of *ler* expression, with **2.17** being more potent than **2.09**. Surprising, the thiourea version of **2.14** (analog **2.13**) was inactive. The removal of the D phenyl group (**2.15**) or its replacement with a morpholine group produced non-active and toxic compounds respectively. Replacing the A ring with a cyclohexyl (**2.16**) or 1,3,4-thiadiazole (**2.19**) gave analogs with agonist activity (activators of *ler* expression). These data suggest that appropriate changes to the A and D rings can produce either agonists or inhibitors.

Table 2.2. Modifications to phenyl rings A and D.

ID	Structure	ler (qPCR)	Pedestal (qPCR)	Toxicity
2.13	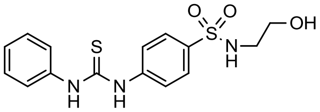	No change	ND	ND
2.14	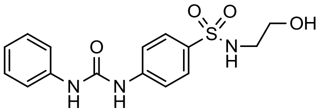	Inhibitor*	ND	ND
2.15#	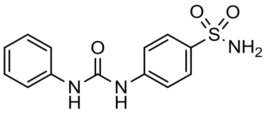	No change	ND	ND

2.16#	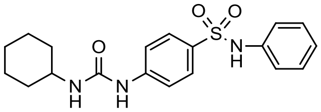	Activator+	ND	ND
2.17#	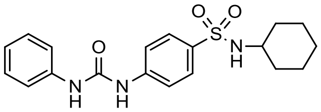	Inhibitor**	No change	ND
2.18#	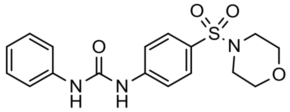	ND	ND	Toxic
2.19#	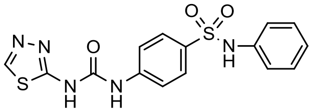	Activator+	ND	ND

* > 2-fold decrease, ** > 10-fold decrease. + > 2-fold increase. ND = not determined. Compounds were tested at 500 nM. # Synthesized by other group members.

2.4.1.4. Addition/Conjugation of Polar Groups

As shown below (Table 2.3), rings A and D were sensitive to electronic and steric changes. Ortho-substitution with a carboxylic acid on ring D (**2.20**) or a methoxy on ring A (**2.23**) was detrimental to the activity of both urea and thiourea lead compounds. Para-substitution with an electron donating dimethylamine group produced a potent inhibitor (**2.21**) of *ler* expression, while para-substitution with the highly flexible triethyleneglycol monomethyl ether (**2.22**) was detrimental to activity. Finally, picoline amine derivative **2.24** was toxic and was not further tested.

Table 2.3. Attachment of polar groups to rings A and D.

ID	Structure	ler (qPCR)	Pedestal (qPCR)	Toxicity
2.20#	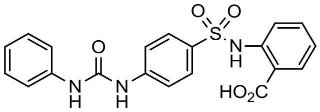	No change	ND	ND

2.21#	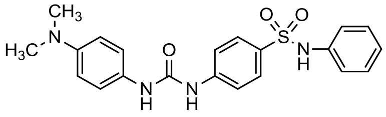	Inhibitor**	ND	ND
2.22#	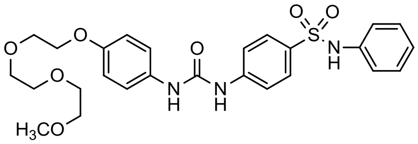	No change	ND	ND
2.23#	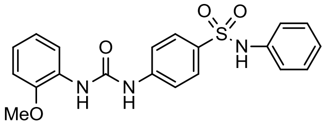	No change	ND	ND
2.24#	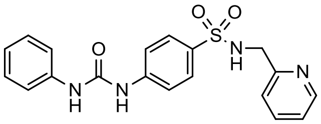	ND	ND	Toxic

* > 2-fold decrease, ** > 10-fold decrease. + > 2-fold increase. ND = not determined. Compounds were tested at 500 nM. # Synthesized by other group members.

2.4.1.5. Summary of SAR Studies on LED209

As shown in Tables 2.1-2.3, fragment B of LED209 is critical for biological activity, and the thiourea can be replaced with a urea with only a little loss in potency. Fragments A and D are sensitive to steric and electronic changes and can determine agonist or inhibitory activity. Changes to fragment C (data not shown, but done by other lab members) are detrimental to activity. Future work will focus on determining the solubility and ADME properties of the active analogs **2.09**, **2.17**, and **2.21**.

2.4.2 Synthesis of Tritium Labeled LED209 for Drug-Receptor Studies

Preliminary mechanistic studies showed that LED209 is a prodrug,[17] i.e, it’s converted to isothiocyanate OM188 in EHEC, and alkylates the K256 and K427 residues of QseC (Scheme 2.1).

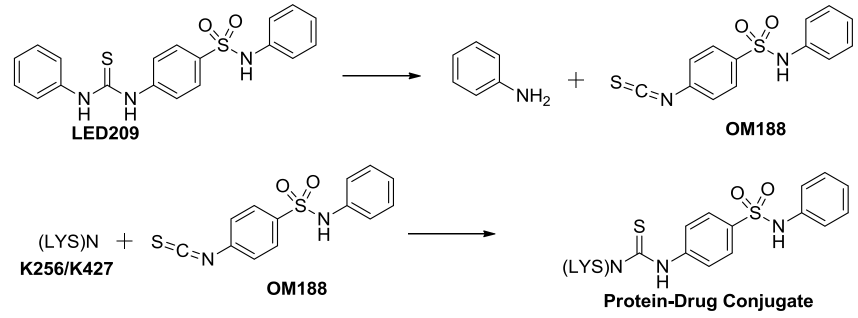

Scheme 2.1
Alkylation of lysine residues by LED209/OM188.

To further verify this mechanism, we proposed isolating a radiolabeled protein-drug conjugate. Based on the proposed mechanism and previous SAR studies, ring D was chosen to possess the radiolabel (Scheme 2.2). To reduce the number of synthetic steps that involved radiolabeled material, our approach to labeled LED209* involved a late stage addition of commercial tritiated aniline* in ethanol to intermediate **2.25** (Scheme 2.2).

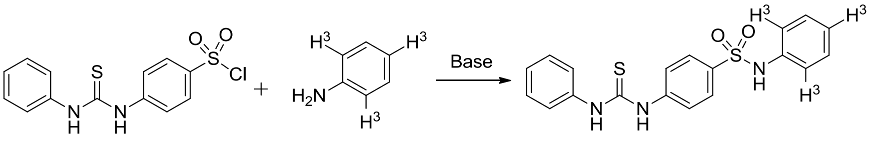

2.25

LED209*

Scheme 2.2
Tritium labeled LED209*

Unfortunately, various efforts to synthesize **2.25** failed (Scheme 2.3). As shown in scheme 2.3, reaction of **2.28** with various chlorinating agents led to activation and hydrolysis of the thiourea to form **2.29**. Furthermore, the addition of aniline to isothiocyanate **2.31** favored addition at the sulfonyl chloride to give **2.33** and LED209.

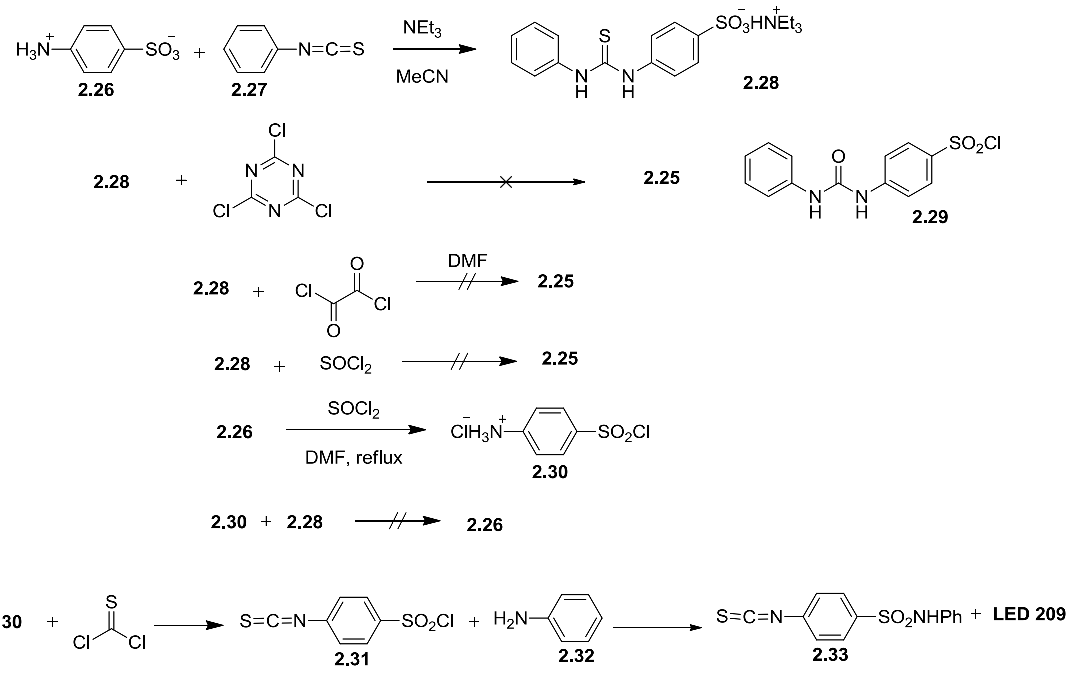
2.26
2.27
NEt3
MeCN
2.28
2.28
2.25
2.29
2.28
DMF
2.25
2.28
SOCl2
2.25
2.26
SOCl2
DMF, reflux
2.30
2.30
2.28
2.26
2.30
2.31
2.32
2.33
LED 209

Scheme 2.3
Failed attempts at the synthesis of **2.25**.

At this stage, I decided to explore a less reactive analog of **2.33**, sulfonyl imidazole **2.34**, (Scheme 2.4) as a precursor to LED209*.

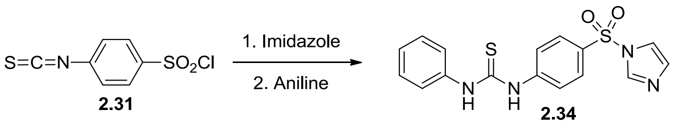
2.31
1. Imidazole
2. Aniline
2.34

Scheme 2.4
Synthesis of sulfimidazolide **2.34** as a surrogate for **2.25**.

With **2.34** in hand, I explored the substitution of the sulfimidazolide with aniline. Test experiments showed that the biological activity of LED209 was not inhibited by LED209 in ethanol containing small amounts of acetone; therefore, acetone was chosen as the solvent for a model substitution reaction. The reaction of sulfimidazolide **2.34** and aniline hydrochloride in the presence of Na_2CO_3 or $NaHCO_3$ produced no product. However, the reaction in the absence of any base gave the desired product in greater than 50% yield. This reaction probably occurs by activation and nucleophilic substitution of the imidazolide by the hydrochloride salt of aniline. Neutralization of the acid by extraneous base prevents product formation.

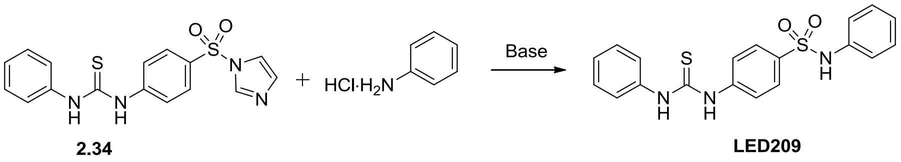

Table 2.4. Conversion of sulfimidazolide **2.34** to LED 209.

Additive	Temperature (°C)	Solvent	Result
$NaHCO_3$	60	Acetone	No reaction
Na_2CO_3	60	Acetone	No reaction
none	40	Acetone	>50%
none	40	Acetone/Ethanol	>50%

Reactions were carried out using 0.07mmol each of **2.34** and aniline hydrochloride over 10 h. The presence of the product was confirmed by thin layer chromatography analysis and ^{1}H NMR of the crude reaction mixture.

Future work will focus on forming LED209* and incubating it with cells.

2.4.3.1. Development of Novel Inhibitors of QseC Mediated Virulence Gene Expression

Due to some of the undesired properties of the LED209 scaffold, *viz.*, poor solubility, undesired chemical reactivity, and the paucity of sites for further chemical modifications, we decided to explore the SAR of other QseC inhibitor scaffolds identified from previous survey studies. Furthermore, the back up to LED209, **2.09** (Table 2.1), was not sufficiently active against the replication of *Salmonella* in infected J774 macrophages, and an alternative was needed. We chose CF308 as a lead due to its moderate activity (500 nM activity) against *ler* expression, better water solubility, and room for further SAR exploration. As with LED209, CF308 was divided into a heterocyclic A fragment, amide B fragment, and phenyl C fragment (Figure 2.8).

Bioactivity in the *Salmonella* assay was determined by comparison of the number of colony forming units (CFU) in non-treated and antagonist treated *Salmonella* infected macrophages.[5]

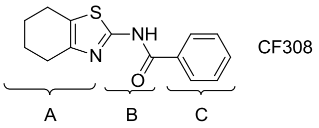

Figure 2.8
Structure and composition of CF308.

Previous SAR studies suggested that the cyclohexyl ring of fragment A was responsible for the loss in biological activity of CF308 against *Salmonella* in infected macrophages. Therefore, 2-thiazole rather than 4,5,6,7-tetrahydrobenzo[d]thiazole analogs were examined.

The SAR study began by modulating the electronic system of fragment C. Analogs **2.35** and **2.36** with electron-withdrawing substituents showed good activity against *Salmonella* but activated *ler* and *eae* expression in EHEC respectively. As in the LED209 series, 1,3,4-thiadiazole **2.37** was devoid of activity against both EHEC and *Salmonella*. Analog **2.38** with an electron-donating substituent showed excellent inhibitory activity in both assays, while the positional isomer **2.40** only showed good activity against EHEC. It should be noted that the rapid metabolism of **2.38** could prevent its development as a future *Salmonella* drug. On the other hand, imidazole derivative **2.39** and thiazole **2.41** activated virulence gene expression in EHEC. These results suggested that the sterics rather than the electronics of fragment C are important for inhibitory activity in the *Salmonella* assay. With **2.39** as a lead, substitutions on the thiazole ring A were examined. Substitution with a *p*-tolyl at the 4-position (**2.42**) or with methyls at the 4- and 5-positions (**2.43**) retained activity against EHEC, but abolished activity against *Salmonella*.

Table 2.5. Biological and metabolic studies of new scaffolds

ID	Structure	GI_{50}(μM)	S9 (min)	Hep. (min)	S. Typhi. (Inv. Macrop.)^{a,b}	EHEC (qPCR)^{a,b}
2.35	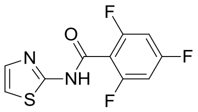	>50	>240	173	-1	ler: +3 eae: 0 stx2: 0
2.36	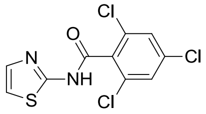	ND	ND	ND	-2	ler: 0 eae: +3 stx2: 0
2.37	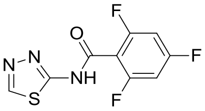	ND	ND	ND	0	ler: 0 eae: 0 stx2: 0
2.38	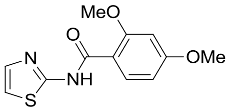	23	34	64	-2	ler: -3 eae: -2 stx2: -3
2.39	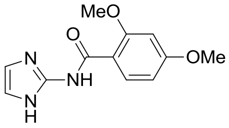	ND	ND	ND	ND	ler: +2 eae: 0 stx2: +2
2.40	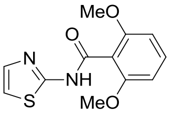	ND	ND	ND	0	ler: -2 eae: 0 stx2: -3
2.41	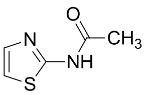	>50	>240	>240	0	ler: +3 eae: 0 stx2: +2
2.42	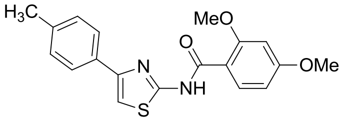	ND	ND	ND	0	ler: -3 eae: -2

						stx2: -2
2.43	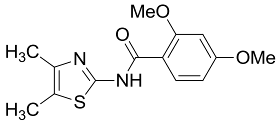	ND	ND	ND	0	ler: -3 eae: -3 stx2: -3

[a]Score of 0, 1, 2, and 3 correspond to not active, active at 500 nM, 5 nM, and 5 pM, respectively.[b] – sign signifies inhibitory activity, + sign signifies agonist activity. > 2-fold change = active. ND = not determined.

From the above results, it could be inferred that fragment C instead of A was more amenable to structural changes. Rather than changes in electron density of fragment C, we focused on bulkiness. Comparison of **2.36** and **2.41** suggests that a sterically bigger group is better than a smaller group. The adamantyl moiety is present in several medicinal agents including antivirals such as amantidine, rimantadine, and tromantadine. The lipophilic nature of the adamantyl makes it a rational choice for inclusion in drugs with membrane-bound targets.

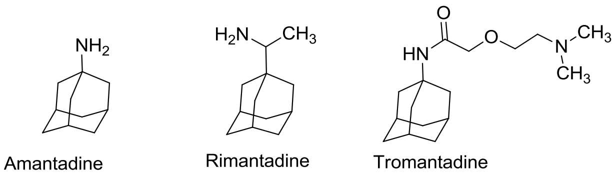

Figure 2.9
Structures of adamantane containing antivirals.

Thus, we decided to begin further explorations of fragment C with adamantyl analog **2.44**. As shown in Table 2.06, bulky **2.44** was a potent inhibitor of EHEC virulence gene expression both *in vitro* and *in vivo*, and a decrease in bulkiness (**2.45-2.47**) was detrimental to activity. A reversal in the connectivity of the amide as exemplified in **2.48**, led to a loss in activity against EHEC and no activity against *Salmonella*. Hydroxylation of the adamantyl (**2.49**) caused a reversal in agonist activity in both EHEC and *Salmonella*. Thus, **2.49** is an activator of viral gene expression and a potential biological research tool. Dimeric compound **2.50** retained activity against EHEC *in vitro*, while dimeric compound **2.52** was the only compound in this series that possessed significant activity against both EHEC and *Salmonella*. The parent adamantyl carboxylic acid was active against EHEC *in vitro* but failed in the *in vivo* assays. This result suggests the involvement of adamantane carboxylic acid in the anti-virulence activity of these analogs. Finally, *N*-methylation of **2.44** (**2.53**) led to a loss in potency. Unfortunately, all of these analogs, except **2.52**, were inactive in the *Salmonella* assay. Sequestration of these analogs in the plasma membrane of macrophages, and/or the inability to reach the target *Salmonella* inside the macrophages could be responsible for the lack of activity of these compounds. Therefore, the adamantyl analogs are most efficacious as EHEC drugs and future analogs were tested in EHEC assays.

Table 2.6. qPCR and survival data for adamantyl scaffolds.

ID	Structure	Genes	*In vitro* Score (qPCR)^{a,b}	*In vivo* Score (Macrophages)^{a,b}	
				Salmonella	EHEC
2.44	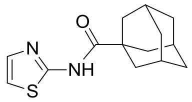	ler	-3	0	Active (-3)
		eae	-3		
		stx2	-3		
2.45	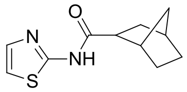	ler	0	0	Inactive (0)
		eae	-1		
		stx2	Activates (+2)		
2.46	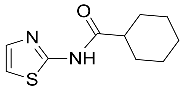	ler	0	0	ND
		eae	0		
		stx2	0		
2.47	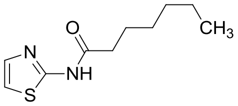	ler	-2	0	ND
		tir	-2		
		stx2	-2		

2.48	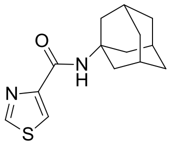	ler	-2	0	Inactive
		tir	-2		
		stx2	0		
2.49	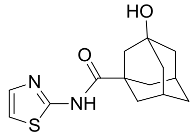	ler	Activates (+2)	Agonist (+2)	agonist
		tir	0		
		stx2	Activates (+3)		
2.50	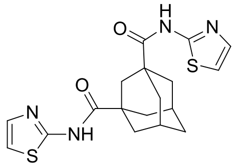	ler	-3	Inactive	Inactive
		tir	-3		
		stx2	-1		
2.51	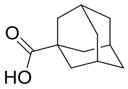	ler	-3	ND	ND
		tir	-3		
		stx2	-3		
2.52	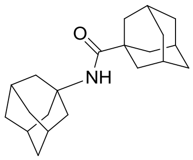	ler	-1	-2	-1
		tir	-1		
		stx2	-1		
2.53	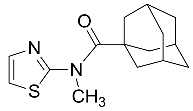	ler	-1	ND	ND
		eae	-1		
		stx2	-1		

[a]Score of 0, 1, 2, and 3 correspond to not active, active at 500 nM, 5 nM, and 5 pM, respectively.[b] – sign signifies inhibitory activity, + sign signifies agonist activity. > 2-fold change = active. ND = not determined.

Metabolic analysis (S9 fraction incubation) of **2.44** showed that it had a short half-life of just 10 minutes (Table 2.7). However, **2.44** was stable *in vitro* in mouse plasma for 24h. We reasoned that hydroxylation of the tertiary carbons on **2.44** by cytochrome P450 was responsible for the short half-life. Indeed, LC-MS analyses of the extracted S9 fraction incubate of **2.44** showed the presence of **2.49**. Therefore, blocking of the tertiary carbons was necessary. To our delight, **2.54** which has two of the three tertiary carbons on the adamantane methylated retained potency against EHEC and was more stable (Table 2.7). With **2.54** as the new lead compound, modifications to the heterocyclic ring were examined.

Imidazole **2.55** retained potency against EHEC at 500 nM but was not tested at 5 pM. On the other hand, oxazole **2.56** stimulated tir expression at 500 nM. Dimethyl substituted analog **2.57** was rapidly metabolized in the S9 fraction assay and was not further tested. Electron-withdrawing groups at the C5 position of the heterocycle retained the biological activity in some cases (**2.58**, **2.60**, and **2.62**). The inactivity of **2.59** and **2.61** suggests a possible steric influence on the biological activity. Also, possible hydrolysis of the ester or the formation of an acidic species could explain the inactivity of **2.59**. The urea analog **2.63** showed no advantage over lead **2.54**. Since **2.58** and **2.60** showed some toxicity against adrenergic receptor, further biological studies will continue with **2.54** and **2.62**.

Table 2.7. Stability and biological activity of adamantyl scaffolds.

ID	Structure	Blood T ½ (min)	S9 T ½ (min)	Hepatocyte T ½ (min)	Hela cell Tox.	EHEC (qPCR)^{a,b}
2.44	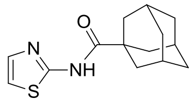 Solubility (646±79 ng/ml, PBS)	ND	10±1	ND	ND	ler: -3 eae: -3 stx2: -3
2.54	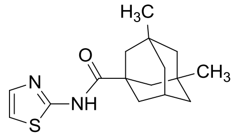	ND	> 240 (385)	80	IC50 = 660 μM	ler: -2 eae: -2 stx2: -2
2.55	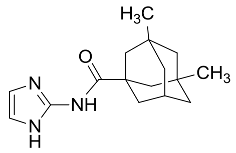	>240	75	71	ND	ler: -1 tir: -1 stx2: -2
2.56	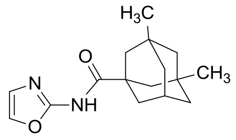	119	52	ND	ND Poor stability	ler: 0 tir: +2 stx2: 0

2.57	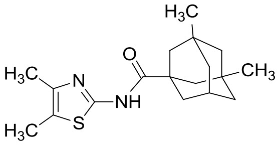	ND	18	ND	ND Poor stability	ND ND ND
2.58	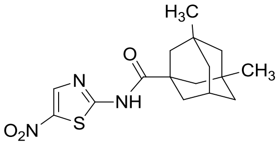	>240	>240	>240	ND	ler: -3 tir: -3 stx2: -3
2.59	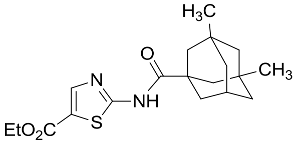	Human: >240 Mice: 7	26	ND	ND	ler: +2 tir: 0 stx2: +2
2.60	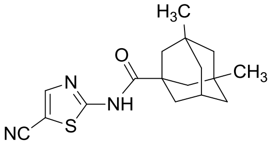	Human: >240 Mice: >240	Mice: >240	ND	ND	ler: -2 tir: -2 stx2: -1
2.61	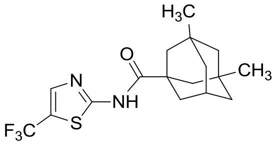	ND	Mice: 248	ND	GI50 = 16.6 μM IC50 > 30 μM	ler: 0 tir: 0 stx2: 0
2.62	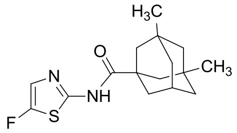		Mice: 92		GI50 = 20.8 μM IC50 > 30 μM	ler: -1 tir: -1 stx2: -1
2.63	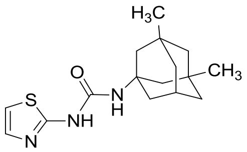	>240	117	>240	ND	ler: +1 tir: 0 stx2: 0

[a]Score of 0, 1, 2, and 3 correspond to not active, active at 500 nM, 5 nM, and 5 pM, respectively.[b] – sign signifies inhibitory activity, + sign signifies agonist activity. > 2-fold change = active. ND = not determined.

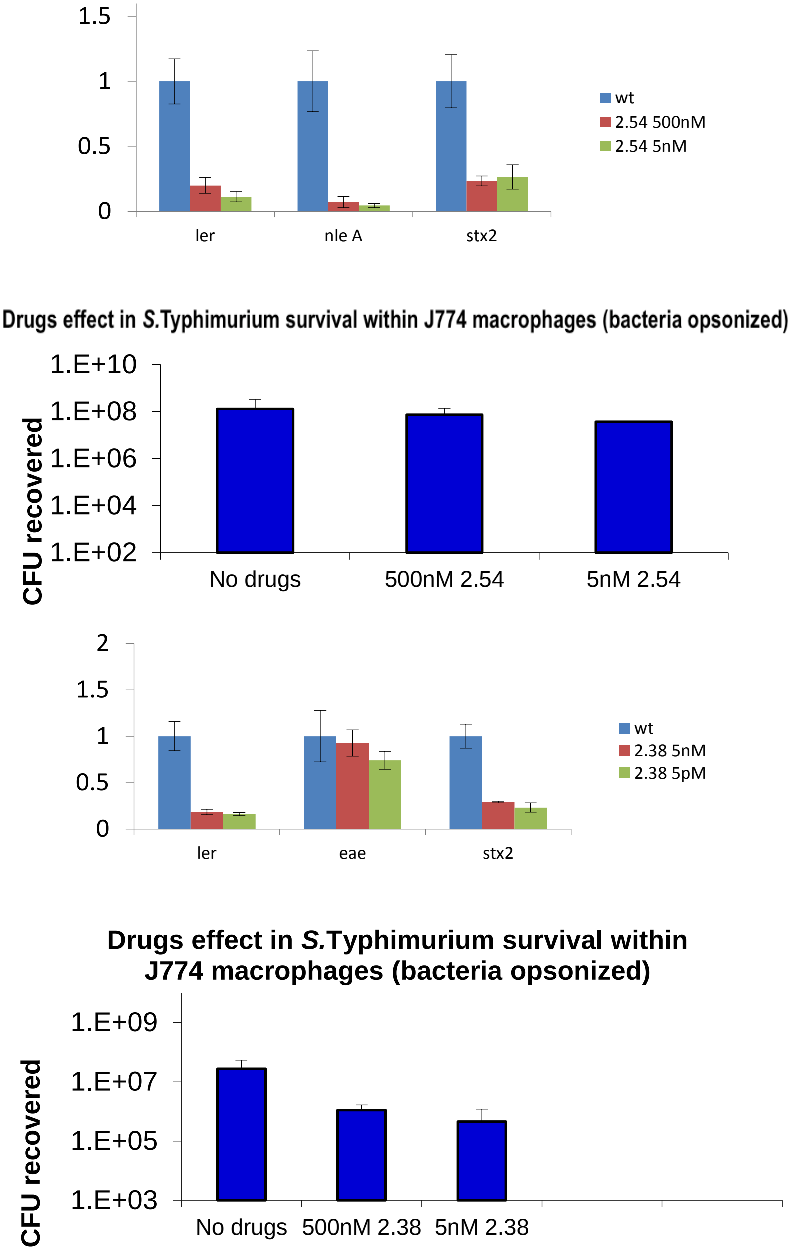

Figure 2.10
Real time qPCR and macrophage survival data for **2.54** and **2.38.**

2.4.3.2 Summary of SAR Study on New Scaffold

A new class of inhibitors of virulence gene expression in EHEC and *Salmonella* were developed through modification of the steric and electronic parameters of CF308. Compound **2.38** was the best drug against *Salmonella*, while **2.54** and **2.62** were the most effective drugs against EHEC. Future work will focus on animal studies of these compounds.

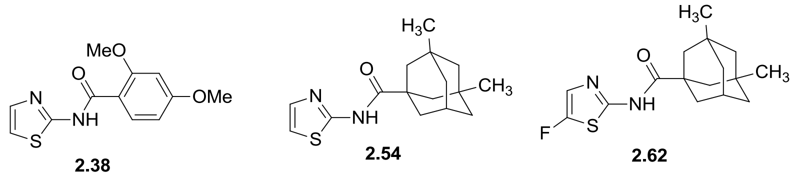

2.38 **2.54** **2.62**

Figure 2.11
Structures of most potent EHEC drugs in this study.

2.5 Conclusion

Two distinct classes of inhibitors of QseC mediated virulence gene expression in *Salmonella* and EHEC were explored. Studies on the first class of inhibitors confirmed the importance of a urea or thiourea moiety for QseC mediated virulence gene expression, and led to the discovery of potential sites for functionalization with polar groups and radiolabels. Biological activity in the second class was highly dependent on pharmacokinetic parameters (such as enzyme metabolism) and target location (in macrophages). Both classes were relatively intolerant to steric congestion but amenable to changes in electron density and polarity, which suggests a small binding site for both inhibitor classes. Although the mechanism of action for the second class of inhibitors is unknown, the presence of potential alkylating sites suggests a similar covalent mode of action as the thiourea class of inhibitors. Of note is the fact that both classes were discovered from the same high-throughput screen. Although covalent modification of certain receptors/targets by drugs is undesired, covalent modification of targets with rapid turn-over frequencies is a powerful and highly effective inhibitory mechanism. In fact, several important drugs such as aspirin, penicillin, and omeprazole covalently modify their targets.[29] Alternatively, hydrogen bonding and hydrophobic interactions may be responsible for binding. Inhibitors of AI-2 binding to LuxPQ with similar chemical structures (Figure 2.12) to the second scaffold were identified through the DOCK6 virtual HTS and optimized *in silico* and *in vitro*.[30] These molecules were reported to bind via hydrogen bonding and hydrophobic interactions. Future work will explore the efficacy of the new scaffold in infected mice, as well as mechanistic studies on the binding site.

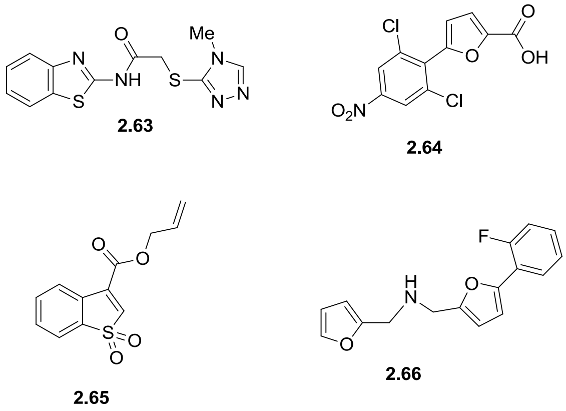

2.63

2.64

2.65

2.66

Figure 2.12
Inhibitors of AI-2 activation of LuxPQ.

Thus, the structural differences of both classes of inhibitors/activators of QseC mediated virulence gene expression discussed above provide some information on potential binding modes to QseC. These findings should be relevant for the development of other anti-virulence chemical probes and clinically relevant bacterial anti-virulence agents.

2.6 Experimental

General Methods and Materials. Proton and carbon nuclear magnetic resonance spectra (^{1}H and ^{13}C NMR) were recorded at 500 MHz and 126 MHz, respectively, or at 400 MHz and 101 MHz, respectively, in $CDCl_3$ with TMS as internal standard, unless otherwise stated. ^{1}H NMR data are reported as follows: chemical shift (ppm), multiplicity (s = singlet, br s = broad singlet, d = doublet, t = triplet, q = quartet, app q = apparent quartet, qn = quintet, app qn = apparent quintet, m = multiplet), h = heptet, and coupling constant (Hz). Melting points were measured using an automated melting point apparatus and are uncorrected. Analytical thin layer chromatography (TLC) used EMD Chemicals TLC silica gel 60 F_{254} plates (0.040-0.063 mm) with visualization by UV light and/or $KMNO_4$ or phosphomolybdic acid (PMA) solution followed by heating. Chromatographic purifications utilized preparative TLC or flash chromatography using pre-packed SiO_2 columns on an automated medium pressure chromatograph. Unless otherwise noted, yields refer to isolated, purified material with spectral data consistent with assigned structures or, if known, were in agreement with published data. All reactions were conducted under an argon atmosphere in oven-dried glassware with magnetic stirring. Reagents were purchased at the highest commercial quality and used without further purification. Reaction solvents were dried by passage through a column of activated, neutral alumina under argon and stored under argon until use.

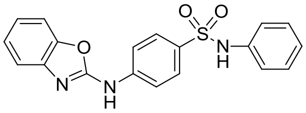

4-(Benzo[d]oxazol-2-ylamino)-N-phenylbenzenesulfonamide

A mixture of 2-chorobenzoxazole (61.9 mg, 0.403 mmol) and 4-amino-N-phenylbenzenesulfonamide (100 mg, 1 equiv) in *o*-xylene (0.62 mL) was refluxed at 155 °C in a sealed tube for 4 h. The reaction was cooled to r.t, diluted with water, extracted 3 times with EtOAc, dried over anhydrous Na_2SO_4, filtered and concentrated by rotary evaporation. The crude product was purified by analytical thin-layer chromatography (TLC). Eluent: EtOAc/hexanes (1:1) to give the product as a tan solid (25.9 mg), 18%, mp: 241.2-245.9 °C (dec).

^{1}H NMR (400 MHz, acetone-d_6) δ 7.98 – 7.90 (m, 2H), 7.82 – 7.73 (m, 2H), 7.45 (ddd, *J* = 7.8, 1.3, 0.6 Hz, 1H), 7.38 (ddd, *J* = 8.0, 1.2, 0.6 Hz, 1H), 7.27 – 7.18 (m, 5H), 7.14 (ddd, *J* = 7.9, 7.5, 1.3 Hz, 2H), 7.07 – 6.97 (m, 1H); ^{13}C NMR (101 MHz, acetone-d_6) δ 158.1, 148.4, 143.7, 143.3, 139.0, 133.8, 130.0, 129.5, 125.2, 125.1, 123.3, 121.6, 118.3, 118.1, 110.0.

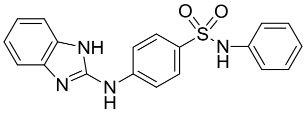

4-((1*H*-Benzo[d]imidazol-2-yl)amino)-*N*-phenylbenzenesulfonamide

A solution of 1,1′-thiocarbonyldiimidazole (34 mg, 90%, 0.172 mmol) and 4-amino-*N*-phenylbenzenesulfonamide (42 mg, 1 equiv) in anhydrous tetrahydrofuran (THF, 2.5 mL) was stirred at rt for 12 h. Benzene-1,2-diamine (18.6 mg, 1 equiv) and dicyclohexylcarbodiimide (53 mg, 1.5 equiv) were added to the reaction, and the mixture was heated at 70 °C for 18 h. The reaction was cooled to r.t. and an aliquot was purified by TLC (70% EtOAc/hexanes) to give the product as a brown paste (20 mg).

^{1}H NMR (400 MHz, acetone-d$_6$) δ 7.99 – 7.87 (m, 2H), 7.76 – 7.64 (m, 2H), 7.32 (s, 2H), 7.20 (d, *J* = 4.3 Hz, 4H), 7.08 – 6.95 (m, 3H), 2.01 (p, *J* = 2.2 Hz, 2H); ^{13}C NMR (101 MHz, acetone-d$_6$) δ 149.3, 144.9, 138.2, 131.1, 129.0, 128.4, 124.1, 120.8, 120.6, 116.4.

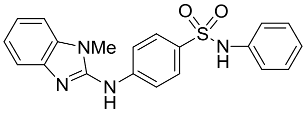

4-((1-Methyl-1*H*-benzo[d]imidazol-2-yl)amino)-*N*-phenylbenzenesulfonamide

The same procedure as above using *N*^{1}-methylbenzene-1,2-diamine (21 mg, 0.172 mmol). Purification by TLC (70% EtOAc/hexanes) gave the product (33 mg, 51%).

^{1}H NMR (400 MHz, DMSO-d$_6$) δ 10.07 (s, 1H), 9.37 (s, 1H), 7.92 (d, *J* = 8.9 Hz, 2H), 7.67 (d, *J* = 8.7 Hz, 2H), 7.43 – 7.35 (m, 1H), 7.35 – 7.28 (m, 1H), 7.19 (dd, *J* = 8.5, 7.2 Hz, 2H), 7.11 – 7.02 (m, 4H), 7.00 – 6.91 (m, 1H), 3.68 (s, 3H); ^{13}C NMR (100 MHz, DMSO-d$_6$) δ 149.2, 144.9, 141.2, 138.1, 134.0, 130.6, 129.1, 128.0, 123.7, 121.1, 120.3, 119.8, 116.9, 116.6, 108.5, 29.1.

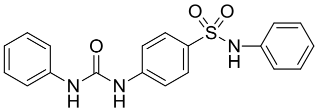

***N*-phenyl-4-(3-phenylureido)benzenesulfonamide**

A mixture of 4-amino-*N*-phenylbenzenesulfonamide[31] (80 mg, 0.322 mmol), phenylisocyanate (38.4 mg, 35 µL, 1equiv) and triethylamine (NEt$_3$, 65.2 mg, 90 µL, 2 equiv) in THF (2 mL) was heated at 60 °C for 12 h. The reaction mixture was concentrated by rotary evaporation, and the residue was purified by TLC (EtOAc/hexanes, 1:1, 2 elutions) to give the title product (44 mg, 37%).

^{1}H NMR (300Mz, acetone-d$_6$): δ 8.78 (br, 1H), 8.12 (br s, 2H), 7.77-7.42 (m, 2H), 7.60-7.49 (m, 5H), 7.42 (d, *J* = 9.0 Hz, 2H), 7.26 (t, *J* = 7.2 Hz, 1H), 7.09 (d, *J* = 8.7 Hz, 2H), 6.99 (t, *J* = 7.2

Hz, 1H); ^{13}C NMR (100 MHz, acetone-d_6) δ 152.4, 140.0, 139.9, 137.3, 132.6, 131.7, 128.9(2), 128.6(2), 127.0 (2), 122.8(2), 122.0, 119.1(2), 118.5(2).

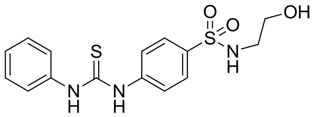

Synthesis of *N*-(2-hydroxyethyl)-4-(3-phenylthioureido)benzenesulfonamide

A mixture of *N*-(2-hydroxyethyl)-4-nitrobenzenesulfonamide[32] (530 mg, 2.15 mmol) and 5% wt Pd/C (53 mg) in anhydrous THF (13 mL) was stirred under hydrogen (1 atmosphere) for 16 h. The reaction was diluted with ethyl acetate and filtered through Celite™. The filtrate was concentrated by rotary evaporation and further dried under high vacuum to give 4-amino-*N*-(2-hydroxyethyl)benzenesulfonamide as a light brown solid (459 mg, 98%). To a solution of 4-amino-*N*-(2-hydroxyethyl)benzenesulfonamide (200 mg, 0.925 mmol) in anhydrous acetonitrile (9 mL) was added phenylisothiocyanate (180 µL, 1 equiv). The reaction was stirred at 70 °C for 24h. The reaction mixture was concentrated in vacuo and purified via TLC (80% EtOAc/hexanes, 2 elutions) to give the title product (22 mg, 7%) as a white solid (mp, 129.2 °C). ^{1}H NMR (400 MHz, methanol-d_4) δ 7.83 – 7.78 (m, 2H), 7.75 – 7.70 (m, 2H), 7.47 – 7.42 (m, 2H), 7.40 – 7.34 (m, 2H), 7.24 – 7.17 (m, 1H), 3.55 (t, J = 6.0 Hz, 2H), 2.96 (t, J = 6.0 Hz, 2H); ^{13}C NMR (100 MHz, methanol-d_4) δ 180.4, 143.4, 138.6, 135.6, 128.5(2), 127.2(2), 125.4, 124.1(2), 123.0(2), 60.4, 44.8.

General Procedure A:

To an oven dried flask containing amine (1 mmol), acid chloride (1 equiv), and *N*,*N*-dimethylaminopyridine (DMAP, 1.2 equiv) was added anhydrous DCM (10 mL). The reaction was continued overnight. After completion as judged by TLC, the reaction was quenched with water, extracted 3 times with dichloromethane, and the combined organic extracts were dried over anhydrous Na_2SO_4. After filtration through a fritted funnel and concentration by rotary evaporation, the crude product was purified via TLC to give the desired product.

General Procedure B:

To an oven dried flask containing amine (1.2 equiv), carboxylic acid (1 mmol), 1-ethyl-3-(3-dimethylaminopropyl)carbodiimide hydrochloride (EDCI.HCl, 1.2 equiv), hydroxybenzotriazole (HOBt, 1.2 equiv) and diisopropylethylamine (DIPEA, 2.4 equiv) was added anhydrous *N*,*N*-dimethylformamide (DMF, 10 mL). The reaction was continued overnight. After completion by TLC, the reaction was quenched with water, extracted 3 times with ethyl acetate, and the combined organic extracts were dried over Na_2SO_4. Following filtration through a fritted funnel and concentration by rotary evaporation, the crude product was purified via TLC to give the desired product.

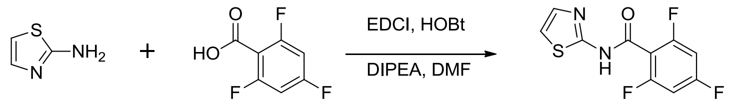

2,4,6-trifluoro-*N*-(thiazol-2-yl)benzamide

The title compound was synthesized according to General Procedure B using thiazol-2-amine (50 mg, 0.48 mmol) and 2,4,6-trifluorobenzoic acid (104 mg, 1.2 equiv). The product was isolated as white needles (23 mg, 25%) after TLC (1:1 EtOAc/hexanes).

1H NMR (400 MHz, DMSO-d_6) δ 13.00 (s, 1H), 7.56 (d, *J* = 3.6 Hz, 1H), 7.44 – 7.33 (m, 3H); ^{13}C NMR (101 MHz, DMSO-d_6) δ 163.3 (dt, ^1J(C-4,F-4) = 251 Hz, ^3J(C-4,F-2) = 15.8 Hz), 159.6 (dd, ^1J(C-2,F-2) = 252 Hz, ^3J(C-2,F-4) = 16.0), 159.5 (dd, ^1J(C-2,F-2) = 252 Hz, ^3J(C-2,F-4) = 16.0), 157.6, 157.3, 137.9, 114.5, 111.1 – 109.7 (m), 101.4 (t, ^2J(C-3,F-2/4) = 26.7 Hz), 101.4 (t, ^{2}J(C-3,F-2/4) = 26.7 Hz); ^{19}F NMR (376 MHz, DMSO-d_6) δ -103.7 (p, 1F, ^{4}J(F-4,F-2) = 8.8 Hz, F-4), -110.0 (t, 2F, ^{4}J(F-2,F-4) = 8.2 Hz, F-2).

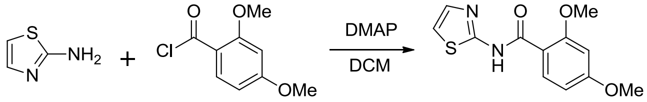

2,4-dimethoxy-*N*-(thiazol-2-yl)benzamide

The title compound was synthesized according to General Procedure A using thiazol-2-amine (50 mg, 0.48 mmol) and 2,4-dimethoxybenzoyl chloride (116 mg, 1.2 equiv). The product was isolated as white crystals (19 mg, 15%, mp: 137.3 °C) after TLC (1:1 EtOAc/hexanes).

^{1}H NMR (400 MHz, acetone-d_6) δ 11.00 (br s), 1H), 8.14 (d, *J* = 8.8 Hz, 1H), 7.48 (d, *J* = 3.6 Hz, 1H), 7.15 (d, *J* = 3.6 Hz, 1H), 6.83 – 6.72 (m, 2H), 4.17 (s, 3H), 3.93 (s, 3H); ^{13}C NMR (101 MHz, acetone-d_6) δ 165.0, 161.9, 159.6, 157.8, 137.8, 133.5, 113.4, 112.0, 106.7, 98.5, 56.2, 55.3, 55.2.

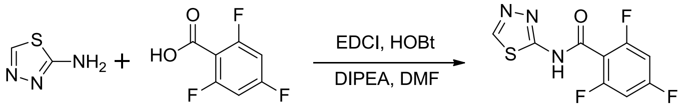

2,4,6-trifluoro-*N*-(1,3,4-thiadiazol-2-yl)benzamide

The title compound was synthesized according to General Procedure B using 1,3,4-thiadiazol-2-amine (150 mg, 1.47 mmol) and 2,4,6-trifluorobenzoic acid (310 mg, 1.2 equiv). The product was isolated as white needles (240 mg, 63%, mp: 198.3 °C) after SiO_2 column chromatography (1:1 EtOAc/hexanes).

^{1}H NMR (400 MHz, DMSO-d_6) δ 13.50 (s, 1H), 9.30 (s, 1H), 7.42 (dddd, *J* = 10.4, 9.4, 3.4, 1.7 Hz, 2H); ^{13}C NMR (100 MHz, DMSO-d_6) δ 163.5 (dt, ^{1}J(C-4,F-4) = 251 Hz, ^{3}J(C-4,F-2) = 15.7 Hz), 159.8 (dd, ^{1}J(C-2,F-2) = 252 Hz, ^{3}J(C-2,F-4) = 16.0), 159.7 (dd, ^{1}J(C-2,F-2) = 252 Hz, ^{3}J(C-

2,F-4) = 16.0), 158.2, 158.1, 149.5, 110.2 – 109.0 (m), 101.6 (t, ^{2}J(C-3,F-2/4) = 26.7 Hz), 101.5 (t, ^{2}J(C-3,F-2/4) = 26.7 Hz); ^{19}F NMR (376 MHz, DMSO-d_6) δ -102.8 – 103.1 (m, 1F, F-4), -109.6 (t, 2F, ^{4}J(F-2,F-4) = 8.4 Hz, F-2).

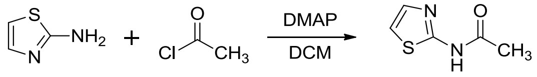

N-(thiazol-2-yl)acetamide

The title compound was synthesized according to General Procedure A using thiazol-2-amine (50 mg, 0.48 mmol) and acetyl chloride (46 mg, 1.2 equiv). The product was isolated as white solid (89 mg, 70%, mp: 191.3 °C) after SiO_2 column chromatography (1:1 EtOAc/hexanes).

^{1}H NMR (400 MHz, $CDCl_3$) δ 12.82 (s, 1H), 7.44 (d, *J* = 3.4 Hz, 1H), 7.00 (d, *J* = 3.6 Hz, 1H), 2.35 (s, 3H); ^{13}C NMR (101 MHz, $CDCl_3$) δ 168.3, 160.5, 136.1, 113.6, 23.2.

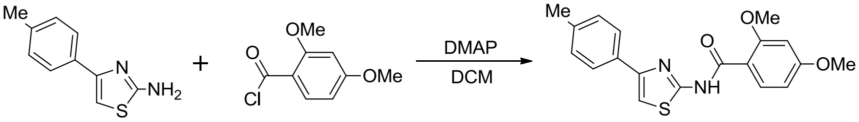

2,4-dimethoxy-*N*-(4-(*p*-tolyl)thiazol-2-yl)benzamide

The title compound was synthesized according to General Procedure A using 4-(*p*-tolyl)thiazol-2-amine (100 mg, 0.53 mmol) and 2,4-dimethoxybenzoyl chloride (126 mg, 1.2 equiv). The product was isolated as white solid (65 mg, 35%, mp: 216.7-216.8 °C) after SiO_2 column chromatography (30-100% EtOAc/hexanes).

^{1}H NMR (400 MHz, DMSO-d_6) δ 11.49 (s, 1H), 7.97 – 7.77 (m, 3H), 7.59 (s, 1H), 7.32 – 7.16 (m, 2H), 6.85 – 6.63 (m, 2H), 4.01 (s, 3H), 3.87 (s, 3H), 3.33 (s, 2H), 2.33 (s, 3H); ^{13}C NMR (101 MHz, DMSO-d_6) δ 164.0, 163.0, 159.1, 157.5, 149.0, 137.1, 132.5, 131.5, 129.2, 125.7, 113.0, 107.5, 106.3, 98.7, 56.5, 55.7, 20.8.

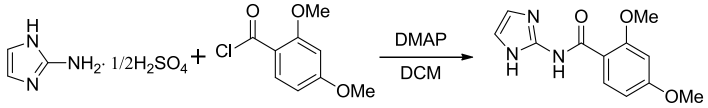

N-(1H-imidazol-2-yl)-2,4-dimethoxybenzamide

The title compound was synthesized according to General Procedure A using the acid salt of 1*H*-imidazol-2-amine (150 mg, 0.53 mmol) and 2,4-dimethoxybenzoyl chloride (199 mg, 1.2 equiv). The product was isolated as white solid (15 mg, 6%, mp: 173.6 °C) after TLC (5% MeOH in DCM).

^{1}H NMR (400 MHz, methanol-d_4:benzene-d_6 (2.7:1)) δ 8.21 (d, *J* = 8.8 Hz, 1H), 6.80 (s, 2H), 6.58 (ddd, *J* = 8.9, 2.4, 1.1 Hz, 1H), 6.53 – 6.47 (m, 1H), 3.81 (d, *J* = 1.4 Hz, 3H), 3.67 (d, *J* = 1.4 Hz, 3H); ^{13}C NMR (100 MHz, methanol-d_4:benzene-d_6 (2.7:1)) δ 166.0, 164.2, 160.5, 142.6, 134.5, 113.2, 107.2, 99.40, 56.4, 56.0.

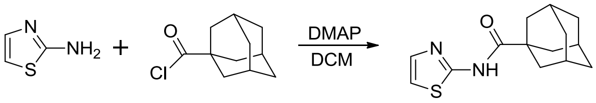

(3*r*,5*r*,7*r*)-*N*-(thiazol-2-yl)adamantane-1-carboxamide

The title compound was synthesized according to General Procedure A using thiazol-2-amine (5.0 g, 50 mmol, 1.2 equiv) and adamantane-1-carbonyl chloride (8.3 g, 42 mmol). The product was isolated as white solid (4.9 g, 45%, mp: 199.5 – 200.0 °C) after purification using a Teledyne Isco Combiflash® *R*f chromatographic system (220 g SiO_2 column: eluted with 50% EtOAc/hexanes).

^{1}H NMR (400 MHz, $CDCl_3$) δ 9.96 (s, 1H), 7.46 (d, *J* = 3.6 Hz, 1H), 6.97 (d, *J* = 3.6 Hz, 1H), 2.18 – 1.98 (m, 3H), 1.92 (d, *J* = 3.1 Hz, 6H), 1.70 (q, *J* = 12.6 Hz, 6H); ^{13}C NMR (101 MHz, $CDCl_3$) δ 176.0, 159.4, 137.0, 113.8, 41.1, 40.4, 38.8, 36.3, 27.9.

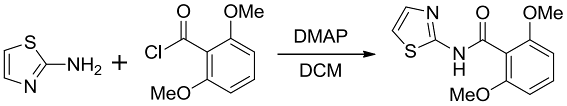

2,6-dimethoxy-*N*-(thiazol-2-yl)benzamide

The title compound was synthesized according to General Procedure A using thiazol-2-amine (100 mg, 0.96 mmol) and 2,6-dimethoxybenzoyl chloride (199 mg, 1.0 equiv). The product was isolated as white solid (23 mg, 10%, mp: 269.2 – 269.3 °C (decomp.)) after purification on SiO_2 column chromatography (1:1 EtOAc/hexanes) and recrystallization in DCM.

^{1}H NMR (400 MHz, methanol-d_4) δ 7.45 – 7.37 (m, 2H), 7.15 (d, *J* = 3.6 Hz, 1H), 6.74 (d, *J* = 8.5 Hz, 2H), 3.83 (s, 6H); ^{13}C NMR (100 MHz, methanol-d_4) δ 164.9, 158.8, 157.6, 136.9, 131.6, 113.6, 113.1, 103.7, 55.0.

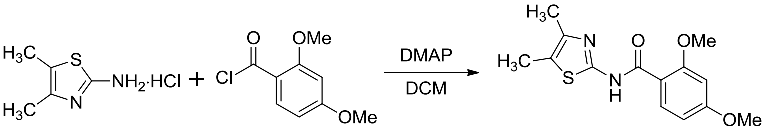

***N*-(4,5-dimethylthiazol-2-yl)-2,4-dimethoxybenzamide**

The title compound was synthesized according to General Procedure A using the acid salt of 4,5-dimethylthiazol-2-amine (100 mg, 0.6 mmol) and 2,4-dimethoxybenzoyl chloride (120 mg, 1.0 equiv). The product was isolated as white solid (26 mg, 15%, mp: 188.8 °C) after TLC (2% MeOH/DCM, eluted twice).

^{1}H NMR (400 MHz, acetone-d_6) δ 10.74 (s, 1H), 8.11 (d, *J* = 8.8 Hz, 1H), 6.78 (d, *J* = 2.3 Hz, 1H), 6.75 (dd, *J* = 8.8, 2.3 Hz, 1H), 4.16 (s, 4H), 3.92 (s, 4H), 2.28 (d, *J* = 1.1 Hz, 4H), 2.18 (d, *J* = 1.0 Hz, 4H); ^{13}C NMR (101 MHz, acetone-d_6) δ 164.8, 161.5, 159.5, 153.4, 142.2, 133.5, 119.2, 112.2, 106.6, 98.5, 56.1, 55.2, 13.7, 9.7.

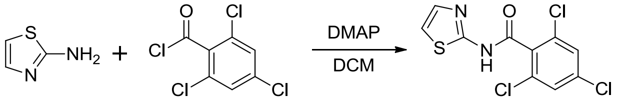

2,4,6-trichloro-*N*-(thiazol-2-yl)benzamide

The title compound was synthesized according to General Procedure A using thiazol-2-amine (150 mg, 1.5 mmol) and 2,4,6-trichlorobenzoyl chloride (439 mg, 1.2 equiv). The product was isolated as white solid (314 mg, 68%, mp: 196.9 °C) after purification using a Teledyne Isco Combiflash® *R*$_f$ chromatographic system (4 g SiO_2 column: eluted with DCM, 5 min; 0-5% MeOH/DCM, 5 min; 5% MeOH/DCM, 4 min).

1H NMR (400 MHz, $CDCl_3$) δ 7.86 (d, *J* = 5.1 Hz, 1H), 7.09 (s, 2H), 6.80 (d, *J* = 5.2 Hz, 1H); ^{13}C NMR (101 MHz, $CDCl_3$) δ 172.3, 167.3, 161.5, 136.6, 135.9, 134.8, 133.7, 132.0, 131.5, 127.4, 127.3, 121.2, 110.8.

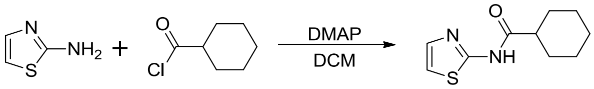

***N*-(thiazol-2-yl)cyclohexanecarboxamide**

To a flask containing thiazol-2-amine (1.2 equiv, 2 mmol) & DMAP (1.1 equiv) in DCM (10 mL) was added cyclohexanecarbonyl chloride (1 equiv, 1.67 mmol) slowly. The reaction was continued overnight. After completion as judged by TLC analysis, the solvent was evaporated and the concentrate was acidified with 10% HCl to bring pH 3. Water was added and the aqueous phase was extracted 2 times with EtOAc. The combined organic phase was dried over $MgSO_4$, filtered through a fritted funnel and concentrated by rotary evaporation. The concentrate was purified using Teledyne Isco Combiflash® *R*$_f$ chromatographic system (12 g, SiO_2 column, eluent: 10%, 6min; 10-30%, 4min; 30%, 5min; EtOAc/hexanes) to give the product as a white solid (344 mg, 98%, mp: 158.8 °C) R$_f$ ~ 0.8, 50% EtOAc/hexanes.

^{1}H NMR (400 MHz, CDCl$_3$) δ 11.75 (br s, 1H), 7.44 (d, *J* = 3.7 Hz, 1H), 7.00 (d, *J* = 3.7 Hz, 1H), 2.47 (tt, *J* = 11.7, 3.6 Hz, 1H), 1.97 (dd, *J* = 13.5, 3.7 Hz, 2H), 1.87 (dq, *J* = 12.9, 3.5 Hz, 2H), 1.73 (dd, *J* = 9.9, 4.2 Hz, 1H), 1.69 – 1.53 (m, 2H), 1.43 – 1.20 (m, 3H); ^{13}C NMR (101 MHz, CDCl$_3$) δ 174.2, 160.0, 135.8, 113.5, 44.9, 29.2, 25.6, 25.5.

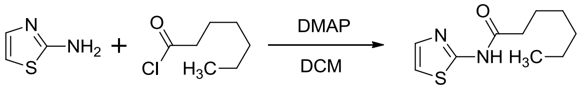

***N*-(thiazol-2-yl)heptanamide**

To a flask containing thiazol-2-amine (1.2 equiv, 2 mmol) & DMAP (1.1 equiv) in DCM (10 mL) was added heptanoyl chloride (1 equiv, 1.67 mmol) slowly. The reaction was continued overnight. After completion as judged by TLC analysis, the solvent was evaporated and the concentrate was acidified with 10% HCl to pH 2. Water and NH_4Cl were added and the aqueous phase was extracted 2 times with EtOAc. The combined organic phase was washed once with water, dried over $MgSO_4$, filtered through a fritted funnel and concentrated by rotary evaporation. The concentrate was purified using a Teledyne Isco Combiflash® *R*$_f$ chromatographic system (12 g SiO_2 column, eluent: 10%, 6min; 10-30%, 6min; 30%, 6min; EtOAc/hexanes) to give the product as a white solid (333 mg, 94%, mp: 96.9 °C). R$_f$ ~ 0.5, 20% EtOAc/hexanes.

^{1}H NMR (400 MHz, CDCl$_3$) δ 12.30 (br s, 1H), 7.43 (d, *J* = 3.6 Hz, 1H), 7.00 (d, *J* = 3.6 Hz, 1H), 2.55 (t, *J* = 7.5 Hz, 2H), 1.77 (p, *J* = 7.4 Hz, 2H), 1.56 – 1.21 (m, 6H), 0.88 (t, *J* = 6.0, 3H); ^{13}C NMR (101 MHz, CDCl$_3$) δ 171.3, 160.1, 135.9, 113.4, 36.2, 31.5, 28.9, 25.1, 22.4, 14.0.

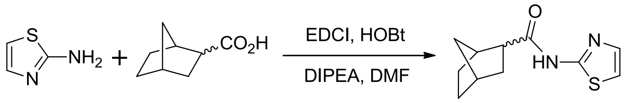

(1*S*,4*R*)-*N*-(thiazol-2-yl)bicyclo[2.2.1]heptane-2-carboxamide

The title compound was synthesized according to General Procedure B using thiazol-2-amine (200 mg, 2.0 mmol, 1.3 equiv) and (1*S*,4*R*)-bicyclo[2.2.1]heptane-2-carboxylic acid (216 mg, 1.54 mmol). The product was isolated as off-white solid (76 mg, 22%, mp: 153.5 °C) after purification on SiO_2 column chromatography (15% EtOAc/hexanes).

^{1}H NMR (400 MHz, $CDCl_3$) δ 12.53 (s, 1H), 7.41 (d, *J* = 3.5 Hz, 1H), 6.99 (d, *J* = 3.6 Hz, 1H), 3.02 (dt, *J* = 10.9, 4.7 Hz, 1H), 2.60 (d, *J* = 3.8 Hz, 1H), 2.57-2.49 (m, 0.3H), 2.35 (t, *J* = 4.4 Hz, 1H), 2.06 (dtd, *J* = 12.2, 4.6, 2.6 Hz, 0.2H), 1.90 (ddd, *J* = 12.6, 4.9, 2.4 Hz, 1H), 1.70 (dddd, *J* = 15.7, 10.4, 5.2, 3.0 Hz, 1H), 1.65 – 1.48 (m, 2H), 1.48 – 1.33 (m, 3H), 1.33 – 1.17 (m, 0.3H); ^{13}C NMR (100 MHz, $CDCl_3$) δ 174.0, 172.6, 160.5, 135.9, 135.9, 113.3, 113.2, 47.8, 47.3, 41.74, 41.5, 40.9, 37.2, 36.4, 35.9, 33.9, 31.0, 29.8, 29.1, 28.8, 24.3.

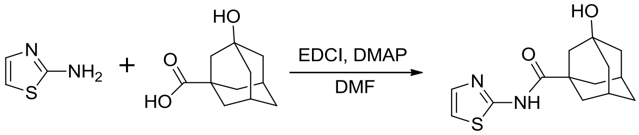

(1*r*,3*s*,5*R*,7*S*)-3-hydroxy-*N*-(thiazol-2-yl)adamantane-1-carboxamide

The title compound was synthesized according to General Procedure B using thiazol-2-amine (150 mg, 1.5 mmol, 1.2 equiv) and (1*r*,3*s*,5*R*,7*S*)-3-hydroxyadamantane-1-carboxylic acid (245 mg, 1.25 mmol). The product was isolated as off-white solid (158 mg, 45%, mp: 205.9-206 °C) after purification using a Teledyne Isco Combiflash® R_f chromatographic system (12 g SiO_2 column: eluted with 40% EtOA/hexanes).

^{1}H NMR (400 MHz, $CDCl_3$) δ 9.03 (s, 1H), 7.44 (s, 1H), 6.97 (s, 1H), 2.37 (s, 2H), 1.94 (s, 2H), 1.88 (s, 3H), 1.77 (s, 4H), 1.65 (s, 2H); ^{13}C NMR (101 MHz, $CDCl_3$) δ 174.4, 159.1, 137.1, 113.8, 68.6, 45.9, 44.6, 44.5, 37.9, 34.9, 30.4.

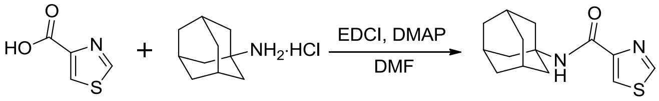

N-((3s,5s,7s)-adamantan-1-yl)thiazole-4-carboxamide

The title compound was synthesized according to General Procedure B using thiazole-4-carboxylic acid (155 mg, 1.2 mmol, 1.2 equiv) and the hydrochloride salt of adamantan-1-amine (188 mg, 1.0 mmol). The product was isolated as white crystals (284 mg, 90%, mp: 170.7 °C) after purification using a Teledyne Isco Combiflash® *R*f chromatographic system (12 g SiO_2 column: eluted with 0-20% EtOAc/hexanes, 5 min; 20% EtOA/hexanes, 5 min).

1H NMR (400 MHz, $CDCl_3$) δ 8.71 (dd, *J* = 2.1, 0.8 Hz, 1H), 8.09 (dd, *J* = 2.1, 0.8 Hz, 1H), 7.17 (s, 1H), 2.22-2.05 (m, 9H), 1.82 – 1.60 (m, 6H); ^{13}C NMR (101 MHz, $CDCl_3$) δ 160.1, 152.5, 152.4, 122.6, 52.2, 41.7, 36.5, 29.6.

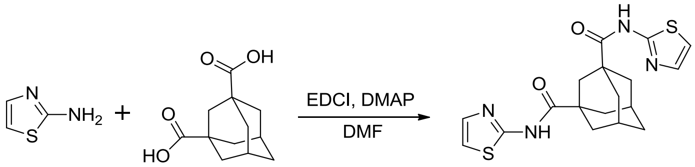

(1*s*,3*s*,5*r*,7*r*)-*N*^{1},*N*^{3}-di(thiazol-2-yl)adamantane-1,3-dicarboxamide

The title compound was synthesized according to General Procedure B using thiazol-2-amine (400 mg, 4.0 mmol, 2.4 equiv) and adamantane-1,3-dicarboxylic acid (373 mg, 1.7 mmol). The product was isolated as white solid (256 mg, 40%, mp: 275.7 °C (decomp.)) after purification using a Teledyne Isco Combiflash® *R*f chromatographic system (12 g SiO_2 column: eluted with

0-30% EtOAc/hexanes, 5 min; 30% EtOA/hexanes, 5 min; 30-50% EtOA/hexanes, 3mins; 50% EtOAc/hexanes, 5 min).

^{1}H NMR (500 MHz, $CDCl_3$) δ 8.88 (s, 2H), 7.45 (d, *J* = 3.3 Hz, 2H), 6.99 (d, *J* = 3.5 Hz, 2H), 2.46 – 2.27 (m, 2H), 2.21 (s, 2H), 2.00 (s, 8H), 1.80 (s, 2H); ^{13}C NMR [100 MHz, $CDCl_3$: DMSO-d_6 (2:1)] δ 174.3, 157.7, 136.3, 111.8, 40.2, 37.5, 36.2, 33.8, 26.8.

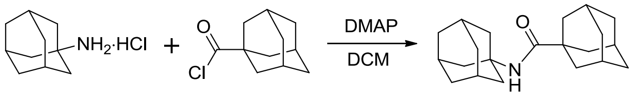

(3*R*,5*R*,7*R*)-*N*-((3*S*,5*S*,7*S*)-adamantan-1-yl)adamantane-1-carboxamide

The title compound was synthesized according to General Procedure A using hydrochloride salt of adamantan-1-amine (225 mg, 1.2 mmol, 1.2 equiv) and adamantane-1-carbonyl chloride (199 mg, 1.0 mmol). The product was isolated as white needles (232 mg, 74%, mp: 305 °C) after purification using a Teledyne Isco Combiflash® *R*f chromatographic system (12 g SiO_2 column: eluted with hexanes, 1 min; 0-10% EtOAc/hexanes, 8 min; 10% EtOAc/hexanes, 8 min).

1H NMR (400 MHz, $CDCl_3$) δ 5.21 (s, 1H), 2.10 – 1.99 (m, 6H), 1.97 (d, *J* = 2.9 Hz, 6H), 1.79 (d, *J* = 2.9 Hz, 6H), 1.76 – 1.61 (m, 12H); ^{13}C NMR (101 MHz, $CDCl_3$) δ 177.3, 51.3, 41.8, 41.0, 39.6, 36.7, 36.6, 29.6, 28.4.

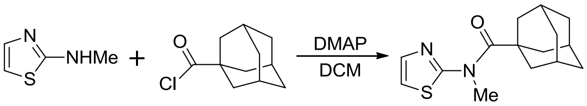

(3*r*,5*r*,7*r*)-*N*-methyl-*N*-(thiazol-2-yl)adamantane-1-carboxamide

The title compound was synthesized according to General Procedure A using *N*-methylthiazol-2-amine (200 mg, 1.75 mmol) and adamantane-1-carbonyl chloride (418 mg, 1.2 equiv). The product was isolated as white microcrystals (301 mg, 62%, mp: 156.2 °C) after purification using a Teledyne Isco Combiflash® R_f chromatographic system (12 g SiO_2 column: eluted with hexanes, 1 min; 0-10% EtOAc/hexanes, 4min; 10% EtOAc/hexanes, 7 min).

1H NMR (400 MHz, $CDCl_3$) δ 7.52 (dd, *J* = 3.6, 1.3 Hz, 1H), 6.99 (dd, *J* = 3.7, 1.3 Hz, 1H), 3.89 (d, *J* = 1.4 Hz, 3H), 2.21 – 2.07 (m, 9H), 1.77 (q, *J* = 2.3 Hz, 6H); ^{13}C NMR (101 MHz, $CDCl_3$) δ 176.2, 161.9, 136.7, 115.1, 43.1, 38.4, 37.1, 36.4, 28.2.

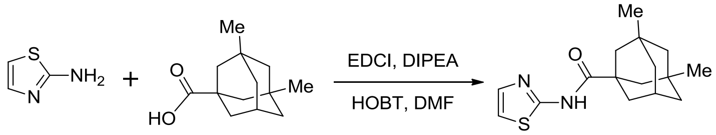

(1*r*,3*R*,5*S*,7*r*)-3,5-dimethyl-*N*-(thiazol-2-yl)adamantane-1-carboxamide

The title compound was synthesized according to General Procedure B using thiazol-2-amine (3.4 g, 33.5 mmol, 1.2 equiv) and 3,5-dimethyladamantane-1-carboxylic acid (6.0 g, 27.9 mmol). The product was isolated as white solid (5.3 g, 66%, mp: 95.0-95.3 °C) after purification using a Teledyne Isco Combiflash® R_f chromatographic system (120 g SiO_2 column: eluted with hexanes, 1 min; 0-20% EtOAc/hexanes, 24min; 20% EtOAc/hexanes, 10 min).

^{1}H NMR (500 MHz, $CDCl_3$) δ 8.88 (s, 1H), 7.44 (d, *J* = 3.6 Hz, 1H), 6.96 (d, *J* = 3.5 Hz, 1H), 2.20 (p, *J* = 3.2 Hz, 1H), 1.88 – 1.70 (m, 2H), 1.70 – 1.48 (m, 12H), 1.40 (t, *J* = 2.5 Hz, 5H), 1.30 – 1.11 (m, 3H), 0.89 (s, 6H); ^{13}C NMR (126 MHz, $CDCl_3$) δ 175.8, 159.3, 137.6, 114.0, 77.6, 50.6, 45.1, 43.2, 42.7, 37.7, 31.3, 30.6, 29.3.

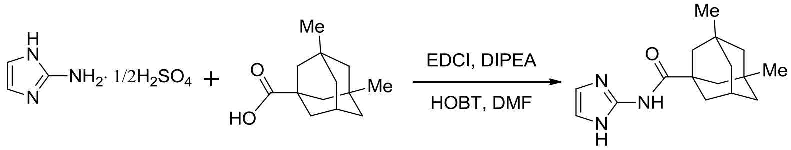

(1*r*,3*R*,5*S*,7*r*)-*N*-(1*H*-imidazol-2-yl)-3,5-dimethyladamantane-1-carboxamide

The title compound was synthesized according to General Procedure B using the acid salt of 1*H*-imidazol-2-amine (200 mg, 1.52 mmol, 1.2 equiv) and 3,5-dimethyladamantane-1-carboxylic acid (262 mg, 1.26 mmol). The title product was isolated as white solid (190.4 mg, 55%, mp: 140.3-140.4 °C) after purification using a Teledyne Isco Combiflash® *R*f chromatographic system (12 g SiO_2 column: eluted with hexanes, 1 min; 0-20% EtOAc/hexanes, 24min; 20% EtOAc/hexanes, 10 min).

^{1}H NMR (400 MHz, $CDCl_3$) δ 6.82 (s, 2H), 2.15 (h, *J* = 3.1 Hz, 1H), 1.85 – 1.73 (m, 2H), 1.56 (q, *J* = 12.3 Hz, 4H), 1.46 – 1.28 (m, 4H), 1.17 (s, 2H), 0.85 (s, 6H); ^{13}C NMR (101 MHz, $CDCl_3$) δ 177.8, 143.1, 50.6, 45.0, 43.4, 42.7, 37.6, 31.2, 30.5, 29.3.

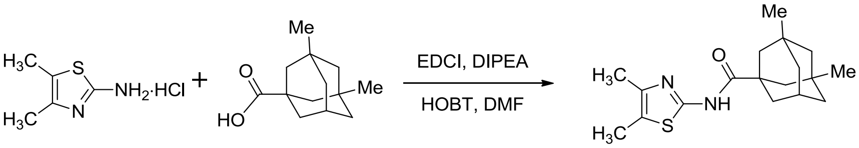

(1*r*,3*R*,5*S*,7*r*)-*N*-(4,5-dimethylthiazol-2-yl)-3,5-dimethyladamantane-1-carboxamide

The title compound was synthesized according to General Procedure B using acid salt of 4,5-dimethylthiazol-2-amine (200 mg, 1.21 mmol, 1.2 equiv) and 3,5-dimethyladamantane-1-carboxylic acid (210 mg, 1.01 mmol). The title product was isolated as white solid (173 mg, 54%, mp: 107.3 °C) after purification using a Teledyne Isco Combiflash® *R*f chromatographic system (12 g SiO_2 column: eluted with hexanes, 1 min; 0-20% EtOAc/hexanes, 24min; 20% EtOAc/hexanes, 10 min).

^{1}H NMR (400 MHz, $CDCl_3$) δ 2.25 (s, 3H), 2.19 (s, 3H), 2.17 – 2.09 (m, 1H), 1.75 – 1.69 (m, 2H), 1.59 – 1.44 (m, 4H), 1.38 – 1.29 (d, *J* = 3.1 Hz, 4H), 1.23 – 1.06 (m, 2H), 0.84 (s, 6H); ^{13}C NMR (101 MHz, $CDCl_3$) δ 174.9, 154.2, 141.7, 120.2, 50.5, 45.1, 42.9, 42.6, 37.6, 31.1, 30.4, 29.2, 14.5, 10.9.

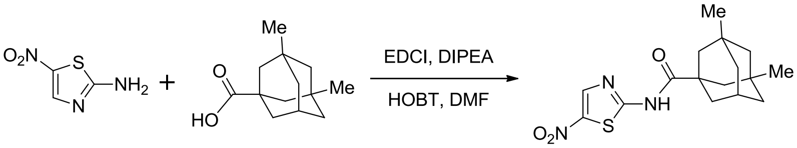

(1*r*,3*R*,5*S*,7*r*)-3,5-dimethyl-*N*-(5-nitrothiazol-2-yl)adamantane-1-carboxamide

The title compound was synthesized according to General Procedure B using 5-nitrothiazol-2-amine (176 mg, 1.21 mmol, 1.2 equiv) and 3,5-dimethyladamantane-1-carboxylic acid (210 mg, 1.0 mmol). The title product was isolated as a yellow solid (326 mg, 96%, mp: 146.1-146.2 °C) after purification using a Teledyne Isco Combiflash® R_f chromatographic system (120 g SiO_2 column: eluted with hexanes, 2 min; 0-20% EtOAc/hexanes, 7 min; 20% EtOAc/hexanes, 2 min).

^{1}H NMR (400 MHz, $CDCl_3$) δ 9.22 (s, 1H), 8.30 (d, *J* = 1.2 Hz, 1H), 2.27 – 2.18 (m, 1H), 1.79 (d, *J* = 3.1 Hz, 2H), 1.66 – 1.52 (m, 4H), 1.45 – 1.38 (m, 4H), 1.22 (tdd, *J* = 13.7, 11.4, 1.7 Hz, 2H), 0.89 (s, 6H); ^{13}C NMR (101 MHz, $CDCl_3$) δ 176.1, 161.3, 140.8, 50.4, 44.9, 43.3, 42.5, 37.5, 31.2, 30.4, 29.1.

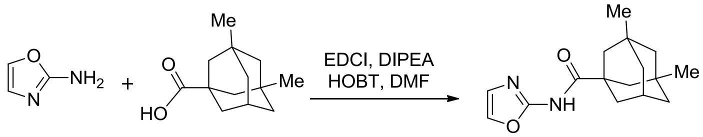

(1*r*,3*R*,5*S*,7*r*)-3,5-dimethyl-*N*-(oxazol-2-yl)adamantane-1-carboxamide

The title compound was synthesized according to General Procedure B using oxazol-2-amine (200 mg, 2.38 mmol, 1.2 equiv) and 3,5-dimethyladamantane-1-carboxylic acid (413 mg, 1.98 mmol). The title product was isolated as a pink oil (65 mg, 24%) after purification via TLC (6% MeOH in DCM).

^{1}H NMR (400 MHz, acetone-d$_6$) δ 9.50 (s, 1H), 7.67 (s, 1H), 7.02 (s, 1H), 2.19 – 2.10 (m, 1H), 1.83 (dd, *J* = 2.9, 1.5 Hz, 2H), 1.62 (q, *J* = 12.4 Hz, 4H), 1.47 – 1.32 (m, 4H), 1.19 (s, 2H), 0.86 (s, 6H); ^{13}C NMR (100 MHz, acetone-d$_6$) δ 176.0, 154.8, 137.0, 127.4, 51.2, 45.5, 44.3, 43.3, 38.0, 31.7, 30.9, 30.3.

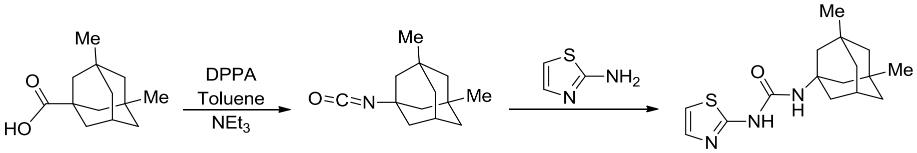

1-[(1*r*,3*R*,5*S*,7*r*)-3,5-dimethyladamantan-1-yl]-3-(thiazol-2-yl)urea

To a solution of 3,5-dimethyladamantane-1-carboxylic acid (300 mg, 1.44 mmol) and triethylamine (1.1 equiv, 220 µL) in anhydrous toluene (10 mL) at rt was added diphenylphosphoryl azide (DPPA, 1.1 equiv, 342 µL). The reaction was continued at 40 °C for 1 h, and at 80 °C for 4 h. The reaction was cooled to rt, thiazol-2-amine (1.1 equiv, 156 mg) was added at once, and the reaction was continued at 80 °C for 19 h. The reaction was cooled to rt, concentrated in vacuo, and purified using a Teledyne Isco Combiflash® *R*f chromatographic system (12 g SiO_2 column: eluted with 0-25% EtOAc/hexanes, 5 min; 25% EtOAc/hexanes, 7 min; 25-100% EtOAc/hexanes, 5 min; 100%, EtOAc,2 min) to give the title product (229 mg, 52%, mp: 71.2 °C) as a white foam.

^{1}H NMR (400 MHz, $CDCl_3$) δ 7.30 (d, *J* = 3.7 Hz, 1H), 6.78 (d, *J* = 3.7 Hz, 1H), 2.22 – 2.14 (m, 1H), 1.96 – 1.90 (m, 2H), 1.80 – 1.64 (m, 4H), 1.45 – 1.28 (m, 4H), 1.18 (dt, *J* = 6.2, 2.0 Hz, 2H), 0.88 (s, 6H); ^{13}C NMR (101 MHz, $CDCl_3$) δ 162.7, 153.5, 136.5, 110.7, 53.1, 50.6, 48.0, 42.6, 40.5, 32.5, 30.1, 30.1.

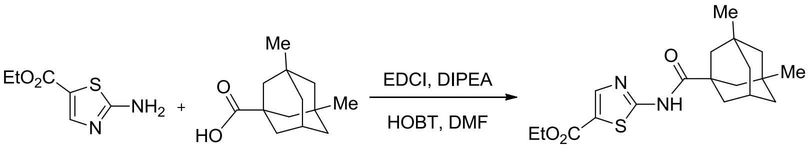

Ethyl 2-((1*r*,3*R*,5*S*,7*r*)-3,5-dimethyladamantane-1-carboxamido)thiazole-5-carboxylate

The title compound was synthesized according to General Procedure B using ethyl 2-aminothiazole-5-carboxylate (208 mg, 1.21 mmol, 1.2 equiv) and 3,5-dimethyladamantane-1-carboxylic acid (210 mg, 1.01 mmol). The title product was isolated as sticky foam (191 mg, 52%) after purification using a Teledyne Isco Combiflash® *R*f chromatographic system (12 g SiO_2 column: eluted with hexanes, 2 min; 0-15% EtOAc/hexanes, 5min; 15% EtOAc/hexanes, 4 min).

^{1}H NMR (400 MHz, $CDCl_3$) δ 10.23 (s, 1H), 8.08 (s, 1H), 4.30 (q, *J* = 7.1 Hz, 2H), 2.17 – 2.08 (m, 1H), 1.77 – 1.70 (m, 2H), 1.60 – 1.45 (m, 4H), 1.36 – 1.28 (m, 7H), 1.20 – 1.06 (m, 2H), 0.81 (s, 6H); ^{13}C NMR (101 MHz, $CDCl_3$) δ 183.2, 176.1, 163.3, 161.9, 144.3, 123.1, 61.2, 50.3, 44.7, 43.2, 42.5, 37.3, 31.0, 30.3, 29.0, 14.3.

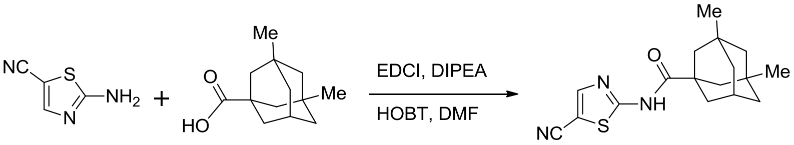

(1*r*,3*R*,5*S*,7*r*)-*N*-(5-cyanothiazol-2-yl)-3,5-dimethyladamantane-1-carboxamide

The title compound was synthesized according to General Procedure B using 2-aminothiazole-5-carbonitrile (151 mg, 1.21 mmol, 1.2 equiv) and 3,5-dimethyladamantane-1-carboxylic acid (210 mg, 1.01 mmol). The title product was isolated as white crystals (174 mg, 55%, mp: 195.1-195.2 °C) after purification using a Teledyne Isco Combiflash® *R*f chromatographic system (12 g SiO_2 column: eluted with hexanes, 1 min; 0-10% EtOAc/hexanes, 5min; 10% EtOAc/hexanes, 8 min). ^{1}H NMR (400 MHz, $CDCl_3$) δ 9.22 (d, *J* = 7.6 Hz, 1H), 7.96 (s, 1H), 2.26 – 2.18 (m, 1H), 1.79 (d, *J* = 3.2 Hz, 2H), 1.65 – 1.52 (m, 4H), 1.45 – 1.38 (m, 4H), 1.29 – 1.16 (m, 2H), 0.90 (s, 6H); ^{13}C NMR (101 MHz, $CDCl_3$) δ 176.0, 161.7, 148.3, 112.9, 100.3, 50.4, 45.0, 43.2, 42.5, 37.6, 31.2, 30.4, 29.1.

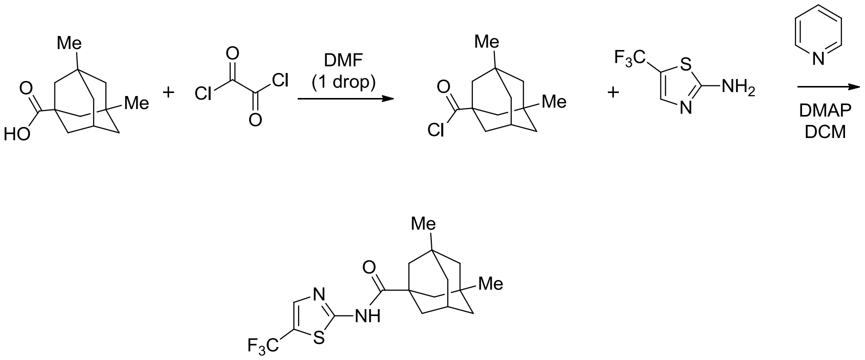

(1*r*,3*R*,5*S*,7*r*)-3,5-dimethyl-*N*-(5-(trifluoromethyl)thiazol-2-yl)adamantane-1-carboxamide

To a vial containing 3,5-dimethyladamantane-1-carboxylic acid (208 mg) was added neat oxalyl chloride (267 μL) to form a clear solution (bubbling evident). Anhydrous DMF (5 μL) was added and the reaction was continued for 1 hour. The reaction was purged with a stream of argon (to get rid of volatile material), concentrated, and dried on high vacuum. The vial was cooled to 0 ^{o}C and pyridine (1 mL) and DMAP (1 equiv., 122 mg) were added. After 3 mins, 5-(trifluoromethyl)thiazol-2-amine (168 mg, 1 equiv.) dissolved in DCM (1 mL) was added, the reaction was warmed to r.t. over 10 mins, and stirred at 60 ^{o}C for 2 hours. The reaction was poured into sat. NH_4Cl solution, extracted with EtOAc (2 X 25 mL), dried over Na_2SO_4, filtered and concentrated. The crude product was purified using a Teledyne Isco Combiflash® R_f chromatographic system (4 g SiO_2 column: eluted with hexanes, 1 min, 0-5% EtOAc/hexanes, 7 mins, 5%, 7 mins to give the title product as a sticky oil (123 mg, 34%).

^{1}H NMR (500 MHz, $CDCl_3$) δ 8.97 (br s, 1H), 7.76 (s, 1H), 2.22 (app p, *J* = 3.2 Hz, 1H), 1.79 (d, *J* = 3.1 Hz, 2H), 1.64-1.51 (m, 4H), 1.44 – 1.39 (m, 4H), 1.29 – 1.15 (m, 2H), 0.90 (s, 6H); ^{13}C NMR (101 MHz, $CDCl_3$) δ 175.9, 161.2, 138.9 (q, $J_{C\text{-}F}$ = 4.4 Hz), 122.4(q, $J_{C\text{-}F}$ = 268 Hz), 120.8, 50.26 , 44.8 (2), 43.0, 42.4 (2), 37.4, 31.0 (2), 30.2 (2), 29.0. ^{19}F NMR (376 MHz, $CDCl_3$) δ -54.5 (s, 3F).

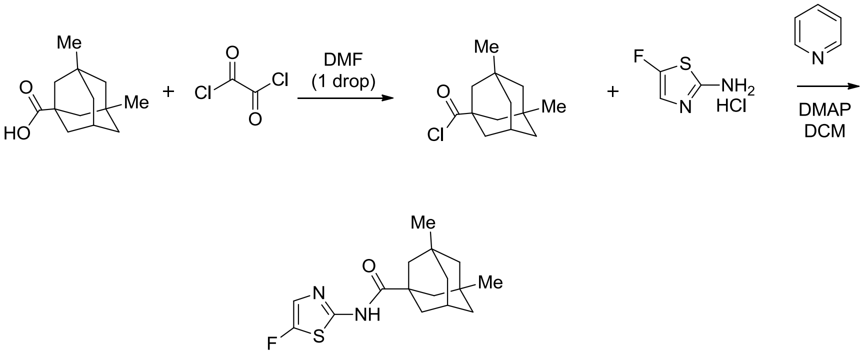

(1*r*,3*R*,5*S*,7*r*)-*N*-(5-fluorothiazol-2-yl)-3,5-dimethyladamantane-1-carboxamide

To a vial containing 3,5-dimethyladamantane-1-carboxylic acid (176 mg, 1.3 equiv) was added neat oxalyl chloride (226 μL) to form a clear solution (bubbling evident).[33] Anhydrous DMF (5 μL) was added and the reaction was continued for 1h. The reaction was purged with a stream of argon (to get rid of volatile material), concentrated, and dried on high vacuum. The vial was cooled to 0 °C and pyridine (1 mL) and DMAP (1 equiv, 79 mg) were added. After 3 mins, 5-fluorothiazol-2-amine hydrochloride (100 mg, 1 equiv.) dissolved in DCM (1 mL) was added, the reaction was warmed to r.t. over 10 mins, and stirred at 60 °C for 2 h. The reaction was poured into sat. NH_4Cl solution, extracted with EtOAc (2 X 25 mL), dried over Na_2SO_4, filtered and concentrated. The crude product was purified using a Teledyne Isco Combiflash® R_f chromatographic system (12 g SiO_2 column: eluted with hexanes, 2 min, 0-5% EtOAc/hexanes, 7 min; 5% EtOAc/hexanes, 5 min) to give the title product (130 mg, 65%, mp: 126.1 °C) as a white solid.

^{1}H NMR (500 MHz, $CDCl_3$) δ 8.53 (br s, 1H), 7.01 (d, J = 2.5 Hz, 1H), 2.20 (app p, J = 3.2 Hz, 1H), 1.77 (d, J = 3.0 Hz, 2H), 1.62 – 1.49 (m, 4H), 1.47 – 1.37 (m, 4H), 1.28-1.14 (m, 2H) 0.88 (s, 6H); ^{13}C NMR (100 MHz, $CDCl_3$) δ 175.3 , 158.7 (d, $J_{C\text{-}F}$ = 293 Hz) , 147.8 (d, $J_{C\text{-}F}$ = 10.8 Hz), 117.4 (d, $J_{C\text{-}F}$ = 12.4 Hz), 50.3 , 44.9 (2) , 42.8 , 42.4 (2) , 37.4 , 31.0 (2) , 30.3 (2), 29.0; ^{19}F NMR (376 MHz, $CDCl_3$) δ -157.3 (s, 1F).

2.7 References

1. Romero, D.; Traxler, M. F.; Lopez, D.; Kolter, R. “Antibiotics as signal molecules”. *Chem. Rev.* **2011**, *111*, 5492-5505.
2. Brown, E. D.; Wright, G. D. “New targets and screening approaches in antimicrobial drug discovery”. *Chem. Rev.* **2005**, *105*, 759-774.
3. Rasko, D. A.; Sperandio, V. “Anti-virulence strategies to combat bacteria-mediated disease”. *Nat. Rev. Drug Discov.* **2010**, *9*, 117-128.
4. Waters, C. M.; Bassler, B. “Quorum sensing: cell-to cell communication in bacteria”. *Annu. Rev. Cell Dev. Biol.* **2005**, *21*, 319-346.

5. Rasko, D. A.; Moreira, C. G.; Li, D.; Reading, N. C. ; Ritchie, J. M.; Waldor, M. K.; Williams, N.; Taussig, R.; Wei, S.; Roth, M.; Hughes, D. T.; Huntley, J. F.; Fina, M. W.; Falck, J. R.; Sperandio, V. "Targeting QseC signaling and virulence for antibiotic development". *Science* **2008**, *321*, 1078-1080.

6. Wopperer, L.; Cardona, S. T.; Huber, B.; Jacobi, C. A.; Valvano, M. A.; Eberl, L. "A quorum-quenching approach to investigate the conversion of quorum-sensing regulated functions within the Burkholderia cepacia complex". *Appl. Environ. Microbiol.* **2006**, *72*, 1579-1587.

7. Balcazar, J. L.; de Blas, I; Ruiz-Zarzuela, I.; Cunningham, D.; Vendrell, D.; Muzquiz, J. L. "The role of probiotics in aquaculture". *Vet. Microbiol.* **2006**, *114*, 173-186.

8. Nakayama, J.; Tanaka, E.; Kariyama, R.; Nagata, K.; Nishiguchi, K.; Mitsuhata, R., et al. "Siomycin attenuates fsr quorum sensing mediated by a gelatinase biosynthesis-activating pheromone in Enterococcus faecalis". *J. Bacteriol.* **2007**, *189*, 1358-1365.

9. Calfee, M. W.; Coleman, J. P.; Pesci, E. C. "Interference with Pseudomonas quinolone signal synthesis inhibits virulence factor expression by Pseudomonas aeruginosa". *Proc. Natl. Acad. Sci. USA* **2001**, *98*, 11633-11637.

10. Murray, E. J.; Crowley, R. C.; Truman, A.; Clarke, S. R.; Cottam, J. A.; Jadhav, G. P.; Steele, V. R.; O'Shea, P.; Lindholm, C.; Cockayne, A.; Chhabra, S. R.; Chan, W. C.; Williams, P. "Targeting Staphylococcus aureus Quorum Sensing with Nonpeptidic Small Molecule Inhibitors". *J. Med. Chem.* **2014**, *57*, 2813-2819.

11. O'Loughlin, C. T.; Miller, L. C.; Siryaporn, A.; Drescher, K.; Semmelhack, M. F.; Bassler, B. L. "A quorum-sensing inhibitor blocks Pseudomonas aeruginosa virulence and biofilm formation". *Proc. Natl. Acad. Sci. USA* **2013**, *110*, 17981-17986.

12. Zhang, L.; Krachler, A. M.; Broberg, C. A.; Li, Y.; Mirzaei, H.; Gilpin, C. J.; Orth, K. "Type III effector VopC mediates invasion for *Vibrio* species". *Cell Reports* **2012**, *1*, 453-460.

13. Yarbrough, M. L.; Li, Y.; Kinch, L. N.; Grishin, N. V.; Ball, H. L.; Orth, K. "AMPylation of Rho GTPases by *Vibrio* VopS disrupts effector binding and downstream signaling". *Science* **2008**, *323*, 269-272.

14. Ivarsson, M. E.; Leroux, J-C.; Castagner, B. "Targeting Bacerial Toxins". *Angew. Chem. Int. Ed.* **2012**, *51*, 2-24.

15. Watanabe, M.; Matsuoka, K.; Kita, E.; Igai, K.; Higashi, N.; Miyagawa, A.; Watanabe, T.; Yanoshita, R.; Samejima, Y.; Terunuma, D.; Natori, Y.; Nishikawa, K. "Oral Therapeutic Agents with Highly Clustered Globotriose for Treatment of Shiga Toxigenic Escherichia coli Infections". *J. Infect. Dis.* **2004**, *189*, 360-368.

16. Maeda, T.; Garcia-Contreras, R.; Pu, M.; Sheng, L.; Garcia, L. R.; Tomas, M.; et al. “Quorum quenching quandry: resistance to antivirulence compounds”. *ISME J*. **2012**, *6*, 493-501.

17. Curtis, M. M.; Russell, R.; Moreira, C. G.; Adebesin, A. M.; Wang, C.; Williams, N. S.; Taussig, R.; Stewart, D.; Zimmern, P.; Lu, B.; Prasad, R. N.; Zhu, C.; Rasko, D. A.; Huntley, J. F.; Falck, J. R.; Sperandio, V. “QseC inhibitors as an antivirulence approach for Gram-negative pathogens”. *MBio.* **2014**, 5, 6, e02165-14.

18. Kaper, J. B.; Elliott, S.; Sperandio, V.; Perna, N. T.; Mayhew, G. F.; Blattner, F. R. “Attaching and effacing intestinal histopathology and the locus of enterocyte effacement”. *In Escherichia coli O157:H7 and other Shiga Toxin-Producing E. coli Strains.* Ed. Kaper, J. B., (ed.). O’Brien, A. D. Washington, DC: *ASM Press* **1998**, 163-182.

19. McDaniel, T. K.; Jarvis, K. G.; Donnenberg, M. S.; Kaper, J. B. “A genetic locus of enterocyte effacement conserved among diverse enterobacterial pathogens”. *Proc. Natl. Acad. Sci. USA* **1995**, *92*, 1664-1668.

20. Wagner, P. L.; Neely, M. N.; Zhang, X.; Acheson, D. W. K.; Waldor, M. K.; Friedman, D. I. “Role for a Phage Promoter in Shiga Toxin 2 Expression from a Pathogenic Escherichia coli Strain”. *J. Bacteriol.* **2001**, *183*, 2081-2085.

21. Sperandio, V.; Torres, A. G.; Kaper, J. B. “Quorum sensing Escherichia coli regulators B and C (QseBC): a novel two component regulatory system involved in the regulation of flagella and motility by quorum sensing in E. coli.” *Mol. Microbiol.* **2002**, *43*, 809-821.

22. Hughes, D. T.; Clarke, M. B.; Yamamoto, K.; Rasko, D. A.; Sperandio, V. “The QseC adrenergic signaling cascade in enterohemorrhagic *E. coli* (EHEC).” PLoS Pathog **2009**, *5*, e1000553.

23. a. Reading, N. C.; Torres A. G.; Kendall, M. M.; Hughes, D. T.; Yamamoto, K.; Sperandio V. “A novel two-component signaling system that activates transcription of an enterohemorrhagic *escherichia coli* effector involved in remodeling of host actin.” *J. Bacteriol.* **2007**, *189*, 2468-2476. b. Reading, N. C.; Rasko, D. A.; Torres A. G.; Sperandio V. “The two-component system QseEF and the membrane protein QseG link adrenergic and stress sensing to bacterial pathogenesis”. *Proc. Natl. Acad. Sci. USA* **2009**, *106*, 5889-5894.

24. Walters, M.; Sircili, M. P.; Sperandio, V. “AI-3 Synthesis is not dependent on luxS in Escherichia coli.” *J. Bacteriol.* **2006**, *188*, 5668-5681.

25. *Autoinducer AI-2 Biosynthesis* 2004, International Union of Biochemistry and Molecular Biology (IUBMB), accessed 21 June, 2015. http://www.chem.qmul.ac.uk/iubmb/enzyme/reaction/misc/AI2.html

26. Zhu, J.; Dizin, E.; Hu, X.; Wavreille, A.; Park, J.; Pei, D. "S-Ribosylhomocysteinase (LuxS) is a mononuclear iron protein." *Biochemistry* **2003**, *42*, 4717-4726.

27. Sperandio, V.; Torres, A. G.; Jarvis, B.; Nataro, J. P.; Kaper, J. B. "Bacteria-host communication: The language of hormones." *Proc. Natl. Acad. Sci. USA* **2003**, *100*, 8951-8956.

28. Jakab, G.; Tancon, C.; Zhang, Z.; Lippert, K. M.; Schreiner, P. R. "(Thio)urea Organocatalyst Equilibrium Acidities in DMSO." *Org. Lett.* **2012**, *14*, 1724-1727.

29. Singh, J.; Petter, R. C.; Baillie, T. A.; Whitty, A. "The resurgence of covalent drugs." *Nat. Rev. Drug Discov.* **2011**, *10*, 307-317.

30. Zhu, P.; Peng, H.; Ni, N.; Wang, B.; Li, M. "Novel AI-2 quorum sensing inhibitors in *Vibrio harveyi* identified through structure-based virtual screening." *Bioorg. Med. Chem. Lett.* **2012**, *22*, 6413-6417.

31. Zheng, X.; Oda, H.; Takamatsu, K.; Sugimoto, Y.; Tai, A.; Akaho, E.; Ali, H. I.; Oshiki, T.; Kakuta, H.; Sasaki, K. "Analgesic agents without gastric damage: Design and synthesis of structurally simple benzenesulfonanilide-type cyclooxyengase-1-selective inhibitors." *Bioorg. Med. Chem.* **2007**, *15*, 1014-1021.

32. Elliott, L. D.; Wrigglesworth, J. W.; Cox, B.; Lloyd-Jones, G. C.; Booker-Milburn, K. I. "2,2-Difunctionalization of alkenes via Pd(II)-catalyzed Aza-Wacker reactions." *Org. Lett.* **2011**, *13*, 728-731.

33. Tian, L.; Tao, J.; Chen, L. "Synthesis of deuterium-labeled simvastatin." *J. Label Compd. Radiopharm* **2011**, *54*, 625-628.

2.8 Spectra

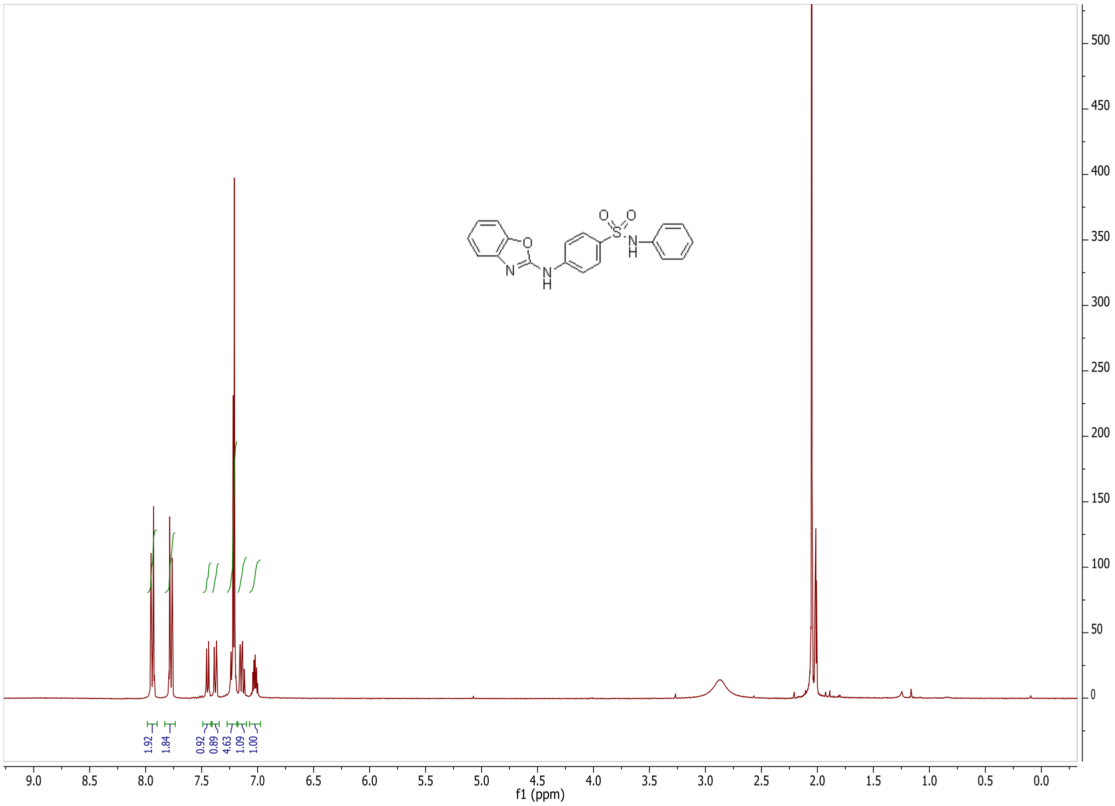
O
O
S
N
H
O
N
N
H
1.92
1.84
0.92
0.89
4.63
1.09
1.00
500
450
400
350
300
250
200
150
100
50
0
9.0
8.5
8.0
7.5
7.0
6.5
6.0
5.5
5.0
4.5
4.0
3.5
3.0
2.5
2.0
1.5
1.0
0.5
0.0
f1 (ppm)

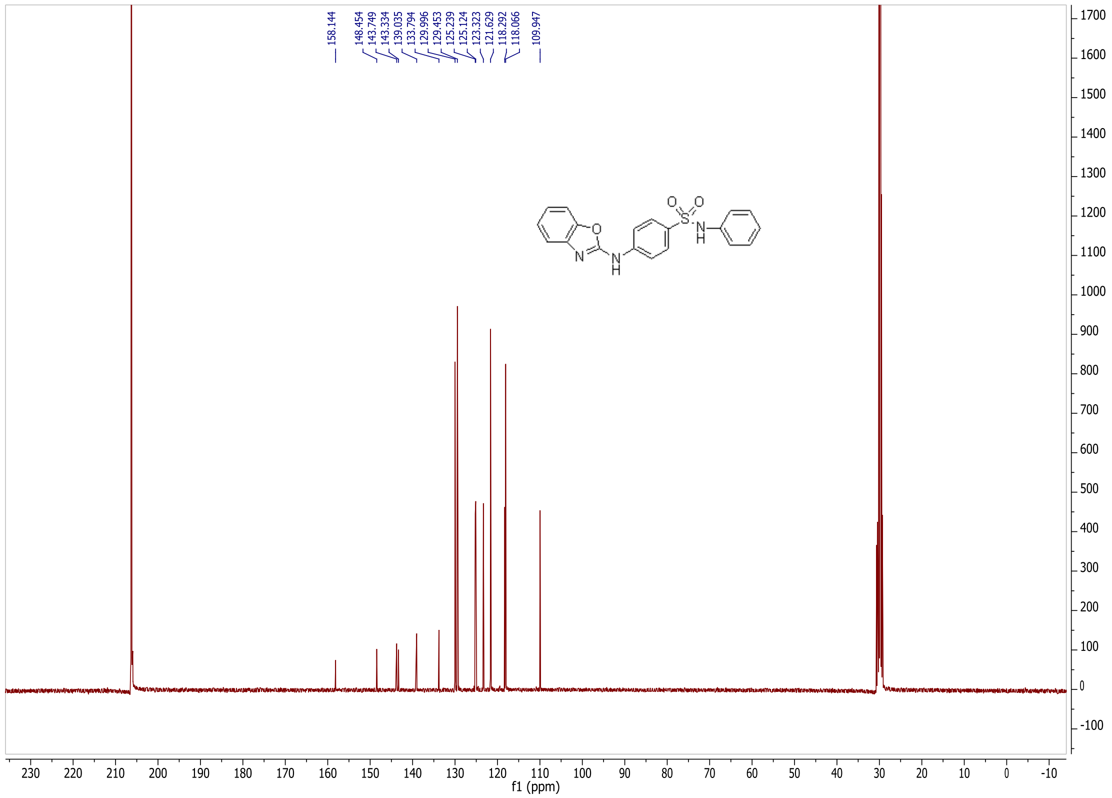
158.144
148.454
143.749
143.334
139.035
133.794
129.996
129.453
125.239
125.124
123.323
121.629
118.292
118.066
109.947
O
N
N
H
O
O
S
N
H
1700
1600
1500
1400
1300
1200
1100
1000
900
800
700
600
500
400
300
200
100
0
-100
230
220
210
200
190
180
170
160
150
140
130
120
110
100
90
80
70
60
50
40
30
20
10
0
-10
f1 (ppm)

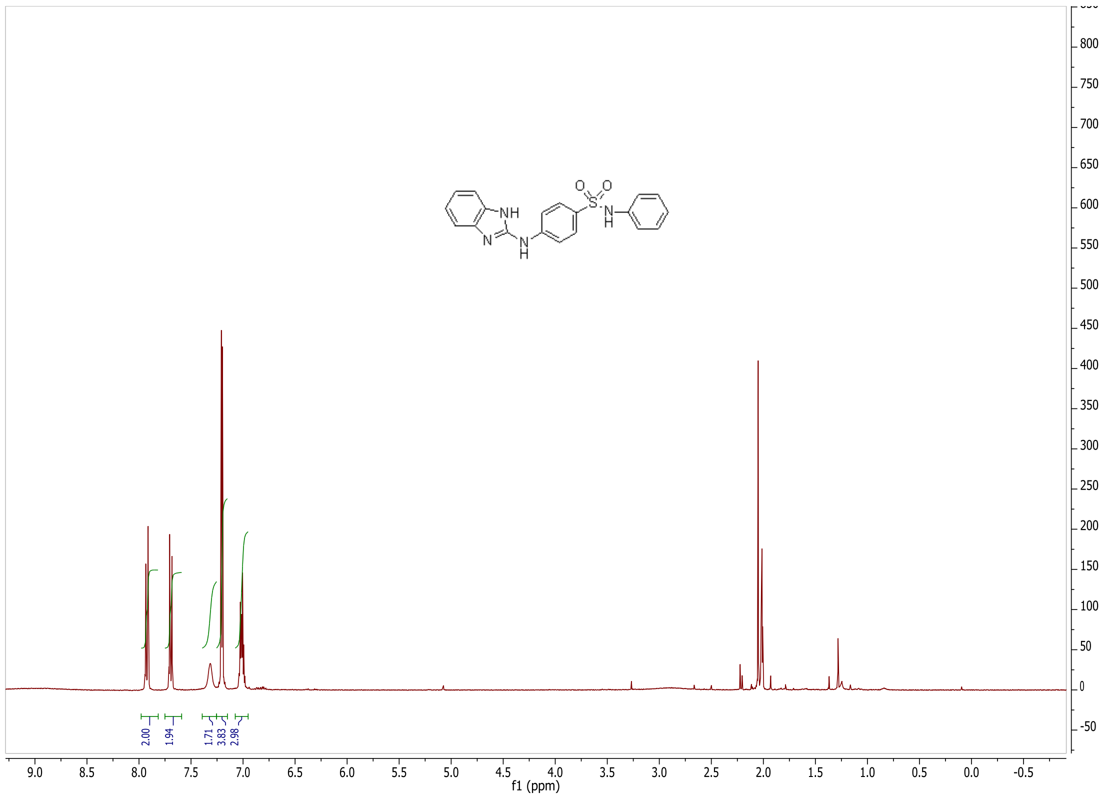
NH
N
N
H
O
O
S
N
H
800
750
700
650
600
550
500
450
400
350
300
250
200
150
100
50
0
-50
2.00
1.94
1.71
3.83
2.98
9.0
8.5
8.0
7.5
7.0
6.5
6.0
5.5
5.0
4.5
4.0
3.5
3.0
2.5
2.0
1.5
1.0
0.5
0.0
-0.5
f1 (ppm)

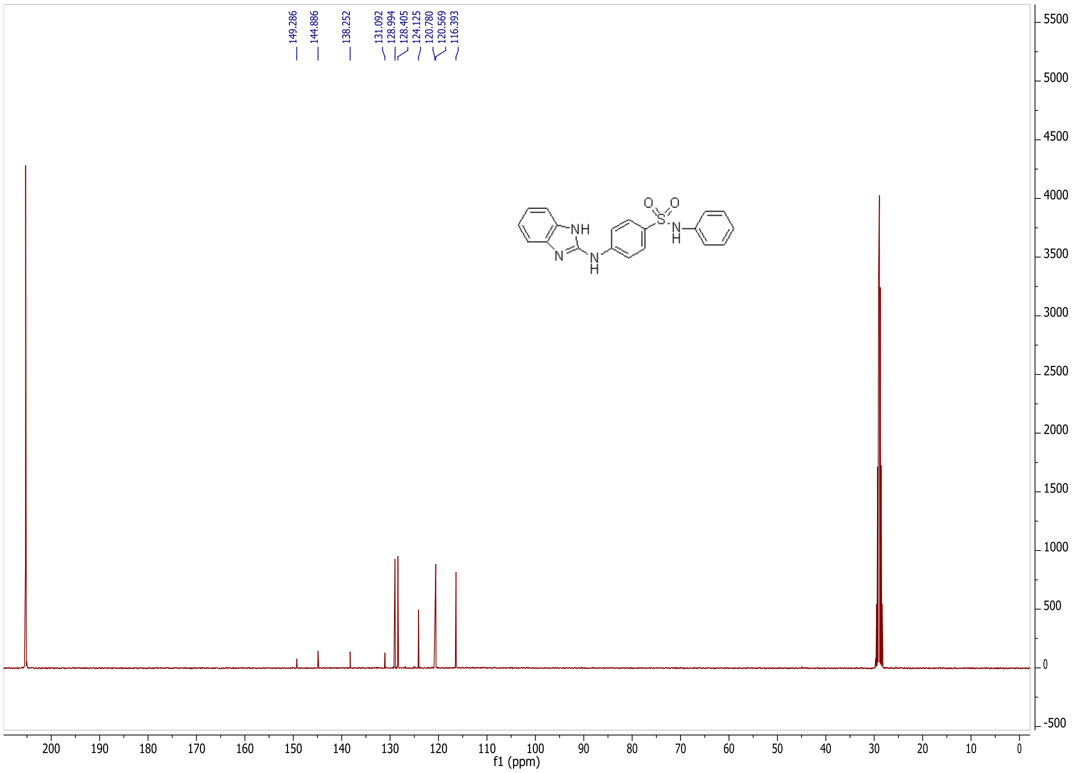
149.286
144.886
138.252
131.092
128.994
128.405
124.125
120.780
120.569
116.393
NH
N
N
H
O
O
S
N
H
5500
5000
4500
4000
3500
3000
2500
2000
1500
1000
500
0
-500
200
190
180
170
160
150
140
130
120
110
100
90
80
70
60
50
40
30
20
10
0
f1 (ppm)

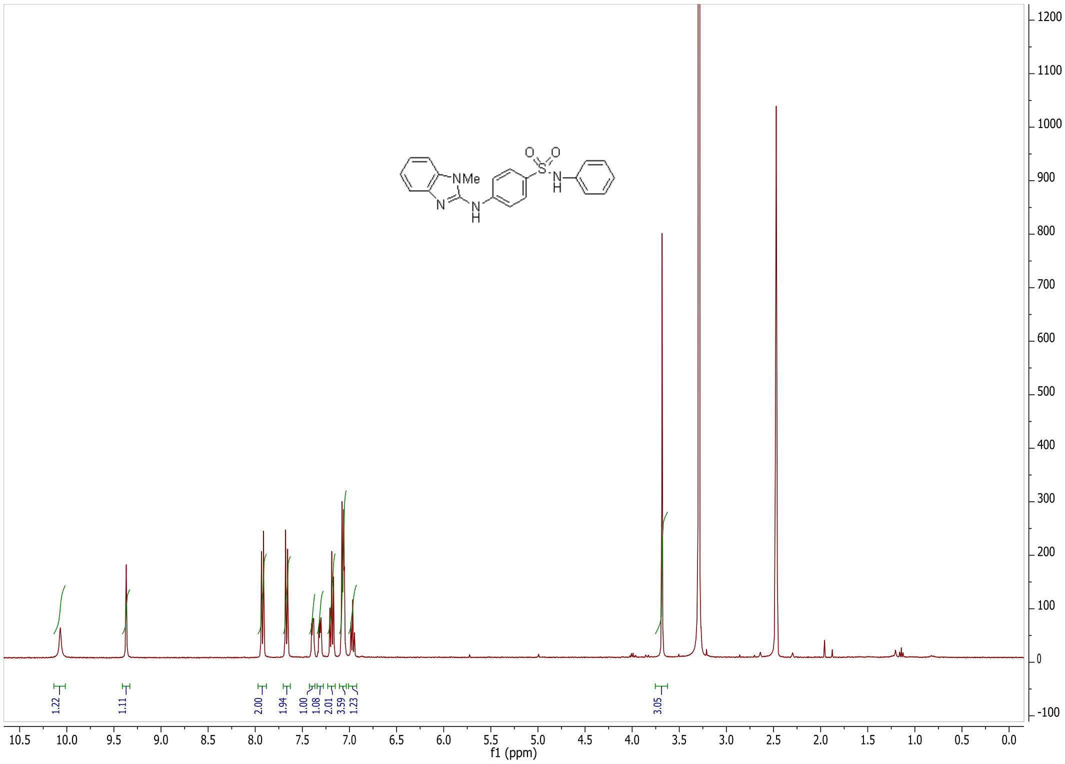
NMe
N
N
H
O
O
S
N
H
1200
1100
1000
900
800
700
600
500
400
300
200
100
0
-100
1.22
1.11
2.00
1.94
1.00
1.08
2.01
3.59
1.23
3.05
10.5
10.0
9.5
9.0
8.5
8.0
7.5
7.0
6.5
6.0
5.5
5.0
4.5
4.0
3.5
3.0
2.5
2.0
1.5
1.0
0.5
0.0
f1 (ppm)

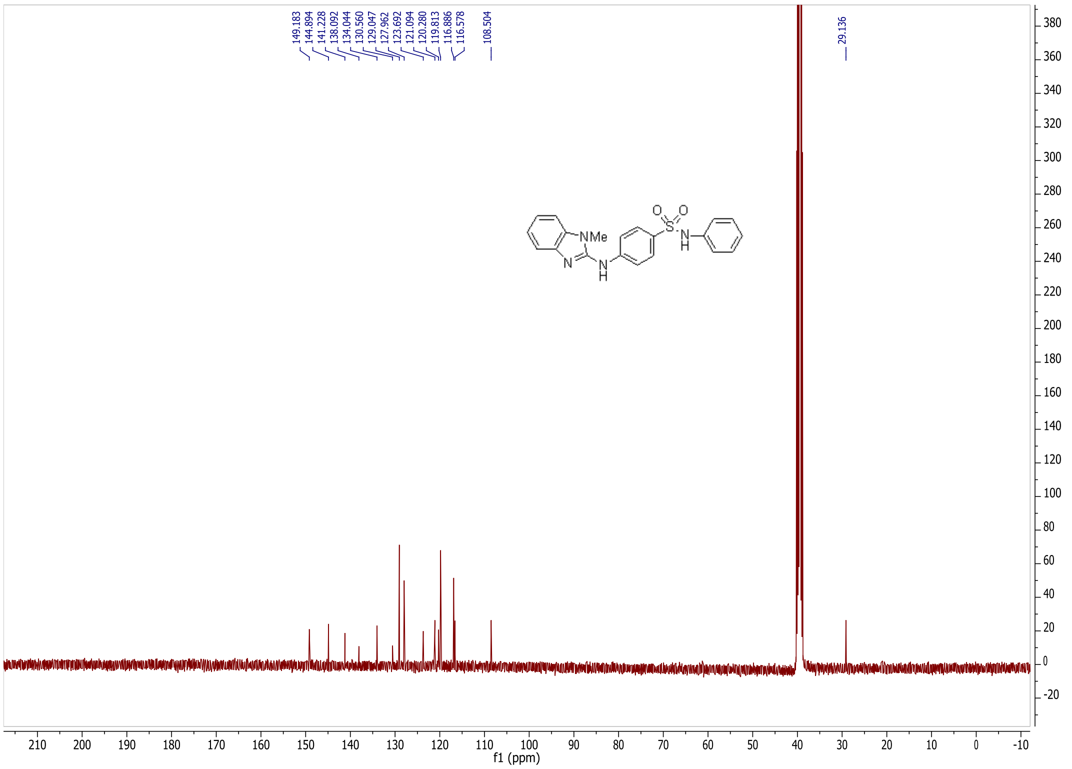
149.183
144.894
141.228
138.092
134.044
130.560
129.047
127.962
123.692
121.094
120.280
119.813
116.886
116.578
108.504
29.136
NMe
N
N
H
O
O
S
N
H
380
360
340
320
300
280
260
240
220
200
180
160
140
120
100
80
60
40
20
0
-20
210
200
190
180
170
160
150
140
130
120
110
100
90
80
70
60
50
40
30
20
10
0
-10
f1 (ppm)

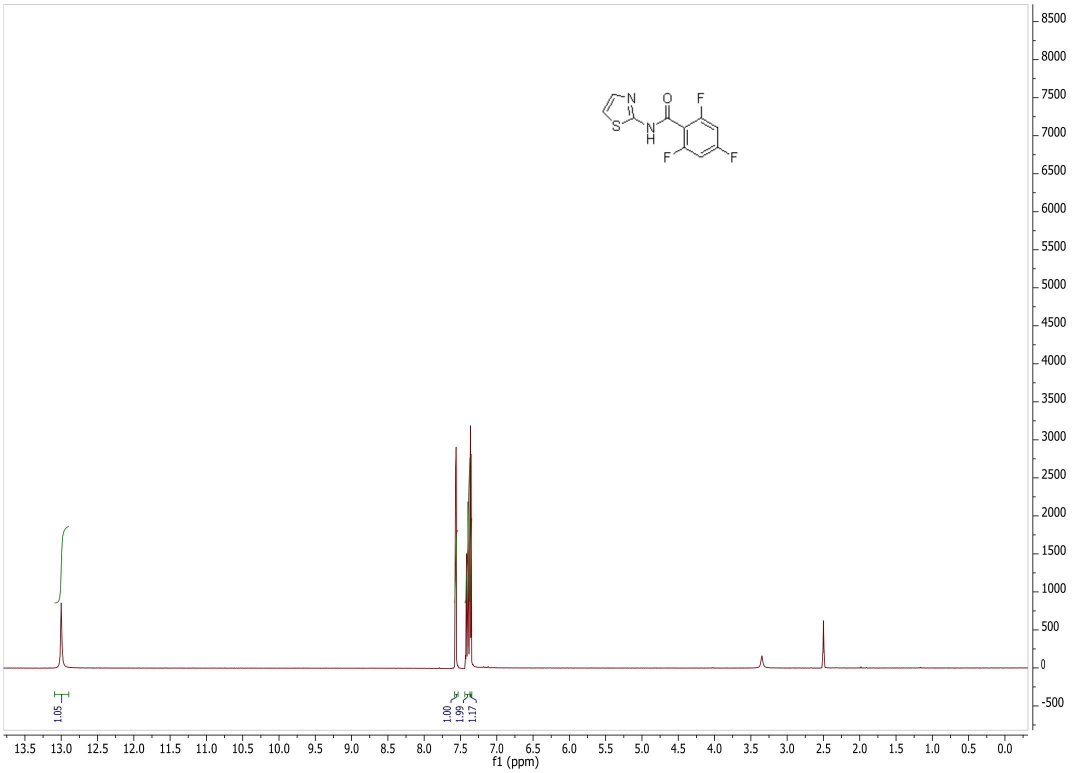
N
S
N
H
O
F
F
F
8500
8000
7500
7000
6500
6000
5500
5000
4500
4000
3500
3000
2500
2000
1500
1000
500
0
-500
1.05
1.00
1.99
1.17
13.5
13.0
12.5
12.0
11.5
11.0
10.5
10.0
9.5
9.0
8.5
8.0
7.5
7.0
6.5
6.0
5.5
5.0
4.5
4.0
3.5
3.0
2.5
2.0
1.5
1.0
0.5
0.0
f1 (ppm)

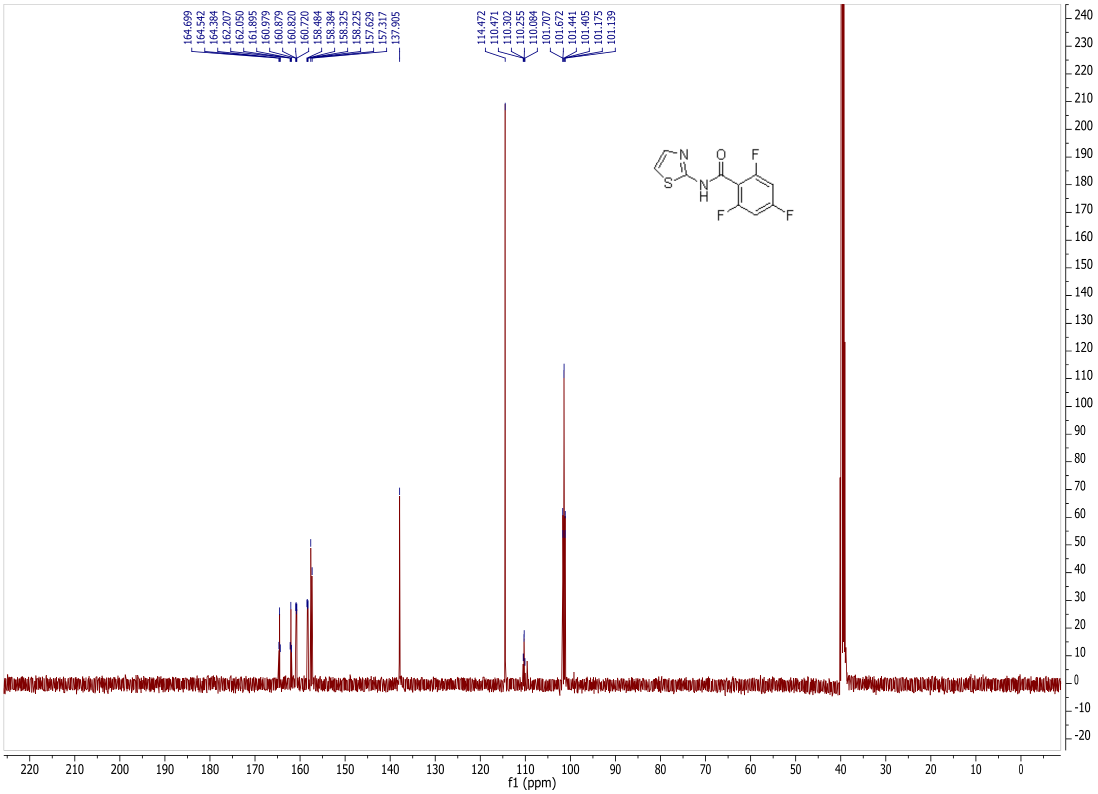
164.699
164.542
164.384
162.207
162.050
161.895
160.979
160.879
160.820
160.720
158.484
158.384
158.325
158.225
157.629
157.317
137.905
114.472
110.471
110.302
110.255
110.084
101.707
101.672
101.441
101.405
101.175
101.139
N
S
O
F
N
H
F
F
f1 (ppm)

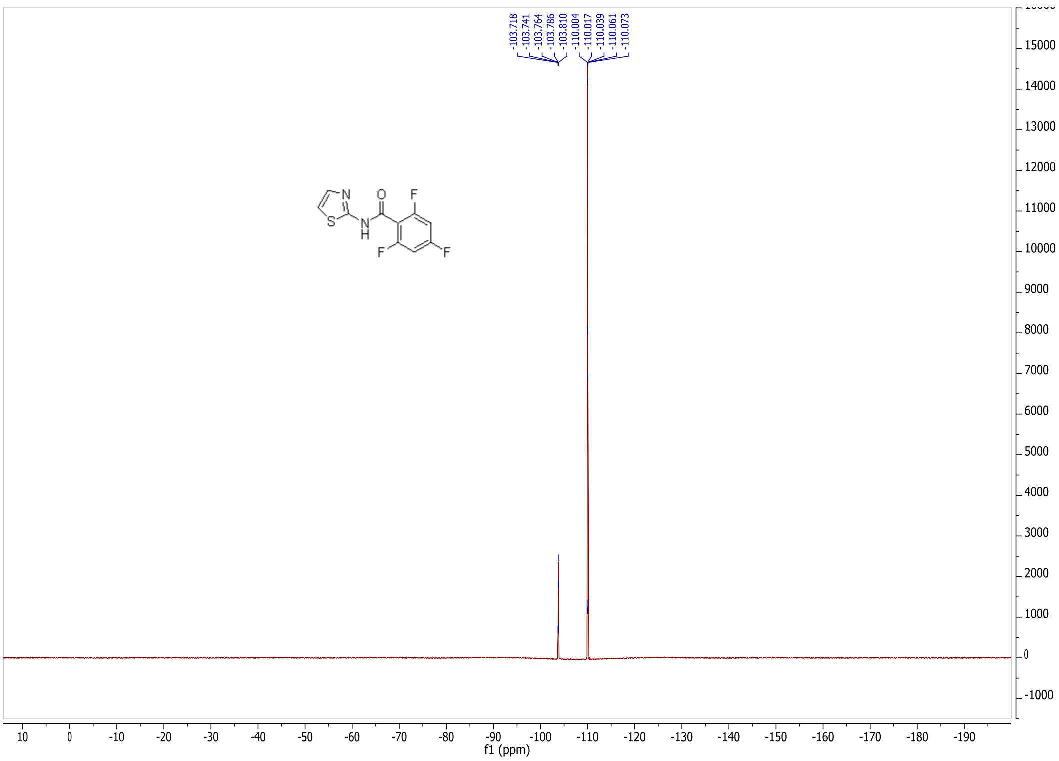
-103.718
-103.741
-103.764
-103.786
-103.810
-110.004
-110.017
-110.039
-110.061
-110.073
N
S
O
F
N
H
F
F
f1 (ppm)

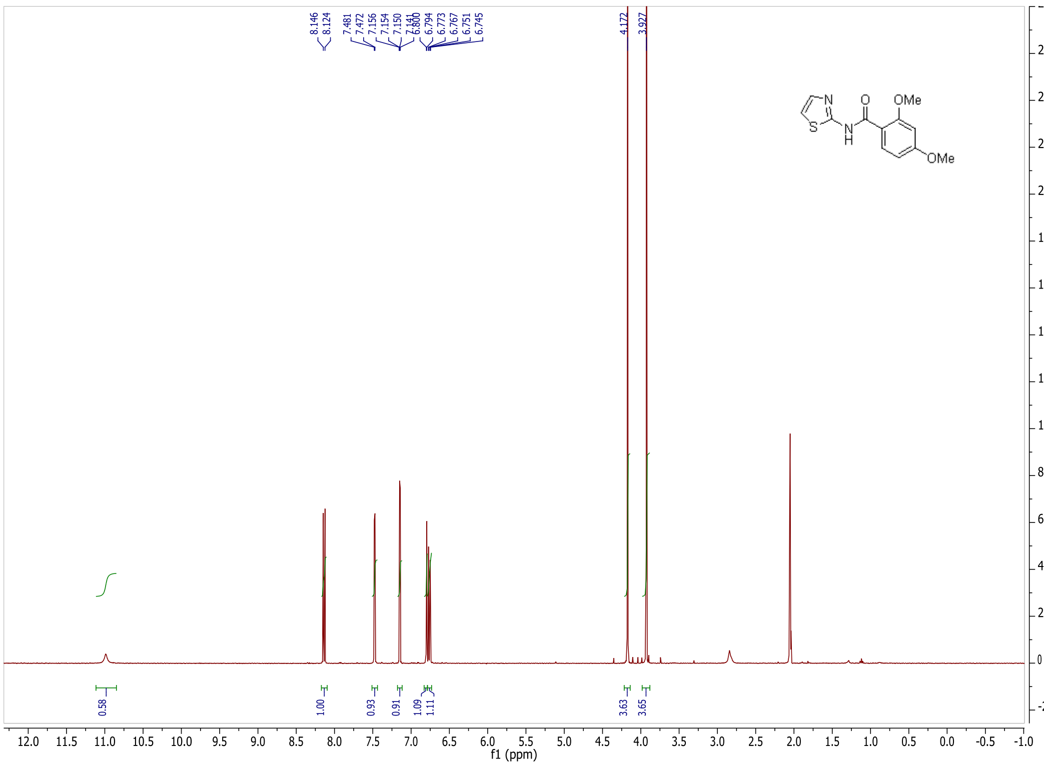
8.146
8.124
7.481
7.472
7.156
7.154
7.150
7.141
6.800
6.794
6.773
6.767
6.751
6.745
4.172
3.927
N
O
OMe
S
H
OMe
0.58
1.00
0.93
0.91
1.09
1.11
3.63
3.65
12.0
11.5
11.0
10.5
10.0
9.5
9.0
8.5
8.0
7.5
7.0
6.5
6.0
5.5
5.0
4.5
4.0
3.5
3.0
2.5
2.0
1.5
1.0
0.5
0.0
-0.5
-1.0
f1 (ppm)
2600
2400
2200
2000
1800
1600
1400
1200
1000
800
600
400
200
0
-200

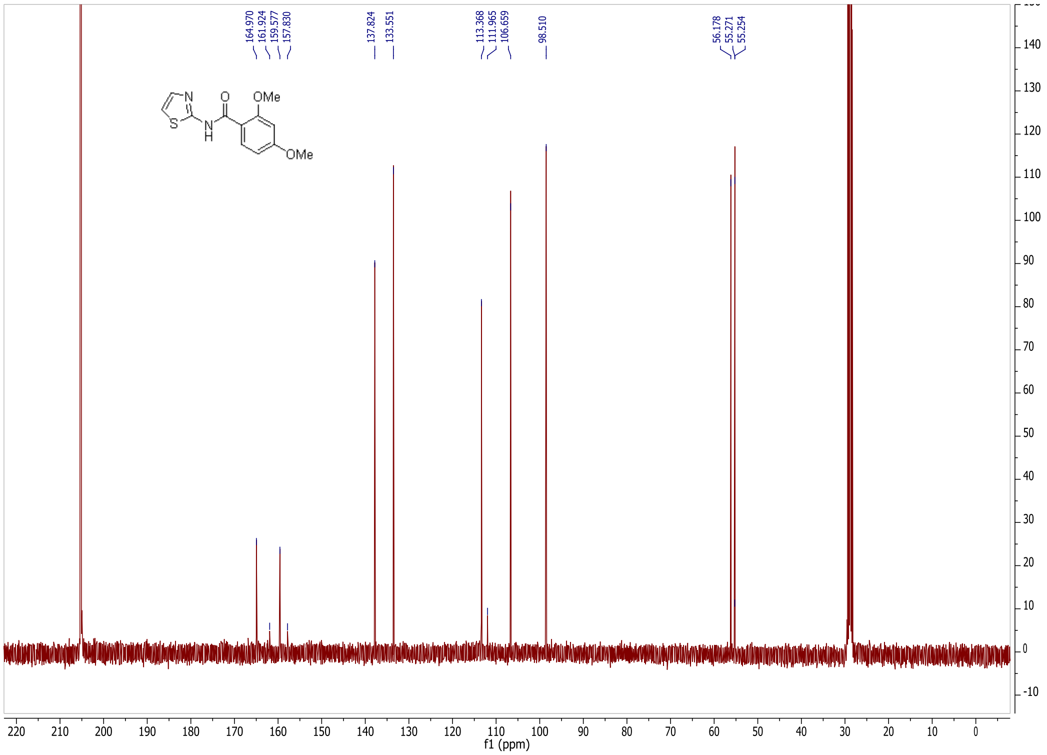
164.970
161.924
159.577
157.830
137.824
133.551
113.368
111.965
106.659
98.510
56.178
55.271
55.254
N
O
OMe
S
H
OMe
220
210
200
190
180
170
160
150
140
130
120
110
100
90
80
70
60
50
40
30
20
10
0
f1 (ppm)
140
130
120
110
100
90
80
70
60
50
40
30
20
10
0
-10

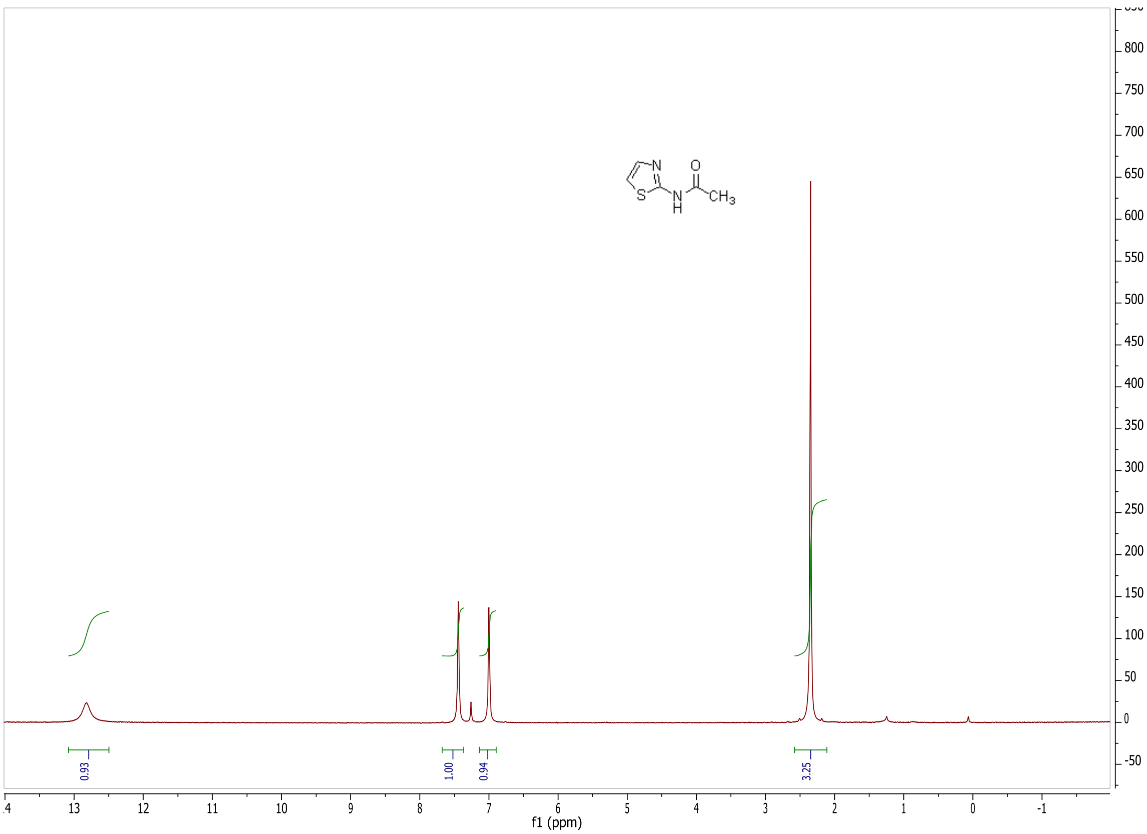

N
O
S
N
H
CH3
0.93
1.00
0.94
3.25
13
12
11
10
9
8
7
6
5
4
3
2
1
0
-1
f1 (ppm)
800
750
700
650
600
550
500
450
400
350
300
250
200
150
100
50
0
-50

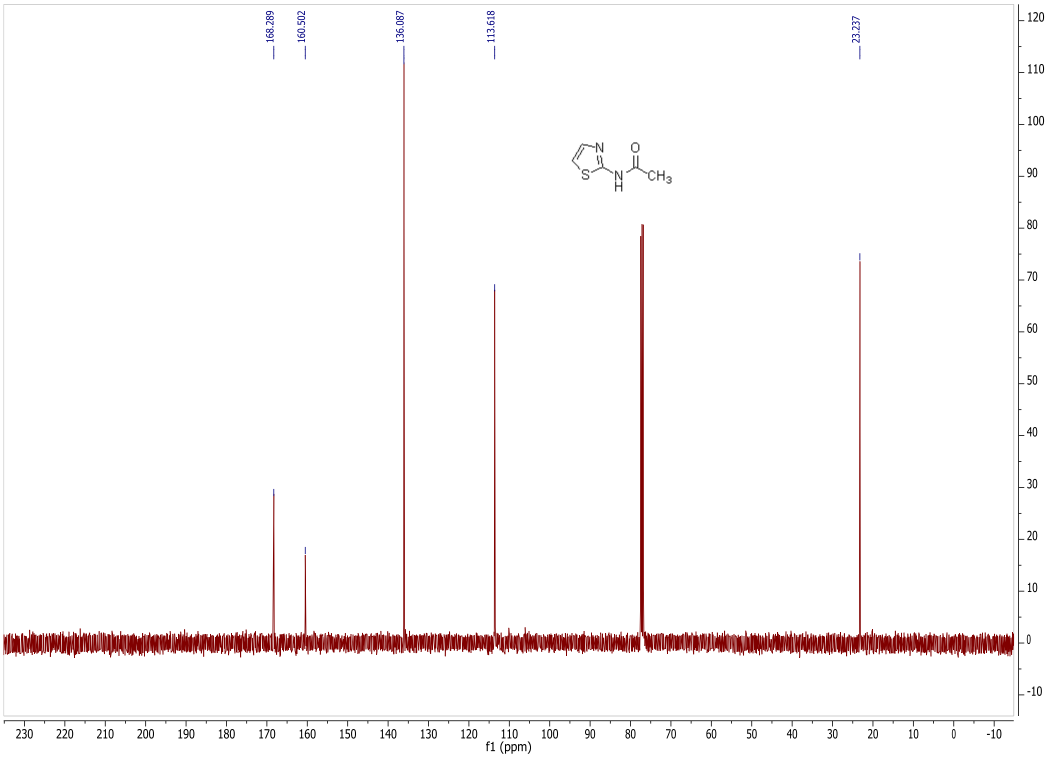

168.289
160.502
136.087
113.618
23.237
N
O
S
N
H
CH3
230
220
210
200
190
180
170
160
150
140
130
120
110
100
90
80
70
60
50
40
30
20
10
0
-10
f1 (ppm)
120
110
100
90
80
70
60
50
40
30
20
10
0
-10

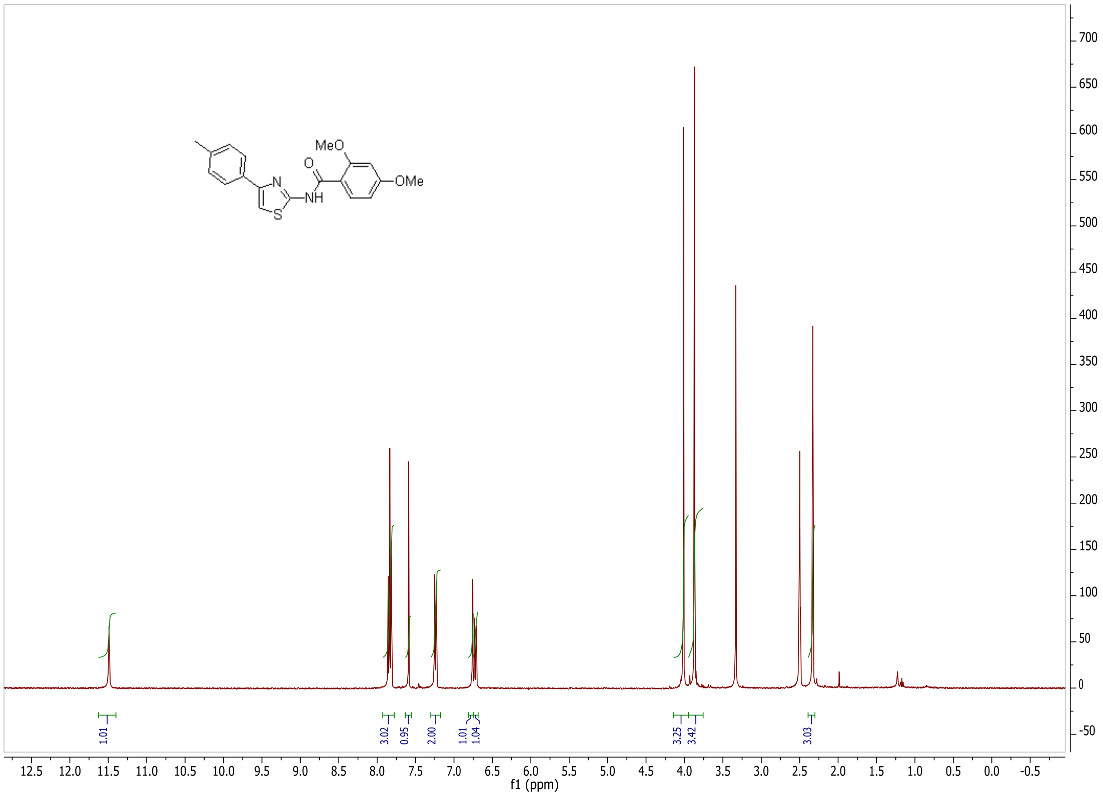
MeO
O
N
NH
S
OMe
1.01
3.02
0.95
2.00
1.01
1.04
3.25
3.42
3.03
12.5 12.0 11.5 11.0 10.5 10.0 9.5 9.0 8.5 8.0 7.5 7.0 6.5 6.0 5.5 5.0 4.5 4.0 3.5 3.0 2.5 2.0 1.5 1.0 0.5 0.0 -0.5
f1 (ppm)
700 650 600 550 500 450 400 350 300 250 200 150 100 50 0 -50

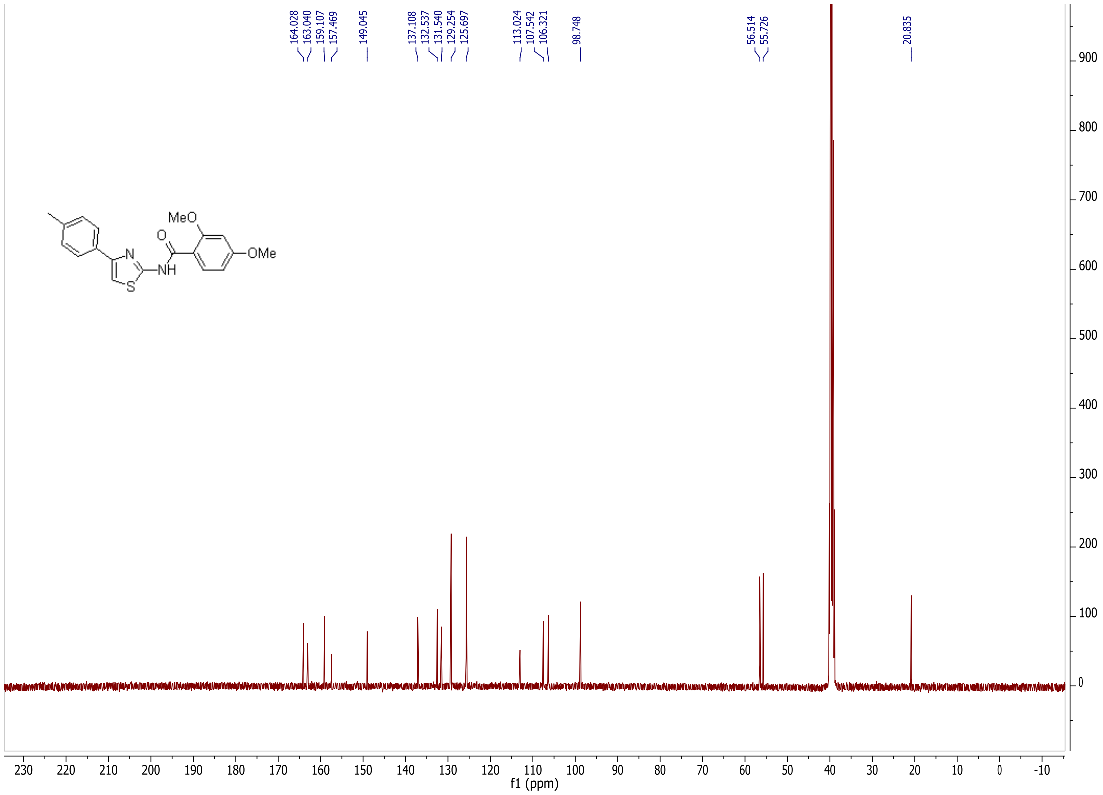
164.028
163.040
159.107
157.469
149.045
137.108
132.537
131.540
129.254
125.697
113.024
107.542
106.321
98.748
56.514
55.726
20.835
MeO
O
N
NH
S
OMe
230 220 210 200 190 180 170 160 150 140 130 120 110 100 90 80 70 60 50 40 30 20 10 0 -10
f1 (ppm)
900 800 700 600 500 400 300 200 100 0

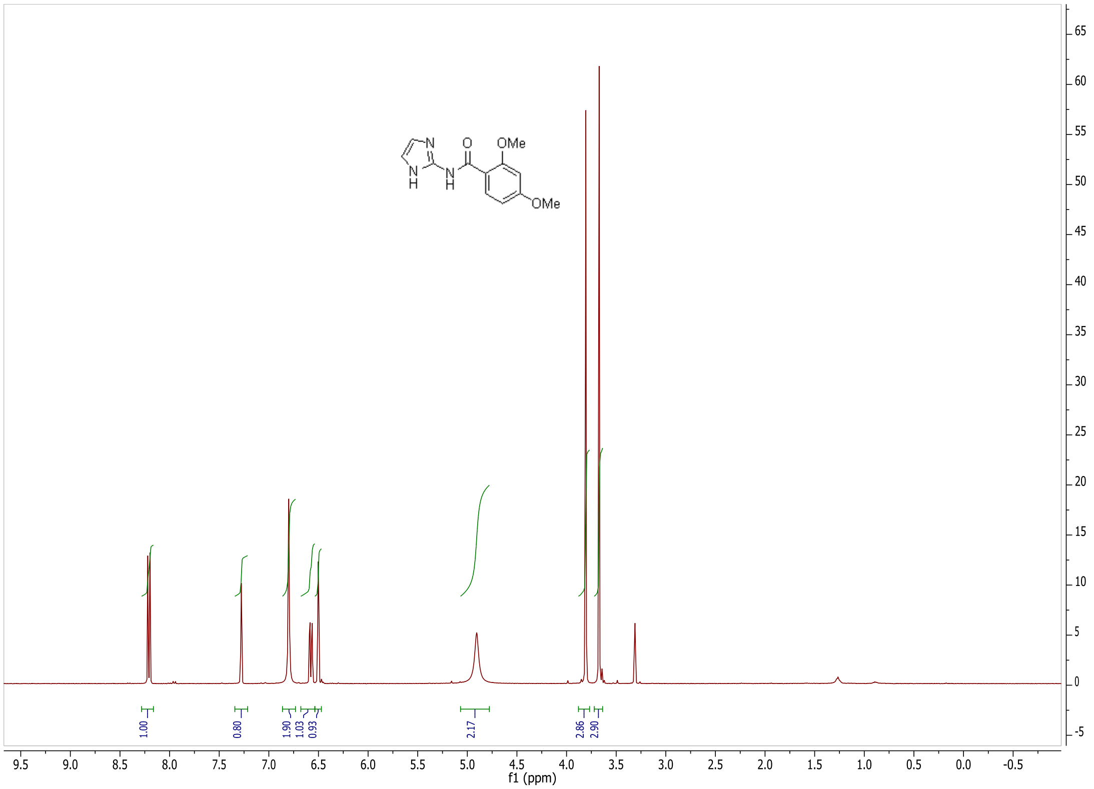
N
O
OMe
N
H
N
H
OMe
1.00
0.80
1.90
1.03
0.93
2.17
2.86
2.90
9.5 9.0 8.5 8.0 7.5 7.0 6.5 6.0 5.5 5.0 4.5 4.0 3.5 3.0 2.5 2.0 1.5 1.0 0.5 0.0 -0.5
f1 (ppm)
65 60 55 50 45 40 35 30 25 20 15 10 5 0 -5

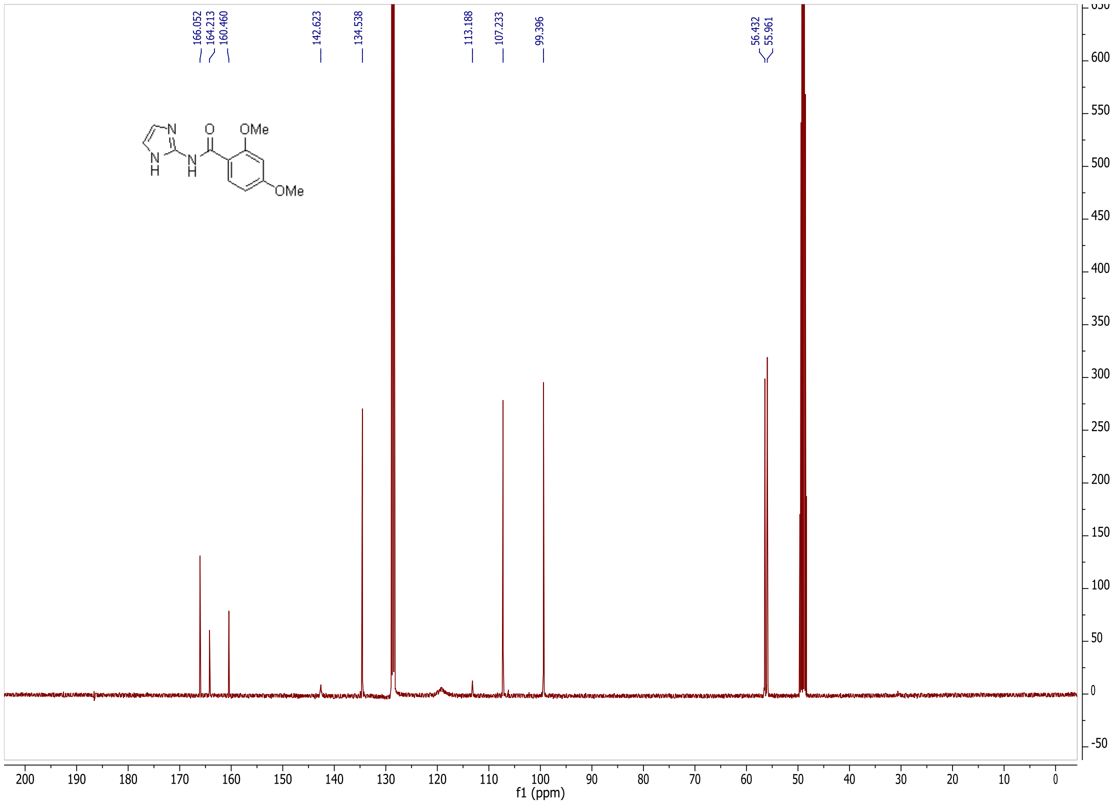
166.052
164.213
160.460
142.623
134.538
113.188
107.233
99.396
56.432
55.961
N
O
OMe
N
H
N
H
OMe
200 190 180 170 160 150 140 130 120 110 100 90 80 70 60 50 40 30 20 10 0
f1 (ppm)
650 600 550 500 450 400 350 300 250 200 150 100 50 0 -50

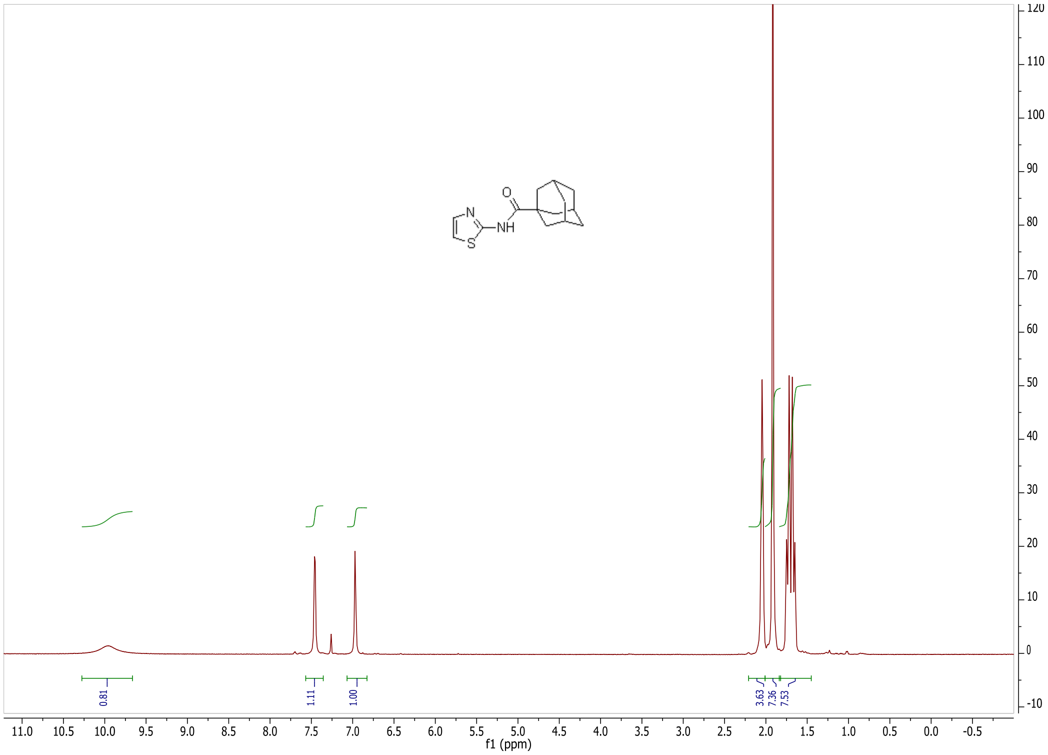
O
N
NH
S
0.81
1.11
1.00
3.63
7.36
7.53
11.0 10.5 10.0 9.5 9.0 8.5 8.0 7.5 7.0 6.5 6.0 5.5 5.0 4.5 4.0 3.5 3.0 2.5 2.0 1.5 1.0 0.5 0.0 -0.5
f1 (ppm)
120 110 100 90 80 70 60 50 40 30 20 10 0 -10

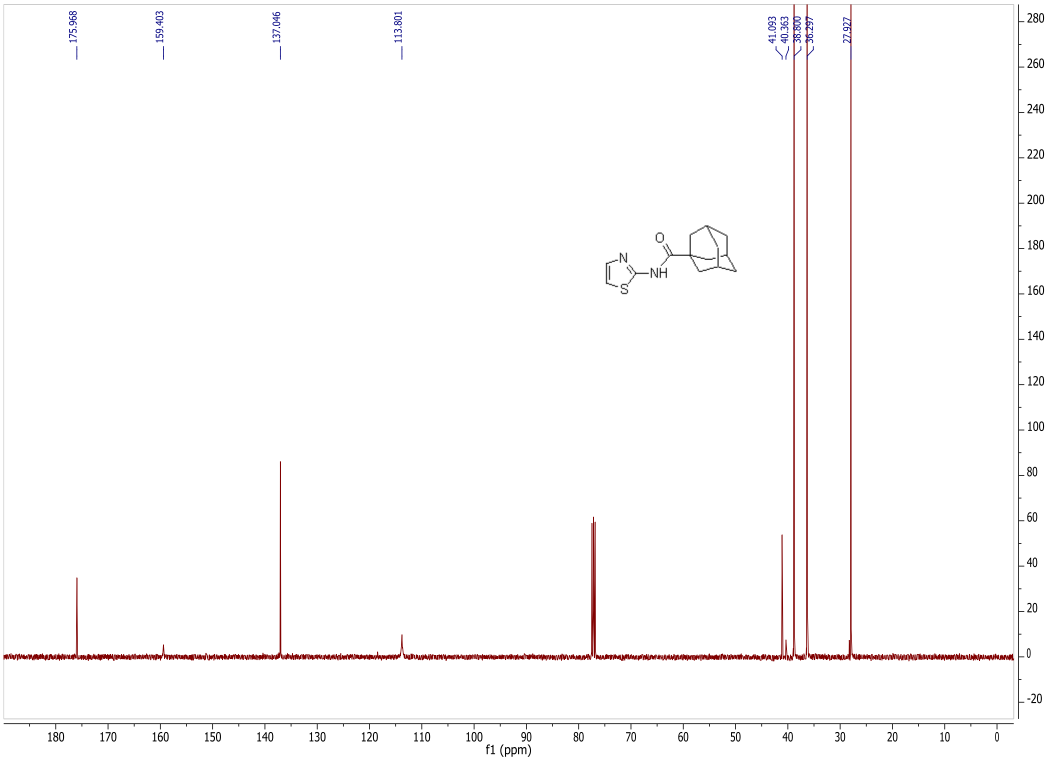
175.968
159.403
137.046
113.801
41.093
40.363
38.800
36.297
27.927
O
N
NH
S
180 170 160 150 140 130 120 110 100 90 80 70 60 50 40 30 20 10 0
f1 (ppm)
280 260 240 220 200 180 160 140 120 100 80 60 40 20 0 -20

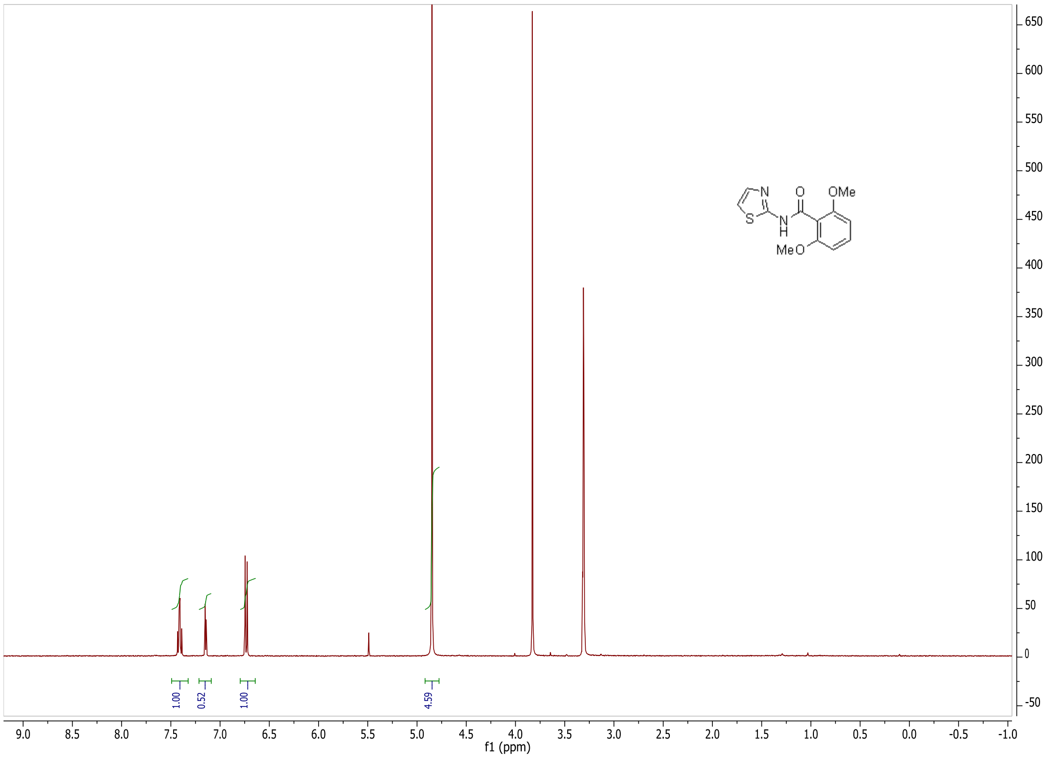
1.00
0.52
1.00
4.59
f1 (ppm)

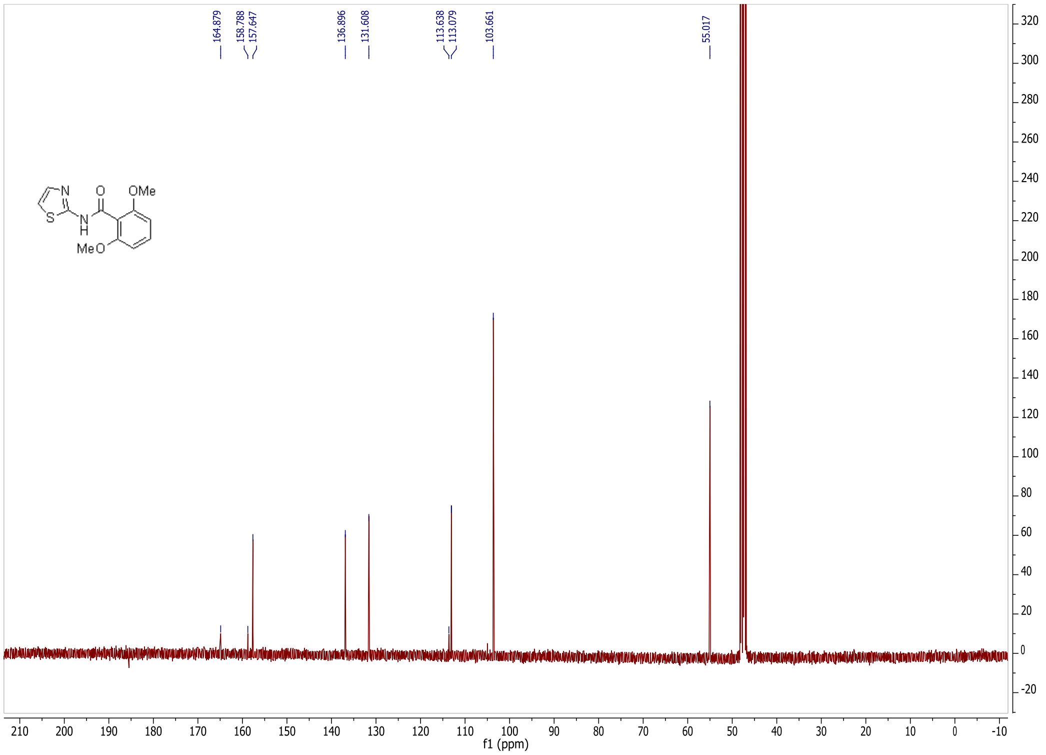
164.879
158.788
157.647
136.896
131.608
113.638
113.079
103.661
55.017
f1 (ppm)

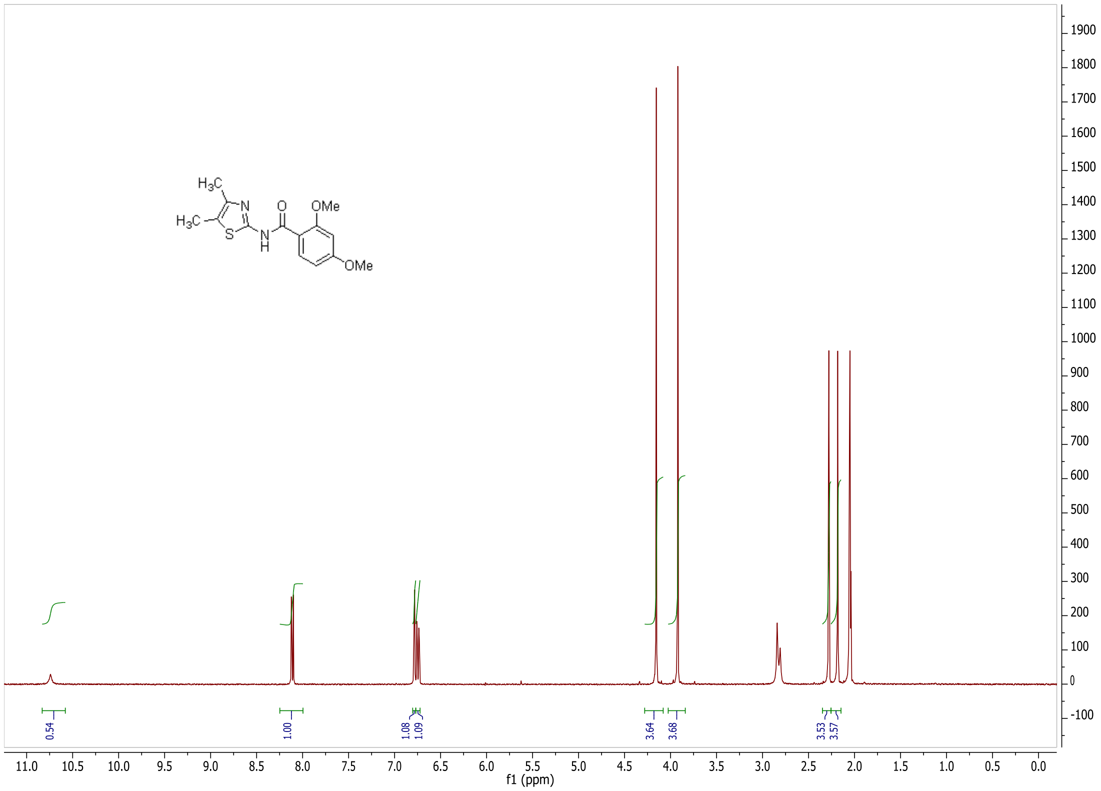

0.54
1.00
1.08
1.09
3.64
3.68
3.53
3.57
f1 (ppm)

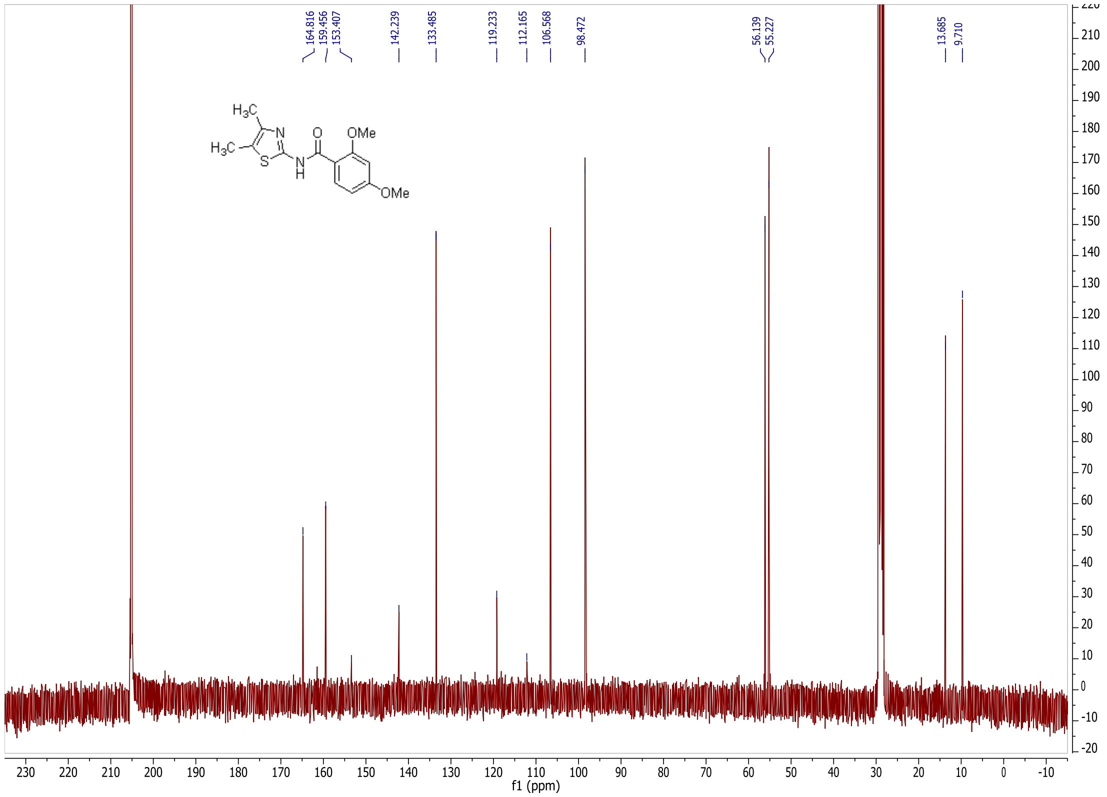

164.816
159.456
153.407
142.239
133.485
119.233
112.165
106.568
98.472
56.139
55.227
13.685
9.710
f1 (ppm)

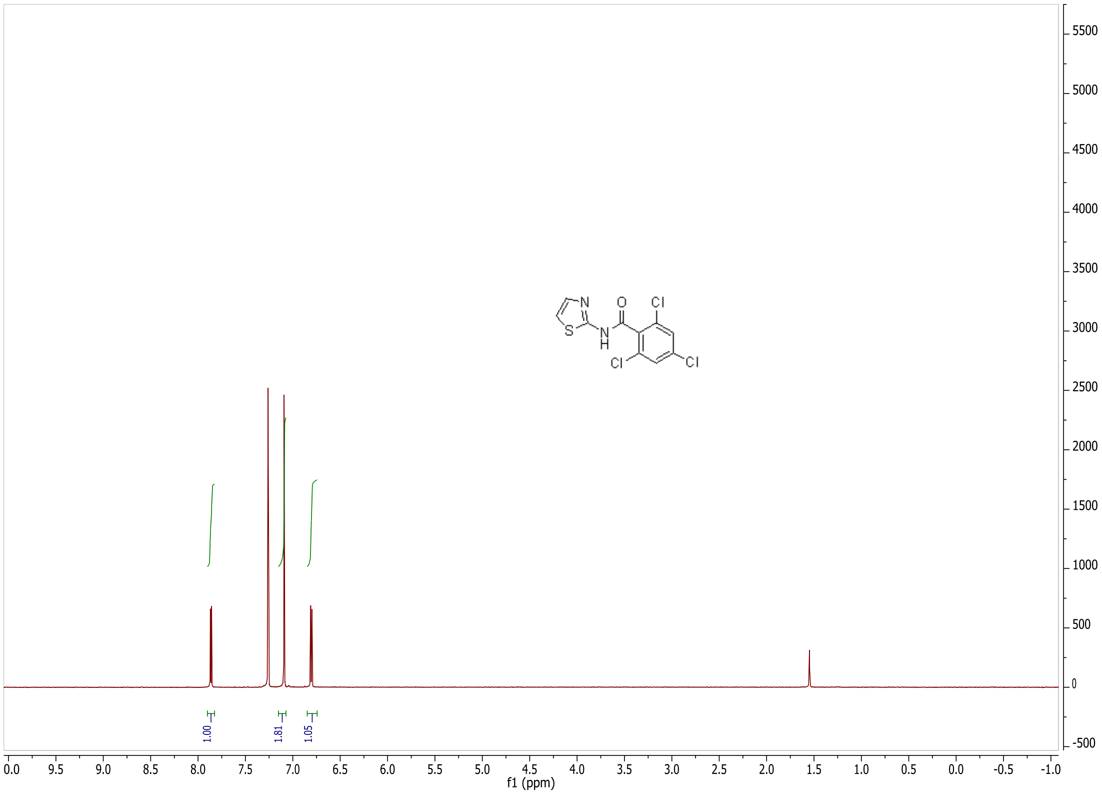
N
O
Cl
S
N
H
Cl
Cl
1.00
1.81
1.05
f1 (ppm)
0.0
9.5
9.0
8.5
8.0
7.5
7.0
6.5
6.0
5.5
5.0
4.5
4.0
3.5
3.0
2.5
2.0
1.5
1.0
0.5
0.0
-0.5
-1.0
5500
5000
4500
4000
3500
3000
2500
2000
1500
1000
500
0
-500

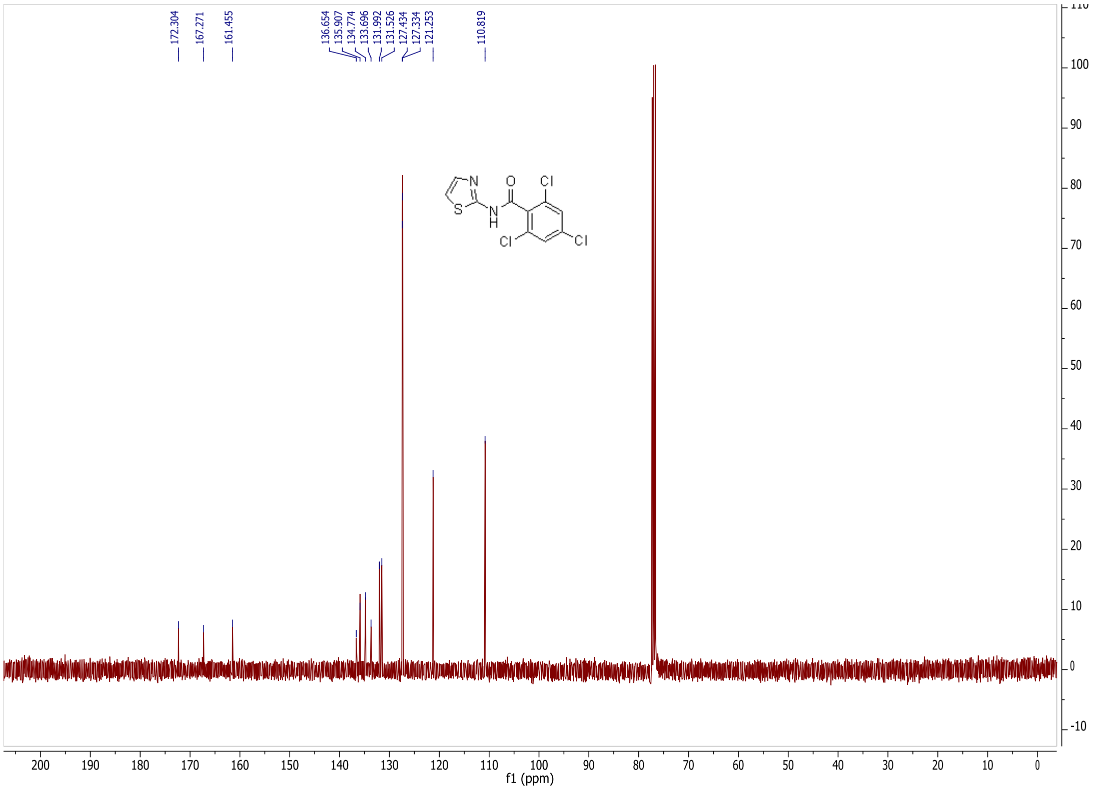
172.304
167.271
161.455
136.654
135.907
134.774
133.696
131.992
131.526
127.434
127.334
121.253
110.819
N
O
Cl
S
N
H
Cl
Cl
f1 (ppm)
200
190
180
170
160
150
140
130
120
110
100
90
80
70
60
50
40
30
20
10
0
110
100
90
80
70
60
50
40
30
20
10
0
-10

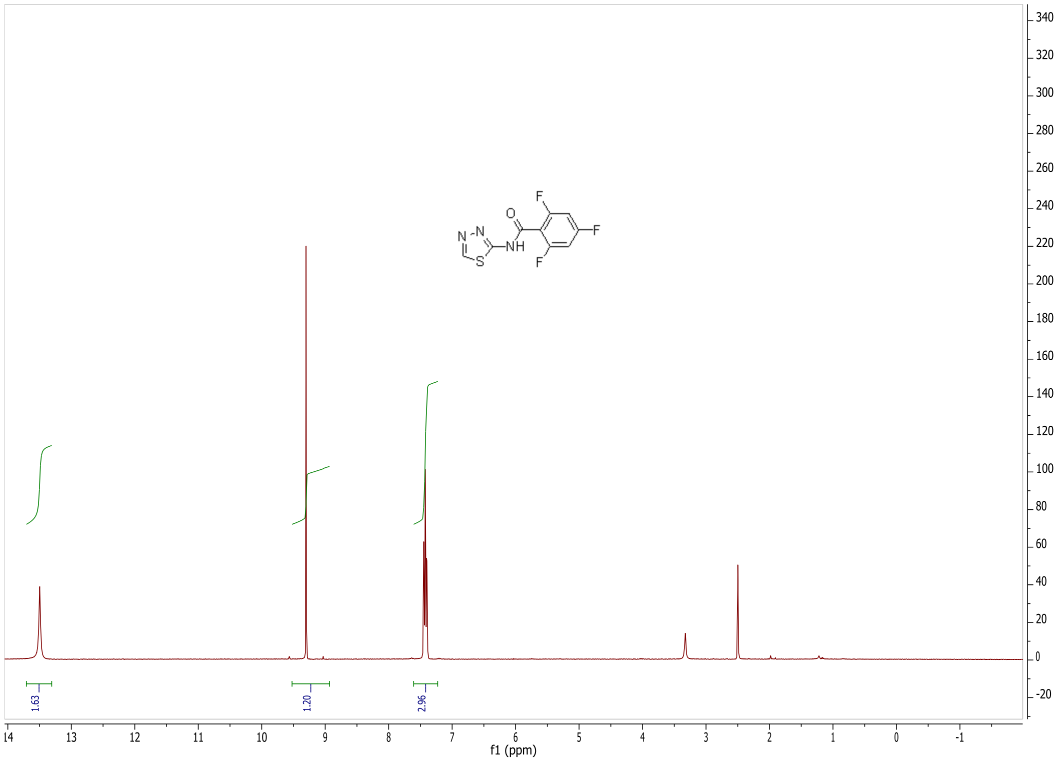

F
O
F
N
N
NH
S
F
1.63
1.20
2.96
14 13 12 11 10 9 8 7 6 5 4 3 2 1 0 -1
f1 (ppm)
340 320 300 280 260 240 220 200 180 160 140 120 100 80 60 40 20 0 -20

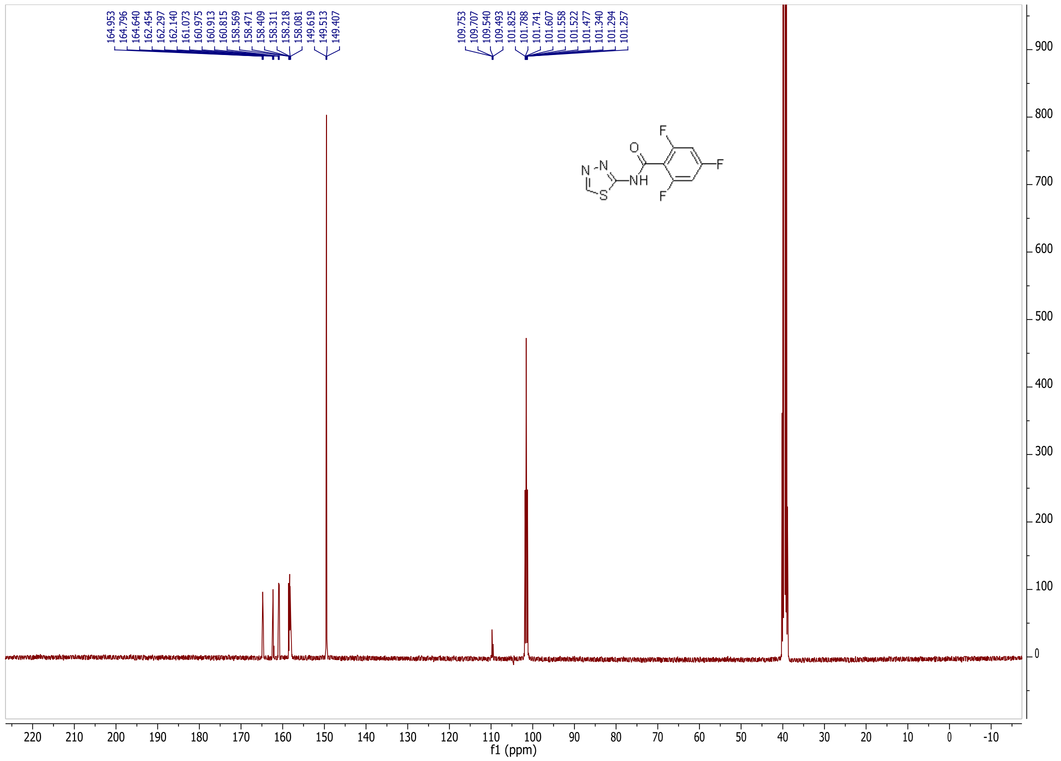

164.953
164.796
164.640
162.454
162.297
162.140
161.073
160.975
160.913
160.815
158.569
158.471
158.409
158.311
158.218
158.081
149.619
149.513
149.407
109.753
109.707
109.540
109.493
101.825
101.788
101.741
101.607
101.558
101.522
101.477
101.340
101.294
101.257
F
O
F
N
N
NH
S
F
220 210 200 190 180 170 160 150 140 130 120 110 100 90 80 70 60 50 40 30 20 10 0 -10
f1 (ppm)
900 800 700 600 500 400 300 200 100 0

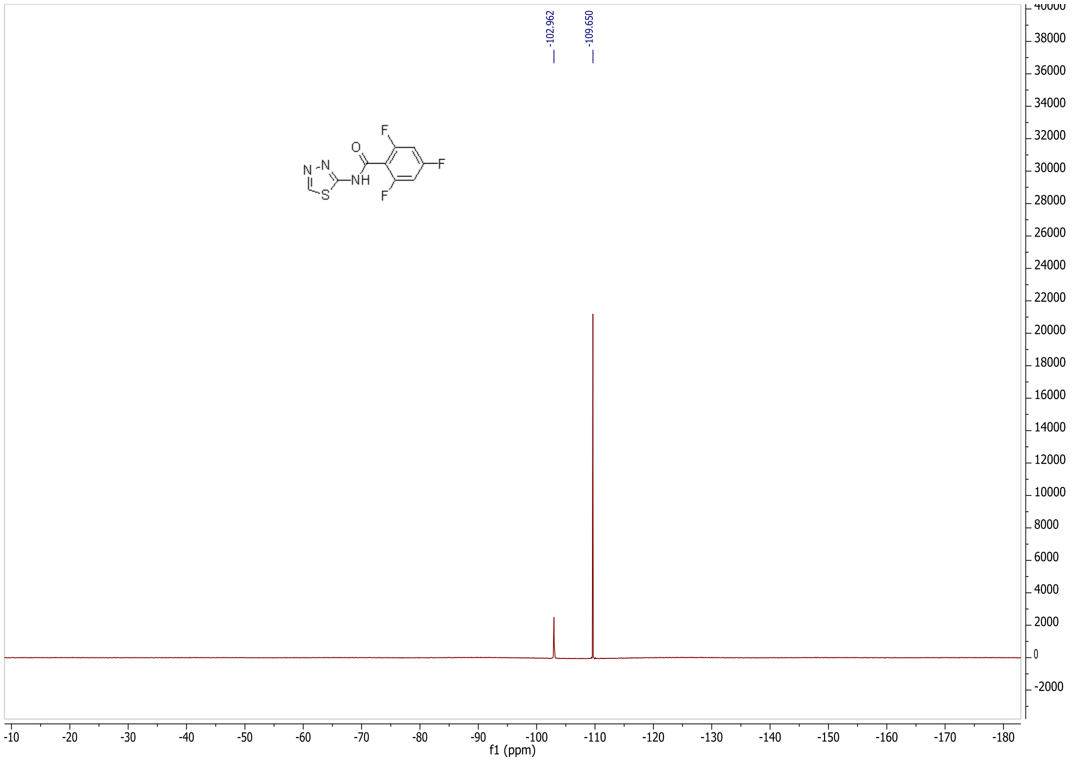
-102.962
-109.650
F
O
N
N
NH
F
S
F
40000
38000
36000
34000
32000
30000
28000
26000
24000
22000
20000
18000
16000
14000
12000
10000
8000
6000
4000
2000
0
-2000
-10
-20
-30
-40
-50
-60
-70
-80
-90
-100
-110
-120
-130
-140
-150
-160
-170
-180
f1 (ppm)

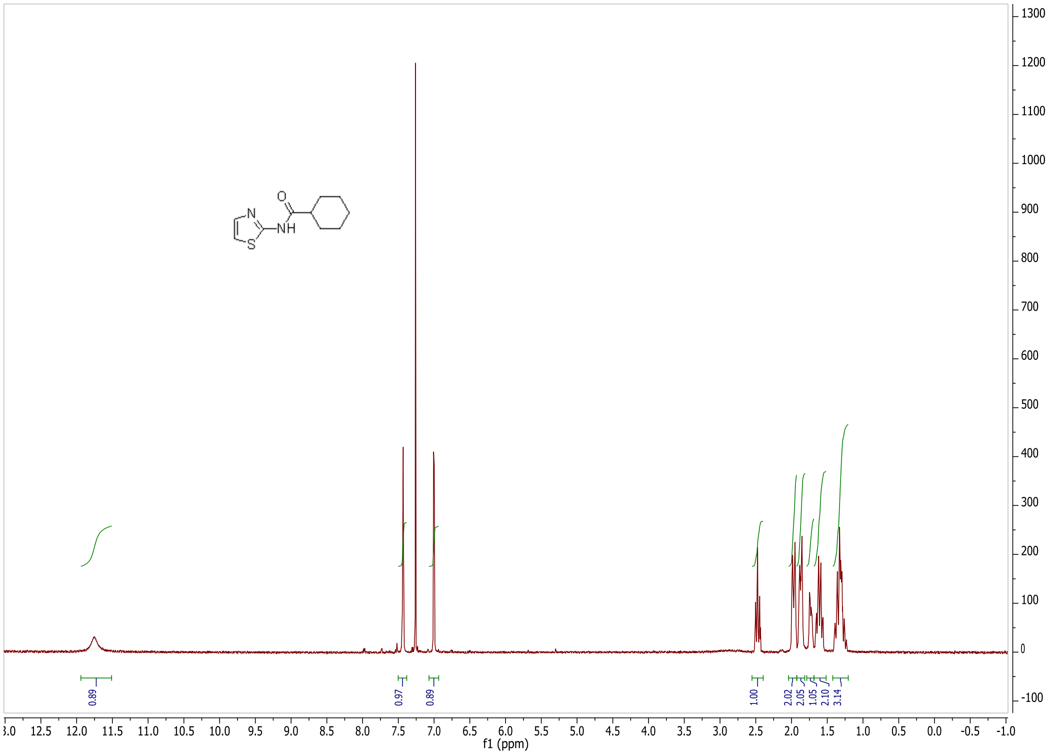
O
N
NH
S
1300
1200
1100
1000
900
800
700
600
500
400
300
200
100
0
-100
0.89
0.97
0.89
1.00
2.02
2.05
1.05
2.10
3.14
13.0
12.5
12.0
11.5
11.0
10.5
10.0
9.5
9.0
8.5
8.0
7.5
7.0
6.5
6.0
5.5
5.0
4.5
4.0
3.5
3.0
2.5
2.0
1.5
1.0
0.5
0.0
-0.5
-1.0
f1 (ppm)

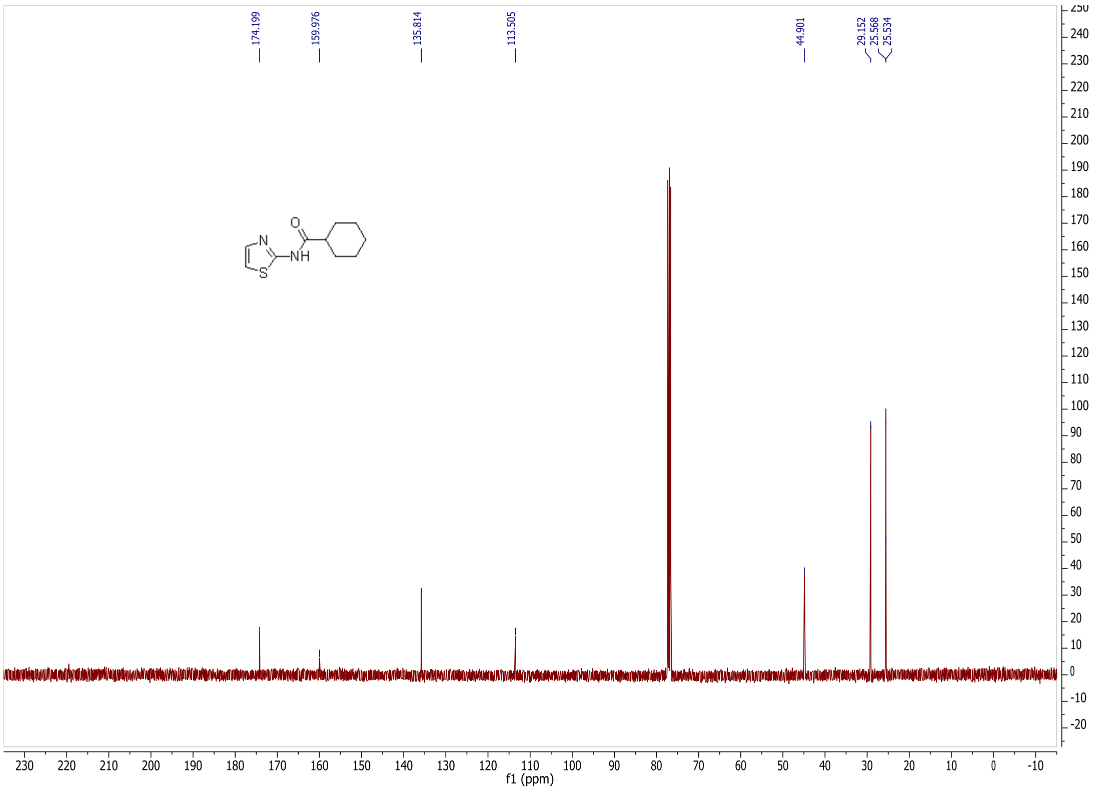
174.199
159.976
135.814
113.505
44.901
29.152
25.568
25.534
O
N
NH
S
f1 (ppm)

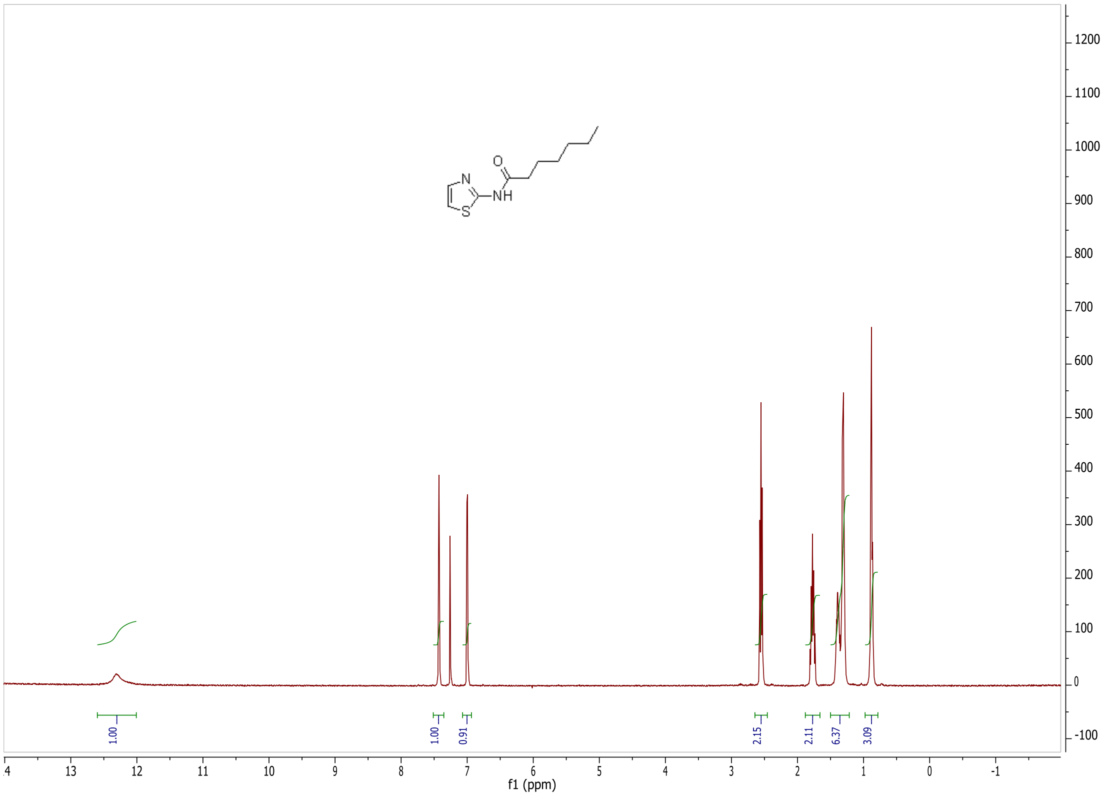
O
N
NH
S
1.00
1.00
0.91
2.15
2.11
6.37
3.09
f1 (ppm)

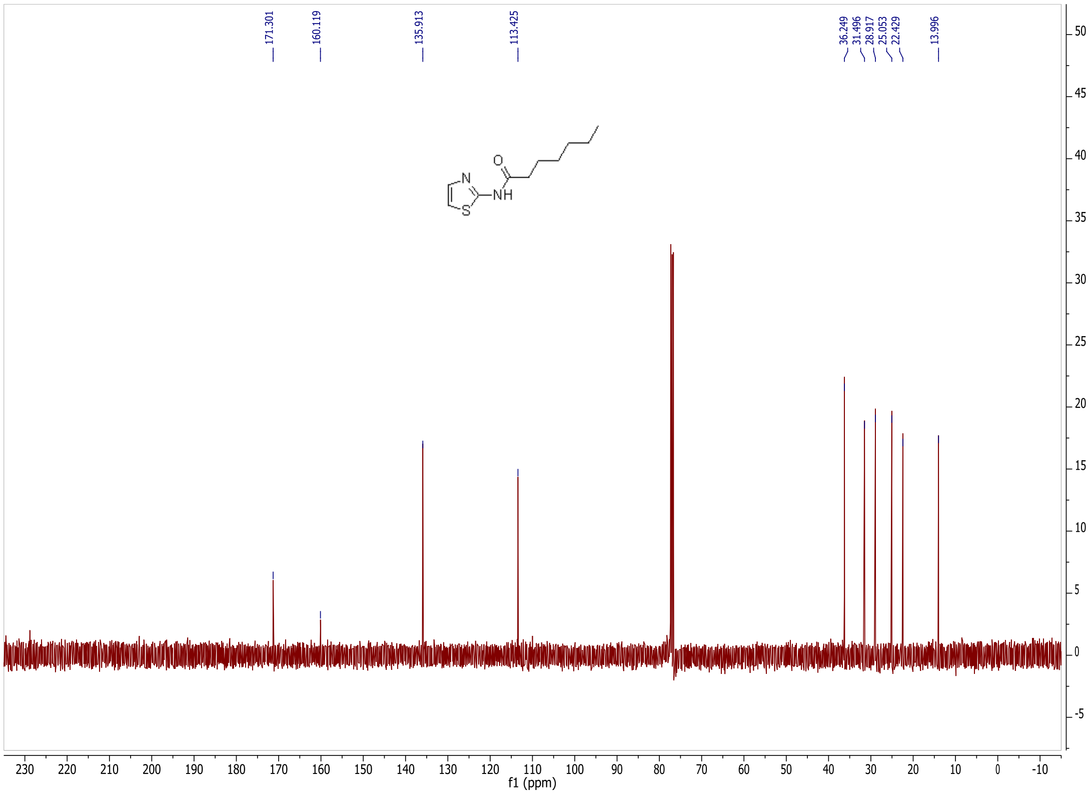
171.301
160.119
135.913
113.425
36.249
31.496
28.917
25.053
22.429
13.996
O
N
NH
S
230 220 210 200 190 180 170 160 150 140 130 120 110 100 90 80 70 60 50 40 30 20 10 0 -10
f1 (ppm)
50 45 40 35 30 25 20 15 10 5 0 -5

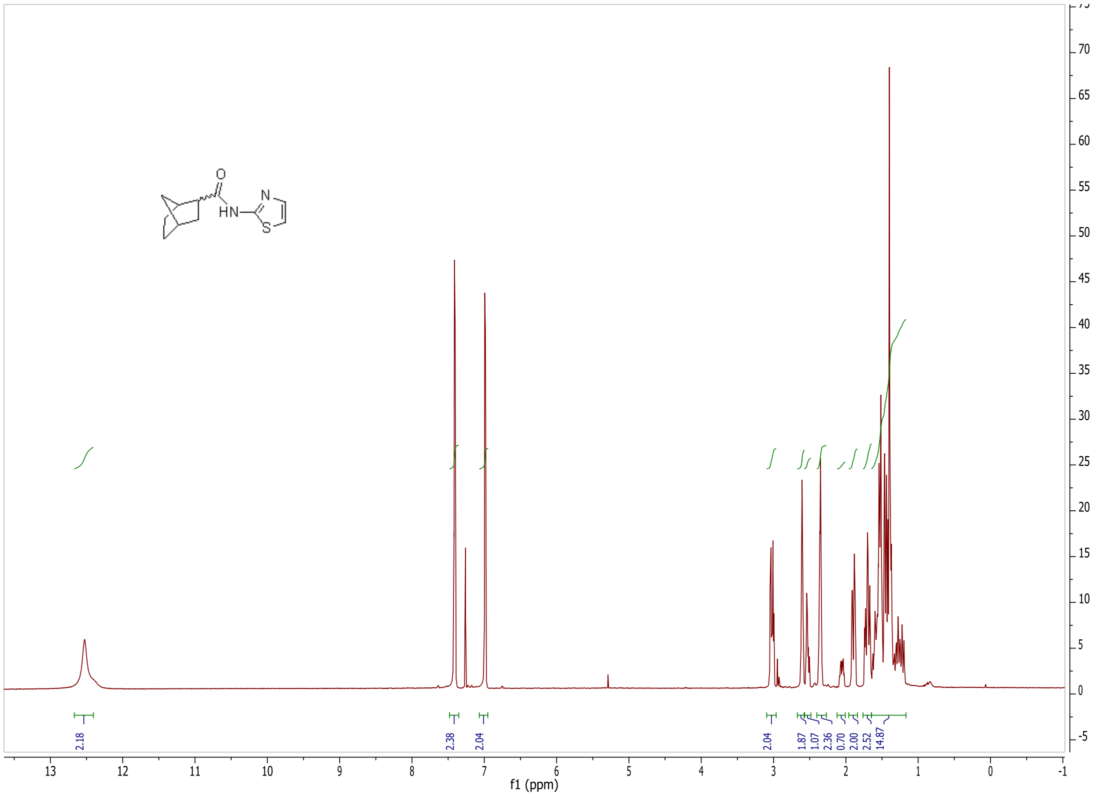
O
N
HN
S
2.18
2.38
2.04
2.04
1.87
1.07
2.36
0.70
2.00
2.52
14.87
13 12 11 10 9 8 7 6 5 4 3 2 1 0 -1
f1 (ppm)
70 65 60 55 50 45 40 35 30 25 20 15 10 5 0 -5

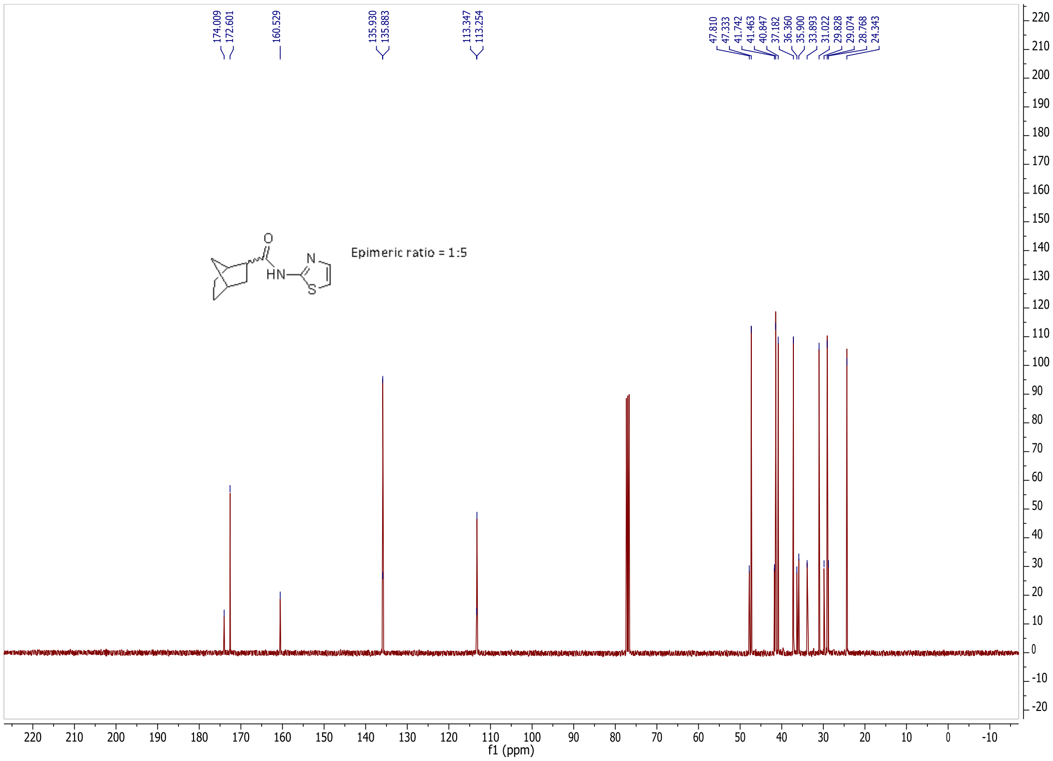
174.009
172.601
160.529
135.930
135.883
113.347
113.254
47.810
47.333
41.742
41.463
40.847
37.182
36.360
35.900
33.893
31.022
29.828
29.074
28.768
24.343
O
HN
N
S
Epimeric ratio = 1:5
220 210 200 190 180 170 160 150 140 130 120 110 100 90 80 70 60 50 40 30 20 10 0 -10 -20
220 210 200 190 180 170 160 150 140 130 120 110 100 90 80 70 60 50 40 30 20 10 0 -10
f1 (ppm)

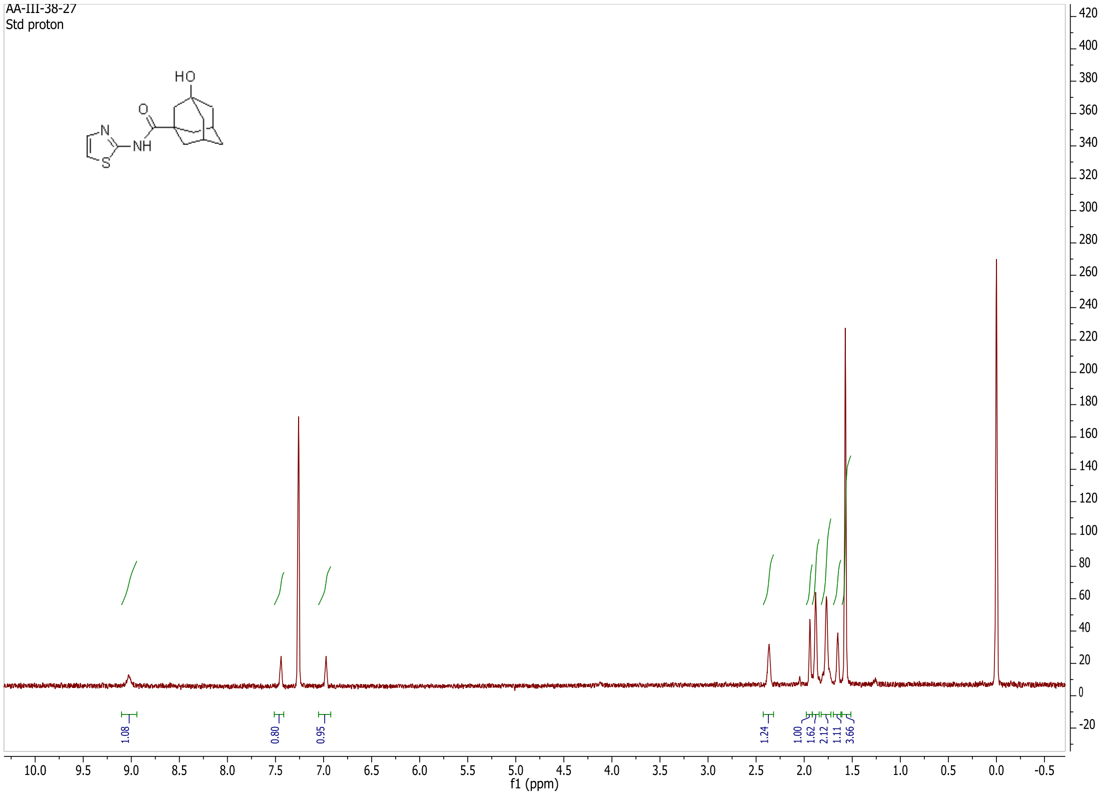
AA-III-38-27
Std proton
HO
O
N
NH
S
420 400 380 360 340 320 300 280 260 240 220 200 180 160 140 120 100 80 60 40 20 0 -20
1.08
0.80
0.95
1.24
1.00
1.62
2.12
1.11
3.66
10.0 9.5 9.0 8.5 8.0 7.5 7.0 6.5 6.0 5.5 5.0 4.5 4.0 3.5 3.0 2.5 2.0 1.5 1.0 0.5 0.0 -0.5
f1 (ppm)

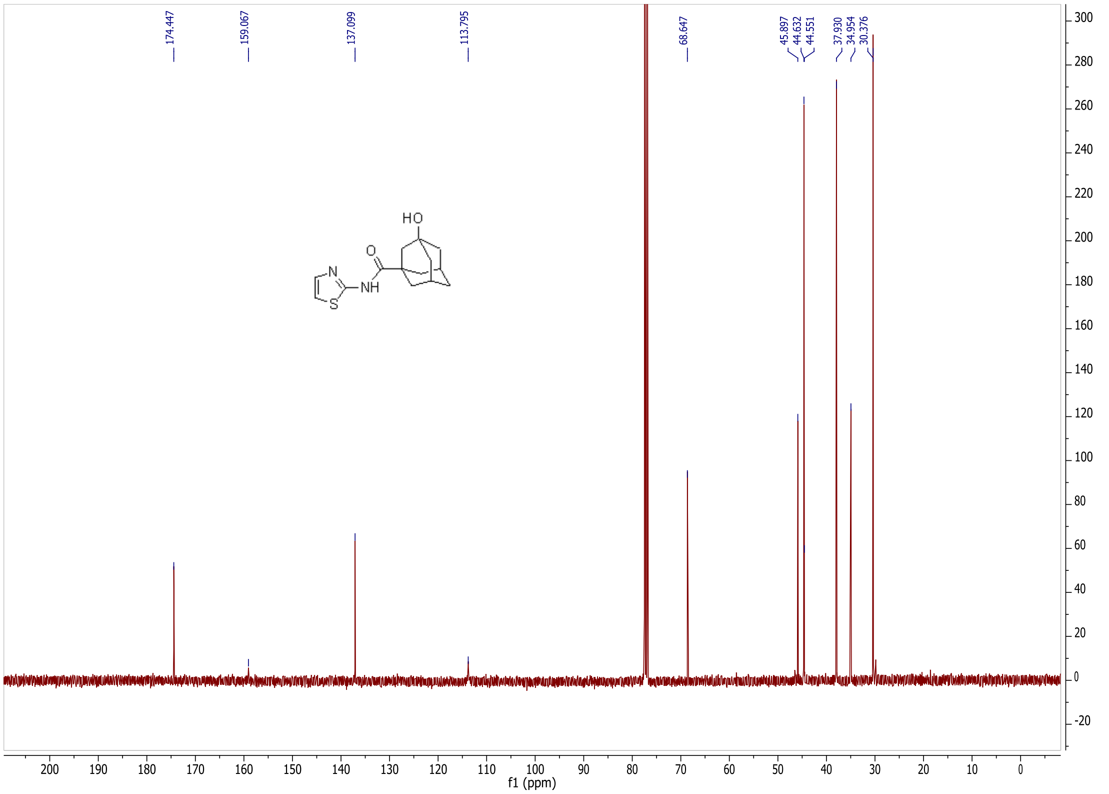
174.447
159.067
137.099
113.795
68.647
45.897
44.632
44.551
37.930
34.954
30.376
HO
O
N
NH
S
300
280
260
240
220
200
180
160
140
120
100
80
60
40
20
0
-20
200 190 180 170 160 150 140 130 120 110 100 90 80 70 60 50 40 30 20 10 0
f1 (ppm)

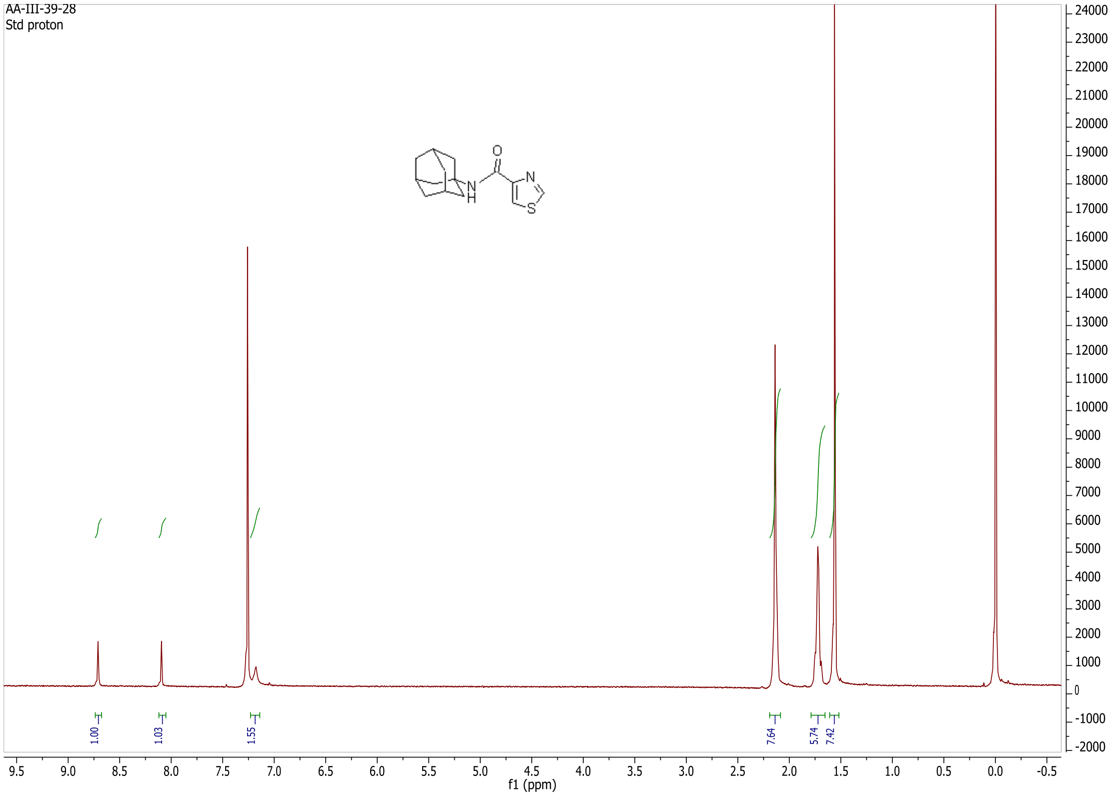
AA-III-39-28
Std proton
O
N
N
H
S
1.00
1.03
1.55
7.64
5.74
7.42
24000
23000
22000
21000
20000
19000
18000
17000
16000
15000
14000
13000
12000
11000
10000
9000
8000
7000
6000
5000
4000
3000
2000
1000
0
-1000
-2000
9.5 9.0 8.5 8.0 7.5 7.0 6.5 6.0 5.5 5.0 4.5 4.0 3.5 3.0 2.5 2.0 1.5 1.0 0.5 0.0 -0.5
f1 (ppm)

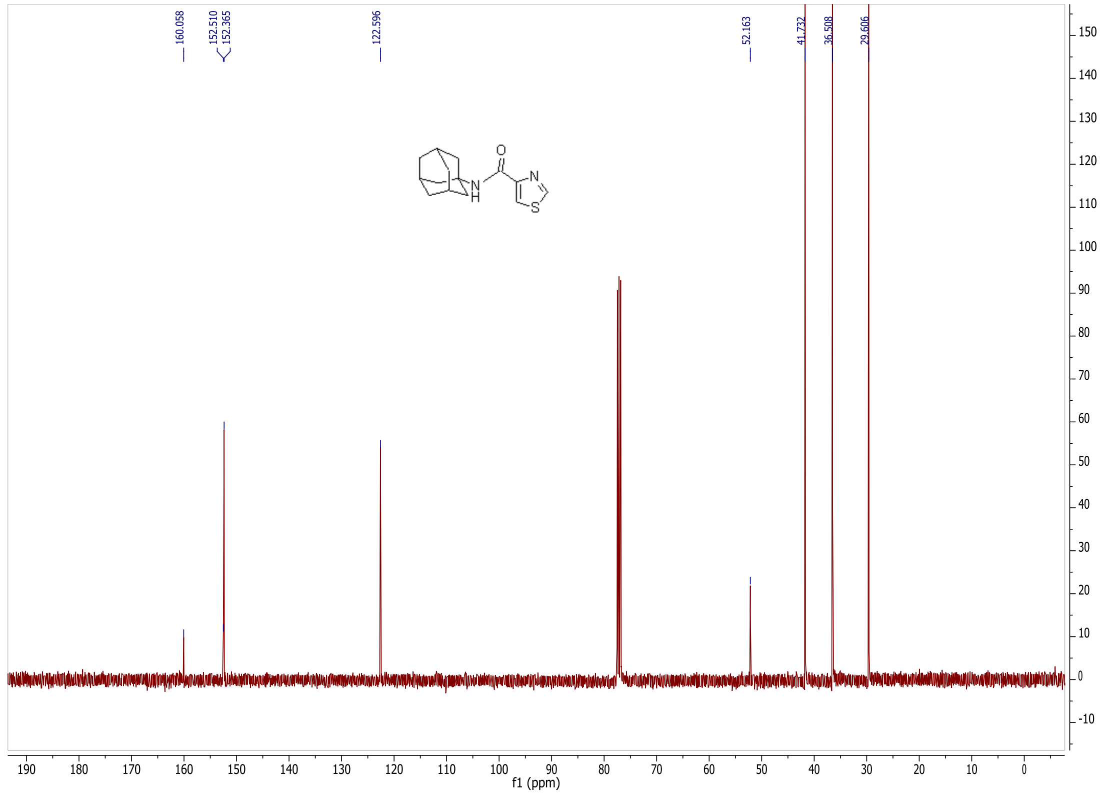
160.058
152.510
152.365
122.596
52.163
41.732
36.508
29.606
O
N
H
N
S
150
140
130
120
110
100
90
80
70
60
50
40
30
20
10
0
-10
190
180
170
160
150
140
130
120
110
100
90
80
70
60
50
40
30
20
10
0
f1 (ppm)

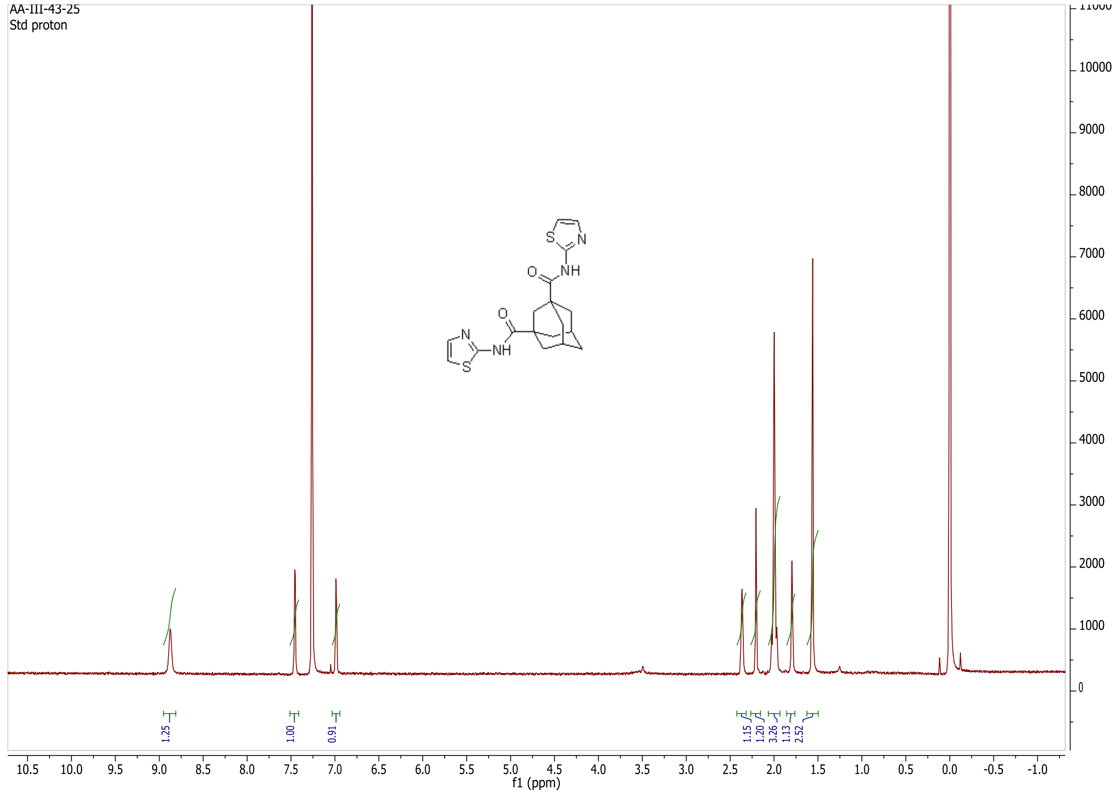
AA-III-43-25
Std proton
S
N
O
NH
O
N
NH
S
11000
10000
9000
8000
7000
6000
5000
4000
3000
2000
1000
0
1.25
1.00
0.91
1.15
1.20
3.26
1.13
2.52
10.5
10.0
9.5
9.0
8.5
8.0
7.5
7.0
6.5
6.0
5.5
5.0
4.5
4.0
3.5
3.0
2.5
2.0
1.5
1.0
0.5
0.0
-0.5
-1.0
f1 (ppm)

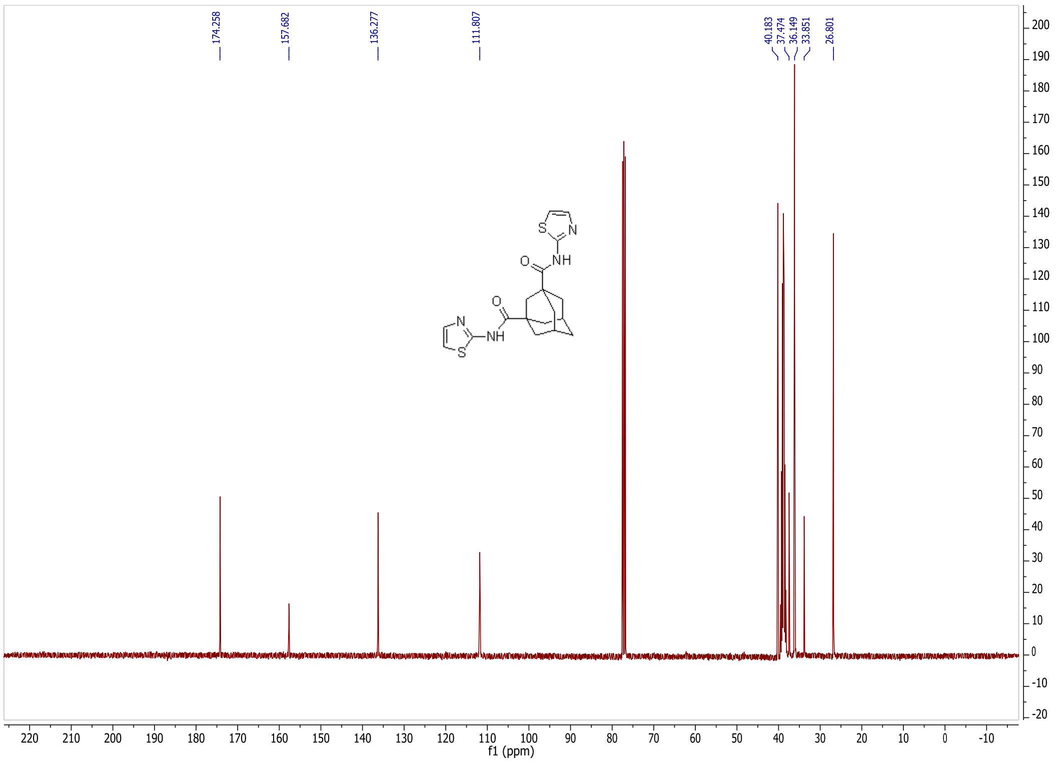
174.258
157.682
136.277
111.807
40.183
37.474
36.149
33.851
26.801
S
N
NH
O
O
N
NH
S
220 210 200 190 180 170 160 150 140 130 120 110 100 90 80 70 60 50 40 30 20 10 0 -10
f1 (ppm)
200 190 180 170 160 150 140 130 120 110 100 90 80 70 60 50 40 30 20 10 0 -10 -20

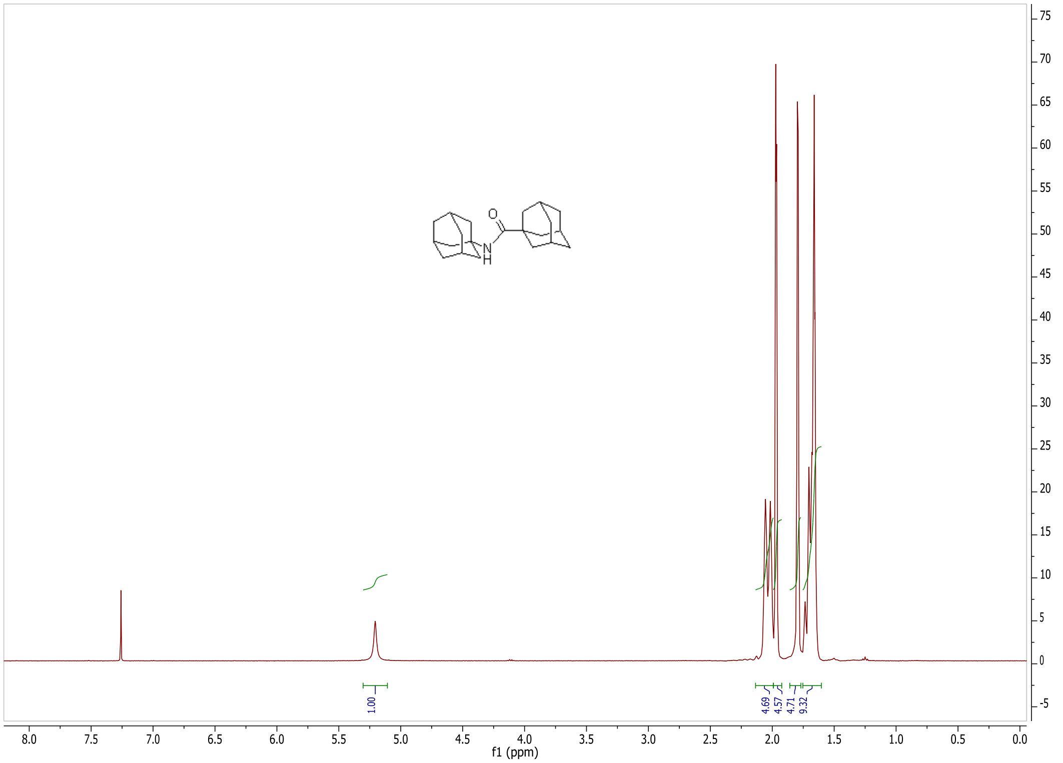
O
N
H
1.00
4.69
4.57
4.71
9.32
8.0 7.5 7.0 6.5 6.0 5.5 5.0 4.5 4.0 3.5 3.0 2.5 2.0 1.5 1.0 0.5 0.0
f1 (ppm)
75 70 65 60 55 50 45 40 35 30 25 20 15 10 5 0 -5

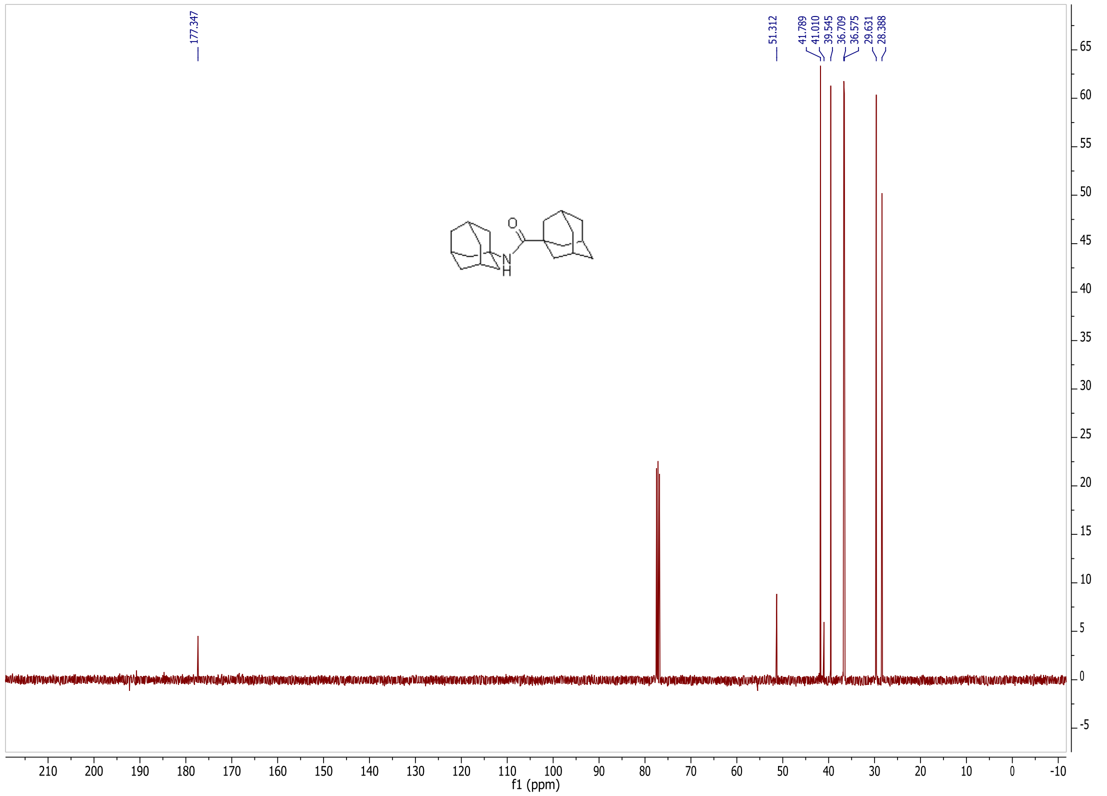
177.347
51.312
41.789
41.010
39.545
36.709
36.575
29.631
28.388
O
N
H
f1 (ppm)

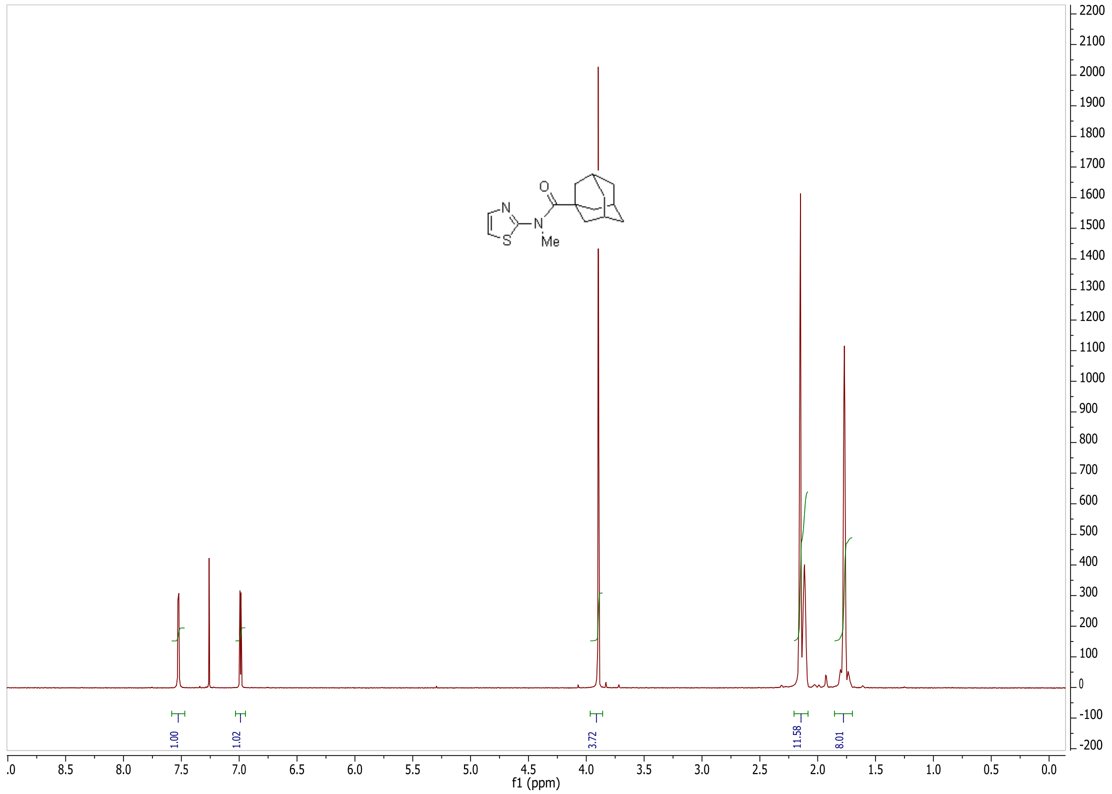
N
S
O
N
Me
1.00
1.02
3.72
11.58
8.01
f1 (ppm)

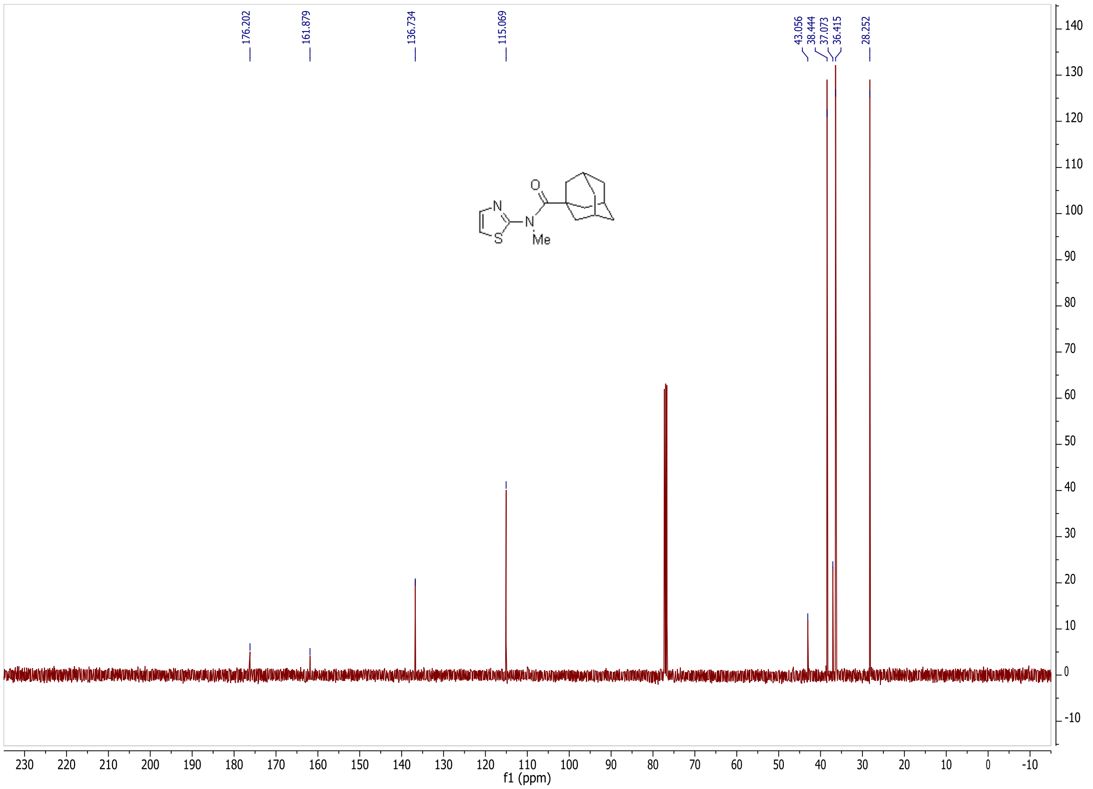
176.202
161.879
136.734
115.069
43.056
38.444
37.073
36.415
28.252
O
N
S
N
Me
230 220 210 200 190 180 170 160 150 140 130 120 110 100 90 80 70 60 50 40 30 20 10 0 -10
f1 (ppm)
140 130 120 110 100 90 80 70 60 50 40 30 20 10 0 -10

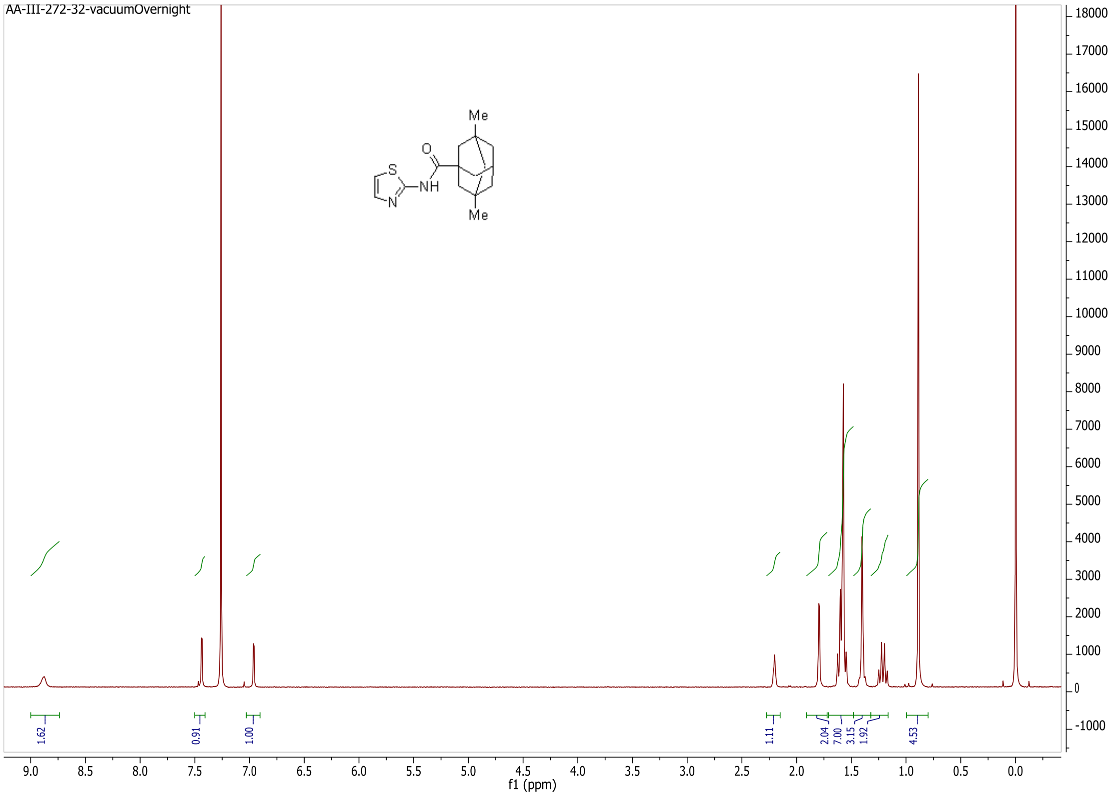
AA-III-272-32-vacuumOvernight
Me
O
S
NH
N
Me
1.62
0.91
1.00
1.11
2.04
7.00
3.15
1.92
4.53
9.0 8.5 8.0 7.5 7.0 6.5 6.0 5.5 5.0 4.5 4.0 3.5 3.0 2.5 2.0 1.5 1.0 0.5 0.0
f1 (ppm)
18000 17000 16000 15000 14000 13000 12000 11000 10000 9000 8000 7000 6000 5000 4000 3000 2000 1000 0 -1000

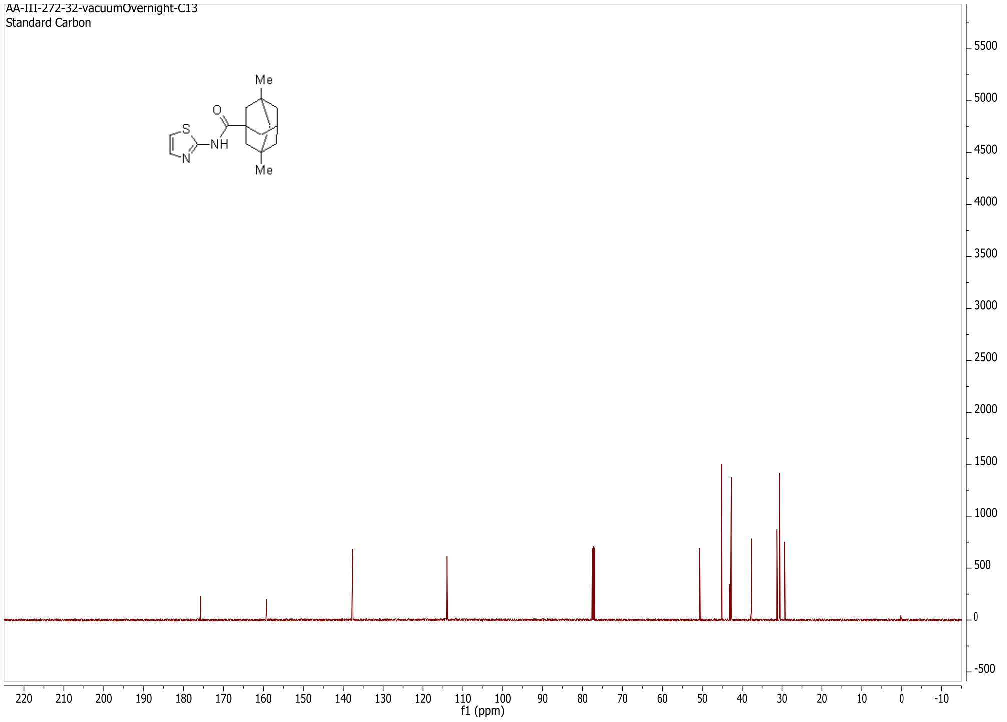
AA-III-272-32-vacuumOvernight-C13
Standard Carbon
Me
O
S
N
NH
Me
5500
5000
4500
4000
3500
3000
2500
2000
1500
1000
500
0
-500
220 210 200 190 180 170 160 150 140 130 120 110 100 90 80 70 60 50 40 30 20 10 0 -10
f1 (ppm)

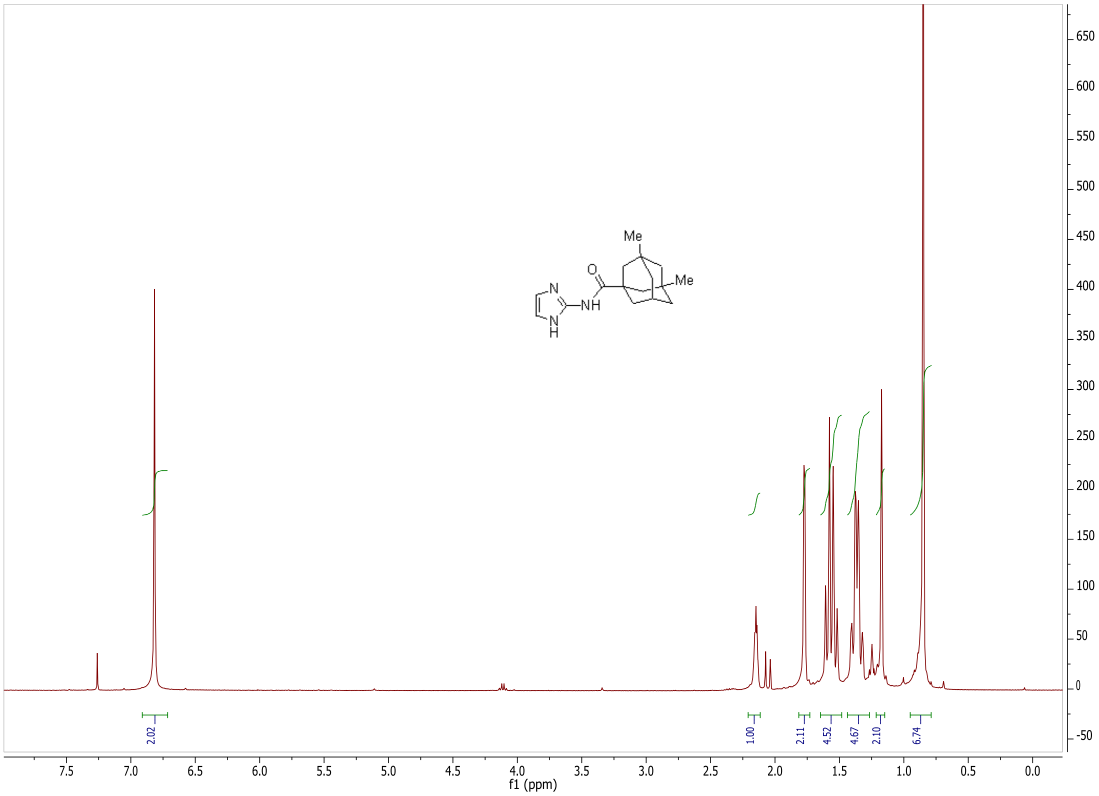
Me
O
N
NH
N
H
Me
650
600
550
500
450
400
350
300
250
200
150
100
50
0
-50
2.02
1.00
2.11
4.52
4.67
2.10
6.74
7.5 7.0 6.5 6.0 5.5 5.0 4.5 4.0 3.5 3.0 2.5 2.0 1.5 1.0 0.5 0.0
f1 (ppm)

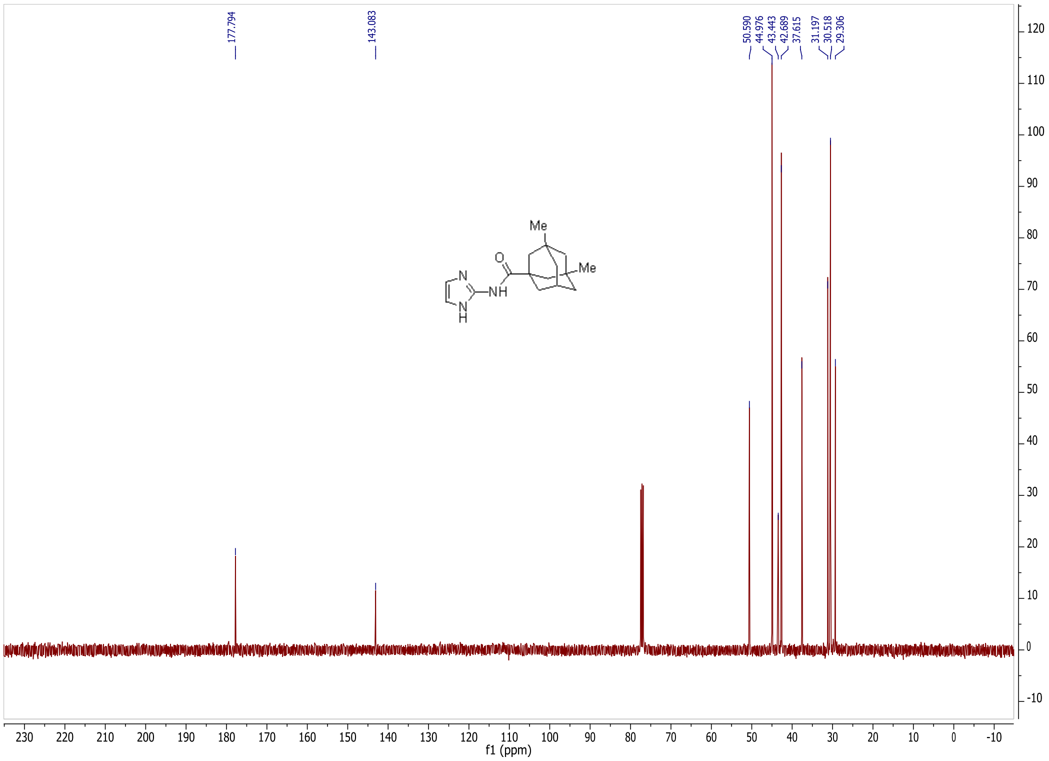
177.794
143.083
50.590
44.976
43.443
42.689
37.615
31.197
30.518
29.306
Me
O
Me
N
NH
N
H
120
110
100
90
80
70
60
50
40
30
20
10
0
-10
230
220
210
200
190
180
170
160
150
140
130
120
110
100
90
80
70
60
50
40
30
20
10
0
-10
f1 (ppm)

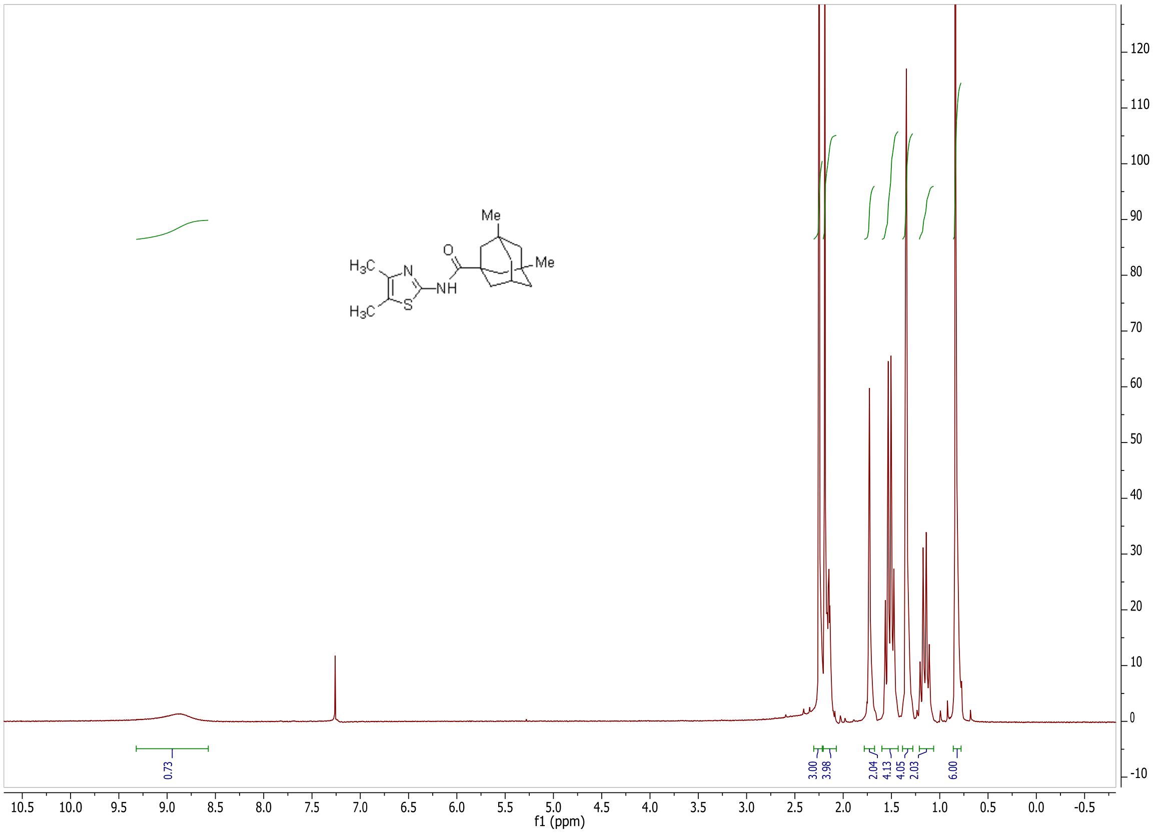
Me
O
H3C
N
Me
NH
H3C
S
0.73
3.00
3.98
2.04
4.13
4.05
2.03
6.00
120
110
100
90
80
70
60
50
40
30
20
10
0
-10
10.5
10.0
9.5
9.0
8.5
8.0
7.5
7.0
6.5
6.0
5.5
5.0
4.5
4.0
3.5
3.0
2.5
2.0
1.5
1.0
0.5
0.0
-0.5
f1 (ppm)

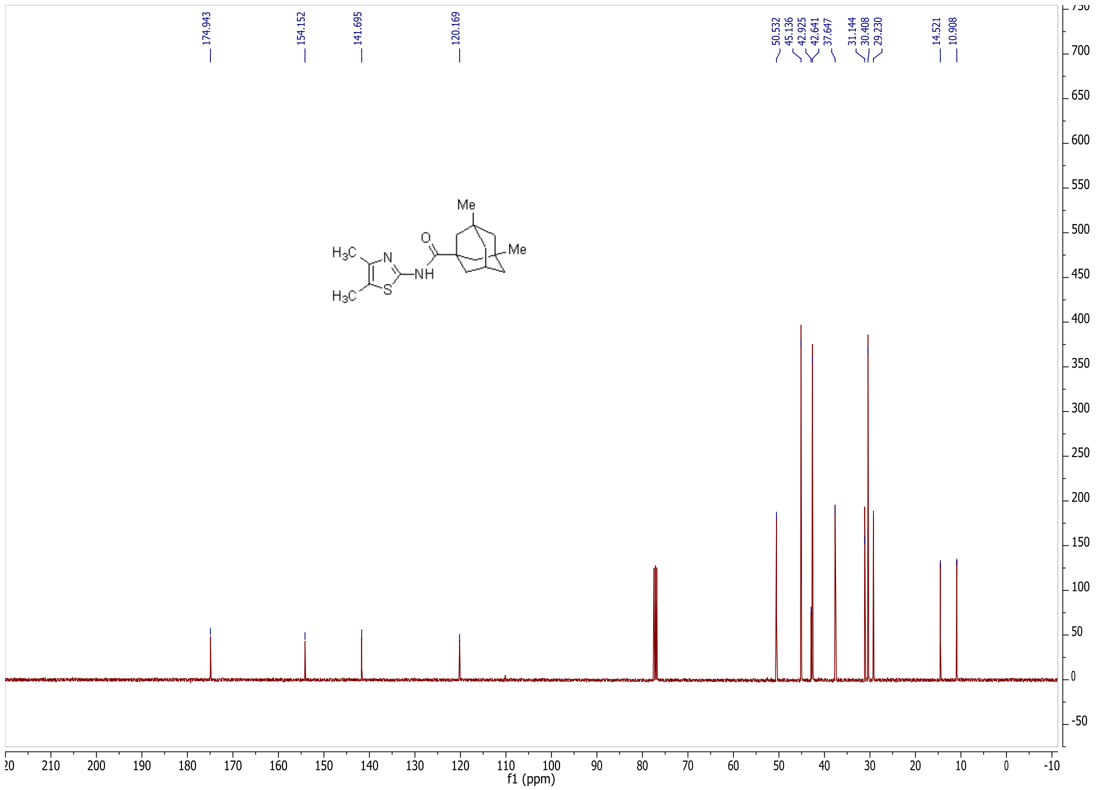
174.943
154.152
141.695
120.169
50.532
45.136
42.925
42.641
37.647
31.144
30.408
29.230
14.521
10.908
Me
O
Me
H3C
N
NH
S
H3C
750
700
650
600
550
500
450
400
350
300
250
200
150
100
50
0
-50
220
210
200
190
180
170
160
150
140
130
120
110
100
90
80
70
60
50
40
30
20
10
0
-10
f1 (ppm)

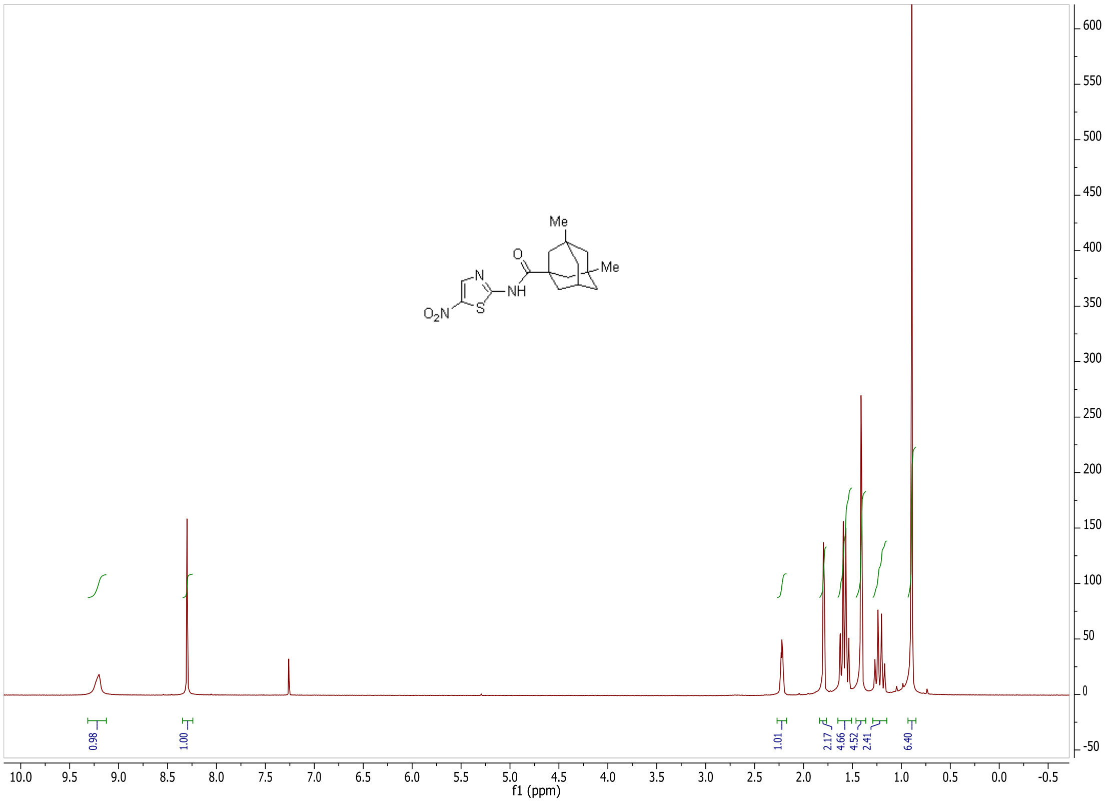
Me
O
N
Me
NH
O2N
S
600
550
500
450
400
350
300
250
200
150
100
50
0
-50
0.98
1.00
1.01
2.17
4.66
4.52
2.41
6.40
10.0
9.5
9.0
8.5
8.0
7.5
7.0
6.5
6.0
5.5
5.0
4.5
4.0
3.5
3.0
2.5
2.0
1.5
1.0
0.5
0.0
-0.5
f1 (ppm)

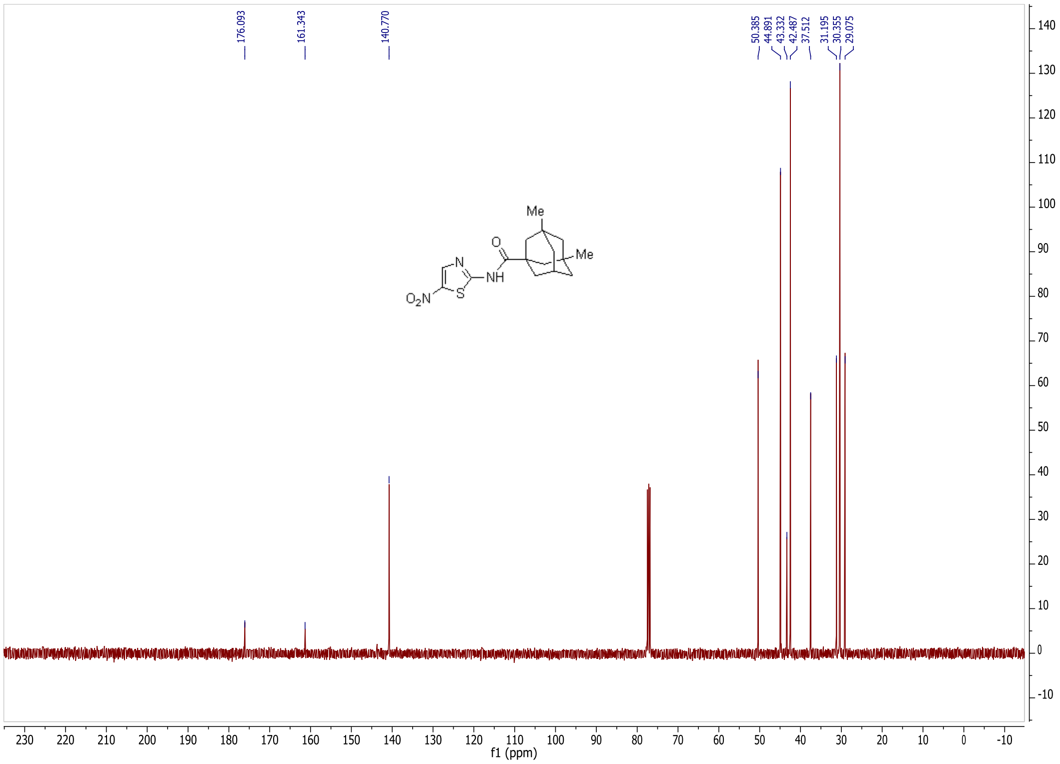
176.093
161.343
140.770
50.385
44.891
43.332
42.487
37.512
31.195
30.355
29.075
Me
O
Me
N
NH
O_2N
S
f1 (ppm)
230 220 210 200 190 180 170 160 150 140 130 120 110 100 90 80 70 60 50 40 30 20 10 0 -10
140 130 120 110 100 90 80 70 60 50 40 30 20 10 0 -10

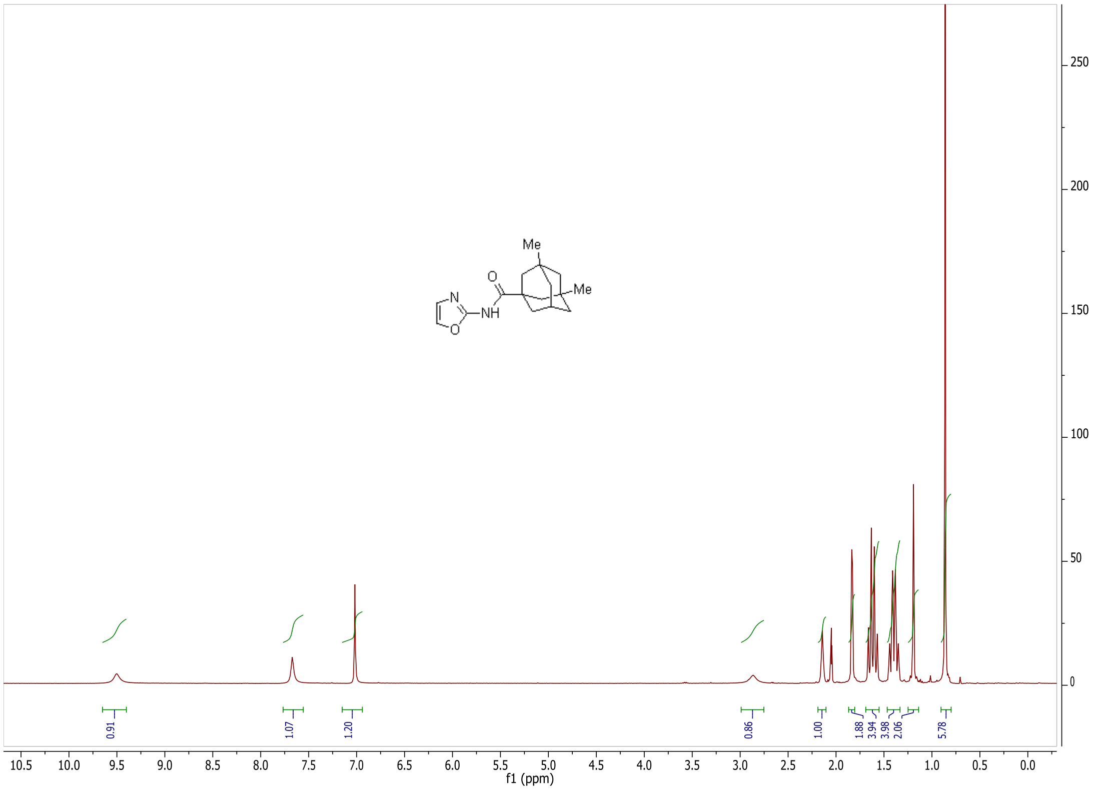
Me
O
Me
N
NH
O
0.91
1.07
1.20
0.86
1.00
1.88
3.94
3.98
2.06
5.78
f1 (ppm)
10.5 10.0 9.5 9.0 8.5 8.0 7.5 7.0 6.5 6.0 5.5 5.0 4.5 4.0 3.5 3.0 2.5 2.0 1.5 1.0 0.5 0.0
250 200 150 100 50 0

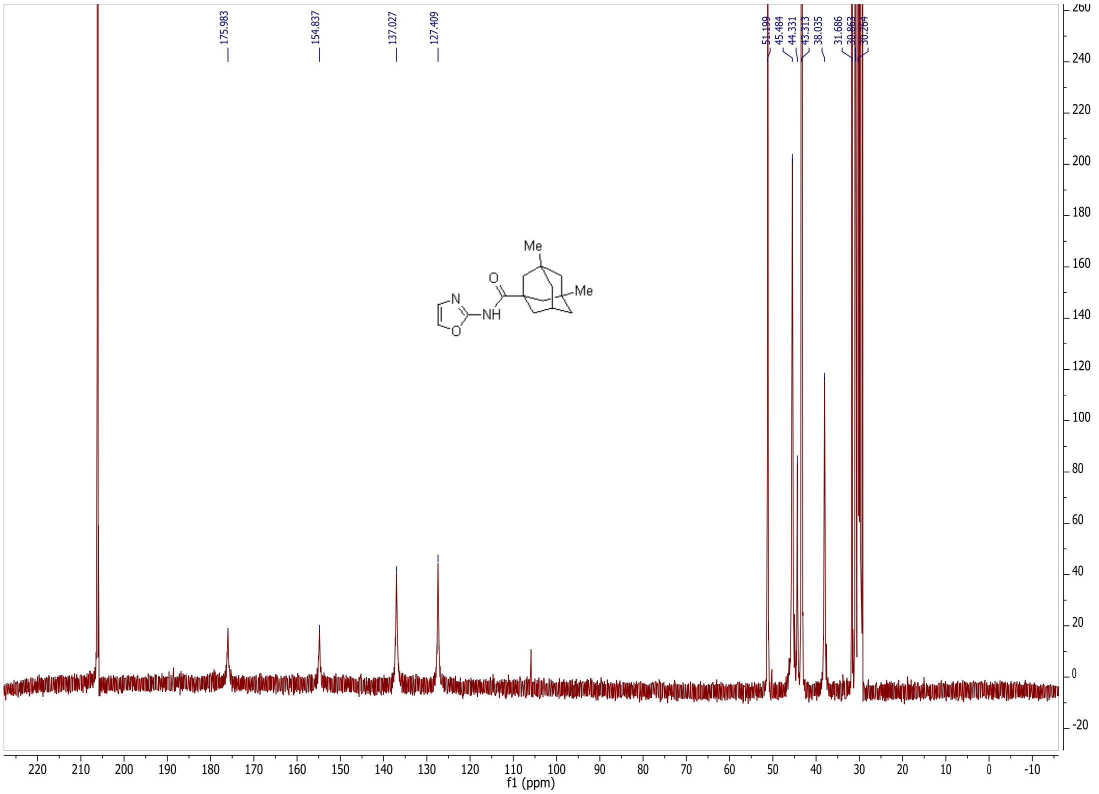
175.983
154.837
137.027
127.409
51.199
45.484
44.331
43.313
38.035
31.686
30.863
30.264
Me
O
N
NH
O
Me
260
240
220
200
180
160
140
120
100
80
60
40
20
0
-20
220 210 200 190 180 170 160 150 140 130 120 110 100 90 80 70 60 50 40 30 20 10 0 -10
f1 (ppm)

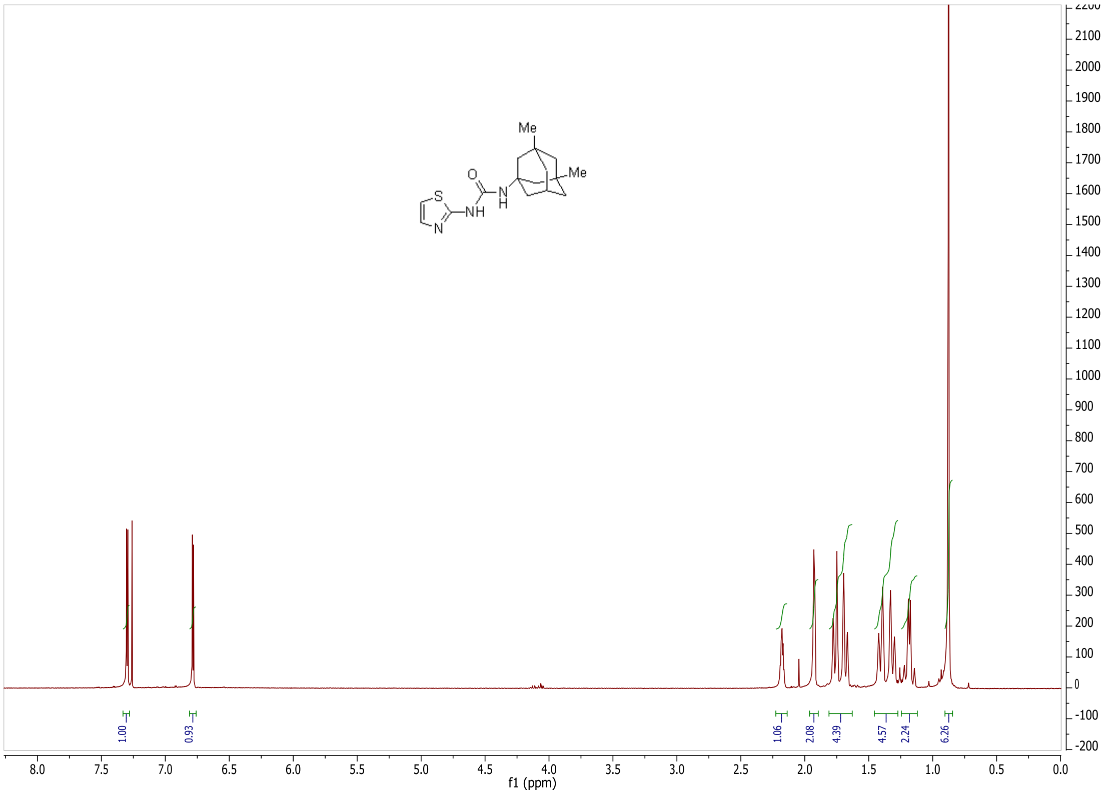
Me
O
S
N
H
NH
N
Me
2200
2100
2000
1900
1800
1700
1600
1500
1400
1300
1200
1100
1000
900
800
700
600
500
400
300
200
100
0
-100
-200
1.00
0.93
1.06
2.08
4.39
4.57
2.24
6.26
8.0 7.5 7.0 6.5 6.0 5.5 5.0 4.5 4.0 3.5 3.0 2.5 2.0 1.5 1.0 0.5 0.0
f1 (ppm)

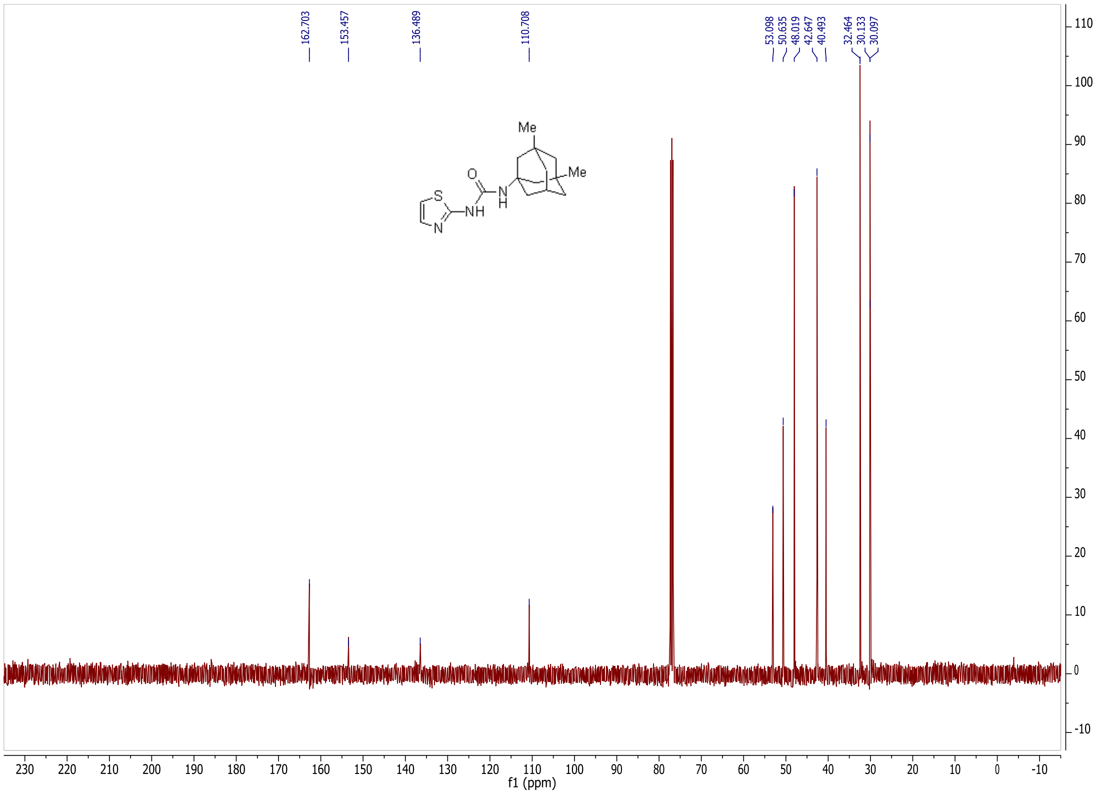
162.703
153.457
136.489
110.708
53.098
50.635
48.019
42.647
40.493
32.464
30.133
30.097
Me
Me
O
S
N
NH
N
H
f1 (ppm)
230 220 210 200 190 180 170 160 150 140 130 120 110 100 90 80 70 60 50 40 30 20 10 0 -10
110 100 90 80 70 60 50 40 30 20 10 0 -10

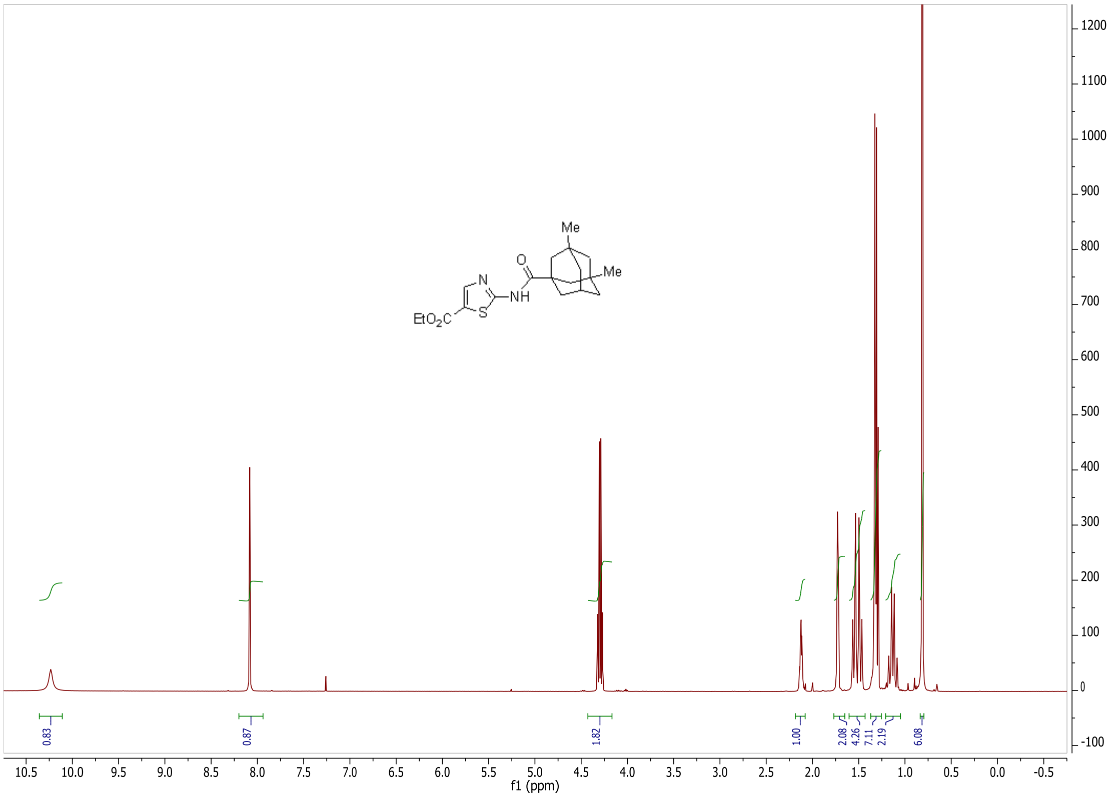
Me
Me
O
N
S
NH
EtO_2C
0.83
0.87
1.82
1.00
2.08
4.26
7.11
2.19
6.08
f1 (ppm)
10.5 10.0 9.5 9.0 8.5 8.0 7.5 7.0 6.5 6.0 5.5 5.0 4.5 4.0 3.5 3.0 2.5 2.0 1.5 1.0 0.5 0.0 -0.5
1200 1100 1000 900 800 700 600 500 400 300 200 100 0 -100

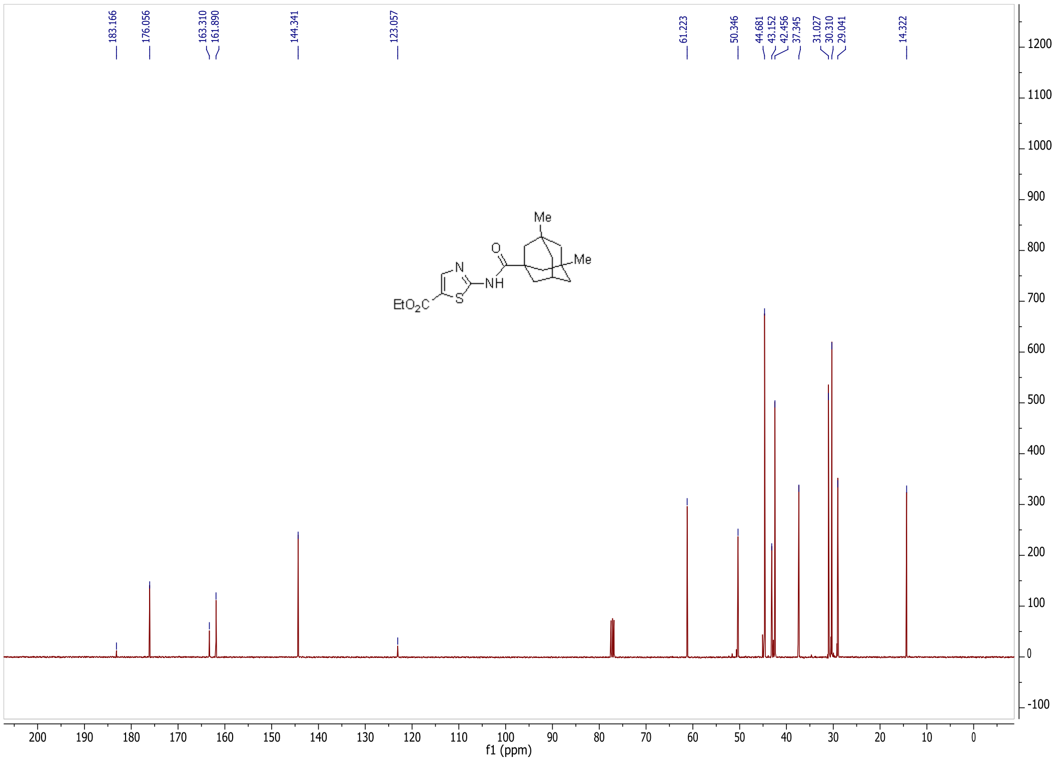
183.166
176.056
163.310
161.890
144.341
123.057
61.223
50.346
44.681
43.152
42.456
37.345
31.027
30.310
29.041
14.322
Me
O
N
Me
NH
S
EtO2C
1200
1100
1000
900
800
700
600
500
400
300
200
100
0
-100
200 190 180 170 160 150 140 130 120 110 100 90 80 70 60 50 40 30 20 10 0
f1 (ppm)

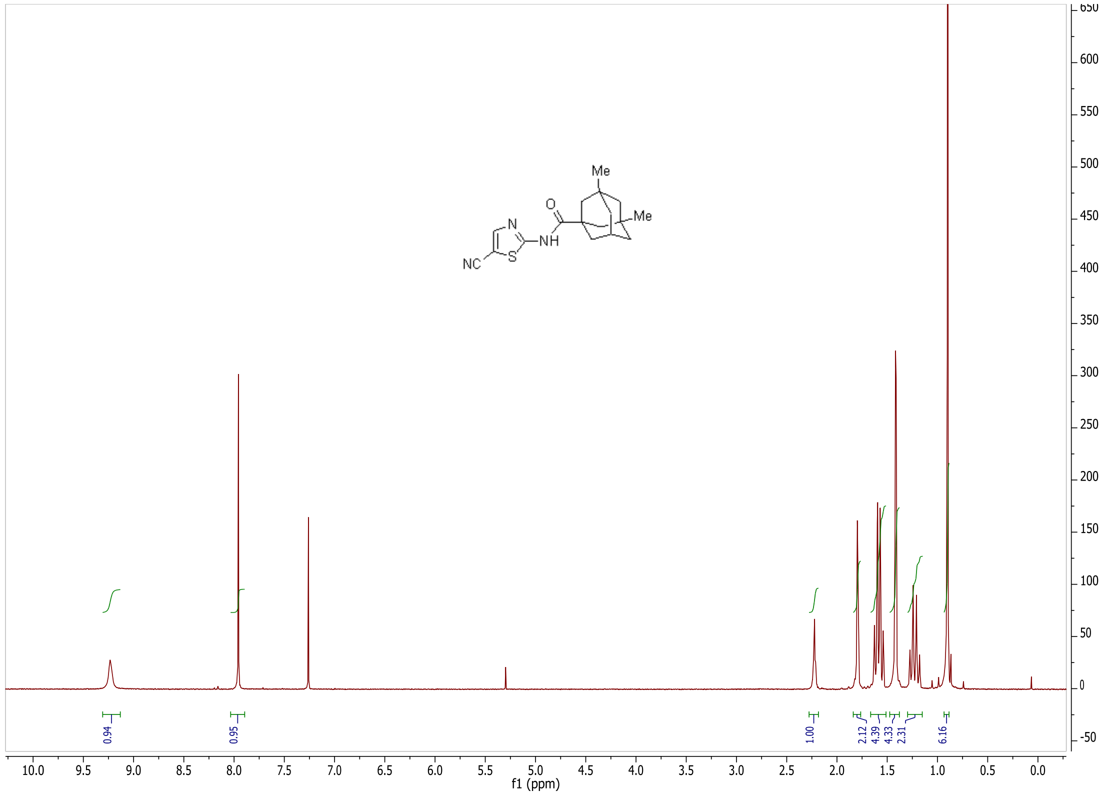
Me
O
N
Me
NH
S
NC
650
600
550
500
450
400
350
300
250
200
150
100
50
0
-50
0.94
0.95
1.00
2.12
4.39
4.33
2.31
6.16
10.0 9.5 9.0 8.5 8.0 7.5 7.0 6.5 6.0 5.5 5.0 4.5 4.0 3.5 3.0 2.5 2.0 1.5 1.0 0.5 0.0
f1 (ppm)

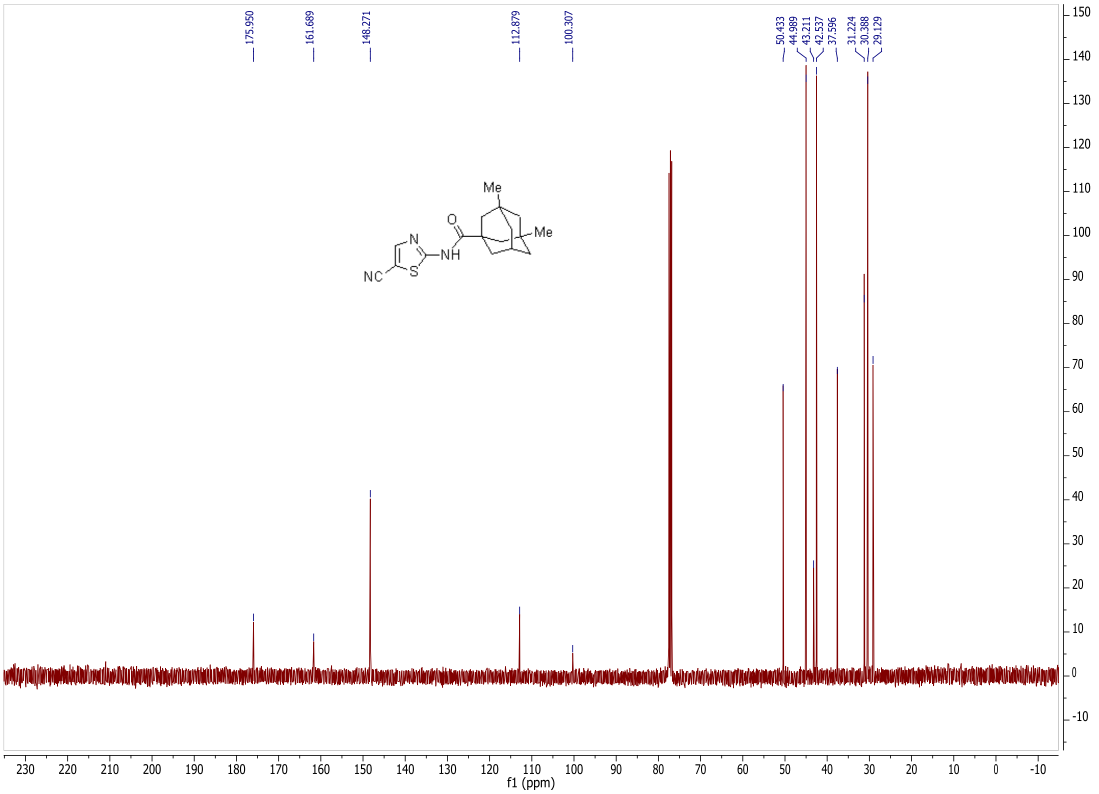
175.950
161.689
148.271
112.879
100.307
50.433
44.989
43.211
42.537
37.596
31.224
30.388
29.129
Me
O
Me
N
NH
NC
S
230 220 210 200 190 180 170 160 150 140 130 120 110 100 90 80 70 60 50 40 30 20 10 0 -10
f1 (ppm)
150 140 130 120 110 100 90 80 70 60 50 40 30 20 10 0 -10

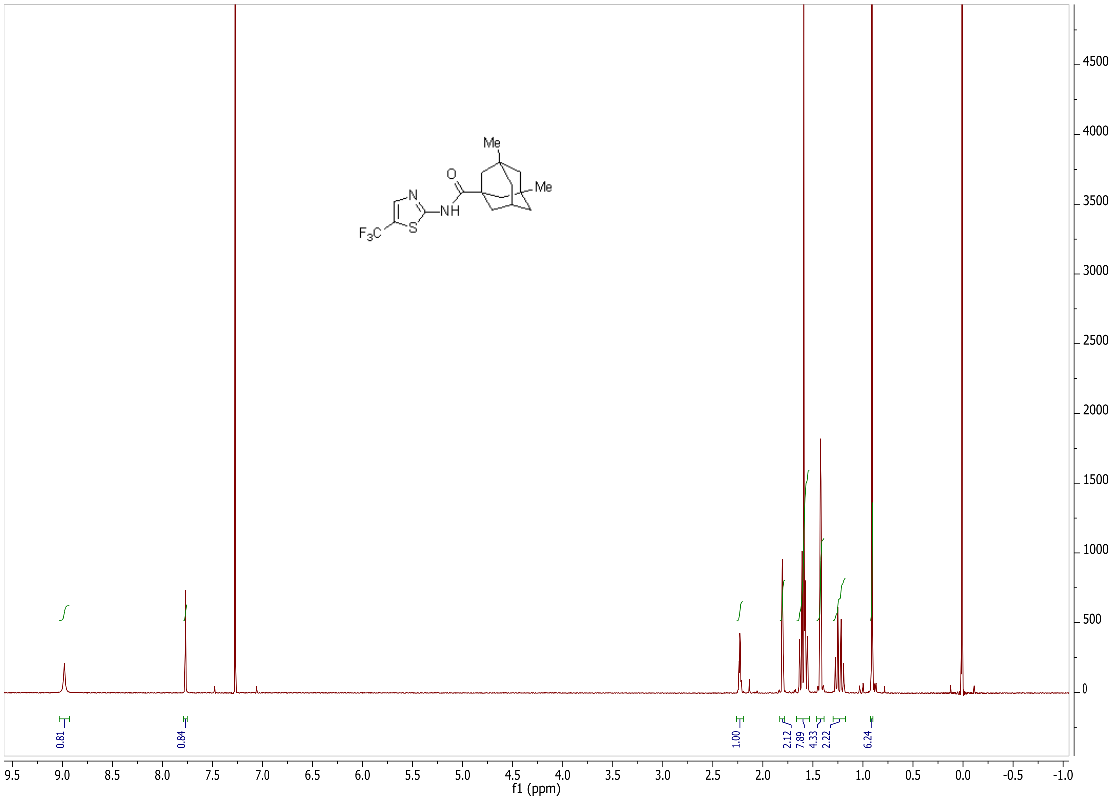
Me
O
Me
N
NH
F3C
S
0.81
0.84
1.00
2.12
7.89
4.33
2.22
6.24
9.5 9.0 8.5 8.0 7.5 7.0 6.5 6.0 5.5 5.0 4.5 4.0 3.5 3.0 2.5 2.0 1.5 1.0 0.5 0.0 -0.5 -1.0
f1 (ppm)
4500 4000 3500 3000 2500 2000 1500 1000 500 0

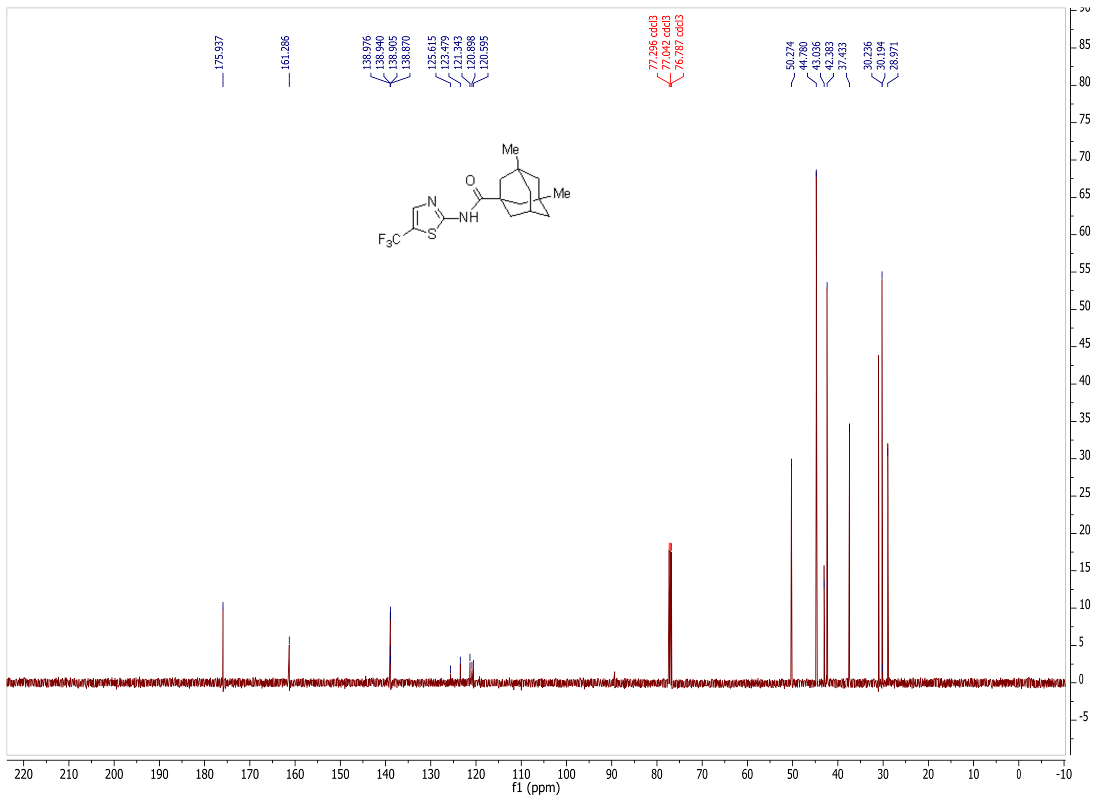
175.937
161.286
138.976
138.940
138.905
138.870
125.615
123.479
121.343
120.898
120.595
77.296 cdcl3
77.042 cdcl3
76.787 cdcl3
50.274
44.780
43.036
42.383
37.433
30.236
30.194
28.971
Me
O
Me
N
NH
S
F_3C
f1 (ppm)

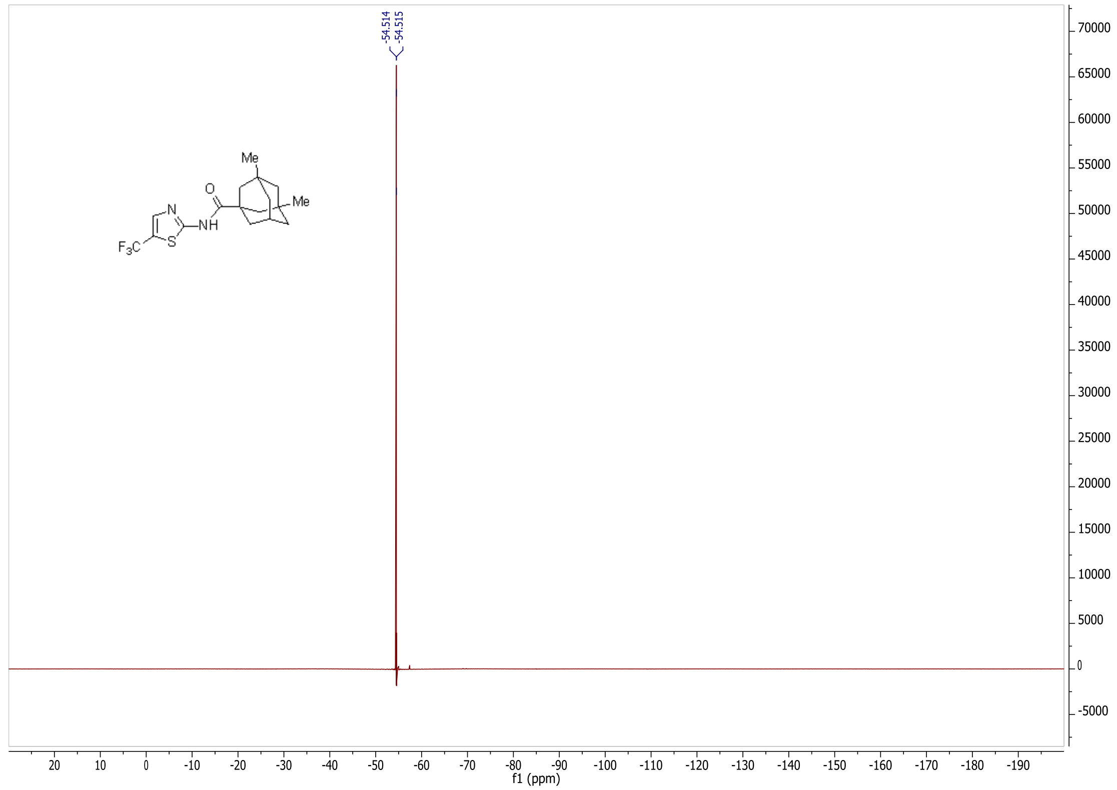
-54.514
-54.515
Me
O
Me
N
NH
S
F_3C
f1 (ppm)

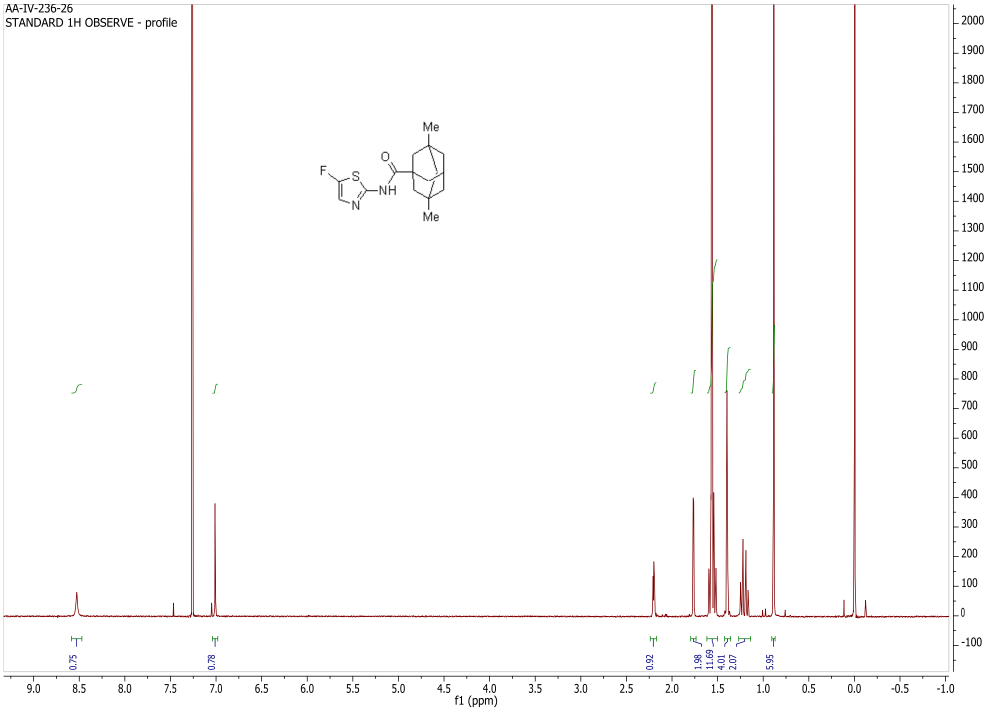
AA-IV-236-26
STANDARD 1H OBSERVE - profile
Me
O
F
S
NH
N
Me
0.75
0.78
0.92
1.98
11.69
4.01
2.07
5.95
9.0 8.5 8.0 7.5 7.0 6.5 6.0 5.5 5.0 4.5 4.0 3.5 3.0 2.5 2.0 1.5 1.0 0.5 0.0 -0.5 -1.0
f1 (ppm)
2000 1900 1800 1700 1600 1500 1400 1300 1200 1100 1000 900 800 700 600 500 400 300 200 100 0 -100

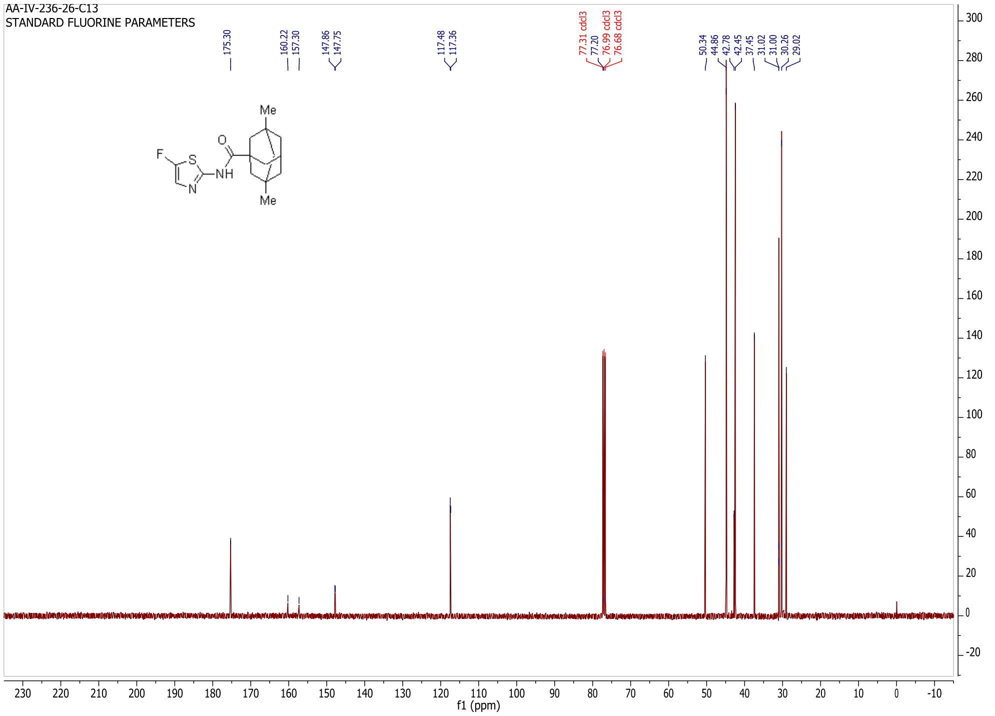
AA-IV-236-26-C13
STANDARD FLUORINE PARAMETERS
175.30
160.22
157.30
147.86
147.75
117.48
117.36
77.31 cdcl3
77.20
76.99 cdcl3
76.68 cdcl3
50.34
44.86
42.78
42.45
37.45
31.02
31.00
30.26
29.02
Me
O
F
S
NH
N
Me
230 220 210 200 190 180 170 160 150 140 130 120 110 100 90 80 70 60 50 40 30 20 10 0 -10
f1 (ppm)
300 280 260 240 220 200 180 160 140 120 100 80 60 40 20 0 -20

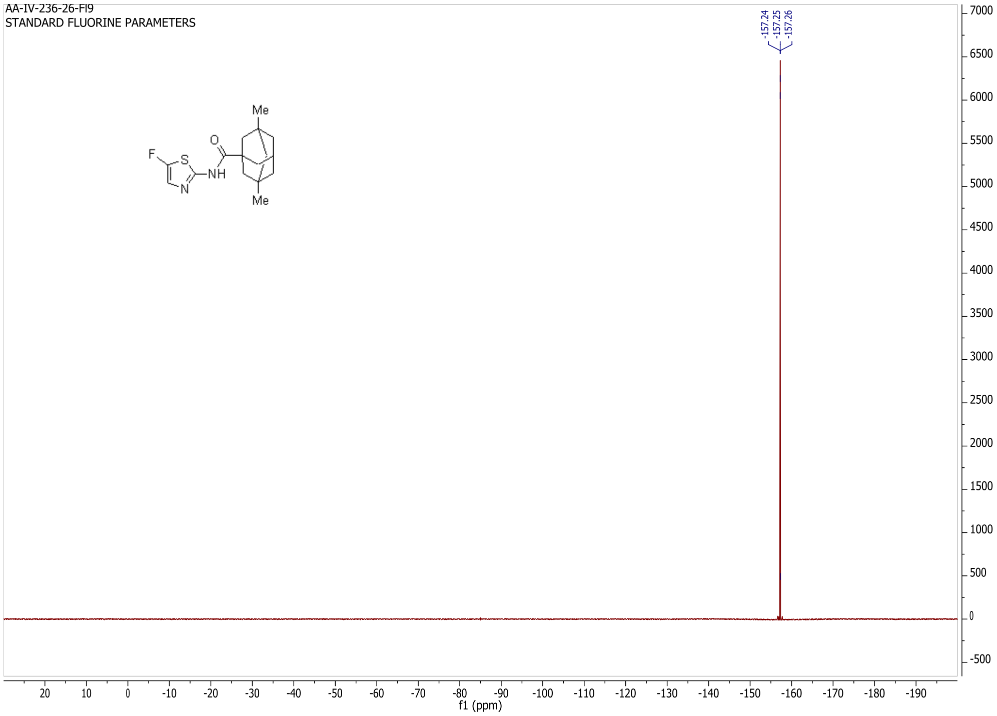
AA-IV-236-26-Fl9
STANDARD FLUORINE PARAMETERS
-157.24
-157.25
-157.26
F
S
N
NH
O
Me
Me
7000
6500
6000
5500
5000
4500
4000
3500
3000
2500
2000
1500
1000
500
0
-500
20
10
0
-10
-20
-30
-40
-50
-60
-70
-80
-90
-100
-110
-120
-130
-140
-150
-160
-170
-180
-190
f1 (ppm)

CHAPTER 3

STUDIES TOWARD A BIOMIMETIC TOTAL SYNTHESIS OF NIGRICANOSIDE A

3.1 Abstract

The stereochemical elucidation and synthesis of nigricanoside A, a potent antimitotic agent, have been active areas of research since its isolation in 2007. The Falck group is pursuing a biomimetic approach to the synthesis of nigricanoside A. This approach takes inspiration from the enzymatic generation and rearrangement of fatty acid hydroperoxides, and this hypothesis was utilized to limit the number of diastereomers to eight out of a possible total of one hundred twenty eight. To achieve the synthetic goal, novel methodologies were undertaken: 1) stereo- and regio-controlled epoxidation of conjugated dienols, 2) stereocontrolled addition of oxygen nucleophiles to the resultant allylic epoxides, and 3) mild etherifications.

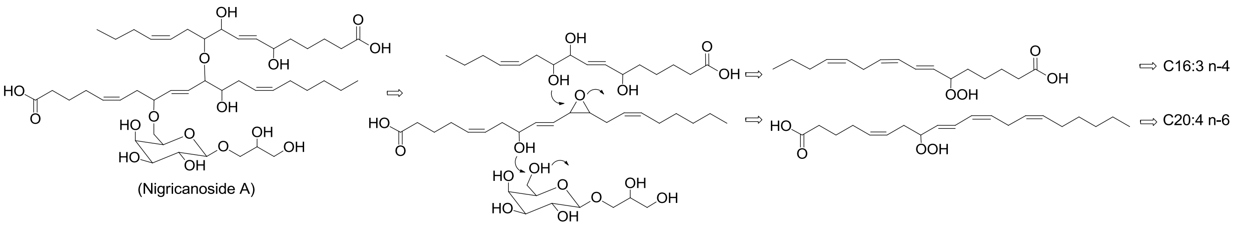

Figure 3.1
Proposed retrobiosynthesis of nigricanoside A.

Reported in this section is the application of a stereocontrolled distal epoxidation methodology, as well as a regioselective allylic epoxide opening reaction to the synthesis of the fatty acid

fragments of nigricanoside A. Also reported is a concise synthesis of the galactopyranoside fragment.

3.2 Introduction

The diversity of various life processes in nature provides scientists with a plethora of inspiration and tools to tackle many of the problems of current interest. This often translates into a better understanding of our environment, and helps us make judicious use of the available limited resources in nature and leads to technological advancements. The prevention and treatment of diseases/health conditions are of paramount importance to scientists in all disciplines. A major focus of their efforts is the development of drugs. In the area of cancer therapy, natural products and natural products inspired agents account for over 47% of approved drugs.[1] Over the years, an increasing awareness of these natural products, coupled with the technological advancements to isolate, elucidate their structure, and synthesize them, have enabled scientists to reach deeper into the "goldmine[2]" of bioactive natural products for the improvement of human and animal health. Despite this, the rarity of many natural products and the complexity of the drug discovery process are major obstacles that must be overcome.[3]

3.2.1 Antimitotic Agents as Cancer Chemotherapeutics

Antimitotic natural products are a well-established class of anticancer compounds.[4] While many of these agents have different mechanisms or sites of action, an important group includes those that directly modulate tubulin dynamics (polymerization and de-polymerization). Indeed, some of these agents are currently being used in clinics for the treatment of cancer, while some of them are currently being studied in clinical trials as potential anti-cancer drugs (Figure 3.2).

Interestingly, antimitotic natural products possess diverse structural motifs, which often translate to different biological potencies, toxicities and selectivity profiles. The lack of effective chemotherapeutic agents for certain cancers (such as brain metastases from lung cancer), combined with the rapid development of resistance to the available agents dictates a need for new anti-cancer agents, especially the highly successful antimitotic agents.

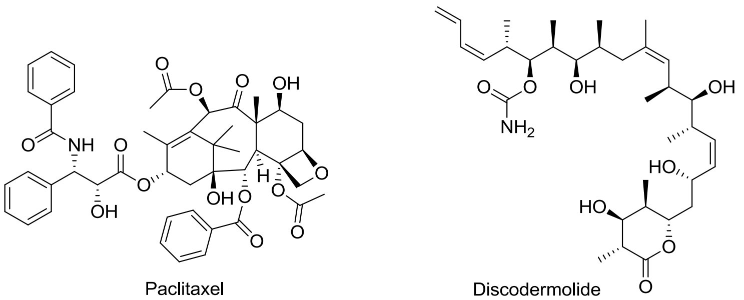

Paclitaxel
available by semi-synthesis
ovarian, breast, lung, etc

Discodermolide
available by synthesis
Clinical Trials

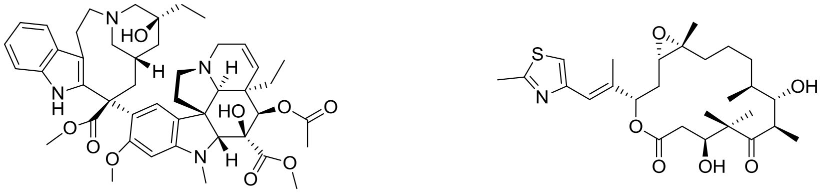

Vinblastine
Hodgkin's lymphoma, testicular cancer, etc

Epothilone B
Metastatic breast cancer

Figure 3.2
Some clinically relevant antimitotic agents.

Most antimitotic natural products were identified during mechanism of action studies following preliminary cytotoxicity assessment. A potentially more productive approach to the identification of new antimitotic agents is a mechanism based approach that involves a direct selection of agents using an antimitotic assay.[5] With this goal, the Anderson and Roberge groups developed a cell based enzyme-linked immunosorbent assay (ELISA)[6] that measures the abundance of phosphorylated nucleolin in compound treated cells as compared to non-treated cells (Figure 3.3). Phosporylated nucleolin is abundant in mitosis-arrested cells. Through this assay, an extract from the marine green alga *Avrainvillea nigricans* was found to possess antimitotic activity. The active principles of the extract, nigricanoside A and B, were identified as the first members of a new class of “ether-linked glycoglycerolipids”[5] through assay guided fractionation and eventual

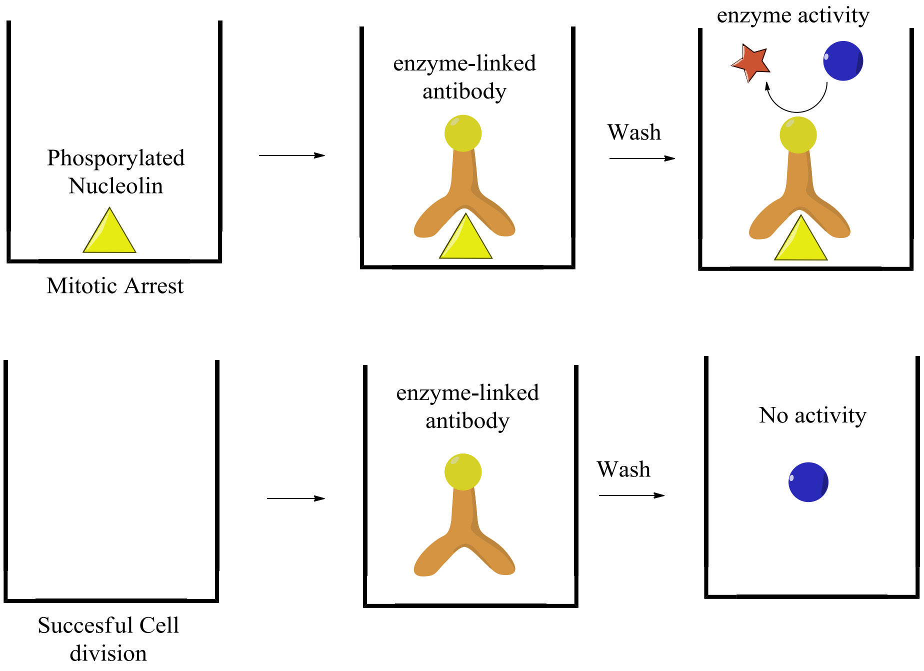
enzyme activity
Phosporylated
Nucleolin
enzyme-linked
antibody
Wash
Mitotic Arrest
enzyme-linked
antibody
Wash
No activity
Succesful Cell
division

Figure 3.3
ELISA of cellular mitotic arrest.

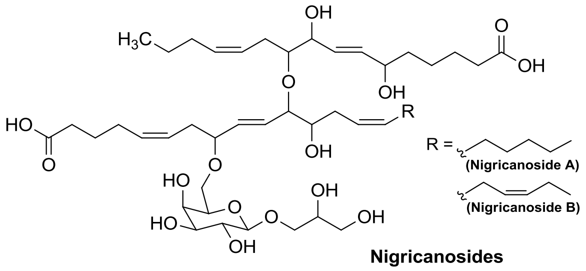
OH
H3C
O
OH
O
OH
HO
R
O
OH
R =
(Nigricanoside A)
(Nigricanoside B)
O
HO
OH
O
HO
O
OH
OH
Nigricanosides

Figure 3.4
Proposed structure of the nigricanosides.

NMR studies. The dimethyl ester of nigriacanoside A was found to arrest human breast cancer MCF-7 cells in mitosis with an IC_{50} of 3 nM. At 10 μM, the diester stimulates the polymerization of pure tubulin *in vitro*, which is a paclitaxel–like activity, and suppresses the growth of MCF-7 and human colon cancer HCT-116 cells with an IC50 ≈ 3 nM. However, further biological and mechanistic studies on this novel class of bioactive natural product were precluded by the minor quantity isolated; less than a milligram of nigricanoside A was obtained after eight years of algal extraction and re-isolation. Further expeditions to obtain more nigricanosides have failed thus far, leaving synthesis as the only alternative to obtaining the nigricanosides. Reported in this section is my foray at providing the nigricanosides via total synthesis for further structural, biological, and mechanistic studies.

3.3 Literature Review

3.3.1 Biomimetic Hypotheses

3.3.1.1. Proposed Stereochemical Assignments

Structurally, the nigricanosides consist of four main parts, namely: 1) an ω-4 C16 tri-oxygenated fatty acid, 2) an ω-6 (nigricanoside A) or ω-3 (nigricanoside B) C20 trioxygenated fatty acid, 3) a galactopyranose, and 4) a glycerol unit.

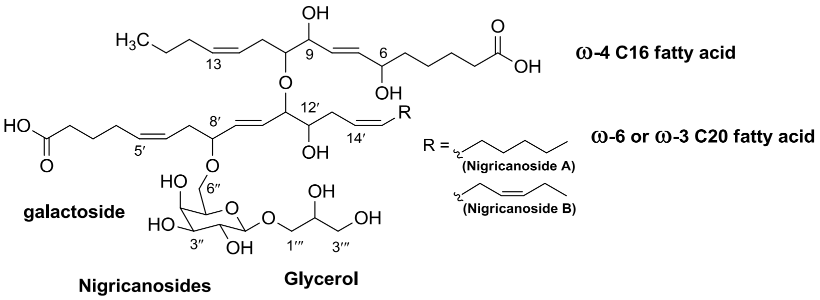

Figure 3.5
Structural composition of the nigricanosides.

ω-4 C-16 Trioxygenated Fatty Acid

Initially, we were skeptical about the correct assignment of the structure of the nigricanosides due to the presence of an ω-4 C16 fatty acid in the assigned structure. Omega-4 fatty acids are rare in nature when compared to the prevalent ω-3, ω-6, and ω-9 fatty acids. However, there are two reports[7,8] of the potential precursor of the C16 fatty acid, which allayed the skepticism surrounding this fragment. We proposed that the C16 tri-oxygenated fatty acid is formed through the action of a lipoxygenase (LOX) as shown in Figure 3.6. The related ω-3 C18 congeners, malyngic[9] and fulgidic[10] acids, as well as the related mueggelone[11] are known natural products (Figure 3.7). As shown in Figure 3.7, the *S* stereochemistry is conserved at the C-13 position of these natural products. Although the stereochemistry of the LOX-metabolized product from a C16 fatty acid could differ from that of the C18 fatty acid, we hypothesized that stereochemical conservation occurs as observed between C20 and C18 fatty acids and therefore focused on the *S* C-10 configuration for the C16 fragment (64 diastereomers).

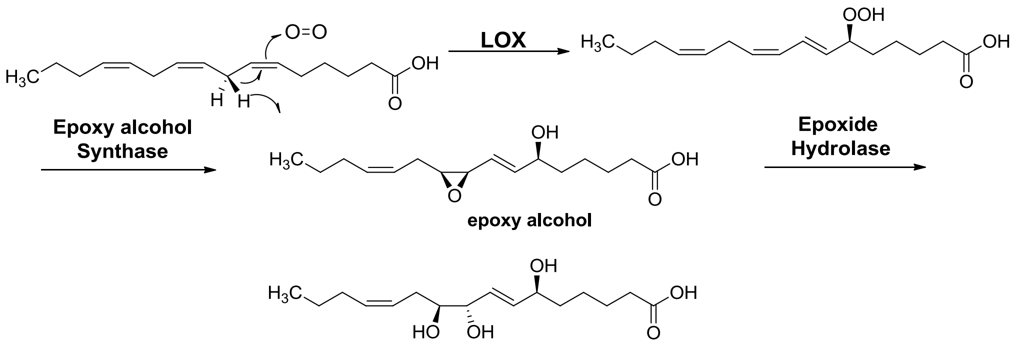
O=O
LOX
Epoxy alcohol Synthase
epoxy alcohol
Epoxide Hydrolase

Figure 3.6
Proposed biosynthesis of ω-4 C16 tri-oxygenated fatty acid of nigricanoside A.

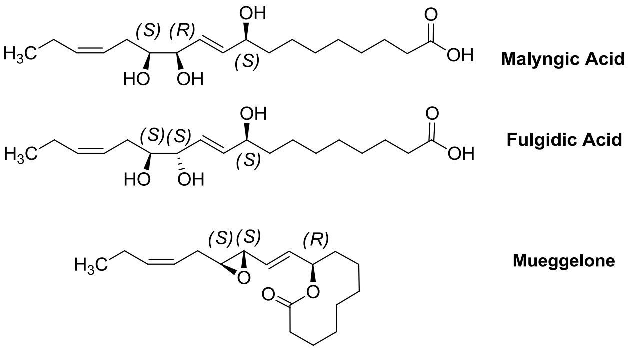
Malyngic Acid
Fulgidic Acid
Mueggelone
(S) (R)
(S)
(S)(S)
(S)
(S)(S)
(R)

Figure 3.7
Structures of known trioxygenated C18 fatty acid metabolites.

ω-6/ω-3 C-16 Trioxygenated Fatty Acid

Likewise, we hypothesized that the C20 tri-oxygenated fatty acid of nigricanoside A is derived from the action of a lipoxygenase on arachidonic acid, while that of nigricanoside B results from a similar enzymatic action on eicosapentaenoic acid. As shown in Figure 3.8, both natural hepoxilin A_3[12] and topsentolide A_2[13] possess the C20 epoxyalcohol motif, but differ in the C-11 stereochemistry. Again, the non-allylic carbinols of both natural products possess the *S* stereochemistry. With an *S* configuration for both the C-10 and C-12 carbinols of the C16 and

C20 fatty acid fragments respectively, one can envision a total of 32 potential diastereomers for nigricanoside A.

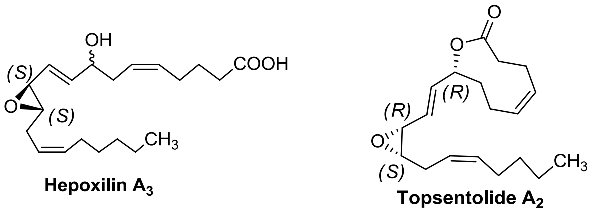

Figure 3.8
Potential precursors of the C20 fragment of the nigricanosides.

Galactopyranoside

Due to the rarity of the L- enantiomer of galactose in nature, our biomimetic hypothesis assumed that the D- enantiomer is present in the nigricanosides. A coupling constant of 7.7 Hz between the H-1" and H-2" protons established the β-anomeric configuration.[5]

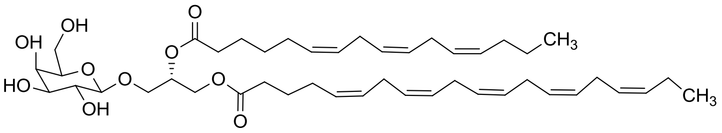

Figure 3.9
Apoptosis-inducing galactolipid from a cultured marine diatom.

Glycerol

The stereochemistry of the C-2‴ position of the glycerol moiety of the nigricanosides was assumed to be *R* by analogy with the natural product isolated by Falkowski and coworkers[8] (Figure 3.9). In addition, a recent synthetic study towards the nigricanosides by Fujiwara and coworkers supports this assumption.[14]

Based on the above hypotheses and precedents, the C-10 and C-12′ carbinols were assigned an *S* configuration, while the C-2‴ carbinol was assigned an *R* configuration (16 stereochemical possibilities). To further limit the stereochemical possibilities to 8, the C-6 carbinol was tentatively assigned an *S* configuration based on analogy with malyngic and fulgidic acids. These remaining eight diastereomers were, therefore, our primary synthetic focus.

3.3.1.2 Ether Linkages

Most of the structural novelty and synthetic convolution of the nigricanosides derive from the unique ether linkages that unify the fatty acids and galactopyranoside moieties. The traditional arrangement of these fragments in monogalactosyldiacylglycerolipids is through ester linkages to glycerol as shown above in Figure 3.9. We hypothesized that the ether linkage between the fatty acid moieties results from the opening of the C20 epoxy alcohol (or epoxy galactoside ether adduct) by the C16 trioxilin (Figure 3.10) under either enzymatic or non-enzymatic conditions (Brønsted/Lewis acid catalysis).

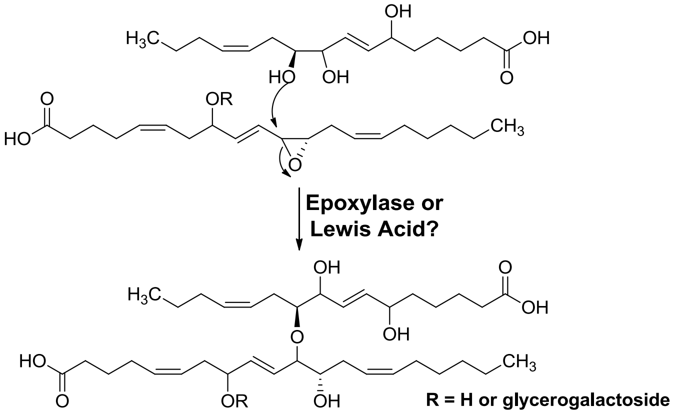

Figure 3.10
Proposed mechanism of formation of fatty acid ether bond.

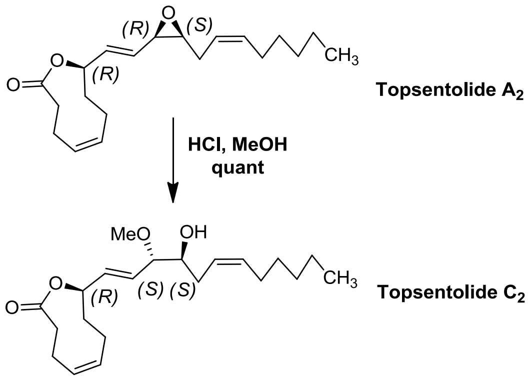
(R)
O
(S)
O
(R)
O
CH3
Topsentolide A2
HCl, MeOH
quant
MeO
OH
O
(R)
(S) (S)
O
CH3
Topsentolide C2

Figure 3.11
Brønsted acid catalyzed transformation of topsentolide A_2 to topsentolide C_2.

The feasibility of a non-enzymatic process was established in the synthesis of the simpler topsentolide C_2[13b] (Figure 3.11). On the other hand, the galactopyranoside to C20 fatty acid ether bond (C8′-O-C6") could arise from different mechanistic pathways which include; a) an interception of a lipoxygenase enzymatic peroxide intermediate, b) a highly stereoselective acid catalyzed dehydrative etherification process, and c) etherification of a metal activated primary phosphate or sulfate (Figure 3.12). These possibilities are currently being explored in my synthetic approach to forming the final ether bonds of the nigricanosides.

a)

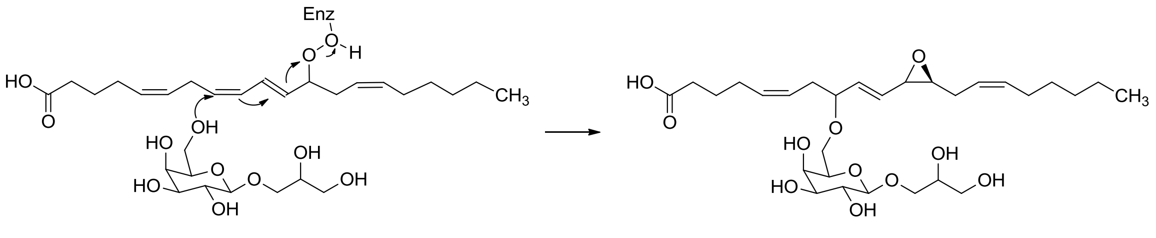
Enz
O
O
H
HO
O
CH3
OH
HO
O
OH
HO
O
OH
OH
HO
O
O
O
CH3
O
HO
O
OH
HO
O
OH
OH

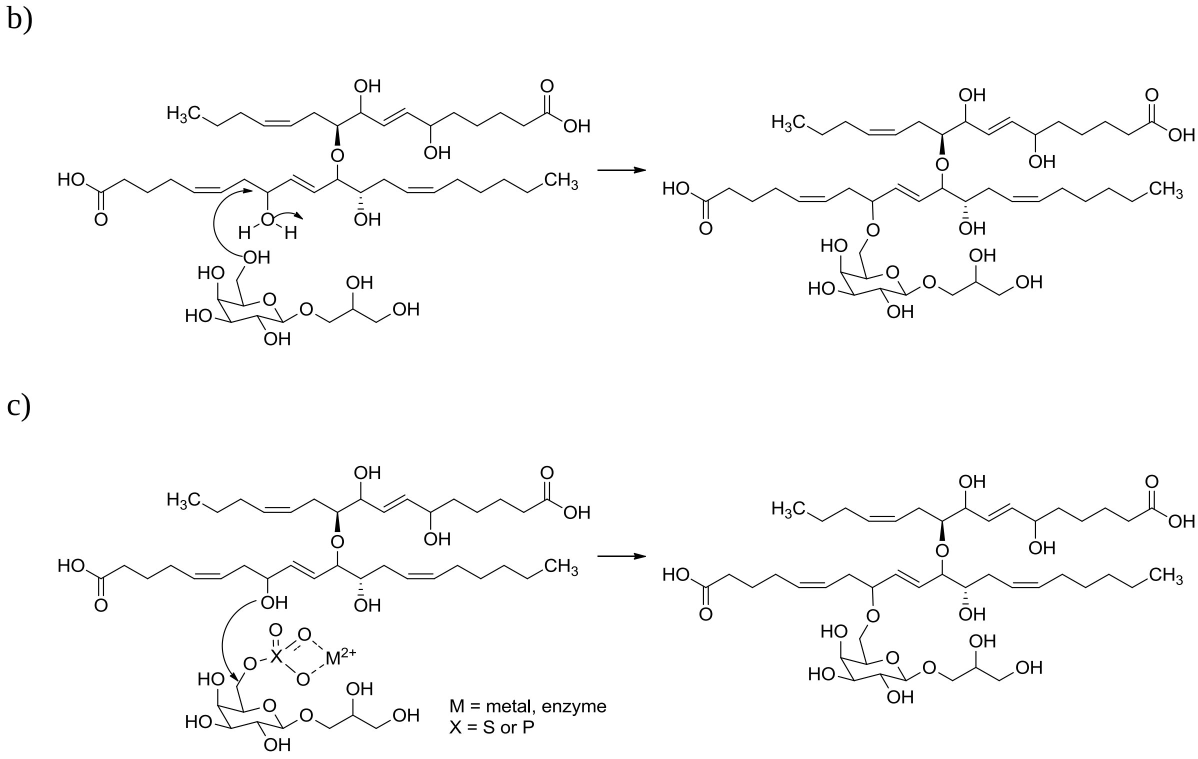

Figure 3.12
Proposed mechanisms for formation of C8’-O-C6’’ etherbond.

3.3.2 Other Synthetic Approaches to the Nigricanosides

MacMillan and Ready Synthesis

In 2009, the MacMillan and Ready groups published on a novel nuclear magnetic resonance (NMR) spectroscopy method[15] that involves multiple simultaneous homonuclear decoupling of coupled protons to simplify ^{1}H NMR spectra and obtain desired coupling constants. In their publication, they proposed utilizing this technology to elucidate the relative stereochemistry of the nigricanosides. In 2015, both groups co-published on the first total synthesis of the nigricanosides (Figure 3.13) and assigned the stereochemistry of nigricanoside A, although minor differences in the NMR spectra of the synthetic and natural material suggest a miss-assignment of the structure.[16] Furthermore, the synthetic material lacked the biological activity of the reported natural product. The C20 fatty acid was determined to be derived from hepoxilin A3 (11*S*, 12*S*) with an erythro configuration of the vicinal diol. The C-8′ configuration was assigned as *S*. By analogy, the C16 trioxilin was assigned as 6*S*, 9*R*, 10*S*. The ether bonds were formed by Williamson etherification, while the stereochemistry of the alcohols of the fatty acid either originated from chiral commercial building blocks, or were established by diastereoselective reactions (reduction and alkylation).

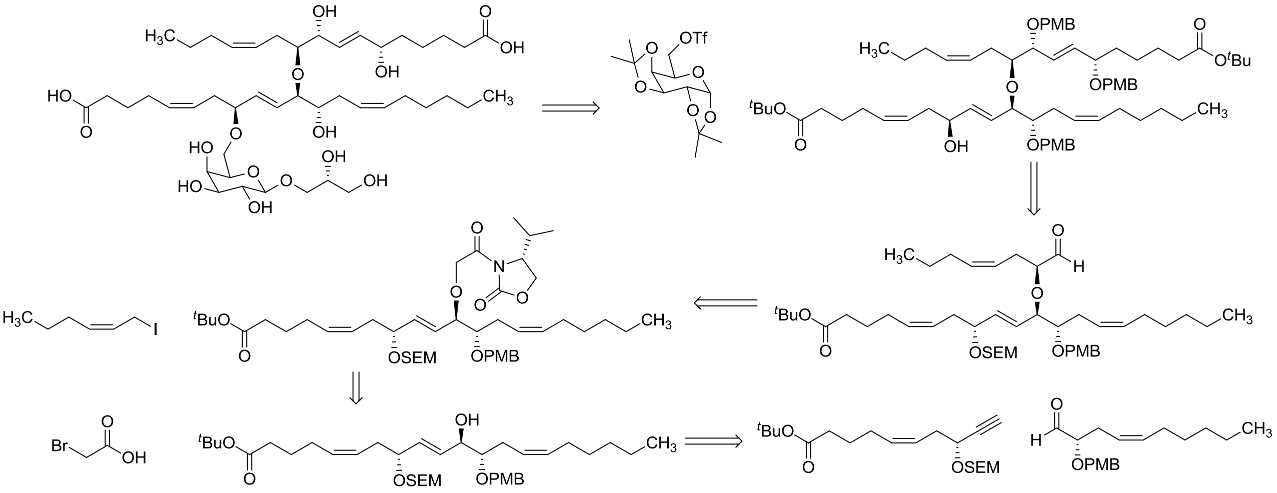

Figure 3.13
MacMillan and Ready synthesis of nigricanoside A.

Yusuke Kurashina and Shigefumi Kuwahara Synthesis of C20 Fragment

In 2012, the Kuwahara group published the first synthetic approach to the fatty acid fragments of the nigricanosides.[17] Their publication culminated in the synthesis of a protected form of the C16 fragment, with a 6*R*, 9*S*, 10*R* triol configuration. The Sharpless asymmetric kinetic resolution, a diastereoselective reduction, and an allylation of a protected α-hydroxyl amide using an Evans chiral auxiliary were used to establish the C-6, C-9 and C-10 stereocenters, respectively.

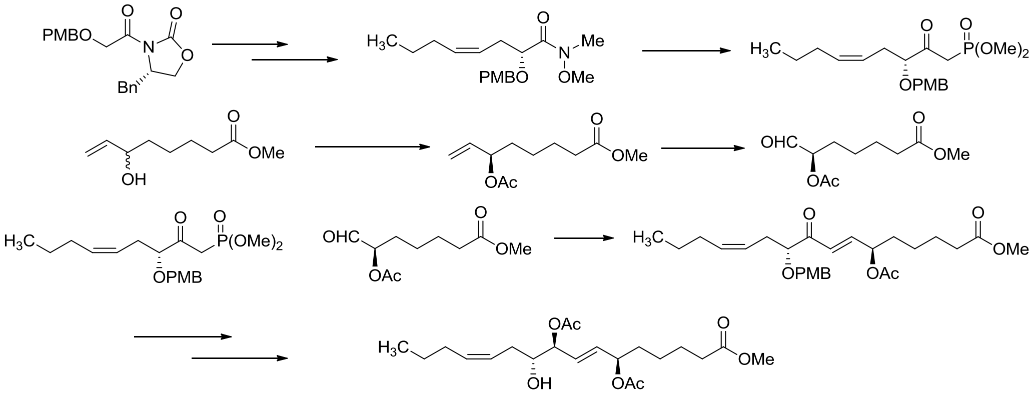

Figure 3.14
Kurashina et al synthesis of protected C16 fragment.

Fujiwara Kenshu Approach

In 2013, the Fujiwara group showed that a stereospecific Ireland-Claisen rearrangement could be employed to construct the C20 fatty acid-galactopyranose ether bond (C8′-O-C6"), although the C20 fatty acid utilized in their study lacked the C11and C12 diol. Spectroscopic studies using an 8′*S*, and 8′*R* analog, prepared in 26 steps, suggested that the C-8′ stereochemistry of the natural material is *S*.[14]

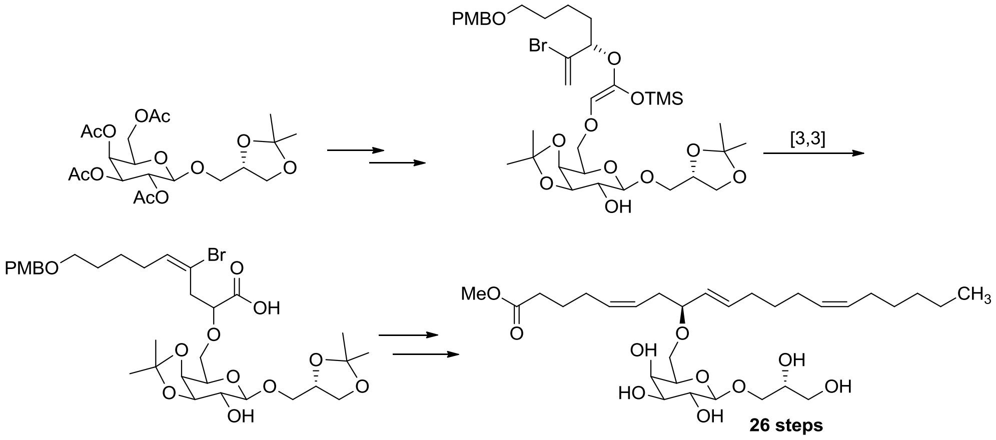

Figure 3.15
Fujiwara and coworkers synthetic approach to the nigricanosides.

3.3.3 Methods

Regio- and Enantioselective Catalytic Monoepoxidation of Conjugated Dienes

Asymmetric epoxidation is one of the most robust ways of bis-functionalizing olefins. Since the pioneering discovery of the Sharpless asymmetric epoxidation by Katsuki and Sharpless,[18] numerous studies have led to an array of catalytic systems for mono-ene and poly-ene epoxidations.[19] However, fewer protocols have found widespread utility for the regio- and enantioselective monoepoxidation of acyclic 2,4-pentadiene-1-ols as a concise pathway to the epoxyol and triol motifs found in the hepoxilins and trioxilins, respectively, as well as several other bioactive natural products (Figure 3.16). In the acyclic 2,4-pentadiene-1-ol polyene system, the Sharpless as well as other functional group directed epoxidation catalysts predominantly epoxidize the proximal olefin.[20]

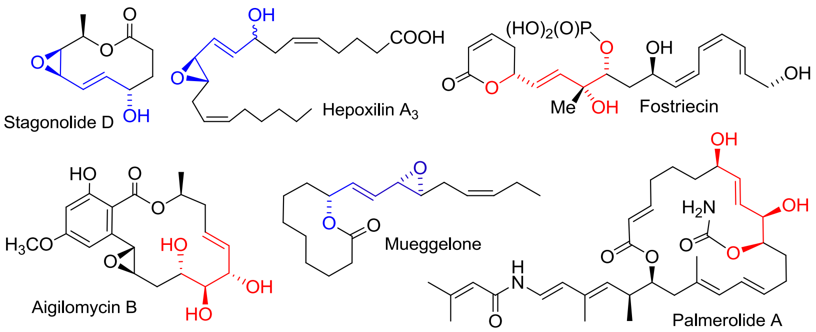

Figure 3.16
Hepoxilin and trioxilin motifs in select bioactive natural products.[20]

On the other hand, the Shi epoxidation catalyst system[21] was reported to favor distal epoxidation; however, the complicated experimental protocol, low yields, and moderate stereoselectivity are drawbacks to the Shi procedure. Recently, the Falck group reported an operationally simple procedure for the regio-and stereoselective monoepoxidation of acyclic 2,4-pentadiene-1-ols.[20]

As discussed below (Scheme 3.7), this methodology was successfully utilized to convert the 2,4-pentadiene-1-ol system present in the C16 and C20 fragments of the nigricanosides to the required epoxy alcohol with high regio-and stereoselectivity. However, the Falck procedure works quite well with conjugated *cis-trans* dienes; the stereoselectivity with *trans-trans* dienes is moderate to modest. Efforts to extend this methodology to *trans-trans* dienes are ongoing.

Etherification of Allylic Epoxides

An important utility of allylic epoxides as synthetic building blocks resides in their subsequent selective transformation into *erythro* and *threo* diols,[22] halohydrins,[23] azidohydrins,[24] amino alcohols,[25] and β-hydroxy ethers,[26] amongst other transformations. Considerable effort in this area of research has led to the development of several regio- and stereoselective protocols. Of relevance to the syntheses of the nigricanosides is the allylic epoxide to diol and β-hydroxy ether transformations. Under carefully controlled conditions (low temperature, low polarity solvents, excess alcohol), several groups have shown that it is possible to stereoselectively open allylic epoxides with alcohols in an S_N2 manner under Lewis acid catalysis, although the regioselectivity (S_N2 vs S_N2') is highly dependent on steric hindrance on both sides of the allylic system.[26] Thus, allylic cis epoxides give the *threo*-product, while allylic *trans*-epoxides give the *erythro*-product stereoselectively.

Complementarily, late transition metal catalyzed epoxide opening reactions often give the product of net retention of configuration at the substituted center either with or without olefin transposition. The stereochemical outcome results from a double inversion of configuration (overall retention of configuration) due to an initial backside attack by the transition metal (blocking the backside) and a subsequent attack at the “frontside” by the incoming nucleophile.

Although the stereoselectivity of this process in cyclic systems is typically high, considerable stereo-erosion can occur in acyclic systems due to a lower barrier to bond rotation.[26e] In 2008, the Miyashita group reported on a highly stereoselective palladium catalyzed etherification of allylic epoxides (Figure 3.17).[26b] By using a chelatable boronate ester, the reacting oxygen nucleophile could be sequestered on the "frontside" of the palladium π–allyl complex for a rapid nucleophilic attack before stereo-erosion occurred. This approach was efficient for a variety of simple primary alcohols, and it was also adapted for the stereoselective conversion of allylic epoxides to diols.[22a]

Also, a rhodium catalyzed stereoselective epoxide ring opening with alcohol nucleophiles was developed by the Lautens group.[26c] Unlike the palladium catalyzed system which gives a net retention of configuration, the rhodium system gives a net inversion of configuration at the reacting center. However, the substrate scope of the rhodium system is limited to cyclic allylic epoxides and acyclic allylic *trans*-epoxides.

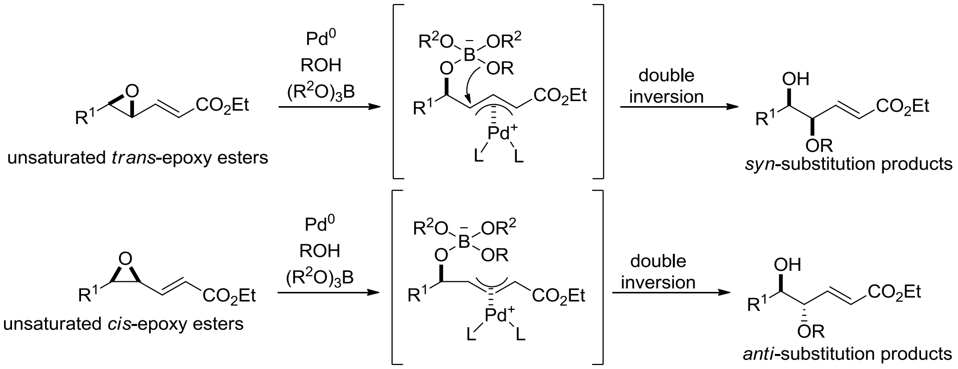
unsaturated trans-epoxy esters
Pd0
ROH
(R2O)3B
double inversion
syn-substitution products
unsaturated cis-epoxy esters
anti-substitution products
CO2Et
R1
OH
OR
Pd+
L

Figure 3.17
Palladium catalyzed etherification of unsaturated α,β-unsaturated γ,δ-epoxy esters.[26b]

Stereospecific Conversion of Diols to Epoxides

Several methods exist for the stereospecific conversion of *vic*-diols to epoxides. The typical method involves direct S_N2 displacement of a halide or activated alcohol (mesylate, tosylate, triflate) by the vicinal hydroxyl group under basic conditions. This leads to an inversion of the reacting center and requires prior differentiation of the vicinal diols. Alternatively, more direct approaches such as the Sharpless procedure[27] can be utilized. The Sharpless procedure involves the conversion of *threo*-diols into regio-isomeric acetoxy-halides through the intermediacy of an orthoester. The *trans*-epoxide is generated by a mild basic hydrolysis (K_2CO_3, MeOH) of the acetate. Other conditions such as the Mitsunobu inversion[28] and various dehydrative conditions can also be employed for the conversion of *vic*-diols to epoxides, although the stereoselectivities are highly substrate dependent. Thus, various methods exist for the conversion of *cis*-epoxides to *trans*-epoxides (or *threo*-diol to *erythro*-diol). These methods should find utility in the syntheses of various stereoisomers of the nigricanosides.

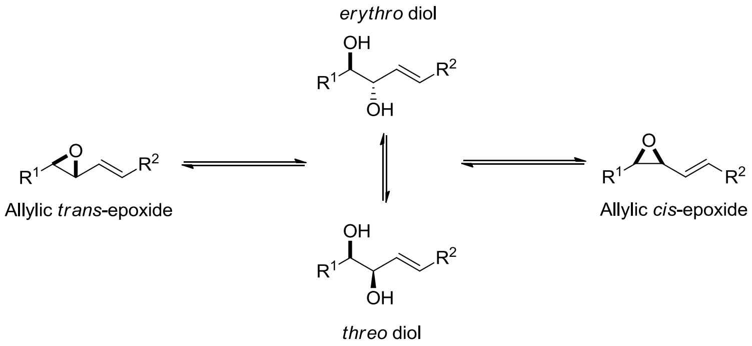

Figure 3.18
Interconversions between allylic epoxides and diols.

3.4 Results and Discussion

Based on the biomimetic hypotheses discussed in the previous section, I focused my attention on the synthesis of the fatty acid fragments with the all *S* diastereomer. My retrosynthetic analysis of protected nigricanoside A is shown below. Disconnection of the C8′-O-C6" ether bond yields protected fatty acid fragment **B** and protected glyceryl galactoside **C**. In the synthetic direction, **C** can be obtained from commercial **E** and **F** in 3 steps through iodination of the anomeric carbon, Ag(I) mediated etherification, and chemoselective deprotection of the primary acetate. Disconnection at the C10-O-C11′ ether linkage of fragment B gives a di-protected triol **K** and allylic epoxide **G**. The latter can be traced back to commercial 5-hexynoic acid and *p*-methoxybenzyl protected *R*-glycidol via regio-, and stereoselective monoepoxidation, two sequential Wittig reactions, and functional group interconversions and protections. On the other hand, allylic epoxide opening, regio-, and stereoselective monoepoxidation, *cis*-selective Wittig olefination, olefin metathesis, and Noyori asymmetric transfer hydrogenation traces **K** to commercial methyl adipoyl chloride **P** and trimethylsilylacetylene **O**.

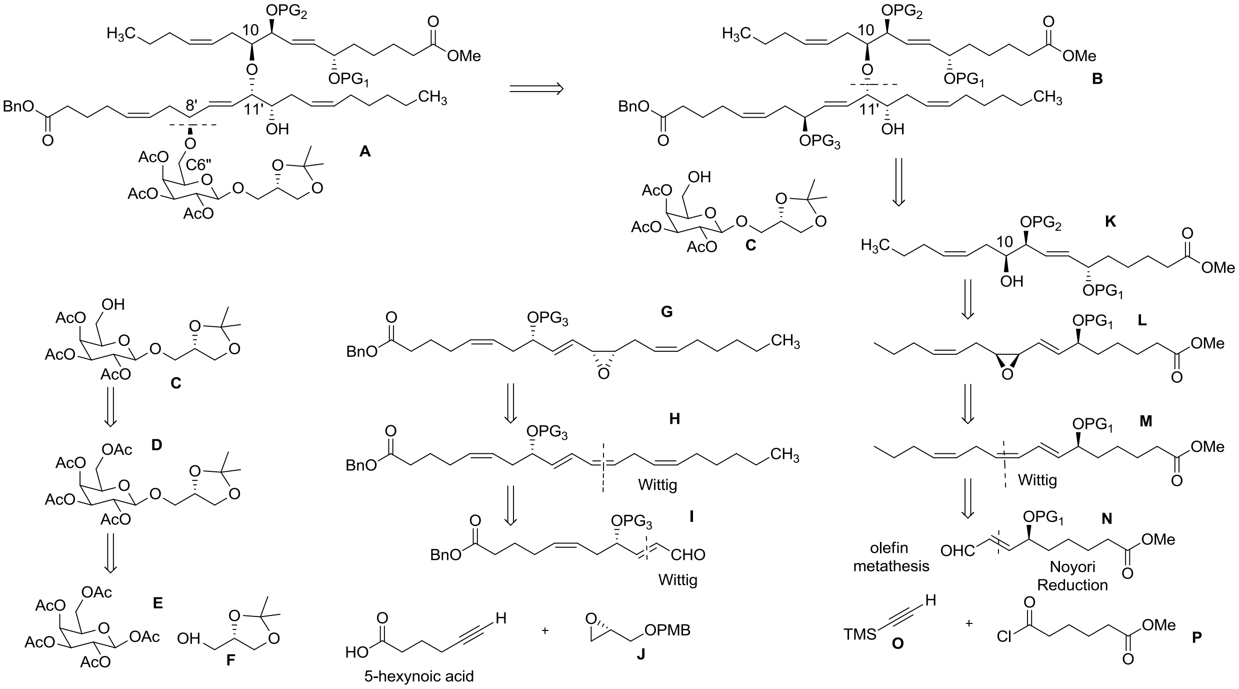
A
B
C
D
E
F
G
H
I
J
K
L
M
N
O
P
OPG_2
OPG_1
OPG_3
10
8'
11'
C6"
Wittig
Wittig
Wittig
olefin metathesis
Noyori Reduction
5-hexynoic acid

Scheme 3.1
Retrosynthetic analysis of nigricanoside A.

3.4.1 Synthesis of the Glyceryl Galactoside Fragment (C)

The synthesis of **C** commenced with iodination of commercial β-D-galactose pentaacetate with triethylsilyl iodide generated from triethylsilane and iodine (Scheme 3.2). The crude 2,3,4,6-tetra-O-acetyl-α-D-galactopyranosyl iodide was reacted with commercial (*S*)-(+)-1,2-isopropylideneglycerol to give galactoside **D** in good yield. Attempted selective deprotection of the primary acetate in **D** with Otera's catalyst in anhydrous methanol gave a significant amount of product in which the C-6 and C-2 acetates were both removed. After exploring various reaction conditions (temperature, solvent, catalyst loading, reaction times and additives), it was discovered that deprotection of the C-2 acetate could be suppressed by using a mixture of isopropanol (IPA) and dichloromethane instead of methanol as the reaction solvent. Thus, **D** could be transformed to **C** in good yield with 5 mol% of Otera's catalyst.

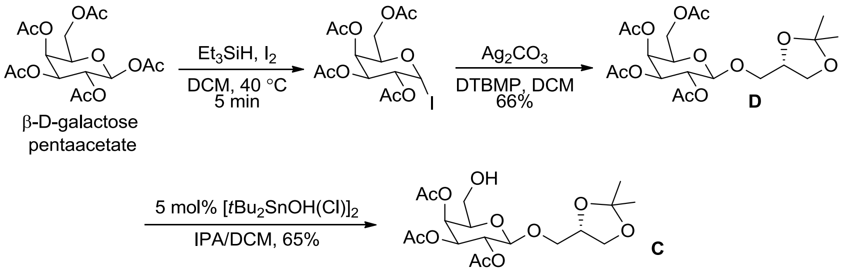

Scheme 3.2
Synthesis of glyceryl galactoside fragment.

3.4.2 Synthesis of C16 Fatty Acid Fragment

A concise and highly efficient synthesis of the C16 fragment of the nigricanosides is shown in Scheme 3.3. Reaction of commercial methyl adipoyl chloride (**P**) with the zinc salt of trimethylsilyl acetylene gave ynone **1** in good yield. Asymmetric reduction of the ketone using the Noyori catalyst *S,S*-TSDPEN[29] in 2-propanol gave propargylic alcohol with excellent ee and yield. Next, the terminal silyl group of **2** was deprotected with K_2CO_3 in methanol to yield propargylic alcohol **3**. I had planned to protect all the free hydroxyl groups of the nigricanosides (except the glycerol fragment) with esters to enable a final global deprotection, so at this stage **3** was protected as the benzoate to give **4** in excellent yield. Semi-hydrogenation with Lindlar catalyst poisoned with quinoline in ethyl acetate gave **5** uneventful. However, attempts to convert allylic benzoate **5** to conjugated aldehyde **6** through a cross metathesis reaction using the Hoveyda-Grubbs 2nd generation catalyst and acrolein was low yielding (~10% conversion by TLC analysis) at rt and reflux conditions. Also, increasing the catalyst loading to 10 mol% and changing the solvent had minor effects on the poor result. Other metathesis catalysts such as the 1st and 2nd generation Grubbs catalysts, and the Zhan catalyst-1B gave similar results.

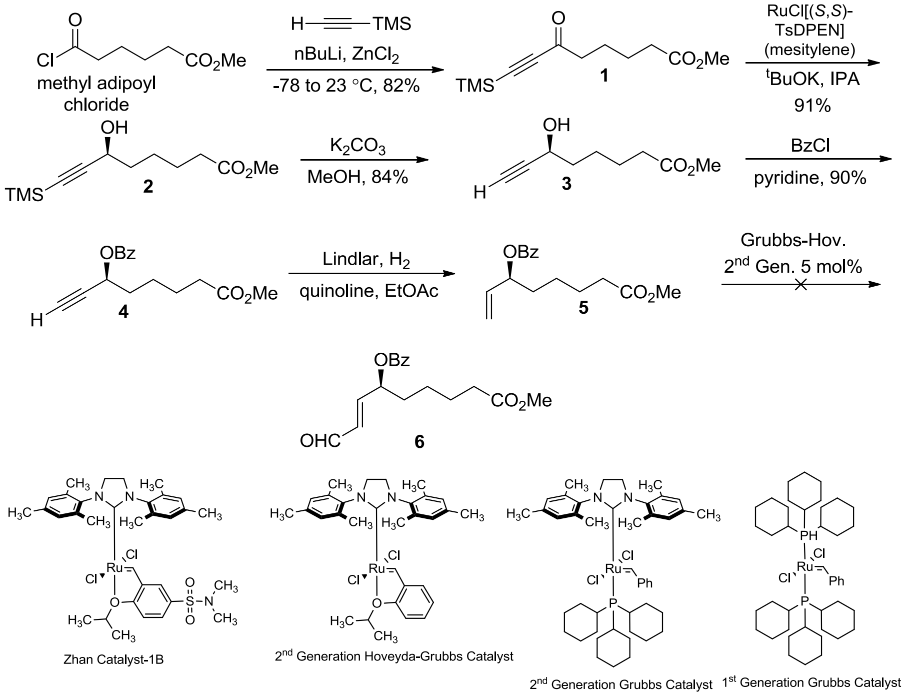

methyl adipoyl chloride
H—≡—TMS
nBuLi, ZnCl2
-78 to 23 °C, 82%
1
RuCl[(S,S)-TsDPEN](mesitylene)
tBuOK, IPA
91%
2
K2CO3
MeOH, 84%
3
BzCl
pyridine, 90%
4
Lindlar, H2
quinoline, EtOAc
5
Grubbs-Hov. 2nd Gen. 5 mol%
6
Zhan Catalyst-1B
2nd Generation Hoveyda-Grubbs Catalyst
2nd Generation Grubbs Catalyst
1st Generation Grubbs Catalyst

Scheme 3.3
Asymmetric synthesis of C16 fatty acid fragment.

Furthermore, the methoxy methyl ether (MOM) protected analog of **5** gave similar results. A close look at the literature suggested that a functional group (apart from an olefin) capable of strongly coordinating to the catalyst should be present on one of the metathesis substrates for an efficient reaction to occur. Thus, the protection of the carbinol in **3** was postponed to a later stage. As shown in Scheme 3.4, Lindlar reduction of **3** gave the semi-reduced product **7**. As predicted, cross-metathesis of the crude product **7** and acrolein with 5 mol% of the Zhan catalyst 1-B gave hydroxyl-aldehyde **8** in 65% yield over the two steps. Protection of the alcohol as its benzoate and subsequent *cis*-selective Wittig olefination gave the desired product in good yield. Thus, the C16 fatty acid chain was constructed in 7 steps.

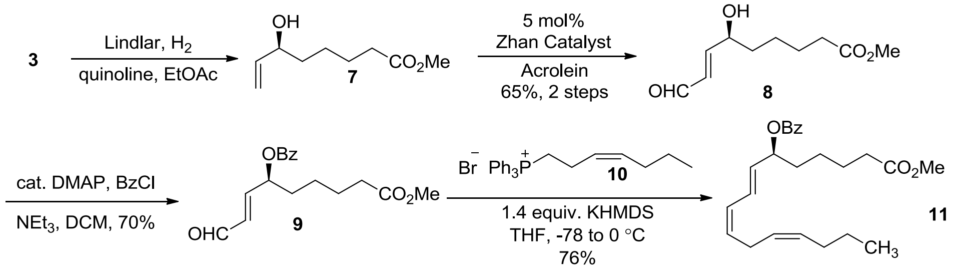
3
Lindlar, H2
quinoline, EtOAc
OH
CO2Me
7
5 mol%
Zhan Catalyst
Acrolein
65%, 2 steps
OH
CO2Me
OHC
8
cat. DMAP, BzCl
NEt3, DCM, 70%
OBz
CO2Me
OHC
9
Br Ph3P
10
1.4 equiv. KHMDS
THF, -78 to 0 °C
76%
OBz
CO2Me
11
CH3

Scheme 3.4
Synthesis of C16 fatty acid fragment contd.

3.4.3 Synthesis of the C20 Fatty Acid Fragment

The synthesis of the C20 fatty acid fragment is shown in Scheme 3.5. Addition of the lithium dianion of 5-hexynoic acid to the known *p*-methoxybenzyl ether protected glycidol **J**[30] gave **12**, which could only be partially purified at this stage. Compound **12** was converted to benzyl ester **13,** whose alkyne was semi-hydrogenated with catalytic P2-Ni/H_2 to give **14**. Protection of the secondary alcohol in **14** as the 2-(azidomethyl)benzoate ester (AZMB) afforded **15** in very good yield. AZMB was chosen to allow selective deprotection in the presence of the C-6 benzoate of the C16 fatty acid. Oxidative removal of the PMB protecting group, Swern oxidation of the resulting primary alcohol **16**, and *trans*-selective Wittig olefination of **17** afforded **18** in good overall yield. Unfortunately, Wittig reaction of **18** using freshly prepared **19** only afforded the desired **20** in low yield. ^{1}H NMR analysis of the side products revealed that the AZMB was cleaved under the Wittig reaction condition to give mostly **21** and **22**. ^{1}H NMR and TLC analyses confirmed that **19** was not contaminated with triphenylphosphine (PPh_3), which could be responsible for the reduction of the azido group and subsequent deprotection of the AZMB.

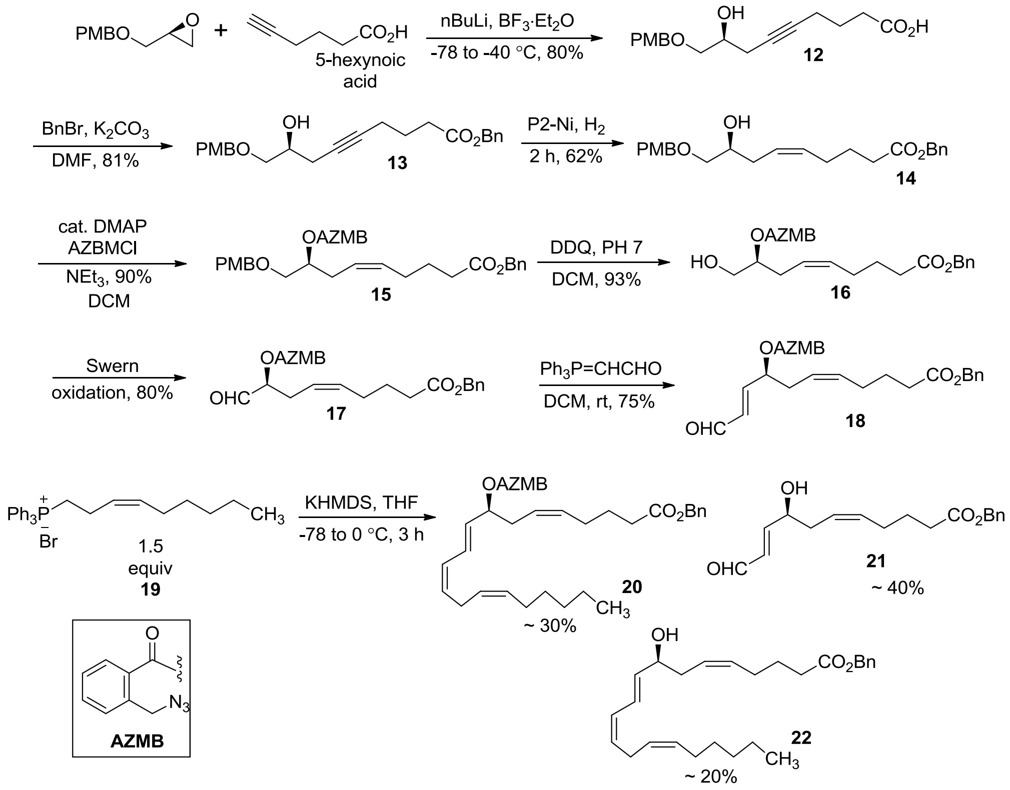
PMBO
+
CO2H
5-hexynoic acid
nBuLi, BF3·Et2O
-78 to -40 °C, 80%
OH
12
BnBr, K2CO3
DMF, 81%
13
CO2Bn
P2-Ni, H2
2 h, 62%
14
cat. DMAP
AZBMCl
NEt3, 90%
DCM
OAZMB
15
DDQ, PH 7
DCM, 93%
HO
16
Swern
oxidation, 80%
OHC
17
Ph3P=CHCHO
DCM, rt, 75%
18
Ph3P
Br
CH3
1.5 equiv
19
KHMDS, THF
-78 to 0 °C, 3 h
20
~ 30%
21
~ 40%
22
~ 20%
O
N3
AZMB

Scheme 3.5
Synthesis of C20 fatty acid fragment.

Therefore, I had to modify the synthetic scheme by replacing the AZMB with a *tert*-butyldimethylsilyl group (Scheme 3.6). With a similar sequence of events as previously described, **14** was successfully converted to aldehyde **26**. To my delight, **26** was smoothly converted to tetraene **27** in very good yield. Thus, the C20 fatty acid chain was constructed in 8 steps from **J**.

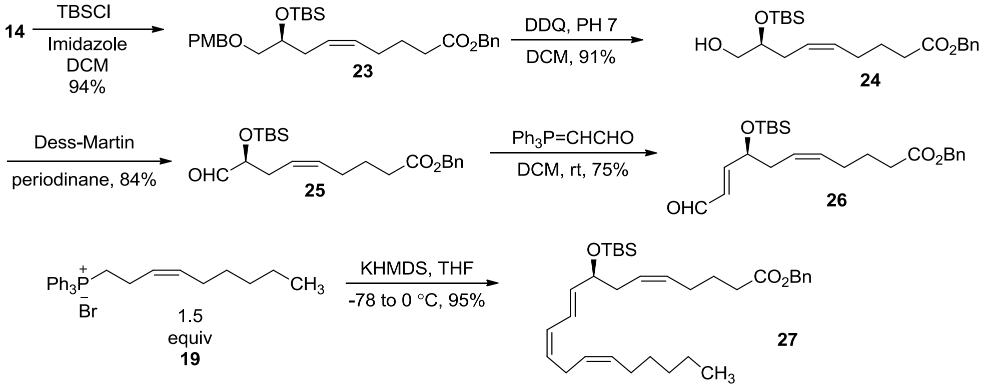
14
TBSCl
Imidazole
DCM
94%
PMBO
OTBS
CO2Bn
23
DDQ, PH 7
DCM, 91%
HO
OTBS
CO2Bn
24
Dess-Martin
periodinane, 84%
OHC
OTBS
CO2Bn
25
Ph3P=CHCHO
DCM, rt, 75%
OTBS
CO2Bn
OHC
26
Ph3P
Br
CH3
1.5
equiv
19
KHMDS, THF
-78 to 0 °C, 95%
OTBS
CO2Bn
27
CH3

Scheme 3.6
Synthesis of C20 fatty acid fragment contd.

3.4.4 Regio- and Stereoselective Epoxidation of 11 and 27

With the assembled C16-triene and C20-tetraene in hand, the Falck epoxidation methodology was examined (Scheme 3.7). As shown in Scheme 3.6, **11** was successfully transformed to **28** in good yield and selectivity, while **27** gave the desired product **29** in moderate yield using the *S*,*S*-salan catalyst.

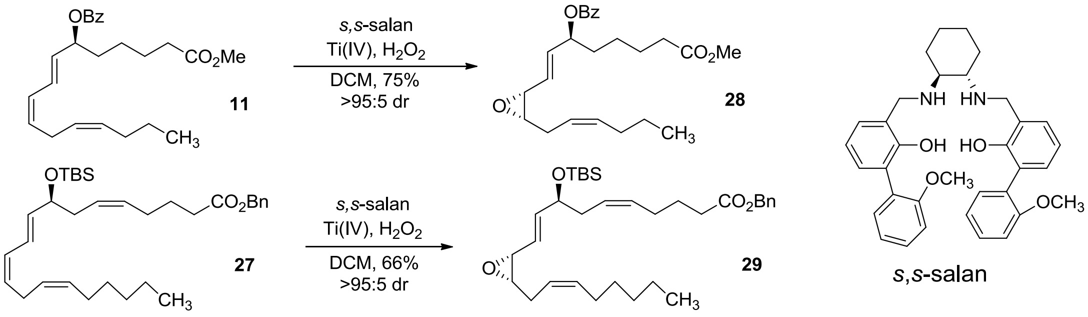
OBz
CO2Me
11
CH3
s,s-salan
Ti(IV), H2O2
DCM, 75%
>95:5 dr
OBz
CO2Me
28
O
CH3
OTBS
CO2Bn
27
CH3
s,s-salan
Ti(IV), H2O2
DCM, 66%
>95:5 dr
OTBS
CO2Bn
29
O
CH3
NH
HN
OH
HO
OCH3
OCH3
s,s-salan

Scheme 3.7
Formation of **28** and **29**.

3.4.5 Allylic Epoxide Opening

My initial studies on the transformation of the C16 epoxy alcohol to a di-protected triol focused on allylic epoxide opening using carboxylates as nucleophiles. This study was performed using the model compound **30**. As shown below (Table 3.1), at best, only a mixture of products could be obtained under Brønsted/Lewis acidic and basic conditions. The mixture of products could have resulted from either ester migration under the reaction conditions, or from an S_N2' process. Therefore, my subsequent studies focused on alcohols as nucleophiles.

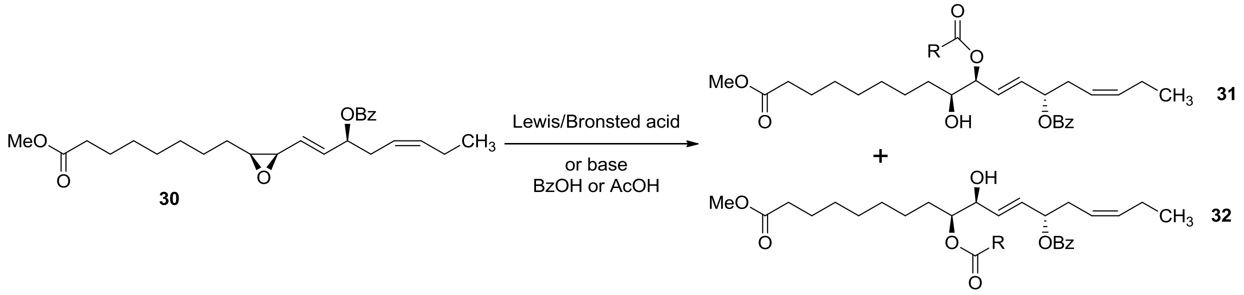
MeO
O
O
OBz
CH3
30
Lewis/Bronsted acid
or base
BzOH or AcOH
MeO
O
R
O
O
OH
OBz
CH3
31
+
MeO
O
OH
O
R
O
OBz
CH3
32

Table 3.1 Allylic epoxide opening with carboxylic/carboxylate nucleophiles

No.	Nucleophile	Acid or Base	Temperature	Result
1	Benzoic acid	$Ti(OiPr)_4$	40 °C	Mixture of products
2	Benzoic acid	$BF_3{\cdot}Et_2O$	0 - 25 °C	Mixture of products
3	Benzoic acid	NEt_3	40 °C	Low conversion
4	Sodium 2-picolinate	None	0 - 40 °C	No reaction
5	Benzoic acid	$ZnEt_2$	40 °C	Mixture of products

As shown in Scheme 3.8a, both *p*-methoxybenzyl alcohol and allyl alcohol were regioselectively etherified with **30** in good yield when an excess of the alcohol was used. However, attempts to form an unsymmetrical *bis*-fatty acid ether or “dimeric ether adduct” by adding **33** to **35** were unsuccessful, presumably due to steric hinderance (Scheme 3.8b). On the other, **34** reacted with **35** under Lewis acid catalysis to give **37** in moderate yield (Scheme 3.8c). These results emphasized the influence of sterics on the efficiency of the “dimerization” and suggested that allyl alcohol was the nucleophile of choice for further evaluation.

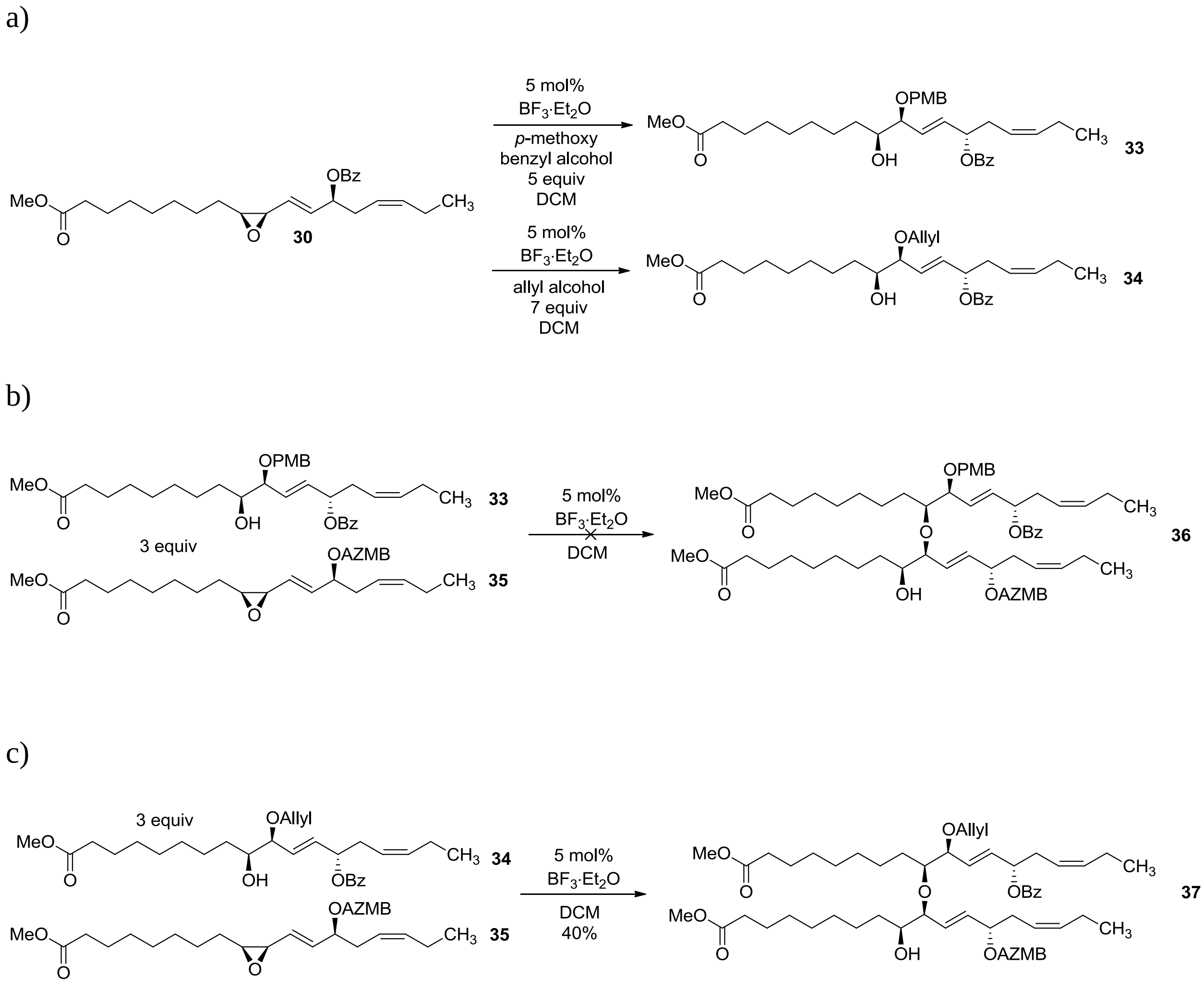

a)
MeO
O
OBz
CH3
O
30
5 mol%
BF3·Et2O
p-methoxy benzyl alcohol
5 equiv
DCM
OPMB
OH
OBz
33
5 mol%
BF3·Et2O
allyl alcohol
7 equiv
DCM
OAllyl
34
b)
33
3 equiv
OAZMB
35
5 mol%
BF3·Et2O
DCM
36
c)
3 equiv
34
35
5 mol%
BF3·Et2O
DCM
40%
37

Scheme 3.8
Allylic epoxide opening with alcohols.

As expected, reaction of allyl alcohol with **28** gave the desired di-protected triol **38** in good yield (Scheme 3.9a). Furthermore, preliminary studies have resulted in the synthesis of **39** in moderate yield over three steps (Scheme 3.9b). Future work will focus on attaching the glyceryl galactoside and completing the total synthesis.

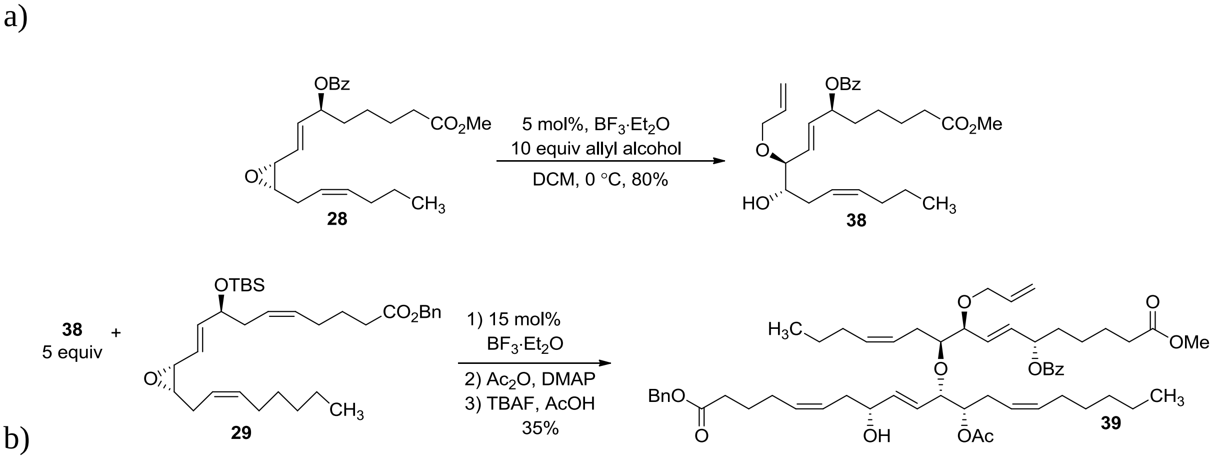
a)
OBz
CO2Me
O
28
CH3
5 mol%, BF3·Et2O
10 equiv allyl alcohol
DCM, 0 °C, 80%
OBz
CO2Me
O
HO
CH3
38
b)
38 +
5 equiv
OTBS
CO2Bn
O
CH3
29
1) 15 mol%
BF3·Et2O
2) Ac2O, DMAP
3) TBAF, AcOH
35%
H3C
O
O
OMe
O
OBz
BnO
O
OH
OAc
CH3
39

Scheme 3.9
Preliminary results on the formation of the *bis*-fatty acid ether of a nigricanoside.

3.5 Conclusion

Supported by literature precedents, our biomimetic approach to the synthesis of nigricanoside A has tentatively reduced the stereochemical uncertainty associated with the structure assignment of this potentially potent antimitotic agent. Our synthetic undertaking led to the development of a novel stereocontrolled distal epoxidation of conjugated dienols, which was successfully applied to the syntheses of both fatty acid fragments of a nigricanoside. Furthermore, promising results with acid catalyzed nucleophilic allylic epoxide openings with allyl alcohol adds merit to our biomimetic hypotheses, and paves a favorable pathway to the completion of this complex total synthesis. Future work will focus on the exploration of various etherifications to attach the synthesized sugar fragment, the completion of the synthesis, and biological studies.

3.6 Experimental

General Methods and Materials. Proton and carbon nuclear magnetic resonance spectra (^{1}H and ^{13}C NMR) were recorded at 500 MHz and 126 MHz, respectively, or at 400 MHz and 101 MHz, respectively, in $CDCl_3$ with TMS as internal standard, unless otherwise stated. ^{1}H NMR data are reported as follows: chemical shift (ppm), multiplicity (s = singlet, br s = broad singlet, d = doublet, t = triplet, q = quartet, app q = apparent quartet, qn = quintet, app qn = apparent quintet, m = multiplet), and coupling constant (Hz). Melting points were measured using an automated melting point apparatus and are uncorrected. Analytical thin layer chromatography (TLC) used EMD Chemicals TLC silica gel 60 F_{254} plates (0.040-0.063 mm) with visualization by UV light and/or $KMNO_4$ or phosphomolybdic acid (PMA) solution followed by heating. Chromatographic purifications utilized preparative TLC or flash chromatography using pre-packed SiO_2 columns on an automated medium pressure chromatograph. Unless otherwise noted, yields refer to isolated, purified material with spectral data consistent with assigned structures or, if known, were in agreement with published data. All reactions were conducted under an argon atmosphere in oven-dried glassware with magnetic stirring. Reagents were purchased at the highest commercial quality and used without further purification. Reaction solvents were dried by passage through a column of activated, neutral alumina under argon and stored under argon until use.

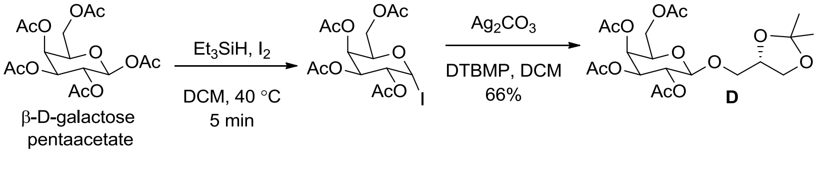

Synthesis of 3-*O*-(2,3,4,6-tetra-*O*-acetyl-β-D-galactopyranosyl)-1,2-*O*-isopropylidene-*sn*-glycerol.

Following literature procedure,[31] anhydrous triethylsilane (Et_3SiH, 3.14 mL, 19.7 mmol, 1.28 equiv) was added slowly over 3 min (caution: exotherm) to a flask containing β-D-galactose pentaacetate (6 g, 15.4 mmol) and I_2 crystals (5.46 g, 21.5 mmol, 1.40 equiv) in DCM (30 mL) at rt. The maroon solution was heated under reflux (42 °C) for 5 min, cooled to rt, and poured into a separatory funnel containing sat. aq. $NaHCO_3$ (20 mL). The organic layer was separated and washed with sat. aq. $Na_2S_2O_3$ solution until the color disappeared. The aqueous washings were extracted with ether (2 × 20 mL), and the combined organic extracts were dried over anhydrous Na_2SO_4, decanted, and concentrated on a rotary evaporator. The residue was further dried under high vacuum for 1 h.

To another flask (oven dried) containing anhydrous $CaSO_4$ (7.70 g), Ag_2CO_3 (6.36 g, 23 mmol), 2,6-di-*tert*-butyl-4-methylpyridine (DTBMP, 1.13 g, 5.50 mmol) and 1,2-*O*-isopropylidene-*sn*-glycerol (1.45 g, 11 mmol) was added DCM (30 mL). The flask was protected from light with aluminum foil and the contents stirred for 1 h under argon. The above crude iodo-galactoside was dissolved in DCM (60 mL) and added slowly (1 h) to the reaction via cannula; the addition was completed with a fresh portion of DCM (10 mL). After 24 h, the reaction was filtered through a pad of Celite™, and the filtrate was concentrated under reduced pressure. The crude product was purified using a Teledyne Isco Combiflash® R_f chromatographic system (120 g SiO_2 column eluted with hexanes, 2 min; 0-30% EtOAc/hexanes, 8 min; 30% EtOAc/hexanes, 50 min) to give the title compound (3.40 g, 66%) as a colorless syrup whose ^1H NMR data were consistent with those reported.[32]

^{1}H NMR (500 MHz, $CDCl_3$) δ 5.39 (dd, *J* = 3.1, 1.7 Hz, 1H), 5.20 (ddd, *J* = 9.2, 8.0, 1.2 Hz, 1H), 5.00 (ddt, *J* = 10.7, 2.8, 1.4 Hz, 1H), 4.57 (dt, *J* = 8.1, 1.3 Hz, 1H), 4.30 – 4.21 (m, 1H), 4.22 – 4.08 (m, 2H), 4.01 (ddd, *J* = 7.7, 6.3, 1.2 Hz, 1H), 3.95 – 3.86 (m, 2H), 3.80 (ddd, *J* = 8.5, 6.0, 1.3 Hz, 1H), 3.63 (ddd, *J* = 10.8, 5.9, 1.3 Hz, 1H), 2.15 (d, *J* = 1.2 Hz, 3H), 2.07 (d, *J* = 1.2 Hz, 3H), 2.05 (d, *J* = 1.1 Hz, 3H), 1.98 (d, *J* = 1.3 Hz, 3H), 1.42 (s, 3H), 1.34 (s, 3H).

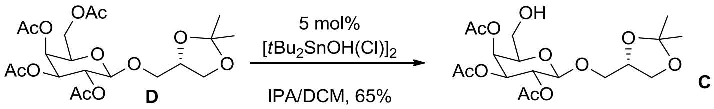

Synthesis of 3-*O*-(2,3,4-tri-*O*-acetyl-β-D-galactopyranosyl)-1,2-*O*-isopropylidene-*sn*-glycerol.

Otera's catalyst ([*t*$Bu_2SnOH(Cl)]_2$,[33] 67 mg, 0.117 mmol, 5 mol%) was added to a solution of **D** (1.08 g, 2.34 mmol) in DCM (8 mL) and IPA (25 mL). The reaction was stirred for 3 days, then concentrated under reduced pressure. The crude product was purified using a Teledyne Isco Combiflash® R_f chromatographic system (40 g SiO_2 column eluted with 0-35% EtOAc/hexanes, 4 min; 35% EtOAc/hexanes, 10 min; 35-50% EtOAc/hexanes, 5 min; 50% EtOAc/hexanes, 15 min) to give the title compound (0.636 g, 65%) as a colorless syrup. $[\alpha]_D^{20}$ = -3.3° (*c* 1.4, EtOH). ^{1}H NMR (400 MHz, $CDCl_3$) δ 5.36 (d, *J* = 3.4 Hz, 1H), 5.22 (dd, *J* = 10.4, 7.9 Hz, 1H), 5.03 (dd, *J* = 10.4, 3.4 Hz, 1H), 4.57 (d, *J* = 8.0 Hz, 1H), 4.31 – 4.22 (m, 1H), 4.01 (dd, *J* = 8.3, 6.5 Hz, 1H), 3.86 (dd, *J* = 10.8, 4.6 Hz, 1H), 3.78 – 3.68 (m, 3H), 3.65 (dd, *J* = 10.8, 5.4 Hz, 1H), 3.52 (dd, *J* = 10.4, 4.9 Hz, 1H), 2.16 (s, 3H), 2.05 (s, 3H), 1.99 (s, 3H), 1.40 (s, 3H), 1.33 (s, 3H); ^{13}C NMR (101 MHz, $CDCl_3$) δ 171.1, 170.1, 169.5, 109.4, 101.6, 74.6, 73.6, 70.9, 69.9, 69.1, 67.8, 66.2, 60.6, 26.6, 25.2, 20.74, 20.7, 20.6.

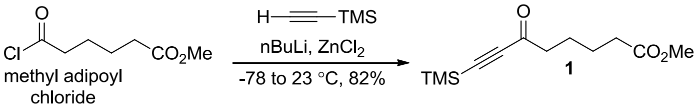

Synthesis of methyl 6-oxo-8-(trimethylsilyl)oct-7-ynoate

Anhydrous $ZnCl_2$ (5.15 g, 37.8 mmol, 1.5 equiv) was dried under high vacuum at 130 °C with stirring for 3 h. The flask was cooled to rt, then THF (60 mL) was added. In a second flask containing a solution of trimethylsilylacetylene (5.34 mL, 37.8 mmol, 1.5 equiv) in THF (30 mL) at -78 °C was added *n*-BuLi (2.5 M in hexanes, 14.1 mL, 35.3 mmol, 1.40 equiv) dropwise. After 30 min, the above $ZnCl_2$ solution was added to the reaction via cannula [the addition was completed with a fresh portion of THF (10 mL)] and stirring was continued at -78 °C for 20 min. The reaction was stirred at 0 °C for 30 min, and then re-cooled to -78 °C. Methyl adipoyl chloride (4.50 g, 25.2 mmol) in THF (20 mL) was added to the reaction via cannula; the addition was completed with a fresh portion of THF (5 mL). The reaction was stirred at 0 °C for 1 h, and at rt for 1 h before being quenched with sat. aq. NH_4Cl (30 mL). The aqueous layer was extracted with Et_2O (2 × 20 mL), the combined organic extracts were dried over anhydrous Na_2SO_4, filtered through a Buchner fritted funnel, and concentrated under reduced pressure. The crude product was purified using a Teledyne Isco Combiflash® R_f chromatographic system (40 g SiO_2 column eluted with hexanes, 3 min; 0-10% EtOAc/hexanes, 7 min; 10% EtOAc/hexanes, 15 min) to give the title compound (5 g, 82%) as a colorless oil whose ^1H NMR data were consistent with those reported.[34]

^1H NMR (500 MHz, $CDCl_3$) δ 3.66 (s, 3H), 2.58 (t, $J = 6.9$ Hz, 2H), 2.33 (t, $J = 7.0$ Hz, 2H), 1.78 – 1.64 (m, 4H), 0.23 (s, 9H).

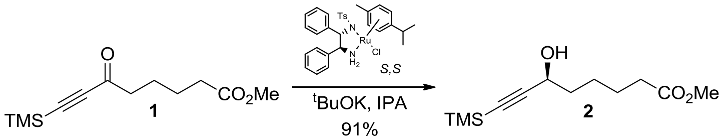

Synthesis of (*S*)-methyl 6-hydroxy-8-(trimethylsilyl)oct-7-ynoate

Potassium *tert*-butoxide (KOtBu, 1.0 M in *t*-BuOH, 0.312 mL, 0.312 mmol, 5 mol%) was added to Noyori's catalyst RuCl(*p*-cymene) [(*S*,*S*)-TS-DPEN] (0.199 g, 0.312 mmol, 5 mol%) followed by anhydrous 2-propanol (IPA, 50 mL). After stirring at rt for 30 min, methyl 6-oxo-8-(trimethylsilyl)oct-7-ynoate (1.5 g, 6.25 mmol) in anhydrous IPA (12 mL) was added to the reaction via cannula. The reaction was continued for 3 h, then concentrated under reduced pressure. The crude product was purified using a Teledyne Isco Combiflash® R_f chromatographic system (12 g SiO_2 column eluted with hexanes, 1 min; 0-10% EtOAc/hexanes, 5 min; 10% EtOAc/hexanes, 10 min; 10-20% EtOAc/hexanes, 5 min; 20% EtOAc/hexanes, 3 min) to give the title compound (1.39 g, 91%, ee ≥99%) as a colorless oil. $[\alpha]_D^{20}$ = -1.8° (*c* 0.5, EtOH), reported value: $[\alpha]_D^{25}$ = -1.8° (*c* 1.2, $CHCl_3$).[34]

^{1}H NMR (400 MHz, $CDCl_3$) δ 4.35 (t, *J* = 6.5 Hz, 1H), 3.66 (s, 3H), 2.32 (t, *J* = 7.5 Hz, 2H), 2.01 – 1.91 (m, 1H), 1.77 – 1.60 (m, 4H), 1.56 – 1.38 (m, 2H), 0.15 (s, 9H); ^{13}C NMR (101 MHz, $CDCl_3$) δ 174.2, 106.7, 89.6, 62.7, 51.7, 37.4, 34.1, 24.8, 24.7, -0.01.

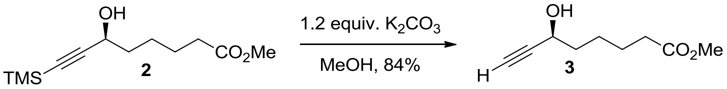

Synthesis of (*S*)-methyl 6-hydroxyoct-7-ynoate

A mixture of (*S*)-methyl 6-hydroxy-8-(trimethylsilyl)oct-7-ynoate (3.64 g, 15.0 mmol) and anhydrous K_2CO_3 (2.49 g, 18.0 mmol, 1.2 equiv) in anhydrous MeOH (60 mL) was stirred at rt for 3 h. The reaction was poured into sat. aq. NH_4Cl (60 mL) and extracted with EtOAc (3 × 30 mL). The combined organic extracts were dried over anhydrous Na_2SO_4, filtered through a Buchner fritted funnel, and concentrated under reduced pressure. The crude product was purified using a Teledyne Isco Combiflash® R_f chromatographic system (40 g SiO_2 column eluted with hexanes, 2 min; 0-20% EtOAc/hexanes, 6 min; 20% EtOAc/hexanes, 15 min; 20-40% EtOAc/hexanes 6 min) to give the title compound (2.16 g, 84%) as a colorless oil. $[\alpha]_D^{20} = -8.6°$ (*c* 0.5, EtOH).

^1H NMR (400 MHz, $CDCl_3$) δ 4.36 (td, *J* = 6.6, 2.1 Hz, 1H), 3.65 (s, 3H), 2.45 (d, *J* = 2.1 Hz, 1H), 2.32 (t, *J* = 7.5 Hz, 3H), 1.78 – 1.59 (m, 4H), 1.53 – 1.41 (m, 2H); ^{13}C NMR (101 MHz, $CDCl_3$) δ 174.2, 84.9, 73.0, 62.0, 51.7, 37.2, 34.0, 24.6, 24.59.

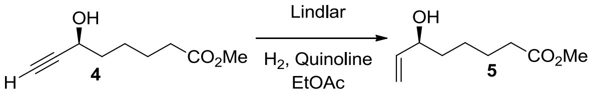

Synthesis of (*S*)-methyl 6-hydroxyoct-7-enoate

A solution of (*S*)-methyl 6-hydroxyoct-7-ynoate (2.00 g, 11.75 mmol) in anhydrous EtOAc (60 mL) was added via cannula to a mixture of Lindlar catalyst (0.150 g) and quinoline (7.00 mL, 59.1 mmol, 5 equiv) in anhydrous EtOAc (57 mL). The reaction was continued under a H_2 atmosphere (1 atm) for 2 h 30 min, filtered through a pad of Celite™, and then washed with cold aq. 1 N HCl (3 × 50 mL), H_2O (50 mL), and brine (30 mL). The aqueous washings were extracted with EtOAc (2 × 20 mL), and the combined organic extracts were dried over anhydrous Na_2SO_4, decanted, and concentrated under reduced pressure. The crude product containing ~ 10% over reduced product (2.00 g) was used in the next step without further purification. $[\alpha]_D^{20} = +11.4°$ (*c* 0.5, EtOH).

Crude: ^{1}H NMR (400 MHz, CDCl$_3$) δ 5.85 (ddd, *J* = 16.9, 10.4, 6.2 Hz, 1H), 5.21 (dt, *J* = 17.2, 1.4 Hz, 1H), 5.09 (dt, *J* = 10.4, 1.3 Hz, 1H), 4.09 (q, *J* = 6.4 Hz, 1H), 3.65 (s, 3H), 2.38 – 2.25 (m, 2H), 1.80 – 1.24 (m, 6H); ^{13}C NMR (101 MHz, CDCl$_3$) δ 174.3, 141.2, 114.8, 73.0, 51.6, 36.6, 34.1, 25.0, 24.9.

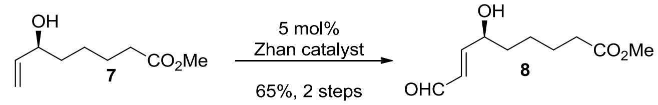

Synthesis of (*S*,*E*)-methyl 6-hydroxy-9-oxonon-7-enoate

A solution of crude (*S*)-methyl 6-hydroxyoct-7-enoate (2.00 g, 11.6 mmol) and anhydrous acrolein (3.88 mL, 58.0 mmol, 5 equiv) in DCM (30 mL) was added via cannula to a solution of Zhan catalyst 1-B (0.426 g, 0.580 mmol, 5 mol%) in DCM (20 mL); the addition was completed with a fresh portion of DCM (8 mL). The reaction was stirred at rt for 24 h, then concentrated in vacuo. The crude product was purified using a Teledyne Isco Combiflash® *R*$_f$ chromatographic system (40 g gold-grade SiO$_2$ column eluted with hexanes, 2 min; 0-30% EtOAc/hexanes, 6 min; 30% EtOAc/hexanes, 12 min; 30-60% EtOAc/hexanes 15 min, 60% EtOAc/hexanes, 5 min) to give the title compound (1.55 g, 65%) as a brown solid. A sample was purified by TLC to give the title compound as a yellow solid (mp, 68.3-68.4 °C). $[\alpha]_D^{20}$ = +37.8° (*c* 0.5, EtOH).

^{1}H NMR (400 MHz, C$_6$D$_6$) δ 9.34 (d, *J* = 7.6 Hz, 1H), 6.17 (ddd, *J* = 15.7, 7.6, 1.5 Hz, 1H), 6.05 (dd, *J* = 15.7, 4.3 Hz, 1H), 3.73 (s, 1H), 3.35 (s, 3H), 2.04 (t, *J* = 7.3 Hz, 2H), 1.52 – 1.33 (m, 2H), 1.22 – 1.01 (m, 4H); ^{13}C NMR (101 MHz, C$_6$D$_6$) δ 192.6, 173.5, 158.5, 130.8, 70.5, 51.1, 36.0, 33.8, 24.9, 24.8.

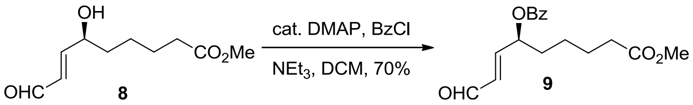

Synthesis of (*S*,*E*)-9-methoxy-1,9-dioxonon-2-en-4-yl benzoate

Triethylamine (1.76 mL, 12.6 mmol, 3 equiv) was added dropwise to a solution of (*S*,*E*)-methyl 6-hydroxy-9-oxonon-7-enoate (0.840 g, 4.20 mmol) and 4-dimethylaminopyridine (DMAP, 0.103 g, 0.840 mmol, 0.2 equiv) in DCM (42 mL) at 0 °C. After 3 min, benzoyl chloride (BzCl, 0.973 mL, 8.39 mmol, 2 equiv) was added slowly to the reaction. The reaction was continued at 0 °C for 3 h and then allowed to gradually warm to rt overnight (15 h). The reaction mixture was washed with sat. aq. $NaHCO_3$ (30 mL) and the aqueous layer was extracted with DCM (3 × 15 mL). The combined organic extracts were dried over anhydrous Na_2SO_4, decanted, and concentrated under reduced pressure. The crude product was purified using a Teledyne Isco Combiflash® R_f chromatographic system (24 g SiO_2 column eluted with hexanes, 1 min; 0-10% EtOAc/hexanes, 7 min; 10% EtOAc/hexanes, 10 min; 10-20% EtOAc/hexanes 5 min, 20%, 8 min) to give the title compound (0.974 g, 70%) as a brown oil. $[\alpha]_D^{20}$ = +51.5° (*c* 0.5, EtOH).

^{1}H NMR (500 MHz, $CDCl_3$) δ 9.59 (d, *J* = 7.7 Hz, 1H), 8.10 – 7.96 (m, 2H), 7.64 – 7.55 (m, 1H), 7.52 – 7.40 (m, 2H), 6.84 (dd, *J* = 15.8, 4.6 Hz, 1H), 6.29 (ddd, *J* = 15.8, 7.7, 1.6 Hz, 1H), 5.78 (tdd, *J* = 6.4, 4.6, 1.6 Hz, 1H), 3.64 (s, 3H), 2.34 (t, *J* = 7.4 Hz, 2H), 1.96 – 1.82 (m, 2H), 1.77 – 1.64 (m, 2H), 1.58 – 1.40 (m, 2H); ^{13}C NMR (101 MHz, $CDCl_3$) δ 193.0, 173.8, 165.6, 153.7, 133.6, 131.7, 129.8, 129.6, 128.6, 72.5, 51.6, 33.8, 33.5, 24.6.

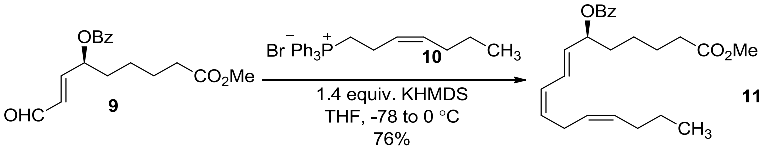

Synthesis of (*S*,7*E*,9*Z*,12*Z*)-1-methoxy-1-oxohexadeca-7,9,12-trien-6-yl benzoate

Potassium bis(trimethylsilyl)amide (0.5 M solution in toluene, 9.50 mL, 4.73 mmol, 1.4 equiv) was added dropwise to a suspension of anhydrous (azeotropically dried by co-evaporation with toluene, 3 × 40 mL) (*Z*)-hept-3-en-1-yltriphenylphosphonium bromide (2.24 g, 5.08 mmol, 1.5 equiv) in anhydrous THF (210 mL) at -78 °C. The cold bath was removed and the reaction (orange solution) was allowed to slowly warm to 0 °C over 1h, and then stirred at rt for 15 min. The reaction was cooled to -78 °C and (*S*,*E*)-9-methoxy-1,9-dioxonon-2-en-4-yl benzoate (1.03 g, 3.38 mmol) in anhydrous THF (25 mL) was added slowly to the reaction via cannula; the addition was completed with a fresh portion of THF (15 mL). The reaction was allowed to slowly warm to 0 °C over 1 h and continued at 0 °C for 30 min. The reaction was quenched with 1M aq. NH_4OAc (20 mL) and concentrated under reduced pressure. The residue was diluted with H_2O (50 mL) and extracted with EtOAc (3 × 20 mL). The combined organic extracts were dried over anhydrous Na_2SO_4, decanted, and concentrated in vacuo. The crude product was purified using a Teledyne Isco Combiflash® R_f chromatographic system (24 g SiO_2 column eluted with hexanes, 5 min; 0-10% EtOAc/hexanes, 13 min; 10% EtOAc/hexanes, 5 min) to give the title compound (1 g, 76%) as a colorless oil. $[\alpha]_D^{20}$ = +107.2° (*c* 0.5, EtOH).

^{1}H NMR (400 MHz, $CDCl_3$) δ 8.09 – 7.93 (m, 2H), 7.56 – 7.46 (m, 1H), 7.40 (tt, *J* = 7.1, 1.3 Hz, 2H), 6.70 – 6.54 (m, 1H), 5.95 (tt, *J* = 11.1, 1.7 Hz, 1H), 5.67 (dd, *J* = 15.1, 7.2 Hz, 1H), 5.60 – 5.49 (m, 1H), 5.47 – 5.23 (m, 3H), 3.60 (s, 3H), 2.98 – 2.81 (m, 2H), 2.29 (t, *J* = 7.5 Hz, 2H), 2.05 – 1.93 (m, 2H), 1.89 – 1.56 (m, 4H), 1.49 – 1.24 (m, 4H), 0.86 (dd, *J* = 7.9, 6.9 Hz, 3H); ^{13}C NMR (100 MHz, $CDCl_3$) δ 173.8, 165.7, 132.8, 131.7, 131.0, 130.6, 129.5, 128.3, 127.9, 127.4, 127.0, 74.9, 51.4, 34.3, 33.8, 29.2, 26.2, 24.7, 22.7, 13.7.

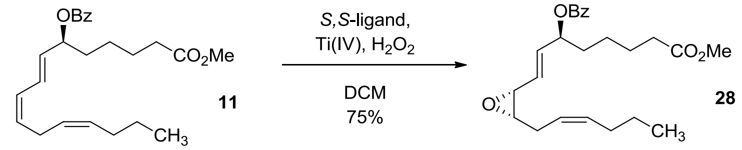

Synthesis of (*S*,*E*)-1-[(2*R*,3*S*)-3-[(*Z*)-hex-2-en-1-yl]oxiran-2-yl]-8-methoxy-8-oxooct-1-en-3-yl benzoate

A solution of *S*,*S*-ligand[20] (0.084 g, 0.156 mmol, 6 mol%) and Ti(*Oi*-Pr)$_4$ (39.3 µL, 0.130 mmol, 5 mol%) in anhydrous DCM (1 mL) was stirred at rt for 1 h. (*S*,7*E*,9*Z*,12*Z*)-1-Methoxy-1-oxohexadeca-7,9,12-trien-6-yl benzoate (1.00 g, 2.60 mmol) was added neat to the yellow solution followed by DCM (6.80 mL), and then the solution was then cooled to 4 °C. Aqueous H_2O_2 (30%, 0.589 mL, 2 equiv) was added dropwise to the reaction, and then the mixture was stirred vigorously at 4 °C overnight (20 h). The reaction was continued at rt for 3 h, diluted with DCM (10 mL), and washed with 10% aq. $Na_2S_2O_3$ (2 × 20 mL). The aqueous layer was extracted with DCM (2 × 20 mL), and the combined organic extracts were dried over anhydrous Na_2SO_4, decanted, and concentrated in vacuo. The crude product was purified using a Teledyne Isco Combiflash® R_f chromatographic system (24 g SiO_2 column, 20 mL/min flow rate, eluted with hexanes containing 2% *tert*-butylamine, 5 min; 0-10% EtOAc/hexanes, 13 min; 10% EtOAc/hexanes, 5 min) to give the title compound (0.781 g, 75%) as a colorless oil. $[\alpha]_D^{20}$ = +22.0° (*c* 0.5, EtOH).

^{1}H NMR (400 MHz, $CDCl_3$) δ 8.02 (dd, 1H, *J* = 8.3, 1.4 Hz), 7.68 –7.47 (m, 1H), 7.53 – 7.25 (m, 1H), 5.95 (ddd, 1H, *J* = 15.6, 6.3, 0.9 Hz), 5.70 (ddd, 1H , *J* = 15.6, 6.7, 1.2 Hz), 5.60 – 5.45 (m, 1H), 5.42 – 5.38 (m, 1H), 5.30 – 5.17 (m, 1H), 3.62 (s, 2H), 3.58 – 3.29 (m, 1H), 3.07 (td, 1H , *J* = 6.4, 4.2 Hz), 2.30 (t, 2H, *J* = 7.5 Hz), 2.21 – 2.01 (m, 1H), 1.91 (dt, 2H, *J* = 7.1, 1.6 Hz), 1.85 – 1.65 (m, 2H), 1.60 – 1.50 (m, 3H), 1.45 – 1.32 (m, 2H), 1.29 (q, 2H, *J* = 7.3 Hz), 0.82 (t, 3H, J = 7.3 Hz); ^{13}C NMR (100 MHz, $CDCl_3$) δ 173.8, 165.6, 134.1, 133.0, 132.7, 130.3, 129.5, 128.3, 126.7, 123.5, 110.0, 73.8, 58.3, 56.0, 51.5, 34.1, 33.8, 29.3, 26.0, 24.7, 22.6, 13.6.

^{1}H NMR (400 MHz, C_6D_6) δ 8.22 – 8.08 (m, 2H), 7.15 – 7.01 (m, 3H), 5.83 (ddd, J = 15.6, 6.3, 0.7 Hz, 1H), 5.72 (ddd, J = 15.5, 6.1, 1.0 Hz, 1H), 5.65 – 5.55 (m, 1H), 5.48 – 5.34 (m, 2H), 3.32 (s, 3H), 3.19 – 3.13 (m, 1H), 2.88 (td, J = 6.3, 4.2 Hz, 1H), 2.38 – 2.26 (m, 1H), 2.14 – 2.04 (m, 1H), 2.01 (t, J = 7.4 Hz, 2H), 1.86 (dddd, J = 8.6, 6.7, 4.5, 1.4 Hz, 2H), 1.64 – 1.39 (m, 4H), 1.30 – 1.14 (m, 4H), 0.80 (t, J = 7.4 Hz, 3H).

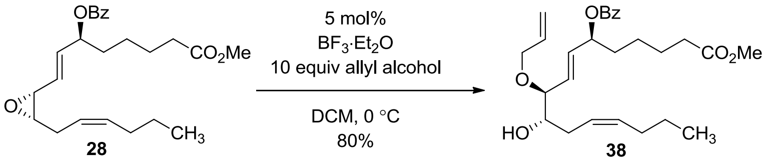

Synthesis of (6*S*,7*E*,9*S*,10*S*,12*Z*)-9-(allyloxy)-10-hydroxy-1-methoxy-1-oxohexadeca-7,12-dien-6-yl benzoate

A solution of $BF_3·Et_2O$ (5.10 µL, 0.041 mmol, 5 mol%) in DCM (46 µL) was added dropwise to a mixture of **28** (330 mg, 0.824 mmol), anhydrous allyl alcohol (0.560 mL, 8.24 mmol, 10 equiv), and 4Å MS (0.280 g) in DCM (0.824 mL) at 0 °C. The reaction was continued at 0 °C for 12 h, then stirred at rt for 30 min. The reaction was quenched with imidazole (8.40 mg, 0.123 mmol, 15 mol%) and filtered through a pad of Celite™ with DCM. The filtrate was concentrated under reduced pressure in a fume hood, and the residue was purified using a Teledyne Isco Combiflash® R_f chromatographic system (12 g SiO_2 column eluted with hexanes, 2 min; 0-10% EtOAc/hexanes, 8 min; 10% EtOAc/hexanes, 5 min, 10-20% EtOAc/hexanes, 10 min) to give the title compound (302 mg, 80%) as a colorless oil. $[\alpha]_D^{20}$ = +7.7° (c 0.5, EtOH).

^{1}H NMR (400 MHz, CDCl$_3$) δ 8.10 – 8.00 (m, 2H), 7.56 (ddt, *J* = 8.0, 6.9, 1.3 Hz, 1H), 7.49 – 7.40 (m, 2H), 5.87 (dddd, *J* = 17.2, 10.4, 6.1, 5.2 Hz, 1H), 5.78 (dd, *J* = 15.6, 6.3 Hz, 1H), 5.64 (ddd, *J* = 15.7, 7.7, 1.0 Hz, 1H), 5.56 – 5.49 (m, 1H), 5.48 – 5.44 (m, 2H), 5.24 (dq, *J* = 17.2, 1.6 Hz, 1H), 5.16 (dq, *J* = 10.4, 1.4 Hz, 1H), 4.05 (ddt, *J* = 12.6, 5.2, 1.5 Hz, 1H), 3.82 (ddt, *J* = 12.7, 6.1, 1.4 Hz, 1H), 3.68 – 3.59 (m, 1H), 3.64 (s, 3H), 3.56 (td, *J* = 7.2, 4.3 Hz, 1H), 2.62 (br s, 1H), 2.32 (t, *J* = 7.4 Hz, 2H), 2.31 – 2.23 (m, 1H), 2.19 – 2.08 (m, 1H), 1.98 – 1.62 (m, 6H), 1.45 (dddd, *J* = 14.2, 11.6, 10.0, 6.8 Hz, 2H), 1.35 – 1.23 (m, 2H), 0.82 (t, *J* = 7.4 Hz, 3H); ^{13}C NMR (101 MHz, CDCl$_3$) δ 174.0, 165.8, 134.6, 133.8, 133.1, 132.3, 130.4, 129.9, 129.7, 128.5, 125.1, 117.4, 82.5, 74.2, 73.5, 69.7, 51.7, 34.3, 34.0, 30.5, 29.5, 24.9, 24.8, 22.8, 13.8.

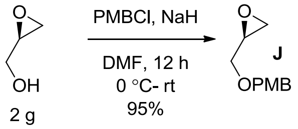

Synthesis of (*R*)-2-[(4-methoxybenzyl)oxymethyl]oxirane

To a suspension of 60% wt NaH in oil (1.1 equiv, 1.19 g, 29.7 mmol) in anhydrous DMF (50 mL) at 0 °C was added neat PMBCl (1.1 equiv, 29.7 mmol, 4.1 mL) dropwise. After 3 min, neat *R*-(-)-glycidol (27 mmol, 1.85 mL) was added slowly over 30 min. The reaction was left to gradually warm to rt in the cold bath. After overnight (12 h), the reaction was re-cooled to 0 °C, carefully quenched with sat. aq. NH$_4$Cl (10 mL), and then allowed to warm to rt. The mixture was poured into a separatory funnel containing sat. aq. NH$_4$Cl (60 mL), and extracted with Et$_2$O (3 × 40 mL). The combined organic extracts were washed with brine (20 mL), dried over anhydrous Na$_2$SO$_4$, filtered through a Buchner fritted funnel, and concentrated on a rotary evaporator. Azeotropoic co-evaporation with toluene was used to remove residual DMF. The residue was purified using a Teledyne Isco Combiflash® *R*$_f$ chromatographic system (40 g SiO$_2$

column eluted with hexanes, 1 min; 0-10% EtOAc/hexanes, 15 min; 10% EtOAc/hexanes, 25 min) and gave the title product (4.98g, 95%) as a colorless oil whose ^{1}H NMR data were consistent with those reported.[30]

^{1}H NMR (500 MHz, $CDCl_3$) δ 7.28 (d, *J* = 8.5 Hz, 2H), 6.88 (d, *J* = 8.5 Hz, 2H), 4.55 (d, *J* = 11.5 Hz, 1H), 4.49 (d, *J* = 11.5 Hz, 1H), 3.81 (s, 3H), 3.73 (dd, *J* = 11.4, 3.1 Hz, 1H), 3.41 (dd, *J* = 11.4, 5.9 Hz, 1H), 3.18 (ddt, *J* = 5.9, 4.0, 2.9 Hz, 1H), 2.84 – 2.72 (m, 1H), 2.61 (dd, *J* = 5.1, 2.7 Hz, 1H).

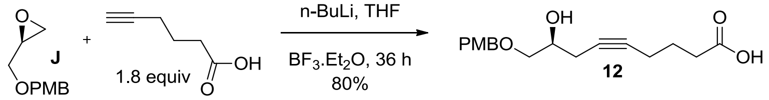

Synthesis of (*S*)-8-hydroxy-9-[(4-methoxybenzyl)oxy]non-5-ynoic acid

n-Butyllithium (2.5M in hexanes, 10.2 mL, 25.5 mmol, 3.4 equiv) was added dropwise to a -78 °C solution of 5-hexynoic acid (1.49 ml, 13.5 mmol, 1.8 equiv) in anhydrous THF (105 mL). The reaction was stirred at -78 °C for 30 min and at 0 °C for 1 h. The reaction was cooled to -78 °C and $BF_3 \cdot Et_2O$ (1.85 mL, 15.0 mmol, 2.0 equiv) was added dropwise to the mixture. After 30 min, a solution of (*S*)-2-[(4-methoxybenzyloxy)methyl]oxirane (J) (2.50 g, 8.10 mmol) in anhydrous THF (16.2 mL) was added slowly to the reaction via cannula. The reaction was stirred at -78 °C for 40 min and then continued at -40 °C for 36 h. The reaction was quenched with sat. aq. NH_4Cl (20 mL), warmed to 0 °C, and acidified to pH 4.0–4.5 with dilute 1N HCl (~ 26 mL). The organic layer was separated, and the aqueous phase was extracted with EtOAc (2 × 20 mL). The combined organic extracts were dried over Na_2SO_4, filtered through a Buchner fritted funnel, and concentrated in vacuo. The crude product was purified using a Teledyne Isco Combiflash® R_f chromatographic system (40 g SiO_2 column eluted with hexanes, 1 min; 0-35%

EtOAc/hexanes, 7 min; 35% EtOAc/hexanes, 10 min; 35-50% EtOAc/hexanes, 5 min; 50% EtOAc/hexanes, 10 min) and the title product (1.84 g, 80%) was obtained as a colorless oil. $[\alpha]_D^{20}$ = +13.6° (*c* 0.5, EtOH).

^{1}H NMR (500 MHz, CDCl$_3$) δ 7.31 – 7.27 (m, 2H), 6.92 – 6.84 (m, 2H), 4.59 – 4.43 (m, 2H), 3.81 (s, 3H), 3.73 (dd, *J* = 11.4, 3.1 Hz, 1H), 3.41 (dd, *J* = 11.4, 5.9 Hz, 1H), 3.20 – 3.15 (m, 1H), 2.80 (t, *J* = 4.6 Hz, 1H), 2.61 (dd, *J* = 5.0, 2.7 Hz, 1H).

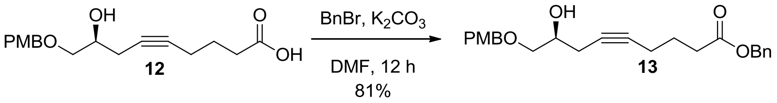

Synthesis of (*S*)-benzyl 8-hydroxy-9-[(4-methoxybenzyl)oxy]non-5-ynoate

A mixture of (*S*)-8-hydroxy-9-[(4-methoxybenzyl)oxy]non-5-ynoic acid (0.748 g, 2.44 mmol) and anhydrous potassium carbonate (K$_2$CO$_3$, 0.438 g, 3.17 mmol, 1.3 equiv) in anhydrous dimethylformamide (DMF, 10 mL) was stirred at rt for 10 min. Benzyl bromide (BnBr, 0.348 ml, 2.93 mmol, 1.2 equiv) was added dropwise, and the mixture was vigorously stirred for 15 h. The reaction mixture was quenched with saturated aqueous NH$_4$Cl (5 mL), diluted with ether (20 mL), and washed with water (20 mL) and brine (20 mL). The aqueous layer was back-extracted with ether (2 × 20 mL). The combined organic extracts were dried over Na$_2$SO$_4$, concentrated under reduced pressure, and the residue was purified using a Teledyne Isco Combiflash® *R*$_f$ chromatographic system (12 g SiO$_2$ column eluted with hexanes, 1 min; 0-20% EtOAc/hexanes, 9 min; 20% EtOAc/hexanes, 5 min, 20-30%, 10 min) to give **13** (0.785g, 81%) as a colorless oil. $[\alpha]_D^{20}$ = +10.2° (*c* 0.5, EtOH).

^{1}H NMR (500 MHz, CDCl$_3$) δ 7.39 – 7.27 (m, 5H), 7.28 – 7.21 (m, 2H), 6.90 – 6.83 (m, 2H), 5.11 (s, 2H), 4.47 (s, 2H), 3.93 – 3.84 (m, 1H), 3.78 (s, 3H), 3.54 (dd, *J* = 9.5, 3.9 Hz, 1H), 3.43

(dd, *J* = 9.6, 6.7 Hz, 1H), 2.57 (d, *J* = 4.5 Hz, 1H), 2.46 (t, *J* = 7.4 Hz, 2H), 2.40 – 2.36 (m, 2H), 2.21 (tt, *J* = 6.9, 2.4 Hz, 2H), 1.81 (qn, *J* = 6.9 Hz, 2H); ^{13}C NMR (101 MHz, $CDCl_3$) δ 173.0, 159.3, 135.9, 130.0, 129.4 (2), 128.6 (2), 128.20, 128.17 (2), 113.8 (2), 81.3, 76.8, 73.0, 72.7, 69.1, 66.2, 55.2, 33.1, 24.0, 23.9, 18.2.

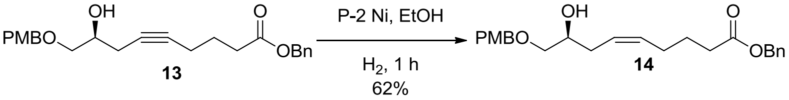

(*S*,*Z*)-benzyl 8-hydroxy-9-(4-methoxybenzyloxy)non-5-enoate

$NaBH_4$ (0.044 g, 1.15 mmol, 0.6 equiv) was added in one portion to a solution of $Ni(OAc)_2$ (0.191 g, 0.768 mmol, 0.4 equiv) in anhydrous EtOH (10 mL) in a two-necked flask under a H_2 atmosphere (1 atm). After 20 minutes, ethylenediamine (EDA, 0.192 ml, 2.88 mmol, 1.5 equiv) was added to the flask, followed by (*S*)-benzyl 8-hydroxy-9-[(4-methoxybenzyl)oxy]non-5-ynoate (0.963 g, 1.92 mmol) in a mixture of anhydrous EtOH/hexanes (10/5 mL). After completion as judged by TLC analysis (1 – 2 h), the reaction was filtered through a column of silica gel eluted with ethyl acetate. The filtrate was concentrated in vacuo to give the crude product (0.603g, 62%) as a colorless oil. $[\alpha]_D^{20}$ = -1.6° (*c* 0.5, EtOH).

^{1}H NMR (400 MHz, $CDCl_3$) δ 7.43 – 7.29 (m, 5H), 7.31 – 7.20 (m, 2H), 6.94 – 6.80 (m, 2H), 5.60 – 5.36 (m, 2H), 5.11 (s, 2H), 4.47 (s, 2H), 3.85 – 3.76 (m, 1H), 3.80 (s, 3H), 3.47 (dd, *J* = 9.4, 3.3 Hz, 1H), 3.32 (dd, *J* = 9.5, 7.4 Hz, 1H), 2.36 (t, *J* = 7.5 Hz, 2H), 2.29 – 2.14 (m, 2H), 2.14 – 2.01 (m, 2H), 1.78 – 1.64 (m, 2H); ^{13}C NMR (101 MHz, $CDCl_3$) δ 173.5, 159.4, 136.1, 131.4, 130.2, 129.5 (2), 128.7 (2), 128.3 (2), 128.3, 126.0, 113.9 (2), 73.8, 73.2, 70.3, 66.3, 55.4, 33.8, 31.4, 26.8, 24.8.

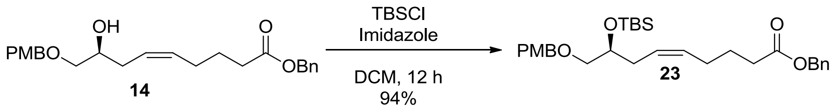

(*S*,*Z*)-benzyl 8-(*tert*-butyldimethylsilyloxy)-9-(4-methoxybenzyloxy)non-5-enoate

tert-Butyldimethylsilyl chloride (TBSCl, 1.68 g, 11.1 mmol, 2 equiv) was added in two portions to a mixture of the above crude (*S*,*Z*)-benzyl 8-hydroxy-9-(4-methoxybenzyloxy)non-5-enoate (2.22 g, 5.57 mmol) and imidazole (1.51 g, 22.2 mmol, 4 equiv) in anhydrous DCM (55 mL) at 0 °C. After 30 min, the cold bath was removed, and the reaction was allowed to gradually warm to rt overnight (20 h). The reaction was quenched with sat. aq. $NaHCO_3$ (5 mL) and diluted with water (30 mL). The organic layer was separated and the aqueous layer was extracted with DCM (2 × 20 mL). The combined organic extracts were dried over Na_2SO_4, concentrated under reduced pressure, and the residue was purified using a Teledyne Isco Combiflash® R_f chromatographic system (40 g SiO_2 column eluted with hexanes, 2 min; 0-7% EtOAc/hexanes, 6 min; 7% EtOAc/hexanes, 5 min) to give **23** (2.7 g, 94%) as a colorless oil. $[\alpha]_D^{20}$ = 3.8° (*c* 0.5, EtOH).

^{1}H NMR (400 MHz, $CDCl_3$) δ 7.42 – 7.28 (m, 5H), 7.29 – 7.18 (m, 2H), 6.92 – 6.81 (m, 2H), 5.52 – 5.32 (m, 2H), 5.11 (s, 2H), 4.44 (s, 2H), 3.84 (t, *J* = 5.7 Hz, 1H), 3.80 (s, 3H), 3.39 – 3.29 (m, 2H), 2.35 (dd, *J* = 8.0, 7.2 Hz, 2H), 2.32 – 2.15 (m, 2H), 2.14 – 2.01 (m, 2H), 1.77 – 1.65 (m, 2H), 0.88 (s, 9H), 0.05 (s, 6H); ^{13}C NMR (101 MHz, $CDCl_3$) δ 173.5, 159.2, 136.2, 130.7, 130.4, 129.3 (2), 128.7 (2), 128.3 (2), 128.28, 126.8, 113.8 (2), 74.1, 73.1, 71.5, 66.2, 55.4, 33.9, 32.7, 26.9, 26.0 (3), 24.9, 18.3, -4.4, -4.6.

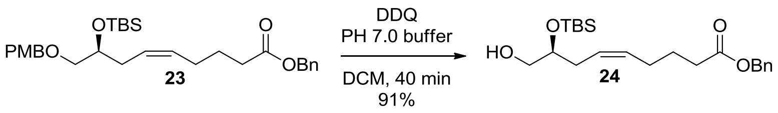

Synthesis of (*S*,*Z*)-benzyl 8-(*tert*-butyldimethylsilyloxy)-9-hydroxynon-5-enoate

2,3-Dichloro-5,6-dicyano-1,4-benzoquinone (DDQ, 1.79 g, 7.90 mmol, 1.5 equiv) was added in 3 portions to a mixture of (*S*,*Z*)-benzyl 8-(*tert*-butyldimethylsilyloxy)-9-(4-methoxybenzyloxy)non-5-enoate (2.7 g, 5.27 mmol) and pH 7.0 buffer (30.4 mL) in DCM (90 mL). After 2 h 30 min, sodium bisulfite (1.64 g, 15.8 mmol, 3 equiv) was added and the reaction was continued for 30 min, then filtered through a pad of Celite™. The filtrate was poured into H_2O (30 mL), the organic layer was separated, and the aqueous layer was extracted with DCM (2 × 20 mL). The combined organic extracts were dried over anhydrous Na_2SO_4, filtered through a Buchner fritted funnel, and concentrated under reduced pressure. The crude material was purified using a Teledyne Isco Combiflash® R_f chromatographic system (40 g SiO_2 column eluted with hexanes, 2min; 0-5% EtOAc/hexanes, 3 min; 5% EtOAc/hexanes, 20 min, 10%, 10 min; 10-20%, 5 min) to give the title product (1.90 g, 91%) as a colorless oil. $[\alpha]_D^{20} = 0.6°$ (*c* 0.5, EtOH). ^{1}H NMR (400 MHz, $CDCl_3$) δ 7.30 – 7.20 (m, 5H), 5.41 – 5.23 (m, 2H), 5.02 (s, 2H), 3.65 (dtd, *J* = 7.1, 5.5, 3.8 Hz, 1H), 3.43 (dd, *J* = 11.0, 3.8 Hz, 1H), 3.33 (dd, *J* = 11.0, 5.3 Hz, 1H), 2.27 (t, *J* = 7.5 Hz, 2H), 2.22 – 2.06 (m, 2H), 1.99 (dt, *J* = 8.3, 6.4 Hz, 2H), 1.77 (s, 1H), 1.68 – 1.54 (m, 2H), 0.81 (s, 9H), -0.01 (s, 6H); ^{13}C NMR (101 MHz, $CDCl_3$) δ 173.5, 136.1, 131.0, 128.7 (2), 128.34 (2), 128.3, 126.1, 72.8, 66.3, 66.0, 33.8, 32.1, 26.8, 26.0 (3), 24.9, 18.2, -4.3, -4.5.

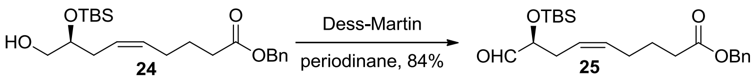

Synthesis of (*S*,*Z*)-benzyl 8-(*tert*-butyldimethylsilyloxy)-9-oxonon-5-enoate

Dess-Martin periodinane (DMP, 2.53 g, 5.96 mmol, 1.2 equiv) was added in 2 portions to a mixture of (*S*,*Z*)-benzyl 8-(*tert*-butyldimethylsilyloxy)-9-hydroxynon-5-enoate and $NaHCO_3$ (0.501 g, 5.96 mmol, 1.2 equiv) in anhydrous DCM (50 mL). After 3 h, the reaction was washed with half-saturated aq. $Na_2S_2O_3$ (2 × 20 mL) and sat. aq. $NaHCO_3$ (2 × 10 mL). The aqueous washings were re-extracted with DCM (3 × 20 mL). The combined organic extracts were dried over anhydrous Na_2SO_4, decanted, and concentrated by rotary evaporation. The crude product was purified using a Teledyne Isco Combiflash® *R*f chromatographic system (40 g SiO_2 column eluted with hexanes, 2 min; 0-5% EtOAc/hexanes, 6 min; 5% EtOAc/hexanes, 15 min) to give the title compound (1.65 g, 84%) as a colorless oil. $[\alpha]_D^{20}$ = 0.8° (*c* 1.0, EtOH).

^{1}H NMR (400 MHz, $CDCl_3$) δ 9.58 (d, *J* = 1.6 Hz, 1H), 7.41 – 7.28 (m, 5H), 5.57 – 5.36 (m, 2H), 5.11 (s, 2H), 3.98 (td, *J* = 6.2, 1.6 Hz, 1H), 2.47 – 2.27 (m, 4H), 2.16 – 2.00 (m, 2H), 1.80 – 1.65 (m, 2H), 0.91 (s, 9H), 0.07 (d, *J* = 5.7 Hz, 6H); ^{13}C NMR (101 MHz, $CDCl_3$) δ 203.9, 173.4, 136.2, 131.9, 128.7 (2), 128.4 (2), 128.3, 124.6, 77.6, 66.3, 33.8, 31.0, 26.8, 25.9 (3), 24.8, 18.3, -4.6, -4.7.

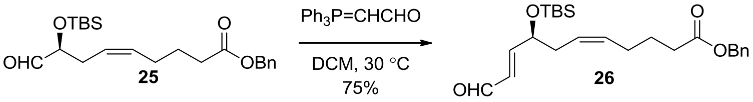

Synthesis of (*S*,5*Z*,9*E*)-benzyl 8-(*tert*-butyldimethylsilyloxy)-11-oxoundeca-5,9-dienoate

A solution of (*S*,*Z*)-benzyl 8-(*tert*-butyldimethylsilyloxy)-9-oxonon-5-enoate (1.68 g, 4.30 mmol) and (triphenylphosphoranylidene)acetaldehyde (95%; 2.52 g, 6.45 mmol, 1.5 equiv) in DCM (30 mL) was stirred at 30 °C for 36 h. The reaction was concentrated using a rotary evaporator, and the residue was purified using a Teledyne Isco Combiflash® *R*f chromatographic system (24 g SiO2 column eluted with hexanes, 2min; 0-5% EtOAc/hexanes, 3 min; 5% EtOAc/hexanes, 15 min, 5-20%, 10 min) to give the title compound contaminated with ~5% double Witting olefination product (1.36 g, ~ 75%) as a colorless oil. $[\alpha]_D^{20}$ = 36.4° (*c* 0.5, EtOH). An analytical sample was purified by TLC to give the title compound as a colorless oil. TLC: 10% EtOAc/hexanes, R_f ~ 0.4.

^{1}H NMR (400 MHz, $CDCl_3$) δ 9.55 (d, *J* = 8.0 Hz, 1H), 7.42 – 7.27 (m, 5H), 6.77 (dd, *J* = 15.5, 4.3 Hz, 1H), 6.27 (ddd, *J* = 15.5, 8.0, 1.6 Hz, 1H), 5.55 – 5.36 (m, 2H), 5.11 (s, 2H), 4.41 (dt, *J* = 6.2, 1.9 Hz, 1H), 2.46 – 2.20 (m, 4H), 2.06 (td, *J* = 7.2, 5.9 Hz, 2H), 1.82 – 1.60 (m, 2H), 0.90 (s, 9H), 0.05 (d, *J* = 11.9 Hz, 6H); ^{13}C NMR (101 MHz, $CDCl_3$) δ 193.7, 173.4, 159.6, 136.1, 131.7, 130.9, 128.7 (2), 128.3 (3), 125.0, 71.6, 66.3, 35.3, 33.7, 26.9, 25.9 (3), 24.7, 18.3, -4.6, -4.7.

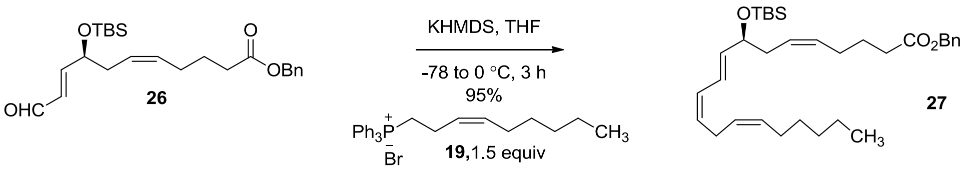

Synthesis of (*S*,5*Z*,9*E*,11*Z*,14*Z*)-benzyl 8-(*tert*-butyldimethylsilyloxy)icosa-5,9,11,14-tetraenoate

Potassium bis(trimethylsilyl)amide (0.5 M solution in toluene, 2.42 mL, 1.21 mmol, 1.4 equiv) was added dropwise to a suspension of anhydrous (azeotropically dried by co-evaporation with toluene, 3× 15 mL) (*Z*)-oct-2-en-1-yltriphenylphosphonium bromide (0.724 g, 1.30 mmol, 1.5 equiv) in anhydrous THF (50 mL) at -78 °C. The cold bath was removed and the reaction (orange solution) was allowed to slowly warm to 0 °C over 1h, and then stirred at rt for 15 min. The reaction was cooled to -78 °C and (*S*,5*Z*,9*E*)-benzyl 8-(*tert*-butyldimethylsilyloxy-11-oxoundeca)-5,9-dienoate (0.360 g, 0.864 mmol) in anhydrous THF (15 mL) was added slowly to the reaction via cannula; the addition was completed with a fresh portion of THF (5 mL). The reaction was allowed to slowly warm to 0 °C over 1 h and continued at 0 °C for 30 min. The reaction was quenched with 1M aq. NH_4OAc (10 mL) and concentrated under reduced pressure.

The residue was diluted with H_2O (30 mL) and extracted with EtOAc (2 × 20 mL). The combined organic extracts were dried over anhydrous Na_2SO_4, decanted, and concentrated in vacuo. The crude product was purified using a Teledyne Isco Combiflash® R_f chromatographic system (24 g SiO_2 column eluted with hexanes, 2 min; 0-5% EtOAc/hexanes, 10 min; 5% EtOAc/hexanes, 2 min) to give the title compound (0.430 g, ~ 95%) as a colorless oil contaminated with <10% of the *E* isomer. $[\alpha]_D^{20} = 19.5°$ (*c* 0.2, EtOH).

^1H NMR (400 MHz, C_6D_6) δ 7.22 (d, *J* = 7.2 Hz, 2H), 7.14 – 7.02 (m, 3H), 6.75 (dd, *J* = 15.2, 11.1 Hz, 1H), 6.09 (t, *J* = 10.9 Hz, 1H), 5.71 (dd, *J* = 15.1, 5.8 Hz, 1H), 5.61 – 5.31 (m, 5H), 5.01 (s, 2H), 4.22 (q, *J* = 6.0 Hz, 1H), 3.02 (t, *J* = 6.6 Hz, 2H), 2.31 (dq, *J* = 22.0, 7.3 Hz, 2H), 2.13 (t, *J* = 7.4 Hz, 2H), 2.05 (q, *J* = 6.7 Hz, 2H), 1.96 (q, *J* = 7.7 Hz, 2H), 1.61 (p, *J* = 7.5 Hz, 2H), 1.44 – 1.17 (m, 6H), 1.03 (s, 9H), 0.89 (t, *J* = 6.7 Hz, 3H), 0.40 (s, 1H), 0.12 (d, *J* = 1.6 Hz, 5H); ^{13}C NMR (101 MHz, C_6D_6) δ 172.7, 137.2, 131.0, 130.8, 130.1, 128.7(2), 128.6 (2), 128.5, 127.7, 126.9, 124.9, 73.3, 66.1, 36.8, 33.7, 31.9, 30.2, 29.7, 27.6, 27.1, 26.6, 26.2 (3), 25.1, 23.0, 18.5, 14.3, -4.1, -4.5.

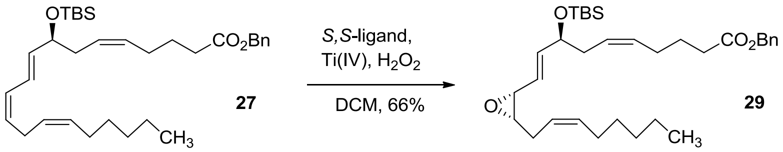

Synthesis of (*S*,5*Z*,9*E*)-benzyl 8-(*tert*-butyldimethylsilyloxy)-10-{(2*R*,3*S*)-3-[(*Z*)-oct-2-en-1-yl]oxiran-2-yl}deca-5,9-dienoate

A solution of *S,S*-ligand[20] (45.4 mg, 0.084 mmol, 6 mol%) and Ti(*Oi*-Pr)$_4$ (21 µL, 0.07 mmol, 5 mol%) in anhydrous DCM (0.735 mL) was stirred at rt for 1 h. Compound **27** (0.735 g, 1.40 mmol) was added neat to the yellow solution followed by DCM (3.46 mL), and then the solution was cooled to 4 °C. Aqueous H_2O_2 (30%, 0.286 mL, 1.8 equiv) was added dropwise to the reaction, and the mixture was stirred vigorously at 4 °C overnight (20 h). The reaction was continued at rt for 3 h, diluted with DCM (10 mL) and washed with 10% aq. $Na_2S_2O_3$ (2 × 10 mL). The aqueous layer was extracted with DCM (2 × 15 mL), and the combined organic extracts were dried over anhydrous Na_2SO_4, decanted, and concentrated in vacuo. The crude product was partially purified using a Teledyne Isco Combiflash® R_f chromatographic system (12 g SiO_2 column, 18 mL/min flow rate, eluted with hexanes containing 1% *tert*-butylamine, 4 min; 0-5% EtOAc/hexanes, 8 min; 5% EtOAc/hexanes, 5 min) to give the title compound (0.500 g, ~ 66%, >95:5 dr) as a pale yellow oil. A sample was further purified by TLC using 10% EtOAc/hexanes containing 2% *tert*-butylamine as eluent. $[\alpha]_D^{20} = 15.2°$ (*c* 0.2, EtOH).

^1H NMR (400 MHz, C_6D_6) δ 7.26 – 7.19 (m, 2H), 7.15 – 7.03 (m, 3H), 5.90 (dd, *J* = 15.6, 5.6 Hz, 1H), 5.71 (ddd, *J* = 15.4, 7.2, 1.3 Hz, 1H), 5.60 – 5.43 (m, 3H), 5.43 – 5.30 (m, 1H), 5.01 (s, 2H), 4.13 (q, *J* = 6.1 Hz, 1H), 3.27 (dd, *J* = 7.2, 4.1 Hz, 1H), 2.93 (td, *J* = 6.3, 4.1 Hz, 1H), 2.55 – 2.41 (m, 1H), 2.33 – 2.17 (m, 3H), 2.13 (t, *J* = 7.4 Hz, 2H), 2.07 – 1.87 (m, 4H), 1.61 (p, *J* = 7.4 Hz, 2H), 1.37 – 1.16 (m, 6H), 0.99 (s, 9H), 0.89 (t, *J* = 6.8 Hz, 3H), 0.08 (s, 6H); ^{13}C NMR (101 MHz, C_6D_6) δ 172.7, 139.4, 136.9, 132.9, 131.0, 128.7 (2), 128.6 (2), 126.6, 124.6, 124.5, 72.8, 66.1, 58.1, 56.2, 36.5, 33.7, 31.8, 29.7, 27.8, 27.1, 26.9, 26.1 (3), 25.1, 23.0, 18.4, 14.3, -4.3, -4.6.

3.7 References

1. Newman, D. J.; Cragg, G. M. Natural products as sources of new drugs over the last 25 years. *J. Nat. Prod.* **2007**, *70*, 461-477.

2. Yadav, V. G. Biosynthonics: Charting the future role of biocatalysis and metabolic engineering in drug discovery. *Ind. Eng. Chem. Res.* **2014**, *53*, 18597-18610.

3. La Clair, J. J.; Loveridge, S. T.; Tenney, K.; O′Neil–Johnson, M.; Chapman, E.; Crews, P. *In situ* natural product discovery via an artificial marine sponge. PLoS One **2014**, *9*, e100474. doi:10.1371/journal.pone.0100474.

4. Nagle, A.; Hur, W.; Gray, N. S. Antimitotic agents of natural origin. *Curr Drug Targets* **2006**, *7*, 305-326.

5. Williams, D. E.; Sturgeon, C. M.; Roberge, M.; Andersen, R. J. Nigricanosides A and B, antimitotic glycolipids isolated from the green alga *Avrainvillea nigricans* collected in Dominica. *J. Am. Chem. Soc.* **2007**, *129*, 5822-5823.

6. Roberge, M.; Cinel, B.; Anderson, H. J.; Lim, L.; Jiang, X.; Xu, L.; Kelly, M. T.; Andersen, R. J. *Cancer Res.* **2000**, *60*, 5052-5058.

7. D′Ippolito, G.; Romano, G.; Caruso, T.; Spinella, A.; Cimino, G.; Fontana, A. Production of octadienal in the marine diatom *Skeletonema costatum*. *Org. Lett.* **2003**, *5*, 885-887.

8. Andrianasolo, E. H.; Haramaty, L.; Vardi, A.; White, E.; Lutz, R.; Falkowski, P. Apoptosis-inducing galactolipids from a cultured marine diatom, *Phaeodactylum tricornutum*. *J. Nat. Prod.* **2008**, *71*, 1197-1201.

9. Cardellina, II J. H.; Moore, R. E. Malyngic acid, a new fatty acid from Lyngbya majuscule. Tetrahedron **1980**, *36*, 993-996.

10. (a) Herz, W.; Kulanthaivel, P. Trihydroxy-C18-acids and a labdane from *Rudbeckia fulgida*. *Phytochemistry* **1985**, *24*, 89-91. (b) Shin, J-S.; Hong, Y.; Lee, H-H.; Ryu, B.; Cho, Y-W.; Kim, N-J.; Jang, D. S.; Lee, K-T. Fulgidic acid isolated from the rhizomes of *Cyperus rotundus* suppresses LPS-induced iNOS, COX-2, TNF-α, and IL-6 expression by AP-1 inactivation in RAW264.7 macrophages. *Biol. Pharm. Bull.* **2015**, *38*, 1081-1086.

11. (a) Papendorf, O.; König, G. M.; Wright, A. D.; Chorus, I.; Oberemm, A. Mueggelone, a novel inhibitor of fish development from the fresh water cyanobacterium *Aphanizomenon flos-aquae*. *J. Nat. Prod.* **1997**, *60*, 1298-1300. (b) Ishigami, K.; Motoyoshi, H.; Kitahara, T. First total synthesis of mueggelone. Tetrahedron Letters **2000**, *41*, 8897-8901.

12. Corey, E. J.; Su, W.-g. Tetrahedron Letters **1984**, *25*, 5119-5122.

13. (a) Luo, X.; Li, F.; Hong, J.; Lee, C.-O.; Sim, C. J.; Im, K. S.; Jung, J. H. *J. Nat. Prod.* **2006**, *69*, 567-571. (b) Towada, R.; Kuwahara, S. Synthesis of topsentolides A_2 and C_2, and non-enzymatic conversion of the former to the latter. Tetrahedron **2014**, *70*, 3774-3781. (c) Towada, R.; Kurashina, Y.; Kuwahara, S. Stereochemical assignment of topsentolide C_2 by stereodivergent synthesis of its four diastereomers. Tetrahedron Letters **2013**, *54*, 6878-6881.

14. Kinashi, N.; Fujiwara, K.; Tsunoda, T.; Katoono, R.; Kawai, H.; Suzuki, T. A stereoselective method for the construction of the C8′-O-C6" ether of nigricanoside-A: synthesis of simple models for the C20 lipid chain/galactosyl glycerol segment. Tetrahedron Letters **2013**, *54*, 4564-4567.

15. Espindola, A-P. D. M.; Crouch, R.; DeBergh, J. R.; Ready, J. M.; MacMillan, J. B. Deconvolution of complex NMR spectra in small molecules by multi frequency homonuclear decoupling (MDEC). *J. Am. Chem. Soc.* **2009**, *131*, 15994-15995.

16. Chen, J.; Koswatta, P.; DeBergh, J. R.; Fu, P.; Pan, E.; MacMillan, J. B.; Ready, J. M. Structure elucidation of nigricanoside A through enantioselective total synthesis. *Chem. Sci.* **2015**, *6*, 2932-2937.

17. Kurashina, Y.; Kuwahara, S. *Biosci. Biotechnol. Biochem.* **2012**, *76*, 605-607.

18. Katsuki, T.; Sharpless, K. B. The first practical method for assymetric epoxidation. *J. Am. Chem. Soc.* **1980**, *102*, 5974-5976.

19. (a) He, J.; Ling, J.; Chiu, P. *Chem. Rev.* **2014**, *114*, 8037-8128. (b) Childers, M. I.; Longo, J. M.; Van Zee, N. J.; LaPointe, A. M.; Coates, G. W. *Chem. Rev.* **2014**, *114*, 8129-8152.

20. Jat, J. L.; De, S. R.; Kumar, G.; Adebesin, A. M.; Gandham, S. K.; Falck, J. R. Regio- and enantioselective catalytic monoepoxidation of conjugated dienes: Synthesis of chiral allylic *cis*-epoxides. *Org. Lett.* **2015**, *17*, 1058-1061.

21. (a) Zhu, Y.; Wang, Q.; Cornwall, R. G.; Shi, Y. *Chem. Rev.* **2014**, *114*, 8199-8256. (b) Burke, C. P.; Shi, Y. *Angew. Chem. Int. Ed.* **2006**, *45*, 4475-4478. (c) Frohn, M.; Dalkiewicz, M.; Tu, Y.; Wang, Z-X.; Shi, Y. Highly region- and enantioselective monoepoxidation of conjugated dienes. *J. Org. Chem.* **1998**, *63*, 2948-2953.

22. (a) Yu, X-Q.; Hirai, A.; Miyashita, M. Palladium-catalyzed stereospecific epoxide-opening reaction of γ,δ-epoxy-α,β-unsaturated esters with boric acid leading to γ,δ-diol derivatives with double inversion of configuration. *Chem. Lett.* **2004**, *33*, 764-765. (b) Gangarajula, S.; Kovela, S.; Jakka, R. Total synthesis and absolute configuration of curvularides A-E. *J. Org. Chem.* **2012**, *77*, 10010-10020. (c) Tamao, K.; Kawachi, A.; Tanaka, Y.; Ohtani, H.; Ito, Y. Synthetic applications of functionalized silyl anions: aminosilyl anions as hydroxyl anion equivalent. Tetrahedron **1996**, *52*, 5765-5772. (d)

Quinkert, G.; Becker, H.; Dürner, G. Substantial refinement of the photochemical synthesis of (+)-Aspicilin. Tetrahedron Letters **1991**, *32*, 7397-7400.

23. (a) Shemet, A.; Sarlah, D.; Carreira, E. M. Stereochemical studies of the opening of chloro vinyl epoxides: Cyclic chloronium ions as intermediates. *Org. Lett.* **2015**, *17*, 1878-1881. (b) Ha, J. D.; Kim, S. Y.; Lee, S. J.; Kang, S. K.; Ahn, J. H.; Kim, S. S.; Choi, J-K. Regio- and stereoselective ring opening of vinyl epoxides with MgBr2. Tetrahedron Letters **2004**, *45*, 5969-5972. (c) Umezawa, T.; Shibata, M.; Kaneko, K.; Okino, T.; Matsuda, F. Asymmetric total synthesis of danicalipin A and evaluation of biological activity. *Org. Lett.* **2011**, *13*, 904-907.

24. (a) Miyashita, M.; Mizutani, T.; Tadano, G.; Iwata, Y.; Miyazawa, M.; Tanino, K. Pd-catalyzed stereospecific azide substitution of α,β-unsaturated γ,δ-epoxy esters with double bond inversion of configuration. *Angew. Chem. Int. Ed.* **2005**, *44*, 5094-5097. (b) Ehara, T.; Fujii, M.; Ono, M.; Akita, H. Total synthesis of (+) methyl β-D-vicenisaminide. Tetrahedron: Asymmetry **2010**, *21*, 494-499.

25. (a) Lindström, U. M.; Somfai, P. Aza-[3,3]-Claisen enolate rearrangement in vinylaziridines: Stereoselective synthesis of mon-, di-, and trisubstituted seven-membered lactams. *Chem. Eur. J.* **2001**, *7*, 94-98.

26. (a) Prestat, G.; Baylon, C.; Heck, M-P.; Mioskowski, C. Lewis acid-catalyzed regiospecific opening of vinyl epoxides by alcohols. Tetrahedron Letters **2000**, *41*, 3829-3831. (b) Yu, X-Q.; Yoshimura, F.; Ito, F.; Sasaki, M.; Hirai, A.; Tanino, K.; Miyashita, M. Palladium-catalyzed stereospecific substitution of α,β-unsaturated γ,δ-epoxy esters by alcohols with double inversion of configuration: Synthesis of 4-alkoxy-5-hydroxy-2-pentenoates. *Angew. Chem. Int. Ed.* **2008**, *47*, 750-754. (c) Fagnou, K.; Lautens, M. Rhodium-catalyzed ring opening of vinyl epoxides with alcohols and aromatic amines. *Org. Lett.* **2000**, *2*, 2319-2321. (d) Gholap, S. L.; Woo, C. M.; Ravikumar, P. C.; Herzon, S. B. Synthesis of the fully glycosylated cyclohexanone core of Lomaiviticin A. *Org. Lett.* **2009**, *11*, 4322-4325. (e) Trost, B. M.; Tenaglia, A. Tin mediated palladium catalyzed regiocontrolled alkylations of vinyl epoxides. Tetrahedron Letters **1988**, *29*, 2931-2934.

27. Kolb, H. C.; Sharpless, B. K. A simplified procedure for the stereospecific transformation of 1,2-diols into epoxides. Tetrahedron **1992**, *48*, 10515-10530.

28. Barrero, A. F.; Alvarez-Manzaneda, E. J.; Chahboun, R. Convenient preparation of carbonyl compounds from 1,2-diols utilizing Mitsunobu conditions. Tetrahedron Letters **2000**, *41*, 1959-1962.

29. Haack, K.-J.; Hashiguchi, S.; Fujii, A.; Ikariya, T.; Noyori, R. *Angew. Chem. Int. Ed.* **1997**, *36*, 285-288.

30. Nicolaou, K. C.; Fylaktakidou, K. C.; Monenschein, H.; Li, Y.; Weyershausen, B.; Mitchell, H. J.; Wei, H.; Guntupalli, P.; Hepworth, D.; Sugita, K. *J. Am. Chem. Soc.* **2003**, *125*, 15433-15442.

31. Pezzella, A.; Ladonisi, A.; Valerio, S.; Panzella, L.; Napolitano, A.; Adinolfi, M.; d'Ischia, M. Disentangling eumelanin "black chromophore": visible absorption changes as signature of oxidation state- and aggregation-dependent dynamic interactions in a model water-soluble 5,6,-dihydroxyindole polymer. *J. Am. Chem. Soc.* **2009**, *131*, 15270-15275.

32. Sias, B.; Ferrato, F.; Grandval, P.; Lafont, D.; Boullanger, P.; De Caro, A.; Leboeuf, B.; Verger, R.; Carrière, F. Human pancreatic lipase-related protein 2 is a galactolipase. *Biochemistry* **2004**, *43*, 10138-10148.

33. (a) Orita, A.; Hamada, Y.; Nakano, T.; Toyoshima, S.; Otera, J. Highly efficient deacetylation by use of the neutral organotin catalyst $[t\mathrm{Bu}_2\mathrm{SnOH(Cl)}]_2$. *Chem. Eur. J.* **2001**, *7*, 3321-3327. (b) Chu, C. K.; Murray, J. D. Hydrolysis products of dibutyltin dichlorides. *J. Chem. Soc. A*, **1971**, 360-367.

34. Huh, C. W.; Roush, W. R. Highly stereoselective and modular syntheses of 10-hydroxytrilobacin and three diastereomers via stereodivergent [3+2]-annulation reactions. *Org. Lett.* **2009**, *11*, 4322-4325.

3.8 Spectra

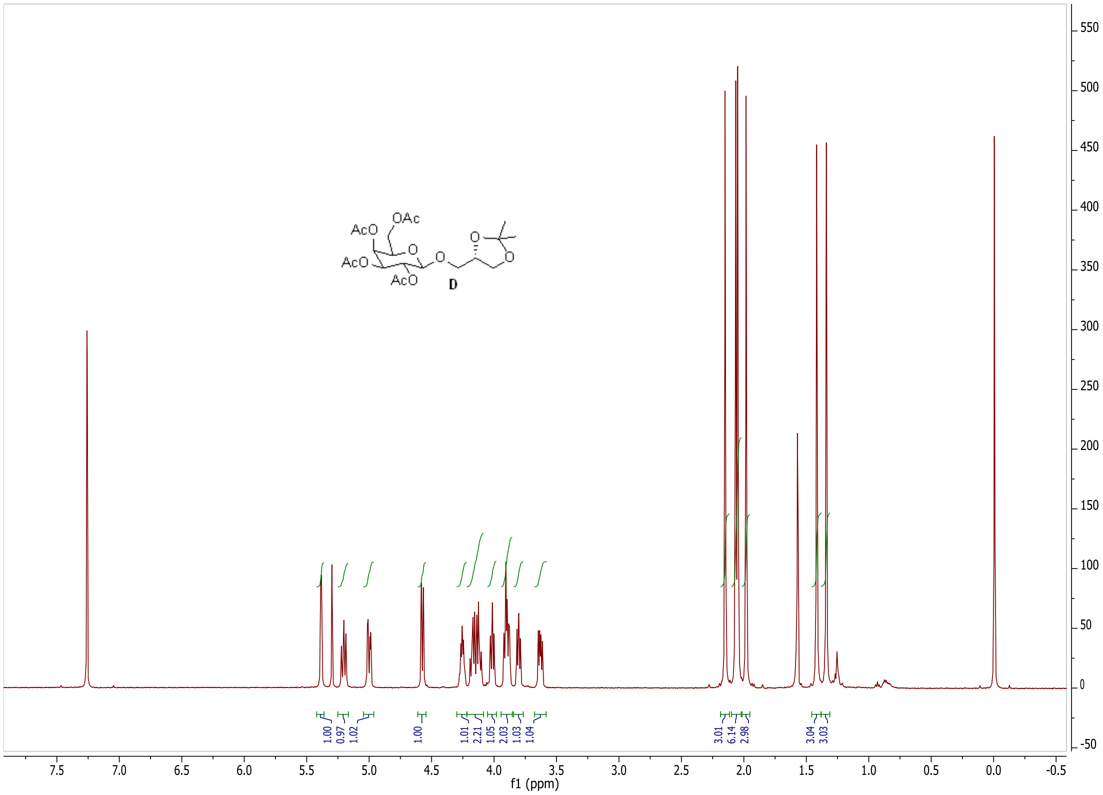
AcO
OAc
AcO
AcO
O
O
O
O
D
1.00
0.97
1.02
1.00
1.01
2.21
1.05
2.03
1.03
1.04
3.01
6.14
2.98
3.04
3.03
550
500
450
400
350
300
250
200
150
100
50
0
-50
7.5
7.0
6.5
6.0
5.5
5.0
4.5
4.0
3.5
3.0
2.5
2.0
1.5
1.0
0.5
0.0
-0.5
f1 (ppm)

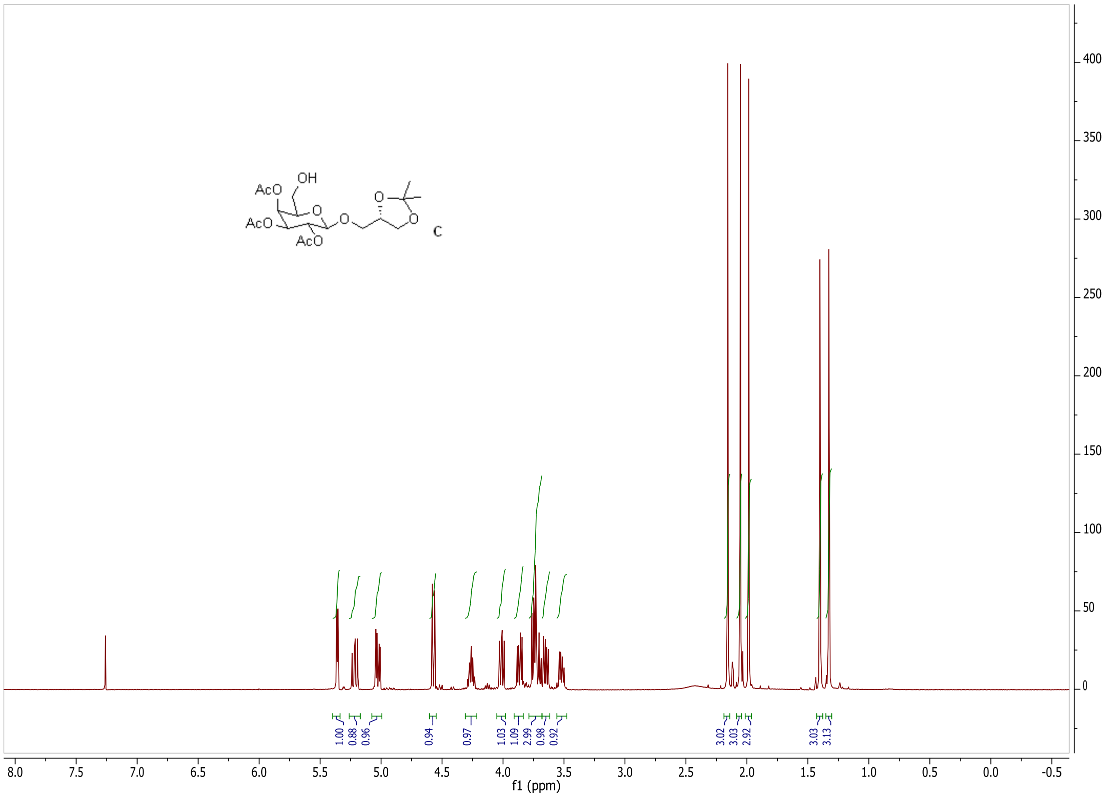
AcO
OH
AcO
O
O
O
O
AcO
C
1.00
0.88
0.96
0.94
0.97
1.03
1.09
2.99
0.98
0.92
3.02
3.03
2.92
3.03
3.13
8.0 7.5 7.0 6.5 6.0 5.5 5.0 4.5 4.0 3.5 3.0 2.5 2.0 1.5 1.0 0.5 0.0 -0.5
f1 (ppm)
400 350 300 250 200 150 100 50 0

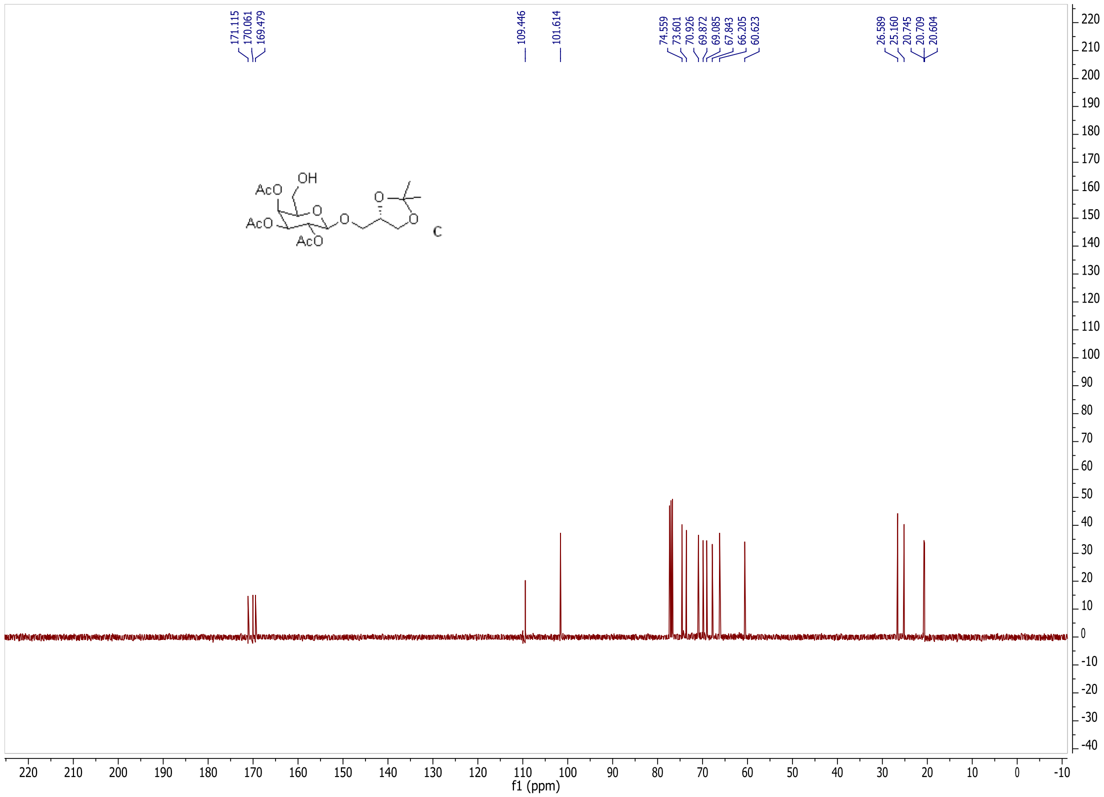
171.115
170.061
169.479
109.446
101.614
74.559
73.601
70.926
69.872
69.085
67.843
66.205
60.623
26.589
25.160
20.745
20.709
20.604
AcO
OH
AcO
O
O
O
O
AcO
C
220 210 200 190 180 170 160 150 140 130 120 110 100 90 80 70 60 50 40 30 20 10 0 -10
f1 (ppm)
220 210 200 190 180 170 160 150 140 130 120 110 100 90 80 70 60 50 40 30 20 10 0 -10 -20 -30 -40

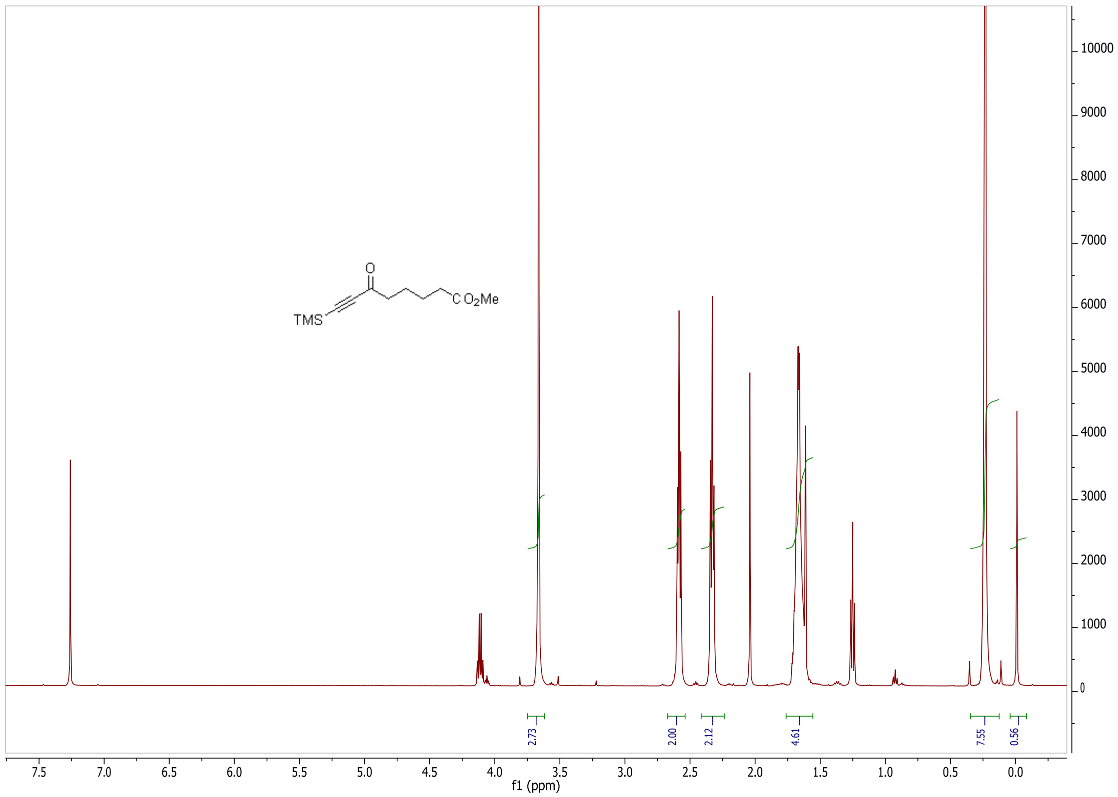
O
TMS
CO2Me
2.73
2.00
2.12
4.61
7.55
0.56
10000
9000
8000
7000
6000
5000
4000
3000
2000
1000
0
7.5
7.0
6.5
6.0
5.5
5.0
4.5
4.0
3.5
3.0
2.5
2.0
1.5
1.0
0.5
0.0
f1 (ppm)

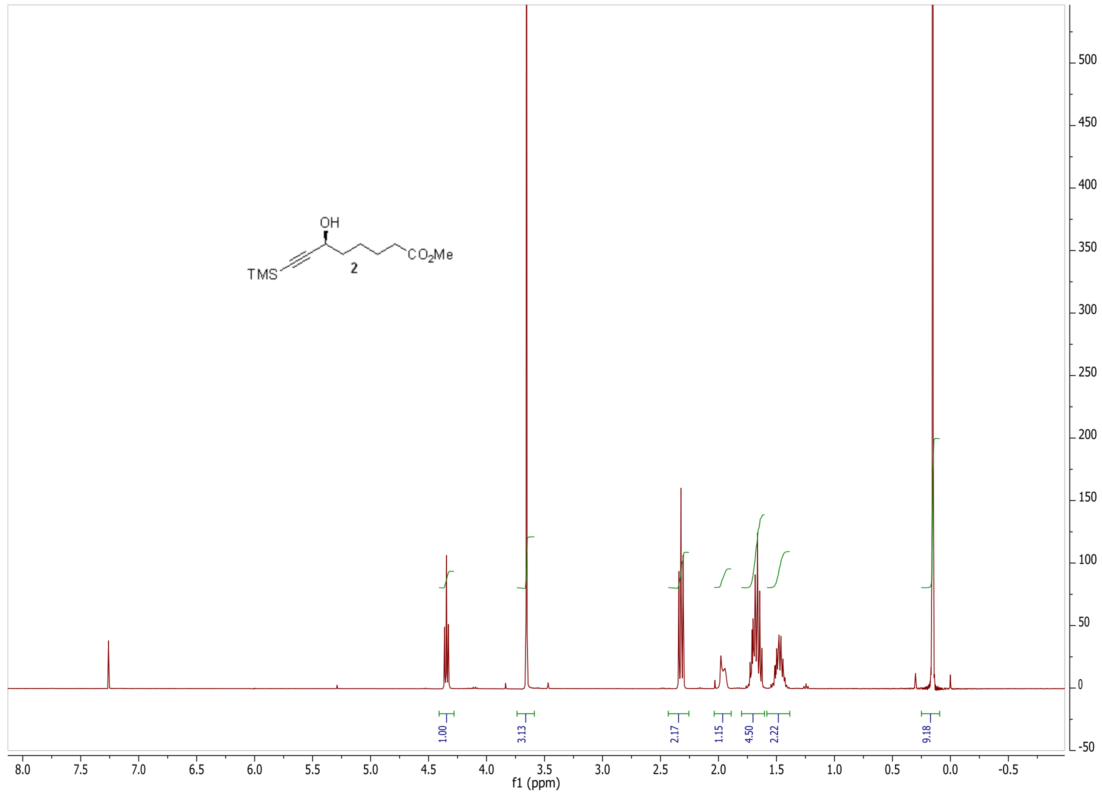
OH
TMS
2
CO2Me
1.00
3.13
2.17
1.15
4.50
2.22
9.18
500
450
400
350
300
250
200
150
100
50
0
-50
8.0
7.5
7.0
6.5
6.0
5.5
5.0
4.5
4.0
3.5
3.0
2.5
2.0
1.5
1.0
0.5
0.0
-0.5
f1 (ppm)

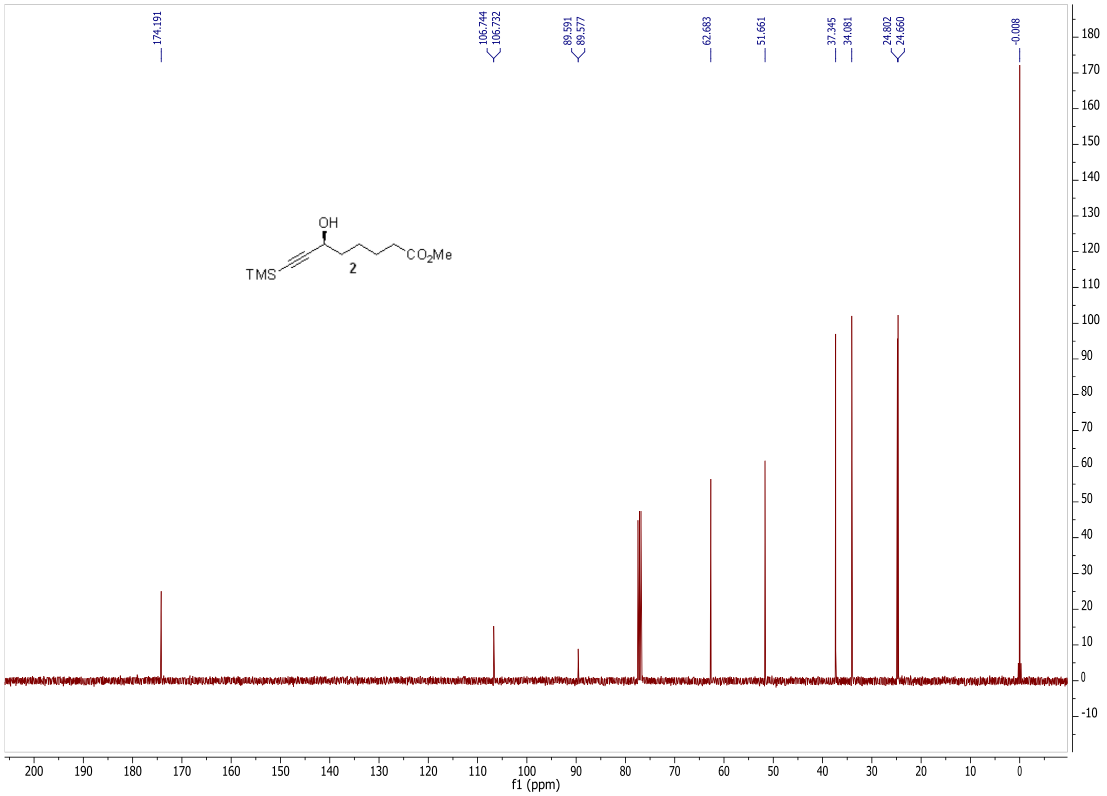
174.191
106.744
106.732
89.591
89.577
62.683
51.661
37.345
34.081
24.802
24.660
-0.008
OH
TMS
2
CO2Me
180
170
160
150
140
130
120
110
100
90
80
70
60
50
40
30
20
10
0
-10
200
190
180
170
160
150
140
130
120
110
100
90
80
70
60
50
40
30
20
10
0
f1 (ppm)

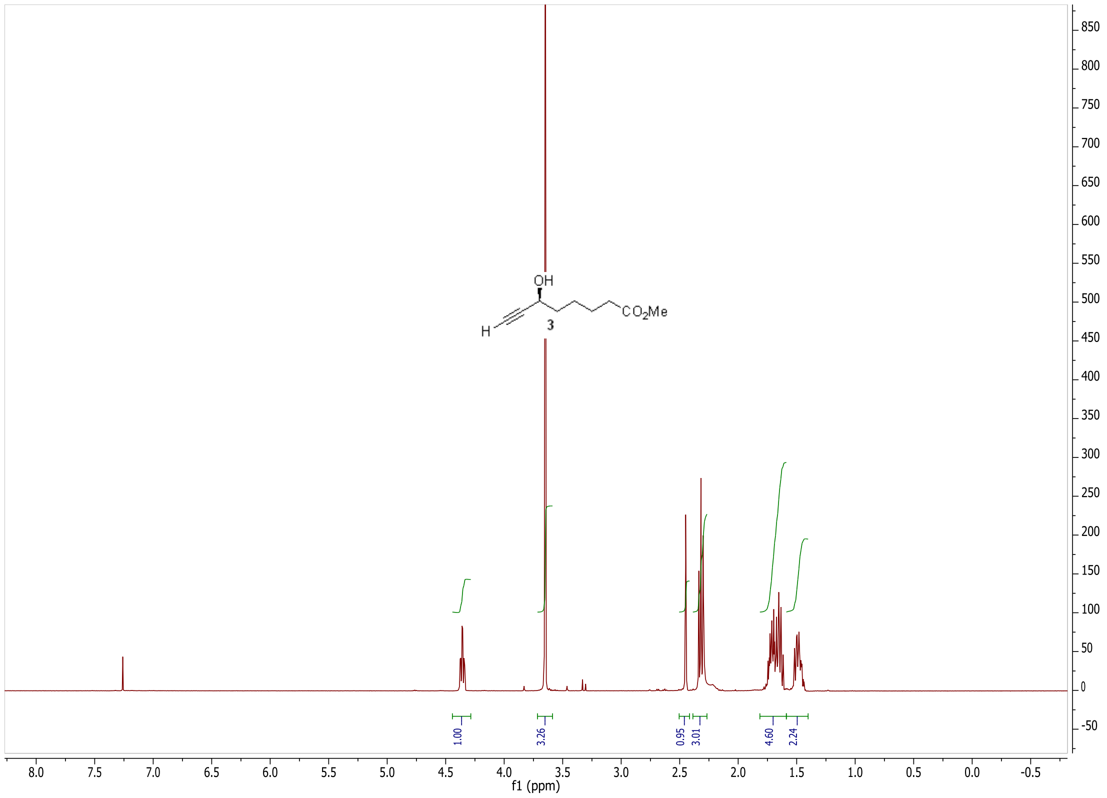
OH
H
3
CO2Me
850
800
750
700
650
600
550
500
450
400
350
300
250
200
150
100
50
0
-50
1.00
3.26
0.95
3.01
4.60
2.24
8.0
7.5
7.0
6.5
6.0
5.5
5.0
4.5
4.0
3.5
3.0
2.5
2.0
1.5
1.0
0.5
0.0
-0.5
f1 (ppm)

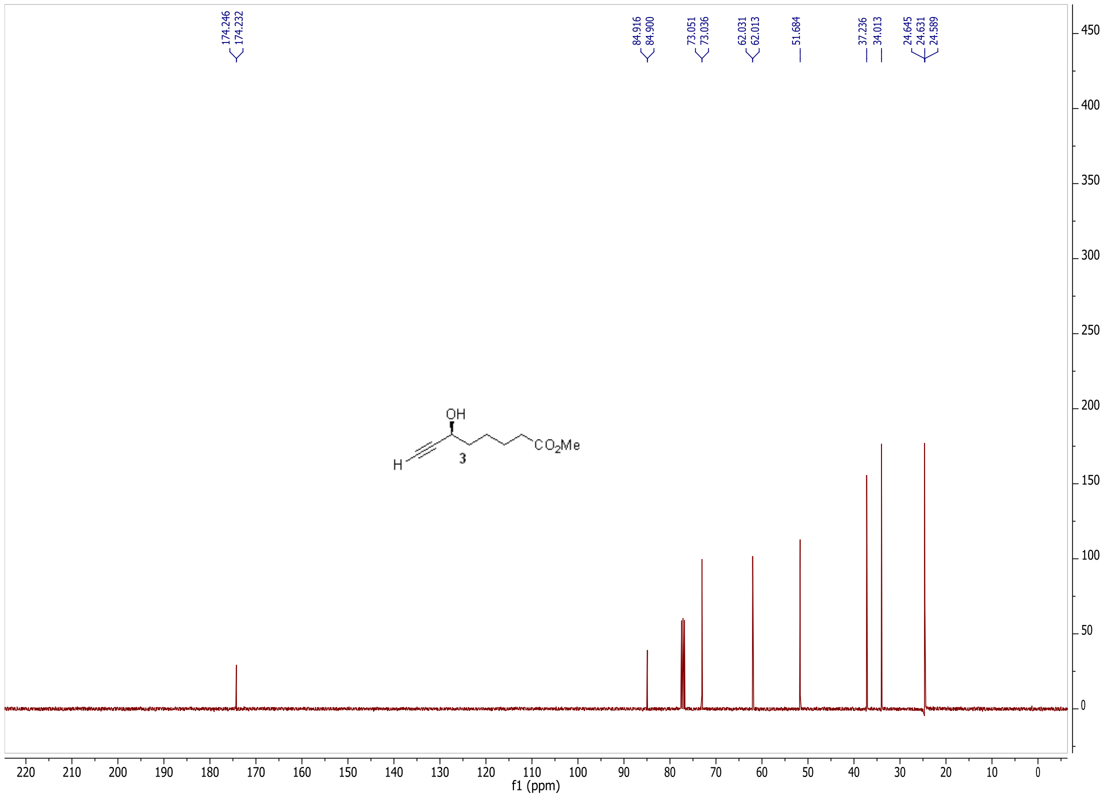
174.246
174.232
84.916
84.900
73.051
73.036
62.031
62.013
51.684
37.236
34.013
24.645
24.631
24.589
OH
H
3
CO2Me
450
400
350
300
250
200
150
100
50
0
220 210 200 190 180 170 160 150 140 130 120 110 100 90 80 70 60 50 40 30 20 10 0
f1 (ppm)

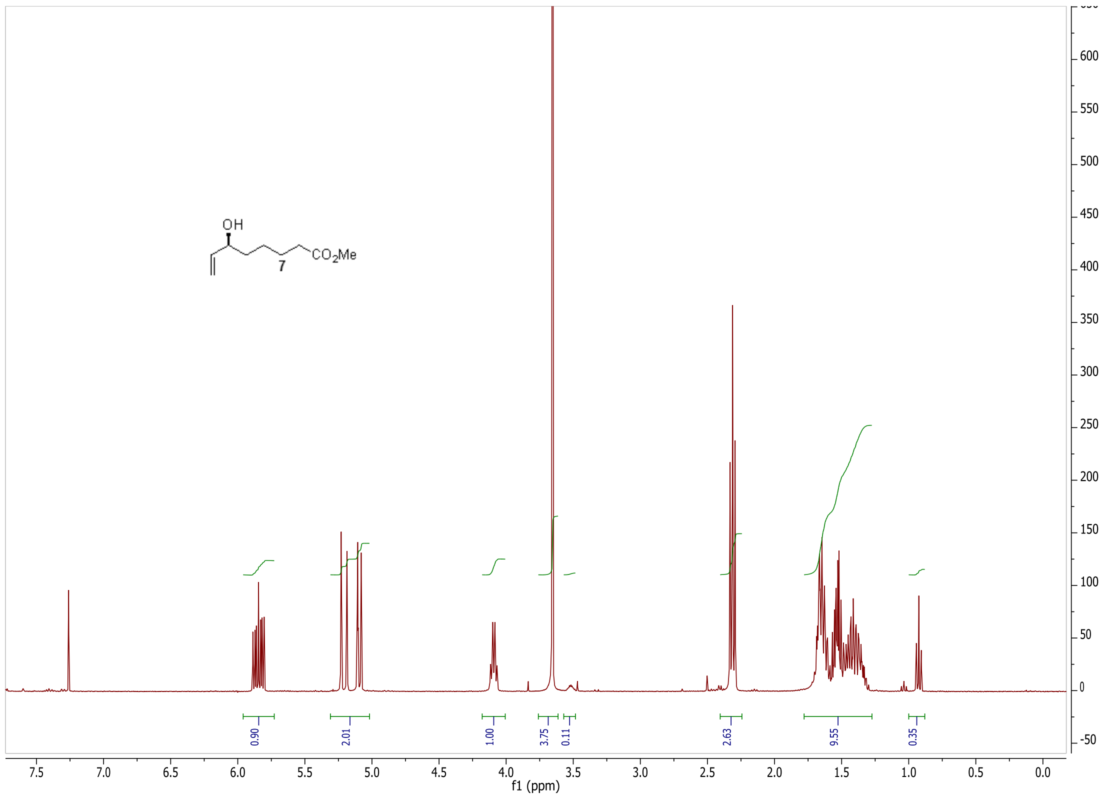
OH
7
CO2Me
600
550
500
450
400
350
300
250
200
150
100
50
0
-50
0.90
2.01
1.00
3.75
0.11
2.63
9.55
0.35
7.5 7.0 6.5 6.0 5.5 5.0 4.5 4.0 3.5 3.0 2.5 2.0 1.5 1.0 0.5 0.0
f1 (ppm)

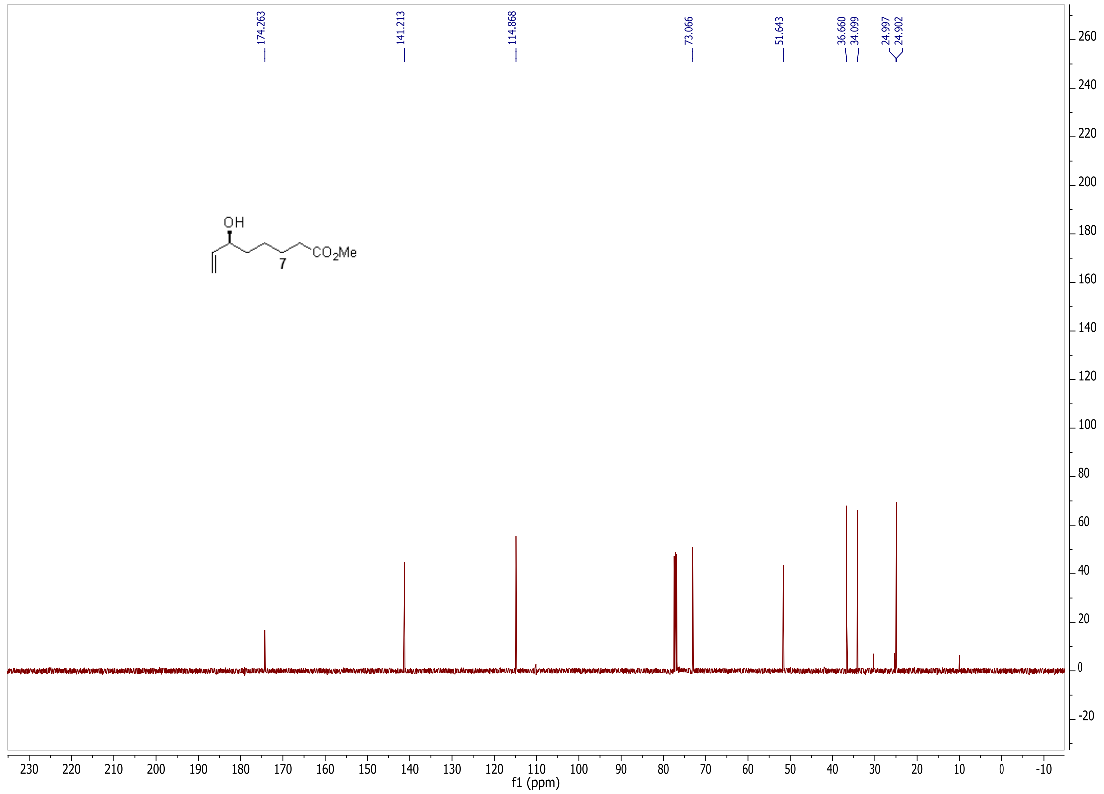
174.263
141.213
114.868
73.066
51.643
36.660
34.099
24.997
24.902
OH
CO$_2$Me
7
f1 (ppm)

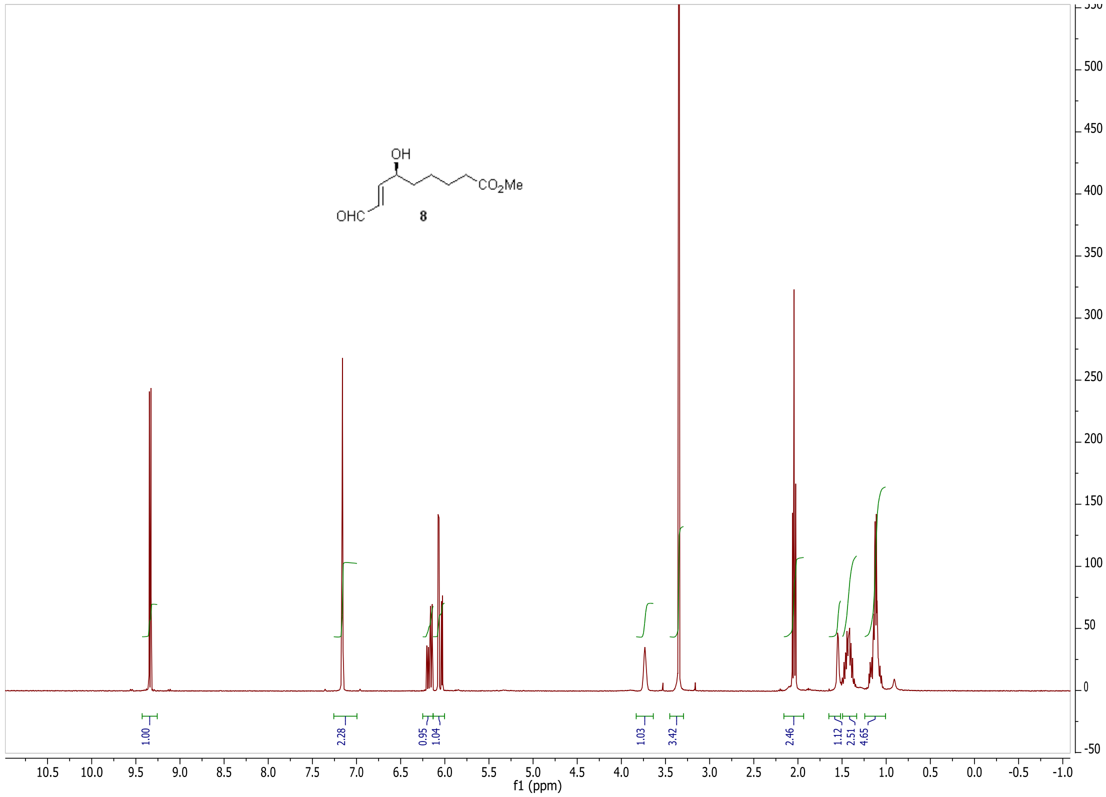
OH
CO$_2$Me
OHC
8
1.00
2.28
0.95
1.04
1.03
3.42
2.46
1.12
2.51
4.65
f1 (ppm)

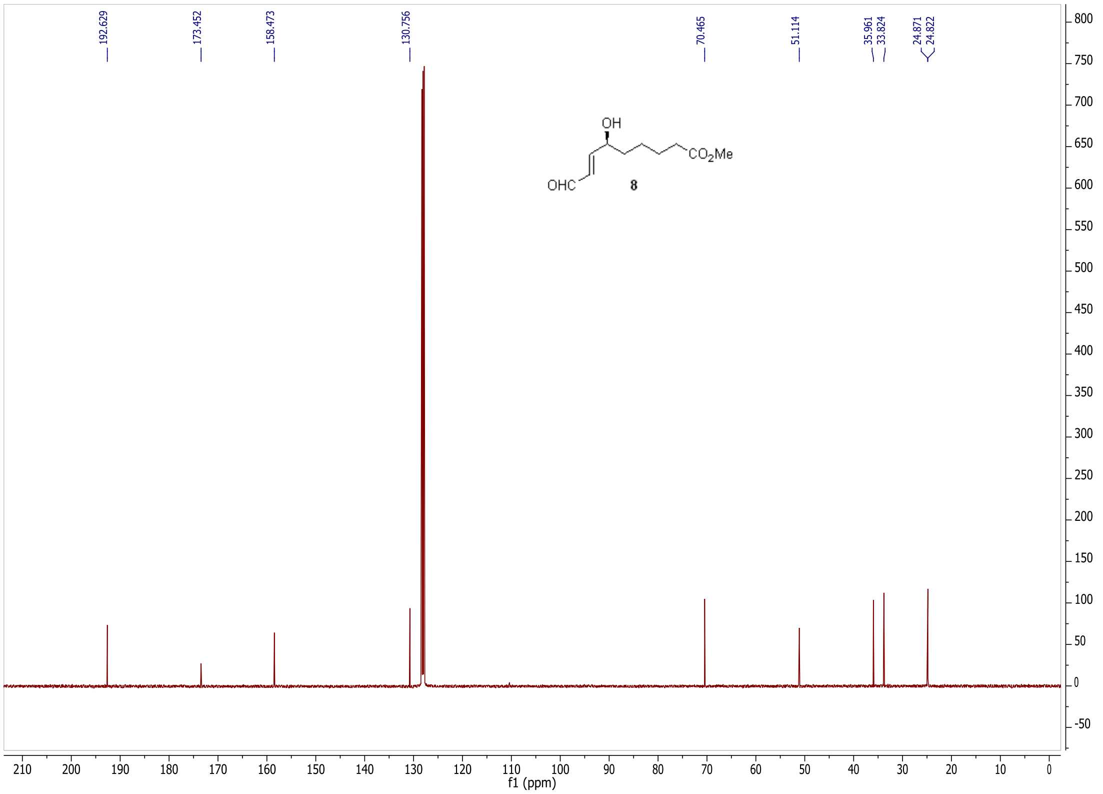
192.629
173.452
158.473
130.756
70.465
51.114
35.961
33.824
24.871
24.822
OH
CO2Me
OHC
8
800
750
700
650
600
550
500
450
400
350
300
250
200
150
100
50
0
-50
210 200 190 180 170 160 150 140 130 120 110 100 90 80 70 60 50 40 30 20 10 0
f1 (ppm)

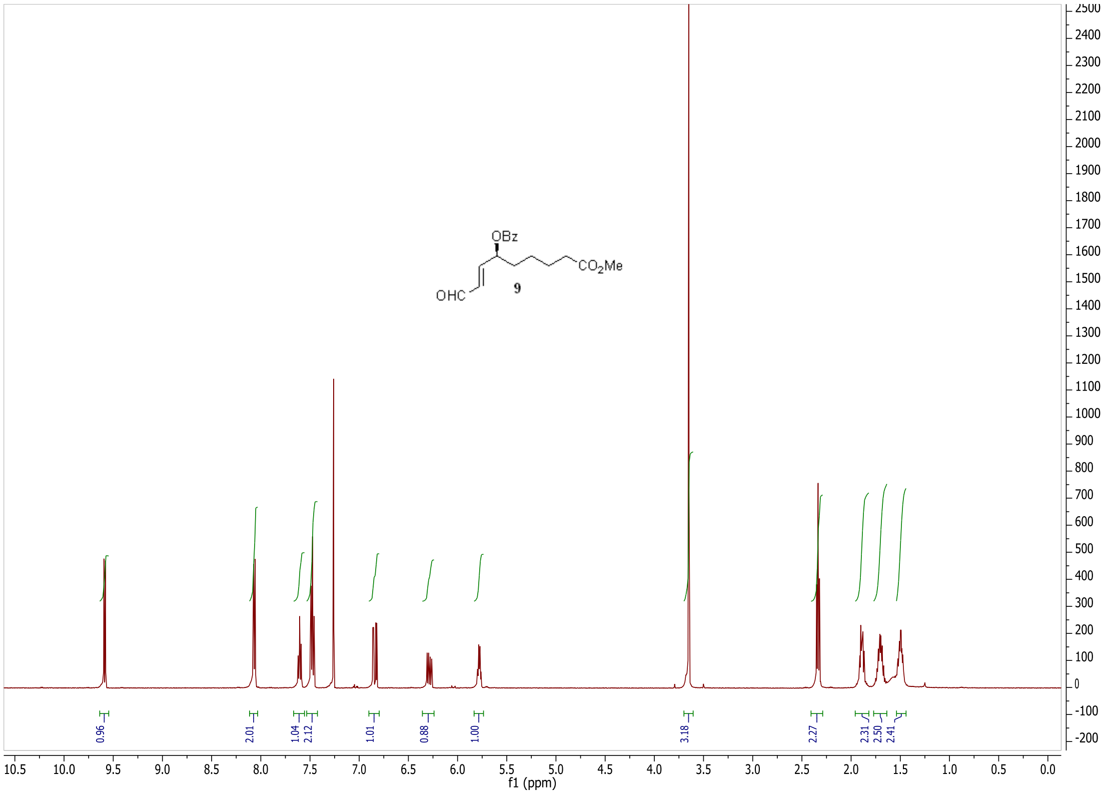
OBz
CO2Me
OHC
9
0.96
2.01
1.04
2.12
1.01
0.88
1.00
3.18
2.27
2.31
2.50
2.41
2500
2400
2300
2200
2100
2000
1900
1800
1700
1600
1500
1400
1300
1200
1100
1000
900
800
700
600
500
400
300
200
100
0
-100
-200
10.5 10.0 9.5 9.0 8.5 8.0 7.5 7.0 6.5 6.0 5.5 5.0 4.5 4.0 3.5 3.0 2.5 2.0 1.5 1.0 0.5 0.0
f1 (ppm)

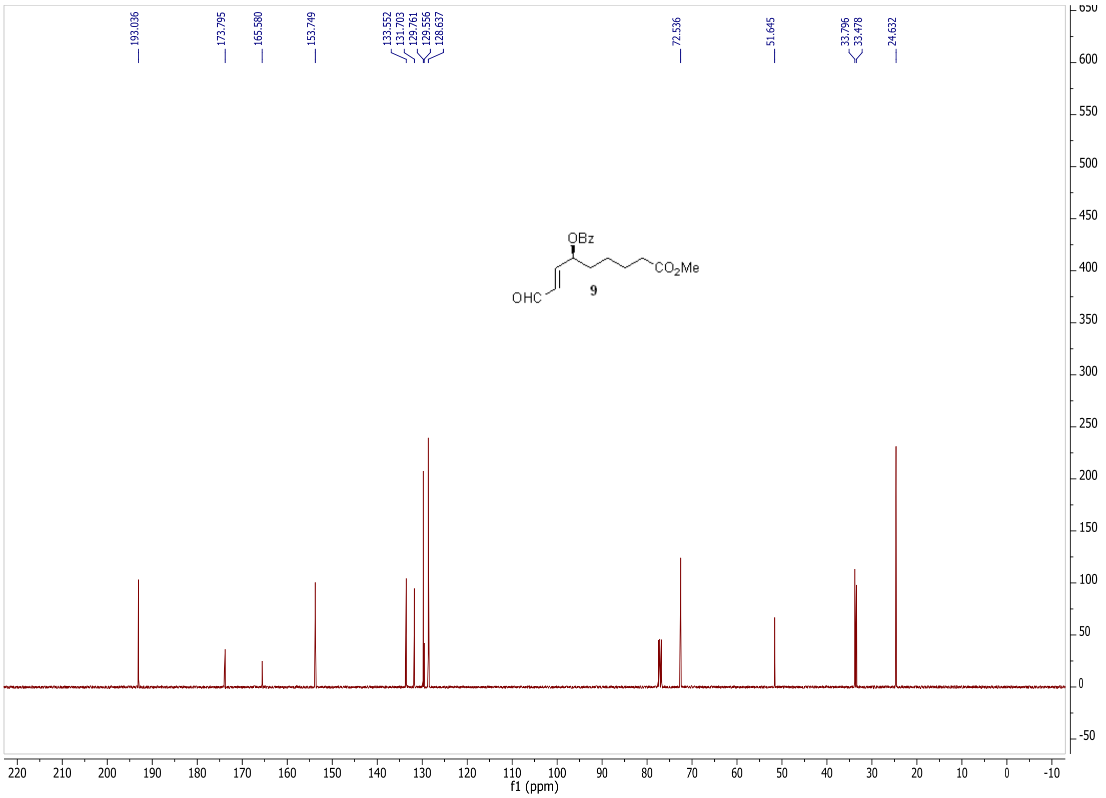
193.036
173.795
165.580
153.749
133.552
131.703
129.761
129.556
128.637
72.536
51.645
33.796
33.478
24.632
OBz
CO2Me
OHC
9
650
600
550
500
450
400
350
300
250
200
150
100
50
0
-50
220 210 200 190 180 170 160 150 140 130 120 110 100 90 80 70 60 50 40 30 20 10 0 -10
f1 (ppm)

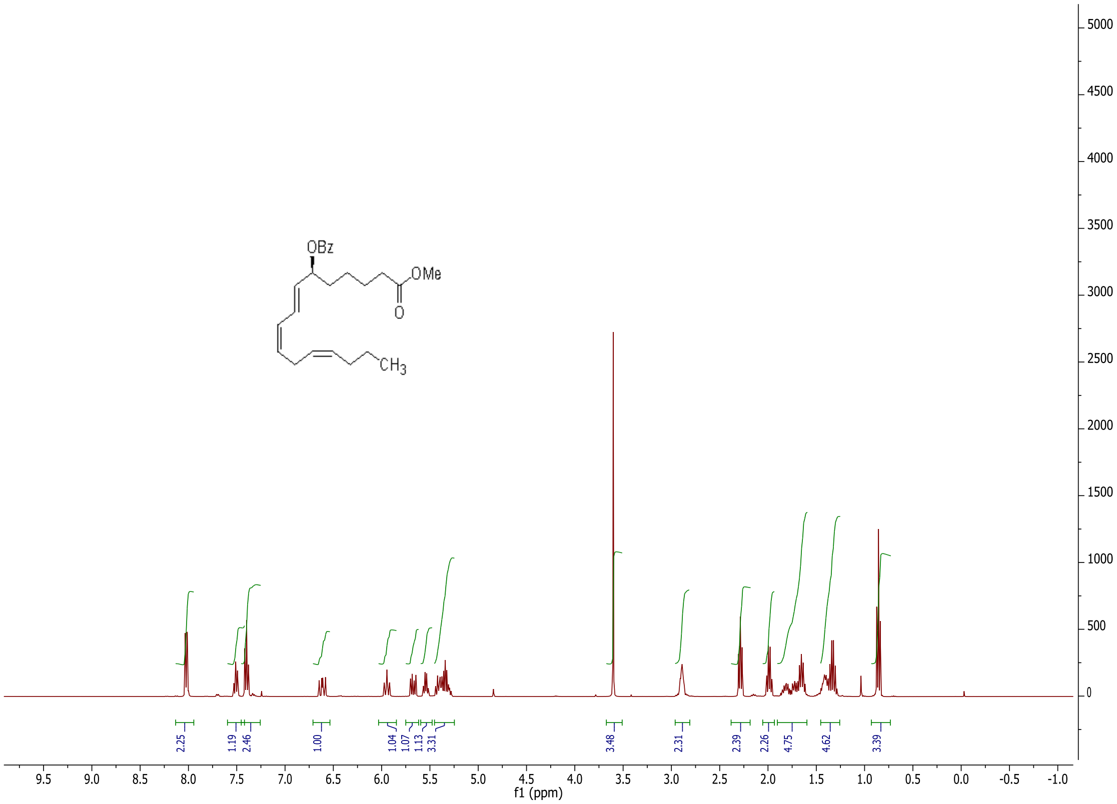
OBz
OMe
O
CH3
5000
4500
4000
3500
3000
2500
2000
1500
1000
500
0
2.25
1.19
2.46
1.00
1.04
1.07
1.13
3.31
3.48
2.31
2.39
2.26
4.75
4.62
3.39
9.5 9.0 8.5 8.0 7.5 7.0 6.5 6.0 5.5 5.0 4.5 4.0 3.5 3.0 2.5 2.0 1.5 1.0 0.5 0.0 -0.5 -1.0
f1 (ppm)

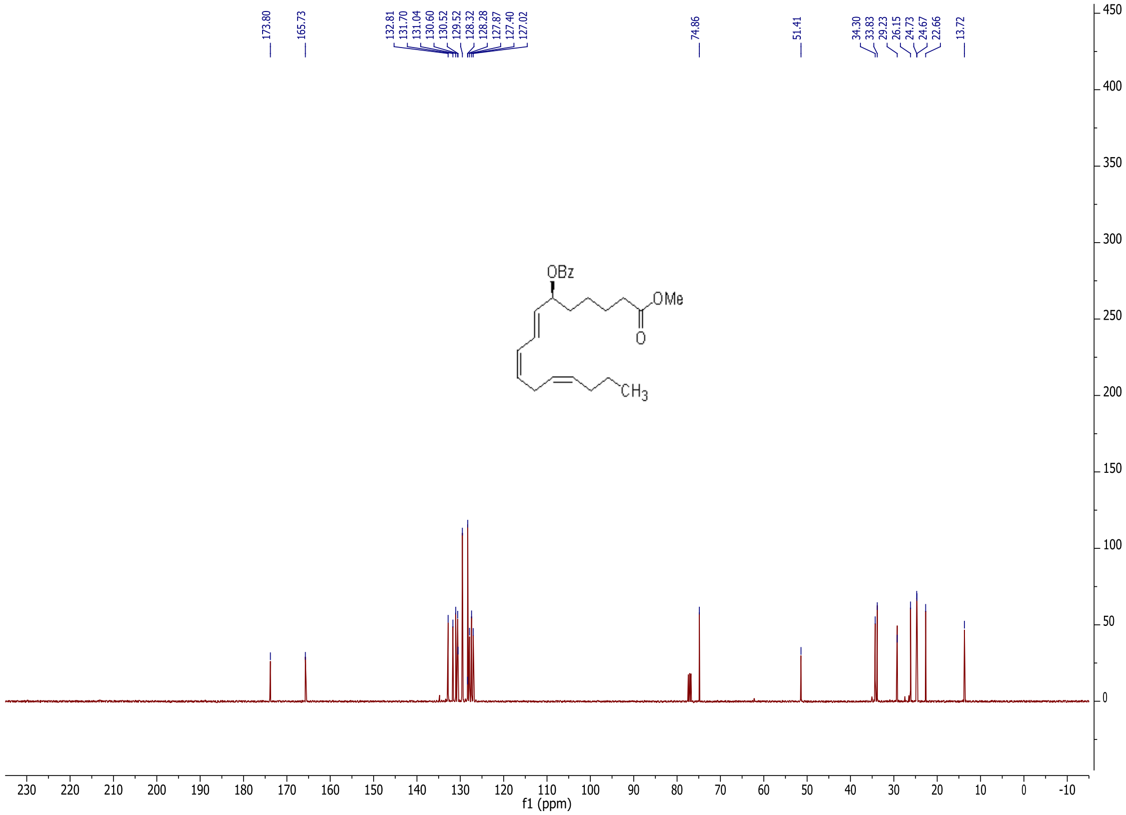
173.80
165.73
132.81
131.70
131.04
130.60
130.52
129.52
128.32
128.28
127.87
127.40
127.02
74.86
51.41
34.30
33.83
29.23
26.15
24.73
24.67
22.66
13.72
OBz
OMe
O
CH3
450
400
350
300
250
200
150
100
50
0
230
220
210
200
190
180
170
160
150
140
130
120
110
100
90
80
70
60
50
40
30
20
10
0
-10
f1 (ppm)

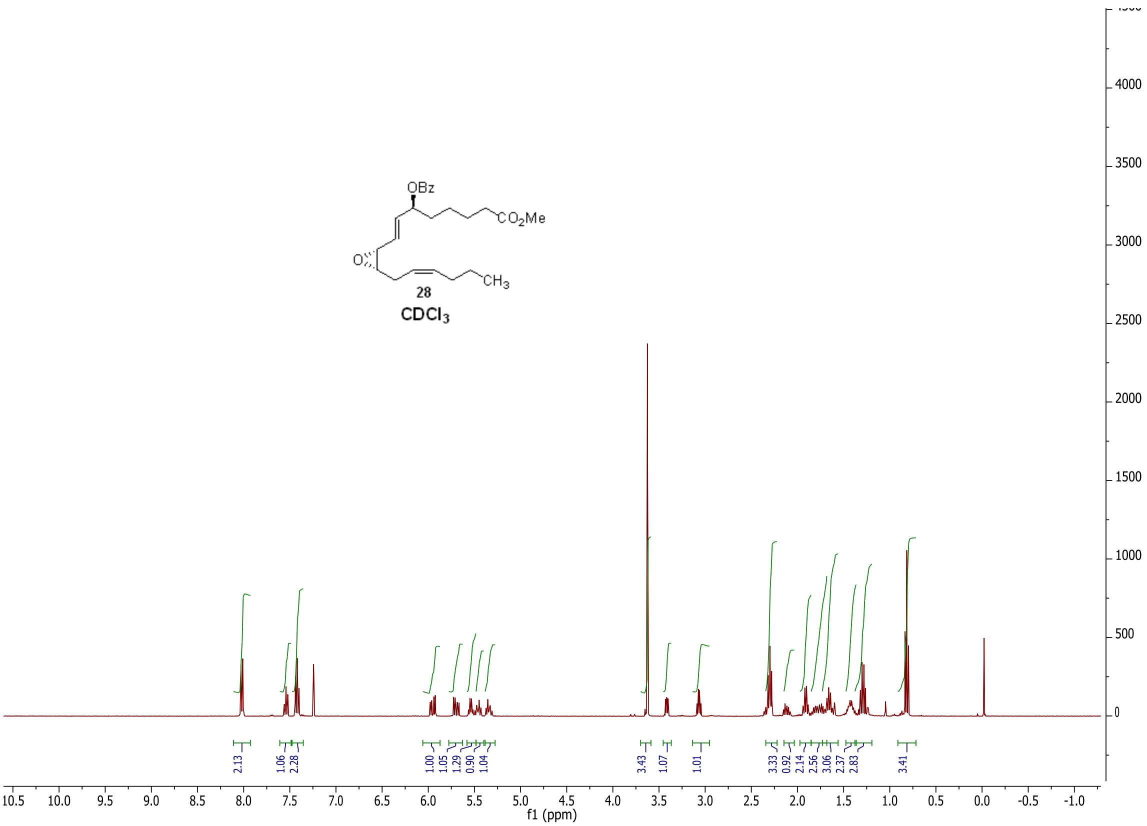
OBz
CO2Me
O
CH3
28
CDCl3
2.13
1.06
2.28
1.00
1.05
1.29
0.90
1.04
3.43
1.07
1.01
3.33
0.92
2.14
2.56
3.06
2.37
2.83
3.41
10.5
10.0
9.5
9.0
8.5
8.0
7.5
7.0
6.5
6.0
5.5
5.0
4.5
4.0
3.5
3.0
2.5
2.0
1.5
1.0
0.5
0.0
-0.5
-1.0
f1 (ppm)
4000
3500
3000
2500
2000
1500
1000
500
0

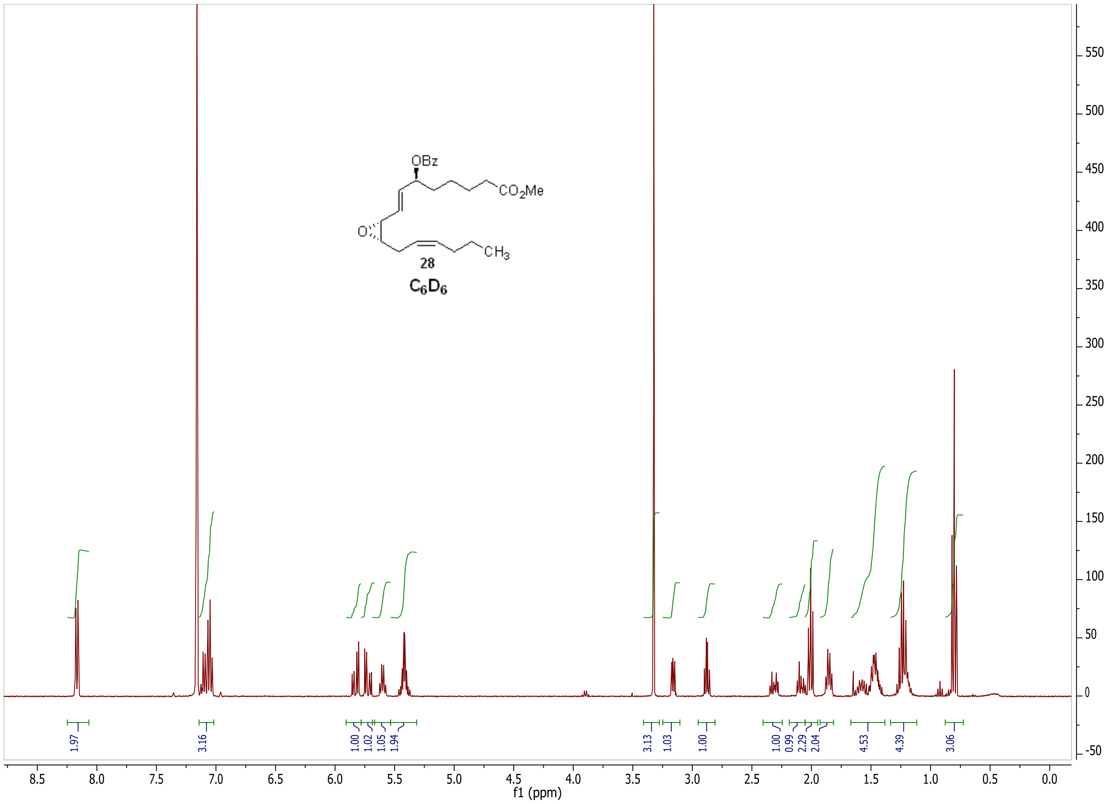
OBz
CO2Me
O
CH3
1.97
3.16
1.00
1.02
1.05
1.94
3.13
1.03
1.00
1.00
0.99
2.29
2.04
4.53
4.39
3.06
8.5
8.0
7.5
7.0
6.5
6.0
5.5
5.0
4.5
4.0
3.5
3.0
2.5
2.0
1.5
1.0
0.5
0.0
f1 (ppm)
550
500
450
400
350
300
250
200
150
100
50
0
-50

28

C_6D_6

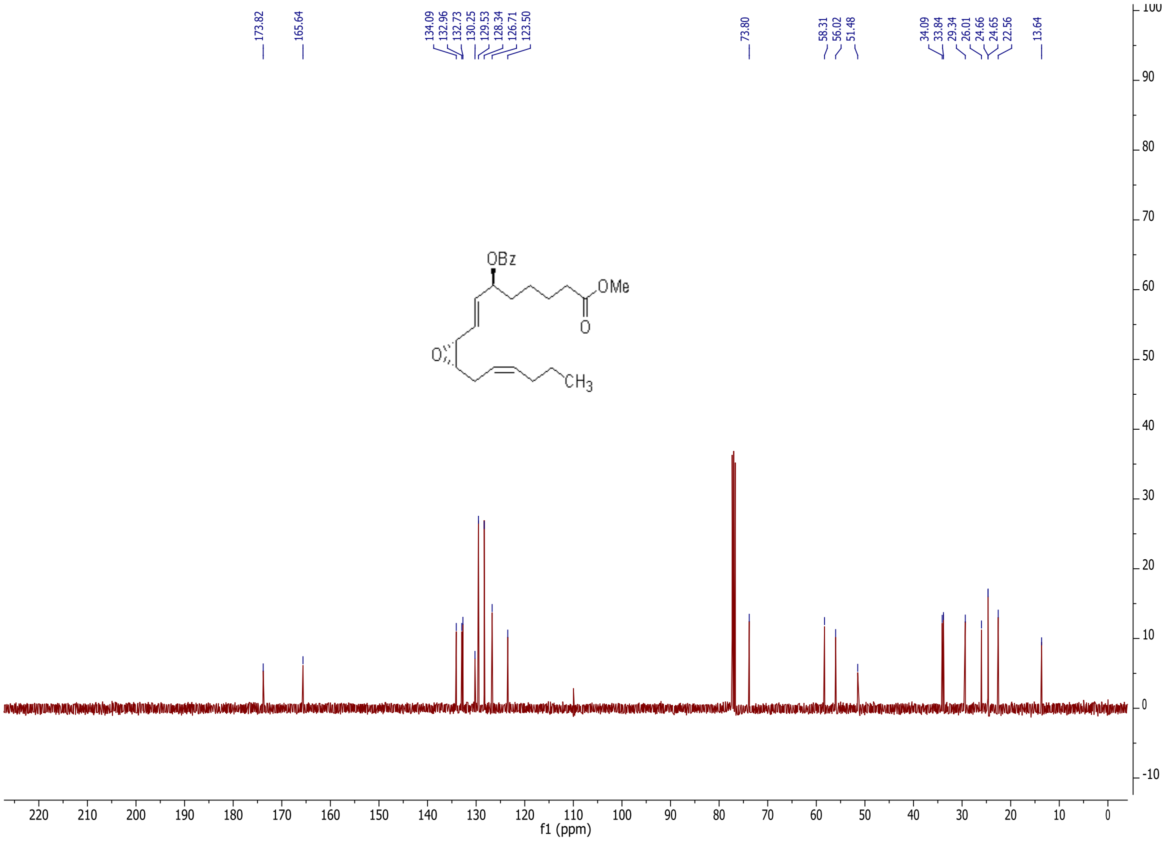
173.82
165.64
134.09
132.96
132.73
130.25
129.53
128.34
126.71
123.50
73.80
58.31
56.02
51.48
34.09
33.84
29.34
26.01
24.66
24.65
22.56
13.64
OBz
OMe
O
O
CH3
100
90
80
70
60
50
40
30
20
10
0
-10
220
210
200
190
180
170
160
150
140
130
120
110
100
90
80
70
60
50
40
30
20
10
0
f1 (ppm)

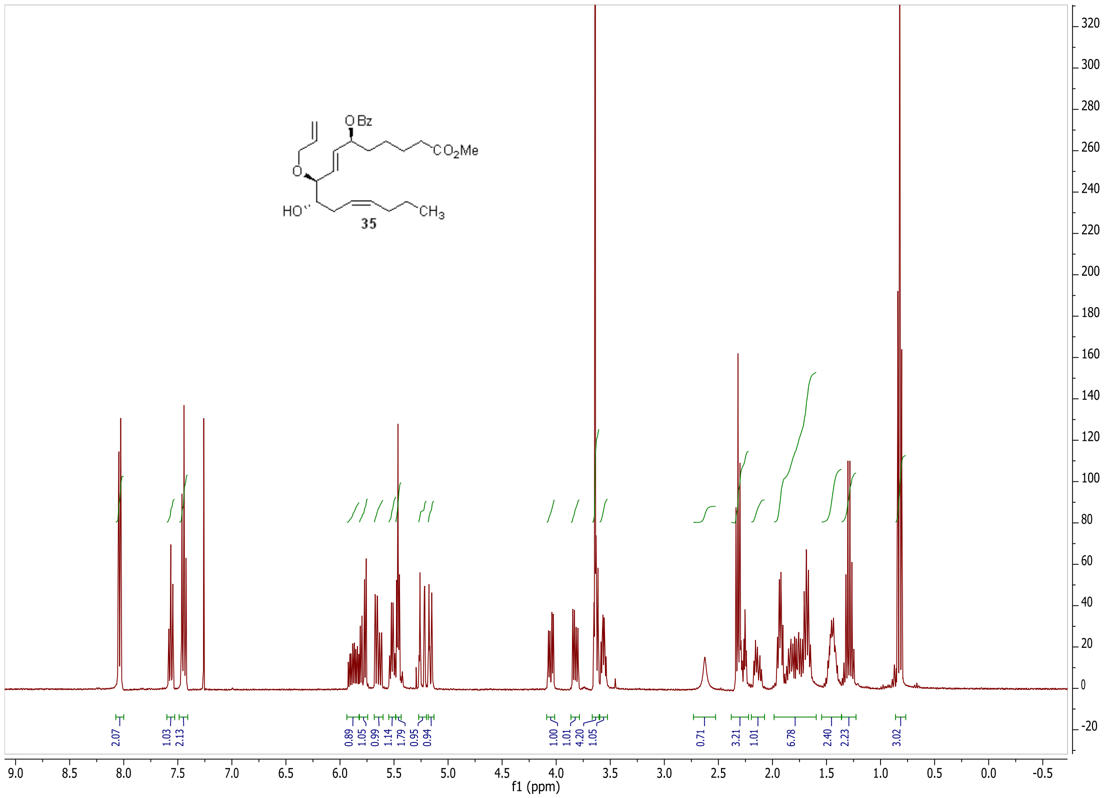
OBz
CO2Me
O
HO
CH3
35
2.07
1.03
2.13
0.89
1.05
0.99
1.14
1.79
0.95
0.94
1.00
1.01
4.20
1.05
0.71
3.21
1.01
6.78
2.40
2.23
3.02
9.0
8.5
8.0
7.5
7.0
6.5
6.0
5.5
5.0
4.5
4.0
3.5
3.0
2.5
2.0
1.5
1.0
0.5
0.0
-0.5
f1 (ppm)
320
300
280
260
240
220
200
180
160
140
120
100
80
60
40
20
0
-20

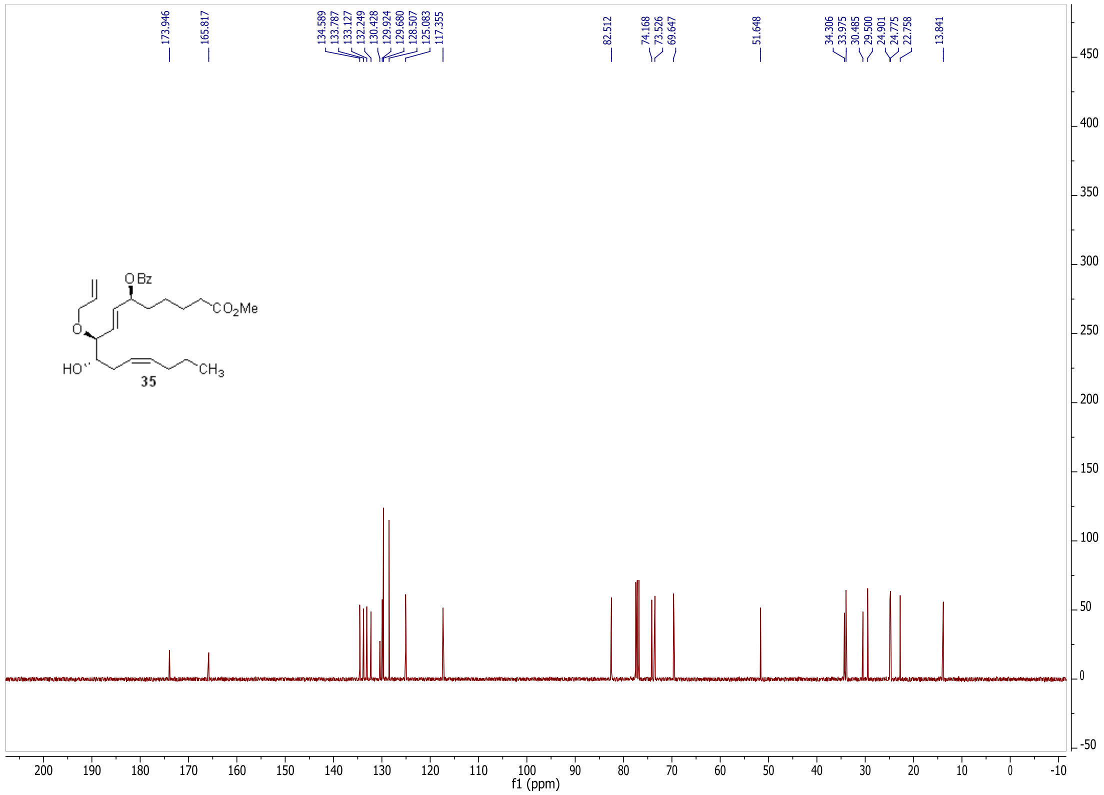
173.946
165.817
134.589
133.787
133.127
132.249
130.428
129.924
129.680
128.507
125.083
117.355
82.512
74.168
73.526
69.647
51.648
34.306
33.975
30.485
29.500
24.901
24.775
22.758
13.841
OBz
CO2Me
O
HO
CH3
35
200
190
180
170
160
150
140
130
120
110
100
90
80
70
60
50
40
30
20
10
0
-10
f1 (ppm)
450
400
350
300
250
200
150
100
50
0
-50

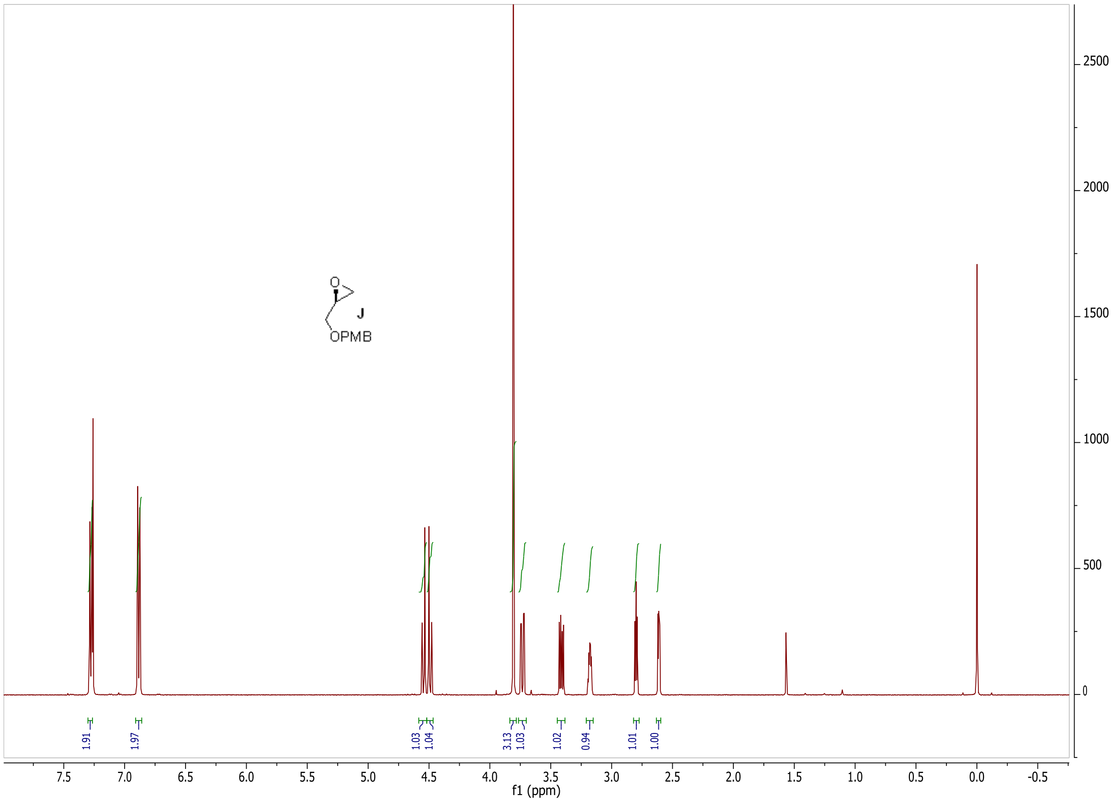
O
J
OPMB
2500
2000
1500
1000
500
0
1.91
1.97
1.03
1.04
3.13
1.03
1.02
0.94
1.01
1.00
7.5
7.0
6.5
6.0
5.5
5.0
4.5
4.0
3.5
3.0
2.5
2.0
1.5
1.0
0.5
0.0
-0.5
f1 (ppm)

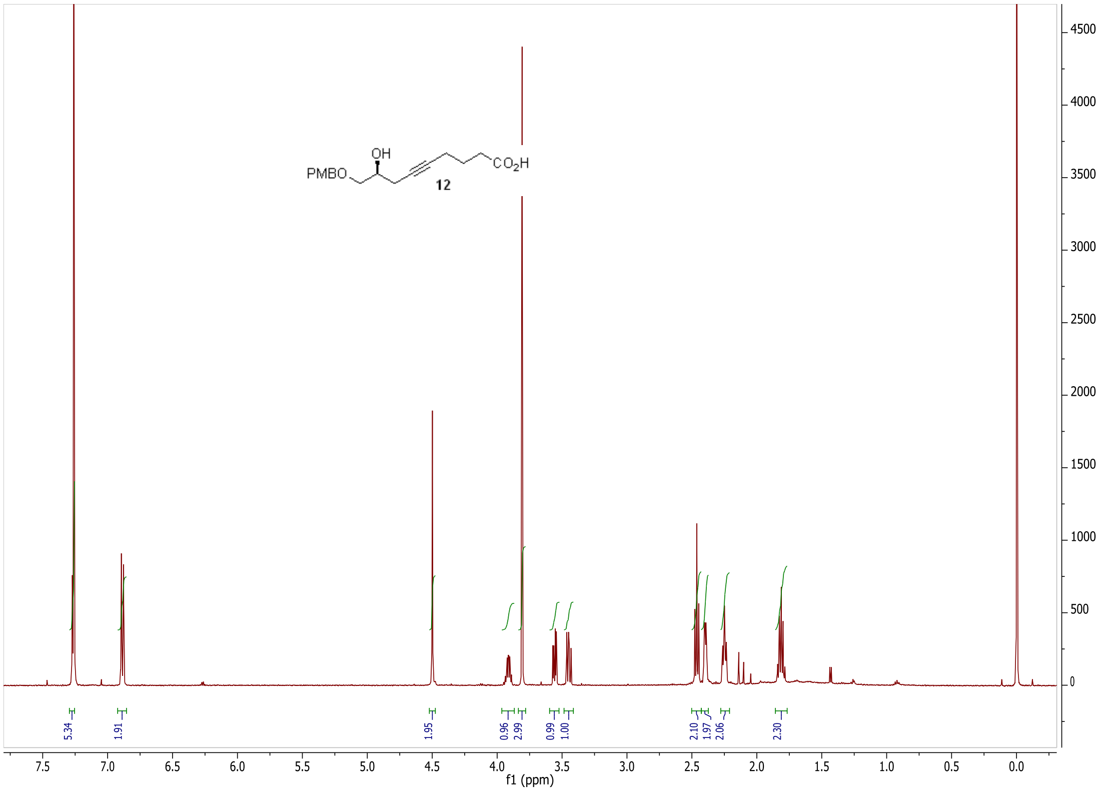
OH
PMBO
CO2H
12
4500
4000
3500
3000
2500
2000
1500
1000
500
0
5.34
1.91
1.95
0.96
2.99
0.99
1.00
2.10
1.97
2.06
2.30
7.5
7.0
6.5
6.0
5.5
5.0
4.5
4.0
3.5
3.0
2.5
2.0
1.5
1.0
0.5
0.0
f1 (ppm)

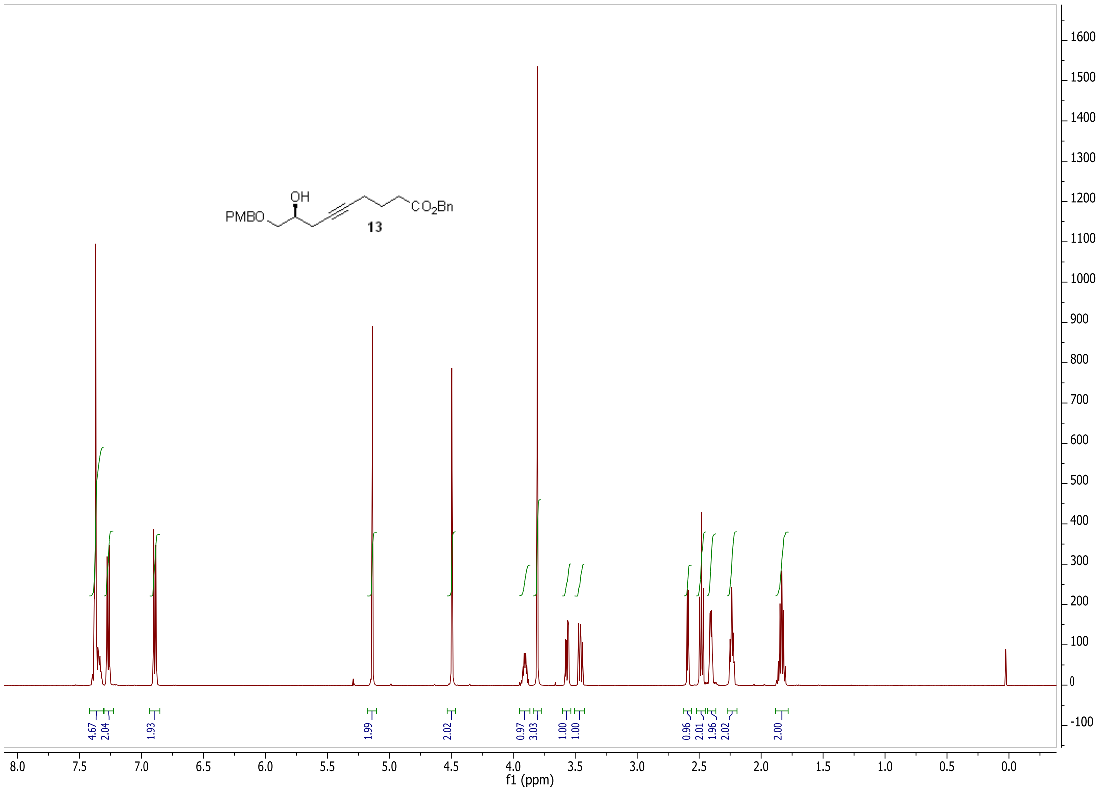
OH
PMBO
CO2Bn
13
4.67
2.04
1.93
1.99
2.02
0.97
3.03
1.00
1.00
0.96
2.01
1.96
2.02
2.00
8.0 7.5 7.0 6.5 6.0 5.5 5.0 4.5 4.0 3.5 3.0 2.5 2.0 1.5 1.0 0.5 0.0
f1 (ppm)
1600 1500 1400 1300 1200 1100 1000 900 800 700 600 500 400 300 200 100 0 -100

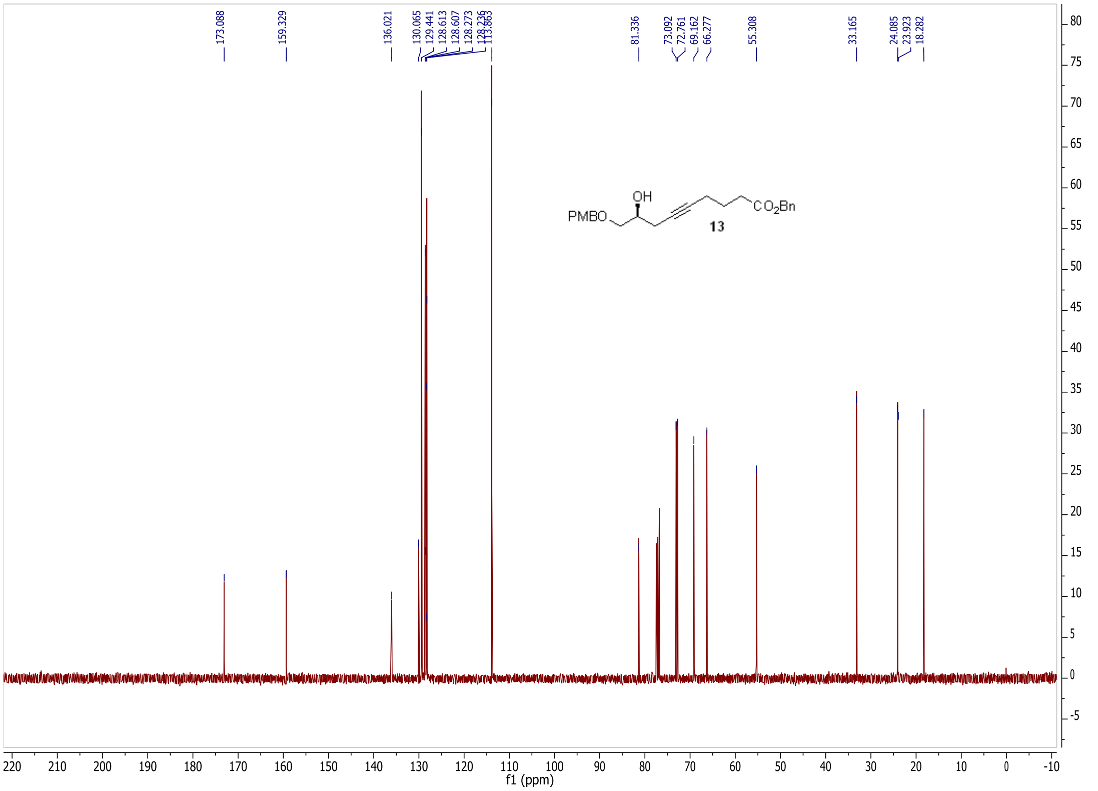
173.088
159.329
136.021
130.065
129.441
128.613
128.607
128.273
128.236
113.863
81.336
73.092
72.761
69.162
66.277
55.308
33.165
24.085
23.923
18.282
OH
PMBO
CO2Bn
13
220 210 200 190 180 170 160 150 140 130 120 110 100 90 80 70 60 50 40 30 20 10 0 -10
f1 (ppm)
80 75 70 65 60 55 50 45 40 35 30 25 20 15 10 5 0 -5

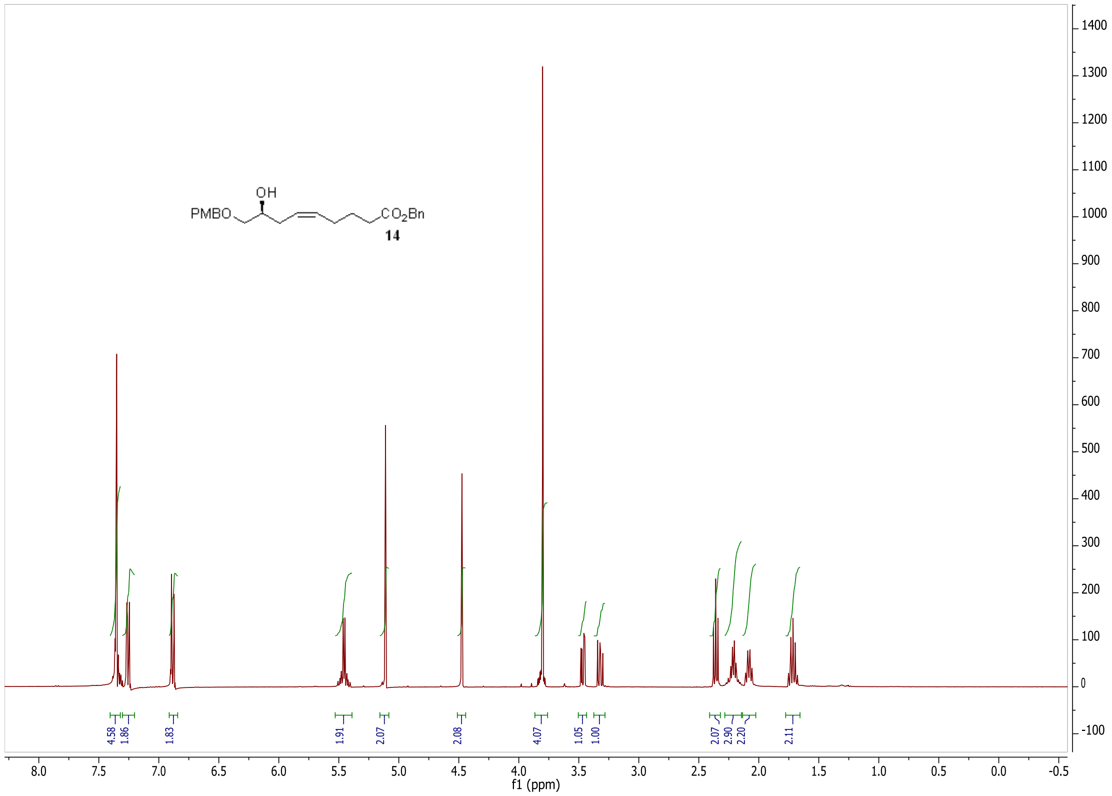
PMBO
OH
CO2Bn
14
4.58
1.86
1.83
1.91
2.07
2.08
4.07
1.05
1.00
2.07
2.90
2.20
2.11
f1 (ppm)

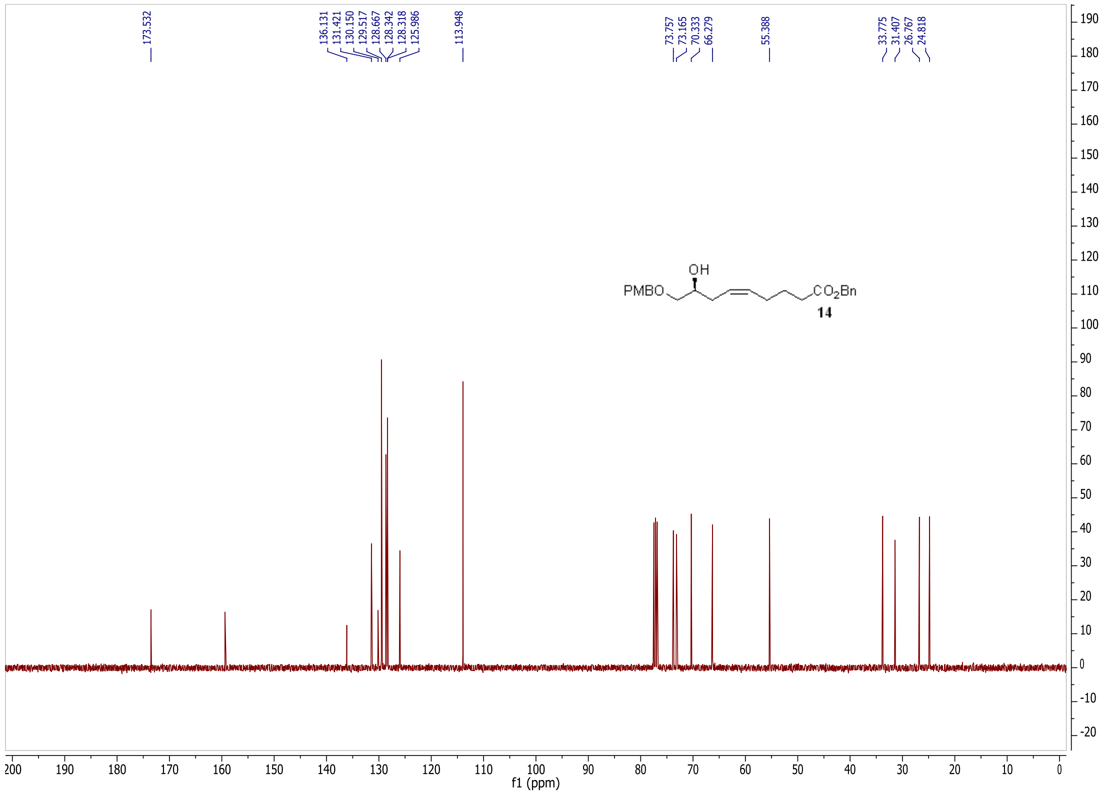
173.532
136.131
131.421
130.150
129.517
128.667
128.342
128.318
125.986
113.948
73.757
73.165
70.333
66.279
55.388
33.775
31.407
26.767
24.818
PMBO
OH
CO2Bn
14
f1 (ppm)

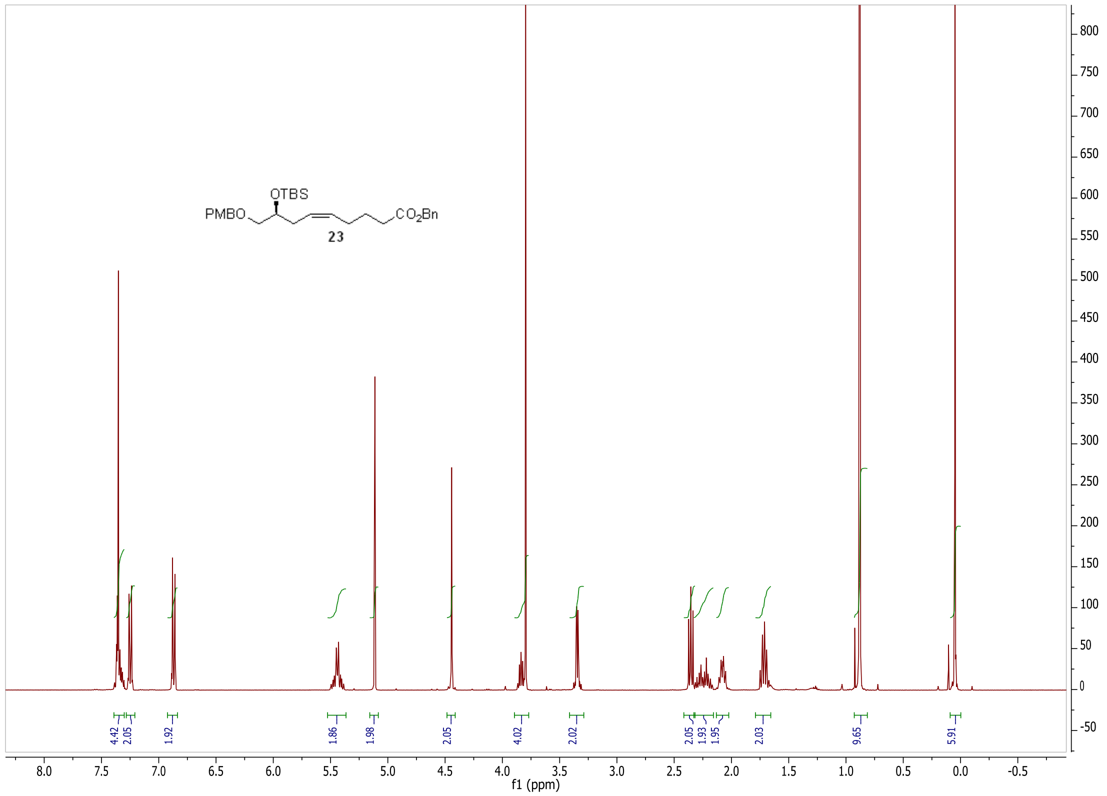
OTBS
PMBO
CO2Bn
23
4.42
2.05
1.92
1.86
1.98
2.05
4.02
2.02
2.05
1.93
1.95
2.03
9.65
5.91
8.0
7.5
7.0
6.5
6.0
5.5
5.0
4.5
4.0
3.5
3.0
2.5
2.0
1.5
1.0
0.5
0.0
-0.5
f1 (ppm)
800
750
700
650
600
550
500
450
400
350
300
250
200
150
100
50
0
-50

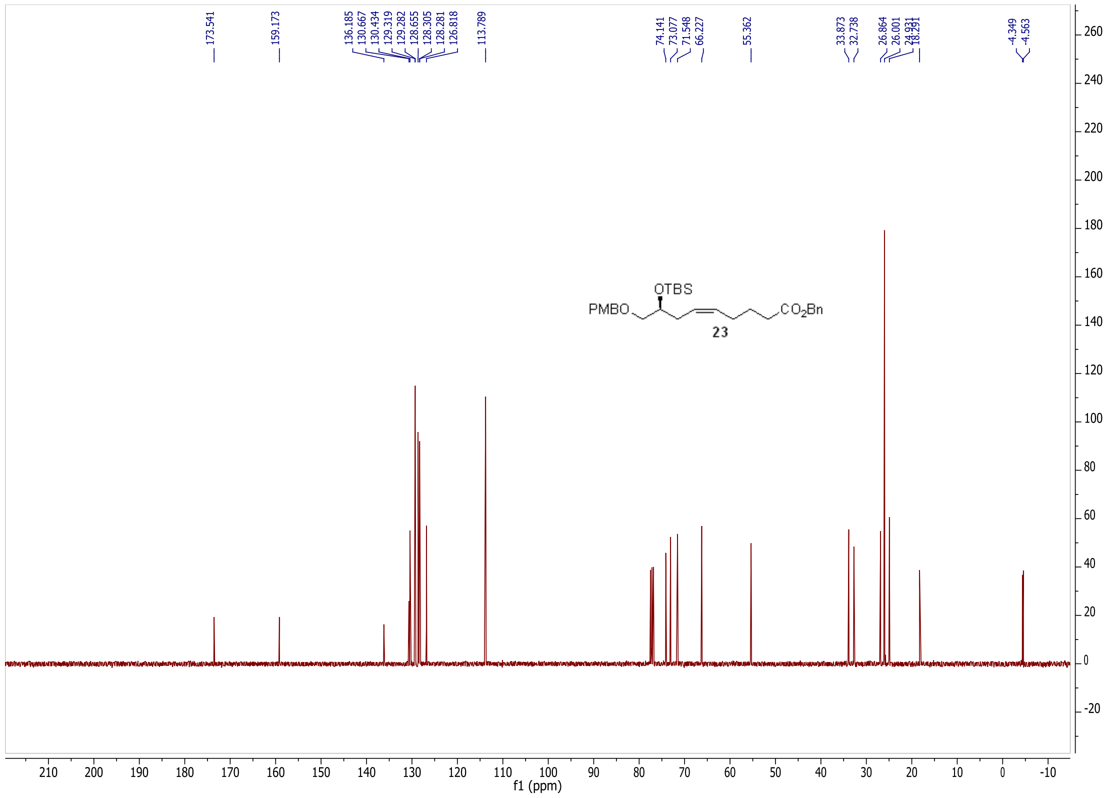
173.541
159.173
136.185
130.667
130.434
129.319
129.282
128.655
128.305
128.281
126.818
113.789
74.141
73.077
71.548
66.227
55.362
33.873
32.738
26.864
26.001
24.931
18.291
-4.349
-4.563
OTBS
PMBO
CO2Bn
23
210
200
190
180
170
160
150
140
130
120
110
100
90
80
70
60
50
40
30
20
10
0
-10
f1 (ppm)
260
240
220
200
180
160
140
120
100
80
60
40
20
0
-20

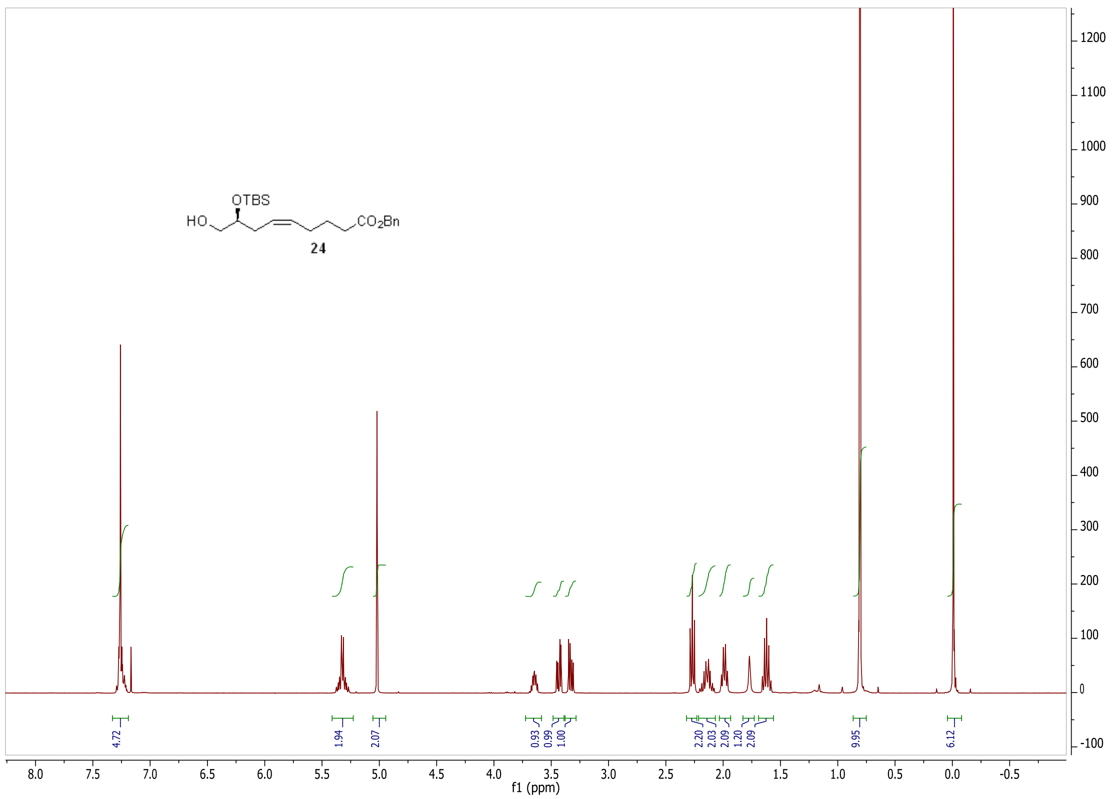
OTBS
HO
CO2Bn
24
4.72
1.94
2.07
0.93
0.99
1.00
2.20
2.03
2.09
1.20
2.09
9.95
6.12
8.0
7.5
7.0
6.5
6.0
5.5
5.0
4.5
4.0
3.5
3.0
2.5
2.0
1.5
1.0
0.5
0.0
-0.5
f1 (ppm)
1200
1100
1000
900
800
700
600
500
400
300
200
100
0
-100

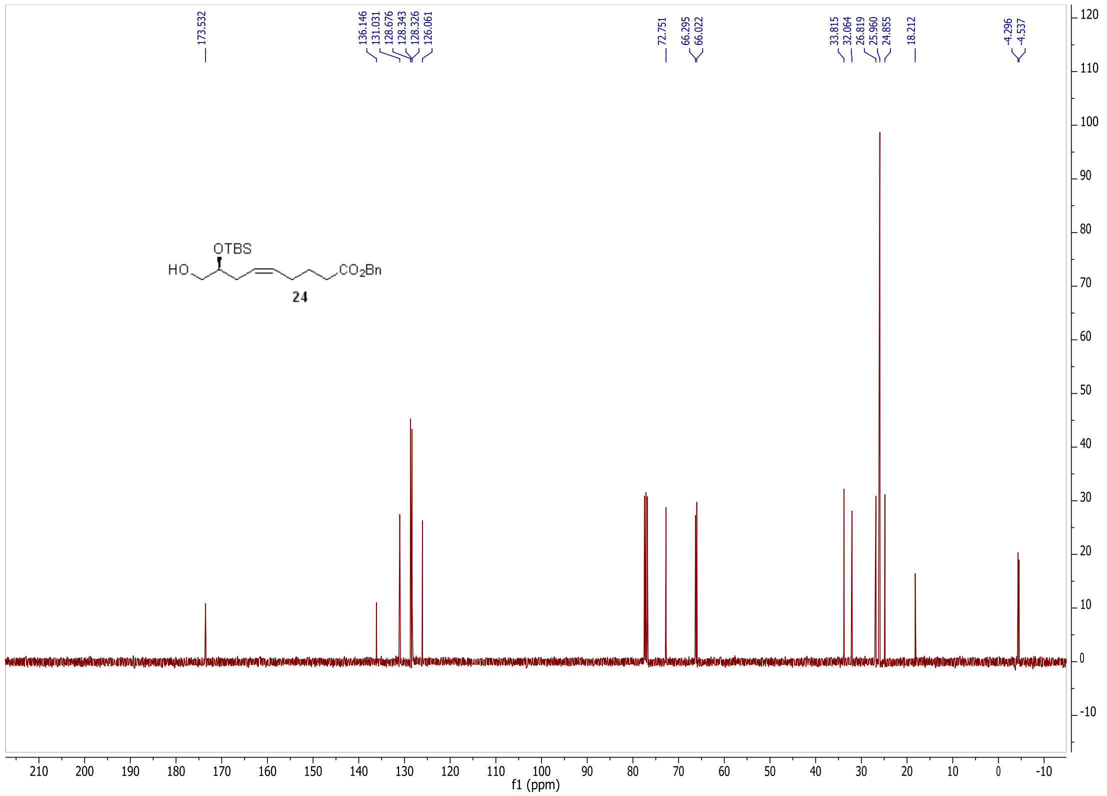
173.532
136.146
131.031
128.676
128.343
128.326
126.061
72.751
66.295
66.022
33.815
32.064
26.819
25.960
24.855
18.212
-4.296
-4.537
OTBS
HO
CO2Bn
24
210
200
190
180
170
160
150
140
130
120
110
100
90
80
70
60
50
40
30
20
10
0
-10
f1 (ppm)
120
110
100
90
80
70
60
50
40
30
20
10
0
-10

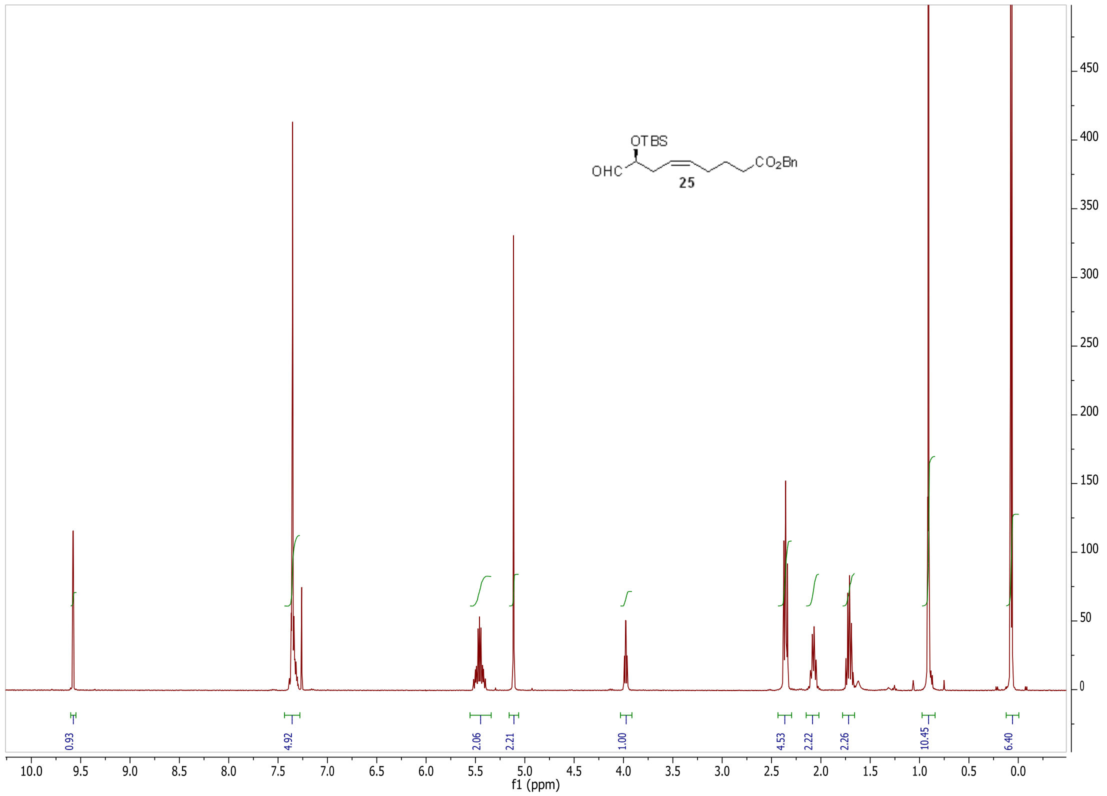
OTBS
OHC
CO2Bn
25
0.93
4.92
2.06
2.21
1.00
4.53
2.22
2.26
10.45
6.40
10.0
9.5
9.0
8.5
8.0
7.5
7.0
6.5
6.0
5.5
5.0
4.5
4.0
3.5
3.0
2.5
2.0
1.5
1.0
0.5
0.0
f1 (ppm)
450
400
350
300
250
200
150
100
50
0

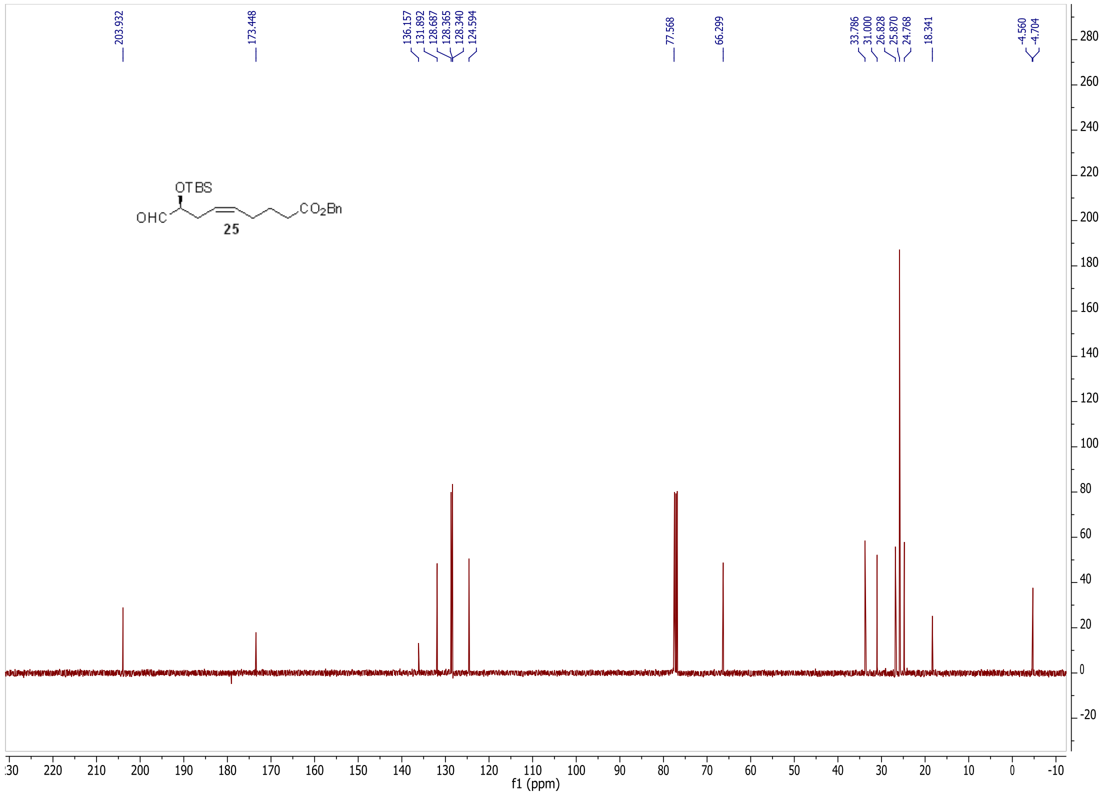
203.932
173.448
136.157
131.892
128.687
128.365
128.340
124.594
77.568
66.299
33.786
31.000
26.828
25.870
24.768
18.341
-4.560
-4.704
OTBS
OHC
CO2Bn
25
230
220
210
200
190
180
170
160
150
140
130
120
110
100
90
80
70
60
50
40
30
20
10
0
-10
f1 (ppm)
280
260
240
220
200
180
160
140
120
100
80
60
40
20
0
-20

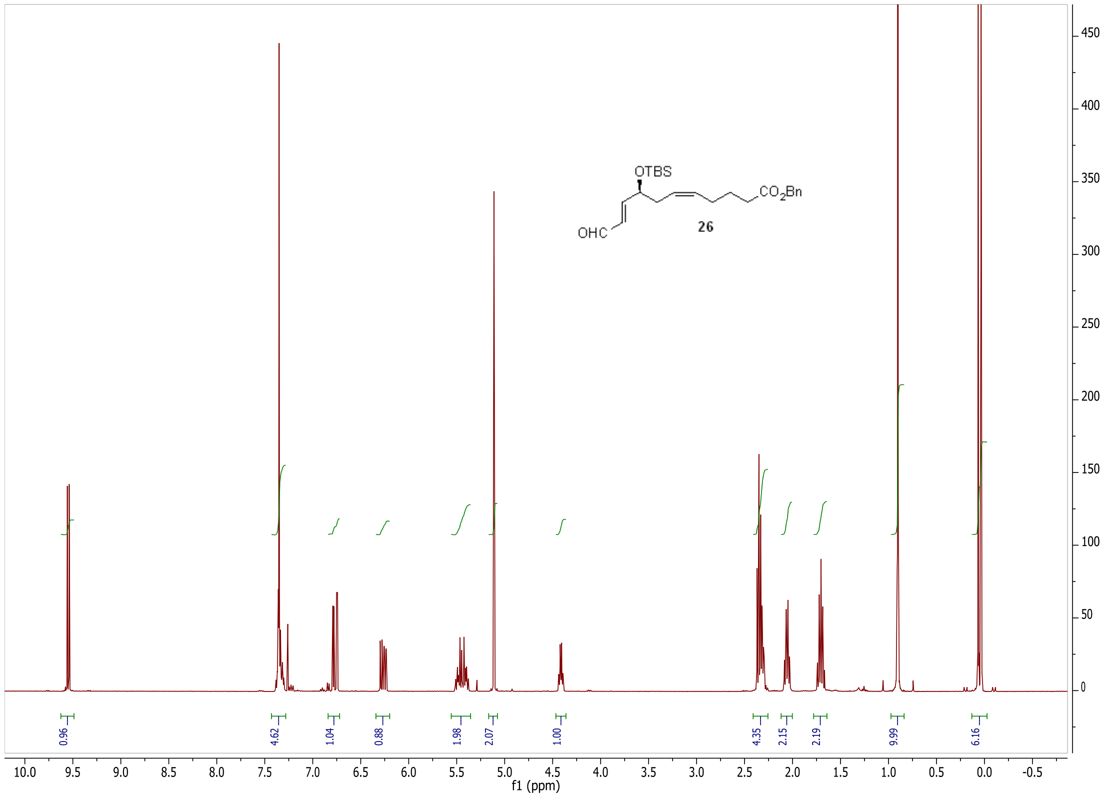
OTBS
CO2Bn
OHC
26
0.96
4.62
1.04
0.88
1.98
2.07
1.00
4.35
2.15
2.19
9.99
6.16
10.0 9.5 9.0 8.5 8.0 7.5 7.0 6.5 6.0 5.5 5.0 4.5 4.0 3.5 3.0 2.5 2.0 1.5 1.0 0.5 0.0 -0.5
f1 (ppm)
450 400 350 300 250 200 150 100 50 0

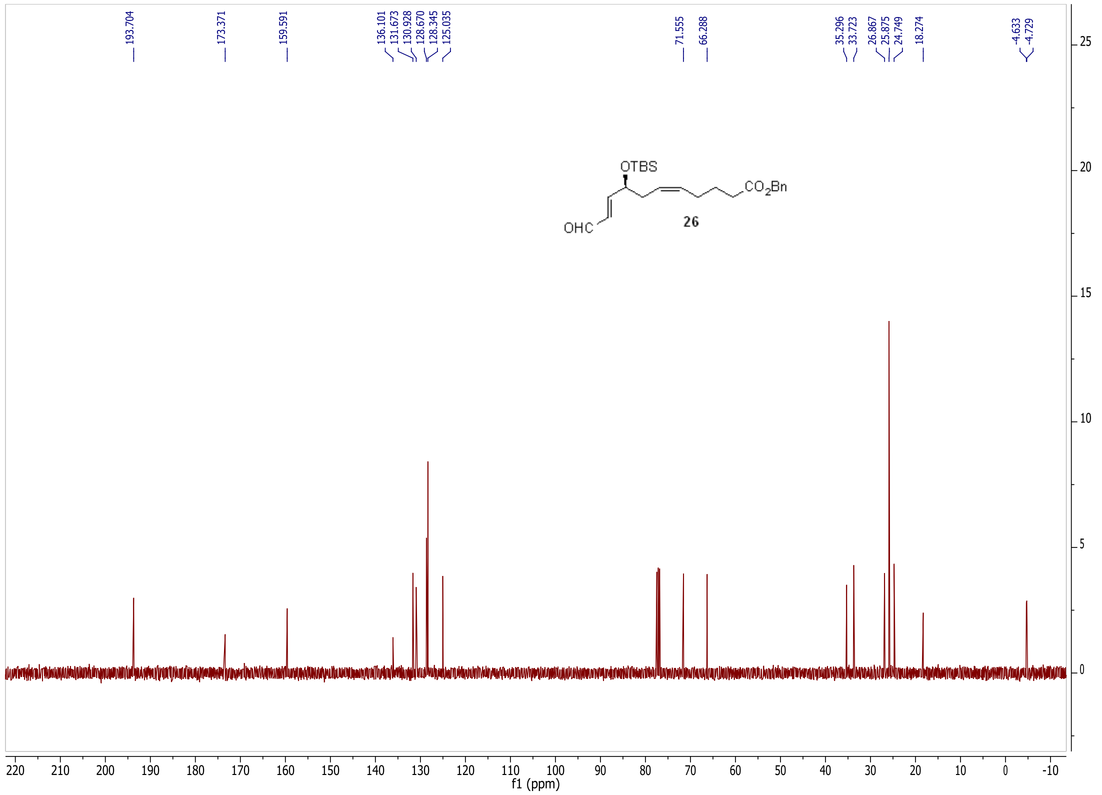
193.704
173.371
159.591
136.101
131.673
130.928
128.670
128.345
125.035
71.555
66.288
35.296
33.723
26.867
25.875
24.749
18.274
-4.633
-4.729
OTBS
CO2Bn
OHC
26
220 210 200 190 180 170 160 150 140 130 120 110 100 90 80 70 60 50 40 30 20 10 0 -10
f1 (ppm)
25 20 15 10 5 0

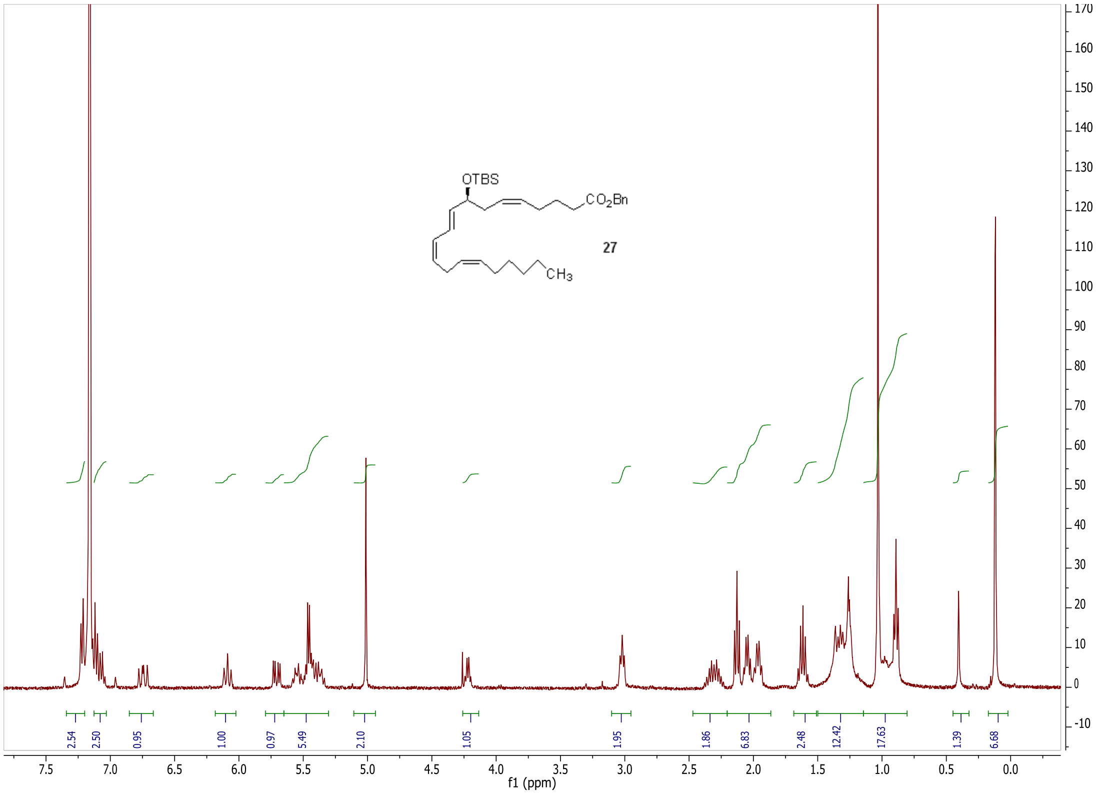
OTBS
CO2Bn
CH3
27
2.54
2.50
0.95
1.00
0.97
5.49
2.10
1.05
1.95
1.86
6.83
2.48
12.42
17.63
1.39
6.68
7.5
7.0
6.5
6.0
5.5
5.0
4.5
4.0
3.5
3.0
2.5
2.0
1.5
1.0
0.5
0.0
f1 (ppm)
170
160
150
140
130
120
110
100
90
80
70
60
50
40
30
20
10
0
-10

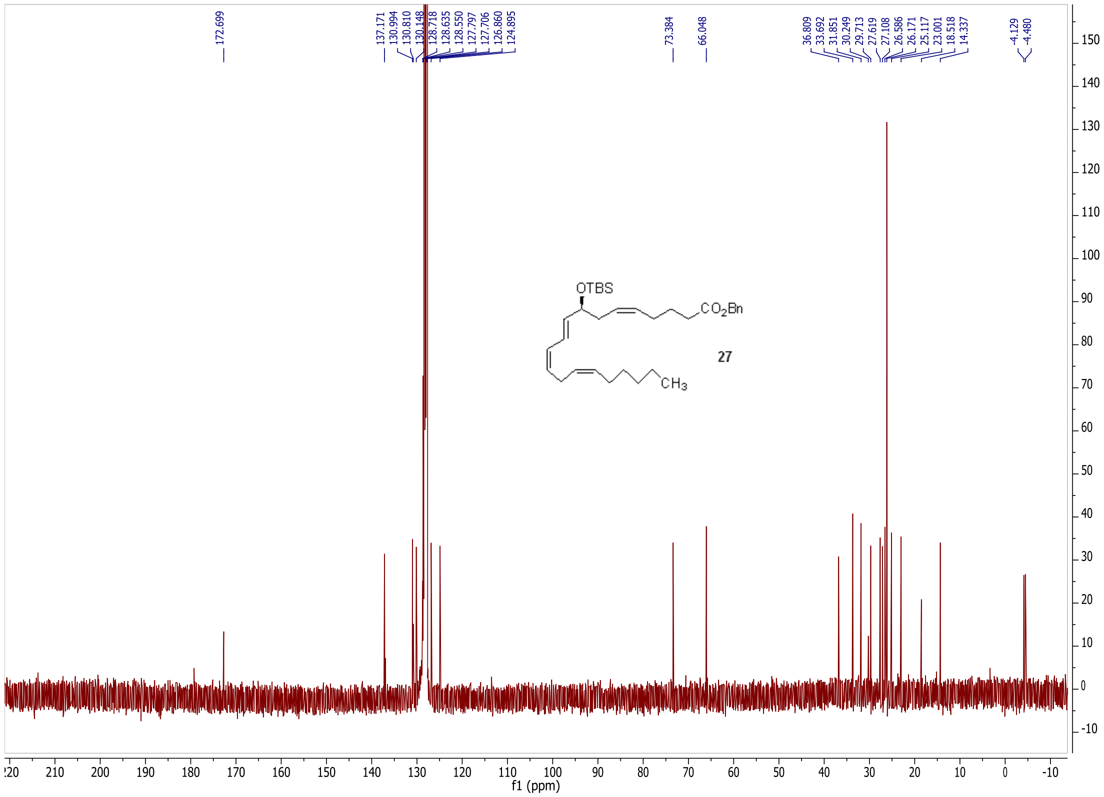
172.699
137.171
130.994
130.810
130.148
128.718
128.635
128.550
127.797
127.706
126.860
124.895
73.384
66.048
36.809
33.692
31.851
30.249
29.713
27.619
27.108
26.586
26.171
25.117
23.001
18.518
14.337
-4.129
-4.480
OTBS
CO2Bn
CH3
27
220
210
200
190
180
170
160
150
140
130
120
110
100
90
80
70
60
50
40
30
20
10
0
-10
f1 (ppm)
150
140
130
120
110
100
90
80
70
60
50
40
30
20
10
0
-10

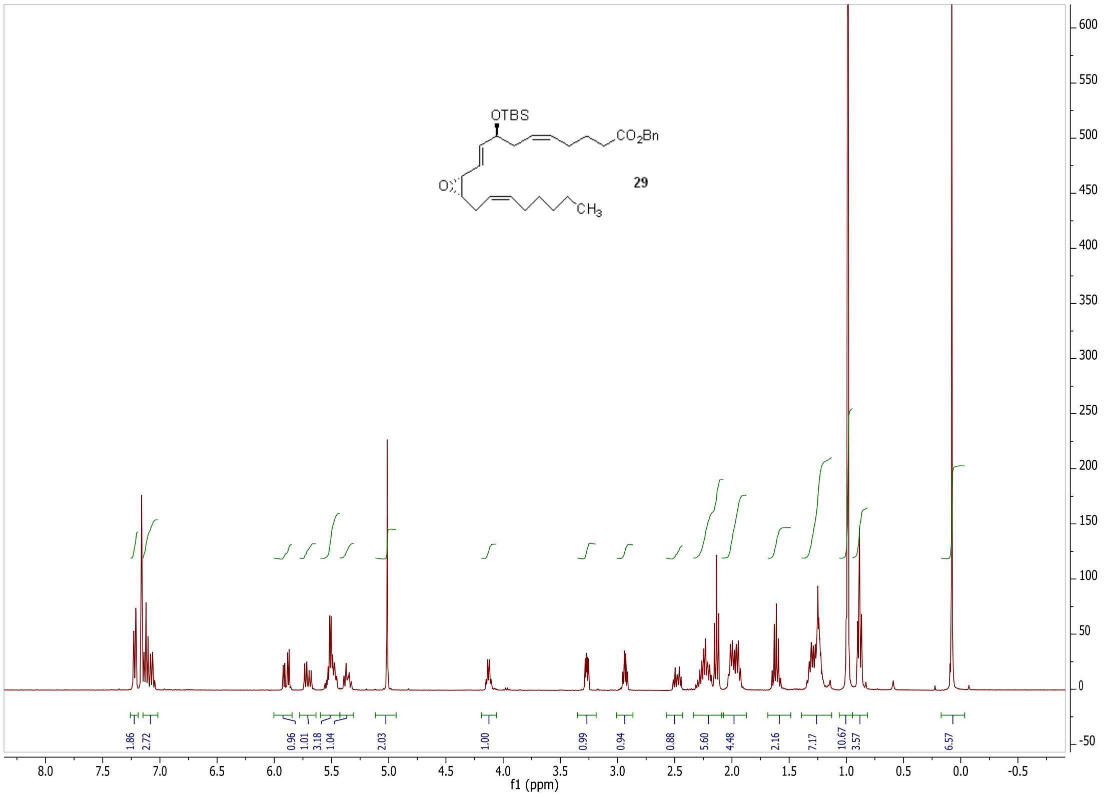
OTBS
CO2Bn
O
CH3
29
1.86
2.72
0.96
1.01
3.18
1.04
2.03
1.00
0.99
0.94
0.88
5.60
4.48
2.16
7.17
10.67
3.57
6.57
8.0
7.5
7.0
6.5
6.0
5.5
5.0
4.5
4.0
3.5
3.0
2.5
2.0
1.5
1.0
0.5
0.0
-0.5
f1 (ppm)
600
550
500
450
400
350
300
250
200
150
100
50
0
-50

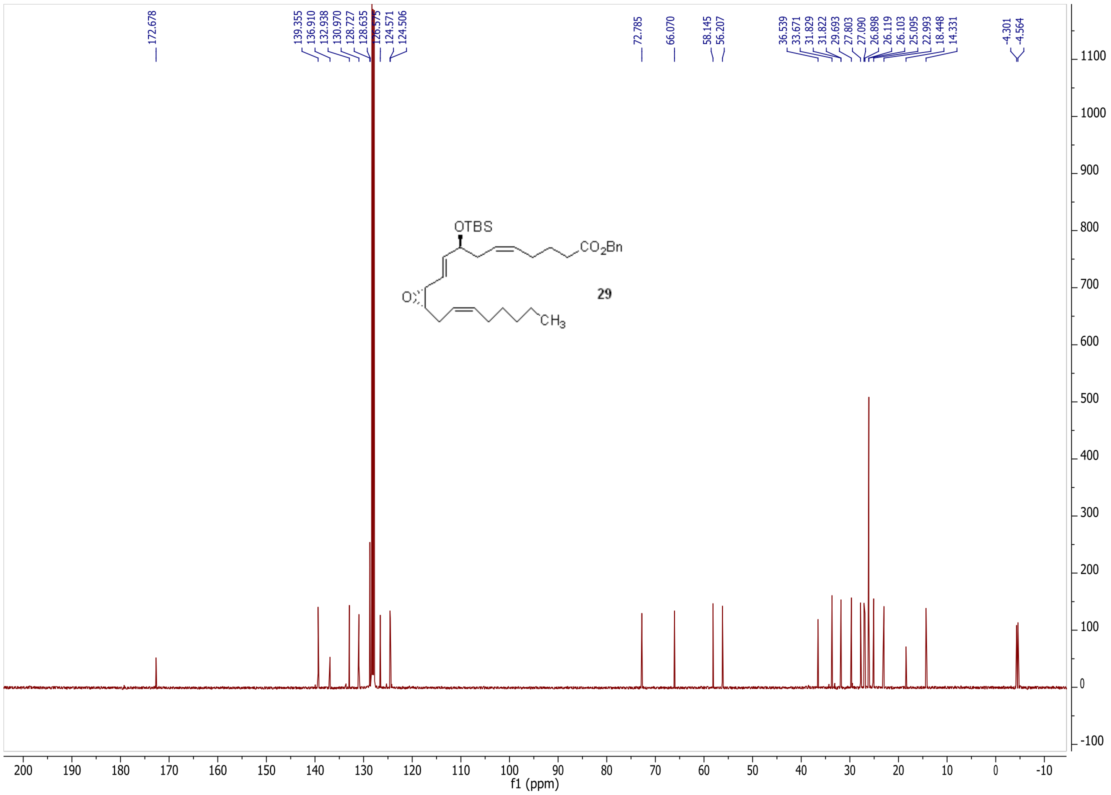
172.678
139.355
136.910
132.938
130.970
128.727
128.635
126.575
124.571
124.506
72.785
66.070
58.145
56.207
36.539
33.671
31.829
31.822
29.693
27.803
27.090
26.898
26.119
26.103
25.095
22.993
18.448
14.331
-4.301
-4.564
OTBS
CO2Bn
O
CH3
29
200
190
180
170
160
150
140
130
120
110
100
90
80
70
60
50
40
30
20
10
0
-10
f1 (ppm)
1100
1000
900
800
700
600
500
400
300
200
100
0
-100

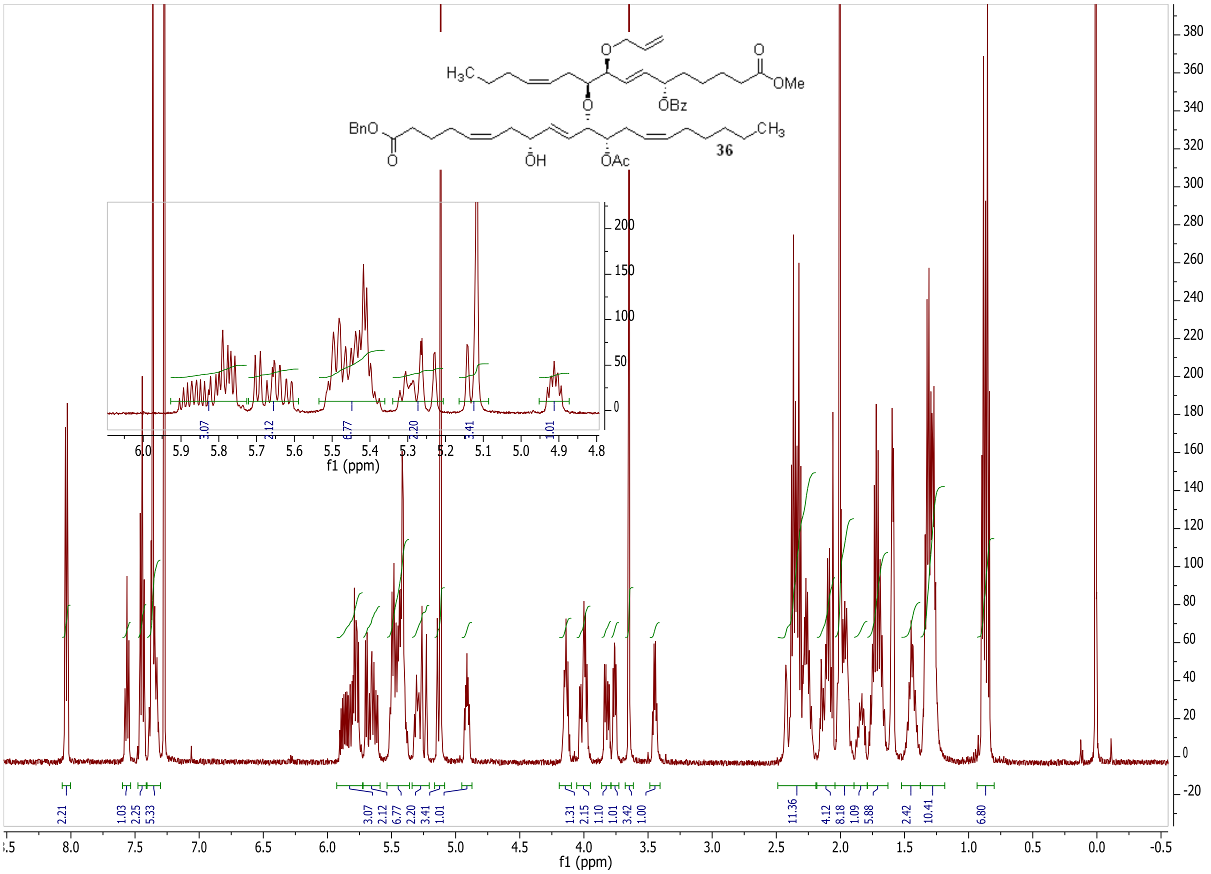
H3C
O
O
OMe
ŌBz
BnO
O
ŌH
ŌAc
CH3
36
6.0
5.9
5.8
5.7
5.6
5.5
5.4
5.3
5.2
5.1
5.0
4.9
4.8
f1 (ppm)
3.07
2.12
6.77
2.20
3.41
1.01
200
150
100
50
0
2.21
1.03
2.25
5.33
3.07
2.12
6.77
2.20
3.41
1.01
1.31
2.15
1.10
1.01
3.42
1.00
11.36
4.12
8.18
1.09
5.88
2.42
10.41
6.80
8.0
7.5
7.0
6.5
6.0
5.5
5.0
4.5
4.0
3.5
3.0
2.5
2.0
1.5
1.0
0.5
0.0
-0.5
f1 (ppm)
380
360
340
320
300
280
260
240
220
200
180
160
140
120
100
80
60
40
20
0
-20

Noyori RacemicBenzoate

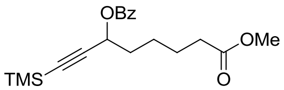

Detector A 254 nm

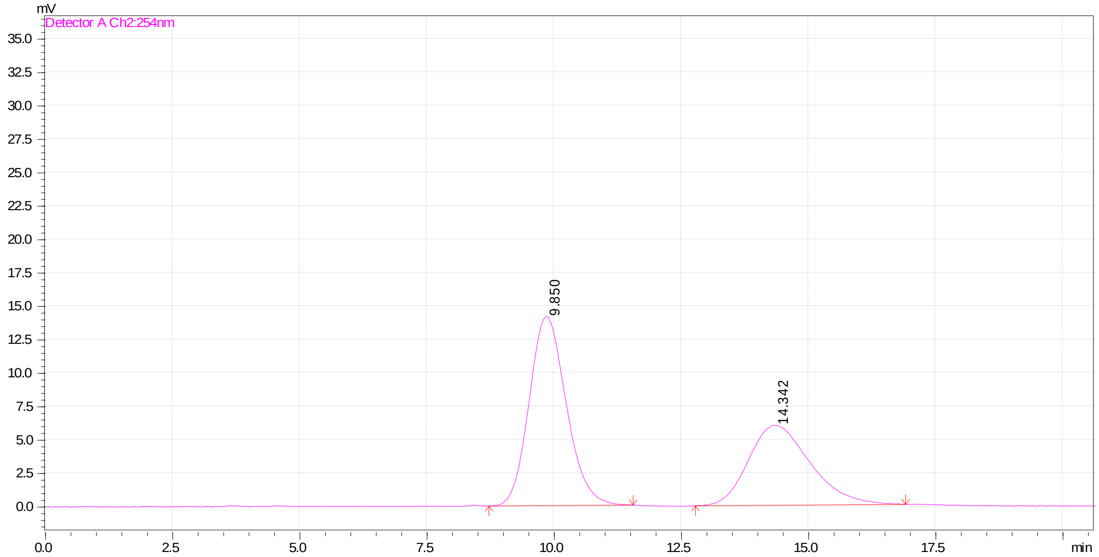

Peak #	Ret. Time	Area	Height	Area%
1	9.85	718641	14156	58.7
2	14.3	505305	5982	41.3

Detector A 205nm

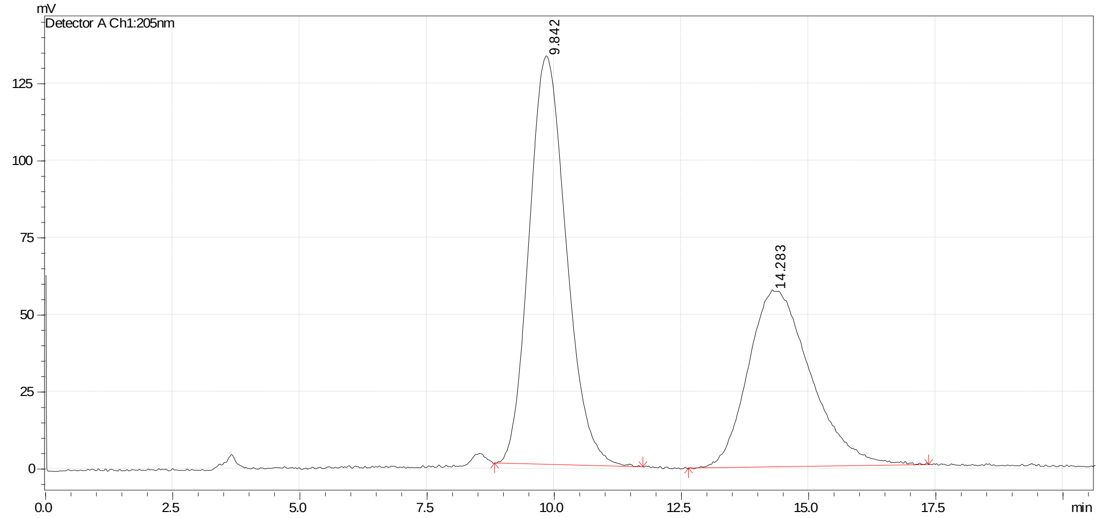

Peak #	Ret. Time	Area	Height	Area%
1	9.84	6757710	132525	58.0
2	14.28	4903154	57383	42.0

Noyori S,S-ligand Benzoate

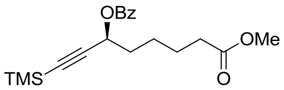

Detector A 205nm

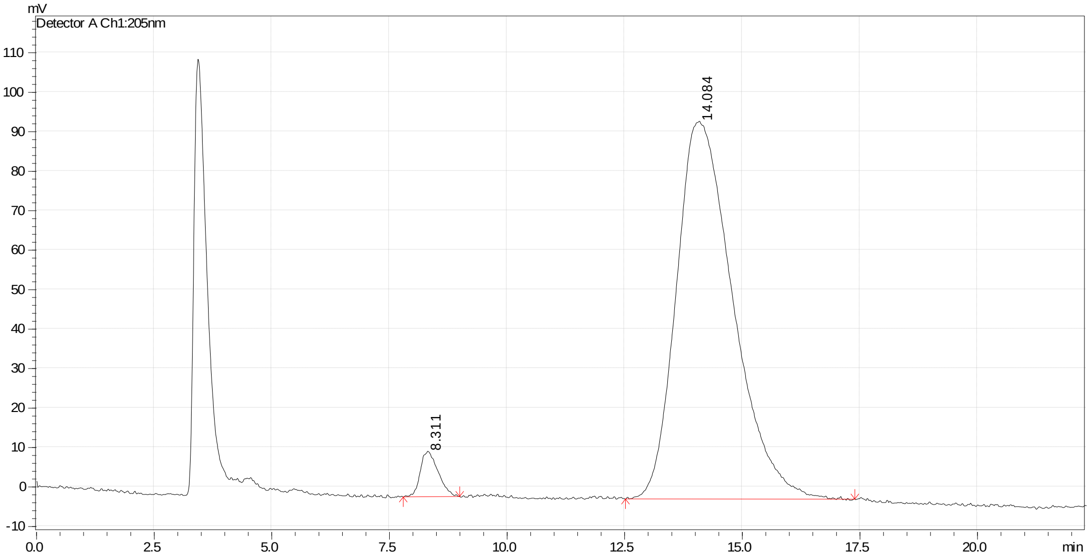

Peak #	Ret. Time	Area	Height	Area%
1	8.31	304700	11538	3.60
2	14.08	8025148	95712	96.4

Detector A 254 nm

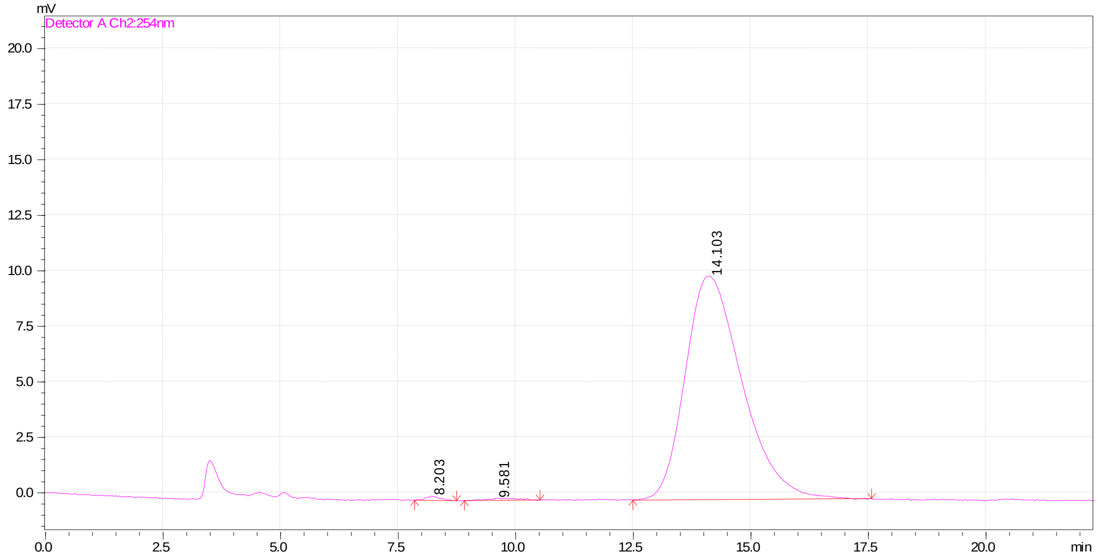

Peak #	Ret. Time	Area	Height	Area%
1	8.20	4185	197	0.49
2	9.58	4028	103	0.47
3	14.10	847885	10066	99.0

ChiralCel OJ-H, 250 X 4.6 mm, 0.375% IPA/hexanes, 1.0 mL/min, 20 µL injection